PROCEEDINGS
OF THE TENTH
ARCTIC AND MARINE OILSPILL PROGRAM
TECHNICAL SEMINAR

JUNE 9-11, 1987

EDMONTON, ALBERTA

87-05961/

Printed in Canada

PROCEEDINGS OF THE TENTH
ARCTIC AND MARINE OILSPILL PROGRAM
TECHNICAL SEMINAR

Seminar Sponsored by
Conservation and Protection
Environment Canada
Seminar held June 9-11, 1987
Edmonton, Alberta

Inquiries relating to technical content of papers in this seminar should be directed to the author(s). Inquiries relating to the AMOP program in general should be directed to:

Technology Development and Technical
Services Branch
Environmental Protection
Conservation and Protection
Ottawa CANADA K1A 0E7

(613) 998-9622

© Minister of Supply and Services Canada 1987
Cat. No. En 40-11/5-1987E
ISBN 0-662-15463-0

TABLE OF CONTENTS

PAGE

SESSION I Properties, Behaviour and Modelling

OIL SUBMERGENCE: WIND/WAVE TANK TESTS AND MODELLING 1

I.A. Buist and S.G. Potter
S.L. Ross Environmental Research
Ottawa, Ontario

OBSERVATIONS AND INITIAL RESULTS FROM A SITE VISIT TO THE "METULA" SPILL 12½ YEARS AFTER THE INCIDENT 21

E.H. Owens
Grampian, Scotland

W. Robson
Calgary, Alberta

B. Humphrey
Seakem Oceanography
Sydney, British Columbia

LONG-TERM FATE OF DISPERSED OIL AT LOW TEMPERATURES IN AN EXPERIMENTAL MESOSCALE TANK 43

E. Pelletier and C. Brochu
INRS - Oceanologie
Rimouski, Quebec

J. Vandermeulen
Bedford Institue of Oceanography
Dartmouth, Nova Scotia

SATURATION/PENETRATION OF NORMAN WELLS CRUDE OIL INTO UKALERK BORROW PIT SAND 63

A.G. Holoboff and R.J. Foster
Esso Resources Canada
Calgary, Alberta

A NOVEL INTERACTIVE OIL SPILL MODEL 79

D.G. Wilson and D. Mackay
University of Toronto
Toronto, Ontario

ENVIRONMENTAL EFFECTS OF OIL SPILL COMBUSTION 91

D. Evans, G. Mulholland,
D. Gross and H. Baum
National Bureau of Standards
Gaithersberg, Maryland

K. Saito
University of Kentucky
Lexington, Kentucky

PAGE

MODELLING OIL SPILLS IN LEADS: WIND/WAVE TANK TESTING AND PRELIMINARY RESULTS 131

I.A. Buist, S.P. Joyce and S.L. Ross
S.L. Ross Environmental Research
Ottawa, Ontario

SESSION II Biological Fate and Effects

FATE AND EFFECTS OF DISPERSED AND NON-DISPERSED OIL ON ARCTIC MUD FLATS 149

P. Sveum
SINTEF
Trondheim, Norway

DEVELOPMENT OF A CONTINUOUS FLOW EXPOSURE SYSTEM FOR OIL EFFECTS TESTING 169

M.S. Hutcheson, R. Odense and R.M. Gershey
Seakem Oceanography
Dartmouth, Nova Scotia

J. Vandermeulen
Bedford Institute of Oceanography
Dartmouth, Nova Scotia

ACCIDENTLY SPILLED GAS-OIL IN A SHORELINE SEDIMENT ON SPITSBERGEN: NATURAL FATE AND ENHANCEMENT OF BIODEGRADATION 177

P. Sveum
SINTEF
Trondheim, Norway

SESSION III Countermeasures

LABORATORY TESTING TO OPTIMIZE THE PERFORMANCE OF A HIGH PRESSURE WATERJET BARRIER 193

L.D. Phillips and A.M. Nawwar
Arctec Canada
Kanata, Ontario

F. Laperrière
Environment Canada
Ottawa, Ontario

PAGE

HIGH PRESSURE WATER JET TESTING FOR OIL CONTAINMENT IN SIMULATED ENVIRONMENTAL CONDITIONS 209

F. Laperriêre and H. Whittaker
Environment Canada
Ottawa, Ontario

M. Yanagisawa and I. Suzuki
Japan Foundation for Shipbuilding Advancement
Tsukuba, Japan

LABORATORY AND TEST TANK EVALUATION OF ELASTOL 223

M.A. Bobra and P.I. Kawamura
Consultchem
Ottawa, Ontario

M.F. Fingas and D. Velicogna
Environment Canada
Ottawa, Ontario

TEST AND EVALUATION OF THE HELITORCH FOR THE IGNITION OF OIL SLICKS 243

A.A. Allen
Spiltec
Anchorage, Alaska

SESSION IV Spill Tracking and Remote Sensing

EVALUATION OF SURFACE DRIFTERS FOR SATELLITE TRACKING OF OIL ON THE SEA SURFACE 267

M. Reed, C. Turner and M. Spaulding
Applied Science Associates
Narragansett, Rhode Island

D. Dorson
Bathy Systems
West Kingston, Rhode Island

CCRS REMOTE SENSING OF THE BEAUFORT SEA DISPERSANT TRIALS 1986 291

W.D. McColl, R.A.E. McGibbon and S.M. Till
Canada Centre for Remote Sensing
Ottawa, Ontario

SESSION V Dispersants

BEAUFORT SEA OIL DISPERSANT TRIAL 307

J.J. Swiss and N. Vanderkooy
Dome Petroleum
Calgary, Alberta

S.D. Gill
COGLA
Ottawa, Ontario

R.H. Goodman and H.M. Brown
Esso Resources Canada
Calgary, Alberta

PAGE

MID-SCALE TESTING OF DISPERSANT EFFECTIVENESS 329

R. Belore
S.L. Ross Environmental Research
Ottawa, Ontario

DISPERSANT TESTING AT THE ENVIRONMENTAL EMERGENCIES TECHNOLOGY DIVISION 343

M.F. Fingas, K.A. Hughes and M.A. Schweitzer
Environment Canada
Ottawa, Ontario

A STUDY OF DISPERSANT EFFECTIVENESS USING ULTRA-UNIFORM DROP-SIZE GENERATOR 357

R. Belore
S.L. Ross Environmental Research
Ottawa, Ontario

A STUDY OF OIL DISPERSION: THE ROLE OF MIXING AND WEATHERING 373

A. Chau and D. Mackay
University of Toronto
Toronto, Ontario

SESSION VI Activity Reports and Recent Spill Experiences

THE ARCO ANCHORAGE OIL SPILL, A REVIEW 385

D.W. Chamberlain, J.L. Siva and E.R. Mancini
Atlantic Richfield Co.
Los Angeles, California

R.A. Levine
ARCO Marine
Long Beach, California

ACS ALASKAN BERING SEA COASTAL RESOURCES MANUAL 397

S.O. Hillman
Standard Alaskan Production
Anchorage, Alaska

W.F. Gusey
Shell Oil
Anchorage, Alaska

D.W. Chamberlain
Atlantic Richfield Co.
Los Angeles, California

PAGE

CONTINUING THE PROGRAM: ALASKA CLEAN SEAS RESEARCH, DEVELOPMENT AND ENGINEERING 407

R.V. Shafer
Alaska Clean Seas
Anchorage, Alaska

ENVIRONMENTAL ATLAS FOR BEAUFORT SEA OIL SPILL RESPONSE 423

D.F. Dickens and I. Bjerkelund
D.F. Dickens and Associates
Vancouver, British Columbia

L. Martin and D. Erickson
Environmental Services Limited
Vancouver, British Columbia

S.G. Potter
S.L. Ross Environmental Research
Ottawa, Ontario

A NEW APPROACH TO EMERGENCY INCIDENT RESPONSE 449

R.H. Goodman
Esso Resources Canada
Calgary, Alberta

W.F. Mackay
Esso Chemical Canada
Toronto, Ontario

R.J. Woznow
Esso Petroleum Canada
Toronto, Ontario

THE USE OF POLYSULFIDE RUBBER MOLDS TO MEASURE OIL STORAGE VOLUMES 459

R.H. Goodman and A.G. Holoboff
Esso Resources Canada
Calgary, Alberta

OIL SUBMERGENCE: WIND/WAVE TANK TESTS AND MODELLING

I.A. Buist and S.G. Potter

S.L. Ross Environmental Research Limited
Ottawa, Ontario

INTRODUCTION

Given appropriate oceanographic conditions and oil properties it is possible for oil slicks to submerge beneath the sea surface. This renders detection, tracking and countermeasures for the spill extremely difficult if not impossible. The objective of this study was to validate and extend the work of previous studies on the formation and submergence of "sinkable" oil forms, and to develop operationally useful process equations to predict the conditions under which an oil spill might be expected to submerge.

Historical Perspective

Several oil spill incidents in the past have had reports of sinking or disappearance of oil slicks. These include the Arrow (Forrester 1971) in which large drops of emulsified Bunker C were detected at depths of up to 80 m; the US/NS Potomac (Petersen 1978) in which the Bunker C formed pancakes that eventually sank; the IXTOC-1 blowout during which large subsurface mats of weathered mousse were observed (Payne and Phillips 1985); the Kurdistan incident which sparked the current interest in oil submergence (C-CORE 1980); the Katina incident in which the heavy fuel oil submerged only to appear on shore later (Rijkwaterstaat 1982); and the recent Thuntank 5 incident in Sweden in which 36 to 40 tons of heavy fuel oil sank in icy waters (OSIR 1987).

The common thread among these incidents is that all involved very low or neutrally buoyant oils or water-in-oil emulsions that, through weathering, formed into particles or mats ranging in size from a millimetre or less to several metres. The criteria for oil submergence seem to be: low or neutral buoyancy and the formation of particulate oil forms.

The State-of-the-Art

Several previous studies have addressed various aspects of sinking or submergence of oil spills. Juszko et al. (1983) and Juszko (1985) have extensively reviewed both the oceanographic conditions conducive to oil submergence and the occurrence and frequency of those conditions in Canadian waters. Mackay et al. (1985 and 1986) presented an excellent literature review on the subject and conducted both small-scale tests with oils and mid-scale tests with surrogates that identified the mechanisms that result in oil submergence. These two most recent studies laid the groundwork for this study.

Other studies (WSL 1978; WSL 1981; S.L. Ross 1984, 1985; S.L. Ross and DMER 1987) have addressed the behaviour and weathering of oils that, when spilled, form into mats and droplets.

Rationale For The Study

To date, the oceanographic conditions studies and the small and mid-scale studies on oil pan/droplet formation and submergence have included extensive theoretical treatment, some small-scale testing and limited meso-scale testing with surrogates. What was required was extensive meso-scale testing with actual oils to validate the previous studies and permit the development of operationally useful equations to predict what percentage of the "slick" is submerged at various depths as a function of environmental conditions.

STUDY METHODS

Test Tank

The experimental portion of the study was conducted in a wind-wave tank (Figure 1) 11 m long, 1.2 m wide and 1.9 m high. The tank was filled with approximately 10,000 L of fresh water to a depth of 0.85 m. Saltwater was not used as it was thought that the oil-water density difference (i.e., buoyancy) rather than absolute densities was the key to submergence processes. This significantly reduced the complexity of the testing.

The tank was fitted with a submerged air-bubbler system in the glass-walled test section to prevent the sticky oils from quickly adhering to the sides of the tank; this permitted test runs of several hours. Waves were generated in the tank by a paddle at one end driven by a continuously variable speed electric motor; Table 1 lists the wave characteristics measured (photographically) for the paddles settings used in the tests.

TABLE 1
TEST WAVE CHARACTERISTICS

WAVE GENERATOR SETTING	WAVE HEIGHT (m)	WAVE LENGTH (m)	STEEPNESS RATIO
40	0.12	4.25	0.055
50	0.14	3.25	0.086
60	0.15	3.20	0.094
80	0.23	1.45	0.33*

* waves were breaking in the test section

Test Oils

Since the majority of Canadian spills involve Bunker C (fuel oil number 6), an oil that offers the greatest potential for sinking, the test program concentrated on it. The properties of the uncut heavy Bunker C used in this study are given in Table 2. The density, and concomitantly viscosity, of the Bunker C were varied by diluting the oil with automotive diesel fuel (see also Table 2). In order to investigate the effect of oil viscosity independent of buoyancy, a waxy Grand Banks crude oil (J-34) was emulsified with different percentages of 35 part per thousand (ppt) artificial seawater.

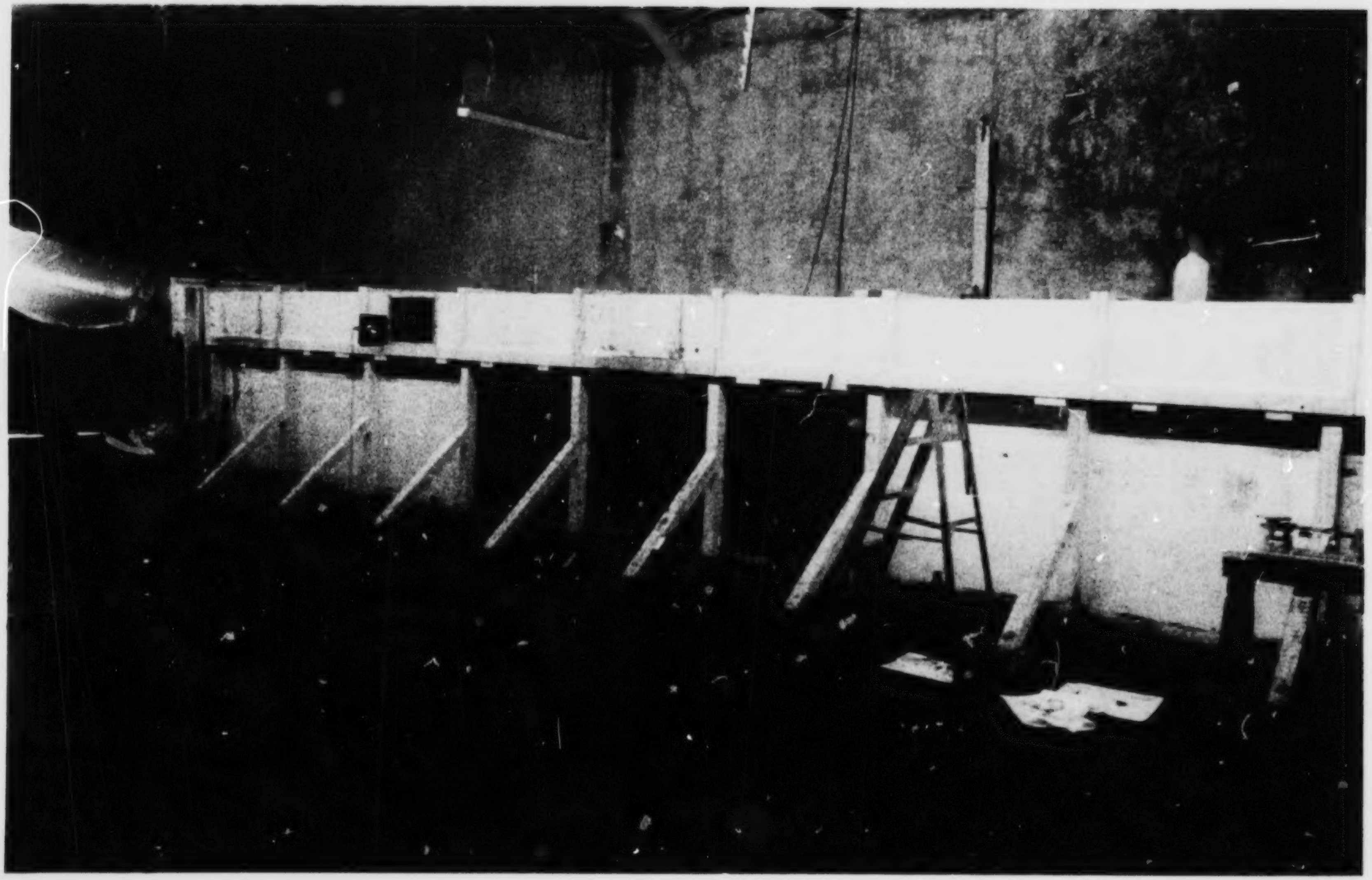

Figure 1 - wind/wave tank

TABLE 2
TEST OIL PHYSICAL PROPERTIES

OIL	TEMPERATURE (°C)	DENSITY (kg/m^3)	VISCOSITY (mPas = cP)
BUNKER C	10	1018	111,000
	5	1022	752,000
	1	1025	2,310,000
AUTO DIESEL	10	831	2.9
	5	835	3.5
	1	837	3.8
J-34	10	881	12,000
(from S.L. Ross	5	885	42,000
and DMER 1987)	1	888	not measured

Test Procedures and Analytical Techniques

A typical test run was conducted as follows. The tank was filled with cold tap water to a depth of 85 cm. A sample of four hundred ml of the test oil was warmed to about 45°C (to facilitate pouring and initial distribution on the water surface), then poured onto a spill plate on the water surface; three or four distinct slicklets were created. Fifteen minutes were allowed for the temperature of the slicklets to equilibrate with the water.

The waves were then turned on at setting 40 (see Table 1); the bubbler was turned on once the slicklets moved towards the walls of the tank or began to drift out of the test section. The behaviour and position of the oil were recorded simultaneously by two video cameras: one positioned above the tank looking down on the test section and one under water at one end of the tank looking along the underside of the slicklets. Still photographs of oil behaviour were taken through the glass walled test section and visual observations were noted throughout each test.

After a 1/2-hour test period with the wave generator setting at 40, it was increased to 50. This procedure was repeated up to a wave generator setting of 80.

Samples for physical property analysis were obtained prior to each run for those tests involving Bunker C (since the change in properties of this oil with exposure is negligible) and after each run for those tests involving crude oil emulsions. Oil density was determined using a Parr Densitometer. Viscosities for the more viscous samples (>20,000 mPas) were determined at 1, 5 and 10°C using a Brookfield viscometer at a shear rate of 0.3 s^{-1}. The viscosities of the more fluid samples were measured, at the test temperature, using cross-arm viscometers. Although attempts were made to measure interfacial tensions using a ring tensiometer, these proved futile for most of the samples because of their high viscosity. Since it is known that interfacial tension varies only slightly as a function of oil type and weathered state, no attempts were made to use more sophisticated techniques.

Although it had originally been planned to measure dispersed oil concentrations and drop sizes, this was abandoned when it was observed that, because of the low buoyancy and high viscosity of the test oils and emulsions, the drops of oil permanently suspended in the water were very large and widely separated. The usual technique for measuring dispersed oil concentration and drop size distribution involves sampling and analysing a small volume of water beneath the slick but is only valid if the small sample is considered to be representative of the whole system. This is the case for homogeneously dispersed oil involving small droplets but is not for heterogeneous distributions such as those observed in these tests.

RESULTS AND DISCUSSION

Blended and Emulsified Oil Properties

Table 3 lists the measured physical properties for the blended or emulsified oil used in each run. The buoyancy ratio (defined as the density difference between oil and water divided by the density of water) ranged from 0.001 (Runs A3 and A9) to 0.042 (Run A5); the oil viscosity ranged from 430 to 842,000 mPas.

TABLE 3
BLENDED AND EMULSIFIED OIL PROPERTIES

RUN	OIL TYPE*	TEST TEMPERATURE (°C)	DENSITY (kg/m^3)	VISCOSITY (mPas)
A1	uncut Bunker C	5.0	1022	752,000
A2	Bunker C/11% diesel	5.5	998	5640
A3	Bunker C/10% diesel	7	999	6280
A4	Bunker C/19% diesel	7.5	981	1480
A5	Bunker C/29% diesel	9	958	430
A6	Bunker C/5% diesel	4	1016	16,300
A7	Bunker C/14% diesel	4	994	2570
A8	J-34/71% salt water	5.5	980	842,000
A9	J-34/85% salt water	9	999	591,000
A10	J-34/78% salt water	9	990	666,000

* blended as mass percent

Summary of General Behaviour

A complete description of each run and results may be found in the project report (S.L. Ross 1987). Based on the observations from the test runs it seems that three criteria must be met for overwashing and transient submergence (i.e., "deep episodes") to occur: firstly, and most obviously, the oil must have a density close to that of the water; secondly the oil must be viscous enough to break into slicklets or blobs that have the potential to be overwashed; and finally the energy in the waves must be sufficient to actually submerge these high density oil forms. The data from these and other tests are next used to develop equations that mathematically describe these processes.

Development of Process Equations

Two groups of process equations have been developed: one to predict whether a given oil in a given sea state will break into slicklets and blobs and to estimate the size of these oil forms; and the second to predict the depth of overwash, maximum transient submergence depth and the distribution of temporarily submerged oil with depth.

Slick Breakage. Raj (1977) presents a mathematical model in which the maximum normal tensile stress in a slick (caused by the stretching and thinning action as waves pass beneath) is compared with the molecular cohesion of the slick to determine whether or not a given slick in a given sea state will break into slicklets. In his analysis, he uses the surface tension (i.e., oil/air interfacial tension) of the slick divided by the slick thickness as a measure of slick cohesion. Unfortunately, this implies that thicker slicks are easier to break than thinner slicks, a result that contradicts intuition and experience. Rather than divide surface tension by slick thickness, it is more appropriate to divide by a measure of the length of surface that the force is acting along; in this case wave amplitude seems reasonable. Starting from Raj's (1977) equation, modified to replace thickness with amplitude, which gives as the slick breakage criteria:

1) $C_1 \sigma / a < 2\mu_o \Gamma_{max}$

where σ = surface tension (N/m)
a = wave amplitude (m)
μ_o = oil viscosity (Pas)
C_1 = a constant
Γ_{max} = maximum strain rate in a slick subjected to a sinusoidal wave (s^{-1})

and substituting:

2) $\Gamma_{max} = W/2(A^2-1)^{1/2}$

where W = wave frequency (rad/s)
A = steepness parameter
$= \dfrac{1 + (\pi s)^2}{2\pi s}$
s = wave steepness
$= 2a/\lambda$
λ = wavelength (m)

and, for deep-water gravity waves:

3) $W = (2\pi(1-s)g/\lambda)^{1/2}$

where g = acceleration of gravity (m/s^2)

yields, for the oil viscosity limit for slick breakage:

4) $\mu_o > C_1 (\sigma^2(A^2-1)/\pi a\ s(1-s)g)^{1/2}$

Examination of the test data (see S.L. Ross 1987a) shows that oils with viscosities less than about 1500 mPas (Runs A4 and A5) did not form into slicklets or blobs at any non-breaking wave condition while oils with viscosities higher than 2500 mPas did. The value of C_1 is thus tentatively set at 30. This gives a minimum oil viscosity for breakage of 2000 mPas at a wave generator setting of 60. As the waves begin to break, A approaches 1 thus predicting, correctly, that even the lowest viscosity oils will fracture, though the mechanism of fracture in breaking waves is not stretching and thinning of the slick.

Equation 4 predicts that, for a given continuous slick on the sea, breakage will occur as the oil weathers (thus increasing the viscosity), as the wave amplitude increases (for a given wave steepness), as the wave steepness increases (for a given amplitude) or as the surface tension of the oil decreases. For the purposes of this study (because of the difficulties encountered in measuring the interfacial tension of viscous oils) the surface tension of any oil is assumed constant at 30 mN/m.

Slicklet/Blob Size. Raj (1977) gives an equation for the strain rate a slick undergoes as sinusoidal waves pass beneath it:

5) $\Gamma(\theta) = W \sin\theta/2(A-\cos\theta)$

where $\theta = Kx$

$= $ angular displacement

$x = $ distance from origin (m)

$K = $ wave number (m^{-1})

$= 2\pi/\lambda$

using the breakage criteria given in equation 1:

6) $C_2\sigma/a = \mu_o W \sin\theta/(A-\cos\theta)$

or

$\sin\theta/(A-\cos\theta) = C_2\sigma/aW\mu_o$

in order to simplify, for x between 0 and $\lambda/8$, θ is between 0 an $\pi/4$. In this range $\sin\theta \approx \theta$ and $\cos\theta \approx 1$ or:

7) $\dfrac{\theta}{(A-1)} \approx C_2\sigma/aW\mu_o$

or

8) $\theta \approx (A-1)C_2\sigma/aW\mu_o$

substituting for 0 and W (for deep-water gravity waves) yields

9) $x = C_2(A-1)\sigma\lambda^{1/2}/\mu_o\pi s(2\pi(1-s)g)^{1/2}$

Figure 2 shows a plot of the data for those runs where slick breakage occurred at wave settings less than 80 (breaking waves make A approach 1), and equation 9 with $C_2 = 3$. Also shown are data from two runs with waxy crude oils (S.L. Ross and DMER 1987). Although the fit is far from perfect, the equation predicts the trends in the data and can be used to obtain order of magnitude estimates of slicklet and blob sizes. Equation 9 is not suitable for use with very viscous oils or emulsions since these behave almost as solids. The viscosity

FIGURE 2 - EXPERIMENTAL SLICK BREAKAGE DATA

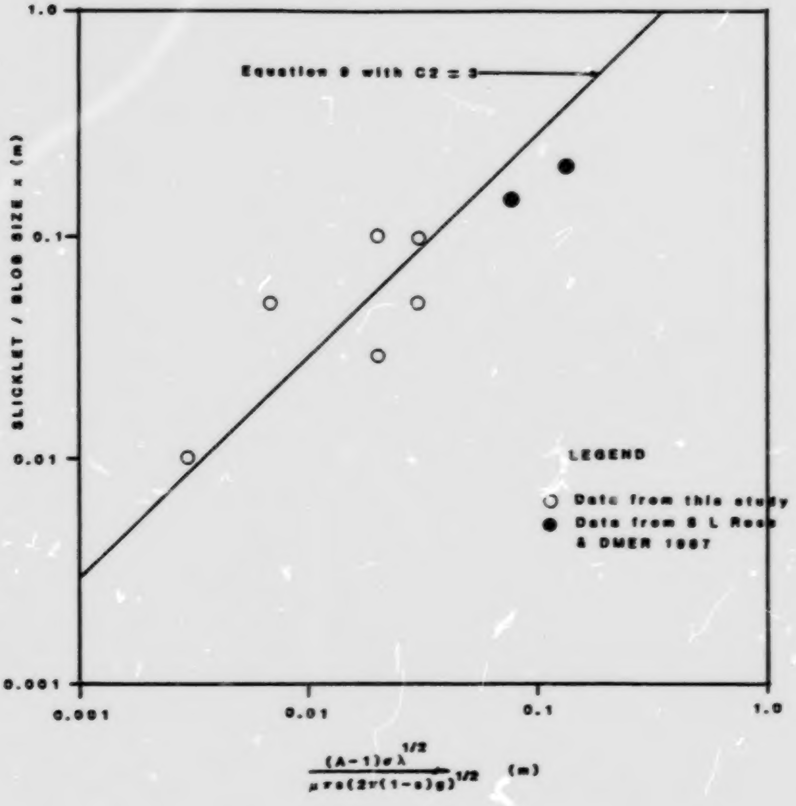

FIGURE 3 - EXPERIMENTAL OVERWASH DATA

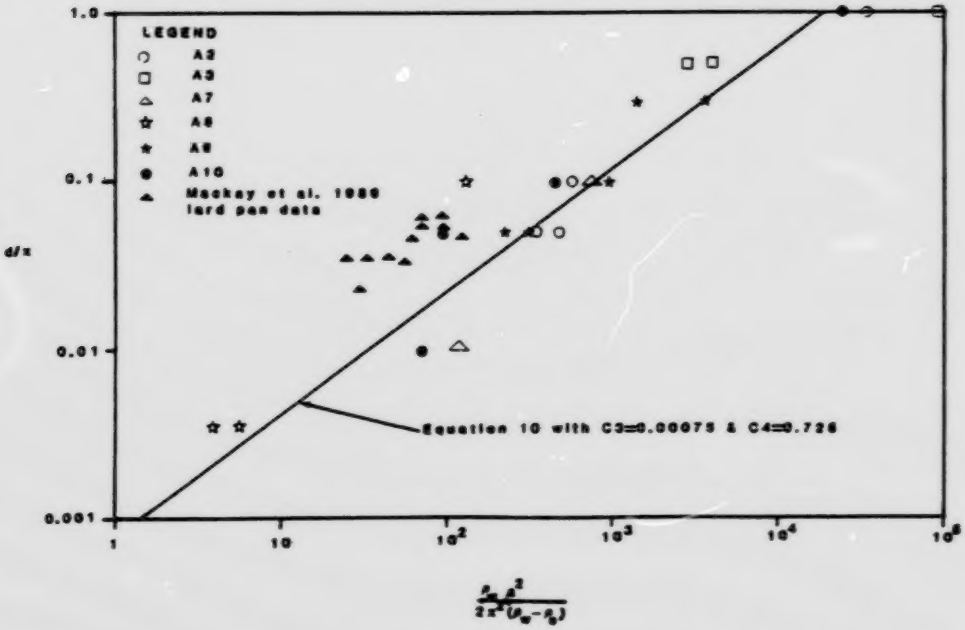

cutoff,above which equation 9 is no longer valid, was arbitrarily chosen as 50,000 mPas.

Overwash Depth. Overwashing is defined as the minimum thickness of water on top of slicklets and blobs in a wave field. By dimensional analysis, including wave energy, oil-water density difference, slicklet/blob size and gravity as factors that influence overwashing in non-breaking waves, it was determined that:

$$10)\quad \frac{d}{x} = C_3(\rho_w\, a^2/2x^2(\rho_w - \rho_o))^{C4}$$

where d = overwash depth (m)

ρ_w = water density (kg/m^3)

ρ_o = oil density (kg/m^3)

Figure 3 shows a plot of the data points for those runs that involved overwashing (i.e., those in which the oil was in the form of slicklets or blobs). Also shown is equation 10 with $C_3 = 7.5 \times 10^{-4}$ and $C_5 = 0.725$ and the data of Mackay et al. (1986) for lard pans. The scatter is due to imprecision in measuring both the submergence depth and slicklet or blob size in a moving system. It should be noted that slicklets in a previous study with viscous, waxy oils (S.L. Ross and DMER 1987) were not overwashed due to their low density relative to the oil used in this study. This is dealt with in the modelling section later by setting the minimum overwash depth as 1 mm (i.e., if equation 10 predicts an overwash less than 1 mm, it is designated as not being overwashed). This cutoff was selected on the basis of observations of runs A8 and A10 during which the slicklets were slowly overwashed. The portions of the slick overwashed by water were covered by a least 1 mm; the above water portions were dry; no areas were covered by less than 1 mm of water. As well, conventional aerial remote sensors for oil spills will not detect oil with more than 1 mm of water overwashing the slick (Fingas 1987).

Equation 10 is intuitively correct in that the overwash depth increases with increasing wave height and oil density and decreases with increasing slicklet size.

Maximum Transient Submergence Depth. Maximum transient submergence depth is defined as the deepest that a buoyant slicklet or blob was propelled during a "deep episode". By dimensional analysis it was found that submergence depth could be correlated with the same factors as overwash depth, i.e.,:

$$11)\quad \frac{d^1}{x} = C_5(\rho_w\, a^2/2x^2(\rho_w - \rho_o))^{C6}$$

where d^1 = maximum transient submergence depth (m)

Figure 4 shows the data from the test runs and equation 11 with $C_5 = 2.9 \times 10^{-2}$ and $C_6 = 0.615$. Also shown are the data of Mackay et al. (1986) for lard pans and the range of data for plastic spheres, both under wave conditions.

FIGURE 4 - EXPERIMENTAL MAXIMUM SUBMERGENCE DATA

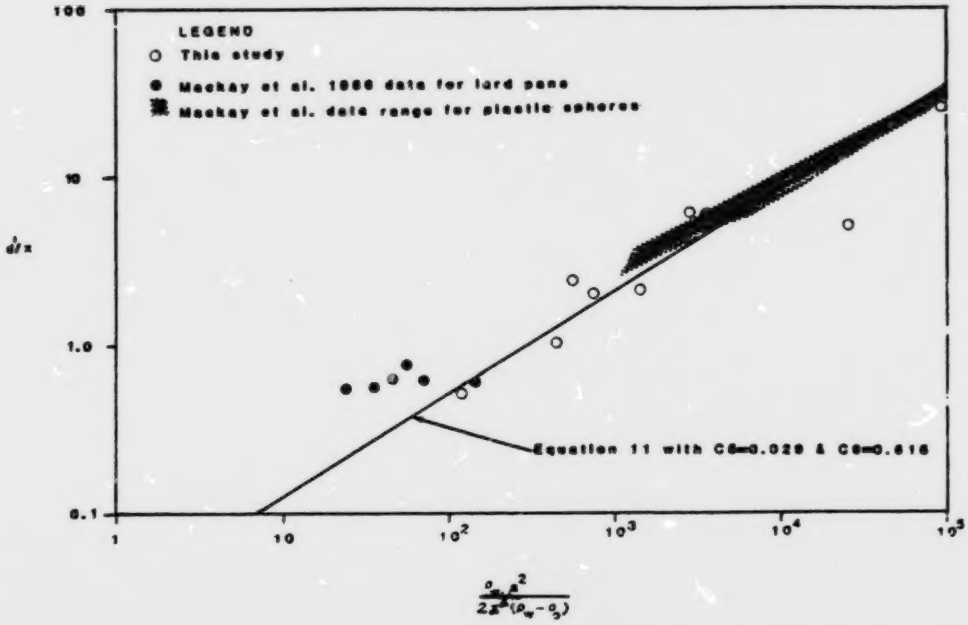

FIGURE 5 - EXAMPLE CALCULATED OIL DEPTH DISTRIBUTIONS

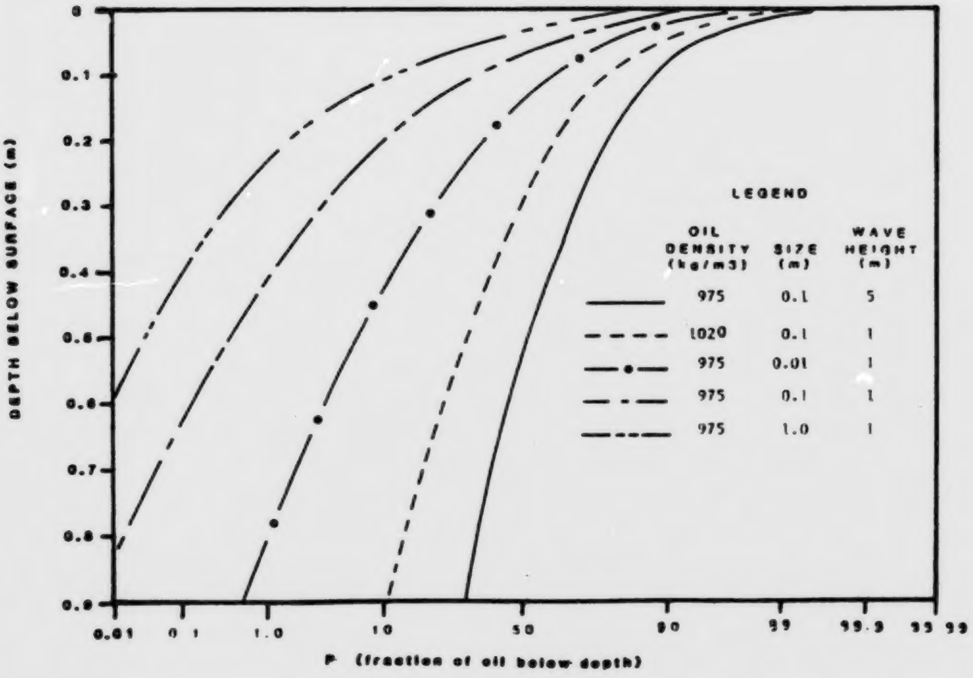

Equation 11 is consistent with the correlations presented by Mackay et al. (1986):

for lard pans,

12) $d^1 = 0.009U^2/(\rho_w - \rho_o)^{0.8}$

with d in cm, the wind speed U in m/s and densities in g/cm^3

and, for plastic spheres,

13) $d^1 = 0.2/(\rho_w - \rho_o)$

Depth Distribution of Oil. The probability of an oil form being below a certain depth d (or alternatively, for a slick containing many slicklets or blobs, the fraction of the oil below depth d) can be expressed as (Mackay et al. 1986).

14) $P = \exp - (d/c)^b$

where P = probability
c = characteristic length (m)
b = a constant

Assuming that equation 10 (overwash depth) represents the depth below which the oil spends 95% of its time and equation 11 (maximum transient submergence depth) represents the depth above which the oil spends 95% of its time, substituting into equation 14 yields:

15) $0.95 = \exp - (7.5 \times 10^{-4} x(\rho_w\ a^2/2x^2(\rho_w - \rho_o)^{0.725}/c)^b$

and

16) $0.05 = \exp - (2.9 \times 10^{-2} \times (\rho_w\ a^2/2x^2(\rho_w - \rho_o)^{0.615}/c)^b$

Solving for c and b gives the probability distribution as:

17) $P = \exp - (91.5d/x(\rho_w\ a^2/2x^2(\rho_w - \rho_o))^{0.64467})$

with b = 1 within the accuracy of the data.

Example distributions for various oil and wave conditions are shown on Figure 5. At a constant oil buoyancy and wave height the effect of increasing slicklet or blob size is to shift the distribution towards the surface; at constant wave height and slicklet size the effect of reducing oil buoyancy is to shift the distribution deeper; at constant buoyancy and slicklet size the effect of increasing wave height is also to shift the distribution deeper.

INCORPORATION INTO AN OIL BEHAVIOUR COMPUTER MODEL

The Oil Fate Model

The purpose of the incorporation of the process equations into a computer model was to allow predictions of submergence behaviour as oil slicks weather, spread and emulsify with time. The approach taken in this study to predict transient oil submergence at sea was to modify an existing oil fate and behaviour model. The main features of this model are presented prior to discussing the modifications. A program listing in Fortran is given in the project report (S.L. Ross 1987a).

The model is based primarily on work performed at the University of Toronto over the past decade; oil spreading is based on the model of Mackay et al. (1979) which utilizes the thick/thin approach; oil evaporation is based on the evaporative exposure approach of Stiver and Mackay (1983), and subsequent oil property changes are determined using the approach of Tebeau et al. (1983); sea state (i.e., wind speed) and oil properties are used to calculate natural dispersion (after S.L. Ross 1984) and emulsification (after Mackay et al. 1979, modified to include a delay until the particular oil weathers to an emulsifiable state). A routine has also been included to assess chemical dispersion effectiveness (S.L. Ross 1987), though this was not used for this study.

In its present form, the model requires a fairly large number of oil property inputs to be used to its full potential. Much of this information is presently available in oil property catalogues published by Environment Canada (S.L. Ross 1985; Bobra and Chung 1986) for many Canadian oils. Work is also underway at the University of Toronto (S.L. Ross and DMER 1987) to develop a technique to fully quantify oil property changes with evaporation using only a simple distillation procedure.

Modifications to Predict Submergence

Data Input and Initialization. The primary modifications to this part of the program included changes to input the sea parameters of swell height (a^1) and wavelength (λ^1), surface water density (ρ_S) and the depth to the pycnocline (d^{11}). In the initialization portion of the program, wave properties are calculated from wind speed (U = m/s at 10 m height), using the following equations given by Raj (1977) for a fully developed sea:

18) RMS waveheight = $a^* = 7.83 \times 10^{-3} U^2$ (m)

19) average wavelength = $\lambda = 1.06 U^2$ (m)

20) average waveheight = $a = 1.77 a^*$

21) wave steepness = $s = 2 a/\lambda$

22) swell steepness = $s^1 = 2 a^1/ \lambda^1$

The program then checks which is steeper, the swell or the waves and uses the amplitude and wavelength of the steeper to calculate the steepness parameter A using the expression given for equation 2.

Mainline. The first step in the mainline calculation program is to check if the oil or emulsion density exceeds that of seawater (1025 kg/m^3); if so the oil sinks and the program terminates. If the oil or emulsion density lies between that of the surface water and 1025 kg/m^3 the oil sinks to the pycnocline depth covering an area equal to the thick slick area calculated for that iteration and the program is terminated.

If the oil density is less than that of the seawater, the program checks to see if the oil or emulsion viscosity exceeds the minimum for slick breakage given by equation 4. If not the program spreads and weathers the oil for one iteration and returns to the beginning; if the oil is viscous enough to break, the size of the slicklets/blobs is calculated using equation 9.

Next the program calculates the overwash depth for the slicklets/blobs using equation 10 (with rms waveheight); if the overwash depth is less than 1 mm the program spreads and weathers the oil for one iteration and returns to the beginning. If the overwash exceeds 1 mm, the program calculates the maximum transient submergence depth from equation 11 and compares it to the pycnocline depth; the lesser of the two is used. The program then calculates the fractions of the oil between the surface and 10 cm deep, between 10 cm deep and 1 m deep, and deeper than 1 m below the surface. The fractions are adjusted if the pycnocline is less than a metre below the surface.

Finally, if the oil is overwashed, the program stops spreading the thick portion of the slick (i.e., the submerged portion); the thin sheen continues to exist on the surface, fed by the submerged slicklets/blobs. This latter feature is based on anecdotal accounts of actual spills rather than laboratory test data. Evaporation, emulsification and natural dispersion of the thick slick are assumed to continue as if the oil were on the surface. These oil fate processes for submerged oil need to be addressed in future studies.

MODELLING RESULTS

Figure 6 shows the predicted behaviour and properties for a crude oil with an initial density of 900 kg/m^3 and initial viscosity of 25 mPas that emulsifies when spilled on water with a surface density of 1020 kg/m^3 in a 5 m/s wind with no swell. Over the time period graphed the oil spreads, evaporates, emulsifies and naturally disperses until after 3 1/2 days about 50% of the original 1000 m^3 spill is left. Figure 7 shows the same spill in the same conditions except that a very steep (s=0.06) swell has been added. In this case, after 18 hours the emulsion becomes viscous enough (2900 mPas) and dense enough (994 kg/m^3) to be broken into slicklets about 2.5 m in diameter overwashed by 2 cm of water. The predicted maximum transient submergence depth is about 0.5 m. Slicklet size decreases slowly with time; both overwash and maximum submergence depth increase with time.

Figure 8 gives the predicted results if the initial oil density is increased to 990 kg/m^3, the surface water density is reduced to 1015 kg/m^3 and all other parameters remain the same. In this situation, the oil breaks up into emulsion slicklets at the same time as the previous case (Figure 7) but the initial overwash and maximum transient submergence depth are about a factor of ten greater. After two days exposure, the emulsion density exceeds that of the surface water and the oil sinks to the pycnocline at a depth of 10 m.

Figure 9 shows the predicted behaviour of the Bunker C spilled by the Kurdistan. Oil property information was taken from C-CORE (1980); environmental information at the time of the spill was obtained from Vandermeulen and Buckley (1985). In the high seas at the time of the incident,

FIGURE 6 - PREDICTED BEHAVIOUR OF 900kg/m3 CRUDE OIL SPILL IN A 5 m/s WIND AND NO SWELL

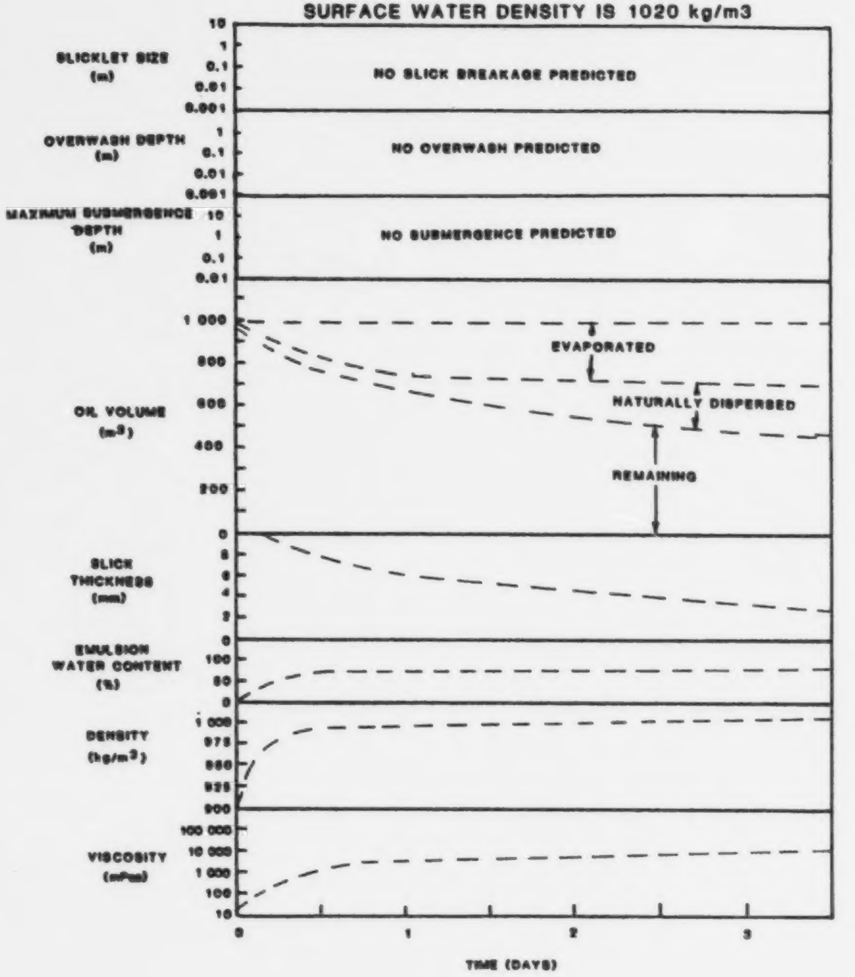

FIGURE 7 - PREDICTED BEHAVIOUR OF 900kg/m3 CRUDE OIL SPILL IN A 5 m/s WIND AND 3m SWELL

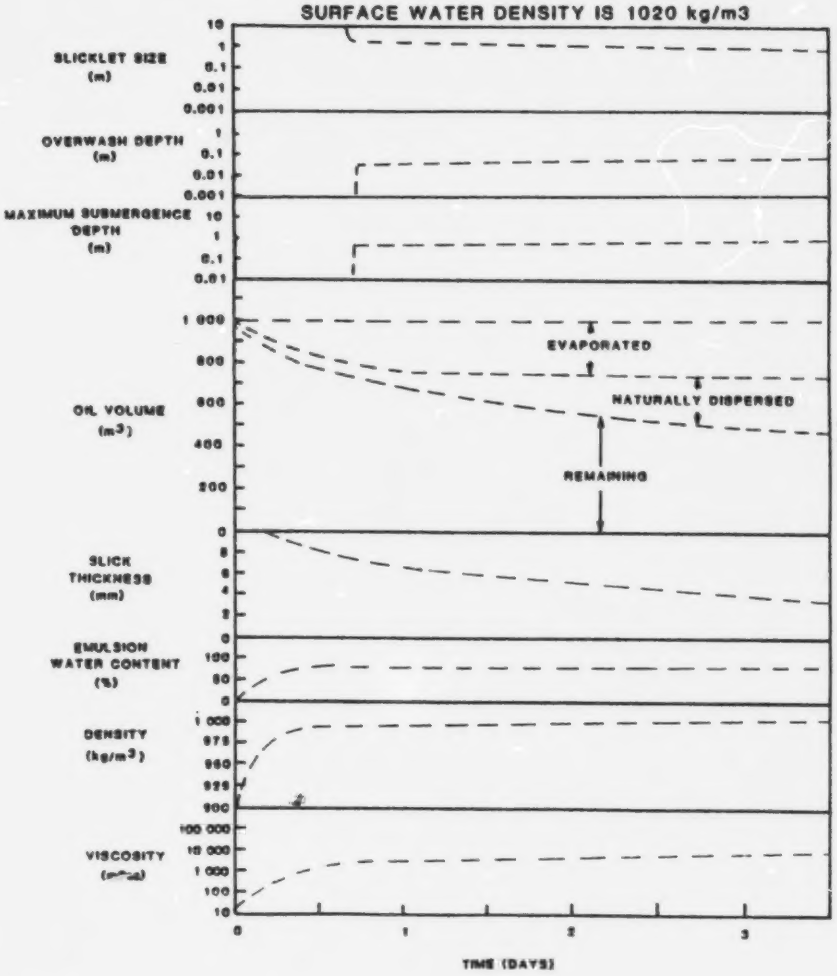

FIGURE 8 - PREDICTED BEHAVIOUR OF 990kg/m3 CRUDE OIL SPILL IN A 5 m/s WIND AND 3m SWELL

SURFACE WATER DENSITY IS 1015 kg/m3

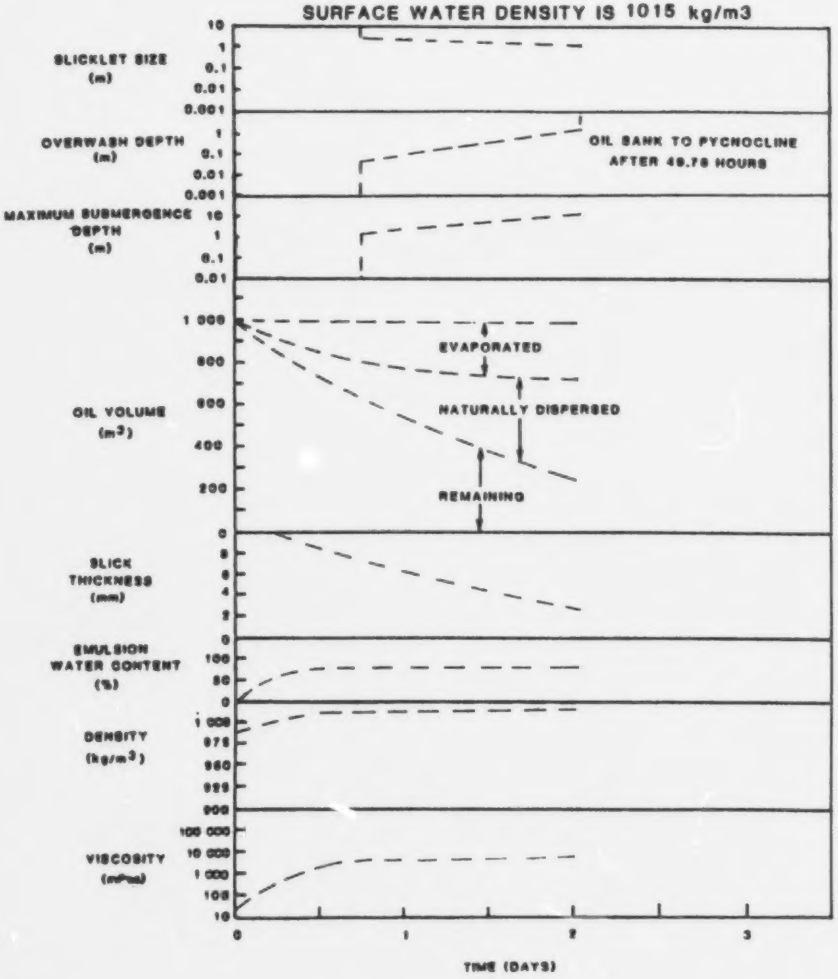

FIGURE 9 - PREDICTED BEHAVIOUR OF KURDISTAN BUNKER C SPILL

SURFACE WATER DENSITY= 1020 kg/m3 ,WIND =10 m/s ,SWELL = 7 m

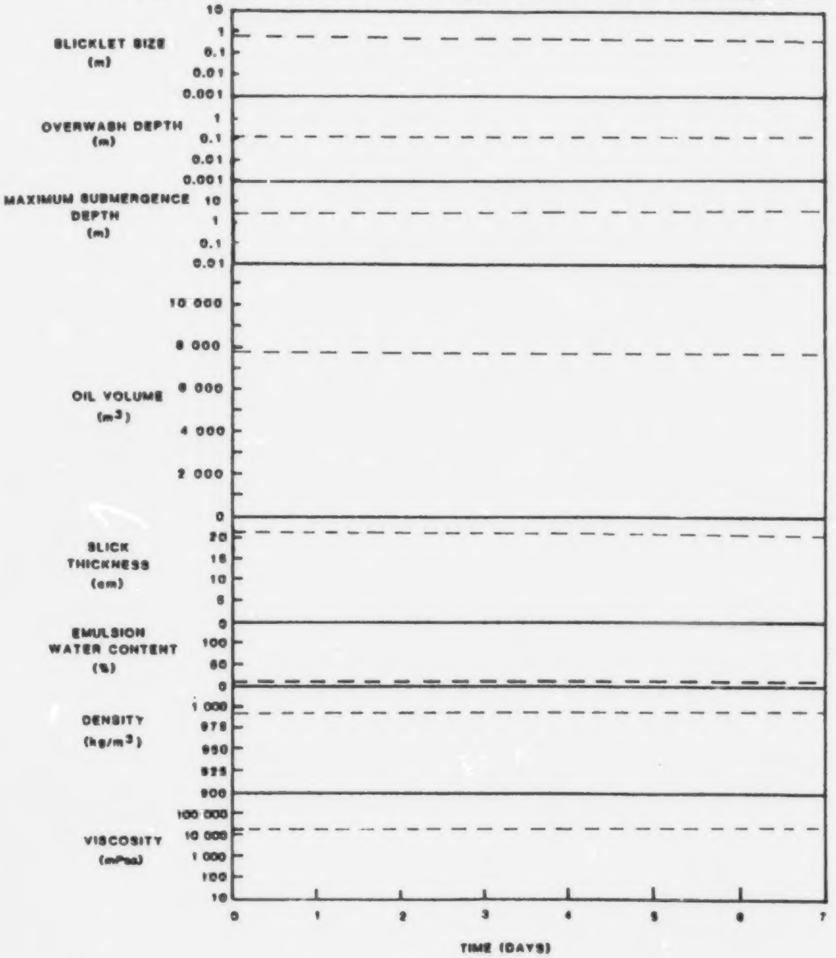

the model predicts that blobs in the size range of 0.6 m would be overwashed by about 10 cm of water. The maximum transient submergence depth is predicted to have been about 2 m. Very little weathering of the Bunker C is predicted thus the oil would survive for long times. These predictions are broadly consistent with the anecdotal accounts given by Reimer (1981).

Simplified Nomograph

In order to obtain quick estimates for emergency response purposes, the process equations have been simplified by substituting the predictive equations for rms waveheight, average waveheight and average wavelength for a fully developed sea into equation 9 to predict slicklet/blob size and equation 10 to predict overwash depth, yielding for non-emulsified oils:

23) $d(cm) = 7.6 \times 10^{-5}\ U^{2.45}\ \ {}_{o}^{0.45}/((\ \ w-\ \ o)/\ \ w)^{0.725}$

and for heavily emulsified oils (which behave as solids and are not "broken" by waves)

24) $d(cm) = 5.9 \times 10^{-4}\ U^{2.9}/((\ \ w-\ \ o)/\ \ w))^{0.725}\ x^{0.45}$

The ratio of overwash depth to maximum transient submergence depth (equation 11 divided by equation 10) is approximately 40 since $C_6 - C_4$ is very small.

Figure 10 shows a nomograph for fully developed sea conditions with a surface water density of 1025 kg/m^3 (35 ppt) based on equation 23 for a range of residual fuel oils. Figure 11 shows a nomograph based on equation 24 for the submergence of emulsion mats/blobs of various sizes.

The residual oil properties used were heavy Bunker C (from this study) medium Bunker C (from data on the Kurdistan spill), light Bunker C (from Bobra and Chung 1986), and heavy Bunker B, or No. 5 fuel oil (from Bobra and Chung 1986). Predictions are given for 1000 kg/m^3 emulsion with mat/blob sizes of 1, 0.1 and 0.01 m.

If oil property information is available during a spill response, equation 23 or 24 can be used to obtain better estimates. If surface salinities are lowered, oil weathering or emulsification is expected to take place or other complicating factors exist, the computer model should be used with the best available input data.

CONCLUSIONS AND RECOMMENDATIONS

The overwashing and transient submergence of oil spills on water depends primarily on the buoyancy of the oil or emulsion, the viscosity of the emulsion and the sea state. A necessary condition for overwashing or transient submergence is that the oil be of sufficiently high viscosity so that it can be broken into discrete slicklets or blobs by wave action. Once this occurs, the degree of overwashing and transient submergence is controlled by the size and buoyancy of the slicklets or blobs and the prevailing sea state. For non-emulsified oils the size of the slicklets or blobs is determined by sea conditions and the surface tension and viscosity of the oil. Emulsions, due to their enormous viscosities, behave almost as solids; emulsion mat or blob sizes are possibly only a function of sea conditions but this is unknown.

FIGURE 10 - OVERWASH / SUBMERGENCE NOMOGRAPH
RESIDUAL FUEL OILS

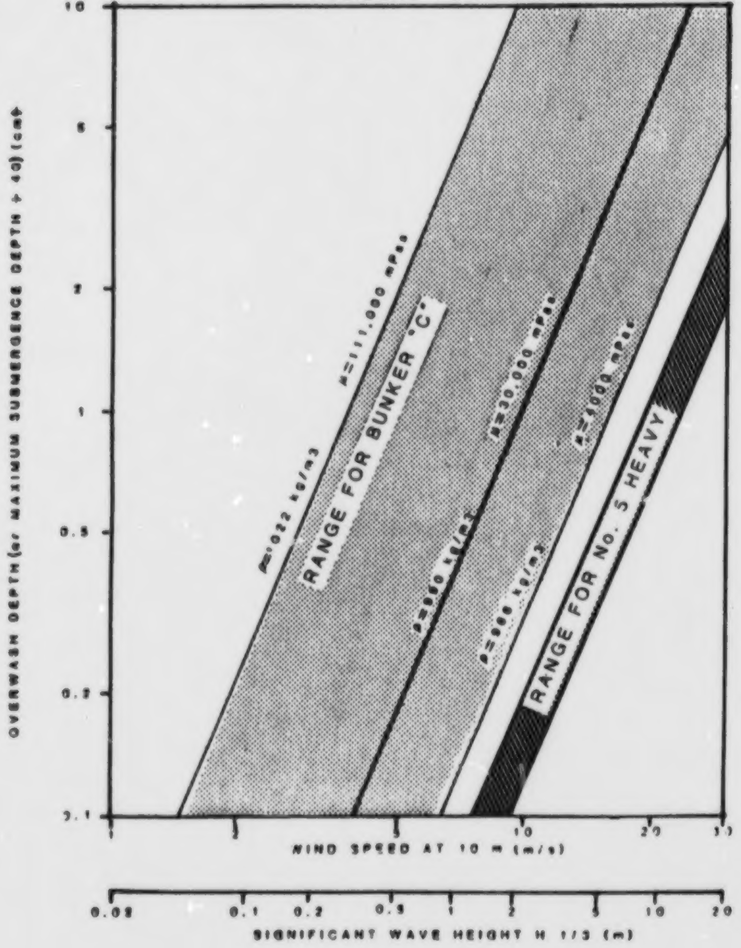

FIGURE 11 - OVERWASH / SUBMERGENCE NOMOGRAPH
EMULSIONS (ρ = 1000 kg/m3)

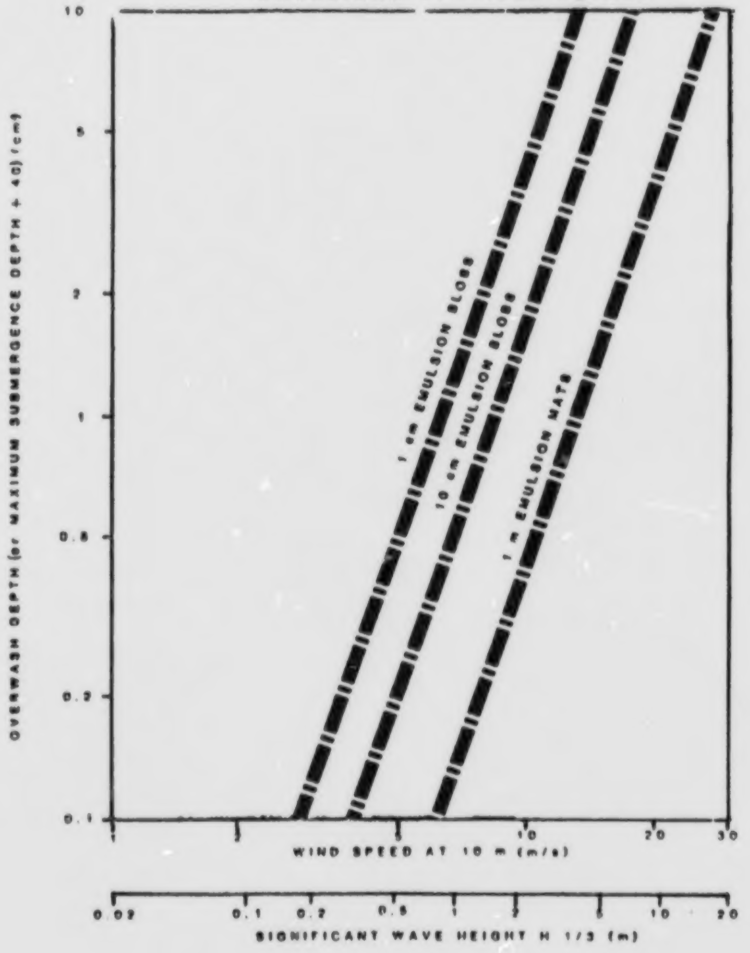

Based on theory and wind/wave tank test results, process equations incorporating oil properties and sea conditions, have been developed to predict: whether or not a particular oil slick will break up into slicklets or blobs, the size of the resultant slicklets and blobs, whether or not they are overwashed by water and to what extent, the maximum transient submergence depth of the slicklets and blobs and their distribution as a function of depth. These process equations have been incorporated into an oil spill fate and behaviour computer model that calculates oil spreading, evaporation, emulsification and natural dispersion to allow state-of-the-art predictions of transient submergence. The process equations were also simplified to provide quick estimates for residual fuel oil spills and a range of emulsion mat sizes.

It is recommended that the models be updated as further field data become available, that a study on the processes of evaporation, emulsification and natural dispersion of submerged oil be undertaken, and that the results of this study be incorporated into an oil spill trajectory model for submerged oil.

REFERENCES

Bobra, M.A. and P.T. Chung. 1986. A catalogue of oil properties. Environmental Emergencies Technology Division, Environment Canada Report EE-77, Ottawa.

C-CORE. 1980. An oilspill in pack ice. Environment Canada report EE-15, Ottawa.

Elliot, A.J. 1986. The influence of near-surface current shears on the spreading of oil. Proceedings of the International Seminar on Chemical and Natural Dispersion of Oil on Sea, SINTEF, Trondheim.

Fingas, M. 1987. (Head Chemistry and Physics, EETD, Environment Canada, Ottawa) personal communication.

Forrester, W.D. Distribution of suspended oil particles following the grounding of the tanker Arrow, J. Marine Res, 29 (2) 1971: p.151-170.

Johansen, O. 1986. DOOSIM - a new simulation model for oil spill management. Proceedings of the International Seminar on Chemical and Natural Dispersion of Oil on Sea, SINTEF, Trondheim.

Juszko, B.A., D.R. Green and J.R. Birch. 1983. A study of the oceanographic conditions suitable for the sinking of oil. Environment Canada. Environmental Protection Service report, Ottawa.

Juszko, B.A. 1985. Determination of oceanographic factors associated with the subsurface movement of oil. Environment Canada report EE-66, Ottawa.

Mackay, D., I.A. Buist, R. Mascarenhas and S. Paterson. 1979. Oil spill processes and models. Report for Environmental Emergency Branch, Department of Fisheries and Environment, Hull, Quebec.

Mackay, D., D. Wilson and Y.C. Poon. 1985. An exploratory study of the buoyancy behaviour of weathered oils in water. Environment Canada report EE-85, Ottawa.

Mackay, D., B. Clark, J. Parsons, C. Yen, B. Ahier and J. Alexander. 1986. A study of factors influencing oil submergence. Draft report to Environment Canada. Ottawa

OSIR (Oil Spill Intelligence Report). 1987. Spilled oil from tanker remains trapped in snow and ice off Swedish coast. Vol. 10, No. 4. 23 January. Cutter Information Corp. Arlington, MA.

Payne, J.R. and C.R. Phillips. 1985. Petroleum spills in the marine environment-the chemistry and formation of water-in-oil emulsions and tar balls. Lewis Publishers Inc. Chelsea, Michigan.

Petersen, H.K. 1978. Fate and effects of Bunker C oil spilled by the USNS Potomac in Melville Bay - Greenland - 1977. Proceedings of the Conference on Assessment of Ecological Impacts of Oil Spills. American Institute of Biological Sciences. Washington, D.C.

Raj, P.P.K. 1977. Theoretical study to determine the sea state limit for the survival of oil slicks on the ocean. U.S. Coast Guard report CG-D-90-77. Washington, D.C.

Reimer, E.M. 1981. "Subsurface" oil movement off the Newfoundland south coast during 1979. C-CORE Publication 81-4. St. John's.

Rijkswaterstaat. 1982. Oil recovery operation in the North Sea involving the oil tanker "Katina" 7-13 June, 1982. Report NZ-R-82.23. The Netherlands.

S.L. Ross Environmental Research Limited. 1984. Hibernia oil spills and their control. Report to Mobil Oil Canada Limited, St. John's.

S.L. Ross Environmental Research Limited. 1985. Spill-related properties of Terra Nova crude oils. Prepared for Petro-Canada Resources, Calgary.

S.L. Ross Environmental Research Limited. 1985. A catalogue of crude oil and oil product properties. Environment Canada report EE-56, Ottawa.

S.L. Ross Environmental Research Limited. 1987. Amauligak seasonal production: the behaviour and control of oil spills. Report to Gulf Canada Corp., Calgary.

S.L. Ross Environmental Research Limited. 1987a. The transient submergence of oil spills: tank testing and modelling. Report to Environment Canada, Dartmouth.

S.L. Ross Environmental Research Limited and D. Mackay Environmental Research Limited. 1987. The behaviour and fate of waxy crude oil spills. Report in preparation for the Environmental Studies Revolving Fund, Ottawa.

Stiver, W. and D. Mackay. 1983. Evaporation rate of spills of hydrocarbons and petroleum mixtures. Environmental Protection Service. Environment Canada, EE-89.

Tebeau, P.A., D. Mackay and W. Stiver. 1983. Testing of crude oils and petroleum products for environmental purposes. Proceedings of the 1983 Oil Spill Conference. San Antonio, TX.

Vandermeulen, J.H. and D.E. Buckley (editors). 1985. The Kurdistan oil spill of March 16-17 1979: activities and observations of the Bedford Institute of Oceanography Response Team. Canadian Technical Report of Hydrography and Ocean Sciences No. 35. Fisheries and Oceans, Ottawa.

Warren Spring Laboratory. 1978. Investigation of factors affecting the fate of North Sea oils discharged at sea. Part 3 - Beatrice crude oil May 1977-March 1978. Stevenage, UK.

Warren Spring Laboratory. 1981. The collection of Beatrice crude oil at sea using the BNOC Ltd. netting and the WSL Springsweep systems. Stevenage, UK.

OBSERVATIONS AND INITIAL RESULTS FROM A SITE VISIT TO THE 'METULA' SPILL 12 YEARS AFTER THE INCIDENT

E.H. OWENS, GEOSCIENCES SERVICES LTD.
W. ROBSON, HALIBURTON LTD.
B. HUMPHREY, SEAKEM OCEANOGRAPHY LTD.

ABSTRACT

The spill of 415,000 barrels of light Arabian crude that resulted from the grounding of the VLCC 'Metula' in August 1974 in the Strait of Magellan was, at that time, the largest oil spill from a tanker. The spill was neither contained nor cleaned up. A field study was conducted in January 1987 in the area of the spill to evaluate the character of any remaining stranded oil and to collect samples for total hydrocarbon and GC analyses. It was believed that an asphalt pavement, observed by one of the authors in 1977 and by Gundlach et al. in 1981, was still present and would be a suitable comparison for data collected on a similar pavement that had formed following the experimental release of oil at Cape Hatt as part of the Baffin Island Oil Spill (BIOS) project.

Oil was found at several locations on the highest sections of the beach. Comparison with observations from the 1977 site visit indicates that there has been considerable natural cleaning at these sites over the past 10 years. The oil that remains is generally a narrow strip that was laid down by high spring tides and is now buried on the landward margin. A major exception to this pattern occurs in the Puerto Espora area on the south shore of the first narrows. Here extensive asphalt pavements remain in the intertidal and supratidal zones over a shoreline length of several kilometers. The surface of these pavements is characterized by a very weathered crust, but the oil contained within the pavements is very fresh in appearance and has a low viscosity in many cases.

INTRODUCTION

1.1 Objective and Rationale

The primary objective of the field study was to visit shoreline locations in the Strait of Magellan, Chile (Figure 1), to record the character of any remaining stranded oil 12 years after the 'Metula' spill and to collect samples for subsequent chemical analyses.

Previous sites visits to this sub-antarctic area had recorded the presence of extensive asphalt pavements on the south shore of the first narrows in the strait. A similar pavement had formed on an intertidal beach in an arctic environment at Cape Hatt following an experimental release of oil as part of the Baffin Island Oil Spill (BIOS) Project (Owens and Robson, 1987). Field studies at Cape Hatt commenced in August 1981 and were repeated in 1982 and 1983, with a further field survey in August 1985. The results from the 'Metula' area would be used to provide a real-world comparison for the data from the BIOS experiment. As part of this overall program a site visit to the 'Amoco Cadiz' area had been carried out in March 1985 to record the character of asphalt pavements that had formed in the mid-latitude temperate environment (Owens and Robson, 1985). The sampling and analytical procedured used in all of these studies are identical in order to provide comparable data sets.

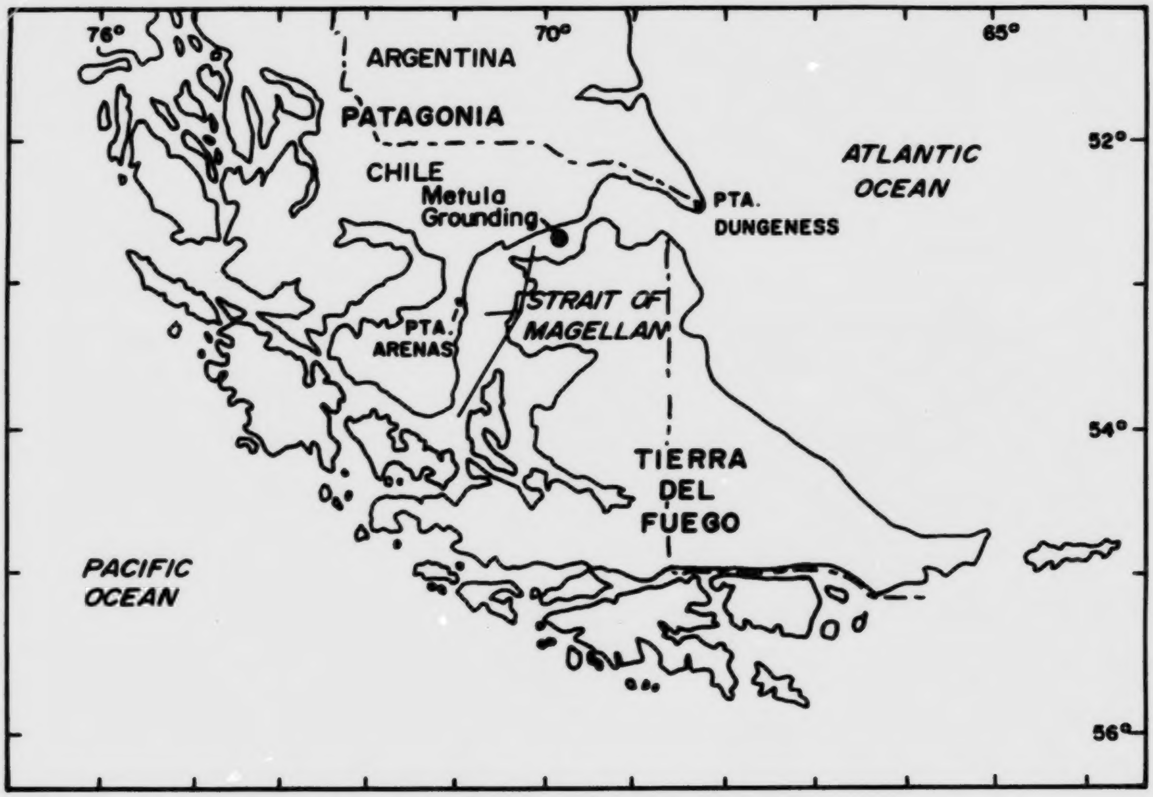
76°
70°
65°
52°
54°
56°
ARGENTINA
PATAGONIA
CHILE
Metula Grounding
PTA. DUNGENESS
ATLANTIC OCEAN
PTA. ARENAS
STRAIT OF MAGELLAN
TIERRA DEL FUEGO
PACIFIC OCEAN

FIGURE 1 LOCATION OF THE "METULA" SPILL SITE (HAYES AND GUNDLACH, 1975)

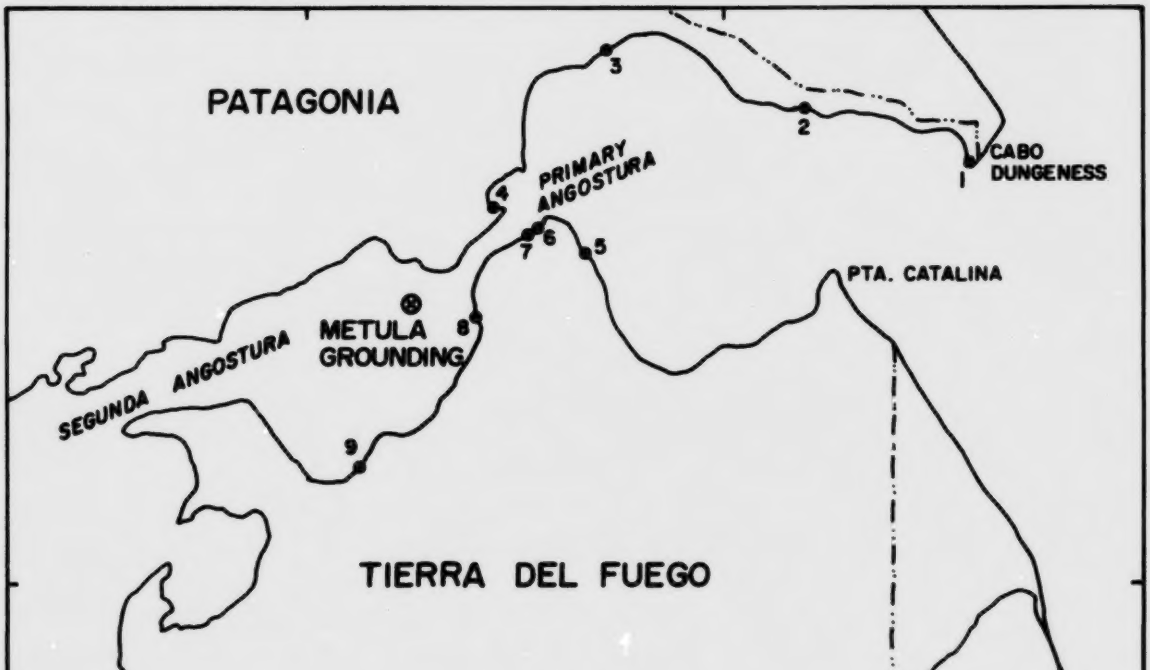
PATAGONIA
3
2
1
CABO DUNGENESS
PRIMARY ANGOSTURA
4
7
6
5
PTA. CATALINA
METULA GROUNDING
8
SEGUNDA ANGOSTURA
9
TIERRA DEL FUEGO
0 10 20 km

FIGURE 2 SHORELINE LOCATIONS VISITED IN JANUARY 1987

1.2 Methods

A total of nine coastal sites were visited in the Eastern Strait of Magellan (Figure 2) (Owens and Robson, 1987). At each site a series of systematic observations were recorded, photographs taken and samples were collected in plastic bags for total hydrocarbon analysis and in cleaned glass jars for GC analysis.

A preliminary set of compositional analyses was obtained for original Metula oil and four selected samples to provide data on the present character of the pavement oil. A small subsample (0.5 g) of oiled sediment was extracted with carbon disulfide, and the extract analysed using a Hewlett-Packard 5830 gas chromatograph fitted with a 25 m SGE BP-5 bonded phase fused silica capillary column and a flame ionization detector (GC/FID). The resolved peaks were identified by comparison to a standard set of n-alkanes analysed in the same manner. Future work will include a total hydrocarbon determination by an infrared spectrophotometric procedure (Owens, Hope and Humphrey, 1986) and more detailed gas chromatographic analysis including fractionation and mass spectrometric determination of selected aromatic hydrocarbons.

2. THE 'METULA' SPILL

2.1 The Spill Incident

The VLCC 'Metula' grounded at full speed during the night of 9 August, 1974 just to the west of the first narrows in the Strait of Magellan, with a cargo of about 1.42 million barrels of light Arabian crude. Oil was spilled from the initial grounding and at intervals until the vessel was refloated on 25 September. This is an area of very strong tidal currents (up to 9 knots) and considerable hull damage was sustained during periods of spring tides on August 11, August 19 and September 4 (Gunnerson and Peter, 1976). The estimated total loss was about 400,000 barrels of crude and 15,000 barrels of bunker C oil. Oil from the 'Metula' was transferred to a small tanker, but no attempts were made to contain or disperse the spilled oil and no shoreline cleanup was undertaken.

The spilled oil was spread rapidly by strong winds and tidal currents and a "Mousse" was observed to have formed. A total of approximately 250 km of shoreline were contaminated, with the most severe impact on the south shores of the Strait in the vicinity of the first narrows (Blount, 1978).

2.2 Environmental Background

Despite the relatively low latitude (53 Deg S.) this is a cold environment with a mean monthly Mid-summer (January) temperature of 11.7 Deg C and a mid-winter (July) temperature of +2.5 Deg C. The shore zone is not affected by severe freezing (Gunnerson and Peter, 1976). Strong westerly winds are characteristic throughout the year with velocities commonly greater than 50 km/hr and frequently greater that 100 km.hr. The mean tidal range near the site of the grounding exceeds 8 m. A large proportion of the spilled oil was released at times of spring high tides and therefore became stranded at many sites above the limits of normal wave action.

The shorelines of the area are characterized by wide sand or sand-gravel beaches and at many locations by wide mud or gravel low-tide terraces. Wave-energy levels at the shoreline vary considerably depending upon exposure to local fetches within the straits and upon the orientation of the coast with respect to waves generated by the dominant westerly winds.

2.3 Previous Studies

Several shoreline surveys and some sampling programs were conducted during the two years immediately following the spill (e.g., Blount, 1976; Hann and Young, 1979; Straughn, 1981) and in 1981 by

Gundlach et al. (1982). Blount collected a series of beach samples which were analyzed for total hydrocarbons and Gundlach et al. reported observations on the extent of the remnant stranded oil and asphalt pavements.

3. SUMMARY OF FIELD OBSERVATIONS

The field site visits were not intended to cover the entire area affected by the 'Metula' oil, and, therefore, do not constitute a systematic or complete survey. However, on the basis of the observations made at the selected locations it is possible to present a review of the character of the remaining stranded oil which in turn provides useful information on the self-cleaning of the beaches of this region. The following paragraphs summarize the observations at the sites where oil was still present on the beach surface in January 1987. A more complete description of each site and photographs of the oil are given in Owens and Robson, 1987.

Punta Malvinas

This site is a spit system on the north shore at the eastern end of the First Narrows (Site 4 - Figure 2). Oil remains on relict recurved ridges in sheltered backshore areas above the normal limit of wave action. Narrow (1 to 2 m wide), hard pebble-cobble pavements were present near the spring high-water level at two locations and on one section the pavement was continuous for about 30 m alongshore. The oil was laid down at a time of high spring-tide water levels in a quiescent backshore location and has been virtually unaffeced by marine processes since that time.

Banco Orange

This exposed beach has a steep pebble beach-face slope and a wide (500+ M) low-tide terrace (Site 5 - Figure 2). A pavement was found in the vicinity of the spring high-water level and was discontinuous alongshore for about 50 m. The pavement was soft and sandy in character, contained shell fragments, varied between 0.5 and 1.0 m in width and was buried on the landward margin by pebble-cobble sediments. An extensive pavement recorded in 1975 by Blount on the inner (landward) margin of the low-tide terrace could not be found.

Puerto Espora

This site has a spit system that has grown approximately 2 km towards the northeast on the south shore of the First Narrows (Site 6 - Figure 2). The most westerly section is a marsh (the West Estuary) that is connected to the ocean by a small tidal creek (Espora Creek). The backbeach section is protected from the ocean by the spit itself and the section referred to as Espora Beach is open directly to marine processes. The area was heavily contaminated by the 'Metula' spill and still contains large amounts of oil. Pavements were found in all sections visited.

In the West Estuary the oil was deposited during spring high tides on the flat upper marsh surface as a 20 to 30 m wide band around the rim of the marsh basin. The upper marsh remains heavily contaminated by a continuous but thin (1 to 2 cm) layer of weathered oil. Some silts have been deposited on the surface of the oil. When samples were collected the oil under the surface crust appeared to be very fresh.

On the south bank of Espora Creek patches of soft sandy-pebble pavement remain between the mean and spring high-water levels. Towards the east this grades into a more continuous pebble-cobble pavement that is about 10 m wide on the upper sections just below and at the spring high-water level. Oil is also present at the spring high-water level at the base of a low backshore scarp. This highest section of pavement varied within a few meters from a soft, sandy deposit that could be broken easily by hand to a hard pebble asphalt that could be sampled only by chipping or chiselling.

The backbeach section, on the mainland in the lee of the spit, had a pavement on the upper beach-face slope that was continuous alongshore for about 700 m. The wideth varied between 5 and 15 m and the pavement was generally 5 to 10 cm, but up to 20 cm, thick. The seaward margin of the pavement usually coincided with a change in sediment type from sand-pebble or pebble-cobble to mud and the upper margin was, in most sections, an eroding scarp except at the western end where the upper parts of the pavement were buried by pebble-cobble sediments. In general, the pavement was harder and contained more pebbles in the upper sections as compared to a softer and more sandy character in the middle sections of the beach-face slope.

At the most easterly end of the backbeach several sections of buried and exposed hard pavements were found above the normal high-water level. In addition, at one location a very soft oil was found above the mean high-water mark. This deposit was characterized by a thin (1 cm) weathered crust with a veneer of fines that overlay a fresh brown mousse which was observed to ooze with a minute of the hole being cut for the sample.

The exposed Espora Beach section has a steep pebble-cobble beach face and a wide (500 m) low-tide terrace of silt and pebble-cobble sediments. A pavement was present on the beach face that was continuous for between 500 and 750 m alongshore. The eastern-most section was 25 m wide and was in the middle to lower portion of the beach-face slope, just landward of the low-tide terrace. The elevation of the pavement on the beach face increased towards the west so that at the westerly end the upper edge of the pavement coincided with the mean high-water level. Again some lower sections of the pavement were soft in character and generally were associated with a light brown mousse that had a dark weathered surface crust. The harder pavement areas had a more pebble character but below the surface also appeared fresh. The low-tide terrace contained considerable amounts of soft mousse-like oil which varied considerably in character. Pebble-cobble areas on the higher elevations of the terrace were often hard whereas the deposits contained more mousse.

Punta Baxa - Rio Oscar

These two sites (8 and 9 respectively on Figure 2) had similar narrow (0.5 to 1.0 m) pavements on the highest parts of the beach at the spring high-water level adjacent to the base of a backshore dune scarp. The pavement was continuous alongshore for about 100 m at Punta Baxa and for 50 m at Rio Oscar. At both sites the pavement was relatively hard and was buried on its landward margin by pebbles and wind-blown sands. Both beaches were oiled during spring tides (Owens, 1978) and all but the highest deposits have now been eroded.

4. PRELIMINARY ANALYTICAL RESULTS

Four oiled beach sediment samples and a sample of original Metula oil were analysed by GC. Table 1 describes the samples, and the resulting chromatograms are presented in Figures 3 a-e.

Table 1.

Figure Number	Sample Number	Site	Location on Beach	Description
3a	METULA			Original oil sample
3b	3	Espora Marsh	Marsh flat above mean high water	Surface sample of thin (1-2 cm) 'latex' layer over fresher oil
3c	8	Espora Spit	Sandy pebble beach near mean high water	2-4 cm subsurface sample from within a soft pavement on upper beach face slope
3d	10	Espora Spit	Sandy pebble beach above spring high water	Surface sample (0-3 cm) of mousse
3e	14	Espora Spit	Sandy pebble beach 5 m below spring high water	Surface sample of very hard pavement

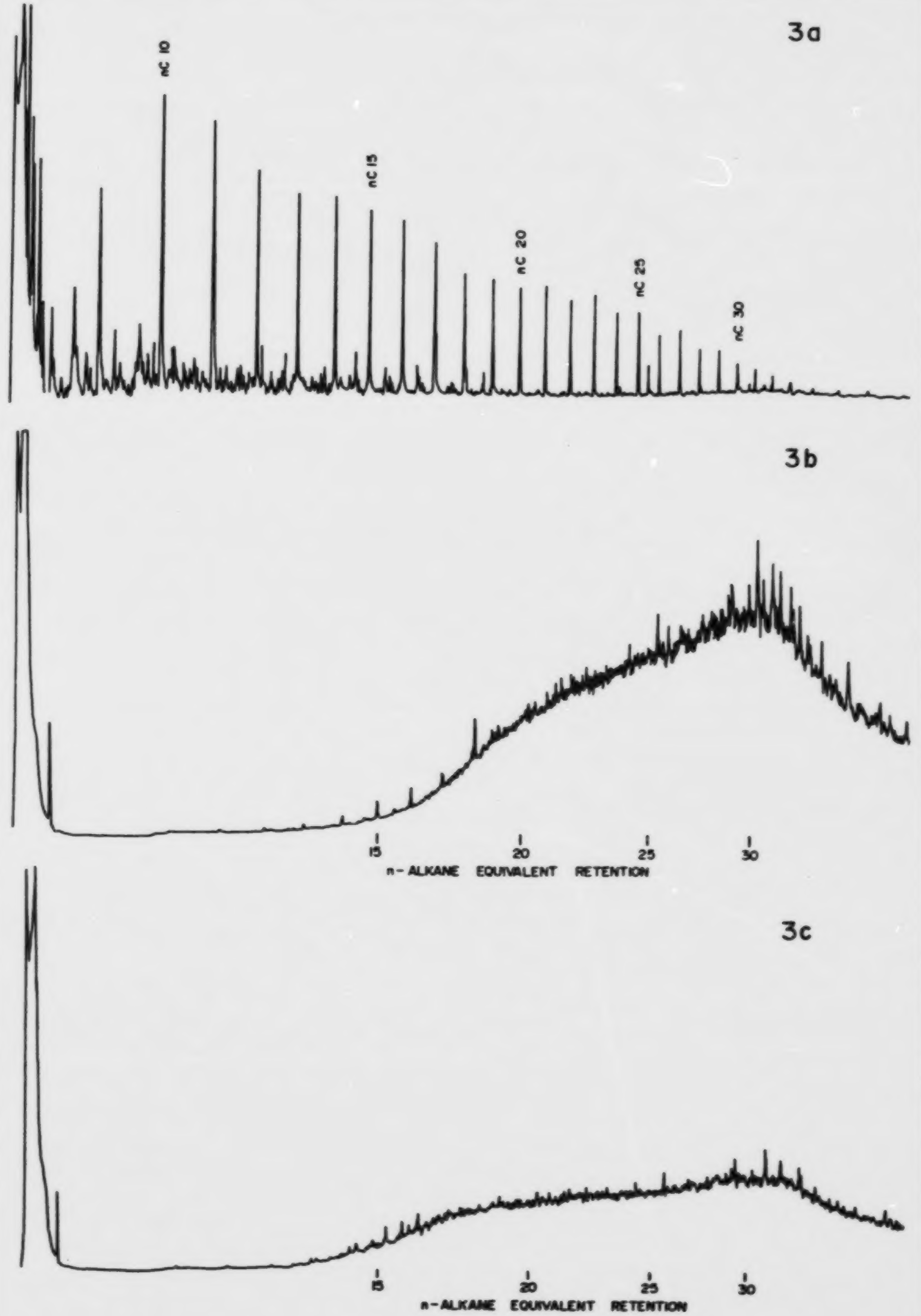

FIGURE 3 HYDROCARBON COMPOSITION

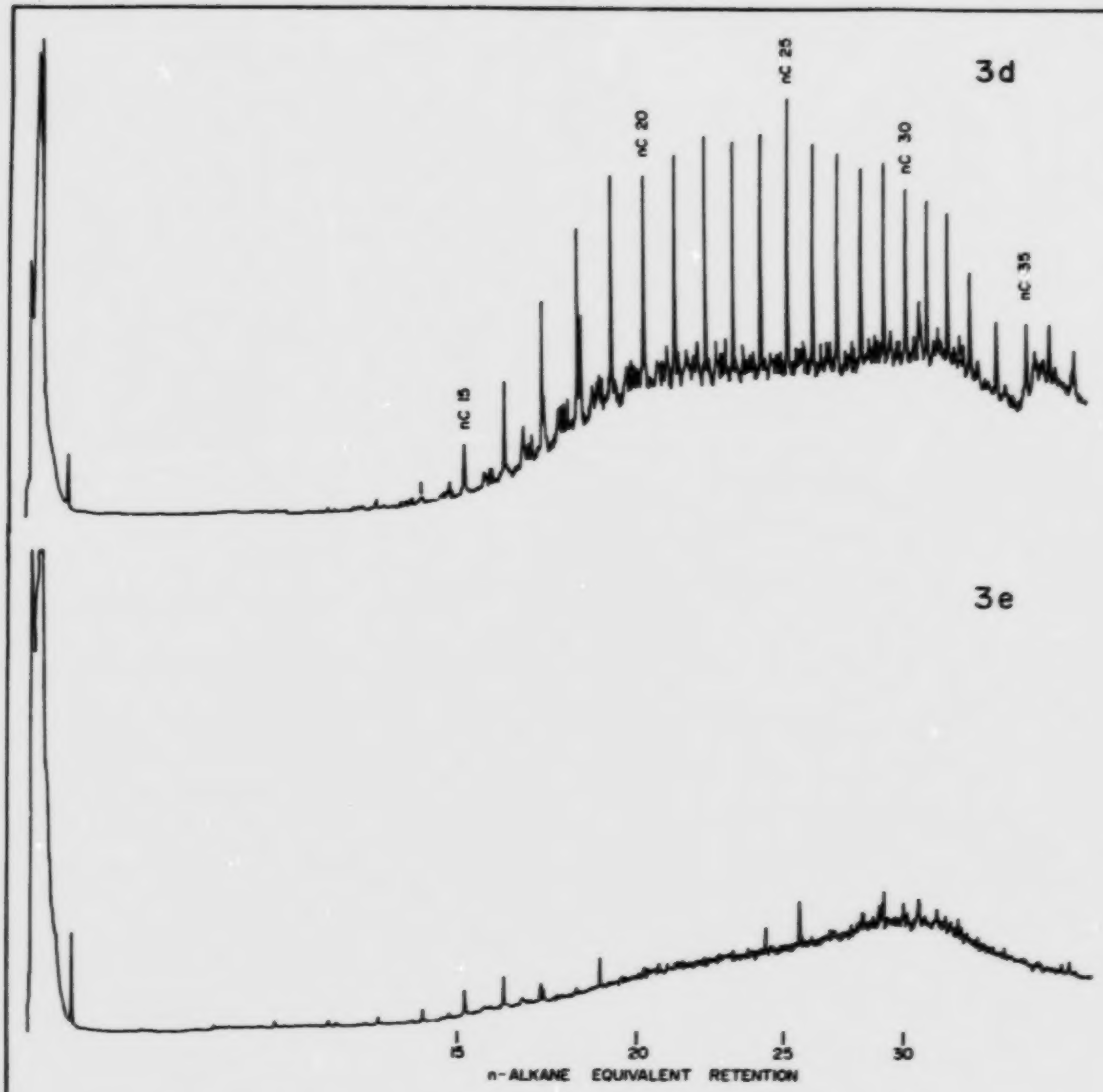

FIGURE 3 HYDROCARBON COMPOSITION

It is clear that all samples collected on January 20, 1987 are weathered relative to original 'Metula' oil. Three of the samples (Figures 3b, c and e) are of pavement material and consist of unresolved complex mixture with essentially no resolved components present. A single sample (Figure 3d, sample 10) indicates that some of the oil on the beach is not heavily weathered, retaining resolved alkanes from n-C 15 and higher. Biodegradation is apparent in this sample, as shown by the apparent loss of n-C 18 relative to phytane, the adjacent peak, when compared to original oil.

5. DISCUSSION

Although this was not a comprehensive survey of the entire coast it is evident that many sections of previously contaminated shoreline are now clean of visible oil and that significant amounts of oil remain at only a few locations. With the exception of the Puerto Espora area, oil was found only on the highest sections of the shoreline, in vicinity of the spring high-water levels. At Puerto Espora oil is present (1) in very large volumes - more than 100 m^3 in total, (2) over the entire area, which includes marsh, sheltered beach and exposed beach environments, (3) in all sections of the beach from the low-water level to the spring high-water level, and (4) generally as a fresh deposit below a weathered surface crust.

The remaining oil is present in a variety of forms that range from fresh, almost fluid and apparently unweathered, mousse and oil to hard pavement that could be sampled only by chipping or chiselling off small fragments. On the basis of this series of non-systematic observations there is an apparent relationship between sediment type and the viscosity of the remnant oil. The softer sections of pavement were generally associated with sands, whereas the harder pavements occurred more frequently with coarser (pebble and cobble) sediments.

Similarities in pavement characteristics between the Cape Hatt study site and the Puerto Espora area (the backbeach and open beach sections) were very evident. Both locations are low wave-energy environments with an intertidal beach-face slope of mixed sediments. At both locations there is (1) a pebble-cobble pavement which is present as a continuous feature in the upper intertidal zone, (2) clear evidence of undercutting and erosion of the upper pavement edge by the action of wave backwash, (3) "fresh" oil within the pavement, and there are (4) sections of soft pavement which can be easily broken off by hand but would not be dented nor show footprints if walked over.

The three pavement samples (Samples 3, 10 and 14) are typical of pavement material seen elsewhere. The presence of only unresolved material has been observed in pavement samples from the 'Amoco Cadiz' spill site (Owens et al, 1986) and from the 'Arrow' site (Humphrey and Vandermeulen, 1986). The pavement material from the BIOS site is substantially less weathered than any of these samples. This is consistent with the difference in time available for weathering at the BIOS site, where only three months per year are warm enough for significant weathering to occur, for a total period of one year of weathering in the four years sampled whereas the other samples had been weathering for many years.

The pavements are not considered to be a major source of secondary contamination, even though the oil is still very fresh in appearance in many cases. The rate of pavement erosion is evidently very slow and any release of oil would be in small quantities and would be weathered by physical processes during erosion.

ACKNOWLEDGEMENTS

This project was encouraged and funded by the Environmental Emergencies Technology Division of Environment Canada. Considerable local assistance was provided by the United Nations International Maritime Organization in Santiago (I. Vergara, Regional Coordinator in marine pollution) and by the Chilean Coast Guard (in particular the Gobernador Maritime in Punta Arenas and the Capitania de La Puerto de Punta Delgada). L. Guzman of the Instituto de La Patagonia in Punta Arenas kindly provided the sample of original 'Metula' oil.

REFERENCES

Blount, A.E., 1978. Two Years After the "Metula" Oil Spill, Strait of Magellan, Chile: Oil Interaction with Coastal Environments. Depart. of Geology, University of South Carolina, Columbia, Tech. Report, No. 16-CRD, 207 p.

Gundlach, E.R., Domeracki, D.D. and Thebeau, L.C., 1982. Persistence of "Metula" Oil in the Strait of Magellan Six and One-half years after the incident. Oil and Petrochemical Poll., 1(1), 37-48.

Gunnerson, G., and Peter, G., 1976. The "Metula" oil spill: NOAA Special Report, Boulder, Colorado, 35 p.

Hann, R.W. Jr. and Young, H.N., 1979. Fate of oil spilled from the super-tanker METULA. Final Rept. to U.S. Coast Guard, Texas A & M Univ., Civil Eng. Dept., College Station, Texas, 149 p.

Humphrey, B. and Vandermuelen, J.H., 1986. Characterization of fifteen year oil stranded oil. Proceedings of the 9th Arctic Marine Oil Spill Program Technical Seminar. Environment Canada, Edmonton. p. 29 - 38.

Owens, E.H., 1978. Mechanical Dispersal of Oil Stranded in the Littoral zone. Journ. Fish. Res. Bd., Canada, 35(5), 563-572.

Owens, E.H., and Robson, W., 1985. The "Amoco Cadiz" Incident: Site Visits Seven Years After the Spill. Environment Canada, Environmental Protection Service, Environmental Emergencies Technology Division, Ottawa, Unpubl. Rept. EE-63, 34 p.

Owens, E.H., Hope, D., and Humphrey, B., 1986. Long-Term Fate and Persistence of Stranded Oil and Cape Hatt, N.W.T. and from the "Amoco Cadiz" Spill - Part I, Cape Hatt Shoreline Study. (BIOS) Baffin Island Oil Spill Working Report 85-1, Environmental Protection Service, Environment Canada, Ottawa.

Owens, E.H. and Robson, W. 1987. Field observations of stranded oil in the Strait of Magellan, Chile, 12-1/2 years after the 'Metula' spill. Environment Canada, Environmental Emergencies Technology Division, Ottawa. Unpub. Rept. EE-89.

Straughn, D., 1981. Intertidal ecological changes after the METULA oil spill. Tech. Rept. No. 4, Allan Hancock Foundation, Inst. for Marine and Coastal Studies, Univ. of Southern California, Los Angeles, 138 p.

Warner, J.S. 1976. Determination of petroleum components in samples from the "Metula" oil spill. U.S. Dept. of Commerce, Boulder, Colorado. NOAA Data Rept. ERL MESA-4, 72 pp.

LONG-TERM FATE OF DISPERSED OIL AT LOW TEMPERATURE IN AN EXPERIMENTAL MESOSCALE TANK

by Emilien Pelletier[1], Charles Brochu[1] and John H. Vandermeulen[2]

[1] Institut National de la Recherche Scientifique,
INRS-Oceanologie, 310 ave des Ursulines, Rimouski (Que), G5L 3A1

[2] Marine Ecology Laboratory,Department of Fisheries & Oceans,
Bedford Institute of Oceanography, Dartmouth (N.S.), B2Y 4A2

INTRODUCTION

The environmental studies associated to the oil exploration and exploitation in extreme weather conditions have received an increasing attention in the last decade (Hillman, 1985). Many research and development projects were settled to solve practical problems caused by sea ice in the field application of classical countermeasure techniques. Among those techniques, the chemical dispersion of oil slicks in presence of frazil ice or below the ice cover has received little attention mainly due to the low effectiveness of most commercial dispersants and also because the long-term behaviour of crude oil dispersed in the water column at very low temperature is almost unknown. Numerous studies on the biodegradation of crude oil in sea water have been reported in the last fifteen years (Table 1). Nevertheless, few of them have been conducted at temperatures below 5°C and none has mentionned experiments below 0°C. Thus, informations about the long-term fate of dispersed crude oil in subarctic and arctic marine environments are sparse and often highly speculative since direct observations have never been obtained. For these reasons, we undertaken the fundamental study of degradation and weathering of dispersed oil two years ago using natural seawater exposed to severe atmospheric conditions.

As long-term experiments at sea or on ice field are difficult to manage and quite expensive, we decided to develop a low cost mesocsale tank which could be used to study the long-term fate and the chronic toxicity of crude oil in severe weather conditions and also in presence of an ice cover. This report describes the results of three weathering experiments conducted in 1986 and 1987.

MATERIALS AND METHODS

The mesoscale tank used for long-term weathering tests has been previously described (Pelletier and Brochu, 1986 and 1987). Modeled on the Mackay-Nadeau-Steelman apparatus, the mesoscale simulator (1,675 L) consists of a double-walled steel container, with either ambient seawater or coolant circulating through the outer chamber. Unfiltered seawater from the St.

TABLE 1. Experimental set-up of selected studies on the oil biodegradation in marine environment.

Volume of seawater (L)	Temperature °C	Oil and additives	Period (days)	References
0.25	20 (controlled)	Arabian light	60	Oudot, 1984
0.125	20 (controlled)	Oil and surfactants	2-3	Robichaux and Myrick, 1972
10.2 X 10^3	0.5-2.5 (*in situ*)	Ekofisk crude	14	Laake, Tjessem and Rein, 1984
20 X 10^3	variable (*in situ*)	Oil and dispersants	120	Marty, Bianchi and Gatellier, 1979
0.10	15 and 25 (cont.)	Libyan crude	45	Olivieri, *et al*. 1976
Continuous flow-through	2-11 (*in situ*)	Oil and fertilizers	50	Horowitz and Atlas, 1977
15.7 X 10^3	??? (*in situ*)	Oil and Corexit 9527	20	Tjessem, Pedersen and Aaberg, 1984
75	3-8 (*in situ*)	Oil and fertilizers	21	Tramier and Sirvins, 1983
65 X 10^3	12-17 (*in situ*)	Oil and Corexit 9527	24	Wong *et al.* 1984
66 X 10^3	11.6-12.8	" " "	15	Cretney *et al*. 1981
0.2	8 (controlled)	" " "	84	Foght, Fedorak and Westlake,1983 Foght and Westlake, 1982 Fedorak and Westlake, 1981

Table 1 (continued)

Volume (L)	Temperature °C	Oil and additives	Period (d)	References
0.5	4 and 14 (cont.)	Kuwait residue	315	Gibbs, 1975 Gibbs, Pugh and Andrews, 1975
0.1	5, 10 ,15 and 25 controlled	Sweden oil	60	Atlas et Bartha, 1972
2	4 and 30 (cont.)	Crude oil	21	Jobson, Cook and Westlake,1972
300	??? (in situ)	Oil and dispersants	25	Gatellier et al. 1973
14-15 X 10^3	0-2 (uncont.)	No.2 fuel oil	23	Gearing and Gearing, 1982
"	20-21	" "	18	" "
"	17-19	" "	8	" "
"	21-23	" "	5.6	" "
60 X 10^3	12 (in situ)	Aromatics and oil	10	Lee et al,1978
8.0 X 10^3	14-19 (uncont.)	Tia Juana crude	17	Gordon et al, 1976
	21-25	" "	10	" "
	24-5	" "	79	" "
	19-16	Guanipa crude	101	" "
	12-3	" "	32	" "

Lawrence Estuary was used to fill the simulator. Ambient air (down to -30°C in winter) was blown over the surface of the contained water column, which favored formation of sea ice in the simulator during the winter months. The apparatus was constructed at field laboratory facilities located on the shore of the St Lawrence Estuary near Rimouski.

Three experiments have been run following the experimental conditions given in Table 2. In all cases, 565 cc of Western Sweet Blend crude oil (EPS standard) and 56.5 cc of Corexit 9527® (a commercial dispersant provided by Esso Canada) were used for the initial dispersion.

A Varian 3400® gas chromatograph equipped with a temperature programmable on-column injector and a flame ionization detector (320 °C) were used for all analyses (Desideri et al.,1984). Hydrocarbons were eluted on a 30 m glass capillary column (0.25 um) coated with a low polarity stationnary phase (DB1). The GC was coupled to a Varian 4270® integrator which was interfaced to a microcomputer Compaq Deskpro® for storage and statistical treatement of chromatographic data.

RESULTS AND DISCUSSION

Physical processes

One of the major objectives of the project was to evaluate the long-term effectiveness of a chemical dispersant at low temperature by estimating the stability of the dispersion. The Figure 1 reports the percentage of dispersed oil remaining in the water column compared to the initial amount used for the dispersion. The % dispersed oil was calculated from the oil concentration measured at sampling level 3 (0.6 m below the surface) assuming an homogeneous distribution of oil in the contained water column. In experiments 1 and 2, very good initial dispersions were obtained (reaching 70% in both cases) using only the low energy provided by the air stream blowing over the water surface. In experiment 3, the dispersion was conducted in presence of frazil ice (5-7 cm) and it was necessary to stir moderately with a wood paddle the oil/ice/water mixture to ensure a relatively good dispersion (50%).

The most stricking feature shown in Figure 1 is the relative similarity of all experimental curves whatever was the initial dispersion level or the water temperature. This behavior indicates that a same physical process, working independently from the initial experimental conditions, was regulating the amount of dispersed oil in the water column.

In such a mesoscale tank , the motion of oil droplets is controlled by buoyancy rather than diffusion. The rate of particle settling is given by Stokes' law:

$$4/3 \ \pi \ a^3 \ \Delta \rho \ g = 6 \ \pi \ \eta_o \ a \ v \qquad \text{Eq. 1}$$

The derivation of Stokes' law assumes that (1) the motion of the spherical particles is very slow to avoid local turbulence generated by particles and minimize the friction, (2) the suspension is very dilute to avoid interactions between particles, and (3) the particles are much much larger

Table 2: Experimental conditions for weathering studies of dispersed crude oil in mesoscale simulator.

Experiment	Dates	Water Temp., °C		Water Salinity	Initial bacterial	notes
no		start	end	°/oo	counts/ cc	
1	18 Nov. 85- 26 March 86	3.4	0.3	28.0	311	90 days with ice cover
2	17 Aug. 86- 20 Oct.86	11.0	3.3	25.5	2400	no ice
3	16 Dec. 86- 20 April 87	-1.7 (ice)	3.0	(28.0)	7286	100 days with ice cover

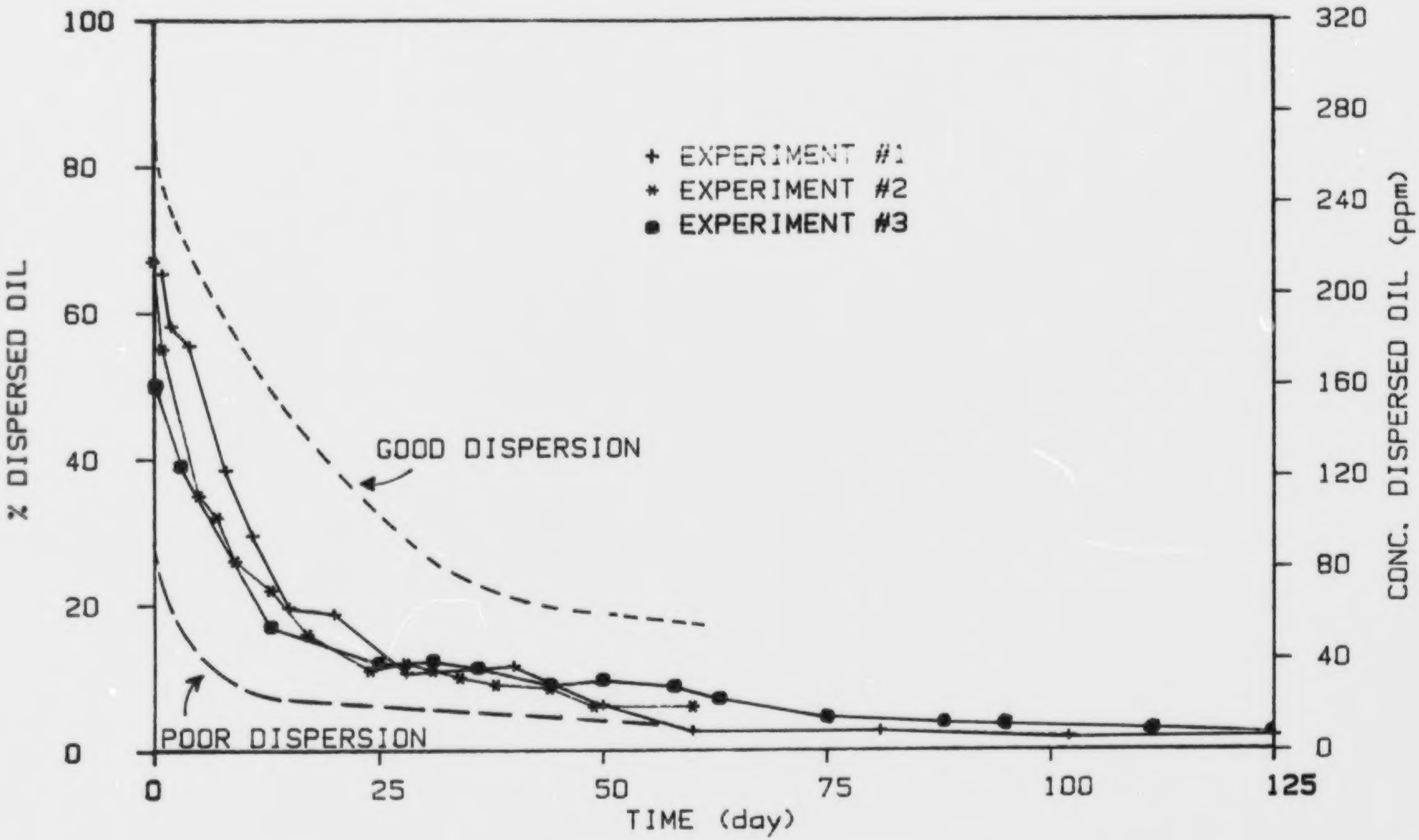

FIGURE 1. Percentage of dispersed oil measured in the contained water colum versus the elapsed time from the initial dispersion. Curves simulating a good dispersion and a poor dispersion are given in dotted lines.

than the molecules of the medium. Keeping in mind these restrictions, the Equation 1 can be used to estimate the diameter of oil droplets rising slowly to the surface:

$$a = \sqrt{\frac{9\,\eta_w\, v}{2\,(\rho_w - \rho_o)\, g}} \qquad \text{Eq. 2}$$

where

a = diameter of oil droplet

η_w = viscosity of seawater $\simeq 1$ Pas $= 1$ kg$\cdot$m$^{-1}\cdot$s^{-2}

v = velocity of the droplet (m$\cdot$s^{-1})

g = 9.81 m^{2}s^{-1}

ρ_w = density of seawater = 1020 kg$\cdot$m^{-3}

ρ_o = density of crude oil = 839 kg$\cdot$m^{-3}

For a given velocity (i.e. $v = 1$ m.day^{-1}), the size of oil droplets travelling from the buttom of the tank up to the sampling level 3, located about 1 meter above the buttom, can be estimated to 5.4 μm. The Figure 2 gives the distribution of oil droplet sizes raising to the surface as calculated by the Stokes' equation for experimental conditions observed in the simulator. The similarity between experimental curves shown in Figure 1 and calculated distribution of Figure 2 indicates a possible direct relationship between the amount of oil in the water column, an experimental parameter, and the calculated size of oil droplets. This relationship is highlighted by data presented in Figure 3 and Table 3 . The linearity of the relationship is not observed right at the beginning of experiments but only few days after the initial dispersion (from day 3 to day 8) due to the restrictions to the application of Stokes' law mentionned above. The regression equations, calculated for data enclosed in large square brackets (Table 3) give the droplet size as a function of the oil concentration in the water column. The correlation coefficient (r) is also given.

The slope of these straight lines is related to the stability of the dispersion. For a fixed amount of oil, the average size of droplets from a less stable dispersion should be larger (inducing an higher slope) than droplets from a very good dispersion (lower slope). This feature is clearly illustrated using simulated curves for a poor and a good dispersion (Figure 1). A good dispersion gives a slope which appproches zero (very slow change in the droplet size) whereas a poor dispersion induces a higher slope and a displacement of the straight line towards the left side of the figure (Figure 4). Experimental data (Table 3) give slopes relatively closed together since the same commercial dispersant and the same crude oil have been used throughout all experiments. Nevertheless, the dispersion in experiment 3 was less stable mainly due to the presence of frazil ice on the surface and seawater temperature below 0°C. As expected, the experimental

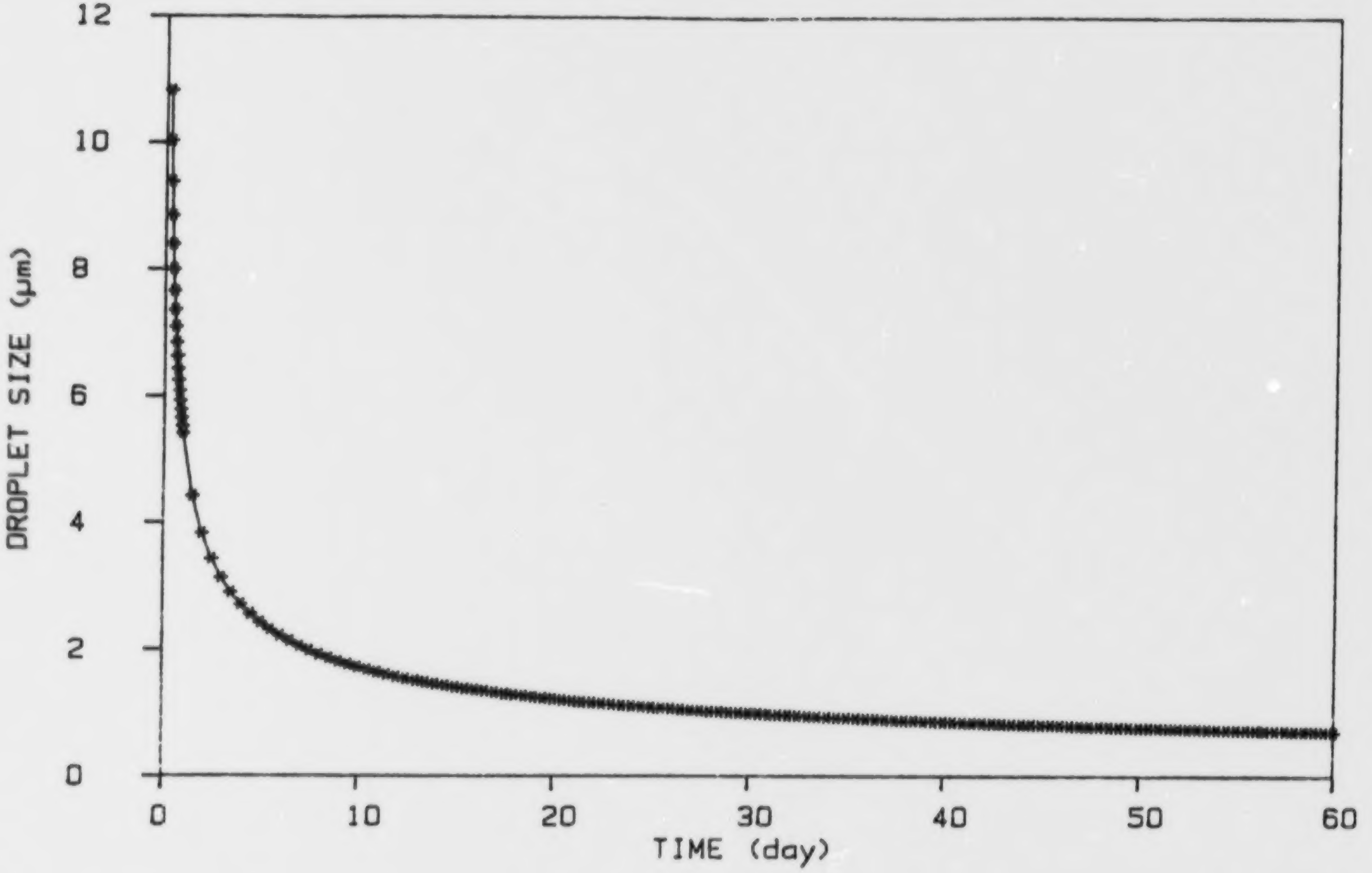

FIGURE 2. Distribution of droplet size (μm) as calculated with the Stokes' equation for experimental conditions observed in the mesoscale simulator over a 60-day period.

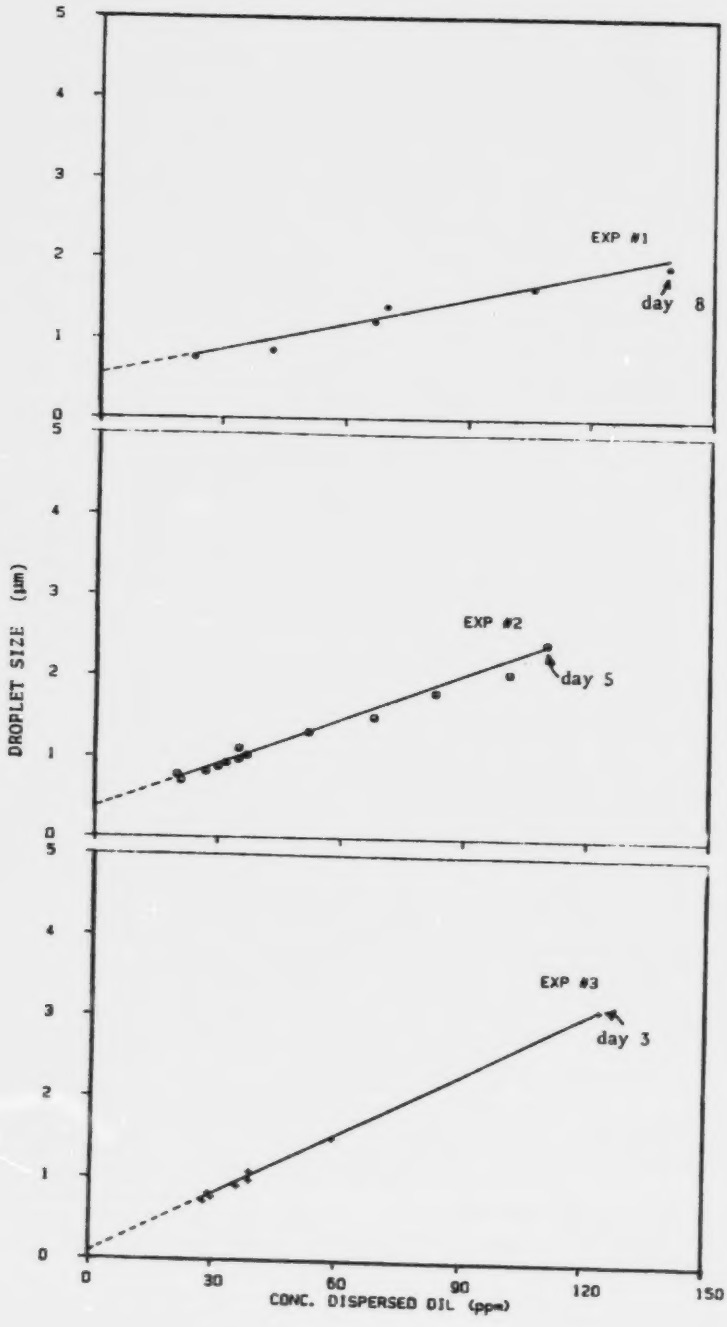

FIGURE 3. Distribution of droplet size (µm) versus the oil concentration observed in three experiments conducted in the mesoscale simulator.

Table 3: Correlation between calculated droplet size and measured oil concentration observed in the mesoscale simulator.

Day	Oil concentration (ppm)	Droplet size (µm)	
EXPERIMENT 1			
0.25	296	10.8	
1	213	5.4	
2	206	3.8	
8	139	1.9	Regression equation:
11	106	1.6	
15	70	1.4	$Y(\mu m) = 0.5 + 1.03\ 10^{-2} X(ppm)$
20	67	1.2	
40	42	0.9	r = 0.982
50	23	0.8	
EXPERIMENT 2			
0.25	211	15.3	
1	174	5.4	
5	110	2.4	
7	101	2.0	
9	83	1.8	
13	68	1.5	
17	52	1.3	Regression equation:
24	35	1.1	
28	37	1.0	$Y(\mu m) = 0.4 + 1.75\ 10^{-2} X(ppm)$
31	35	1.0	
34	32	0.9	r = 0.993
38	30	0.9	
44	27	0.8	
49	20	0.8	
60	21	0.7	
EXPERIMENT 3			
3	124	3.1	
13	59	1.5	
25	39	1.1	Regression equation:
31	39	1.0	
36	36	0.9	$Y(\mu m) = 0.04 + 2.49\ 10^{-2} X(ppm)$
44	29	0.8	
50	30	0.8	r = 0.999
58	28	0.7	

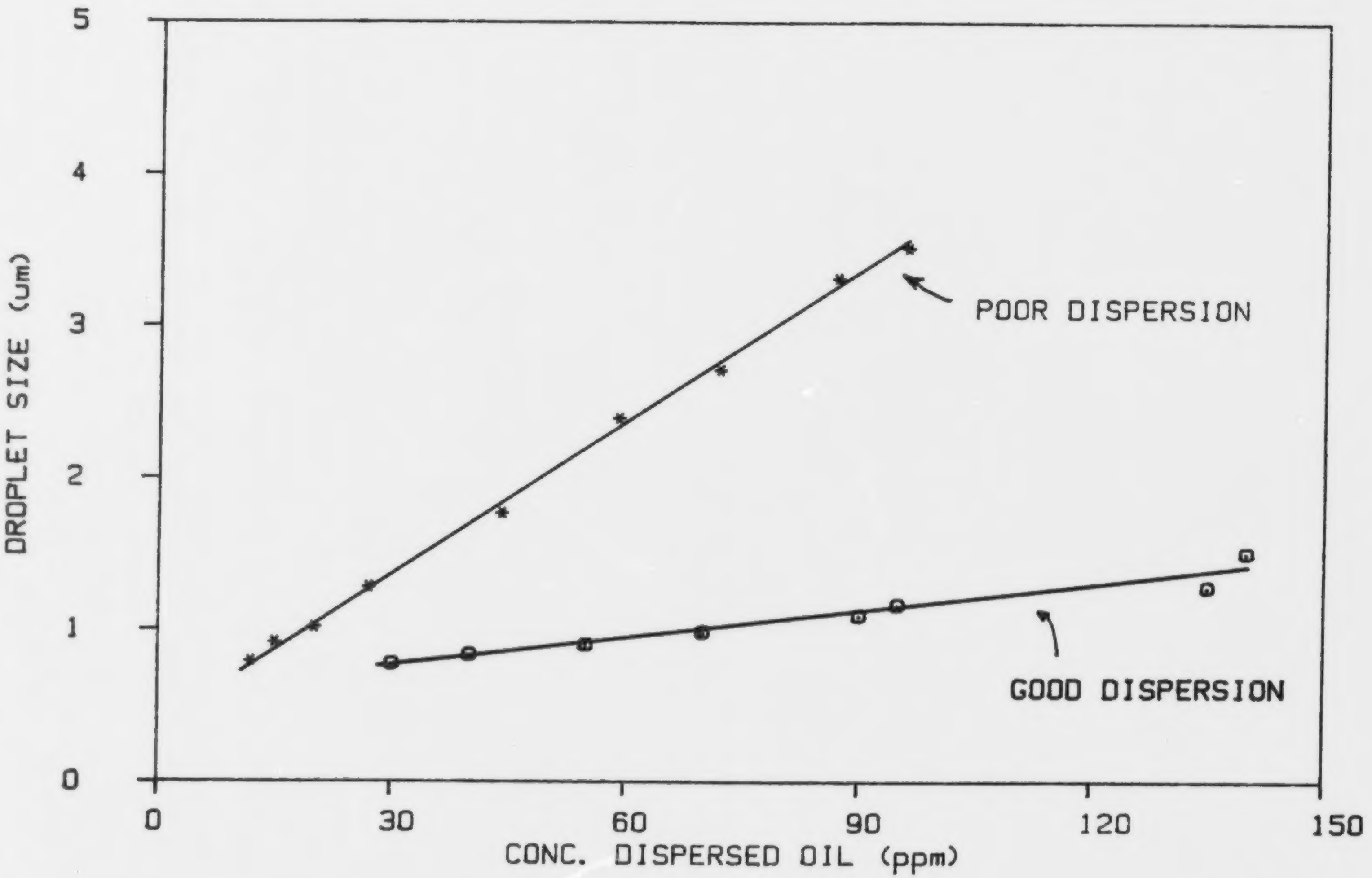

FIGURE 4. Distribution of droplet size (μm) versus the concentration of dispersed oil for a good and a poor dispersion over a 60-day period.

slope observed for experiment 3 (Table 3) is almost twice the average slope of experiments 1 and 2. The correlation in the experiment 3 was the best of all (r = 0.999) because the water column was rapidly covered by ice after the dispersion and no more external agent came to disturb the slow boyancy of droplets.

Weathering processes

Among the other factors affecting the concentration of oil in the water column, evaporation and biodegradation were monitored by regular analysis of different hydrocarbon fractions of dispersed oil by gas chromatography. Some GC data and weathering ratios are given in Tables 4 to 7. Light linear alkanes and isoprenoids are listed with their respective retention time and peak height (arbitrary units).

The Saturated Hydrocarbon Weathering Ratio (SHWR) is the ratio of the sum of n-alkanes from C10 to C25 over the sum of n-alkanes from n-C17 to n-C25. The biodegradation ratio (ALK/ISO) is given by the ratio of the sum of n-alkanes from C14 to C18 over the sum of 5 isoprenoids in the same boiling range (Boehm et al.,1984). Two other biodegradation ratios, C17/pristane and C18/phytane, are also given. The Pristane/Phytane ratio gives information about the production of biogenic pristane-rich hydrocarbons versus the presence of petrogenic phytane-rich hydrocarbons.

The hydrocarbon parameters of unweathered Western Sweet Blend crude oil are given in Table 4. In a usual weathering process, the SHWR decreases and approches 1.0 as low-boiling alkanes are lost by evaporation. In both winter experiments (Tables 5 and 7), the SHWRs were unchanged which means that evaporation was negligible during the dispersion process mainly due to low temperature of seawater at the beginning of each experiment (Table 2). The SHWR was significantly lowered in experiment 2 (Table 6) because the dispersion was conducted at 11.0°C. All biodegradation ratios were also strongly lowered during the fall experiment (Table 6) indicating that an important biodegradation process occured in the first 60 days. Finally, the Pristane/Phytane ratio was closed to 1 in all samples indicating no important production of biogenic material during the course of these experiments. Few biodegradation activity were detected in experiments 1 and 3 even after 50 days.

CONCLUSION

These results highlight some interesting fundamental features about the long-term fate of dispersed oil under experimental conditions:

1)The seawater temperature is not a determining factor in the dispersion stability but the presence of frazil ice reduced strongly the dispersant effectiveness due to the wave damping induced by the ice.

2)In absence of diffusion and convection, the main mechanism controlling the oil concentration in the contained water column is the buoyancy.

3)Few days after the initial dispersion, the rising of oil droplets can be

TABLE 4. Chromatographic data for the Western Sweet Blend crude oil (EPS standard) as used in experiments 1 to 3 before the dispersion.

NAME	RETENTION TIME (min)	HEIGHT
C10	10.84	34616
C11	14.6	31875
C12	18.16	27275
C13	21.48	26643
ISO1	23.92	14605
C14	24.6	30248
ISO2	26.5	14739
C15	27.55	34632
C16	30.34	28301
ISO3	31.72	10779
C17	32.99	28381
PRIST	33.21	17720
C18	35.12	33045
PHYTH	35.33	18144
C19	36.79	35195
C20	38.21	33389
C21	39.49	29349
C22	40.65	26909
C23	41.74	23200
C24	42.64	34317
C25	43.22	34317

SHWR= 1.77

ALK/ISO= 2.03

C17/PRISTANE= 1.60

C18/PHYTANE= 1.82

PRISTANE/PHYTANE= .98

TABLE 5. GC data and weathering ratios of dispersed crude oil measured at day 50 in experiment 1.

NAME	RETENTION TIME (min)	HEIGHT
C10	10.84	14701
C11	14.6	55384
C12	18.14	38392
C13	21.47	20451
ISO1	23.91	21851
C14	24.58	28520
ISO2	26.48	19061
C15	27.53	34659
C16	30.32	27355
ISO3	31.7	14144
C17	32.97	29568
PRIST	33.2	23352
C18	35.1	32765
PHYTH	35.31	22811
C19	36.85	25429
C20	38.2	32880
C21	39.47	30152
C22	40.64	23355
C23	41.73	34333
C24	42.63	34544
C25	43.2	34544

SHWR= 1.79

ALK/ISO= 1.51

C17/PRISTANE= 1.27

C18/PHYTANE= 1.43

PRISTANE/PHYTANE= 1.02

TABLE 6. GC data and weathering ratios of dispersed crude oil measured at day 60 in experiment 2.

NAME	RETENTION TIME (min)	HEIGHT
C10	10.82	3691
C11	—	—
C12	18.14	3296
C13	21.47	6384
ISO1	23.91	13480
C14	24.59	16339
ISO2	26.49	17547
C15	27.53	21595
C16	30.32	19144
ISO3	31.71	14923
C17	32.98	18416
PRIST	33.2	24019
C18	35.11	21896
PHYTH	35.32	25693
C19	36.78	21243
C20	38.21	19560
C21	39.48	16115
C22	40.65	14592
C23	41.74	8901
C24	42.7	10448
C25	43.21	10448

SHWR= 1.50

ALK/ISO= 1.01

C17/PRISTANE= .77

C18/PHYTANE= .85

PRISTANE/PHYTANE= .93

TABLE 7. GC data and weathering ratios of dispersed crude oil measured at day 50 in experiment 3.

NAME	RETENTION TIME (min)	HEIGHT
C10	10.79	9040
C11	14.53	20683
C12	18.07	42608
C13	21.39	40656
ISO1	23.83	30747
C14	24.51	51915
ISO2	26.41	30551
C15	27.46	61870
C16	30.25	51157
ISO3	31.63	16924
C17	32.91	46496
PRIST	33.13	33129
C18	35.05	50452
PHYTH	35.27	36043
C19	36.74	49314
C20	38.16	46162
C21	39.44	38539
C22	40.61	30176
C23	41.7	31063
C24	42.6	34368
C25	43.19	34368

SHWR= 1.77

ALK/ISO= 1.78

C17/PRISTANE= 1.40

C18/PHYTANE= 1.40

PRISTANE/PHYTANE= .91

described with a simple mathematical relationship, the Stokes' equation, which means that contributions from other physical mechanisms, as flocculation and dissolution, to the removal of oil from the water column are negligible.

4)The long-term stability of a dispersion (i.e. the dispersant effectiveness) can be evaluated by plotting the calculated droplet size versus the concentration of dispersed oil. As the relationship is linear in absence of external disturbance, the experimental period could be reduce to 3 weeks without lost of accuracy.

5)In winter experiments, evaporation and biodegradation do not contribute to the weathering process.

6)In fall experiment, the effects of both processes on the chemical composition of dispersed oil are easily detected by GC analysis. Their relative contributions to the removal of oil from the water column are not clear at the present time.

ACKNOWLEDGMENT

The financial support for this study was provided by the Environmental Revolving Funds (contract 406-99-04) and the National Sciences and Engineering Research Council of Canada (strategic grant).

REFERENCES CITED

Atlas, R.M. and R. Bartha, 1972. Biodegradation of petroleum in seawater at low temperature. Canadian Journal of Microbiology, 18:1851-1855

Bohem, P., W. Steinhauer, D. Cobb, S. Duffy and J. Brown, 1984. Chemistry 2: Analytical Biogeochemistry - 1983 Study Results. BIOS Working Report 83-2; 139p. EPS, Environmewnt Canada, Ottawa.

Cretney, W.J., R.W. Macdonald, C.S. Wong, D.R. Green, B. Withehouse, and G.G. Geesey, 1981. Biodegradation of a chemically dispersed crude oil. Proceeding of the 1981 Oil Spill Conference, American Petroleum Institute, Washington, D.C., 37-43

Desideri, P.G., L. Lepri, D. Heimler, S. Giannessi and L. Checchini, 1984. Concentration, separation and determination of hydrocarbons in sea water. Journal of Chromatography, 284:167-178

Fedorak, P.M. and D.W.S. Westlake, 1981. Microbial degradation of aromatics and saturates in Prudhoe Bay crude oil as determined by glass capillary gas chromatography. Canadian Journal of Microbiology, 27:432-443

Foght, J.M. and D.W.S. Westlake, 1982. Effect of the dispersant Corexit 9527 on the microbial degradation of Prudhoe Bay oil. Canadian Journal of Microbiology, 28:117-122

Foght, J.M., P.M. Fedorak, and D.W.S. Westlake, 1983. Effect of the dispersant Corexit 9527 on the microbial degradation of sulfur heterocycles in Prudhoe Bay oil. Canadian Journal of Microbiology, 29:623-627

Gatellier, C.R., J.L. Oudin, P. Fusey, J.C. Lacaze and M.L. Priou, 1973. Experimental ecosystems to measure fate of oil spills dispersed by surface active products. Proceeding of Joint Conference on Prevention and control of Oil Spills, American Petroleum Institute, Washington, D.C., 497-504

Gearing, P.J. and J.N. Gearing, 1982. Behaviour of no 2 fuel oil in the water column of controlled ecosystems. Marine Environmental Research, 6:115-132.

Gibbs, C.F. 1975. Quantitative studies in marine biodegradation of oil I. Nutrient limitation at 14°C. Proceeding of the Royal Society of London, B. 188:61-82

Gibbs, C.F., K.B. Pugh and A.R. Andrews, 1975. Quantitative studies on marine biodegradation of oil. II. Effect of temperature. Proceeding of the Royal Society of London, B. 188:83-94

Gordon, D.C., P.D. Keizer, W.R. Hardstaff and D. G. Aldous, 1976. Fate of crude oil spilled on seawater contained in outdoor tanks. Environmental Science and Technology, 10:580-585

Green,D.R., J. Buckley and B. Humphrey, 1982. Le devenir du pétrole dispersé par voie chimique dans la mer. Rapport sur deux expériences menées sur le terrain. Service de la protection de l'environnement, rapport SPE 4-EC-82-5F, Environnement Canada, 88pp.

Hillman, S.O. 1985. Arctic spill response improvements: A 1985 review of Arctic research and edvelopment. Proceeding of the 1981 Oil Spill Conference, American Institute of Petroleum, Washington, D.C., 411-414.

Horowitz, A. and R. M. Atlas, 1977. Continuous open flow-through system as a model for oil degradation in the Arctic Ocean. Applied and Environmental Microbiology, 647-653

Jobson, A., F.D. Cook, and W.S. Westlake, 1972. Microbial utilization of crude oil. Apllied Microbiology, 23:1082-1089.

Laake, M., K. Tjessem and K. Rein, 1984. Fate of a tritiated Ekofisk crude oil in a controlled experiment with North Sea plankton, Environmental Science and Technology, 18:641-647

Lee, R.F., W.S. Gardner, J.W. Anderson, J.W. Blaylock and J. Barwell-Clarke, 1978. Fate of polycyclic aromatic hydrocarbons in controlled ecosystem enclosures. Environmental science and Technology, 12:832-838

Marty, D., A. Bianchi and C. Gatellier, 1979. Effects of three oil spill dispersants on marine bacterial populations. 1. Preliminary study. Quantitative evolution of aerobes. Marine Pollution Bulletin, 10:285-287

Olivieri, R., P. Bacchin, A. Robertiello, N. Oddo, L. Degen and A. Tonolo, 1976. Microbial degradation of oil spills enhanced by a slow-release fertilizer. Applied and Environmental Microbiology, 629-634

Oudot, J. 1984. Rates of microbial degradation of petroleum components as determined by computerized capillary gas chromatography and computerized mass spectrometry. Marine Environmental Research, 13:277-302.

Pelletier, E. and C. Brochu, 1986. Simulation of biodegradation under an ice cover. Proceed. 9th AMOP Technical Seminar, Edmonton, 141-150.

Pelletier, E. and C. Brochu, 1987. Oil dispersion and weathering in a mesoscale simulator. Environmental Studies Revolving Funds Report, Ottawa (in preparation).

Robichaux, T.J. and H.N. Myrick, 1972. Chemical enhancement of the biodegradation of crude-oil pollutants, Journal of Petroleum Technology, 16-20

Tjessem, K., D. Pedersen and A. Aaberg, 1984. On the environmental fate of a dispersed Ekofisk crude oil in sea-immersed plastic columns. Water Research, 18:1129-1136

Tramier, B. and A. Sirvins, 1983. Enhanced oil biodegradation: a new operational tool to control spills. Proceeding of the 1983 Oil Spill Conference, American Institute of Petroleum, Washington, D.C., 115-119

Wong, C.S., F.A. Whitney, W.J. Cretney, K. Lee, F. McLaughlin, J.Wu, T. Fu and D. Zhuang. 1984. An experimental marine ecosystem response to crude oil and Corexit 9527: Part 1 -Fate of chemically dispersed crude oil. Marine Environmental Research, 13:247-263

SATURATION/PENETRATION OF NORMAN WELLS CRUDE OIL INTO UKALERK BORROW PIT SAND

by

A.G. Holoboff & R.J. Foster
Esso Resources Canada Limited, Calgary

ABSTRACT

In the unlikely event of a blow out at Esso's Caisson Retained Island (CRI) the CRI infill material would be penetrated by oil thus acting as a large storage tank. This report presents experimental data on the saturation, permeability of the sand, and oil-front velocity when oil is applied to the sand-pack surface. The volume of oil absorbed by the sand varied from from 26-32% of the sand volume, and permeabilities varied from 4×10^{-3} to 9×10^{-3} cm/sec. The oil-front movement rate was as high as 0.025 cm/sec when oil displaced trapped air in the sand, and dropped as low as 0.001 cm/sec when displacing water. A typical Arctic oil, Norman Wells (a relatively light crude) was used in these experiments.

This report will describe the experimental apparatus and summarize the data collected during the experiment. Results of this program give a clearer understanding of the holding capacity and rate of penetration of the fill material used at the CRI Amerk Site.

1.0 INTRODUCTION

Esso's Caisson Retained Island (CRI) at Amerk is more similar to a land-based drilling operation than the typical floating structure. In the unlikely event that a blowout occurs, while drilling from the CRI, oil would flow onto the sand-fill material and not directly into the ocean. The voids in the sand fill material represent a storage area for spilled oil. In order to determine how much oil can be stored in the sand and how rapidly that oil will penetrate this fill, experiments were conducted at Esso's Research department on the Ukalerk fill material, used in the caisson at the Amerk site. Norman Wells crude oil was used in the experiment. It is a light crude with properties similar to those of oils discovered in the Beaufort. Ukalerk sand represents a typical fill material for the CRI in the Southern Beaufort Sea.

2.0 EXPERIMENTAL METHODS

2.1 Laboratory Equipment

The laboratory equipment (Figure 1) consisted of a Lucite cylinder, 130 cm high and 29 cm inside diameter, equipped with an overflow reservoir to control the water level in the sand. The top of the cylinder was fitted with a sampling collar with a welded jar ring to hold the glass sample container. A movable piston inside the cylinder was used to raise the sand so that a 1 mm thick slice could be removed, using a sharp scraper, into the sample collar. The sample was then brushed into a sample jar.

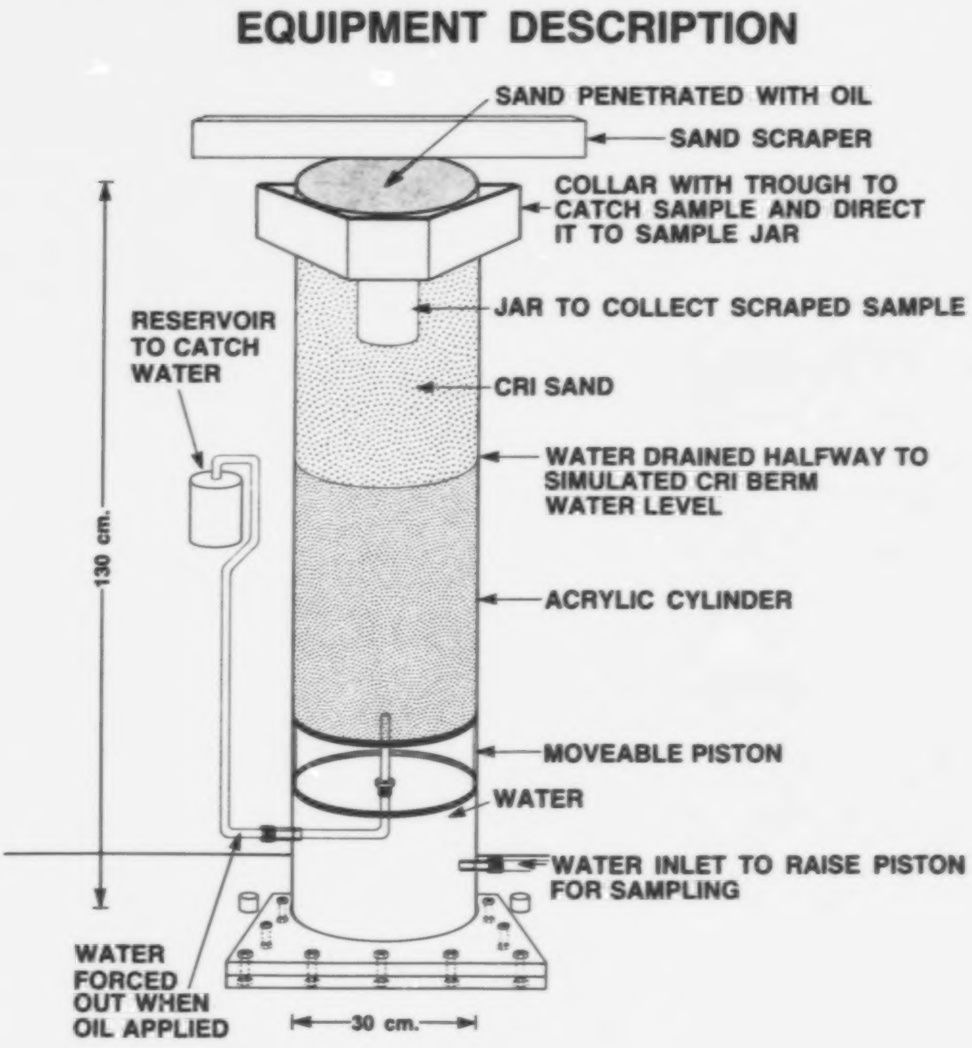
EQUIPMENT DESCRIPTION
SAND PENETRATED WITH OIL
SAND SCRAPER
COLLAR WITH TROUGH TO CATCH SAMPLE AND DIRECT IT TO SAMPLE JAR
JAR TO COLLECT SCRAPED SAMPLE
RESERVOIR TO CATCH WATER
CRI SAND
WATER DRAINED HALFWAY TO SIMULATED CRI BERM WATER LEVEL
130 cm.
ACRYLIC CYLINDER
MOVEABLE PISTON
WATER
WATER INLET TO RAISE PISTON FOR SAMPLING
WATER FORCED OUT WHEN OIL APPLIED
30 cm.

FIGURE 1 Sand Cylinder

2.2 Experimental Program

An initial experiment was performed to test the equipment, to establish experimental procedures, and to confirm suitability of the chosen experimental parameters. The steps of the experiment were:

1. The movable piston was positioned at the bottom of the acrylic cylinder and the cylinder was filled with tap water to within 30 cm of the top (Figure 2).

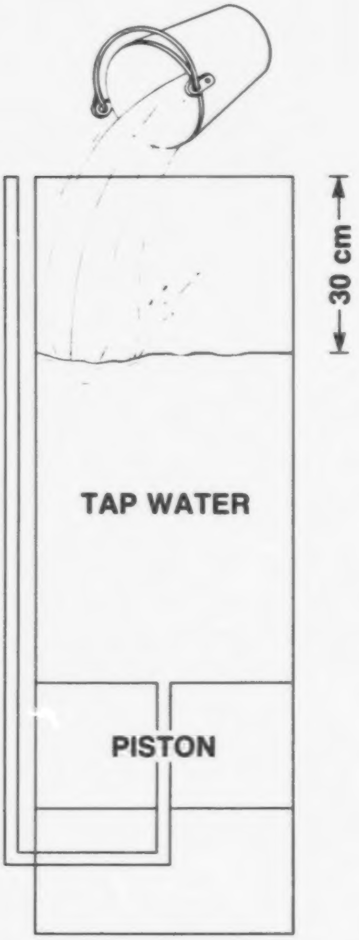

FIGURE 2 Cylinder Filled with Tap Water

2. Ukalerk sand was poured on top of the water column using a two kilogram scoop (Figure 3). Surplus water was removed from the top to allow for additional sand (Figure 4). This procedure was continued until the sand in the column was 49 cm deep. This procedure was used to simulate the placing of sand in the CRI where sand was hydraulically pumped into the center of the caisson ring, which contained seawater.

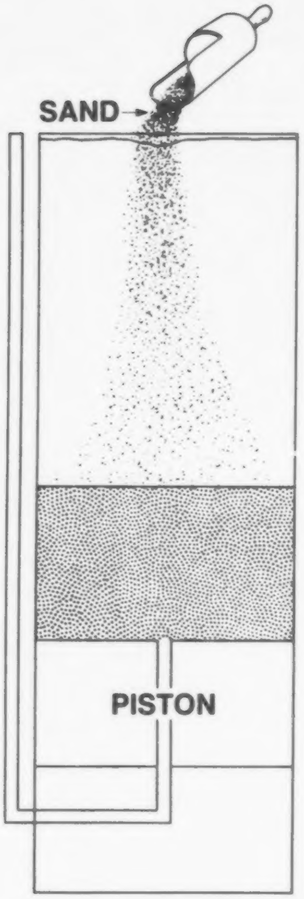

FIGURE 3 Sand Placement

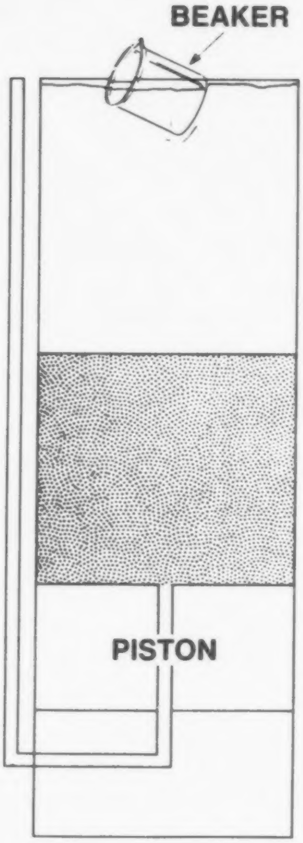

FIGURE 4 Surplus Water Removed to Allow for more Sand

3. The sand was not compacted.

4. The water was removed from the sand pack, through the drain in the bottom of the movable piston, to half height (Figure 5).

5. Oil was applied to the sand surface in 2.5 Litre volumes until the sand pack was saturated and oil had reached the outlet of the reservoir (Figure 6). The movement of the oil through the sand was observed through the transparent acrylic cylinder wall. Depth measurements were taken at several points around the cylinder during the course of the experiment.

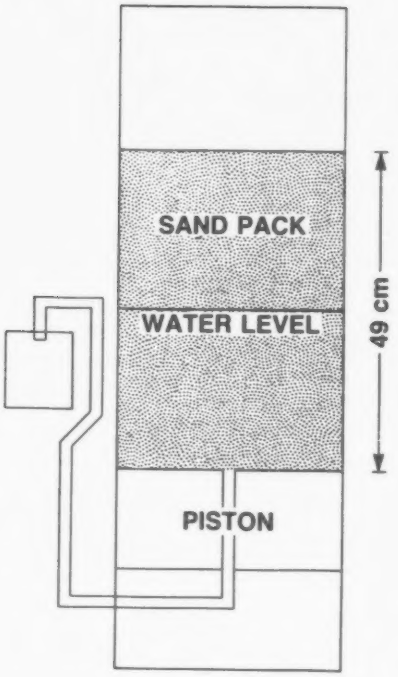

FIGURE 5 Water Drained From Sand Pack to Half Height

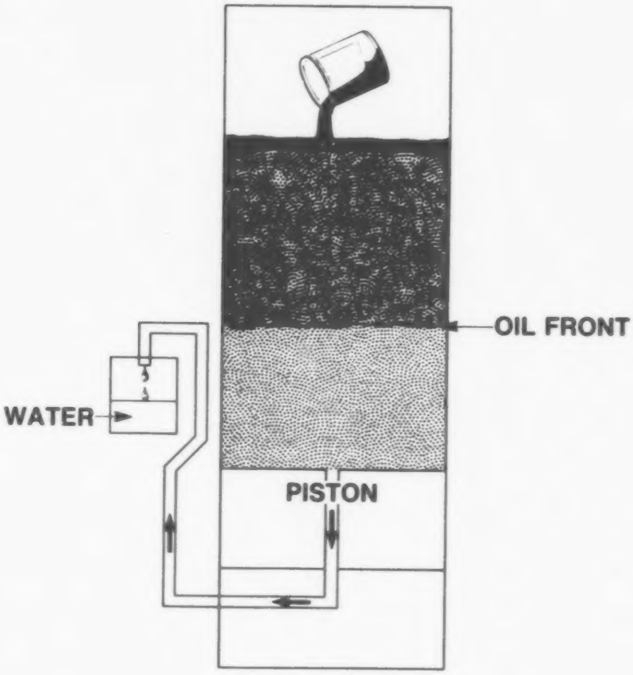

FIGURE 6 Oil Applied in 2.5 Litre Volumes. Water Being Driven Out of Sand Pack

6. Surplus oil was skimmed off the sand surface using a small beaker (Figure 7). A small depression was made to facilitate the removal of surplus oil from the sand surface. Afterwards the depression was filled in and the sand surface levelled smooth with an 8 cm width spatula.

7. The sand pack was raised to the top of the cylinder and the sand was scraped off in 1 mm slices by sliding a sharp scraper across the top of the cylinder (Figure 8). The recovered sand was brushed into a 900 ml jar. The 1 mm slices were taken from many different depths throughout the sand pack in intervals varying from 0.5 to 2 cm. (Closer together at the top and further apart at the bottom.)

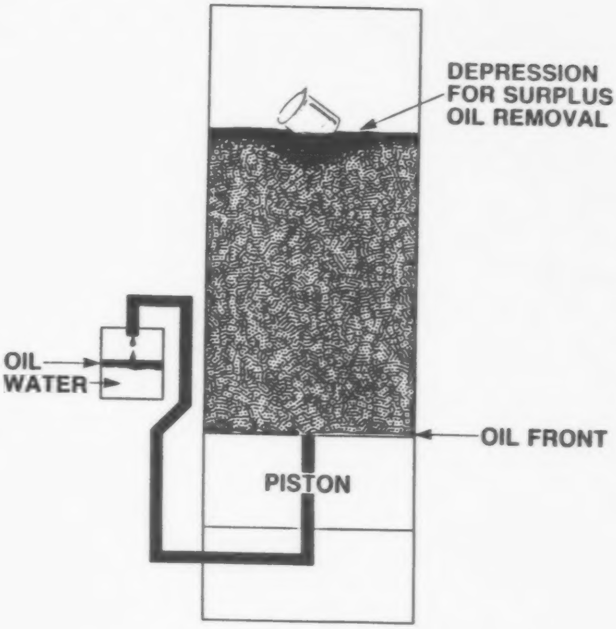
DEPRESSION FOR SURPLUS OIL REMOVAL
OIL
WATER
OIL FRONT
PISTON

FIGURE 7 Surplus Oil Skimmed Off Surface When Sand Pack Saturated With Oil

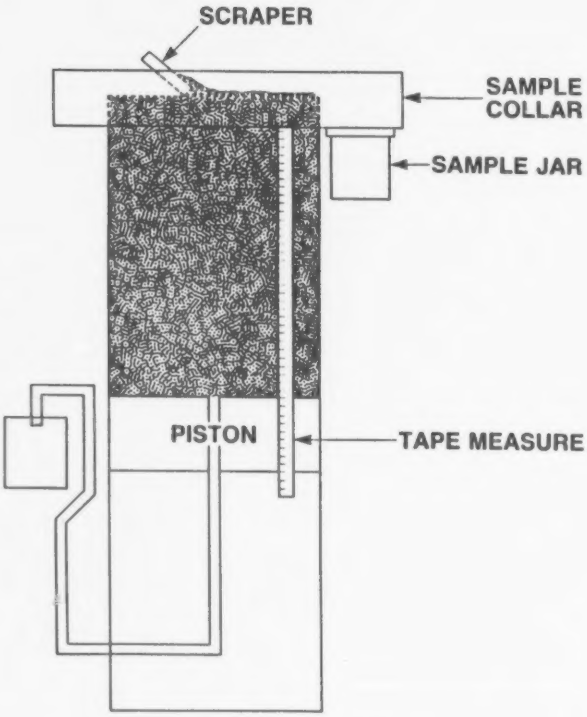
SCRAPER
SAMPLE COLLAR
SAMPLE JAR
PISTON
TAPE MEASURE

FIGURE 8 Sand Pack Raised to Top - 1 mm Slices Scraped Off With Sharp Knife

8. The oil in the sand slices was analyzed for its hydrocarbon content by toluene extraction using the Soxhlet apparatus (Figure 9) to provide a second measure of the total oil content in the sand. (The first measure being the total volume of oil added to the column during the experiment minus the oil removed in step 6.)

FIGURE 9 Soxhlet Extraction Apparatus

The oil used in this and all subsequent tests was unweathered "Norman Wells," light Arctic crude, chosen for its availability. (Table 1 presents the properties.)

Table 1

Properties of Unweathered Norman Wells Oil

Viscosities		(cps)	Flash Point °C	Pour Point °C	API Gravity @ 20°C API	Density
-10°C	0°C	15°C				
30	20	10	<-30	<-50	35-40	0.987

After running one preliminary test, two other tests were run with the following variations:

1. Test 2 sand pack was modified by replacing the wet drained sand above the water line with dry sand (Figure 10). This was used since sand in the CRI is dry. The sand depth was increased to 62 cm in order to observe any differences of a deeper sand pack.

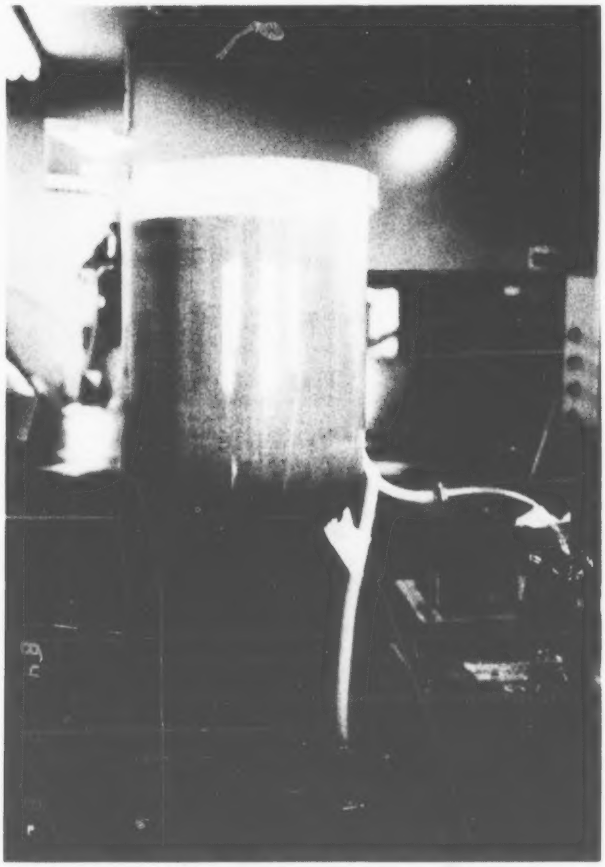

FIGURE 10 Cylinder Filled With Dry Sand Above Water Line

2. Test 3 sand pack depth was increased to 93 cm and air dried for four weeks using an electric fan to simulate atmospheric drying conditions at the CRI site. A 5 cm crust which formed on top was broken up and the sand pack was dried for an extra day.

3.0 OBSERVATIONS

Test 1

A total of 12.4 litres of oil was applied to the surface of the 49 cm sand pack over a period of 6 hours. The oil penetrated to a depth of 35 cm (Figure 11 shows the oil front). Initially, there were some air bubbles rising through the sand column and bubbling up through the oil reservoir. An additional 5 litres were applied and the sand pack was left to saturate to the maximum depth overnight. The next morning there was a total of 1.6 litres of oil on the sand surface and in the outlet reservoir, leaving a total of 10.8 litres of oil saturated in the sand pack.

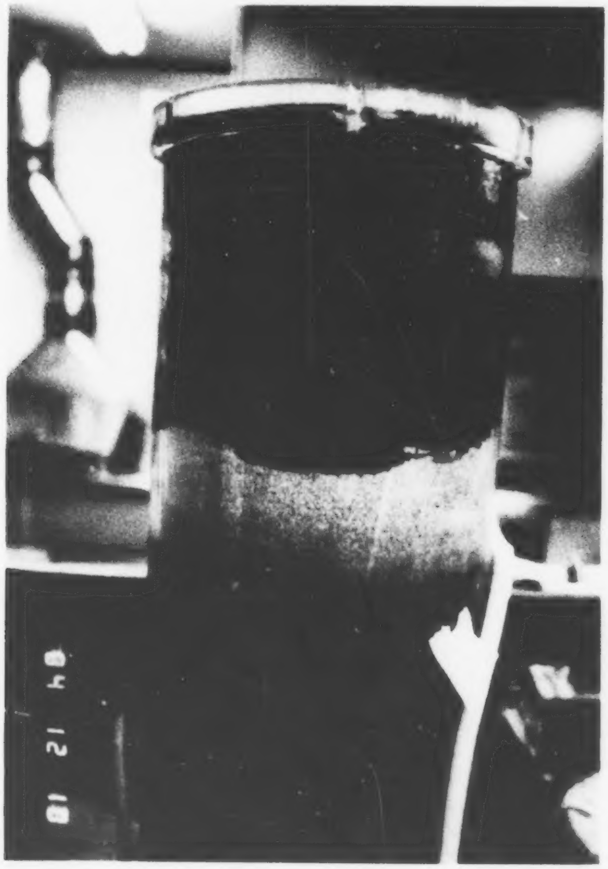

FIGURE 11 Penetration of Oil Front Through Dry Sand Pack Material

Test 2

Fifteen litres of oil were applied to the surface of the 62 cm sand pack over a period of 8.6 hours before oil was observed at the outlet reservoir. There were significantly more air bubbles rising through the sand column than in Test 1 because of the dry sand fill in the upper part of the sand column used in this test (Figure 12 shows air bubbles on the oil surface). One litre of oil was skimmed off the surface of the sand leaving 14 litres of oil in the sand pack.

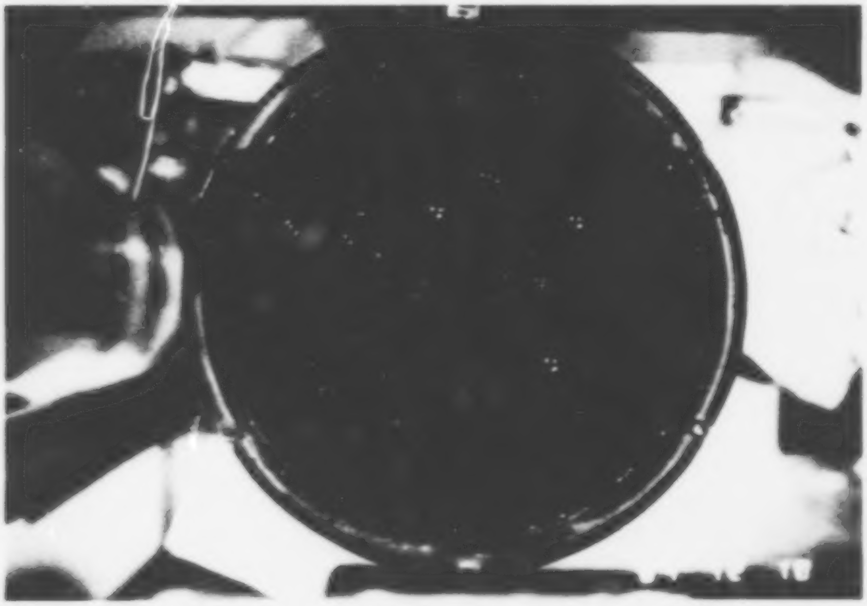

FIGURE 12 Air Bubbles Escaping From Sand Pack and Reaching the Oil surface

Test 3

A total of 29.9 litres of oil was applied to the 93 cm sand pack, 22.4 litres over a period of eleven hours and then an additional 7.5 litres were applied the following day, before oil was observed coming into the overflow reservoir. Two litres of oil were skimmed of the top leaving a total of 20.4 litres being saturated in the oil pack. Air bubbles were observed coming out of the sand column as in Test 2.

Figure 13 shows the oil front movement for the 3 tests.

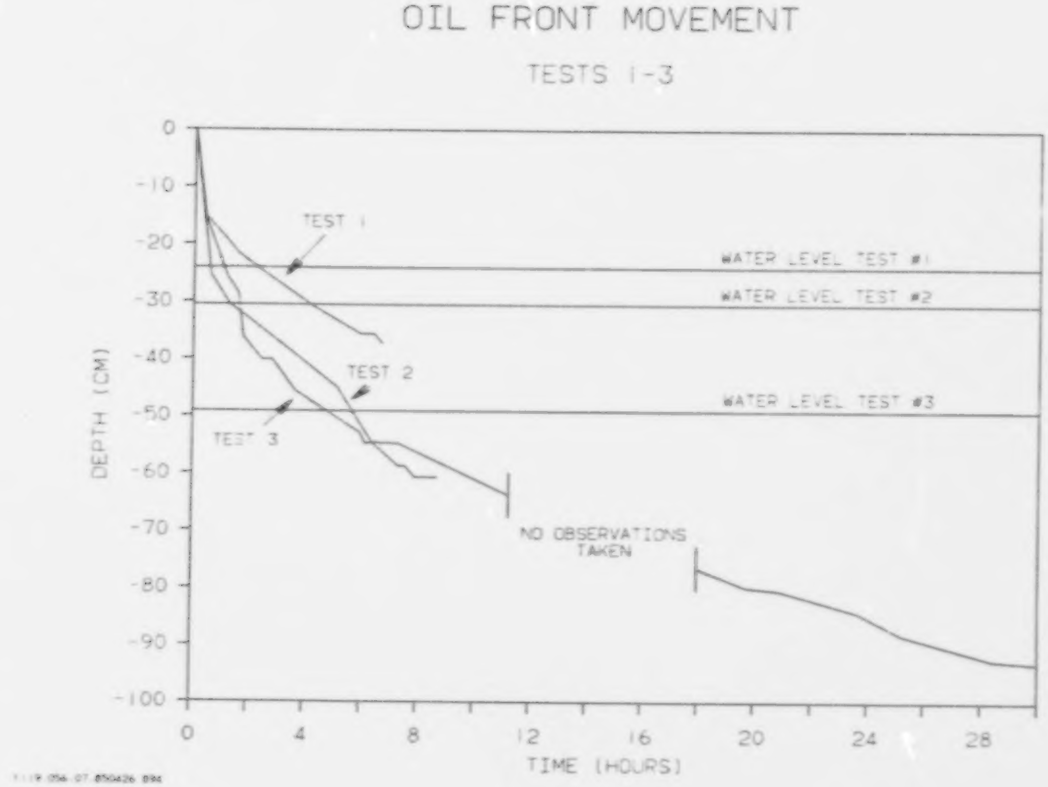

FIGURE 13 Oil Front Movement (Tests 1-3)

4.0 DISCUSSION

Saturation of Ukalerk Sand

The sand saturation, calculated using data from the sand slices analysed for their hydrocarbon content, varied from 26% to 32% of sand volume (Table 2). Based on the volume of oil applied the saturation was 4-6% higher then the volume of oil in the sand slices indicating evaporation of the oil from the reservoir on top of the sand pack. Norman Wells crude evaporates at an average rate of 1% per hour during the first 24 hours (Table 3).

TABLE 2
Sand Pack Saturation

Test No.	Oil Applied ℓ	Oil Applied % of Sand Volume	Sand Slices %
1	12.4	32	26
2	15.0	36	32
3	22.4	36	32

TABLE 3
Evaporation of Norman Wells Crude Oil

Beaker No.	Initial Weight of Oil GMS	Weight of Oil After 24 hours GMS	Weight Loss In 24 hours %	Weight Loss Per Hour %
1	81.4	58.4	28	1
2	81.9	57.1	30	1
3	82.0	57.4	30	1
4	81.9	57.1	30	1
5	81.9	57.4	30	1

Oil Penetration of Ukalerk Sand

The three tests performed had permeabilities varying from 3×10^{-3} to 9×10^{-3} cm/s (Table 4).

TABLE 4
Permeability Coefficients (k) and Oil Front Velocities

Test No.	Oil Front Movement cm	Time Hours	Permeability Coefficients cm/s	Oil Front Velocities cm/s
1	14	0.5*		0.007
	28	3.3*	0.006	0.002
	35	6.4*	0.004	0.002
2	5	0.1*		0.013
	20	0.7*		0.008
	28	1.4*		0.006
	40	2.8*		0.004
	53	6.0	0.007	0.002
	61	8.6	0.007	0.002
3	5	0.1*		0.025
	16	0.4*		0.011
	32	1.7*		0.005
	45	5.0	0.009	0.003
	56	8.1	0.008	0.002
	63	11.3	0.009	0.002
	84	23.8	0.005	0.001
	93	30.2	0.003	0.001

---

* Oil Displacing Trapped Air

The permeabilities in Table 4 are indicative of fine sand mixed with clay (Table 5) a characterization of soils described by Tschebotarioff (1973).

TABLE 5
Permeability Coefficient (k) of Different Soils (Lambe, 1951)

Permeability:	10+2	10	10-2	10-4	10-6	10-8 cm/s
Soil Type:	Gravel	Sand	Very fine sands and silts. Mixtures of both with clay			Clay

The coefficient of permeability k (cm/s) was computed using the equation in Lambe (1951, 1979). To convert from cm/s to Darcy multiply cm/s by 1.045×10^3.

$$k = 2.3\ aL/A(t1-t0)\ \log 10\ h0/h1$$

in which:
a = cross-sectional area of the standpipe,
L = length of soil sample in permeameter*,
A = cross-sectional area of the permeameter,
$t0$ = time when water in standpipe is at ho,
$t1$ = time when water in standpipe is at h1,
$h0, h1$ = the heads between which the permeability is determined.

For this experiment, the equation was simplified as follows; since $a = A$:

$$k = 2.3\ L/(t1 - t0)\ \log 10\ h0/h1$$

in which:
L = length of soil sample in cylinder
$t0$ = time when the oil in the cylinder is at h0
$t1$ = time when oil in the cylinder at h1
$h0, h1$ = the heads between which the permeability is determined (see Figure 14).

---

* Apparatus for determining permeability (Lambe, 1951, 1979)

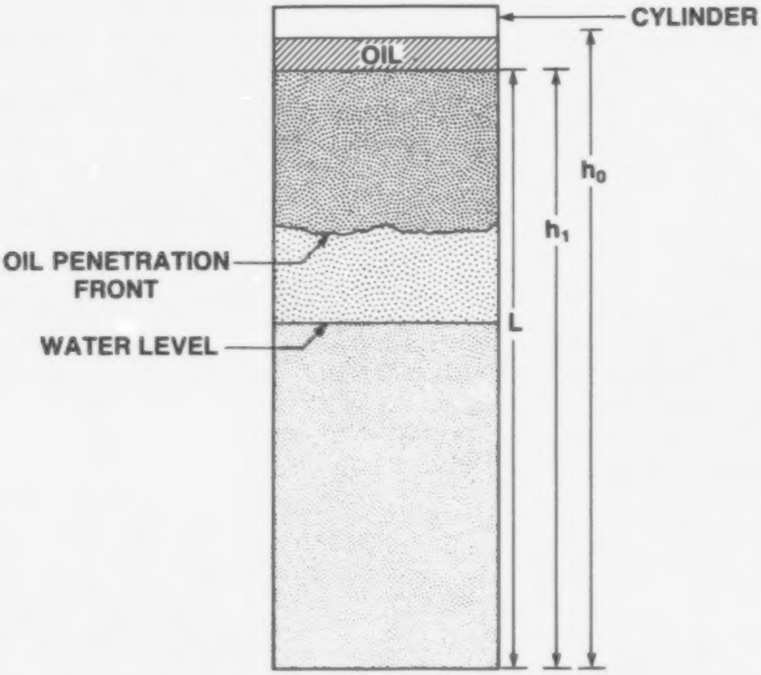
CYLINDER
OIL
h0
h1
L
OIL PENETRATION FRONT
WATER LEVEL

FIGURE 14 Modified Variable Head Permeability Test

The initial oil penetration front velocities when oil was moving through the dry sand pack displacing air varied from 0.008 to 0.025 cm/s. When the oil began to displace the water in the sand pack, there was a significant decrease in rate of oil front movement to as low as 0.001 m/s (Figure 15).

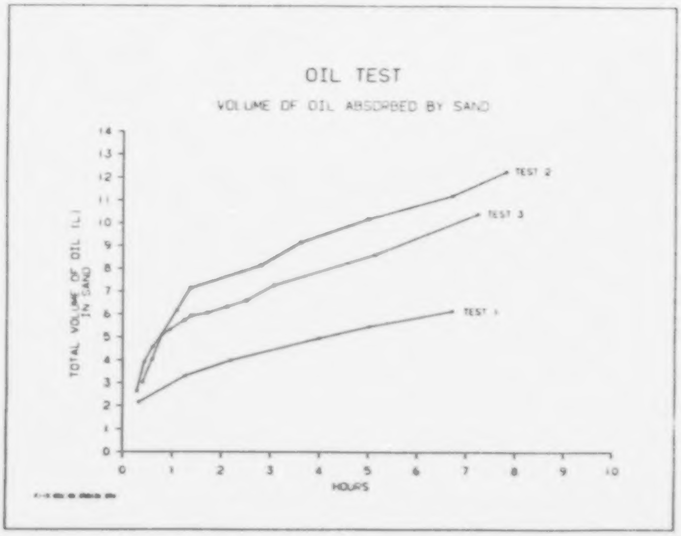

FIGURE 15 Volume of Oil Absorbed by Sand Pack Over Time

5.0 CONCLUSIONS

Based on a saturation of 26 to 32% the Ukalerk sand at the Amerk CRI site could hold from 5,000 to 6,200 m^3 of oil. At the lower and upper blowout rates of 200 to 800 m^3/day it would take 6.5 to 31 days to saturate the sand berm to the mean water level.

Acknowledgments

The authors would like to thank the Research Department of Esso Resources Canada Limited for the funding of this program. In particular, they would like to thank J.C. McDougall and Dr. R.H. Goodman for their continued support. They are also grateful for analysis work carried out by John Macleod, Analytical Chemistry, apparatus maintenance by the Machine Shop staff and typing by A. Kilpatrick.

References

1. PEABODY, C.H., HOLOBOFF, A.G., "Penetration of Oil Into Beach Sands" (1984). Calgary, Alberta.

2. LAMBE, T. William, "Soil Testing for Engineers" (1951). J. Wiley & Sons, Toronto, Ontario.

3. TSCHEBOTARIOFF, Gregory P., "Foundations, Retaining and Earth Structures" (1973). McGraw-Hill, Toronto, Ontario.

4. LAMBE, T. William, WHITMAN, Robert V., "Soil Mechanics, SI Version (1979). J. Wiley & Sons, Toronto, Ontario.

A NOVEL INTERACTIVE OIL SPILL MODEL

David G. Wilson and **Donald Mackay**
University of Toronto
Toronto, Ontario

INTRODUCTION:

The past two decades have seen heightened concern for our environment and for the effects of oil spills on it. This awareness and concern, brought about, in part, by a number of oil spill disasters, has resulted in a new wave of scientific and technical thought. Not only is the production of petroleum resources accepted as important but their safe transport, disposal and utilization is also seen to be essential. Consequently, the prevention, and prediction of the behaviour of oil spills has come to the forefront of chemical technology. In turn, the development and deployment of computer models in order to predict the behaviour of oil spills, and hence facilitate assessment of effects, recovery or countermeasures has been of growing importance.

Early spill models were simple and consisted largely of algebraic or simple ordered differential equations for such phenomena as flow, evaporation, diffusion or spreading. While these models were useful as approximations of oil behaviour they were found to be lacking in terms of actual applicability to real spill scenarios. The main shortcomings of such models were their inability to account for significant variations in environmental conditions. Also, the early models usually treated only a few of the many physical and chemical phenomena that an oil spill experiences. Hence, they suffered from the very feature that was intended to be their strength; simplicity. Their ease in formulation, comprehension and use was offset by their lack of accuracy in predicting spill behaviour as well as their inability to account for dynamic environmental conditions.

The early models, while not entirely satisfactory, were successful in initiating the well thought out modelling of oil spills and effectively laid the groundwork for later, more complicated models. This second wave of models attempted to overcome the problems inherent in the simple models. Large quantities of environmental and geographical data were combined with complex analytical and numerical techniques for predicting chemical behaviour. However, while the simple models were too general to predict spill behaviour accurately, the complex models were either too site-specific or too situation-specific. Also, even if a spill scenario specific to a particular model occured, the model itself would often be far too complex to permit its rapid and efficient use. While many of the analytical techniques used in such models were quite innovative and perceptive, it was often only the designer of such a model who was capable of using them. Although these complex models overcame the gross oversimplifications of their predecessors they still, for the most part, were rarely able to cope with dynamic environmental conditions. Hence, this capability remains as one of the most important facets of any model of oil spill behaviour. Further, the models often suffered from an inability to be updated while running to include available information about present conditions.

Thus, the further development of oil spill modelling is limited by the extremes of oversimplicity or overcomplexity. The lesson to be learned from the previous work on models is that the key to a successful model lies in how easily and how often it can be used. That is, the ideal model must be simple enough that any number of people can use it effectively and efficiently for a large number of spill situations, encompassing changes in spill as well as environmental status over the course of the lifetime of the spill. One proposed solution is the expert system similar to those that have been implemented for diagnosis of diseases or location of mineral resources (Van Horn 1986). The ideal expert system would require a massive data base describing the likely behaviour of any chemical under any environmental condition in any location. Such a system would interact with the user who would input all available spill and environmental data. The expert system would be programmed to predict spill behaviour based on available input and then specify further data requirements necessary to refine its prediction. The advantage of an expert system over a knowledge based system is that the expert system weighs the relative merits of a number of possible correct solutions and provides a level of accuracy for each solution. In addition a true expert system "learns" from previous decisions it has had to make. A purely knowledge based system requires a match of inputted data with the data or scenarios programmed into the system and is incapable of making a prediction based on an incomplete set of data. However, a complete expert system requires prohibitively large quantities of computer storage space, time and money to develop. Many of the expert systems presently in use in other fields have cost millions of dollars and have required many years to develop. There is also the added drawback that there are a limited number of computers that would be capable of running such a complicated program.

A compelling case can, however, be made for developing a hybrid of traditional and expert systems that contains many of its advantages while avoiding some of the major difficulties inherent in an expert system, namely the unwieldy nature of such a model and the difficulty in developing it. This "new generation" of chemical and oil spill model could be run on a small personal computer and would be user interactive. It would consist of a number of spill descriptors or characteristics such as spill area and thickness as well as physical/chemical characteristics such as density, viscosity or solubility. In addition, the model would also include the relevant spill processes or events and their respective governing equations. This would include such processes as evaporation, spreading or dissolution. Hence, by the co-ordination of spill descriptions with the particular spill processes that affect them, an oil spill and the changes that it undergoes may be modelled. By allowing the user to choose which processes to consider, and by updating the status of the spill over time, the model becomes dynamic and thorough without loss of ease of use.

In this paper such a model is developed. "ATOM" is An Interactive Time-segmented Oilspill Model which combines the features of ease of use, computing power, a knowledge base, user interaction and simple governing equations. By relying on established models and correlations combined with user interaction capability ATOM provides a comprehensive and flexible treatment of oil spill behaviour as well as the capability to accept data from many competing and interacting, and as yet poorly quantified, processes.

Literature Review:

There have been a large number of oil spill behaviour models produced during the past two decades. Mackay (1984) provided a review of oil spill models and commented on some of their strengths and weaknesses. The majority of models apply only to specific processes, locations or oils, however a number of comprehensive oil spill models have been produced, a number of which are of interest.

Mackay et al (1982) produced an Arctic marine oil spill model that treats the evaporation, dispersion, emulsification, drift and spreading of a number of oils. Payne and Kirstein (1984) produced a similar model which treats the same spill processsess. However, while the Mackay model considered the oil as a whole, the Payne model used a TBP (true boiling point) separation of the oil into a number of components for which average properties were assigned. Further, the Payne model is user interactive, allowing the user to input important environmental and spill data.

Both the Mackay and Payne models have the benefit of ease of use and utilization of simple sub-models. Also, by use of the TBP separation of the oil the Payne model is able to predict compositional changes in the oil. However, neither model considers such important processes as shoreline and grease ice interaction. Page and Stamps (1987) developed a computer oil spill model that considers tidal currents, wind induced motion, dispersion, evaporation, diffusion and beaching. While this model is quite comprehensive it does not allow the user to update oil properties if the model predictions contradict actual observations.

Hence, the models mentioned are illustrative of the vast array of oil spill models in existence in that while all of the models have their own particular strengths they fail to address a complete range of spill processess, properties and user interactions simulataneously. This problem is derived from the approach of these models in which the simpler processes can be written as differential equations and solved analytically or numerically. The models also allow the inclusion of a few processes simultaneously.

But as knowledge of oil spill behaviour increases it is desirable to include processes which cannot easily be described by differential equations. Processes such as interaction with ice and shorelines and changes in the oil regime due to interfacial tension variations fall into this category. There is also a need to update and correct the model and allow for changes in environmental factors such as wind velocity or water temperature. Consequently, the solution of such a system of differential equations becomes prohibitively complex.

Thus, a new approach is needed which tolerates some loss in model accuracy in order to allow the inclusion of more processes using the intuitive capabilities of the user.

Basic Theory and Structure:

The focal point of this model is its usage of a time segmented basis which allows the user to specify the relevant environmental conditions and physical/chemical processes applicable to the spill. The model utilizes a "compartmentalized" approach which allows for simple but comprehensive coverage of spill behaviour. By allowing for simple sub-models or governing equations for each spill process the user can treat each process independently. Because the program is user interactive on a time segment basis, the user may update spill conditions after each specified time segment and hence, in effect, monitor the spill's dynamic behaviour. In addition this model may also be adapted to accept a more complex model for any particular process compartment should such a site or situation specific model exist. Such flexibility allows the model itself to improve in the future.

The ATOM model operates on a simple mass balance basis. The oil spilled has defined physical and chemical properties such as density, viscosity, vapour pressure and solubility. Physical features of the spill such as spill volume, area, thickness, mass and location are also defined. Such properties are the descriptors of the spill itself. An oil spill which is a mixture of pure components has each component treated separately with regard to the above properties but combined together in the appropriate manner to provide overall or average properties for the spill.

A list of processes or phenomena which could affect the descriptors is also assembled. Processes such as evaporation, spreading, biodegradation, dissolution, emulsification, drifting or interaction with shorelines or ice, are considered with regard to the descriptors affected. In turn, each process's effect on each descriptor is represented by a governing equation. In most cases the effect of a certain process on a certain descriptor may be calculated with a simple algebraic expression and many of the processes have no effect on some of the descriptors. For example the evaporation equation affects volume but not area. Spreading affects area but not volume. Hence, the model requires governing equations to treat only the process/descriptor combinations that are relevant to the successful and accurate modelling of the oil spill.

Initially, the program requests the necessary spill information and oil data as well as environmental conditions. The program also requests the user to input the magnitude of time segments to be considered as well as which processes are to be considered. For each process additional information may be requested in order to satisfy its governing equation. For example, if the spreading and drifting processes were to be considered, the program would request information on wind and water current velocities. Similarly, for evaporation the program would require specific wind and temperature conditions in that area. The program then calculates the effect of the designated processes over the alotted time segment, updates the values of the relevant descriptors and performs a mass balance on the oil. New values for the oil descriptors are calculated and are assigned to the spill. The program then asks which processes are to be considered for the next time segment, including any new processes to be considered or any to be neglected. There is a possibility that some of the calculated values for each descriptor may be contradicted by actual observations of the spill at any time during the spill. Consequently, after each time segment, the program will request any changes in any descriptors to be inputted so as to allow their adjustment to agree with actual observations.

Thus, by choice of an appropriate time increment, the spill may be monitored and modelled even as the characteristics of the spill change. However, it may be desirable to guide the user who may lack knowledge of what processes are likely to occur in different spill situations. Hence, before the calculations for each time segment are performed the program considers the available information on the nature of the oil and the spill itself. By use of criterion built into the program the model is able to suggest which processes are likely to be the most important and which are not likely to be a factor. This still allows the user to include a process, which was initially neglected, at a later time should it eventually become important. It is also possible that the user may lack knowledge of what an appropriate length for a time segment may be. To aid the user the model is programmed to recognize that certain processes tend to occur more rapidly than others. For example, if an oil is very volatile then evaporation would tend to occur very rapidly although other processes such as biodegradation may occur much more slowly. By calculating appropriate time segments for each process the model requires only that the user identify which processes he wishes to consider. The program is then able to recommend the shortest approximate time segment from the processes being considered.

The individual process equations are assumed to be independent. Each process equation is a simple first order differential equation and is solved independently. Its effect on the oil spill is quantified before the next process equation is considered. Small time increments and an ordered heirarchy of processes are used to reduce inaccuracies resulting from this approach. For example, by considering natural dispersion before evaporation the oil that is entrained below the water surface is not considered in the evaporation equation. This reflects the real spill situation. The treatment of each process with a simple, independent, first order differential equation allows for rapid calculations and avoids a complicated numerical methods solution. A sample program menu is illustrated in Figure 1.

8.3 Oil Descriptors:

As previously discussed, in order to ascertain the status or condition of the oil at any given time it is necessary to consider a set of descriptors of the spill. The descriptors have been chosen on the basis of their importance to the user or to spill behaviour and their ability to be correlated to basic physical and chemical properties of the oil. Also of importance is the relative ease and accuracy in calculating the changes in these descriptors as a result of influence from spill processes. Use of the "matrix approach" allows each component of the oil to be treated separately as a pure component. Proper combination of the components allows for average descriptors for the oil to be calculated.

The descriptors used in "ATOM" are:

PRIMARY	SECONDARY	AUXILIARY
Volume	Density	Area
Mass	Vapour Pressure	Thickness
Mass Fraction	Solubility	% Emulsion
No. of Moles	Molar Volume	Emulsion Volume
	Viscosity	Spill Rate
	Molecular Weight	Volume on Shore
		Volume Dispersed
		Volume in Ice
		Emulsion Density
		Emulsion Viscosity

```
DO YOU WISH TO ENTER OIL COMPOSITION (Y or N)? N

OILS AVAILABLE IN PROGRAM LIBRARY ARE [1] DIESEL FUEL
                                      [2] NORMAN WELLS
                                      [3] .......

CHOOSE OIL MOST SIMILAR TO ACTUAL SPILLED OIL (BY #)   1


ENTER VOLUME OF OIL SPILLED (in m^3), AND RATE OF SPILLAGE (in m^3/hr, enter 0
for rate of spill if it is not a continuous spill) [_,_]  1000,20

ENTER WATER TEMPERATURE (Deg C) AND WIND SPEED (km/hr)   3,10

IS WATER SALT OR FRESH (LAKE,RIVER,ICE RUNOFF ETC.)(S or F) ? S

                  [Calculating initial properties.  Please Wait]



  DO YOU WISH TO ENTER INITIAL SLICK AREA (Y or N)? N

THE ENVIRONMENTAL PROCESSES WHICH MAY AFFECT THE SPILL ARE:
--------------------------------------------------------------
1) BIODEGRADATION     (B)           6) EMULSIFICATION       (EM)
2) DISSOLUTION        (DS)          7) COUNTERMEASURES      (CM)
3) WAVE DISPERSION    (DP)          8) GREASE ICE EFFECTS   (IC)
4) SHORELINE EFFECTS  (SL)          9) SPREADING            (SP)
5) EVAPORATION        (E)          10) DRIFT                (DR)

PROGRAM RECOMMENDS THAT THE FOLLOWING PROCESSESS BE CONSIDERED
--------------------------------------------------------------
EVAPORATION     SPREADING       DRIFTING

[COUNTERMEASURES: only while countermeasure in progress, GREASE ICE EFFECTS: if
oil has entered heavybrash and grease ice, SHORE EFFECTS: after oil is on shore

PROGRAM RECOMMENDS THAT THE FOLLOWING PROCESS(ES) BE DISCONTINUED:
-----------------------------------------------------------------

CHOOSE APPROPRIATE PROCESSES IN GIVEN ORDER [1-10], BY INITIAL (eg DS)

CHOOSE PROCESS(ES) YOU WISH TO CONSIDER (one at a time, 0 when finished)
```

Figure 1   Initial Sample Menu for ATOM Program

Initial volume and spill rate are user inputs at the beginning of the program. The user may also input the mass fractions for each of the individual components of the oil or refer to the program library in which the mass fraction distributions for a number of oils are contained. The initial volume is converted to an initial mass using an average oil density (obtained by correlation). The mass fraction distribution is then multiplied by the overall mass of the oil to obtain masses for each element or component. The individual masses are converted to individual volumes and moles using the density and molecular weight for each component (obtained by correlation).

Secondary descriptors are obtained by correlations to oil component carbon number, structural class and environmental temperature.

The auxiliary descriptors are so named because of their derivation from the primary and secondary descriptors.

The model allows user interaction to alter primary descriptors or auxiliary descriptors after each time segment. The secondary descriptors pertain to the individual "pure" components and hence are constant. However, changes in the primary or auxiliary descriptors may alter the distribution of components and hence change the average values for the secondary descriptors and therefore for the oil itself.

In addition environmental factors such as temperature wind and oceanic conditions are requested.

Model Equations:

The ability of "ATOM" to model oil spill behaviour accurately is dependent upon the accuracy of the individual process equations. As already indicated it is not desirable to have governing equations that are too site or situation specific, nor is it desirable to have equations that are so general that they provide very little indication of the true behaviour of the spill. This stipulation makes the choice of governing equations somewhat subjective. However, the nature of this model, which is to allow for replacement of governing equations or submodels as superior ones are developed, provides flexibility in choice of governing equations as well as the opportunity for model improvement. Figure 2 illustrates some of the possible spill processes and the spill characteristics they are likely to affect.

The governing equations are simple algebraic equations and are solved independently in the model. However, the use of time segments of variable length over which each equation is solved provides a good approximation of the interaction between spill processes over the duration of the spill.

A number of governing equations and submodels have been compiled and may be considered to be a satisfactory initial skeleton framework for the model. It is expected that better equations and submodels will be proposed which may be superior in given locations or situations.

MODEL EVENTS

	SPILL PROCESSES									
SPILL DESCRIPTORS	EVAPORATION	DISSOLUTION	BIODEGRADATION	DISPERSION	EMULSIFICATION	SHORELINES	GREASE ICE	DRIFTING	SPREADING	COUNTERMEASURES
Volume	*	*	*	*	*	*	*			*
Mass	*	*	*	*	*	*	*			*
Mass Fraction	*	*	*	*	*	*	*			*
No. of Moles	*	*	*	*	*	*	*			*
Density	*	*	*		*					
Vapour Press.	*	*	*							
Solubility	*	*	*							
Molar Volume	*	*	*							
Viscosity	*	*	*		*					
Molecular Wt.	*	*	*		*					
Area									*	
Thickness	*	*	*	*		*	*		*	*
Spill Rate										*

Figure 2 Table of Spill Processes and Descriptors Showing Dependence of Spill Descriptors on Spill Processes

Model Knowledge Base:

An important aspect of "ATOM" is the ability of the program to function as a knowledge base by advising the user which processess and time segments should be chosen. The knowledge base is divided into three distinct sections. The ability to advise which processes should be considered, the ability to advise which processes should be discontinued and the ability to advise on the size of the time segment required comprise the knowledge base.

In order to advise the user on choice of spill processes the program relies on knowledge of environmental conditions as well as knowledge of the nature of the spill processes. Because of its importance as an oil removal process, consideration of evaporation is always advised at the onset of a spill. Similarly, because of the importance of spill area in determining the effects of spill processes such as evaporation, spreading is always advised to be a process choice in the program. If the spill is continuous then it is especially important that spreading be an advised choice throughout the duration of the program. Conversely, biodegradation and dissolution typically remove so little of the spill that they are never advised as process choices.

Although the program will advise which processes should be considered, based on various criteria, the user is free to choose any processes he desires. Hence, the ability of the program to advise which processes should be discontinued is of equal importance. The basic criterion for discontinuation of a process is a 5% removal criterion. That is, if a spill process fails to remove more than five percent of the spill in a 24 hour period then the program will advise its discontinuation. This feature allows the user to disregard a previously considered process and thus hasten execution of the program for the following time segment. The five percent criterion has been chosen arbitrarily as the minimum level of significant removal of oil.

Recommendations regarding choice of time segments are facilitated by assigning "characteristic times" to each of the spill processess. A characteristic time represents the period of time required for a significant change in oil properties (volume or composition) to occur as a result of that particular process. Arbitrarily, a five percent change in oil volume has been assigned as the measure of the change which a characteristic time represents. After the user has choosen the processes he wishes to consider as well as inputted all relevant environmental information then the characteristic times for each process are compared by the program and the shortest time is recommended to the user. The recommended time will help a user to gain an idea of the approximate appropriate time frame that should be considered to maximize the accuracy of the model. It is likely that the user will have, from his own observations and model output, the ability to judge the size of future time segments more accurately than the program and hence the advice of the program should only serve as a guide or as an alternative to tedious deliberations over the subject.

Discussion:

Although the ATOM spill model has the great advantages of simplicity and the capability to interact with the user, its greatest asset may be its own adaptability and flexibility. While conventional models immediately begin to be outdated upon their very completion this new form of spill model can evolve with changing modelling techniques. That is, the "modular" form of this type of model allows for any of the governing equations or submodels to be replaced by more accurate or convenient governing equations or submodels, as they are developed. This is the same mechanism that permits the incorporation of site or situation specific submodels in the present form of the model where appropriate. This feature is valuable since there may be processes, so far considered irrelevant, or new artificial processes, spawned by technological breakthroughs, which it may be desirable to include in the model in the future. This form of model has the advantage that it acknowledges and accommodates the dynamic nature of modelling by allowing for such improvements or alterations in the model itself.

Thus, the distinguishing feature of this model is that rather than relying on new analytical techniques or computer programming methods, it provides a skeleton or framework for existing submodels or governing equations as well as future submodels or processes. It is simple yet comprehensive and adaptable to more complicated submodels.

8.8 Conclusions:

In conclusion, while ATOM, in its present state of development, relies on general correlations and contains some simplifications of physical and chemical processes it provides a method and framework for the creation of a simple, comprehensive model for oil spills. This model has the capability to interact with the user to follow the dynamic nature of a spill. By allowing for user input to update or correct spill descriptors and processes, at different times during the spill, the overall accuracy of the model is improved. The structure of ATOM also allows for improvement of the model through the addition of new or improved submodels, governing equations or chemical properties.

Validation of the spill model using the Amoco Cadiz spill as an example demonstrates that ATOM is capable of providing an acceptable approximation of the fate of an oil spilled under dynamic environmental conditions.

REFERENCES

Mackay, D., Buist, I., Mascarenhas, R., Paterson, S., Oil Spill Processes and Models, Research and Development Div., Environmental Emergency Branch, Environmental Impact Control Directorate, Environmental Protection Service, Environment Canada, Ottawa, Canada, Report EE-8, (1980)

Mackay, D., Shiu, W.Y., Hossain, K., Stiver, W., McCurdy, D., Paterson, S., Tebeau, P.A., Development and Calibration of An Oil Spill Behaviour Model, Department of Chemical Engineering and Applied Chemistry, University of Toronto, Toronto, Ont., Report prepared for U.S. Department of Transportation, United States Coast Gaurd, Sept. (1982)

Mackay, D., Uses and Abuses of Oil Spill Models, Institute for Environmental Studies, University of Toronto, Toronto, Proceedings 7th Arctic Marine Oil Spill Program Technical Seminar, June 12-14,(1984), Edmonton, Alta.

NOAA/EPA, The Amoco Cadiz Oil Spill, U.S. Dept. of Commerce, U.S. Govt. Printing Office, Washington, D.C., April (1978)

Payne, J.R., Kirstein, B.E., Oil Weathering on Open Ocean Computer Model, Environmental Assessment of The Alaskan Continental Shelf, U.S. Dept. of Commerce, Juneau, Alaska, Vol. 22, February (1984)

Payne, J.R., McNabb, D., Kirstein, B.E., Redding, R., Lambach, J.L., Phillips, C.R., Hachmeister, L.E., Martin, S., Development of a Predictive Model for the Weathering of Oil In The Presence of Sea Ice, Applied Environmental Science Division, JRB Associates, Science Applications International Corp., La Jolla, Cal., November, (1984)

Van Horn,M., The Waite Group, Understanding Expert Systems, Bantam Books Inc., New York, (1986)

ENVIRONMENTAL EFFECTS OF OIL SPILL COMBUSTION

D. Evans, G Mulholland, D. Gross, and H. Baum
Center for Fire Research, U.S. National Bureau of Standards
Gaithersburg, Maryland 20899

and

K. Saito
Department of Mechanical Engineering, University of Kentucky
Lexington, Kentucky 40506

ABSTRACT

Experimentation and analysis have been performed to quantify the combustion of crude oil on water. The burning behavior of three crude oils -- ALBERTA SWEET, LA ROSA, and MURBAN, were studied using 1.2 m diameter pool burns. In smaller 0.6 m diameter pool fires using ALBERTA SWEET, combustion products were collected for extensive chemical analysis. This analysis showed that about 10% of the crude oil was converted to smoke in the combustion process. The CO concentration was a factor of 25 lower than the primary gaseous product CO_2, and the emission of NO and NO_x were less than one thousandth the concentration of CO_2. The PAH content of the smoke was enriched in the larger molecular weight species in comparison with the original fuel. A methodology was developed with which the down wind dispersal of smoke generated by one or more oil spill fires in close proximity may be predicted. Initial results that demonstrate the capability of the analysis are presented.

BACKGROUND

In 1985, the Center for Fire Research (CFR) at the U.S. National Bureau of Standards (NBS) began studies of oil spill combustion under support from the Minerals Management Service (MMS) of the U.S. Department of the Interior. This work seeks to quantify the processes involved in oil spill combustion on open waters and in water filled channels formed in broken ice including measurements of smoke production and prediction of smoke dispersal. Added support from the U.S. Coast Guard and Environment Canada has allowed the study to be broadened in scope and increased in detail.

The long range goal of the research program is to provide measurements and means to make quantitative predictions of (a) the fraction of oil in a spill that can be consumed by an in-situ combustion process, (b) the characteristics of the residual oil, and (c) the characteristics of the combustion product flow from the burning oil. It is hoped that this information may be cast into a form that is usable by local officials and oil spill response professionals as part of the decision making process in the event of an oil spill.

Last year's study included results from experiments to quantify the burning of 0.60 m diameter oil pool fires. Measurements of burning rate, thermal radiation emission, smoke production and the chemical composition of both the oil and the burn residue were reported [1]. Calculations were performed to estimate the surface wind velocities that could be generated by multiple fires distributed over a large area as might be expected during the burning of an oil pool confined by broken ice in the arctic. This year's effort is the first in a two year program to quantify (a) the thermal properties and burning characteristics of the crude oil, (b) the physical and chemical properties of the smoke generated in the combustion process, and (c) the expected dispersal of the soot through the atmosphere and deposition down wind of the oil fires. This report summarizes results from these three main research thrusts all of which are at the mid-point of the two year effort.

EXPERIMENTAL FACILITIES

Crude oil burn tests were conducted in the CFR large-scale test building using both the large and small calorimeter hoods. The small hood facility could accommodate oil pool fires up to 0.6 m in diameter. This hood was used to collect all smoke and gas samples for quantitative analysis. Details of this experimental gas and soot sampling installation were reported previously [1]. A new controlled dilution probe, shown in Figure 1, was added to the exhaust stack of the small calorimeter hood for the present studies. This probe is used to cool and dilute the gas sampled from the stack by adding a mass flow of chilled air approximately twice the mass flow of the combustion products sampled. With the addition of this probe to the existing system two sampling conditions for the soot could be examined. The previous system maintained the gas sample at the nominal 100 °C from the stack to the filters where soot samples were deposited. The new system cools and dilutes the sample such that at the filters the temperature is within 2 °C of ambient temperature.

For larger test burns, a steel pan measuring 1.20 m in diameter and 0.30 m in height was installed under the large calorimeter hood, as shown in Figure 2. The pan was elevated 0.6 m above the platform floor by means of blocks to allow for the introduction of instrumentation and for supply and drainage of water through the bottom of the pan. A predetermined quantity of oil was floated on the water surface the level of which could be controlled to maintain a burning surface 10 mm to 12 mm below the pan rim. Perforated steel plates were arranged to form an artificial "floor" at the level of the pan rim. This was intended to limit, but not to completely exclude, air supply from below the pan rim, and also to allow for liquid spillover during test periods where energetic boiling was expected to occur based on results of previous smaller scale burns [1]. An annular trough containing a layer of moist sand was located around the pan below the perforated plates to contain any spillover or splattered droplets of burning oil. Sorbent pads of oleophilic polypropylene fiber were used to adsorb the oil remaining on the water surface after each test in order to determine the weight of the residue.

Instrumentation was provided for the measurement of flame temperature; oil and water temperature; energy release rate; radiation feedback from the flames to the liquid surface; and radiation from the flames to the surrounding. Placement of this instrumentation is shown in Figure 2. All thermocouples were of the metallic-sheathed, mineral-insulated type. Two specially-designed thermocouple rakes were commercially fabricated and were mounted to provide temperature measurement along two vertical axes which included the entire oil layer depth plus positions in the fuel-rich air above the oil and in the water. As shown in Figure 3, each thermocouple rake consisted of 13 thermocouples the top seven of which were spaced at 1.5 mm separation. At the lower positions that extended to 76.2 mm below the top thermocouple, spacing was gradually increased to 3.1 mm, 6.3 mm, 12.7 mm, and 25.4 mm. The in-pool radiometers were commercially fabricated instruments of

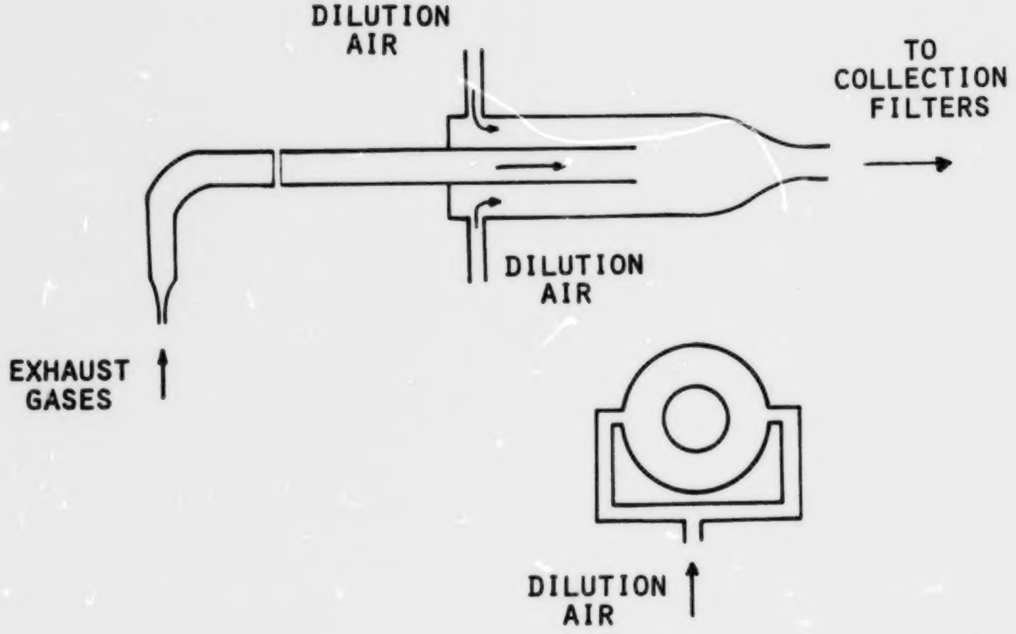
DILUTION
AIR
TO
COLLECTION
FILTERS
DILUTION
AIR
EXHAUST
GASES
DILUTION
AIR

FIGURE 1. SCHEMATIC OF SMOKE DILUTION SYSTEM.

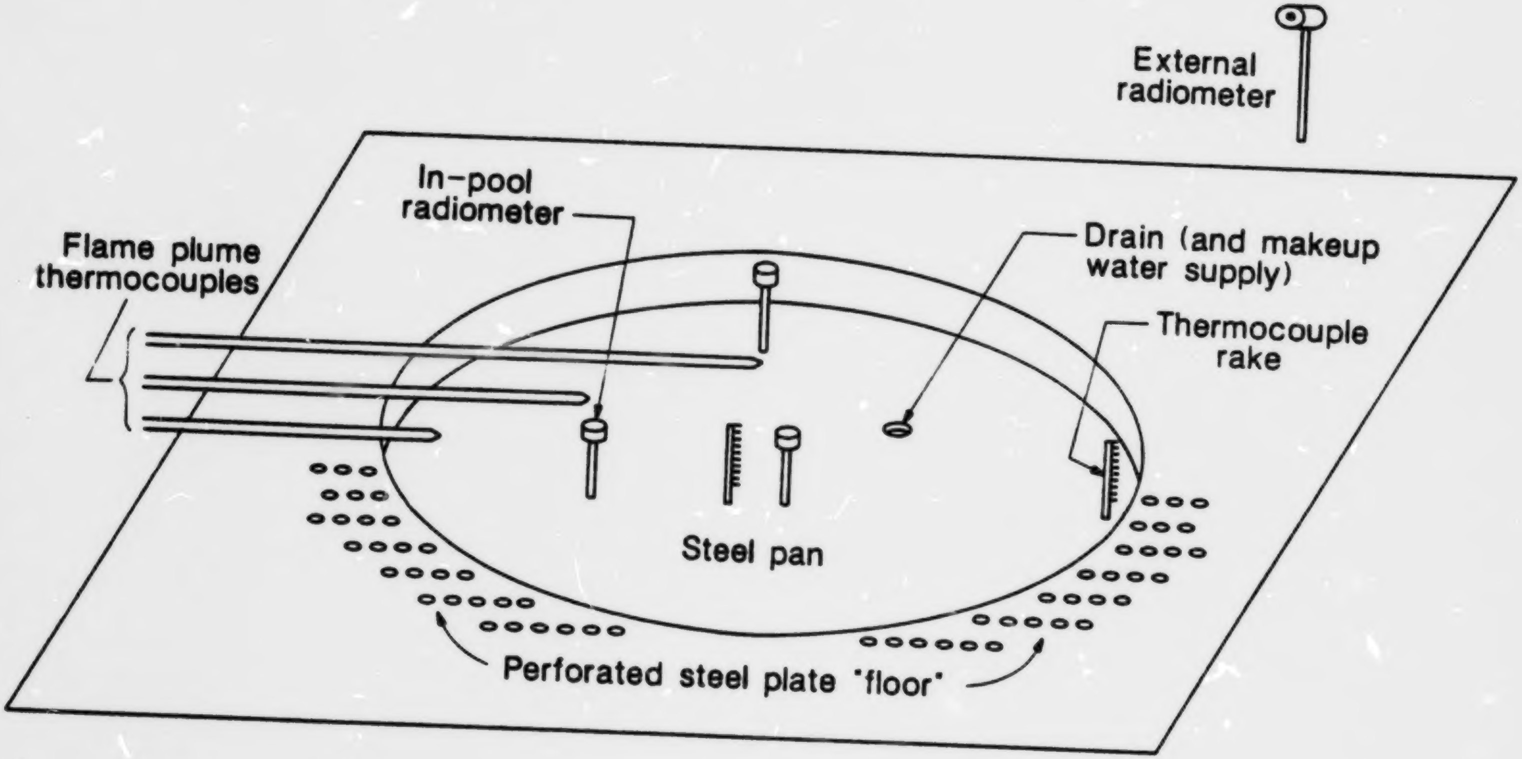
External radiometer
In-pool radiometer
Flame plume thermocouples
Drain (and makeup water supply)
Thermocouple rake
Steel pan
Perforated steel plate 'floor'

FIGURE 2. DIAGRAMMATIC SKETCH OF EXPERIMENTAL ARRANGEMENT.

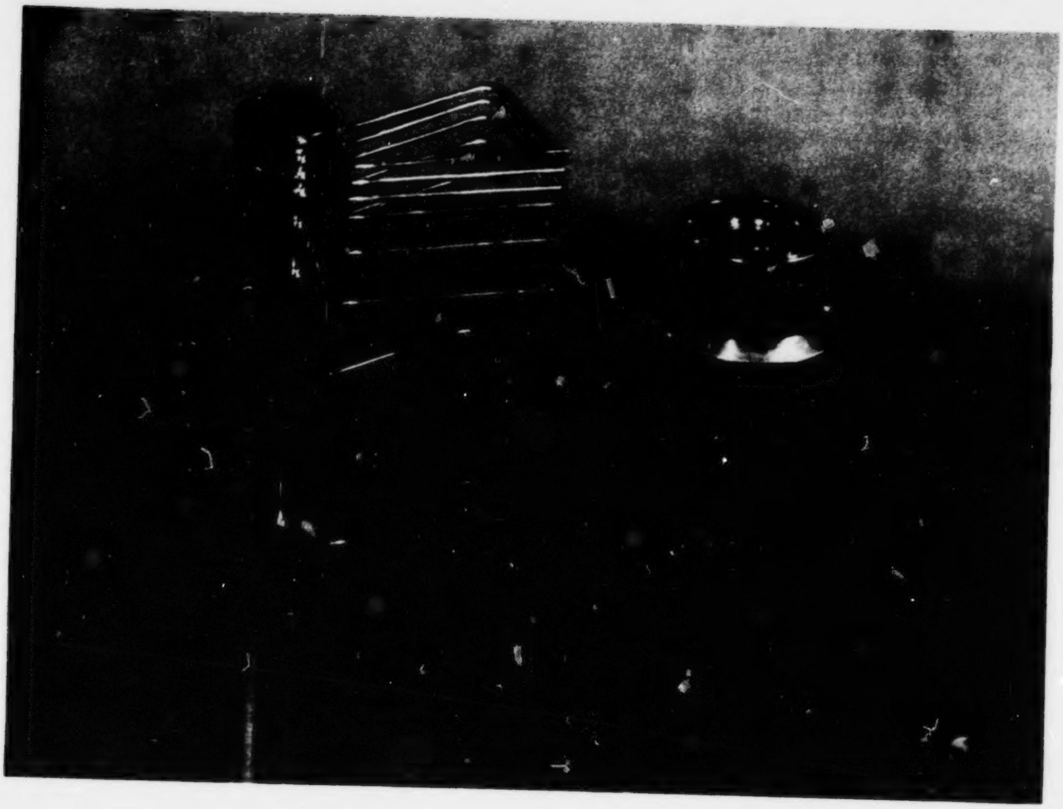

FIGURE 3. THERMOCOUPLE RAKE FOR MEASUREMENT OF OIL-WATER LAYER TEMPERATURE.

the Schmidt-Boelter type, provided with Irtran windows and nitrogen gas purging as well as water cooling. They were positioned approximately 25 mm above the oil surface facing up at the center, at a quarter-point, and near the rim of the pan.

The energy release rate of the fires burned under this hood are determined using the oxygen consumption calorimeter technique. The energy release rate is calculated from measured decreases in oxygen concentration in the total flow of gases through the stack [2].

CRUDE OIL MATERIALS

The burning characteristics of three types of crude oils were investigated in the large calorimeter -- ALBERTA SWEET, LA ROSA and MURBAN. These oils were obtained from supplies at the EPA-OHMSETT facility in New Jersey. According to available oil property information [3], reproduced in Table 1, these oils differ in composition, notably in the percent of the heavier wax plus asphaltene fractions, with ALBERTA SWEET crude being the lowest and LA ROSA crude being the highest.

TABLE 1
PROPERTIES OF OILS (TYPICAL DATA)

CRUDE OIL	DENSITY kg/m^3	PERCENTAGE BY WEIGHT			
		PARAFFINS	AROMATICS	WAX	ASPHALTENES
ALBERTA SWEET *	839	84.4	12.8		1.8
LA ROSA	911	66.1	23.2	9.9	6.2
MURBAN	824	81.4	16.6	5.7	0.8

---

* Composition analysis provided by Environment Canada

Important thermal characteristics of the crude oils used in this study are being measured. The thermal conductivity of each oil was measured using the transient hot-wire method [4]. In this method the thermal conductivity of the liquid is determined by comparing the measured time dependent temperature change of a wire submerged in the liquid reservoir at known initial temperature with the known analytic solution. The measured results for the three oils over the temperature range 0 °C to 50 °C are shown in Figure 4.

BURNING CHARACTERISTICS

The burning characteristics of the three crude oils were measured in burns under the large calorimeter hood. The use of a 1.2 m diameter pan permitted controlled burning experiments to be conducted under conditions representative of the radiation-dominated, turbulent flow regime of larger pool fires. Each oil was studied at four initial layer thicknesses -- 2 mm, 5 mm, 10 mm, and 25 mm. In each test a pre-weighed sample of oil, corresponding to the desired oil layer thickness, was floated on the water

Table 2. Summary of Burning Data in 1.2 m dia Pan

Test	Oil Layer		Maximum Plume Temperature °C	Maximum Heat Release Rate		Maximum Radiation Feedback		Maximum External Radiation (2m) kW/m^2	Oil Residue kg
	Thickness mm	Weight kg		MW	kW/m^2	Center kW/m^2	Rim kW/m^2		
MURBAN									
M04	2	1.94	678	1.20	1060	21.6	38.4	7.2	0.76
M01	5	4.86	878	2.00	1770	64.0	34.1	11.0	0.83
M02	10	9.72	934	2.11	1860	68.8	31.6	11.8	0.81
M03	25	24.3	955	2.07	1830	69.9	44.0	16.5	1.19
ALBERTA SWEET									
A04	2	1.87	707	0.97	860	53.8	43.3	6.2	0.62
A01	5	4.68	864	2.14	1890	62.2	34.0	11.1	0.64
A02	10	9.36	883	2.84	2510	80.6	--	14.4	0.77
A03	25	23.4	967	2.55	2260	47.3	35.5	13.3	0.96
LA ROSA									
L04	2	2.08	484	0.60	530	29.2	30.8	4.0	1.22
L01	5	5.20	896	2.43	2150	35.5	30.8	12.4	0.81
L02	10	10.4	932	3.27	2890	39.8	32.8	13.8	0.99
L03	25	26.0	931	2.85	2520	32.4	42.2	15.0	0.66

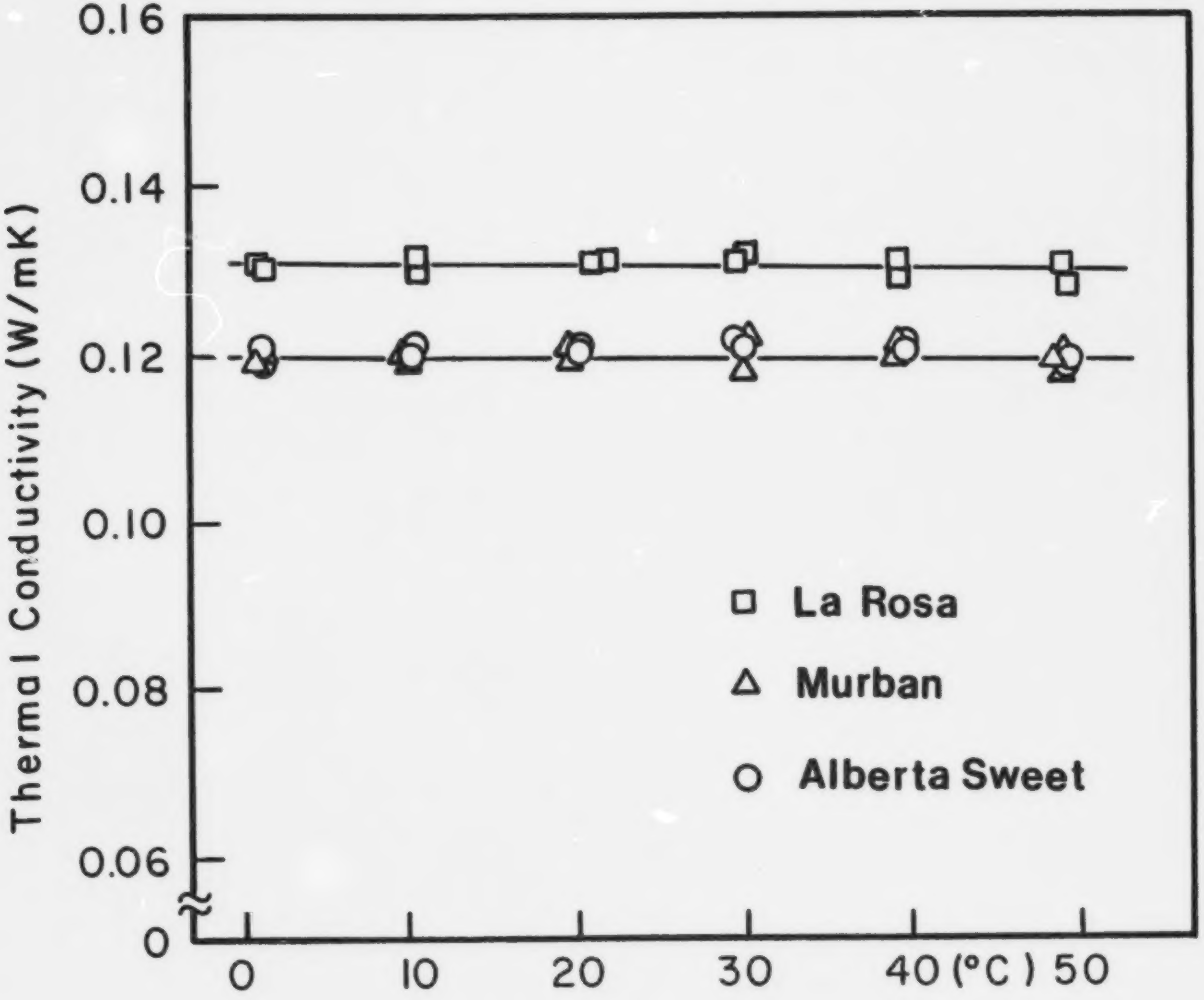

FIGURE 4. THERMAL CONDUCTIVITY OF CRUDE OILS.

surface. The oil level control device was operated in most tests to maintain the oil surface nominally 12 mm below the top of the pan rim. At this depth, the two top thermocouples on the rakes were above the oil surface at the start of each test. As soon as the surface was calm and stabilized and all instrumentation was in operating condition (usually within 2 minutes), an ignition flame was applied to the oil surface. All temperatures, radiation levels, heat release rate and exhaust gas measurements were scanned automatically at 5 second intervals and recorded on magnetic tape. After burning ceased, a pre-weighed sorbent pad was placed on the surface to adsorb the residual oil and then the oil soaked pad was reweighed. No attempt was made to capture oil which had splattered over the pan rim or to account for water picked up by the sorbent pad. Oil which remained on the radiometers, thermocouples, and pan surfaces was removed with solvent-moistened napkins, prior to the next test. Photographs showing the typical sequence in a burn are reproduced in Figure 5.

To date, 12 tests have been completed. Although the data have not been completely analyzed and evaluated, a summary of selected data is given in Table 2. Principal emphasis in this report will be on discussion of measured flame-plume temperature, energy release rate, and radiation feedback to the oil surface.

For a given crude oil, the maximum recorded flame-plume temperature increased slightly with oil layer thickness. As shown in Figure 6 for the MURBAN crude, the flame temperature did not reach a steady state condition for oil layer thicknesses of 2 mm and 5 mm, but approached a steady-state value (before reaching a peak) for the larger thicknesses. The peak temperature corresponding to the vigorous burning period prior to the end of burning was approximately 100 °C to 150 °C above the "steady-state" temperature.

The maximum recorded energy release rate also increased with oil layer thickness, but then decreased for the 25 mm layer. The energy release rate for the MURBAN crude exhibited an approach to steady-state for the 10 mm and 25 mm layer thicknesses prior to reaching a peak value during the vigorous burning period (see Figure 7). The quasi-steady-state energy release rate for the MURBAN crude was approximately 0.95 MW (840 kW/m^2), actually decreasing noticeably prior to the rapid increase in burning corresponding to a peak level of 2.1 MW (1860 kW/m^2) prior to burnout. The decrease in energy release rate during the steady burning phase (100 to 500) seconds appears to be associated with the changing composition of the crude oil towards the heavier fractions and the concurrent decreased combustion efficiency leading to the apparent generation of more smoke. The corresponding values of steady-state and peak energy release rates for the ALBERTA SWEET crude were 1.15 MW (1000 kW/m^2) and 2.7 MW (2400 kW/m^2). These values are significantly greater than the area specific energy release rate for MURBAN crude measured in the 0.6 m diameter pan (720 kW/m^2). The peak energy release rate for the LA ROSA crude was approximately 50% greater than for the MURBAN crude.

There was a similar increase in the recorded peak levels of radiant heat feedback to the MURBAN crude oil surface as a function of oil layer thickness (see Figure 8). However, for the ALBERTA SWEET and LA ROSA crudes, the peak levels of feedback radiation at the center appeared to be lower for the 25 mm layer than for the 10 mm layer. Also,the recorded level of feedback radiation did not follow the same temporal pattern of the peaks of the flame temperature and the energy release rate, particularly for the 10 mm and 25 mm layer depths. Several problems with the present radiation measurement system must be overcome to obtain more reliable data. One problem is with the splattering of

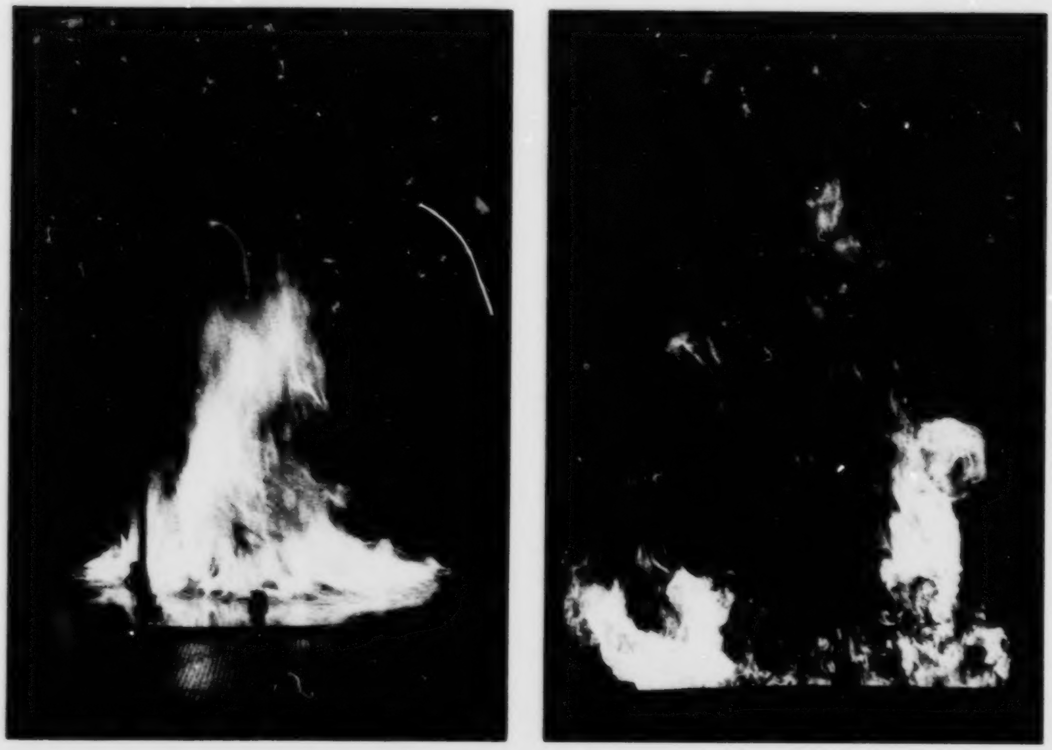

T = 1.0 MIN.
FIRE GROWTH PERIOD

T = 2.0 MIN.
START OF STEADY-STATE BURNING PERIOD

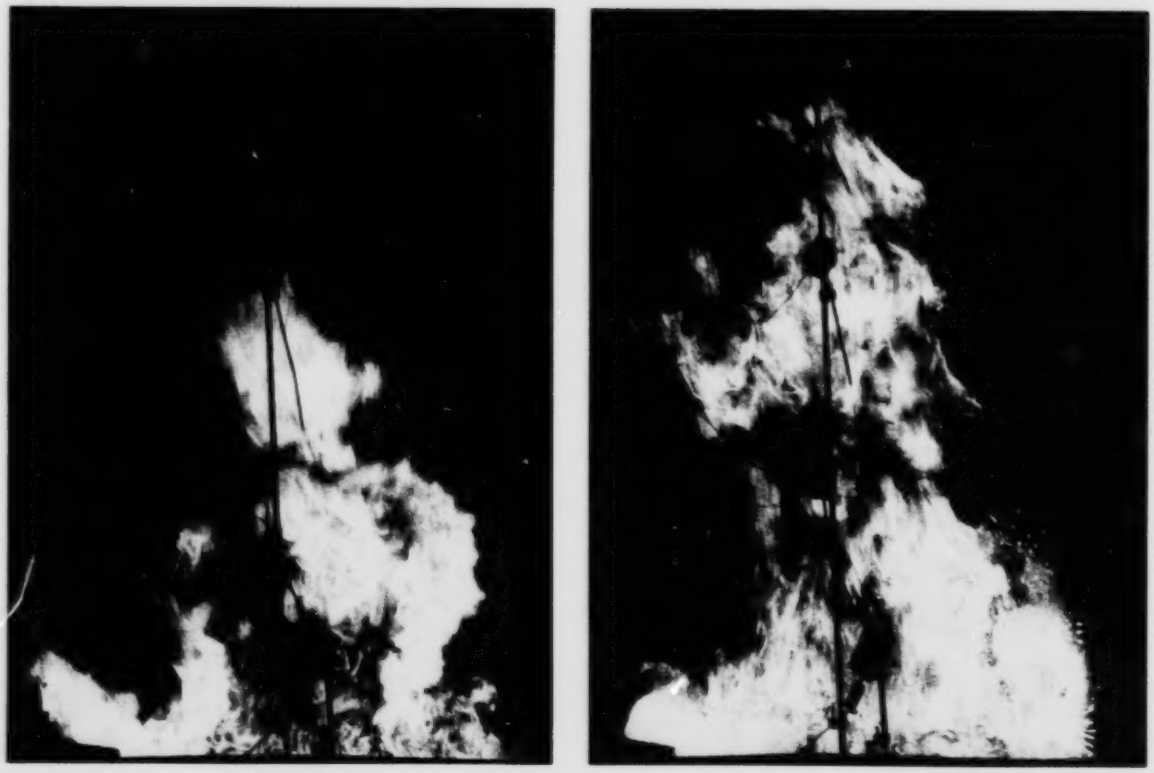

T = 3.0 MIN.
NEAR END OF STEADY-STATE BURNING PERIOD

T = 4.0 MIN.
VIGOROUS BURNING PERIOD

FIGURE 5. BURN SEQUENCE FOR 10 MM THICK LAYER OF LA ROSA CRUDE OIL

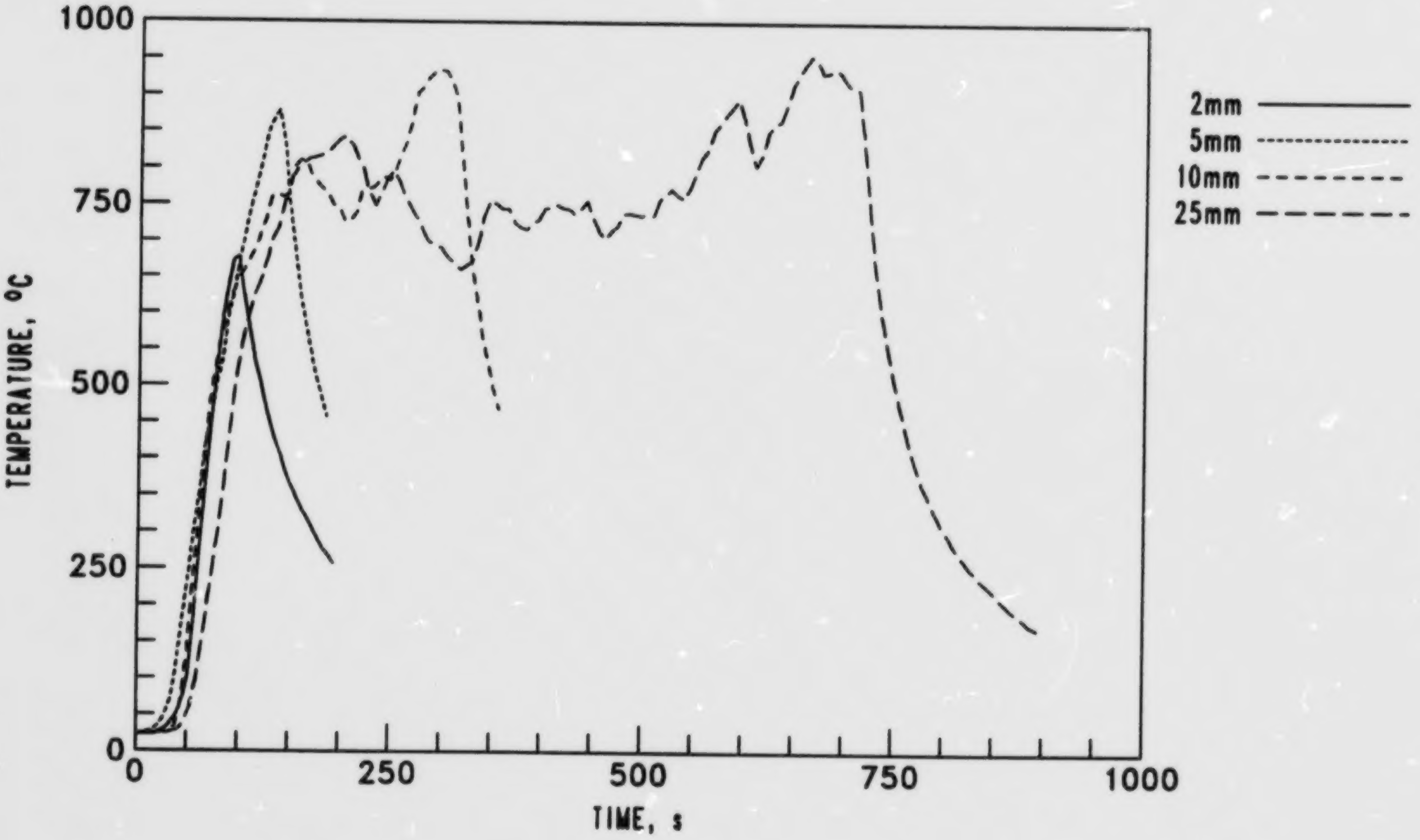

FIGURE 6. FLAME PLUME TEMPERATURE FOR MURBAN CRUDE AT DIFFERENT LAYER THICKNESSES.

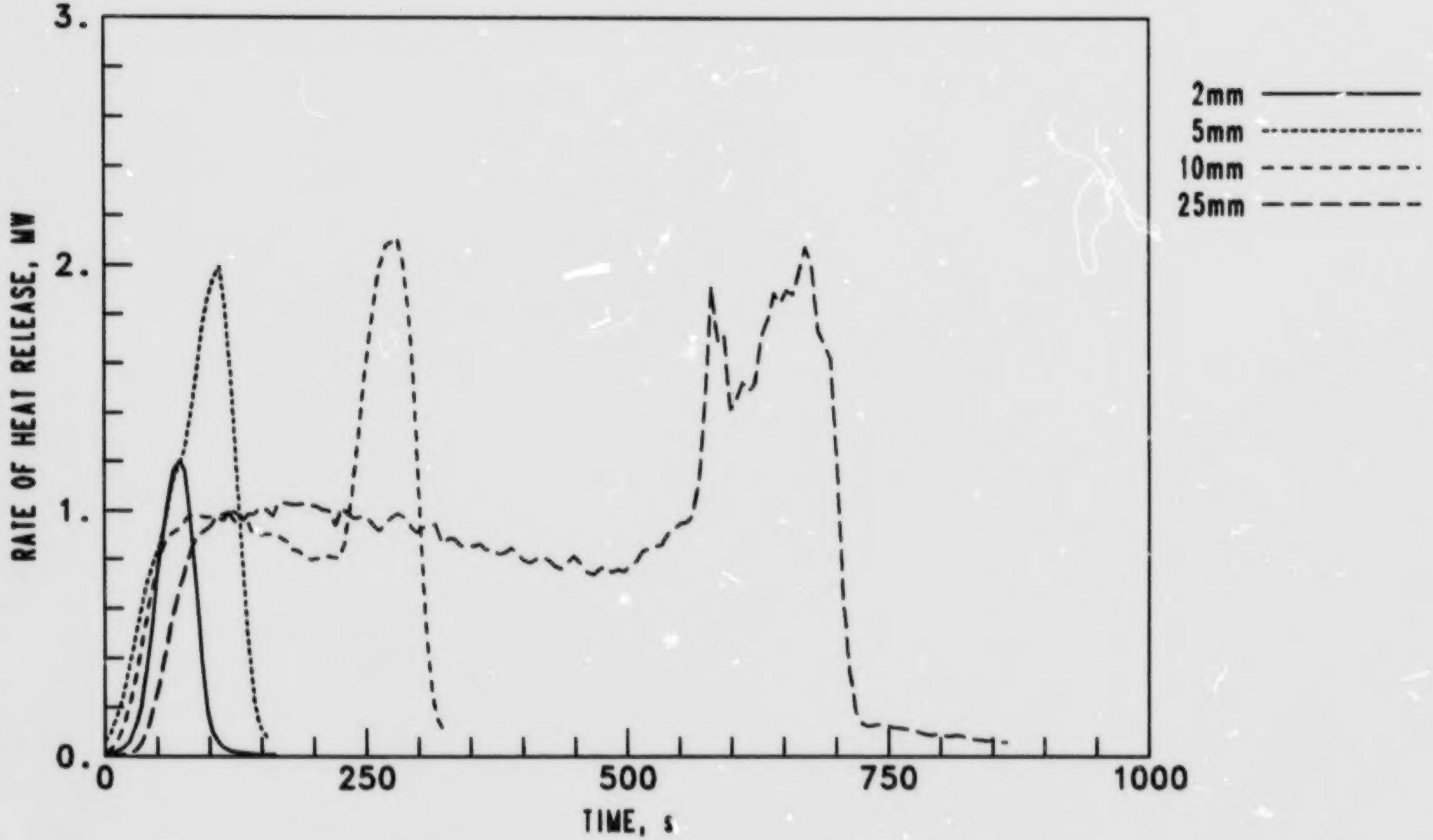

FIGURE 7. ENERGY RELEASE RATE FOR MURBAN CRUDE AT DIFFERENT LAYER THICKNESS.

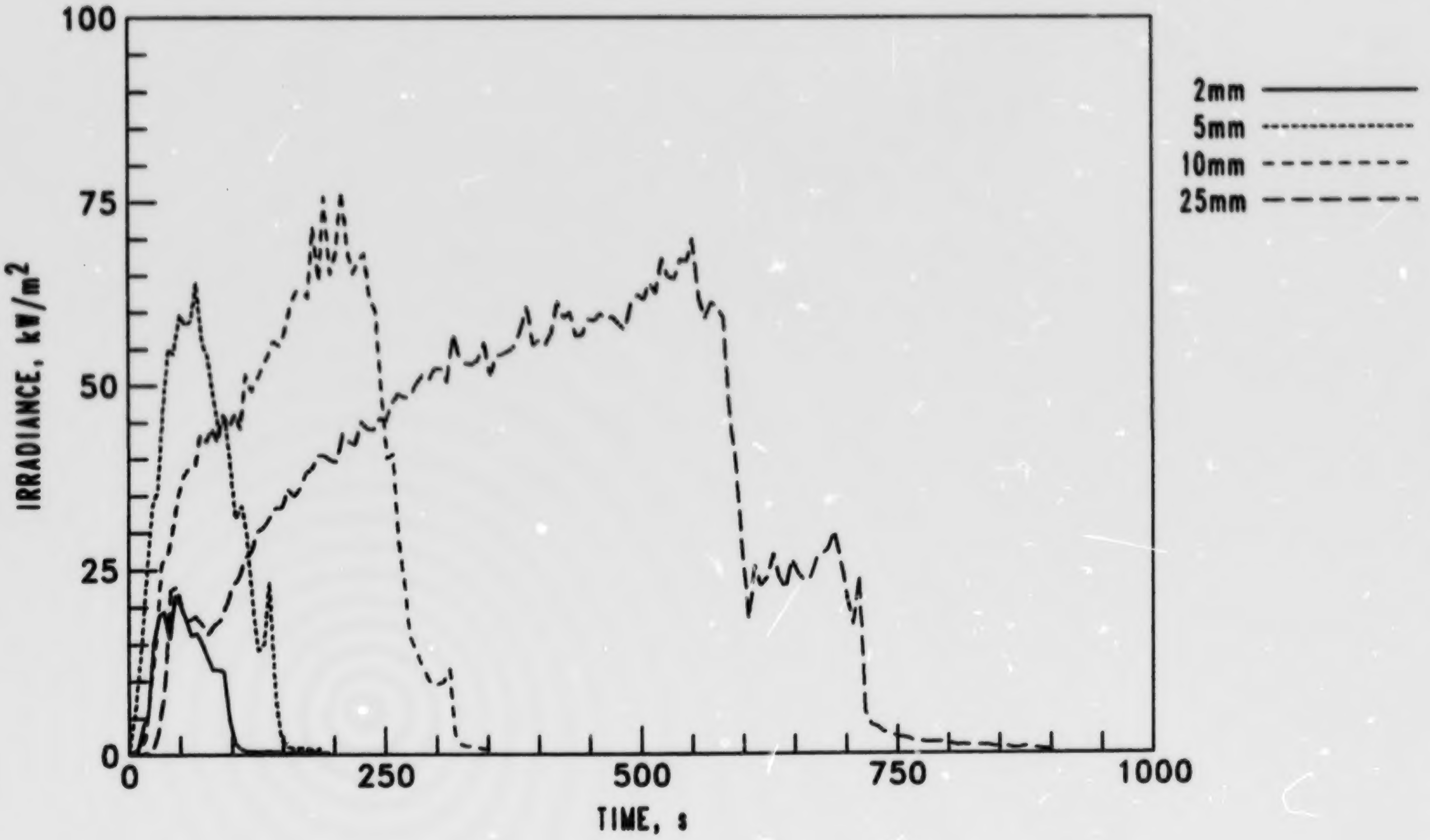

FIGURE 8. RECORDED RADIATION FEEDBACK TO CENTER OF PAN FOR MURBAN CRUDE AT DIFFERENT LAYER THICKNESSES.

oil from the pool up onto the radiometers during the vigorous burning period near the end of the test. The other is the nitrogen purging of the radiometers interfering with the normal burning. Intense burning due to fire whirls induced by the nitrogen flow immediately above the radiometers may significantly influence the readings.

The following observations were noted during this series of tests:

1. Ignition
With the ALBERTA SWEET crude oil, ignition was immediate with active and rapid flaming involving the entire oil layer. With the LA ROSA crude, there was a delay of approximately 60 to 90 seconds before the flaming spread to involve the entire surface. The response of the MURBAN crude was intermediate.

2. Fire whirls
Local intense burning, usually with strong vortex motion, was observed in the vicinity of the gas-purged radiometers. This appeared to be the result of the air-aspirating effect of the nitrogen jet used to minimize oil condensation on the radiometer window. This may be noted in the photographic sequence of the 10 mm LA ROSA burn test shown in Figure 5. Although this activity was very localized and did not appear to affect the overall measurements of external radiation, some in-pool radiation feedback measurements may be affected. Knowledge of this effect may be of interest where methods for increasing local rates of burning are being considered.

3. Oil splatter
During the vigorous burning period, boiling water and oil droplets splattered up and out of the pan. The LA ROSA and the MURBAN crudes caused extensive splattering, with flaming droplets from the former approaching 1 m in height. The splattering occurred at the end of the test when the remaining thin layer of oil contained a greater percentage of higher boiling point fractions. The increased surface temperature and thin oil thickness caused boiling in the water sublayer.

4. Smoke
The quantity of smoke observed within the flame mass appeared to be greater as the oil layer thickness was increased and smoke appeared to be generated at a greater rate and closer to the oil surface late in the test. The LA ROSA and MURBAN had noticeably more smoke than ALBERTA SWEET.

5. Boilover
With the MURBAN and LA ROSA crudes at an oil layer thickness of 25 mm, boilover occurred at the end the test. In the test with 25 mm initial layer depth of LA ROSA, the boilover was relatively intense and considerable oil spilled or splattered out over the rim of the pan. The ALBERTA SWEET crude exhibited only a minor tendency to boilover.

6. Residue
The oil residue remaining following burnout varied with the type of oil and the layer thickness. With one exception, more oil remained from the thickest (25 mm) layer of each oil and slightly more residue remained with the LA ROSA crude than with the other oils. The measured residue for all tests ranged from 0.6 kg to 1.2 kg corresponding to a layer depth of approximately 0.6 mm to 1.2 mm.

The effectiveness of combustion as an oil spill mitigation tool depends critically upon the feedback of radiation from the flames to the burning oil surface. This project is attempting to emphasize this measurement, particularly since prior investigations reported in the literature [5,6] have experienced experimental difficulties and analytical models have never been fully validated. This study has not been completely immune to similar experimental problems, but significant progress is being made. Initial indications are that radiation feedback to the surface may range from less than 2 percent to more than 5 percent depending upon the type of oil and its layer thickness. Based on initial estimates of the temperature gradients at the oil surface (22 °C/mm to 50 °C/mm), and the measured thermal conductivity of the crudes (0.12 W/mK to 0.13 W/mK), the rate of heat conduction into the oil is approximately 2 kW/m^2 to 6 kW/m^2 or less than 20 percent of the radiant energy approaching the surface in these tests. A better estimation will be available with additional tests, improved instrumentation, completion of energy balances, and comparison with a flame radiation model which accounts for radiant energy blockage by the cool fuel vapor-rich zone above the oil surface [7]. Examination of the effects of water temperature, oil spill weathering, and wind on the combustion process will require additional experimentation and calculations.

SMOKE CHARACTERISTICS

The focus of this part of the project is the chemical characterization of the smoke produced by burning crude oil. The measurements include the organic versus elemental carbon in the smoke, the quantity of selected polynuclear aromatic (PAH) compounds in the smoke, and the amount of CO_2, CO, NO, and NO_x emitted. Much of the analysis effort was concentrated on the PAH analysis. These materials are of environmental concern, because some have been reported to be carcinogenic to animals [8]. The results of the PAH analysis are compared with the PAH component of the fuel itself.

In all tests in this series, ALBERTA SWEET crude oil was burned in a 0.6 m diameter pool. Approximately 9 liters of crude oil were burned in each test, which corresponded to a fuel depth of about 30 mm. The sample burning time was found to be about fifteen minutes. Smoke samples were collected on filters heated to match the stack temperature, about 100 °C, using a heated transfer line described in last year's report [1]. The first smoke sample was collected from the time of visually steady burning, typically one minute into the burn, for about six minutes. The collection of a second sample began immediately thereafter and lasted for about another six minutes. Smoke samples were also diluted before collection with air cooled to about 10 °C to simulate the cooling that would naturally occur in a rising smoke plume. In this case, both filter samples were collected in parallel over about thirteen minutes of the burn. The filter collections in all the tests were completed before the rapid burning at the end of the test.

Smoke Emission Measurements

The results of the smoke emission measurements are contained in Table 3. The smoke yield, ϵ, which is defined as the mass of smoke aerosol generated per mass of fuel consumed, is found to have a value of about 0.10. This is similar to the value found in previous test with PRUDHOE BAY crude oil [1]. the value of ϵ increases in going from sample 1 to sample 2 indicating that

TABLE 3. SUMMARY OF SMOKE EMISSION DATA FOR 60 CM DIAMETER ALBERTA SWEET CRUDE OIL POOL FIRES

Property	Test H-1 sample 1	Test H-1 sample 2	Test H-4 sample 1	Test H-4 sample 2	average
dQ/dt, kW	217	172	234	191	204
dm/dt, g/s	5.27	4.40	5.63	4.93	5.06
H, KJ/g	37.4	39.8	41.7	38.8	39.4
ϵ_1	0.076	0.119	0.100	0.110	0.101
ϵ_2	0.070	0.110	0.089	0.101	0.093
K_s, m^2/g	9.2	9.3	(6.4)	9.8	9.4
K_f, m^2/g	0.70	1.10	0.64	1.08	0.88

Property	Test C-5	Test C-7	average
dQ/dt, kW	205	203	204
dm/dt, g/s	4.98	5.57	5.28
H, KJ/g	41.1	36.3	38.7
ϵ_1	0.087	0.079	0.083
ϵ_2	0.080	0.079	0.080
K_s, m^2/g	10.2	10.9	10.6
K_f, m^2/g	0.88	0.86	0.87

Legend:

H-1 and H-4 refer to identical crude oil burns in which the filter collection system was heated to about 100 °C.

C-5 and C-7 refer to identical crude oil burns in which the smoke is cooled to ambient temperature in a sampling dilution system.

dQ/dt - heat release rate of the fuel.

dm/dt - burning rate of the fuel.

H - heat of combustion.

ϵ_1 and ϵ_2 refer to the smoke yield based on a flux method and a carbon balance method [1], respectively.

K_f and K_s are defined in the section entitled Smoke Emission Measurements.

the smoke emission increases as the fuel presumably distills leaving the sootier component for the later stage of burning.

One important parameters in regard to visibility effects of the smoke is the specific extinction coefficient relative to the fuel, K_f.

$$K_f = K/(\dot{m}_f/\dot{V}) \quad , \qquad (1)$$

where K is the extinction coefficient per meter, m_f is the fuel mass loss rate, and $\dot{V}$ is the volumetric flow rate through the duct. As a heuristic example, a K_f value of 1 m^2/g means that if the smoke produced by one gram of material were collected over a 1 m^2 area, the light incident on this area would be blocked by the smoke ($I/I_0 = e^{-1}$). The value of K_f increases from about 0.7 to 1.1 m^2/g for the second collection period for both H-1 and H-4 indicating again that the fire becomes sootier as the burning proceeds. The average value of K_f, 0.87 m^2/g, is close to the value obtained with Prudhoe Bay crude oil, 0.96 m^2/g.

A second optical property of interest is the extinction coefficient per mass concentration of the smoke, K_s, defined by

$$K_s = K/m_s \quad , \qquad (2)$$

where m_s is the mass concentration of smoke. The quantity K_s is an intrinsic property of the smoke depending on (a) the optical properties of the smoke, (b) the size distribution of the smoke, and (c) the wavelength of light. The average value of 9.4 m^2/g obtained from the first two tests is in good agreement with the value obtained for PRUDHOE BAY crude oil, 9.1 m^2/g.

The smoke collected in tests C-5 and C-7 was first diluted and thus cooled by the probe illustrated in Figure 1. The mass flow of ice cooled dilution air is approximately twice the mass flow of the air sampled from the stack. The manifold temperature just prior to the filter is observed to be within two °C of the ambient temperature. The value of ϵ obtained under these conditions is 15% to 20% less than the value obtained for the heated, undiluted sample. Normally, one would expect an increase in ϵ with dilution by cool air resulting from the condensation of organic vapors. The PAH analysis discussed below clearly shows that the higher vapor pressure PAH's are greatly enriched in the diluted sample compared to the high temperature sample. The observed decrease in these tests may be the result of smoke deposition by thermophoresis in the entrance portion of the diluter and by turbulent flow in the mixing region of the diluter.

Gas Emission Measurements

The emission of CO, CO_2, NO, and NO_x was monitored during selected tests. The concentrations of CO and CO_2 were measured by standard gas analysis instrumentation based on nondispersive infrared spectroscopy. The smoke aerosol was filtered and the moisture condensed out with a dry ice trap before the sampled gas entered the CO and CO_2 analyzers. The analysis of the nitrogen oxides is based on the reaction of ozone with the oxides and detection of the resulting chemiluminescence with a photocell. The CO_2 accounts for over 95% of the gaseous products measured as indicated in Table 4. The other principal product of combustion, H_2O, was not measured. The volume fraction of CO, NO, and NO_x relative to CO_2 were found to be about 0.038, 1.5×10^{-4}, and 4×10^{-4}, respectively. The concentrations of NO and NO_x were just above the detection threshold.

TABLE 4. GASEOUS EMISSION FROM ALBERTA SWEET CRUDE OIL

Species	C-6 ppm	C-7 ppm	C-6 fract.[a]	C-7 fract.[a]
CO_2	4604	4906		
CO	174	187	0.038	0.038
NO	0.7	0.7	$1.6x10^{-4}$	$1.5x^{-4}$
NO_x	2.3	1.7	$5.0x10^{-4}$	$4.0x^{-4}$

---

[a] Volume fraction of gas species relative to CO_2.

Elemental and Organic Carbon Analysis

Smoke aerosol produced by flaming combustion is composed of a graphitic or so called elemental carbon fraction and an organic carbon fraction. Smoke samples were collected on quartz fiber filters and sent to a contract laboratory for thermal-optical analysis for organic/elemental carbon [9]. Standard precautions were taken to avoid sample contamination before sample collection by heating the filter for several hours at 700 °C and also heating the aluminum foil used to line the sample containers (petri dishes) to 500 °C for several hours. The organic fraction of the sample is determined by heating the sample in pure helium in four temperature steps up to 770 °C. The pyrolysis products flow through a heated catalyst and are converted to CO_2, which is detected by nondispersive infrared spectroscopy. The second stage of the analysis consists of reducing the temperature to 525 °C and introducing O_2 (2%). The temperature is increased in two steps to 770 °C and the elemental carbon is oxidized to CO and CO_2. Ultimately all of the carbon is converted to CO_2 by the catalyst.

The optical absorbance of the sample is used to determine whether elemental carbon is being produced by pyrolytic conversion of the organic carbon and also to correct for this effect. The maximum deposit of elemental carbon that allows light to be transmitted through the sample is about 15 $\mu g/cm^2$. As indicated in Table 5, the elemental carbon content of the smoke is over 90%. The large blank reading for the high temperature filter sample may result from the diffusion of condensible organic vapors from the filter manifold onto the filter. No sample is drawn through the blank filter, but there is an open path between the manifold and the filter. The fact that the high temperature collection yields a slightly lower elemental carbon content may be an artifact resulting from vapor diffusion.

Analysis of Polynuclear Aromatic Hydrocarbons

Eight smoke samples weighing 10 mg to 15 mg each were deposited on teflon filters and were analyzed for 15 polynuclear aromatic hydrocarbons (PAH's) using combined liquid and gas chromatographic techniques. Wise and Benner from the Center for Analytical Chemistry (NBS) performed the analysis on four of the samples by a method previously used by them in quantifying the PAH content of two standard reference air particulate samples [10]. The PAH concentration in the smoke for samples similar to those analyzed at NBS were

TABLE 5. ORGANIC/ELEMENTAL ANALYSIS OF SMOKE FROM BURNING OF ALBERTA SWEET CRUDE OIL

Sample No.	org. carbon $\mu g/cm^2$	elem. carbon $\mu g/cm^2$	% elem. carbon[a]
H-3[b], blank	3.80±0.46	0.41±0.22	
H-3, #1	6.18±0.51	29.29±1.66	92
H-3, #2	5.18±0.46	17.71±1.09	93
H-3, #2 repeat	5.29±0.46	19.86±1.19	93
C-5, blank	0.78±0.24	0.22±0.21	
C-5, #1	0.97±0.25	12.95±0.85	99
C-5, #1 repeat	0.80±0.24	13.37±0.87	100
C-5, #2	2.76±0.24	43.02±2.35	96

[a] The blank values are subtracted from the sample values in determining the percent elemental carbon.

[b] H refers to filter heated to about 100 °C and C to filter at near ambient conditions.

analyzed at the laboratories of Environment Canada in Ottawa. A preliminary analysis of heteroatomic PAHs was also made by Environment Canada.

Sample Preparation. At NBS the samples were spiked with internal standards (phenanthrene-d_{10} and 1-n-butylpyrene) and Soxhlet extracted with dichloromethane (DCM) for approximately 20 hours. The extracts were concentrated by rotary evaporation to less than 5 ml and further concentrated under nitrogen to dryness. The residues were dissolved in 1 mL of DCM and approximately half of each extract was pipetted onto a silica cartridge (Sep-Pak, Waters, Assoc., Milford, MA)[1] and eluted with 15 mL of a solution of 10% DCM in pentane. This chromatography is performed to isolate an enriched PAH fraction. The eluates were concentrated to dryness under nitrogen and were dissolved in 1 mL of a solution of 5% DCM in pentane. The samples were separated into subfractions by normal-phase LC on a semi-preparative aminosilane liquid chromatographic column (μBondapak NH_2, Waters Assoc., Milford, MA) using 5% DCM in pentane as the mobile phase operated at a flow rate of 5 mL/min. Collection of an aromatic fraction was begun just before the elution of phenanthrene (30 mL) and was continued until well after the elution of coronene (200 mL total collected). Elution volumes of these two PAHs were determined prior to sample injection. The fractionated samples were concentrated by rotary evaporation, transferred to 100 μL vials, further concentrated to dryness under nitrogen and the residues dissolved in DCM.

---

[1] Certain commercial equipment, instruments, and materials are identified in this paper to specify adequately the experimental procedure. In no case does such identification imply recommendation or endorsement by the National Bureau of Standards, nor does it imply that the material or equipment identified is necessarily the best available for the purpose.

Gas Chromatographic Quantification. Capillary gas chromatography with flame ionization detection (GC-FID) was used at NBS for the measurement of 15 PAHs in the four filter extracts. Each of the four extracts was chromatographed in duplicate injecting approximately 1 μL onto a 30 m x 0.25 mm i.d. fused silica capillary column (DB-5, 0.25 μm phase thickness, J&W Scientific, Inc.) using helium as the carrier gas (20 psi). The injector and detector temperatures were 300 °C and 320 °C, respectively, and the split flow was set at 30 mL/min. The temperature program used in the study was the following: 150 °C (hold for 2 min) ramp at 4 °C/min to 280 °C (hold for 15 min). The PAHs were determined by comparison of peak areas of the analytes with those of the internal standards. Typical GC-FID chromatograms for the four samples and a blank are shown in Figures 9-13. The blank (Figure 9) had been spiked with the same amount of internal standards as the samples and proved to be virtually free of any impurity except for a compound that eluted at approximately 14 minutes. Fortunately, this artifact did not cause any difficulty in the quantification of the fifteen PAHs. The names and structures of PAHs for selected peaks in the chromatogram are given in Figure 12. It is also seen in Figure 12 that the smaller PAHs are eluted from the column first.

Environment Canada has made a preliminary analysis for nitrogen containing PAHs by GC analysis with a phosphorous detector. In sample 7,#2, the following results were obtained: nitro-fluorene (15 μg/g), nitro-anthracene (5 μg/g), nitro-fluoranthene (14 μg/g), and nitro-benzo[a]pyrene (7 μg/g). Nitrogen containing PAHs were not detected in the other samples, presumably, because the concentrations were below the 4 μg/g detection limit of the analysis technique. No evidence of nitrogen containing PAHs was found in the crude oil itself at a detection limit of about 0.2 μg/g.

Results and Discussion. Concentrations of 18 PAHs are shown in Tables 6 and 7 based on results from both (NBS) and Environment Canada (EC). The NBS results for the samples collected at the higher temperature (H-2, #1 and #2) suggest some preferential losses of the more volatile PAH during sample work-up since the concentrations calculated versus phenanthrene-d_{10} were a factor of two greater than those calculated versus 1-n-butylpyrene. One has difficulty explaining these apparent losses, since the samples were prepared in the same manner as the ambient temperature samples, which showed good agreement between concentrations calculated using the two internal standards. Reported concentrations of phenanthrene for H-2 were calculated using phenanthrene-d_{10} as the internal standard, since its volatility is similar to that of phenanthrene. In all other cases, 1-n-butylpyrene was used.

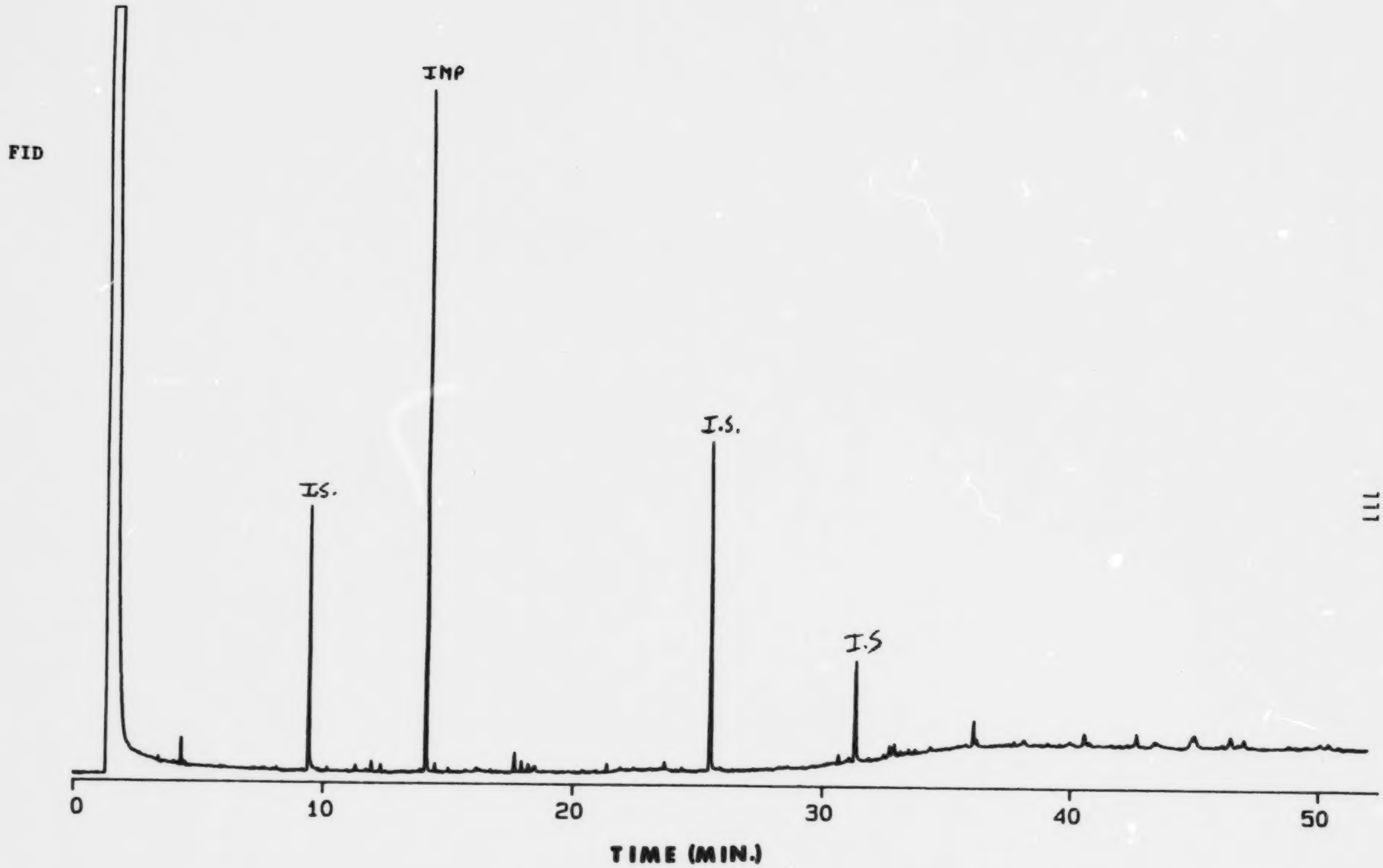

FIGURE 9. GAS CHROMATOGRAM OF TYPICAL BLANK SAMPLE WITH I.S. INDICATING INTERNAL STANDARD AND IMP INDICATING AN IMPURITY.

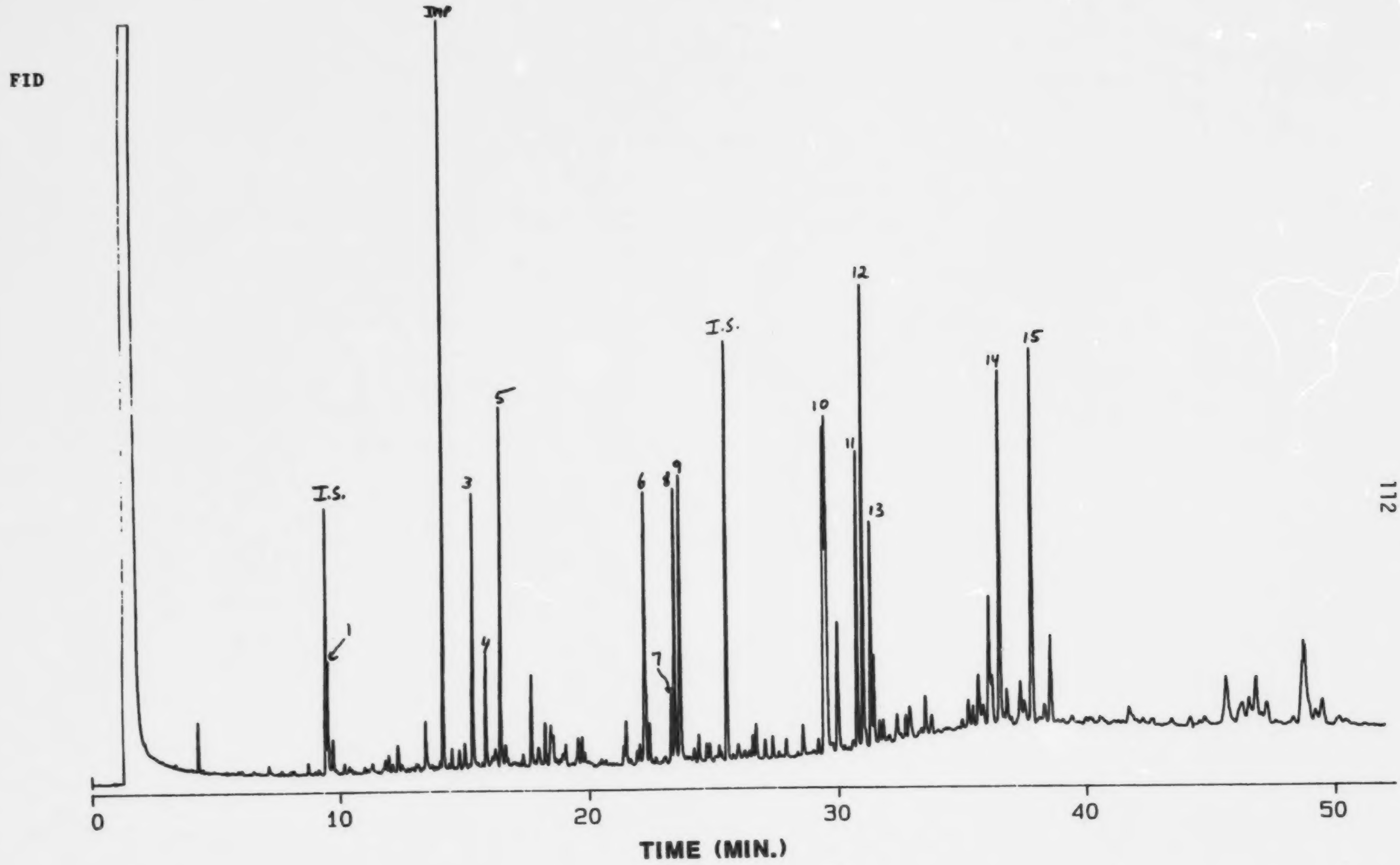

FIGURE 10. GAS CHROMATOGRAM OF THE FIRST SMOKE SAMPLE COLLECTED AT 100°C (H-2,#1). THE PAHS ASSOCIATED WITH THE PEAKS ARE IDENTIFIED IN TABLE 6

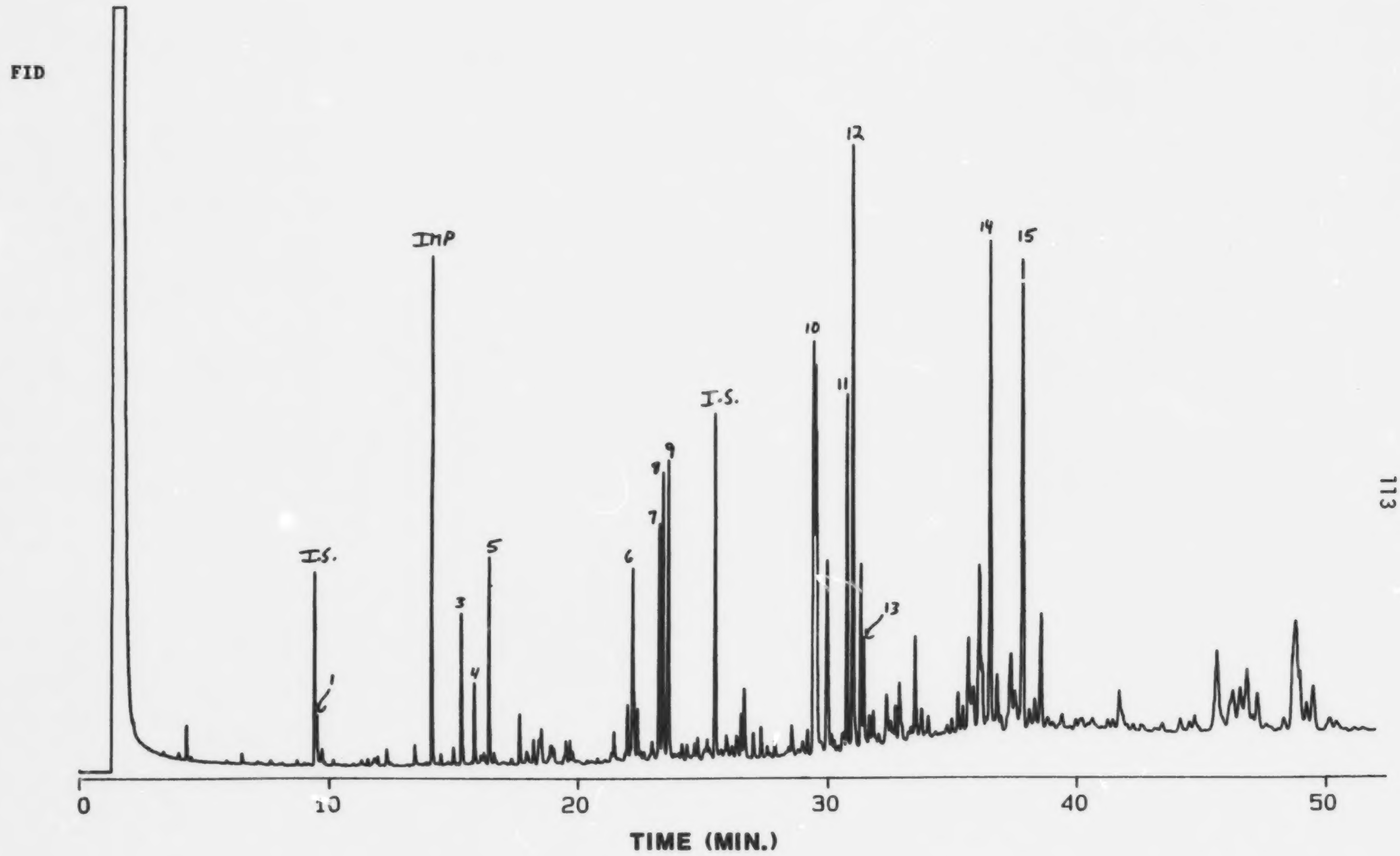

FIGURE 11. GAS CHROMATOGRAM OF THE SECOND SMOKE SAMPLE COLLECTED AT 100°C (H-2,#2).

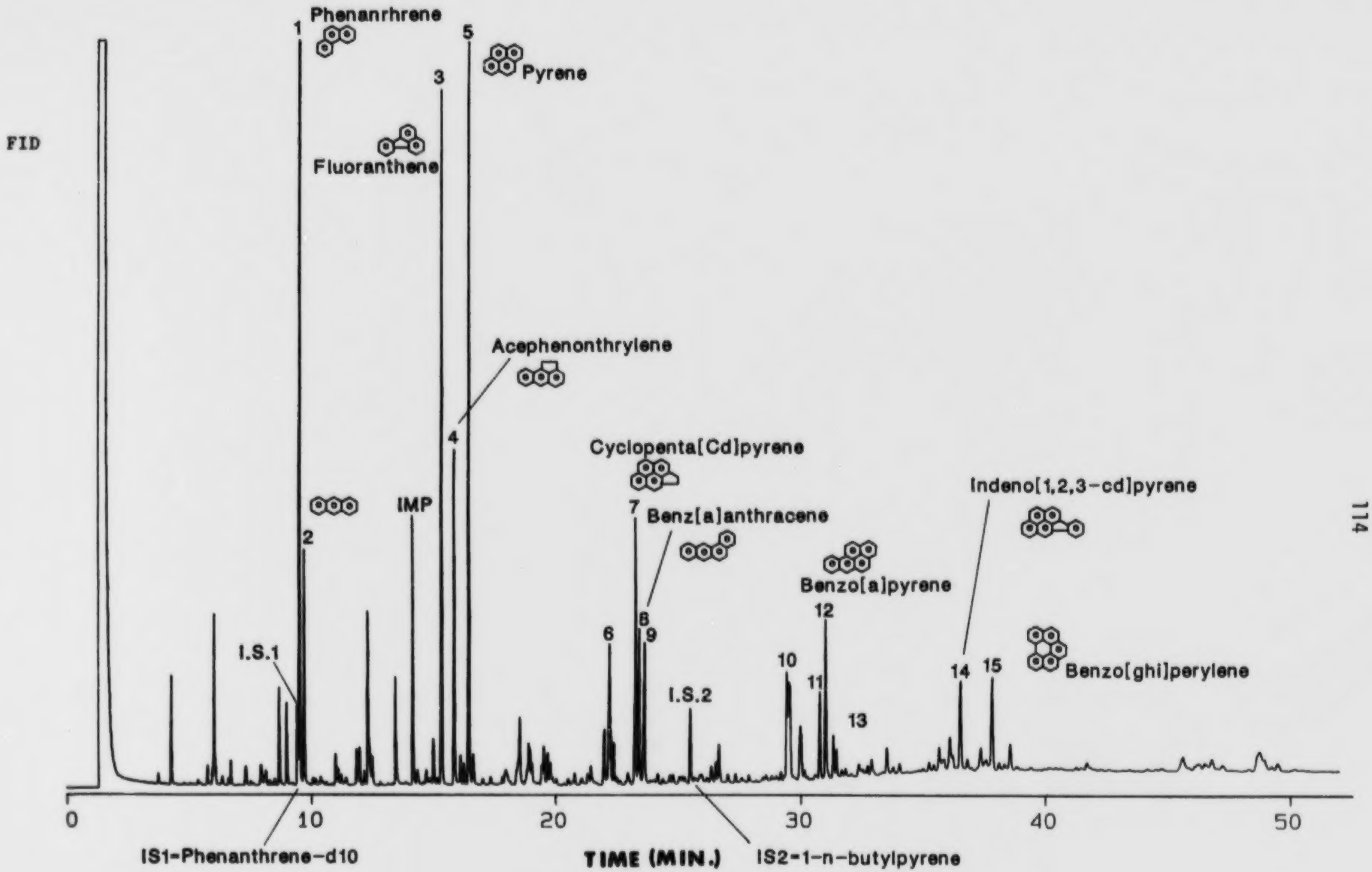

FIGURE 12. GAS CHROMATOGRAM OF SMOKE SAMPLE COLLECTED AT AMBIENT TEMPERATURE (C-5,#1).

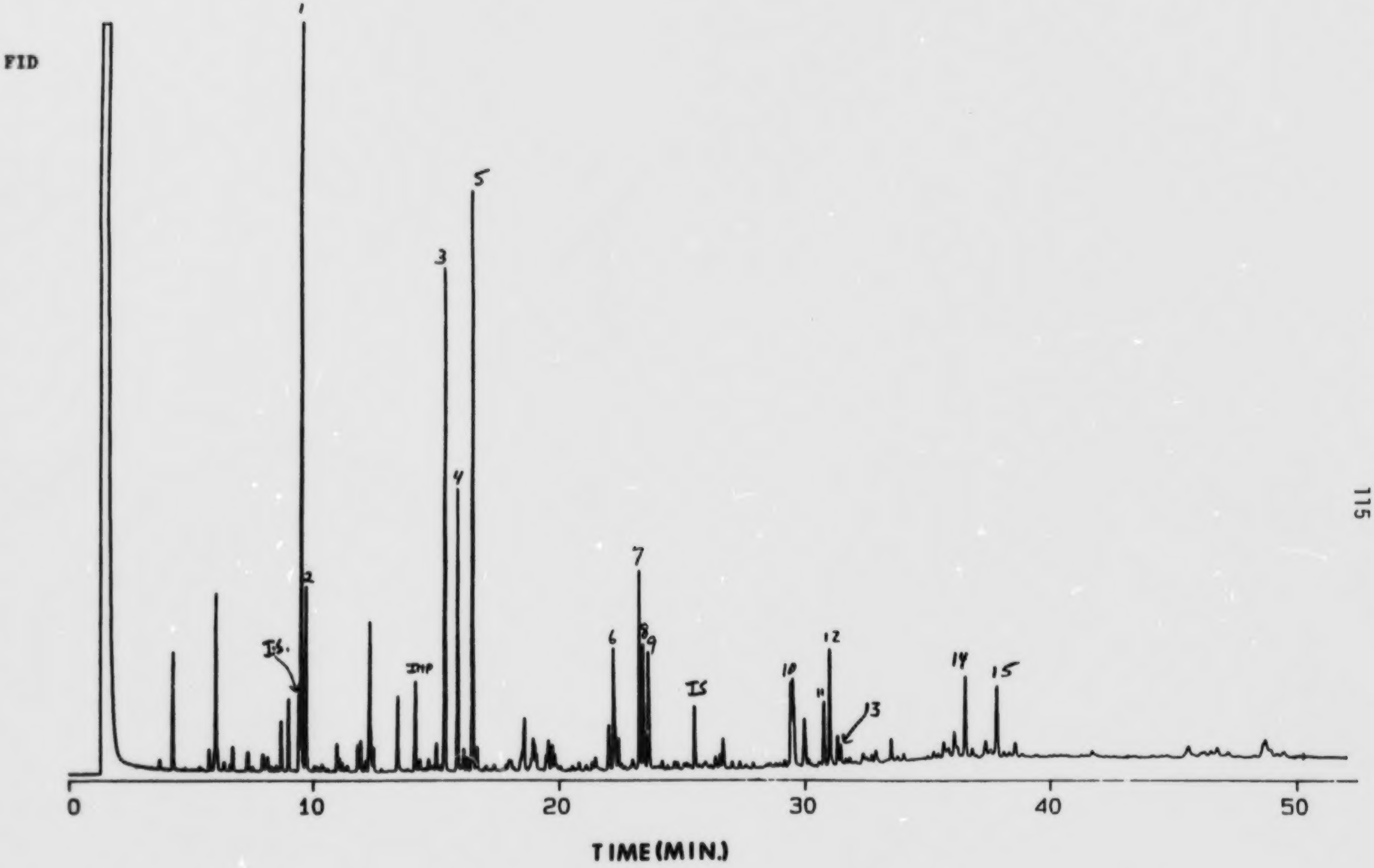

FIGURE 13. GAS CHROMATOGRAM OF SECOND SMOKE SAMPLE COLLECTED AT AMBIENT TEMPERATURE (C-5,#2).

TABLE 6. MEAN PAH CONCENTRATION FOR ALBERTA SWEET CRUDE OIL SMOKE SAMPLES COLLECTED AT 100 °C[a]

No.[b]	PAH	H-2,#1 μg/g[c]	H-2,#2 μg/g	H-4,#1 μg/g	H-4,#2 μg/g
	Acenaphthylene			3	2
	Acenaphthene			N.D.	N.D.
	Fluorene			4	3
1.	Phenanthrene	31[d]	21[d]	94[g]	58[g]
2.	Anthracene	N.D.[e]	N.D.		
3.	Fluoranthene	47	37	213	126
4.	Acephenanthrylene	22	22		
5.	Pyrene	65	49	259	152
6.	Benzo[ghi] fluoranthene	69	65		
7.	Cyclopenta[cd] pyrene	24	108		
8.	Benz[a]anthracene	63	87	88	176
9.	Chrysene/ Triphenylene	71	87	95	186
10.	Benzo[b,j,k] fluoranthene	187	351	491	515
11.	Benzo[e]pyrene	66	106	92	224
12.	Benzo[a]pyrene	113	204	73	189
13.	Perylene	19	38	18	52
14.	Indeno[1,2,3-cd] pyrene	112	219	251	752
15.	Benzo[ghi]perylene	127	235	87	240
Total PAH Conc.[f]		901	1434	1761	2670

---

[a] The samples H-2 analyzed at NBS and H-4 were analyzed by EC.

[b] Peak identification numbers for Figures 10-13.

[c] μg of PAH/g of smoke; uncertainty estimated to be ±10% of the reported concentration for samples H-2.

[d] Concentration calculated using phenanthrene-d$_{10}$ as the internal standard; all other concentrations computed based on 1-n-butylpyrene as the internal standard for samples H-2.

[e] Not detected.

[f] Only PAHs common to both analyzes (NBS and EC) are included in the sum.

[g] This number represents the sum of penanthrene and anthracene.

TABLE 7. MEAN PAH CONCENTRATION FOR ALBERTA SWEET CRUDE OIL SMOKE SAMPLES COLLECTED AT AMBIENT TEMPERATURE[a]

No.[b]	PAH	C-5,#1 µg/g[c]	C-5,#2 µg/g	C-7,#1 µg/g	C-7,#2 µg/g
	Acenaphthylene			35	59
	Acenaphthene			N.D.	1.2
	Fluorene			126	140
1.	Phenanthrene	905	1040	1217[e]	1223[e]
2.	Anthracene	257	291		
3.	Fluoranthene	695	725	738	721
4.	Acephenanthrylene	384	397		
5.	Pyrene	903	839	795	779
6.	Benzo[ghi] fluoranthene	243	220		
7.	Cyclopenta[cd] pyrene	535	538		
8.	Benz[a]anthracene	217	222	237	223
9.	Chrysene/ Triphenylene	215	226	219	217
10.	Benzo[b,j,k] fluoranthene	384	394	421	410
11.	Benzo[e]pyrene	122	121	179	173
12.	Benzo[a]pyrene	238	184	206	196
13.	Perylene	42	41	45	47
14.	Indeno[1,2,3-cd] pyrene	185	188	535	532
15.	Benzo[ghi]perylene	209	206	176	175
	Total PAH Conc.[d]	4372	4186	4768	4696

---

[a] The samples C-5 were analyzed at the National Bureau of Standards and the samples C-7 were analyzed by Environment Canada.

[b] Peak identification numbers for Figures 10-13.

[c] µg of PAH/g of smoke; uncertainty estimated to be ±10% of the reported concentration for samples C-5.

[d] Only PAHs common to both analyzes (NBS and EC) are included in the sum.

[e] This number represents the sum of phenanthrene and anthracene.

The analysis performed by EC involved spiking the samples with 5 internal standards: anthracene-d_{10}, pyrene-d_{10}, benz[a]anthracene-d_{12}, perylene-d_{12}, and fluoranthene-d_{10}. The recovery percent used in the analysis was the average of the first four internal standards given above and corresponded to a value of 60 to 70%. The recovery percent of fluoranthene-d_{10} was 20% to 60% larger than the other standards and was not included. Generally speaking, there was more variability in the recovery percent for these smoke samples than is typically observed by EC for other samples.

Two diluted samples were collected simultaneously throughout most of the 900 second test in order to obtain enough sample for analysis. This is the reason for the good agreement between C-5,#1 and C-5,#2 and between C-7,#1 and C-7,#2 in Table 7. The high temperature samples were obtained sequentially. It appears from Table 6 that the sample H-2,#2 and sample H-4,#2, which are collected in the latter part of the burn, are enriched in the larger, lower vapor pressure PAHs.

It is apparent from both the Figures 10-13 and Tables 6 and 7 that the samples collected at the lower temperature are enriched in PAH content. The sum of selected PAH concentrations for 12 species listed in Table 7 is 4200 to 4800 μg/g smoke for the diluted sample and 900 to 2700 μg/g smoke for the high temperature collection. For the three and four ring PAHs, the enrichment for the lower temperature sample is at least a factor of 15 greater than the high temperature samples based on the NBS analysis and a factor of 3-20 enrichment base on EC. The enrichment in anthracene and fluoranthene observed in these tests is at least a factor of 2 greater than observed for PAH collected as a function of filter temperature in the laminar premixed sooting combustion of benzene [11].

The agreement between the NBS and EC results for the diluted samples is typically 10-20% with Indeno[1,2,3-cd]pyrene as the one exception. There is also a significant difference between laboratories for this species for the high temperature collection. Overall the EC results for the high temperature collection are about twice the NBS results with the largest differences observed for the smaller PAHs.

It is expected that the diluted samples better represent the chemistry of smoke collected downwind of a crude oil burn given the cooling the smoke would naturally experience as the smoke plume rises up and entrains air. The combustion conditions including flame size, availability of O_2, and the degree of mixing together with the fuel chemistry have been shown to affect the PAH emission [11].

It is known that the crude oil fuels themselves have a PAH component. It is of interest to compare the amount of selected PAHs per gram of fuel versus the amounts of PAHs collected in the smoke per gram of fuel consumed. As seen in Table 8, the relative concentration of the PAHs is different in the fuel compared to the smoke. For example, the concentration of phenanthrene plus anthracene in the fuel (296 μg/g) is about 2 times greater than for the smoke (133 μg/g fuel burned), while the concentration of benzo[a]pyrene (BaP) is a factor of three lower for the fuel (5 μg/g) compared to the smoke (18 μg/g). This indicates that the combustion process itself is generating specific PAHs and that the PAH content of the fuel will not represent the distribution of PAHs emitted. There is about a four-fold enrichment of the four-six ring PAHs in the smoke compared to the crude oil.

BaP has been used as a surrogate for the overall carcinogenic effect of PAHs. The higher BaP concentration in the smoke relative to the fuel is of environmental concern; however, several key issues must be addressed before a

TABLE 8. COMPARISON OF PAH CONTENT OF ALBERTA SWEET CRUDE OIL AND SMOKE FROM BURNED OIL

No.[a]	PAH	Crude Oil µg/g[b]	Smoke µg/g[c]
	Acenaphthylene	61	
	Acenaphthene	N.D.	
	Fluorene	188	
1.	Phenanthrene	296[d]	104
2.	Anthracene		29
3.	Fluoranthene	22	73
4.	Acephenanthrylene		40
5.	Pyrene	21	84
6.	Benzo[ghi] fluoranthene		22
7.	Cyclopenta[cd] pyrene		54
8.	Benz[a]anthracene	N.D.	22
9.	Chrysene/ Triphenylene	30	23
10.	Benzo[b,j,k] fluoranthene	N.D.	39
11.	Benzo[e]pyrene	21	12
12.	Benzo[a]pyrene	5	18
13.	Perylene	N.D.	4
14.	Indeno[1,2,3-cd] pyrene	N.D.	19
15.	Benzo[ghi]perylene	N.D.	21
Total Conc. of PAHs		395	448

---

[a] Peak identification numbers for Figures 10-13.

[b] µg PAH/g crude oil. Analysis performed by Environment Canada.

[c] µg PAH/g of crude oil burned assuming smoke emission factor, ε, of 0.10 and PAH emission data from C-5, #2. Analysis performed by NBS.

[d] This number represents the sum of penanthrene and anthracene.

full assessment of PAH emission can be made. The effect of burning rate on PAH emission should be analyzed. Smoke was not collected during the very rapid burning stage near the end of a test, but this burning phase may be dominant in a large fire with a thin oil layer. Preliminary data indicate for the first time the existence of nitrogen containing PAHs in smoke from burning crude oil. The concentration is apparently low being at the lower limit of the present analysis, so that additional analysis at great resolution is need to clearly evaluate the present findings. An analysis of the vapor phase PAHs should be made to complete the present analysis that has concentrated on condensed phase products.

PLUME DISPERSAL ANALYSIS

The object of this analysis is to develop a methodology which will permit the prediction of smoke dispersal generated by one or more oil spill fires in close proximity. In order to allow for the possibility of large composite fires, there are three main ingredients that must be taken into account in the analysis. They are the stratification of the atmosphere, ambient winds, and the properties of the initial fire plume. The scale of the phenomena to be considered is roughly 1-3 kilometers in the vertical (the plume rise height), a comparable spread laterally in a direction perpendicular to the ambient wind, and anywhere from 20 to 200 kilometers in the downwind direction.

Given the scale of these plumes, the Reynolds or Grashof numbers of the associated flow patterns are enormous, and a description which omits molecular diffusion of mass, momentum and energy is reasonable. The transport of smoke aerosol, the object of primary interest, is dominated by large scale advection. We are not concerned with the initial establishment of the plumes, so that a steady state picture of the dispersal process is appropriate. Under these circumstances the equations expressing the conservation of mass, momentum, and energy in the flow take the form:

$$(\vec{U} \cdot \nabla) \rho + \rho \nabla \cdot \vec{U} = 0$$

$$\rho \left\{ (\vec{U} \cdot \nabla) \vec{U} \right\} + \nabla P - \rho \vec{g} = 0 \qquad (3)$$

$$\rho C_p (\vec{U} \cdot \nabla) T - (\vec{U} \cdot \nabla) P = 0$$

Here ρ, $\vec{U}$, P, and T are respectively the density, velocity, pressure and temperature in the atmosphere. The quantity $\vec{g}$ is the gravitational acceleration and C_p the specific heat of the gas. The conservation laws are supplemented by an equation of state

$$P = \rho RT \qquad (4)$$

This system of equations must be solved subject to boundary conditions which introduce the three ingredients which characterize the flow of interest. The ambient atmosphere is stratified with a scale height H given by:

$$H = P_o/\rho_o g \qquad (5)$$

Here, the subscript indicates reference sea level values. The ambient atmosphere is assumed to vary on a larger scale in the horizontal directions than any length scale of interest in this study. The atmosphere then will depend only upon the vertical variable in the form y/H. Thus, far from any fire plume:

$$\begin{aligned} P &= P_o \ \hat{P}_a(\hat{y}) \\ \rho &= \rho_o \ \hat{\rho}_a(\hat{y}) \qquad (6) \\ \hat{y} &= y/H \end{aligned}$$

The ambient wind is assumed to vary with height but flow in a constant direction. The windward direction is the x-direction, the vertical coordinate is y, and the lateral direction perpendicular to x and y is z. The corresponding velocity components are u, v, w. Thus:

$$\vec{x} = (x,y,z)$$

$$\vec{U} = (u,v,w)$$

The boundary condition far from any plume can then be expressed in the form:

$$\begin{aligned} u &= U_o \hat{u}_a(y) \\ & \qquad\qquad (7) \\ v &= w = 0 \end{aligned}$$

Finally, the input from the fire plumes must be prescribed. It is not possible to calculate anything in or near the combustion zone based on equations (3) and (4), since the small scale physical and chemical processes are not described by these equations. There is no point appending the additional terms required, since we cannot even solve the above equations without further approximation. Instead, the vertical velocities and temperatures characteristic of a fire of prescribed strength are used as input variables. McCaffrey [12] has developed a set of correlations for fire plume velocities and temperatures which are ideal for this purpose. These correlations have been used to calculate inflow velocities into oil spill fires by the authors [1]. The time average vertical velocity and temperature distributions have the form:

$$\begin{aligned} v &= (gD)^{1/2} \ V\ (y/D) \exp\left[-(r/R)^2\right] \\ (T - T_o)/T_o &= \theta\ (y/D) \exp\left[-\alpha(r/R)^2\right] \\ D &= (Q/\rho_o C_p \sqrt{g})^{2/5} \qquad (8) \\ r^2 &= (x - x_c)^2 + (z - z_c)^2 \end{aligned}$$

Here Q is the total rate of heat release from the fire centered at (x_c, z_c). The plume centerline velocity V (y/D), temperature θ (y/D), and width R(y/D), together with the ratio of velocity to thermal profile with α are given by McCaffrey [12].

Note that there is no need to use these plume input functions at ground level. In practice, it would be desirable to select an attitude y_o where the excess temperature is sufficiently small and the plume sufficiently broad that equations (3) can be adequately solved in the presence of the wind that disperses the plume. As y_o increases, this condition becomes easier to meet for a given fire (or fires). On the other hand, we wish to begin the calculation at an altitude sufficiently low so that the wind has not yet had much of an effect on the plume, and distinct fire plumes have not yet merged. For individual fires in the range 10^2 - 10^3 MW, this altitude should typically be in the range 50 - 150 M.

As mentioned above, it is necessary to simplify equations (3) if reasonably accurate numerical solutions are to be obtained without prodigious computational efforts. As a practical matter, it is much easier to solve these equations if the numerical method can march in the direction of the wind and solve a two-dimensional problem in each cross flow plane. Moreover, we would like to reduce the equations to an equivalent incompressible form previously used to study flows generated by enclosure fires [13,14]. To this end, it is more convenient to work with the potential temperature θ, rather than the temperature itself. By definition we have:

$$T = T_o \; (P/P_o)^{(\gamma-1)/\gamma} \theta \tag{9}$$

The energy equation and equation of state now take the following form:

$$\begin{aligned} &(\vec{U}\cdot\nabla)\,\theta = 0 \\ &(P/P_o)^{1/\gamma} = (\rho/\rho_o)\,\theta \end{aligned} \tag{10}$$

In order to simplify the equations to the form desired, we introduce dimensionless dependent variables and a small parameter δ as follows:

$$\begin{aligned} &\theta = 1 + \delta\, \hat{\theta}_A(\hat{y}) + \delta\, \theta\, (\hat{x},\hat{y},\hat{z}) + \cdots \\ &\rho/\rho_o = \hat{\rho}_A\, (\hat{y}) + \hat{\rho}\, (\hat{x},\hat{y},\hat{z}) + \cdots \\ &P/P_o = \hat{P}_A\, (\hat{y}) + \delta \hat{P}\, (\hat{x},\hat{y},\hat{z}) + \cdots \\ &(v,w) = V_o\, (\hat{v}[\hat{x},\hat{y},\hat{z}] + \cdots,\ \hat{w}[\hat{x},\hat{y},\hat{z}] + \cdots) \\ &u = U_o \left\{ 1 + \delta^2 \hat{u}_A\, (\hat{y}) + \delta^2 \hat{u}(\hat{x},\hat{y},\hat{z}) + \cdots \right\} \end{aligned} \tag{11}$$

The parameter δ is defined by the relations:

$$\begin{aligned} \delta &= Q/\rho_o C p T_o H^2 V_o \\ H &= P_o/\rho_o g \\ V_o &= (Qg^2/P_o C p T_o)^{1/3} \end{aligned} \qquad (12)$$

Finally, the independent variables are defined in terms of the scale height and δ:

$$x = (H/\delta)\,\hat{x},\quad y = H\hat{y},\quad z = H\hat{z} \qquad (13)$$

We also assume that the ambient wind U_o is much larger than Vo by a factor of order of magnitude δ. Thus we can introduce a parameter K of order unity in δ such that:

$$V_o = \delta K U_o \qquad (14)$$

The scaling laws implied by the expansion defined in equations (11)-(14) are consistent with the following physical picture. The atmospheric motion is nearly but not quite adiabatic. The small excess temperature remaining in the plume and departures in the ambient atmosphere from neutral stability (adiabaticity) are responsible. Similarly, the atmospheric winds are nearly uniform and much larger than the vertical buoyancy induced velocity. However, since we are interested in downwind dispersal over distances much larger than the plume rises, the buoyancy effects cannot be neglected. When all these relations are substituted into the first two of equations (3) and equations (10), the following dimensionless system results:

$$\begin{aligned} &\frac{\partial \hat{v}}{\partial \hat{y}} + \frac{\partial \hat{w}}{\partial \hat{z}} + \frac{d \log \hat{\rho}_A \, \hat{v}}{d\hat{y}} = 0 \\ &\frac{\partial \hat{v}}{\partial \hat{t}} + \hat{v}\frac{\partial \hat{v}}{\partial \hat{y}} + \hat{w}\frac{\partial \hat{v}}{\partial \hat{z}} + \frac{\partial \Phi}{\partial \hat{y}} - \hat{\theta} = 0 \\ &\frac{\partial \hat{v}}{\partial \hat{t}} + \hat{v}\frac{\partial \hat{v}}{\partial \hat{y}} + \hat{w}\frac{\partial \hat{v}}{\partial \hat{z}} + \frac{\partial \Phi}{\partial \hat{z}} = 0 \\ &\frac{\partial \hat{\theta}}{\partial \hat{t}} + \hat{v}\frac{\partial \hat{\theta}}{\partial \hat{y}} + \hat{w}\frac{\partial \hat{\theta}}{\partial \hat{z}} + \hat{v}\frac{\partial \hat{\theta}_A}{\partial \hat{y}} = 0 \end{aligned} \qquad (15)$$

Two new variables have been introduced into equations (15). They are:

$$\begin{aligned} &\hat{t} = K\hat{x} \\ &\Phi = \left\{ - \int_0^{\hat{y}} \rho_A(\hat{y})\;\Phi_A\;(\hat{y})\,d\hat{y} + \hat{P} \right\} / \rho_A \end{aligned} \qquad (16)$$

Those final substitutions have generated a system of equations very close to those solved by Baum et.al. [13]. The system is now explicitly two dimensional and time dependent with suitably scaled distance downwind playing the role of time. There are two significant differences, which will require modifications to earlier calculations before quantitative predictions can be made. First, the ambient stratification as by $\hat{\theta}_A$ and ρ_A appear in the equations in a fundamental way. Second, the enclosure walls built into the calculations in Ref. [13] must be removed. Still, the equations are close enough that it is worthwhile to see the kind of results which emerge from a related enclosure fire computation.

In order to make the calculations equivalent, we consider the problem of a "thermal" generated in the enclosure. To see why this is necessary consider the "floor" boundary conditions represented by equations (8). Since x is now the time like variable, the Gaussian forms used to represent the velocity and temperature profiles imply that the vertical velocity and temperature introduced at the floor of the two dimensional enclosure must be turned on and off rapidly. Figure 14 shows (potential) temperature contours shortly after the pulse is turned on. Recalling that the frame of reference is now a plane sweeping downstream with the ambient wind velocity, Figure 15 shows the plume just downwind of the fire. It is now bent over and barely connected to the "ground". Figure 16 shows the initial development of the typical counter-rotating vortex pair in the plume as it rises above the datum level much further downstream. Finally, in Figure 17 the vortex structure is quite pronounced. The plume structure this distance downstream would probably be strongly modified by stratification and the presence of plumes generated by other fires. Some indication of the latter effect might be inferred by considering this sequence to represent an infinite periodic array of plumes aligned perpendicular to the wind. However, definitive answers can only come from calculations based exactly on equations (15) with appropriate boundary conditions. Future work will focus on this problem.

SUMMARY

An experimental facility was completed to examine the burning conditions of crude oil in a 1.2 m diameter pool fire configuration. This facility permitted controlled burning experiments to be conducted under conditions representative of the radiation-dominated, turbulent flow regime of larger pool fires that might occur on the open ocean or in pools confined by broken ice. Tests with three different crude oils, ALBERTA SWEET, LA ROSA, and MURBAN were conducted using initial oil depths of 2 mm, 4 mm, 10 mm and 25 mm floated on a deep water layer.

At oil depths of 10 mm and 25 mm each oil exhibited two distinct burning stages. The first was associated with a progressive vaporization of the burning oil layer and the other with more intense, short duration burning in which the oil surface was churned and splattered by boiling water under the thin oil layer. For MURBAN crude oil, the steady burning resulted in energy release rates of 840 kW/m^2 which increased to 1860 kW/m^2 during the vigorous burning before extinction. Residual oil left on the water surface at the end of natural burning corresponded to a uniform layer depth of 0.6 mm to 1.2 mm. The rate of heat conduction into the oil during burning was estimated to be less than 20 percent of the incident radiant energy directed at the surface. Additional tests are planned to characterize the radiation to the oil surface. Several instrumentation problems must be overcome in order to obtain more

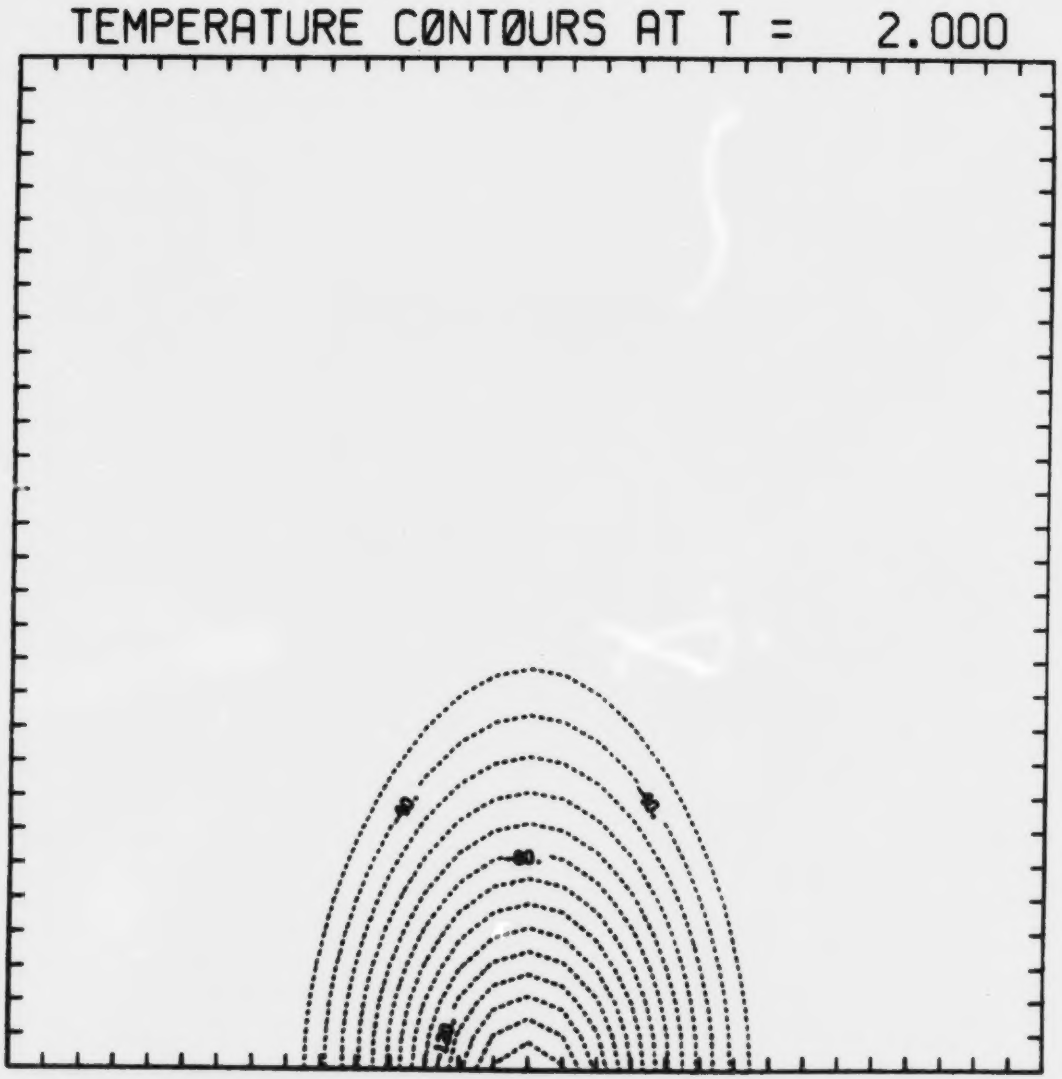

FIGURE 14. TEMPERATURE CONTOURS AT FRONT OF WIND BLOWN PLUME USING TRANSIENT ENCLOSURE FLOW ANALOGY.

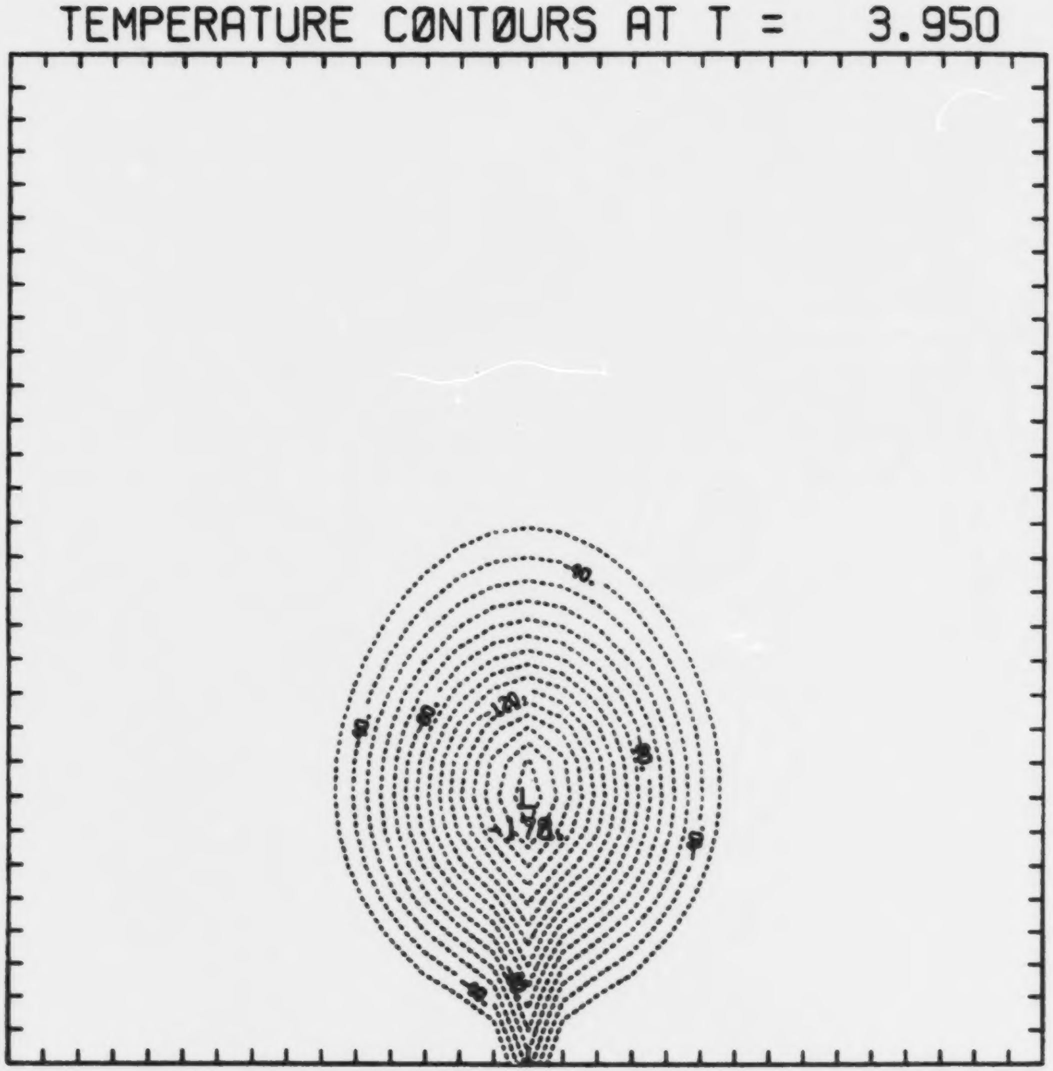

FIGURE 15. TEMPERATURE CONTOURS JUST DOWNWIND OF FIRE USING TRANSIENT ENCLOSURE FLOW ANALOGY.

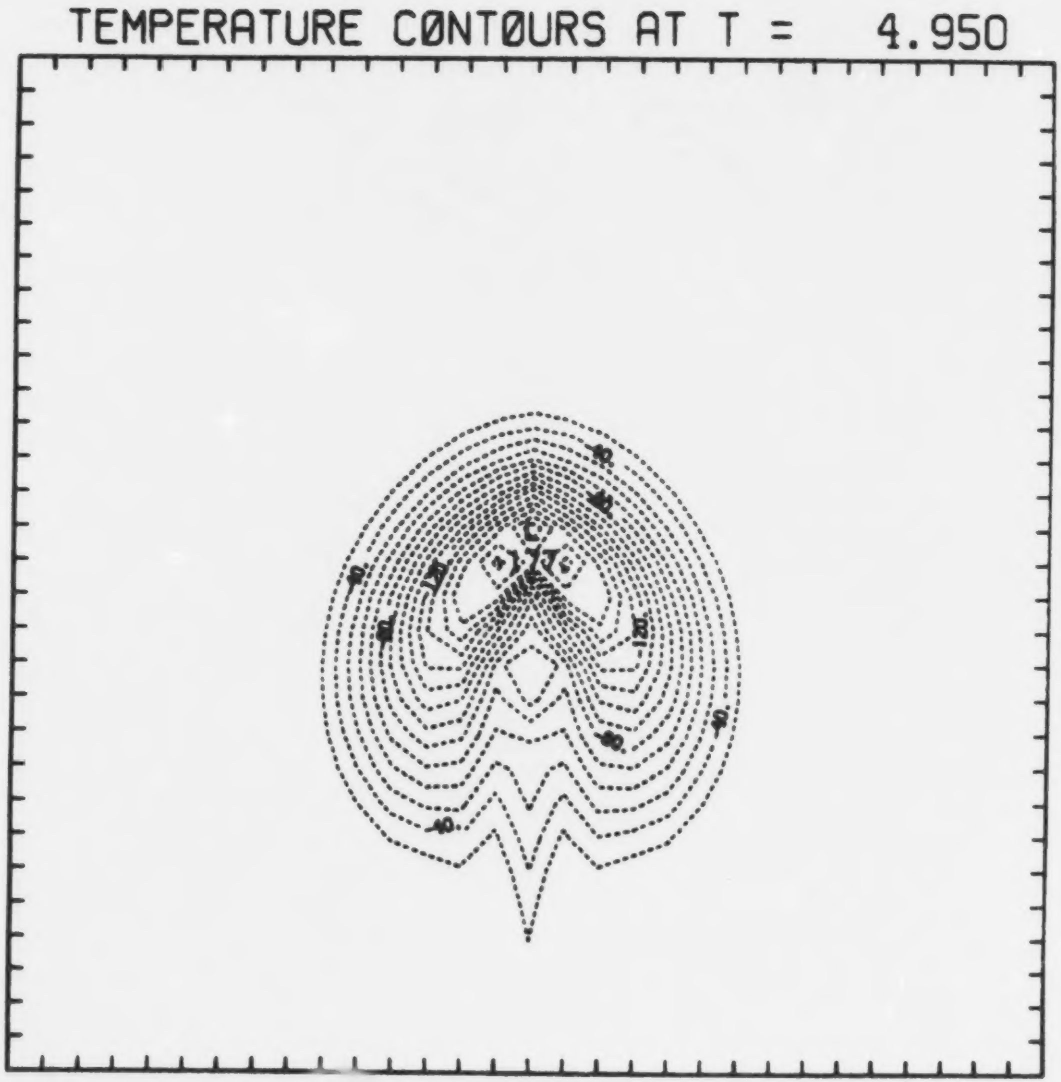

FIGURE 16. TEMPERATURE CONTOURS AT POINT OF VORTEX PAIR FORMATION USING TRANSIENT ENCLOSURE FLOW ANALOGY.

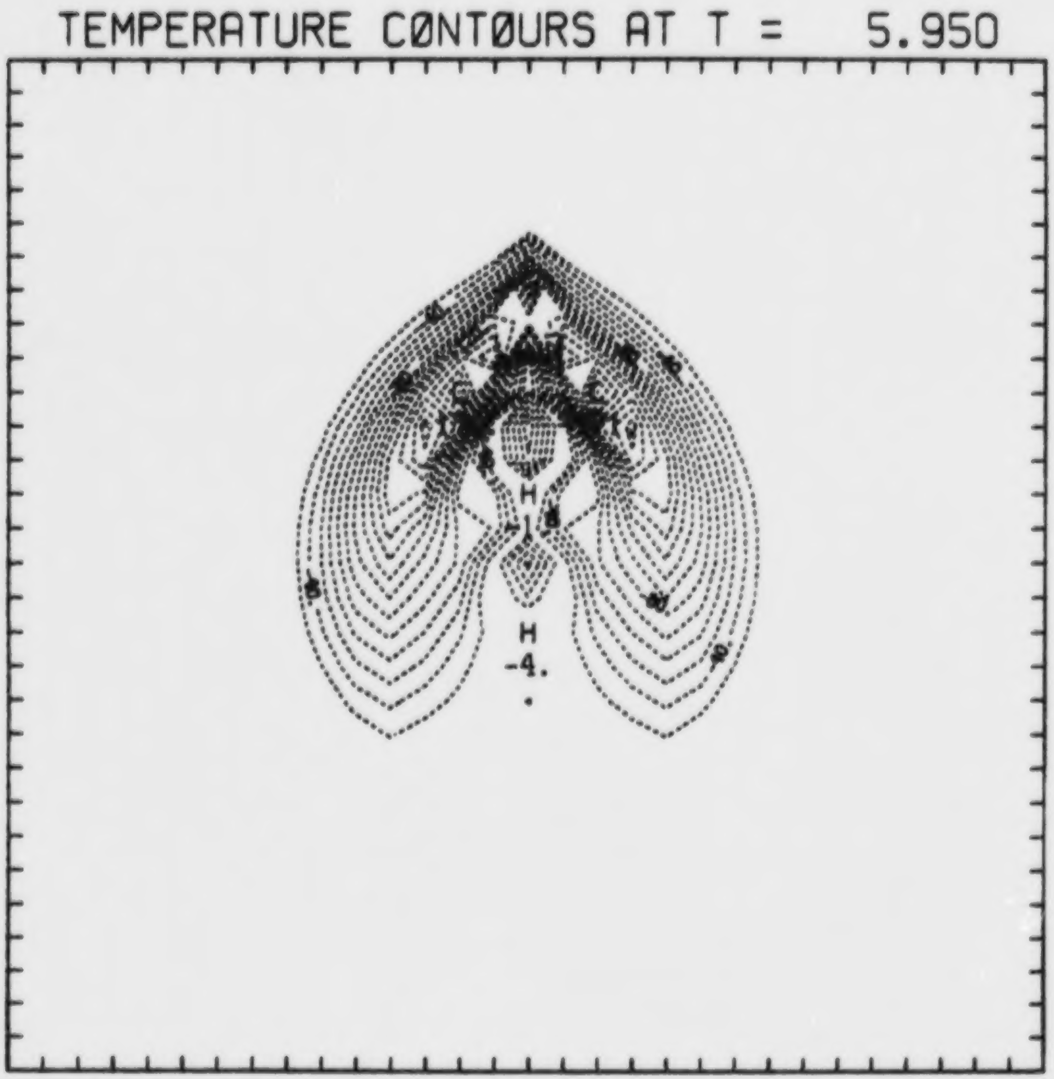

FIGURE 17. FAR DOWNWIND TEMPERATURE CONTOURS USING TRANSIENT ENCLOSURE FLOW ANALOGY.

reliable data. This new data will be used in an analysis of the surface energy balance for the burning crude oil.

The burning of ALBERTA SWEET crude oil results in a high smoke emission with ϵ about 0.10 (10% conversion to smoke). The smoke has a high elemental carbon component in excess of 90% resulting in a highly absorbing soot with a specific extinction coefficient, K_s, of 9.4 m^2/g. These values are similar to the values reported last year for PRUDHOE BAY crude oil. Over the 900 second period of burning, the values of both ϵ and K_f, the specific extinction coefficient relative to the fuel, increase and also the PAH emission shifts from smaller to larger structures as the fuel burns. Perhaps all of these effects are a result of a fractionation of the fuel with the sootier component burning last.

The primary gaseous product of combustion is CO_2 with the CO concentration about a factor of 25 lower than CO_2. The emission of NO and NO_x are less than one thousandth the concentration of CO_2.

Independent analyses of the PAH content of the smoke by the National Bureau of Standards and Environment Canada showed the same trends and had good overall agreement for 12 individual PAHs. The PAH content of the smoke was enriched in the larger species in comparison with the fuel. The concentration of benzo[a]pyrene, which is often used as a surrogate for the carcinogenic effect of PAH, was found to be three times greater in the crude oil smoke per gram of fuel consumed compared to the crude oil itself. The concentrations of the three ring PAHs were found to be very sensitive to the filter collection temperature. Thus, it is important to use a diluter when sampling the PAHs to simulate the conditions existing in a rising smoke plume.

Nitrogen containing PAHs have been observed in one of four crude oil smoke samples at concentrations near the lower limit of detection for the present analysis. This is a preliminary result obtained by Environment Canada and additional higher resolution analysis is needed.

An analysis of the dispersal of fire plumes by atmospheric winds was presented. It was demonstrated that as the plume buoyancy weakens with altitude and the plume gets bent over by ambient winds, the equations describing the dispersal process are greatly simplified. Physically, they are equivalent to studying the two-dimensional but time dependent process by which a buoyant thermal equilibrates with a stratified atmosphere at rest. Sample results of a similar process occurring inside an enclosure have been shown. This approximate model can be used to calculate realistic dispersion of oil spill combustion generated smoke with moderate sized computing resources.

ACKNOWLEDGEMENT

This work was supported under the joint sponsorship of the Minerals Management Service, U.S. Department of the Interior, Environmental Protection Service, Environment Canada, and the Office of Research and Development, U.S. Coast Guard.

Special thanks is extended to Mr. Edward Tennyson who was instrumental in organizing this program of research. Dr. M. F. Fingas was especially helpful in consultations about the chemistry and analysis of crude oils. The assistance of Mr. B. Benner and Dr. S. Wise was indispensible in the analysis for PAH compounds in the crude oil and soot.

The authors also wish to thank the many individuals on the CFR staff involved with the large scale testing effort among them were Dr. K. M. Tu, Mr. N. Bryner, Mr. J. S. Steel, and Mr. R. Zile.

REFERENCES

1. Evans, D., Baum, H., McCaffrey, B., Mulholland, G., Harkleroad, M., and Manders, W., "Combustion of Oil on Water", Proceedings of the Ninth Arctic Marine Oilspill Program Technical Seminar, June 10-12, 1986, Edmonton, Alberta, Ministry of Supply and Services Canada Cat. No. EN 40-11/5, 1986, 301 (1986).
2. Huggett, C., Fire and Materials 4, 61 (1980)
3. Bobra, M. A. and Chung, P.T., "A Catalogue of Oil Properties," Environment Canada Report No. EE-77, March 1986.
4. Healy, J. J., de Groot, J. J., and Kestin, J., Physica 82C, 392 (1982)
5. Yumoto, T, "Heat Transfer from Flame to Fuel Surface in Large Pool Fires," Combustion and Flame, 17, 108-110 (1970)
6. Petty, S. E. "Combustion of Crude Oil on Water," Fire Safety Journal, 5, 123-134 (1983)
7. Brosmer, M. A. and Tien, C. L. "Radiative Energy Blockage in Large Pool Fires," Combustion Science and Technology, 51, 21-37, 1987
8. Boyland, E., The Toxicology of Soot, Soot in Combustion Systems and its Toxic Properties, ed. by J. Lahaye and G. Prado, Plenum Press, New York, 13, 1981.
9. Johnson, R. L., Shah, J. J., Cary, R. A., and Huntzicker, J. J., An Automated Thermal-Optical Method for the Analysis of Carbonaceous Aerosol, in ACS Symposium Series, No. 167, Atmospheric Aerosol: Source/Air Quality Relationships, ed. by E. S. Macias and P. K. Hopke, 1981.
10. Wise, S. A., Benner, B. A., Chesler, S. N., Hilpert, L. R., Vogt, C. R., and May W. E., Characterization of the Polycyclic Aromatic Hydrocarbons from Two Standard Reference Material Air Particulate Samples, Anal. Chem., 58, 3068, (1986).
11. Longwell, J. P., Polycyclic Aromatic Hydrocarbons and Soot from Practical Combustion Systems, Soot in Combustion Systems and its Toxic Properties, ed. by J. Lahaye and G. Prado, Plenum Press, New York, 37, 1981
12. McCaffrey, B.J., "Momentum Implications for Buoyant Diffusion Flames", Combustion and Flame 52, 149 (1983).
13. Baum, H.R., Rehm, R.G., and Mulholland, G.W., "Computation of Fire Induced Flow and Smoke Coagulation", Nineteenth Symposium (International) on Combustion, The Combustion Institute, Pittsburgh, 921 (1982).
14. Baum, H.R., and Rehm, R.G., "Calculations of Three Dimensional Buoyant Plumes in Enclosure", Combustion Science and Tech. 40, 55, (1984).

MODELLING OIL SPILLS IN LEADS: WIND/WAVE TANK TESTING AND PRELIMINARY RESULTS

I.A. Buist, S.P. Joyce and S.L. Ross

S.L. Ross Environmental Research Limited
Ottawa, Ontario

INTRODUCTION

Several research programs have been devoted to the modelling of oil spills in Arctic waters. These have resulted in a number of oil spill fate models that tend to fall into certain categories as defined by Mackay (1986): (i) open-water trajectory models which may include interaction with shorelines; (ii) open-water behaviour models which describe the changing properties and configuration of oil spills with time; (iii) descriptions of oil behaviour on shore; (iv) descriptions of oil behaviour in rising blowout plumes beneath open water or an ice-covered surface; and (v) descriptions of oil movement under ice. There is, however, a lack of model capability treating the situation in which a spill on water is subjected to freezing conditions or a developing ice field (Bobra and Fingas 1986).

Spilled oil would be exposed to such a developing ice field if it found its way into pack ice leads in below-freezing temperatures. Leads are long linear regions of open water formed when sheets of pack ice diverge. These leads will often open and close depending on wind stresses, water currents, and ship traffic. Birds, seals, polar bears, and walrus often gather in these open water areas making leads one of the most biologically sensitive areas in ice-covered waters.

Various experimental studies have investigated the fate of oil spilled on water or in ice during freezing conditions. Perhaps the earliest of these was conducted near Ottawa in 1972 (Scott and Chatterjee 1973). These tests involved pouring 100 litres of Norman Wells crude onto a 13 m^2 area of open fresh water on an ice covered pond. Weather conditions were monitored continuously, as were the physical and chemical properties of the oil as time progressed. For the first 12 days following the release, the air temperature was generally in the 0°C range and no freezing occurred. On day 13, colder temperatures and snowfall led to incorporation of the weathered oil into slush and the eventual encapsulation of the oil in frozen slush.

Similar results were obtained on a larger scale as part of the Balaena Bay experiments (NORCOR 1975). In this experiment 400 litres of Norman Wells crude was spilled in a 36 m^2 open water area. The oil was mixed with blowing snow in -10 to -40°C temperatures to form oiled slush and was eventually encapsulated. In this and the 1972 experiment, the oil remained on the surface and was affected primarily by evaporation until snowfall caused an oil-snow mulch to develop and encapsulate the oil by freezing. These experimental results were verified at an actual spill in Buzzards Bay (Deslauriers 1978) where the effect of snow greatly hindered cleanup and restricted aerial observation.

Cold room wave tank tests were performed by Martin (1980) to investigate the interaction of Prudhoe Bay crude oil with grease ice. It was observed that oil released in front of the grease ice was rapidly transported into the ice and pumped onto the ice beyond the "dead" zone where wave action was damped out. Some oil droplets remained circulating in the grease ice ahead of the dead zone.

This pumping action was also noted by Metge and Telford (1979) and during the Kurdistan spill (C-CORE 1980).

The fate of oil in a closing lead was investigated by MacNeill and Goodman (1985). In this experiment, leads 1 m wide were created in an outdoor test basin containing 30 cm thick ice. Oil was poured into the leads and they were manually closed at varying rates. It was concluded that very little oil ends up beneath the ice surface and that the amount pumped onto the surface of the adjoining edges increases with increasing closure rate from 20% at 6 cm/s to 80% at 12 cm/s. It was noted that lead closure did not cause oil to flow along the lead using a viscous crude for a test oil.

Small scale tests were performed by Wilson and Mackay (1986) in a hoop tank apparatus to investigate the incorporation of various oils in developing grease ice under agitated conditions. They concluded that the amount of oil entrained in ice was increased as a function of the density and viscosity of the oil, the presence of sufficient turbulence, the formation of water-in-oil emulsions and the fineness of the ice particle size (the optimum size was 5 mm). They also indicated that under quiescent conditions, the presence of an oil slick may delay the onset of freezing, though under agitated conditions it may not.

OBJECTIVE OF STUDY

The objective of the study was to develop a computer model to predict the amount of oil available for countermeasures as a function of time, initial oil properties and environmental conditions, in the event of a significant oil spill in a pack ice lead. A review of the above and other past work indicated that more experimental data would be required to construct the model. Information was still missing on 1) the spreading rate and wind herding of oil on frazil and grease ice over a range of development stages; 2) weathering rates of oil in freezing situations; and 3) data on the fraction of oil remaining as a surface slick as a function of freezing. Before modelling could proceed it was necessary to develop experimental information in these missing areas. This was accomplished by conducting work in the wind/wave tank at the S.L. Ross laboratory and at the National Research Council outdoor manoeuvering basin in Ottawa. This paper presents the results of the wind/wave tank studies.

EXPERIMENTAL METHODOLOGY

Wind/Wave Tank as a Simulator

Figure 1 shows the wind/wave tank at the S.L. Ross laboratory. The tank is 11 m long by 1.2 m wide by 1.2 m deep. A large fan and ductwork allow the passage of outside air over the water surface at varying wind speeds. A wave paddle is used to mechanically generate waves of varying amplitude and period. The tank was fitted with a 40 cm wooden barrier 7.2 m from the upwind edge. This section of the tank simulates a small 1.2 m wide section of a pack ice lead at the downwind edge.

Ice formation in the freshwater tank was found to be very similar to ice formation in actual pack ice leads as described by Dickins et al. (1986). Ice crystals formed in the open water area and drifted down the length of the tank to pile up against the fixed barrier to formed grease ice. Without mechanically generated waves the grease ice eventually forms a dense dead zone where it behaved as a solid. Allowed to continue, the entire tank became covered with slush ice which formed a hard impermeable layer on the surface.

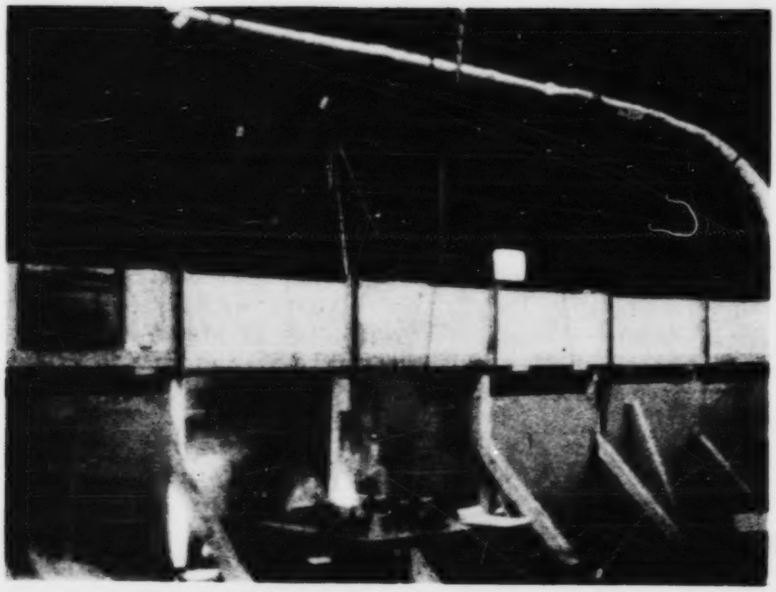

FIGURE 1

Wind/wave tank

		S_1			S_2		
		I_1	I_2	I_3	I_1	I_2	I_3
W_1	O_1		Run 9		Run 1 Run 2	Run 3	Run 4
	O_2					Run 13	
	O_3					Run 8	Run 12
W_2	O_1				Run 7	Run 6	Run 5
	O_2				Run 14		
	O_3					Run 10	Run 11

Figure 2 : Test Matrix

O_1, O_2, O_3 - Oil Type

I_1, I_2, I_3 - Initial Ice Maturity

W_1, W_2 - Wave Condition

S_1, S_2 - Wind Speed

In the presence of mechanically generated waves the same grease ice formation was observed but eventually became so thick that circulation within the ice was suppressed and the surface froze into chunks of "pancake" ice floating over a grease ice layer. The pancakes formed in the tank were generally circular with a diameter of about 30 cm and slightly turned up edges. This phenomenon of pancake ice formation was well documented by Martin (1980) and Metge and Telford (1979).

The wind/wave tank set-up can be considered to be an approximate full-scale representation of a spill situation in which a lead has opened up and oil has found its way into the open water or forming ice field. Since the oil in this situation will quickly spread and drift to the downwind edge of the lead, the tests in the wind/wave tank can be used to predict the fate and behaviour of the oil at the downwind edge as the ice growth progresses under the influence of a variety of different environmental conditions.

Test Matrix

The ability of an ice field to retain quantities of oil within its structure is presumably a function of the oil's density, viscosity, and interfacial tension as well as the thickness of the oil layer, the porosity of the ice field and the level of turbulence present.

The four easily adjusted variables of: windspeed, oil type and volume, wave height, and initial ice maturity were chosen to form the test matrix (Figure 2) since they incorporate all of the parameters thought to affect the interaction of oil and developing ice. Since each run took up to 24 hours under the right conditions, it was not possible nor was it thought necessary to do all of the tests in the matrix.

One crude oil, Mixed Sweet Western (MSW) and two mixtures of Bunker C and automotive diesel were used as test oils. Table 1 shows the properties of the oil types.

Three distinct ice maturities were identified. I_1 represents no initial ice present. I_2 is a covering of grease ice at the barrier up to about 15 cm thick and to 50 cm from the barrier. The I_3 condition occurred after the transition from slush-like grease ice to a semi-solid but malleable mass of dense grease ice. When waves were present, the I_3 condition was pancake ice.

TABLE 1: TEST OIL PROPERTIES

Oil Type	**Test Temp.**	**Density (g/cm^3)**	**Dynamic Viscosity (mPas)**	**Kinematic Viscosity (mm^2/s)**
Bunker C[1]	1°C	1.025	2,310,000	2,253,658
Diesel[2]	0°C	0.838	3.9	4.65
MSW[2]	0°C	0.847	47.3	55.9
Bunker C/19% Diesel[1]	7.5°C	0.981	1480	1509
Bunker C/55% Diesel[3]	2°C	0.917	71.8	78.3

Source
1. Submergence Report (S.L. Ross 1987); 2. Catalogue of Oil Properties (Bobra and Chung 1986); 3. Measured

Two wave conditions, W_1 = no waves generated by the wave paddle and W_2 = mechanically generated waves, were also used as test variables. The windspeeds S_1 and S_2 were 3.5 m/s and 7 m/s respectively measured with a hot-filament anemometer at 30 cm above the ice surface.

Experimental Method

The tank was filled with approximately 10,000 L of tap water to a depth of 0.85 m. The proper initial ice conditions were allowed to develop for each run with the artificial barrier in place and the blower turned on. If no initial ice was called for then the water was allowed to cool until ice crystals just started to appear. The inlet air temperature, the air temperature at the barrier and the water temperature were all recorded just prior to adding oil and at regular intervals thereafter. One litre of the test oil was added at room temperature with the fan momentarily shut off using a spill plate. The oil was spilled at least 1 m from the barrier so it could spread and cool before the wind herded it into the developing ice. The first five minutes of each run were recorded on video tape in order to observe wind herding behaviour.

When the wave paddle was not used, the experiment was allowed to continue until the surface of the tank was completely frozen over (including the area underneath the slick). When waves were artificially generated, the experiment was allowed to continue until the amount of oil remaining as a surface slick was thought to have reached equilibrium. The wave generator was then shut off and the surface of the tank allowed to freeze solid for analysis.

At the completion of each run, the area and thickness of the surface slick was measured or estimated. The slick was then removed with sorbent material from the surface of the ice. The remaining oil frozen in the ice was then separated and measured when possible or its percentage of the total was estimated. A short video tape was taken for each run before and after the surface slick was removed.

RESULTS

Figures 3 through 5 show numerical data for each run. A short description of each experiment follows.

Run 1

This initial run was primarily to evaluate and make changes to the test procedure. 500 ml of Mixed Sweet Western (MSW) was initially spilled. The water temperature in the tank was 2.5°C and the air temperature at the tank inlet and above the test area were -2.5 and 0.5°C respectively. There was no ice initially present and the wave generator was off. Another 500 ml of MSW was added 20 minutes later to bring the slick volume and area to a more reasonable level. The slick quickly spread and drifted to the barrier and the edges of the slick were swirling back into the centre in a cyclic motion. This unnatural behaviour was corrected for subsequent runs by moving the barrier farther down the tank. New ice crystals were forming 30 minutes after the start of the test and the tank was completely frozen over in 6 hours when the air temperature over the slick had dropped to -6°C. There was no oil incorporated into the developing ice in this run.

		S_1			S_2		
		I_1	I_2	I_3	I_1	I_2	I_3
W_1	O_1		0%		0%	6%	1%
	O_2					8%	
	O_3					0%	0%
W_2	O_1				20%	10%	2%
	O_2				30%		
	O_3					5%	1%

Figure 3 : Percentage of original volume frozen into ice

		S_1			S_2		
		I_1	I_2	I_3	I_1	I_2	I_3
W_1	O_1		8592		3120	3960	3456
	O_2					7200	
	O_3					960	255
W_2	O_1				3600	5100	14400
	O_2				5400		
	O_3					1700	4800

Figure 4 : Final surface area of slick (cm^2)

		S_1			S_2		
		I_1	I_2	I_3	I_1	I_2	I_3
W_1	O_1		0 (+3)		-7 (2)	-2 (0)	-7 (-3)
	O_2					-2 (+2)	
	O_3					-8 (-3)	-2 (1.5)
W_2	O_1				-16 (-9)	-6 (-2)	-5 (-1.5)
	O_2				-1 (1)		
	O_3					-4.5 (-1)	-1.5 (0)

T_{inlet}
(T_{air})

Figure 5 : Average temperatures during run

Run 2

Run 2 was a repeat of Run 1 with the barrier moved farther down and using one litre of test oil. The temperatures during the run were -8 and -3.5°C for the inlet and test area temperatures and 1.5°C for the water temperature. Ice started forming 2 hours and 10 minutes after the fan was started. After 3 hours and 20 minutes, the slick was on top of a fairly solid mass of grease ice. After 7 hours and 30 minutes the tank was completely covered with solid ice about 8 mm thick. Below this, there was a layer of fine crystals approximately 3 cm thick. A thickness sample of the surface slick showed it to be about 1 mm, although there seemed to be thicker patches present. All of the oil with the exception of a few scattered drops remained on the surface of the ice. The area of the surface slick was about 3120 cm^2 and it was located up against the barrier in the same position and shape as the wind originally herded it to before the ice growth.

Run 3

This run was similar to Run 2 except that an initial covering of slush ice was allowed to build up to 40 cm from the barrier before spilling the 1 L of MSW. The air temperature above the water was -3°C. The oil quickly herded to the edge of the grease ice and then slowly migrated across the surface of the grease ice to the barrier. It took about 3 minutes for the oil to completely spread on top of the slush ice. After 8 hours and 30 minutes the tank was frozen over and again the surface slick was found to have an area of 3960 cm^2 next to the barrier where the wind had originally herded it. After cleaning the surface slick with sorbent pads, it was found that a significant amount of oil had become trapped in the slush ice that was initially present. This remaining oil was removed and had a mass of approximately 54 g or slightly more than 6% of the original volume.

Run 4

Again 1 L of MSW was spilled under conditions of no waves and a windspeed of 7 m/s. This time there was about 80 cm of consolidated grease ice initially present. The air temperature was -3°C over the slick. The slick was quickly herded to the ice edge as in the previous run but then spread more slowly on top of it. Once the entire slick was on top of the ice, the spreading stopped completely. There was very little sideways spreading and the slick did not expand the full width of the tank. The run was stopped after about 1 1/2 hours since the surface slick was completely on top of the ice and was no longer exposed to developing ice. It was found that a small amount of oil was frozen into the ice at the water/ice edge. This made up less than 1% of the slick volume. The final area of the surface slick was about 3456 cm^2 and it was easily removed from the surface with sorbent pads.

Run 5

This began the series of experiments on the MSW oil type with waves being generated. Run 5 had a wave generator setting of 50 which corresponded to an amplitude of about 50 mm at the barrier and a wave period of 1.58 seconds. In this run there was a 1 m wide covering of slush ice in the tank just starting to form pancakes. The air temperature was -2°C. The slush ice thickness was about 20 cm. The oil quickly herded to the ice edge and then made its way to the barrier through the slush-filled spaces between pancakes within about 6 minutes. As the oil moved through the pancake ice field most of it was pumped onto the top of pancakes by the opening and closing motion of the spaces. The wave generator was stopped after 2 hours and the tank was allowed to freeze over. It was found that about 80% of the oil was deposited on top of the pancakes. Most of the remainder was stuck to the sides of the tank and the barrier. About 14 g was measured that was frozen in the ice (mostly at the edges of the pancakes) or less than 2% of the total volume. The area covered by the slick was about 14400 cm^2. It seemed to be evenly distributed throughout the initial ice cover.

Run 6

1 L of MSW was spilled with an initial grease ice cover to 50 cm from the barrier. The wave generator setting was again 50 and the waves at the barrier were 60 mm in height. The slick was herded quickly right across the top of the slush ice to the barrier. After 40 minutes, pancakes started to form and the crust around the edges was largely saturated with oil. There was evidence of weak (black) emulsion formation at the barrier and at the edges of the tank. The surface slick took up an area of 6100 cm^2. It was estimated that about 10% of the oil was frozen in the ice; mostly in the form of small droplets 1-2 mm in diameter. These were evenly distributed beneath the slick.

Run 7

The wave generator was set at 60 for a wave period of 1.36 seconds and a wave of 65 mm at the barrier. One litre of MSW was spilled with no ice initially present. The inlet temperature was extremely cold at -16°C giving an air temperature over the water of -9°C. In less than 2 hours, there was a covering of slush ice about 20 cm thick starting to form pancakes. The action of the waves on the oil against the barrier caused a significant amount of dispersion throughout the depth of the tank. This caused some of the oil to go under the barrier (which extended about 20 cm under water) and resurface or get trapped on the other side. Again there was weak emulsion formation noted at the edges of the tank. It was estimated that about 20% of the original oil volume became trapped in the ice.

Run 8

Run 8 was a repeat of the conditions of Run 3 (i.e. initial slush ice and a windspeed of 7 m/s) except a heavy Bunker C/diesel blend oil was used. The air temperature was -3 through most of the run. The heavy oil was quickly herded into one ribbon about 50 to 80 mm wide and 10 mm thick located at the edge of the ice. After 5 minutes, this slick slowly rolled up inside the grease ice border, The surface of the tank froze after 2 1/2 hours and the slick was removed easily from the ice surface with a spatula. As in the other experiments without waves, the oil slick remained in the same location as the wind originally herded it to.

Run 9

1 L of MSW was spilled with an initial grease ice cover and a slow windspeed of 3.5 m/s. The inlet temperature was 0°C and the temperature over the slick was +3 so the experiment was run overnight to get cold enough temperatures. It was noted that the slow windspeed did not herd the slick toward the barrier very much and natural spreading determined its area. After 14 hours the surface slick area was 8592 cm^2 and there was no oil at all in the ice underneath.

Run 10

1 L of Heavy Bunker C/diesel mix (O_3) was spilled with an initial slush ice cover about 40 cm wide and a wave generator setting of 50. The air temperature was +1.5 at the beginning of the run and dropped to -6 after 4 hours. The heavy viscous oil formed a ribbon at the grease ice edge as in Run 8 that slowly made its way to the barrier. From here the oil spread along both edges of the tank,

sticking to the walls along the way. There was very little emulsification as there was with the crude oil, 0_1. At the completion of the run, there was only about 30% of the oil remaining as a surface slick with approximately 5% frozen in the ice and 65% stuck to the sides of the tank and the barrier underwater.

Run 11

1L of 0_3 was added to the open water ahead of a 72 cm wide area of 11 cm thick pancake ice. The waves generator was set at 50 and the waves were 50 mm high at the barrier. The air temperature was -0.5°C. After 30 minutes the pancake ice had consolidated into 2 large chunks and most of the oil was in the space between them and on the adjacent edges. There was some migration down the space to the tank edges but the oil never did spread all the way to the barrier. After about 4 hours, the surface slick was removed with a spatula and sorbents. It was found that about 1% of the oil was trapped in the ice in scattered globs.

Run 12

An extremely heavy oil was mixed with 86% Bunker C and 14% Diesel for this run giving it a density of 0.995 g/cm^3 and a viscosity of 2570 mPas at 10°C. This oil was spilled in front of a consolidated grease ice area in order to see if the wind would push it underneath the ice edge. The wave generator was turned off. The oil formed a large blob about 3 cm thick at the edge of the ice and it floated low in the water but would not roll under or over the ice edge. After 15 hours, the ice around the blob was at least 3.5 cm thick but there was no ice underneath the oil. None of the oil was completely encapsulated in the ice although it was sunk in about 1.5 cm.

Run 13

The 45% Bunker C diesel mix, 0_2 was added to the open water ahead of a small area of grease ice. The wave generator was off. The air temperature was +2 at the time of the release but there were colder temperatures overnight. The slick was herded quickly over the grease ice to the barrier and remained there as the ice developed. After 12 hours, it was found that about 8% of the oil was frozen in the ice in fairly large blobs and distributed throughout the area where the original slush ice was.

Run 14

0_2 was used in this experiment with the wave generator setting at 50 and no initial ice present. The air temperature was +1 at the beginning and dropped to 0 later. Figure 6 shows the results of this run after 11 hours. Most of the oil was on the surface either as a slick on top of the pancakes or in the form of a weak emulsion at the edges of the tank. An estimated 30% was frozen in the ice in small drops about 3-5 mm diameter, however as can be seen from Figure 7. This was largely due to the crystals scraping away at oil on the sides of the tank. Finer droplets were distributed throughout the ice cover.

Run 15

The purpose of Run 15 was to investigate the behaviour of a highly viscous oil. Hibernia B-27 was chosen since it is a waxy crude with a high viscosity but a density comparable to that of the MSW. It was added to the open water ahead of a grease ice area to 65 cm from the barrier. The oil migrated very slowly onto the slush ice surface. Figure 8 shows the slick shortly after release. About 1/2 of the slick was pushed on top of the ice and the rest stayed in open water. Slush ice eventually formed underneath it and stopped spreading

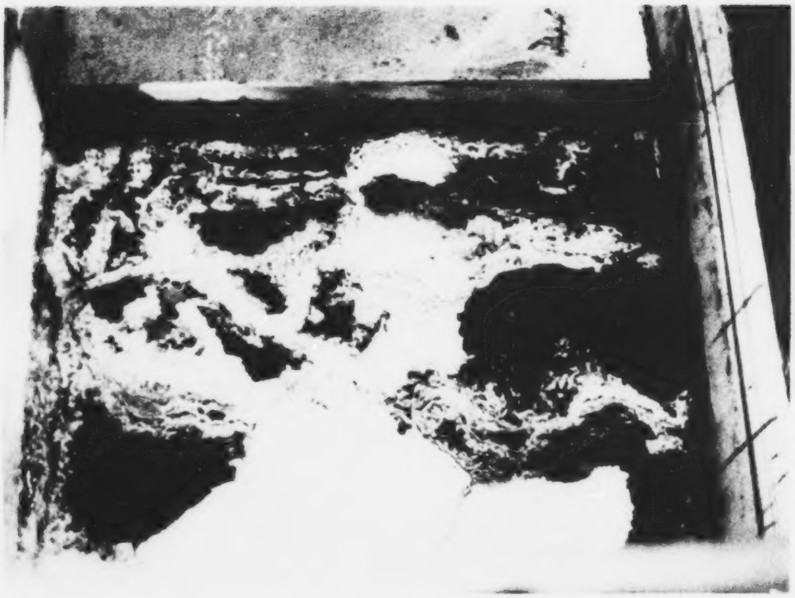

Figure 6: Oiled pancake ice; top view

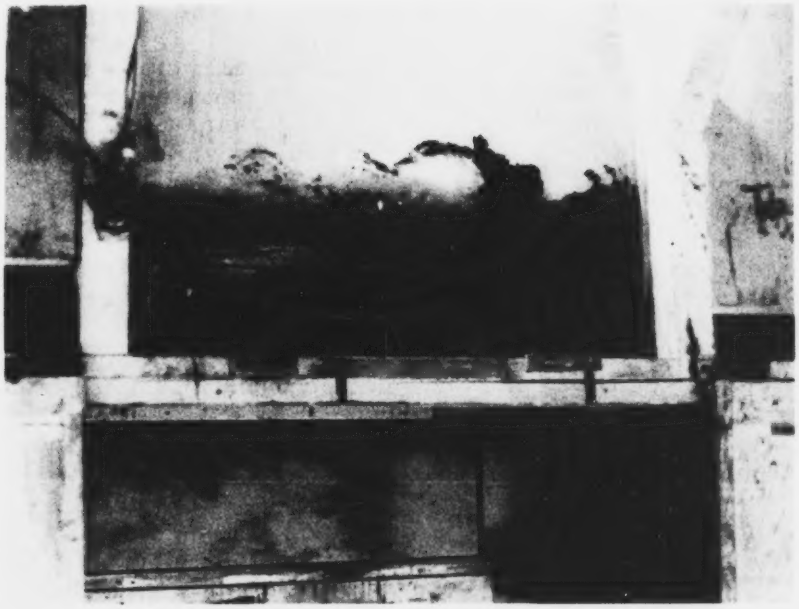

Figure 7: Oiled pancake ice; side view

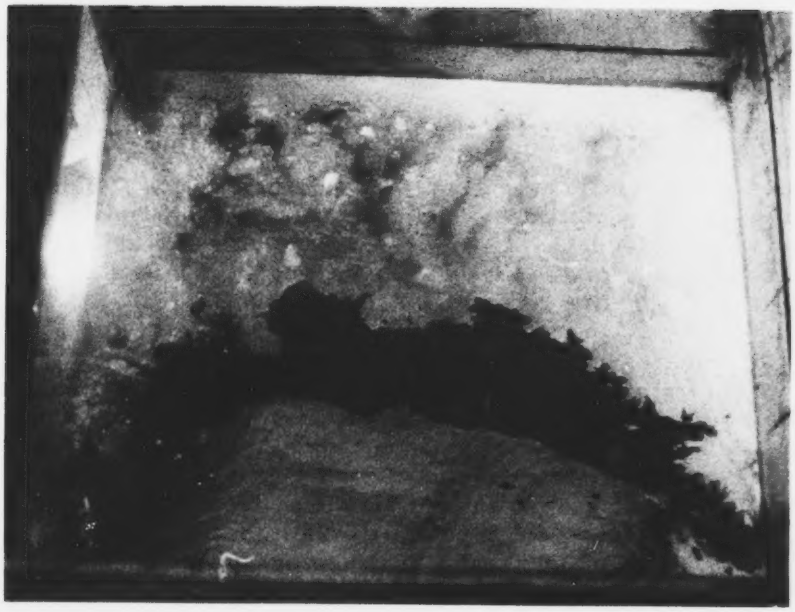

Figure 8: Wind herding of the slick into grease ice

altogether. 12 hours later the slick had moved about 20 cm forward but its area had not changed. The slick was easily removed from the surface of the ice and it was noted that it left a fairly deep impression in the ice surface.

DISCUSSION OF RESULTS

Effect of Wind Speed

Wind speed affects a number of processes that are important to oil fate and behaviour. Information already exists on: 1) the rate of evaporation (Mackay 1980), ii) the grease ice thickness and coverage time for a lead (Dickins et al. 1986), iii) the wave heights for a given lead, which were treated as a separate variable in these experiments, iv) the drift rate and final location of the slick, and v) the slick thickness and area due to wind herding (Energetex 1981). What remained to be determined from these experiments was the effect of wind on the distribution of oil in developing ice situations.

In order to accomplish this, it was originally thought that three different windspeeds would be required in the tank tests. After the first few experiments, however, it was decided that only two windspeeds would be required. In fact, only one test was performed with a windspeed of 3.5 m/s and all of the others were done at 7 m/s. The reasons for this were:

1. It was discovered that with the I_3 initial ice condition and no waves, the oil slick would quickly migrate across the open water and any fresh grease ice until it reached the dense dead zone. This effectively stopped spreading and drift. Similar behaviour was noted by Wilson (1979). Therefore, for modelling purposes, the dead zone can be treated as impermeable and wind herded slick thicknesses can be calculated from data on wind herding against a fixed barrier from experiments by Energetex (1981).
2. Difficulties were encountered in freezing the tank using windspeeds lower than 7 m/s, which was the maximum speed attainable with the blower used.
3. Other tests for this project conducted at a larger, outdoor tank in Ottawa (not discussed in this paper) provided good data on the behaviour of oil in freezing situations under quiescent and low wind speed conditions.
4. The one experiment with a 3.5 m/s windspeed showed a larger surface slick area as expected and no oil frozen into the ice. Lower windspeeds were not expected to give more useful results.

Effect of Oil Type

An oil's density and viscosity seem to be important for determining the amount of oil frozen in ice: density because it determines the buoyancy of the oil in the water or the water/grease ice mixture, and viscosity because it determines the oil's ability to break up into small enough particles to migrate through the porous grease ice and also because it affects the thickness of the slick. A higher oil density will increase the amount of oil frozen in the ice as shown consistently in the experiments for 0_1 and 0_2. These oils have similar viscosities but 0_2 is more dense. This relationship was also found by Wilson & Mackay (1986). The effect of viscosity is not as clear. There appears to be two different processes by which oil can become incorporated into the ice. The first is by infiltration from above as in Runs 3 and 13 where there were no waves and an initial grease ice cover. In this case the low viscosity oil tends to be encapsulated in large globs; a low viscosity seems to permit the oil to move through the ice crystals more freely. The highly viscous 0_3 was not encapsulated at all in run 8.

The second process was noted only when waves were generated. This involves dispersion of the slick into the water column and a resurfacing of the oil droplets to become trapped in the grease ice. In this case, a high viscosity would inhibit resurfacing through the grease ice, thus encapsulating the oil. The result is an even distribution of 1-2 mm diameter oil droplets in the final ice cover. This was the explanation used by Wilson and Mackay (1986) in their bench scale mixing experiments. However, the high viscosity may also somewhat inhibit dispersion of the slick to begin with. The experiments showed that there was more encapsulation with a non-viscous oil for the same wave and ice conditions. It therefore must be concluded that the amount of oil frozen in the ice decreases with viscosity by virtue of both processes.

Effect of Wave Condition

Waves are a significant factor in the interaction of oil and ice not only because they provide mixing energy but because they affect the process of ice formation and also induce dispersion of the slick into the water column. As previously mentioned, pancake ice forms in the presence of waves while a dense dead zone forms without them.

It was found that the fraction of oil incorporated into ice is increased considerably by wave action. Waves also have a large effect on the spreading of the slick. The oil seems to be able to spread readily in the slush around pancake ice as shown in Runs 5 and 11.

The experiments without waves showed that the slick rarely exceeds its wind herded slick area in all ice conditions. The pancake ice generated by waves caused two dimensional spreading that was not stopped until the oil was pumped on top of the pancakes or expanded to fill the test area of the tank.

Effect of Initial Ice Maturity

In the presence of mechanically generated waves, it was found that the amount of oil in the ice decreased with ice maturity. The major factor in determining the amount in the ice under wave conditions was dispersion of the slick and subsequent resurfacing of the droplets. This dispersion only happened when there was no ice present and to a lesser extent when there was slush ice present. The slush ice may dampen the wave action and also limit the downwelling currents necessary for dispersion. It is reasonable to assume that the final amount in the ice was related to the amount of time that the slick was exposed to open water dispersion or dampened slush ice dispersion. The presence of an initial ice cover only reduces or eliminates this exposure time. In addition, most of the dispersion occurred at the artificial barrier (which may not adequately represent a real lead situation) and when the slick was released in front of pancake ice, most of the slick was immobilized on the surface by the time the leading edge reached the barrier.

Without waves present, the effect of an initial ice cover was not the same. Significant amounts of oil in ice were found only when there was an initial grease ice covering. The oil moved into the grease ice layer from above probably because the density of the oil was very close to that of the grease ice. Thus, the oil has very little buoyancy in the grease ice and globs may sink and become encapsulated as the ice growth progresses.

OIL FATE MODEL

Assumptions and Scope

The model treats a situation in which a lead has opened up and oil is spilled sometime during the refreezing of the open lead. It does not consider closing leads since these account for only 17% of lead movements (Dickins et al. 1986) and would result in almost complete encapsulation of the oil into a pressure ridge except at high closure rates. Lead openings will not affect the ultimate fate of the oil since ice coverage time is independent of lead width (Dickins et al. 1986). The opening rate is also too unpredictable to be used as an input to the program.

Precipitation in the form of snow has been shown (Scott and Chatterjee 1973, Norcor 1975, S.L. Ross and D.F. Dickins 1987) to cause an oiled slush to form and completely encapsulate the oil, leaving no oil on the surface.

It is also assumed that temperature, windspeed, and wind direction are constant during the time it takes for the lead to freeze over. There is no accommodation of water currents which are typically small in leads, although this could be added to the model at a later date.

Emulsification is not considered in the model. Although some weak emulsions were formed in the wind/wave tank experiments, this was mostly due to the motion of the ice chunks with oil against the sides of the tank. It is not expected that such behaviour would be observed in an actual lead.

Changes to an Existing Model

At the time of writing the oil in leads computer model is being developed using an existing open-water oil fate model (S.L. Ross 1987a and 1987b) as a framework. The model was originally written in Fortran and was used to predict open water spreading, dispersion, evaporation and emulsification of spilled oil as well as chemical dispersion effectiveness. The model is based primarily on work performed at the University of Toronto over the past decade. Spreading is based on the model of Mackay et al. (1979) which utilizes the thick/thin approach. Oil evaporation is based on the evaporative exposure approach of Stiver and Mackay (1983) and subsequent oil property changes are determined using the approach of Tebeau et al. (1983). The routines for emulsification and dispersion are not used for the oil-in-leads model since they were developed for an open sea with mature wave conditions based primarily on wind speed. Leads are more quiescent environments that develop smaller waves over a limited fetch.

The model uses a large number of oil properties as input parameters. Much of this information is presently available in oil property catalogues published by Environment Canada (S.L. Ross 1985, Bobra and Chung 1986) or many Canadian oils. Other inputs include environmental conditions such as wind speed, water temperature and air temperature. The conditions of the spill include the spill volume and duration (batch spill or delayed release) and the geometry and initial ice conditions of the lead.

The model computes the behaviour of the oil in finite time steps of 100 seconds. During each program pass, an evaporation routine calculates a new fraction evaporated and a new oil volume and makes changes to the oil properties. The new slick area and thickness is calculated by a spreading routine. Also in each program pass, there is an increase in the area of the lead covered by grease ice. Depending on the spill conditions, a small amount of oil may become encapsulated in the developing grease ice and thus will be removed from the total volume available for evaporation and spreading. The program terminates when the lead is completely frozen over.

Ice Growth. The ice growth routine was developed using equations for grease ice formations reported by Dickins et al. (1986). These equations are:

$$P = 1.2 + 0.0312\ U\ (Tw - Ta) \qquad (1)$$

and

$$P = 3.0 + 0.0204\ U\ (Tw - Ta) \qquad (2)$$

where

P = production rate (kg/m^2/h)

U = wind speed (m/s)

Tw = water temperature (^{o}C)

Ta = air temperature (^{o}C)

U(Tw - Ta) = wind chill factor (^{o}C m/s)

Equation (1) is used for mild conditions (wind chill less than 200 ^{o}Cm/s), and equation (2) for severe conditions (wind chill greater than 200 ^{o}Cm/s), The final coverage thickness is estimated by H (m) = 0.06 U where U is the windspeed in m/s. The rate of ice cover can be calculated using the density of the grease ice (ρ_i) and the final thickness of the cover (H) as:

$$dA_I = \frac{P}{\rho_i H} \qquad (3)$$

where A_I is the ice coverage area in m^2 of ice per m^2 of open water remaining per hour. If the width of the lead (W) is known, the differential linear grease ice cover for one 100 second program pass is calculated by:

$$dL = \frac{P\ A_W}{\rho_i\ H\ W} \times 100 \times \frac{1}{3600} \qquad (4)$$

in linear metres of grease ice, where A_W is the open water area.

Spreading. During the time that the oil is in open water, the thick/thin spreading routine is called every 100 seconds. In small leads without mature wave conditions, the slick is allowed to spread until the centre of the slick reaches the grease ice edge. At this point it is assumed that the leading edge of the slick will have reached the dead zone and spreading is stopped.

Wind Herding. The oil slick on the open water is estimated to drift at 3% of the wind speed. Eventually it will encounter the downwind edge of the lead where drift and spreading will stop but wind herding will determine the final slick thickness. Energetex Engineering (1981) performed a series of experiments on wind herding of fresh and aged Prudhoe Bay crude oil. They found that the wind herded oil thickness is primarily a function of the initial oil thickness and the windspeed. The empirical equation is:

$$T_H = 1.01\ T_I + 0.72U \tag{5}$$

where

T_H = herded thickness (mm)

T_I = initial thickness (mm)

U = wind speed (m/s)

has been derived from Energetex data for fresh Prudhoe Bay crude oil and shows a good correlation for initial thickness between 1 and 6 mm and windspeeds between 2.78 and 8.3 m/s.

Wind herding in the oil in leads model thickens the oil slick to the calculated herded thickness based on equation (5). No further spreading takes place but the slick will be thinned by evaporation.

Fraction Frozen into Ice. The wind/wave tank tests showed that a small percentage of the oil slick may become trapped in the developing grease ice. We visualize a volume of oil becoming trapped during each program iteration in the differential area of new ice growth based on the slick thickness and area in contact. This fraction encapsulated is increased by a density factor:

$$K_1 + K_2\rho_o \tag{6}$$

and decreased by a viscosity factor:

$$K_3 + K_4\mu_o \tag{7}$$

The fraction (F) of the oil in contact that becomes encapsulated is then given by

$$F = (K_1 + K_2\rho_o) - (K_3 + K_4\mu_o) \tag{8}$$

or

$$F = K_1 + K_2\rho_o - K_4\mu_o \tag{9}$$

where

ρ_o = density of oil,

μ_o = viscosity

Substituting from the experimental results and solving for the constants yields values of:

$K = -0.19966$

$K_2 = 0.31053$

$K_4 = 0.0000709$

The differential volume encapsulated is then given by:

$$dV = (-0.19966 + 0.31053\rho_o - 0.0000709\mu_o)\ dA_I.T_H \tag{10}$$

where dA_I is the differential ice area for that program pass and T_H is the wind herded slick thickness.

CONCLUSIONS

Oil can become incorporated into a developing ice field in two ways: 1) by dispersion of the slick into the water column and subsequent resurfacing of the droplets to become trapped in the crystal structure of the grease ice. 2) by infiltration from above the developing ice due to a density difference between the slush ice/water mixture and the oil.

The amount of oil frozen into the ice is increased by a high density, a low viscosity, wave energy and the time the slick is exposed to open water dispersion.

Without significant wave energy the growing ice forms a dead zone which is an effective barrier to spreading oil slicks. The final slick area will be similar to its wind herded area on open water against a fixed barrier.

Pancake ice formed in the presence of waves reduces wind herding but allows slow two dimensional spreading in the cracks between the floes. Most of the oil is eventually pumped onto the surface of the pancakes.

REFERENCES

Bobra, M.A. and P.T. Chung. 1986. A catalogue of oil properties. Environmental Emergencies Technology Division, Environment Canada Report EE-77, Ottawa.

Buist, I.A., W.M. Pistruzak and D.F. Dickins. 1980. Dome Petroleum's oil and gas under sea ice study. Proceedings of the 1981 U.S. Oil Spill Conference. American Petroleum Institute, Washington, D.C.

D.F. Dickins Associates Limited. 1986. Pack ice in Canadian waters: dimension and dynamics of leads and floes. (unpublished). Environment Canada Report EE-82. Ottawa.

Energetex Engineering. 1981. Burning of crude oil under wind herding conditions. Canadian Marine Drilling Limited, Calgary.

Mackay, D., I.A. Buist, R. Mascarenhas and S.Paterson. 1979. Oil spill processes and models. Report for Environmental Emergency Branch, Department of Fisheries and Environment, Hull, Quebec.

Mackay, D. 1984. The fate and behaviour of oil in cold climates. Department of Chemical Engineering and Applied Chemistry. Report to Environment Canada, Ottawa.

Mackay, D. 1985. Uses and abuses of oil spill models. Proceedings of the 7th Arctic Marine Oilspill Program Technical Seminar. Environment Canada, Ottawa.

MacNeil, M. and R.H. Goodman. 1985. Motion of oil in leads. Proceedings of the 8th Arctic marine Oilspill Program Technical Seminar. Environment Canada, Ottawa.

Nelson, W. and A. Allen. 1981. The physical interaction and cleanup of crude oil with slush and solid first year sea ice. ABSORB.

Schulze, R. 1985. Oil spreading in pancake and grease ice. Proceedings of the 8th Arctic Marine Oilspill Program Technical Seminar. Environment Canada, Ottawa.

Scott, B.F. and R.M Chatterjee. 1973. Behaviour of oil under Canadian climatic conditions. Part 1 - Oil on water under ice-forming conditions.

S.L. Ross Environmental Research Limited. 1985. A catalogue of crude oil and oil product properties. Environment Canada report EE-56, Ottawa.

S.L. Ross Environmental Research Limited. 1987. The transient submergence of oil spills: tank testing and modelling.

S.L. Ross Environmental Research Limited. 1987. Field research spills to investigate the physical and chemical fate of oil in pack ice. Environmental Studies Revolving Funds. in press.

S.L. Ross Environmental Research Limited and D.F. Dickins Associates Limited. 1987. Study of oil spills in leads: tank testing and modelling. in progress.

Tebeau, P.A., D. Mackay and W.Stiver. 1983. Testing of crude oils and petroleum products for environmental purposes. Proceedings of the 1983 Oil Spill Conference. San Antonio, TX.

Wilson, D.G. and D. Mackay. 1986. The behaviour of oil in freezing situations. Proceedings of the 9th Arctic Marine Oilspill Program Technical Seminar. Environment Canada, Ottawa. p.51.

FATE AND EFFECTS OF DISPERSED AND NON DISPERSED OIL ON ARCTIC MUD FLATS

Per Sveum

SINTEF
Applied Chemistry Division
N-7034 TRONDHEIM
NORWAY

INTRODUCTION

The arctic parts of Norway has hitherto been without extensive oil explotation activity, and the only threaths in terms of oil pollution have been from the general activity. However, the oil activity are gradually moving north. Consequently the oil companies and the government meet other environmental problems, both connected to exploration, production technology and oil spill contingency.

Shoreline clean-up operations on the coast of the Norwegian mainland have proved to be very laborious and thus expensive. It is difficult to adapt how similar operations can be carried out in to the Norwegian Arctic, which is more or less unpopulated and without infrastructure.

It is therefore important to develop alternative clean-up strategies to cope with these problems in the Arctic. Such strategies must include other means of priority, and clean-up techniques that consumes a minimum of labour.

SINTEF has earlier studied enhanced biodegradation on several backshore systems on Spitsbergen. These studies included treatment of oil contaminated backshore meadows with fertilizers to enhance biodegradation, and treatment of oil contaminated wracked seaweed with sorbents to diminish contamination of animals and to enhance biodegradation.

Dispersants have been mostly applied after oil pollution incidents on the sea. In some cases, however, the use of dispersants on the sea shore has been used to such an extend and with such harmful effects that a long lasting bad reputation has been established. The most serious spills in this connection have been the Torrey Canyon and the Amoco Cadiz oil spills where the amounts of dispersants used were considerable (Bocard et al 1979, Wells et al 1984, Southward 1979, Southward & Soutward 1978). Later studies on shoreline use of dispersants have revealed less drastic results for 2. generation dispersants, and for use on more or less exposed rocky shores. The Oman crude oil spill from Juliana were treated with dispersants on the shore.

The main idea of the present experiments have been to evaluate how three different dispersants affects the biodegradation of oil, the physical removal of oil and the sediment living microfauna and flora of oil contaminated mudflats on Spitsbergen.

MATERIAL AND METHODS

STUDY SITE

The study was carried out on a mud-flat which is part of the Kvadehuken lagoon system in the other part of Kongsfjorden on Spitsbergen (Cf.map fig. 1). The mud-flats have earlier been studied from an ecological pont of view (Sveum and Sendstad 1984), and these investigation has been of fundamental importance when the present experiments were designed. Table 1 summarises the basic characteristics of the sediments.

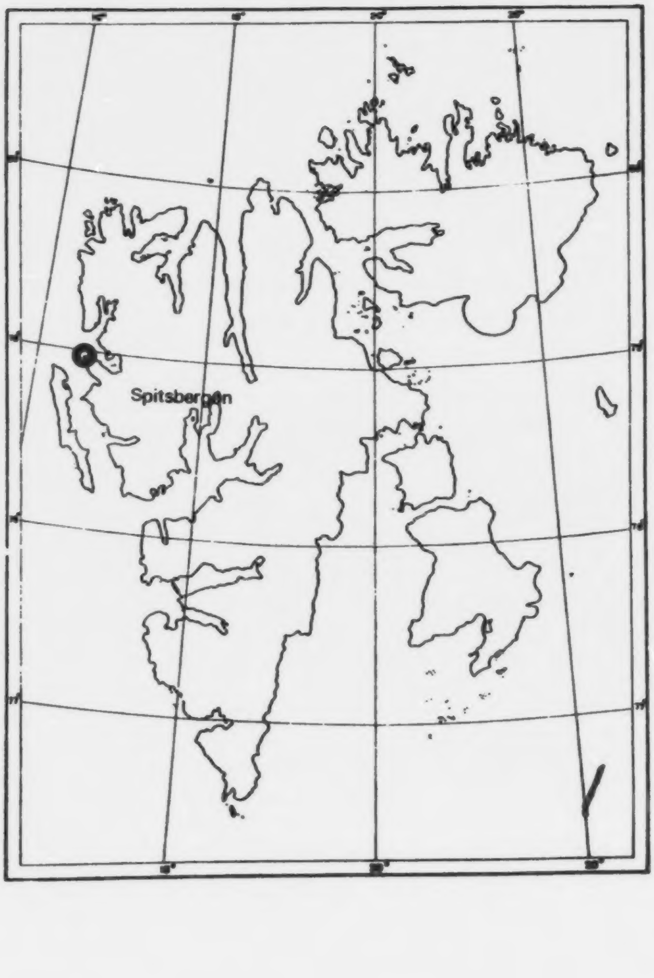

Figure 1. Map showing the location of the mud-flat which has been used for the study.

Table 1. Characteristics of mud-flat sediments in the outer Kvadehuken lagoon (from Sveum and Sendstad 1984).

Sediment stratum	Particle size (mean)	Redox condition	pH values	Loss of iqnition (%)
0-1 cm	121.14±36.54	- 40→ +200	6.4-7.5	3.4±0.42
1-3 cm	95.36±18.26	-120→ 40	6.0-7.2	4.4±0.37
3- cm	93.3 ±16.5	-115→ +110	6.2-7.0	2.6±0.34

The lagoon under study is partly open, which is the case with most real lagoons on Spitsbergen.

EXPERIMENTAL DESIGN

The experimental plots were kept separated through perforated polyethylene frames which was pressed into the upper 5 centimeters of the sediment. The perforation enabled a more or less free transfer of water in and out of the frames during the tidal motion. The level of the frames in the sediment was far above the level of the permafrost.

A mixture of Statfjord A + B crude oil was used in the experiment. Three different treatment chemicals were used, i.e. Finasol OSR5, BP 1100 WD and Corexit 7664. Doses of oil and chemicals are given in table 2.

Table 2. Dosage amounts of oil and dispersants used in the experimental plots.

Exp. plot	Description	Oil	Dispersant
f0	Unpolluted control	No	No
f1	Oil only	4 liters	No
f2	Oil + Finasol OSR4	4 "	0.6 liters
f3	Oil + BP1100 WD	4 "	0.6 "
f4	Oil + Corexit 7664	4 "	0.6 "

Each plot was replicated, and one of each were covered to shelter from radiation.

No attempts were done to simulate natural dispersion of oil. The oil and the water/dispersant was mixed throughouly by hand before contamination of the sediment.

METHODS

Sampling was carried out with 5 ml disposable plastic syringes with the top removed.

The total number of bacteria was enumerated with epifluorescence (EF) microscopy and acridine orange as the stain (AO) (Trolldernier 1972). The metabollically active fraction was enumerated using EF and fluorescein diacetate (Lundgren 1982).

The total community respiration was measured on an infrared gaz analyser modified for septum injection from samples incubated in vitro at 5^0C, in glass vessels with a volume of 100 ml. Gas samples were taken sequentially and the respiration was calculated from linear regression analysis.

Nematods are extracted from the sediment samples with the modified wet funnel technique as described by Barrron (1982). The animals was ascribed trophical groups acording to Wieser (1961) from slide mounted specimens.

The total oil content in the sediments are given as the difference between organic content in the experimental plot and the mean organic content in the reference plot at each sampling time. Organics were determined by combution of samples at 600^0C for 24 hours.

The nC_{17}/pristane and nC_{18}/phytane ratios were found after extraction of the sediment samples with freon, and GC-analysis.

RESULTS

MICROBIOLICAL STUDIES

Microbial abundance in the uncontaminated mud-flat sediments studied here has earlier been reported by Sveum and Sendstad (1983). Fungal hyphae was not found in amounts to be quantified. During the present study these observations were validated. Length of fungal hyphae was therefore checked sporadically during the study in the experimental plots, and was not found to reach a higher level than in the clean sediment. This implies that fungi most likely play an insignificant role in the biodegradation of oil in the mud-flat sediments studied. This is constsent with the results of Song et al. (1986) for sandy loam oil biodegradation

Bacterial numbers in the upper and middle strata of the 5 plots were counted every week. Results are given in figure 2 to 6.

There is a significant increase in the bacterial abundance in the upper stratum of the oil contaminated segments compared to the reference without oil. This demonstrates that the aerobic microflora of Spitsbergen mud-flat sediments are able to use oil as a growth medium. In the middle stratum a decrease is found, and the level never reaches that found in the uncontaminated middle sediment. It therefore seems reasonable to conclude that oil alone has a negative effect on the total anaerobic microflora, but as no attemt has been made to quantify the fraction of possible oil degraders, it is impossible to tell whether the remaining bacterial cells can degrade the oil. However, while there is a significant decrease in the metabolically active bacterial fraction of the upper aerobic stratum, the decrease is significant in the middle anaerobic stratum.

Compared to the untreated oil contaminated experimental plot, the OSR5 treated plot has a lower increase. The increase in the metabolically active fraction is however higher. The results is very similar also for BP 1100 WD, but with a lower metabollically active fraction in the middle sediment. In the upper stratum there is a slight decrease in the active fraction. The Corexit 7664 treated plot has a response more similar to that found in the plot with only oil. The inactivation of cells is, however, relatively higher. In the anoxic part of the sediment the metabollically active fraction are however at the same level as that found in the clean anoxic sediment.

Liu (1983) found that dispersants applied to the marine environment had no effect on the microbial environment. Traxler et al (1983) found that dispersants themselves were easily decomposed and increased the decomposition of crude oil when mixed. No harmfull effects on oil degrading bacteria were recorded. Similar effects were also recorded by Traxler and Bhattachanga (1977).

TOTAL RESPIRATION

Total community respiration was measured four times with approximately three weeks between each measurement.

Compared to the reference, an incraese is found in the oil contaminated sediment in both the studied strata (Figure 7). Among the chemically treated plots OSR5 gives the highest increase in community respiration. Corexit gives a level of respiration comparable to the clean sediment in the upper sediment, while a sligtly higher level is observed in the middle sediment. The highest level of "anaerobic" respiration is found in the plot treated with BP 1100WD.

The total community respiration is a measure of the total biological activity of the sediment. Levels might be difficult to evaluate, especially for complex systems. However, in systems contaminated with oil a decrease in diversity and total biomass are often recorded, and an increase in the total community respiration will indicate that the decomposers in the system utilizes the introduced source of carbon. A temporary increase in total respiration after contamination, if recorded together with extensive mortality of biota, can imply that the biota is supplied with easily decomposable recent organic material as animal and/or microfloral tissue. If, however, as can be recorded in the present study the increase in respiration is permanent, this is likely to be connected to the fate of the contaminant itself.

It is, however, not possible to conclude that the highest level of respiration indicates the highest level of oil and degradation, as the toxic effect of dispersants, oil, intermediate decomposition products (biological or photochemical) of oil and dispersants might cause toxic effects on biota over time, and thus continious input of easily decomposable recent organic material. The increased level of respiration found in the Corexit treated contaminated plot can possibly be explained from this.

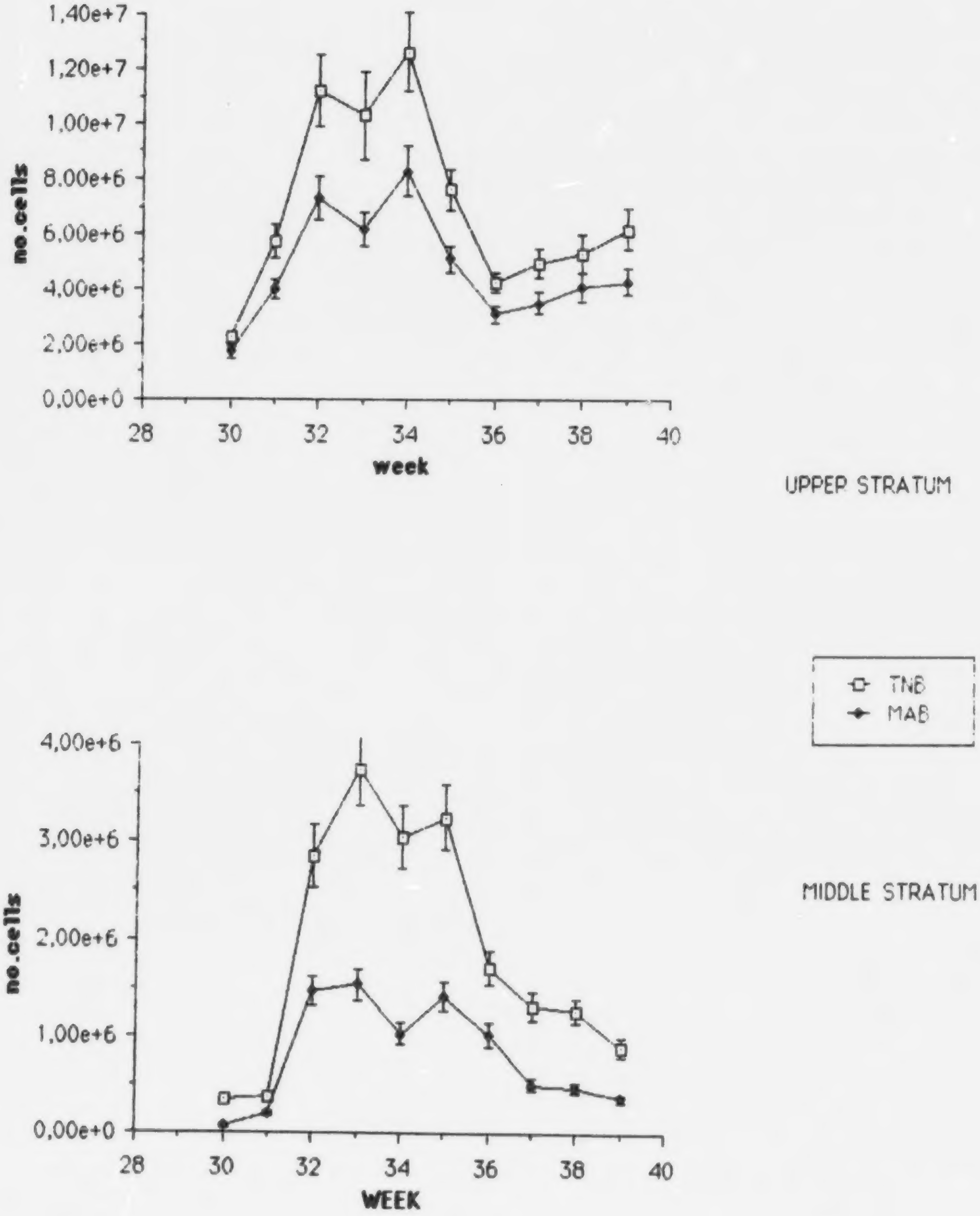

Figure 2. Bacterial abundance in the reference plot (f0) from weekly direct counts during the experimental periode. TNB=total number of bacteria. MAB=number of metabolically active bacteria.

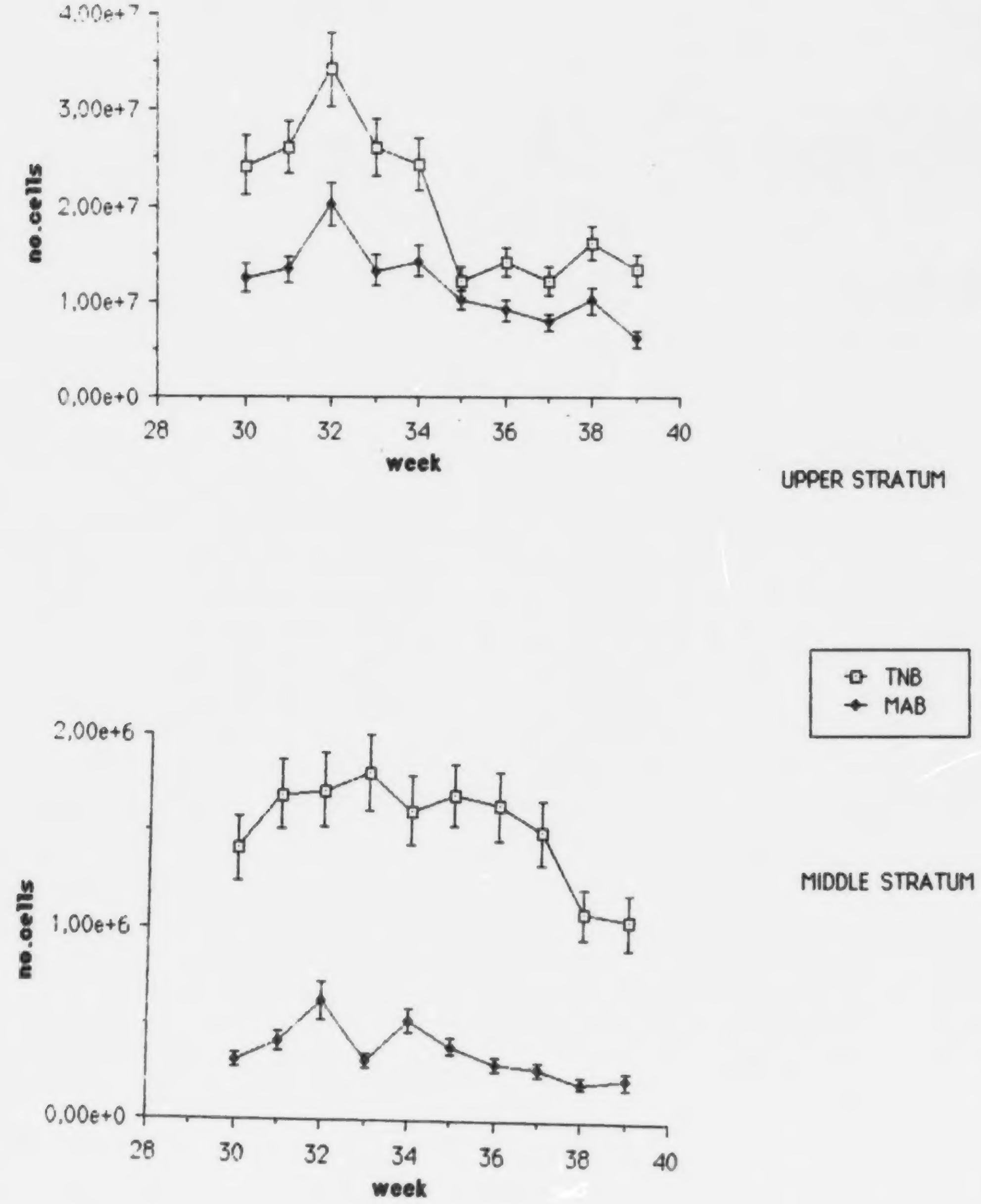

Figure 3. Bacterial abundance in the oil (f1) plot from weekly direct counts during the experimental periode. TBN=total number of bacteria. MAB=number of metabolically active bacteria.

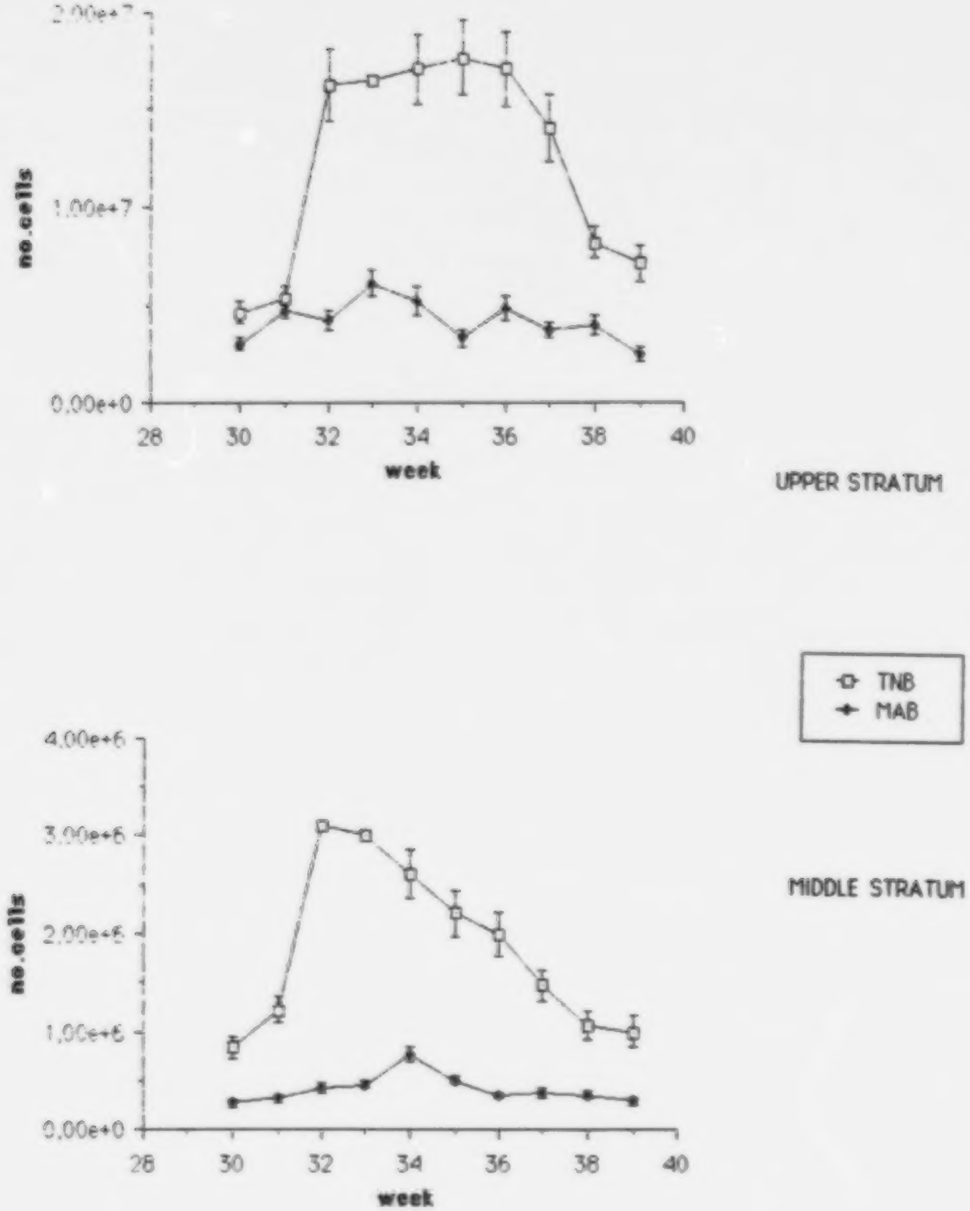

Figure 4. Bacterial abundance in the oil + Finasol OSR5 (f2) plot from weekly direct counts during the experimental periode. TBN=total number of bacteria. MAB=number of metabolically active bacteria.

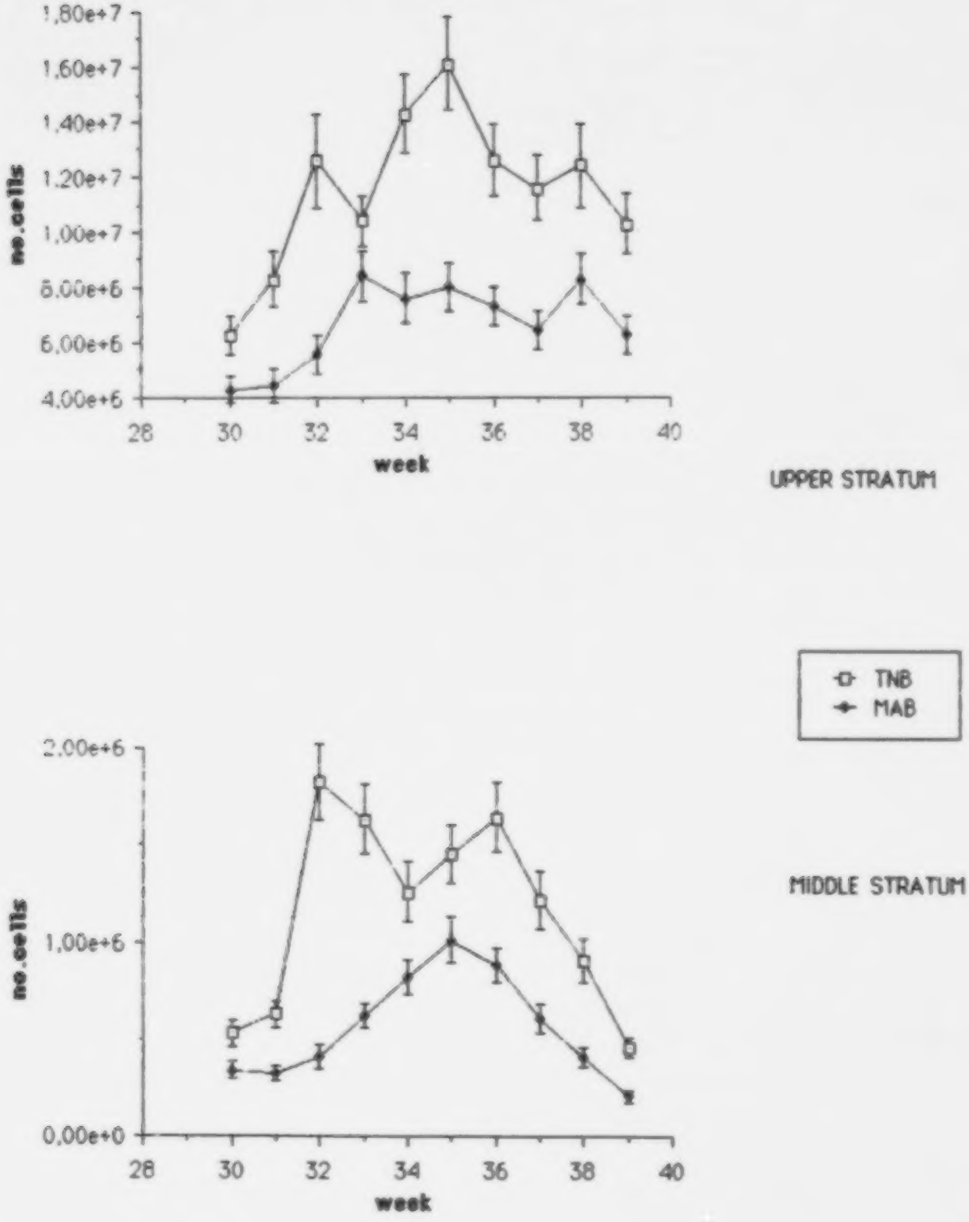

Figure 5. Bacterial abundace in the oil + BP1100WD (f3) plot from weekly direct counts during the experimental periode. TBN=total number of bacteria. MAB=number of metabolically active bacteria.

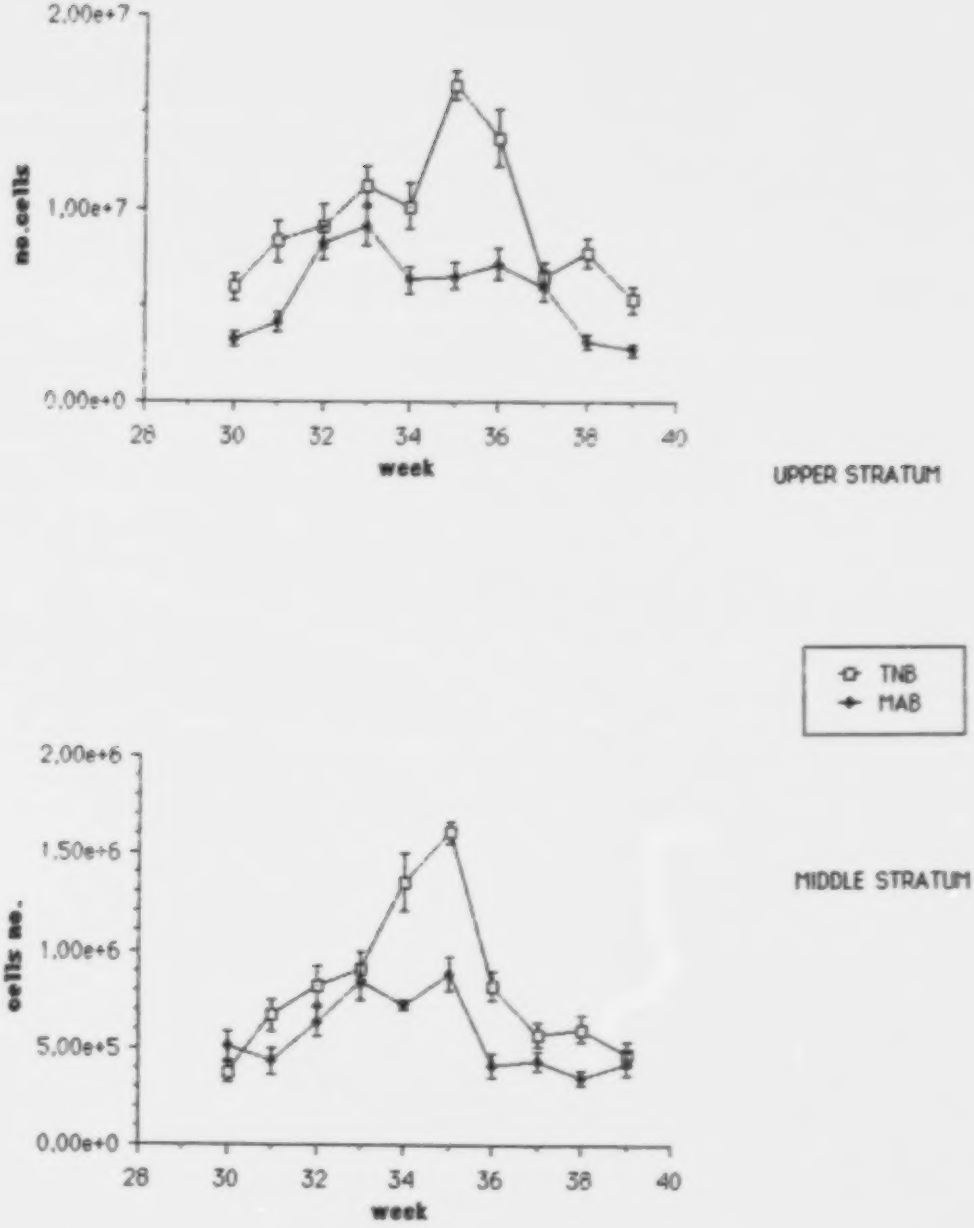

Figure 6. Bacterial abundance in the oil + Corexit 7664 (f4) plot from weekly direct counts during the experimental periode. TNB=total number of bacteria. MAB=number of metabolically active bacteria.

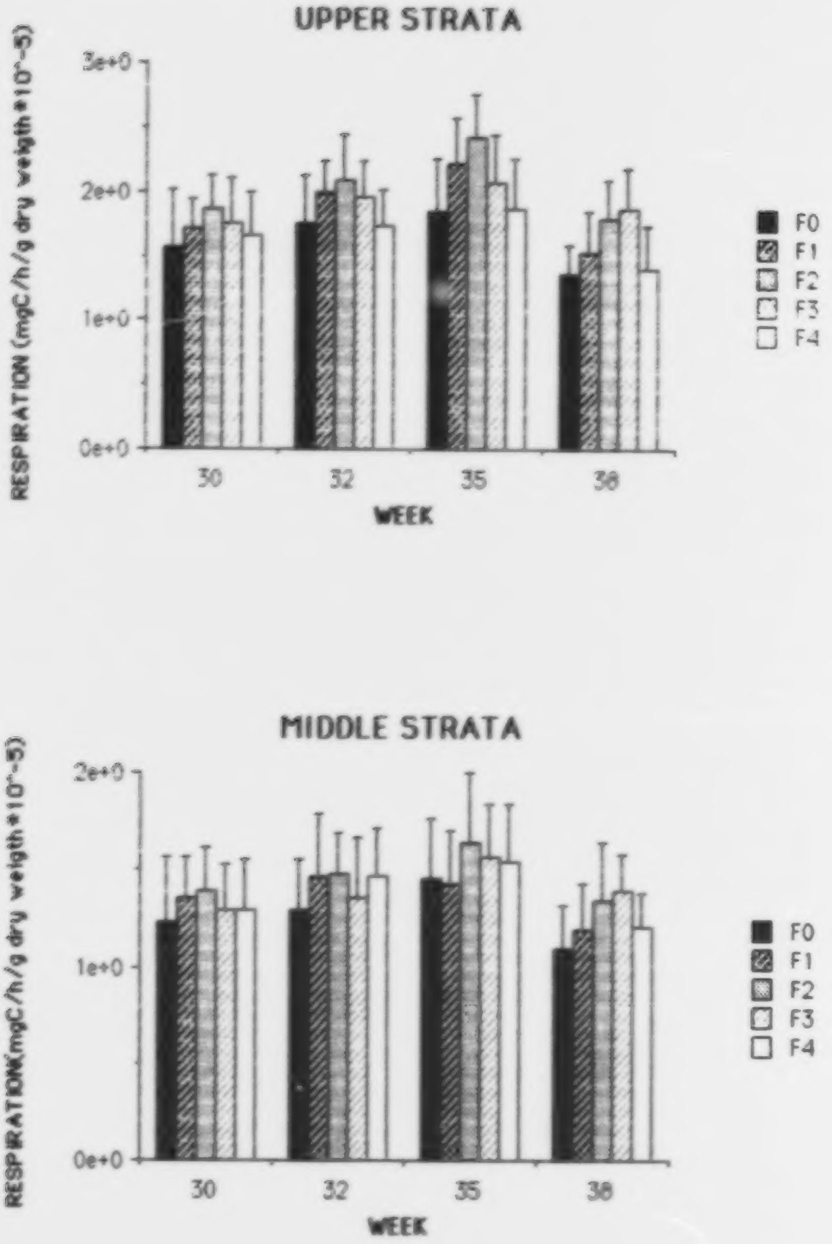

Figure 7. Total community respiration in the experimental plots and the experimental plots during the experimental period.

MICROFAUNA

The microfauna study in the experimental plots has been restricted to the nematods only and to the upper stratum. Earlier studies in these sediments indicated that the abundance in the lower strata is much lower (Sveum and Sendstad 1984). Nematods were extracted from the sediments at three times during the experimental periode.

Microfauna plays an important part of the decomposer systems by grazing on the microbial biomass, and thus mineralizing nutrients. Oil is defficient in nutrients like nitrogen and phosphorous. Mineralisation of essential nutrients are thus un important prerequisite for biological degradation of spilled oil. It is therefore importante to study effects on presumably important microbial grazers to gain understanding of the decomposition of spilled oil and of nutrient dynamics assosiated with these processes.

The importance of nematoda as microbial grazers has been stressed by several authors (e.g. Coleman and Yeates 1982). As a target for study, nematods are useful as trophic groups, e.g. bacterial grazers can be distinguished by their mouthparts. Other groups can be of importance in nutrient cycling as well, but only nematods are treated in this study. The importance of the microfauna for oil biodegradation has been demonstrated in laboratory studies by Huang et al. 1981, who enhanced biodegradation by supplying protozoa to decomposing oil.

Compared to the clean sediment, there is a general decrease in the abundance in nematoda all the oil contaminated plots (Figure 8). The decrease is higher in the plots treated with OSR5 than in the plots which are either untreated (i.e. oil alone) or treated with Corexit 7664. There is a change in trophic structure towards a higher fraction of bacterial feeders in all the polluted plots.

Earlier studies on Spitsbergen have showed decreased abundance of Nematoda, and also an increase in the relative fraction of bacterial grazers after oil contamination. Boucher (1980) found an increase in total number of nematods in bottom sediment contaminated with oil after the Amoco Cadiz incident, however with a decrease in the diversity of the group, which probably was related to an increase in bacterial feeders.

PHYSICAL BEHAVIOR OF THE OIL

The main goal of any treatment of oil on shorelines is to remove as much oil as possible from the sediment surface and the sediment itself. The oil contents of each plot each week are given in figure 9 and 10.

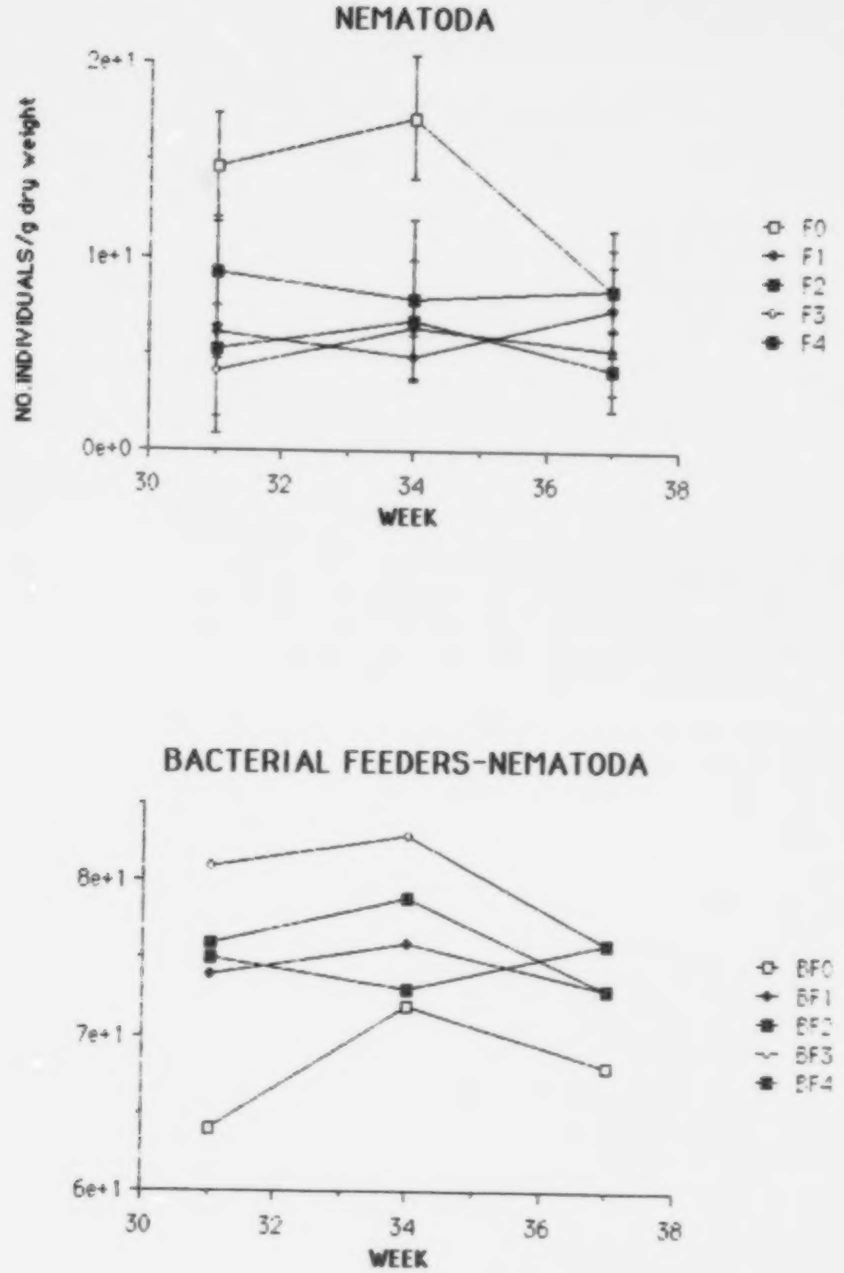

Figure 8. Nematod abundance as recorded at three sampling times during the experimental period and the trophic structure measured at each time.

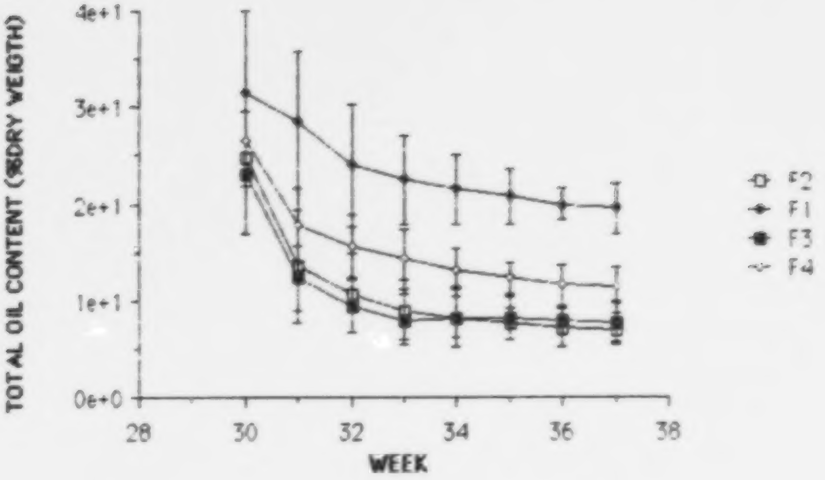

Figure 9. Oil content in the upper stratum of the experimental plots as a function of time.

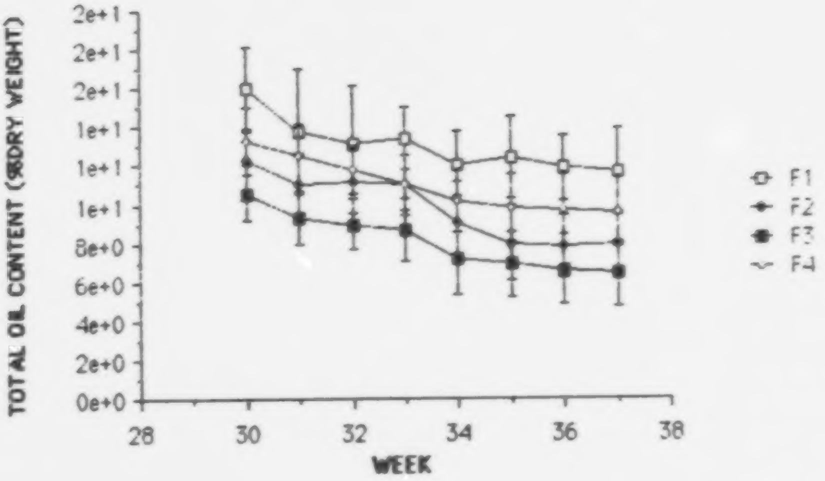

Figure 10. Oil content in the upper stratum of the experimental plots as a function of time.

Penetration and washout from shoreline sediments are essensial topics in connection with the use of dispersants on the shore (Wells et al 1984).

The total content of oil in the sediment has been taken as the difference in loss of ignition between the reference site without oil and the oil contaminated plots. The two upper strata were dealt with separately.

OSR5 and BP 1100 WD gave the highest degree and removal of oil from the sediment. The untreated oil gave much lower values. However, Corexit which shows the chemical lowest efficiency is also significantly better in this respect than no treatment of the oil.

Page et al (1984) found that dispersed oil reaches the sediment in the littoral zone due to loss of the shorter carbon chain compounds and an increase in specific weight. Model studies including simulation of tidal movements by Anderson et al (1984) showed that dispersed oil did not penetrate below about 3 cm. Other studies have demonstrated a penetration down to about 6 cm for untreated oil, while the addition of dispersants increased both rate and depth of penetration (Dörjes 1984a,b; Farke 1984, 1985a, b).

In the present study only the two upper sediment strata were studied from the physical oil removal point of view. However, a few samples were taken initialy to detemine the depth of penetration. The results are given in table 3.

Table 3. Penetration of oil in the mud-flat sediment.

Exp.Plot	Description	Dept. of penetration (cm)
f1	Oil only	3.2
f2	Oil+Finasol OSR5	5.6
f3	Oil+BP1100WD	4.7
f4	Oil+Corexit 7664	4.3

It should be noted that the penetration of the oil was measured after 2 tidal cycles. Penetration increases according to the series crude oil < oil+Corexit 7664 < oil+BP1100WD < oil+OSR5. This implies that there is a connection between the initial rate of physical removal of the oil and the depth of penetration.

The dependency of dispersants, in terms of efficiency upon variable temperature and salinity, has been demonstrated by several authors (e.g. Lethinen and Vesala 1984). This will be of primary importance on shorelines where both these factors will vary due to tidal movements and freshwater supply from the adjacent land areas. It is difficult to assume any effects on either salinity or the temperature in this study. However, the salinity in the interstitial water was found to vary between about $14^0/_{00}$ and $36^0/_{00}$, while the temperature of the water varied from 0.5^0C to about 5^0C. As the products applied in the study have been designed for temperatures above that pertaining during this experiment, the results obtained should be considered more as an indication of potential than as limits of effiency.

BIOLOGICAL DEGRADATION

The degree of biodegradation of the oil was evaluated at the experimental termination in October. The nC$_{17}$/pristane and nC$_{18}$/phytane rations have been used for these evaluations. It should be noted that these analyses have been carried on samples containing a mixture of the upper and middle strata. The results are given in table 4.

Plot	nC17/pristane	nC17/phytane
F0 (LIGHT)	1.44,1.53	1.51,1.56
F0 (DARKNESS)	2.11,1.58	1.42,1.79
F2 (LIGHT)	1.44,1.26	1.77,1.54
F2 (DARKNESS)	1.31,1.13	1.55,1.19
F3 (LIGHT)	1.04,1.13	1.19,1.32
F3 (DARKNESS)	1.30,1,31	1.28,1.47
F4 (LIGHT)	0.82,0.88	0.88,1.04
F4 (DARKNESS)	1.19,1.00	1.34,1.04

Table 4. Biodegradation of the oil in the experimental plot evaluated by the nC$_{17}$/pristane and nC$_{18}$/phytane ratios. The light exposed and sheltered plots are treated separately.

The light exposed and the light sheltered plots have been treated separately. Although a larger number of analysis may have given a better basis for conclusions, the tendency of the analyses performed are quite clear.

Comparison between sheltered and exposed experimental plots reveals that light exposure enhances degradation, also when evaluated by biodegradation markers. This imply the possibility of photochemically induced toxic effect on the decomposers, however, only the unsheltered plots were studied with respect to microbioloby.

The highest degradation are found in the oil treated with BP 1100 WD and Corexit 7664. The difference between the plot with oil alone and that treated with OSR5 seems to be less pronounced especially when exposed to light.

When treated with BP 1100 WD or Corexit 7664 there is a unambigious tendency towards a higher biodegradation as indicated by both the applied ratios. In the plot with oil alone this tendency is less clear, and in the plot treated with OSR5 the opposite tendency is found when judged from the nC_{18}/phytane ratio.

CONCLUSION

The microflora that inhabits the studied arctic mud-flats on Spitsbergen responds to oil pollution with an increase in microbial numbers. The addition of the dispersants OSR5 enhances the increase in cell numbers. Despite the large increase in bacterial cells in sediments treated with OSR5, the increase in the metabolically active bacterial fraction is larger when the oil is trated with Corexit 7664.

The number of nematods in the sediment decreases after oil contamiation, and also with the treatments of different dispersants. However, the relative fraction of bacterial feeding nematods increases in all the contaminated plots. There is a connection between relative toxicity of oil and dispersant and the metabolically active fraction of bacterial cells.

The biological degradation of the aliphatics is most extensive in the plots treated with dispersants. Dispersants enhances biodegradation and Corexit 7664 which is found to give the largest increase in metabollically active bacterial cell number, also enhances biodegradation of the aliphatics mostly.

The biodegradation of the aliphatics is found to be higher under light exposure than in darkness.

Treatment with dispersants enhances physical removal of oil from the sediment. The physical removal can be described with an inverse hyperbolic curve. The most toxic dispersants, OSR5 and BP1100WD, are the most efficicent dispersants in terms of oil removal. However, even the less toxic dispersant, Corexit 7664, increases the physical removal relative to no treatment.

Altogether the results of these experiments indicate that the use of chemical treatment methods might be a strategy worth considering on arctic mud-flat sediments. There might be a potential for the development of a low toxic nutrient containing chemicals that enhances both physical removal and biodegradation of the oil.

REFERENCES

Andersen, J.W. et al 1984; "Recommended Methods for Testing the Fate and Effects of Dispersed Oil in Marine Sediments", from "Oil Spill Chemical Dispersants: Research, Experience and Recommendation", STP 840, ed. T.E. Allen, ASTM, Philadelphia.

Bocard, D.C. et al. 1979; "Cleaning products used in operations after the Amoco Cadiz disaster", Am.Pet Inst.Publ., Proc. from 1979 Oil Spill Conference.

Bocard, C. et al. 1984; "Chemical Oil Dispersion in Trial at Sea and in Laboratory Tests: The Key Role of Dilution Processes" from "Oil Spill Chemical Dispersants: Research, Experience and Recommendations" STP 840, ed. Tom E. Allen, ASTM, Philadelphia.

Bryan, G.W. 1969; "The effects of oil-spill removers ("detergents") on the gastropod Nucella Plaillus on a rocky shore and in the laboratory", Marine Biological Association of the United Journal 49 (4).

Danielsen, A., Denstad, J.P., Halmø, G., Hoddø, T., Klokk, T., Marion, D.van, Sveum, P. & A.V. Aarset, 1985. Oljesøl på strand - effektivitet og biologiske effekter av opprenskningsmetoder. PFO prosjekt 1713.

Dewling, R.T., Amaral e Silva, Q.C. 1979; "Impact of dispersant use during the Brazilian Marina incident", Am.Pet.Inst.Publ. 4308. Proc. 1979 Oil Spill Conference.

Dørjes, J. 1984; "Experimentale Untersuchungen zur Wirkung von Rohøl und Rohøl/Tensid Gemischen im Økosystem Wattenmeer. Einfürung und abiotische Parameter", Senckenbergiana marit. 16 (1/6), Senckenberg am Meer 418.

Dørjes, J. 1984; "Experimental Untersuchungen zur Wirkung von Rohøl und Rohøl/Tensid Gemischen im Økosystem Wattenmeer. Zuzammenfassung und Schlussfoerungen", Senckenbergiana marit. 16 (1/6), Senckenberg am Meer 418.

Harris, G.W., Wells, P.G. 1980; "A Laboratory Effectiveness Testing of Oil Spill Dispersants", in Proc. Third. AMOP Tech.Seminar, Environment Canada, Edmonton, Alberta.

Honma, Y., Kitami, T. 1974; "The Juliana oil pollution on shore life and effects of several oil spill removers on some fishes and sea urchin egg in the laboratory", Annual Report of the Sado Marine Biological Station Niigata University.

Huang, T.C., Chang, M.C. and Alexander, M. 1981. Effect of Protozoa on Bacterial Degredation of an Aromatic Compound. Appl.Environ.Microbiol. 41:229-232.

Lundgren, B. 1981; "Fluorescein diacetate as a stain of metabolically active bacteria in soil". Oikos 36:17-22.

Page, D.S. et al. 1984; "Tidal Area Dispersant Project: Fate of Dispersed and Undispersed Oil in two Nearshore Test Spills", in "Oil Spill Chemical Dispersants; Research, Experience and Recommendations", STP 840, ed. T.E.

Allen, ASTM; Philadelphia.

Southward, A.J., Soutward, E.C. 1978; "Recolonization of Rocky Shores in Cornwall after use of toxic dispersants to clean up the Torrey Canyon spill", Fisheries Research Board. Journ. 35 (5).

Southward, A.J. 1979; "Cyclic fluctuations in population density during eleven years. Recolonisation of Rocky Shore in West Cornwall following the Torrey Canyon Oil-spill in 1967", 13th. Europ.mar.biol.symp., Isle of Man.

Straugham, D. 1971; "The influence of oil and detergents on recolonization in the upper intertidal zone", API/EPA Conf.

Sveum, P. and Sendstad, E. 1984; "Oil pollution at Spitsbergen. Ecological studies of dominant shoreline types". SINTEF-report STF21 A84073. (In Norwegian).

Sveum, P. and Sendstad, E. 1985. "Oil polluted seaweeds in the Arctic". Proc. 8 AMOP. Tech.Seminar.

Trolldenier, G. 1972; "Fluorescencemikroscopischer Zahlungen von Bodenbakterien. I. Historischer Uberblick und Beschreibung eines Verfahrens zur Zahlung von Bodenbakterien in Trockenpraparaten nach Fahrbung mit Acridinorange.Zentrbl.Bakt.Hyg.Abt. II. 127:25-40.

Wells, P.G. et al. 1984; "Uniform Methods for Exposure Regimes in Aquatic Toxicology Experiments with Chemically Dispersed Oils", from "Oil Spill Chemical Dispersants; Research, Experience and Recommendations", STP 840, ed. T.E. Allen, ASTM, Philadelphia.

Wieser, W. 1953; "Die Beziehung zwischen Mundhohlengestalt, Ernärgungsweise und Vorkommen bei freilebenden Marinen Nematoden. Eine ökomorphologiische Studie". Ark.Zool.Ser II, 4:436-484.

DEVELOPMENT OF A CONTINUOUS FLOW EXPOSURE SYSTEM FOR OIL EFFECTS TESTING

Michael S. Hutcheson, Remi Odense and Robert M. Gershey
Seakem Oceanography Ltd.
Dartmouth, Nova Scotia

and

John Vandermeulen
Fisheries and Oceans Canada
Dartmouth, Nova Scotia

ABSTRACT

The first phase of a multi-year study into the effects of petroleum hydrocarbons on Atlantic salmon (Salmo salar) has been to design and construct an oil exposure system. The design criteria for the system were that it be continuous-flow, produce a water-accomodated fraction (WAF) of a crude oil in relatively large volumes, have a low particulate oil content and produce a consistent concentration of oil in the WAF.

The system produces up to about 2.0 L min^{-1} of WAF in a three chambered, gravity flow system: oil/seawater mixing tank, separation tank and constant head toxicant delivery tank. Each chamber is a rectangular 100 L glass aquarium. The crude oil is pumped into Chamber 1 where it is vigorously mixed with the seawater. A motor driven impeller enhances mixing in the first quarter of this chamber. The oil/water mixture then overflows a baffle and flows under a second baffle into the last half of the tank where some separation of particulates occurs. An overflow standpipe skims off the surface layer of oil and the mixture is drawn off subsurface to the separation chamber. The oil-water mixture flows the length of the separation chamber with particulates which rise to the surface being drawn off by an overflow standpipe. The WAF flows out to the constant head delivery chamber through a subsurface discharge. From there, the 100% WAF is metered to exposure tanks through adjustable height overflow tubes.

Typical measured oil concentrations (IR) in the 100% WAF produced are 6-7 mg L^{-1}. There were few non-background particles with diameters greater than 64 u in the WAF in the constant head chamber and exposure solutions. Oil particulates had diameters in the 16-64 u region with a peak at 32 u and were present in particle concentrations of approximately 0.15 ppm.

INTRODUCTION

Toxicological studies with petroleum hydrocarbons pose some unique methodological problems primarily resulting from the high volatility of hydrocarbon compounds. The determination of lethal concentrations of substances is based upon exposures to constant concentrations of the toxicant over defined periods of time. Standardly used terms such as 96 hour LC50 all refer to the concentration of a substance required to produce 50% mortality in the test species within given exposure times. Exposures can be made where one batch of the toxicant is used in a static mode, the batch can be replaced with fresh toxicant at defined time intervals, or fresh toxicant solution can continually be supplied to the exposure chamber. The costs and skill required to perform these tests increases from static to flow-through conditions. The flow-through mode is the exposure of choice with petroleum hydrocarbons where the need to maintain constant exposure concentrations exists with volatile compounds. This paper describes a continuous-flow system for the preparation of a water-accomodated fraction of a waxy crude oil in seawater. Its uniqueness stems from its ability to accept a waxy crude, in contrast to other systems reported in the literature which have been used with fuel oils and lighter crude oils.

The variety of systems available for preparing oil-water solutions has been summarized by the National Research Council (1985). Our requirement for a water-accomodated fraction composed primarily of dissolved hydrocarbon components but also containing some smaller oil particulates led us to incorporate the essential elements of Vanderhorst et al.'s (1977) system which included contactor, separation and metering tanks. The system developed provides for initial vigorous mechanical mixing of the oil with seawater, additional contact through baffle-directed flow and separation tanks to permit the segregation of larger particulates from the water mass.

Other continuous-flow systems have used Prudhoe Bay crude oil producing mixtures with total petroleum hydrocarbon concentrations (IR) of 0.14 mg L^{-1} (Bean et al., 1980), and No. 2 fuel oils where mixtures with up to 3 mg L^{-1} (Hyland et al., 1977) have been produced. Vanderhorst et al.'s (1977) system had the capacity to produce up to 4320 L d^{-1} of an oil-water mixture from # 2 fuel oil containing between 0.4-1.6 mg L^{-1} of total hydrocarbons (IR).

EXPOSURE SYSTEM DESCRIPTION

This system was designed to continually produce a water-accomodated fraction of Hibernia crude oil in seawater. The capabilities and specifications of the system are as follows:

design WAF production capacity	3000 L d^{-1}
exposure temperature	10 °C
oil consumption rate	2.4 L d^{-1}
total seawater requirements	17,400 L d^{-1}
exposure tank capacity	250 L
exposure tank turnover rate	5 tank vol d^{-1}

The exposure system is presented in Figure 1. A flow-through seawater source is required to operate the system. Sand-filtered Bedford Basin seawater at an ambient salinity of approximately 30 o/oo passes through two in-line filters (50 and 10 u) to a constant head tank. From that point, flow in the system is driven by gravity. Water leaving the head tank passes into a contact chamber (Tank 1) just above the rotating blades of a variable speed stirring motor impeller. Oil is pumped through long-life oil resistant tubing with a peristaltic pump into the contact chamber above the blade. Oil is effectively broken into small particles by the impeller blades. The contents of this chamber flow over and under consecutively

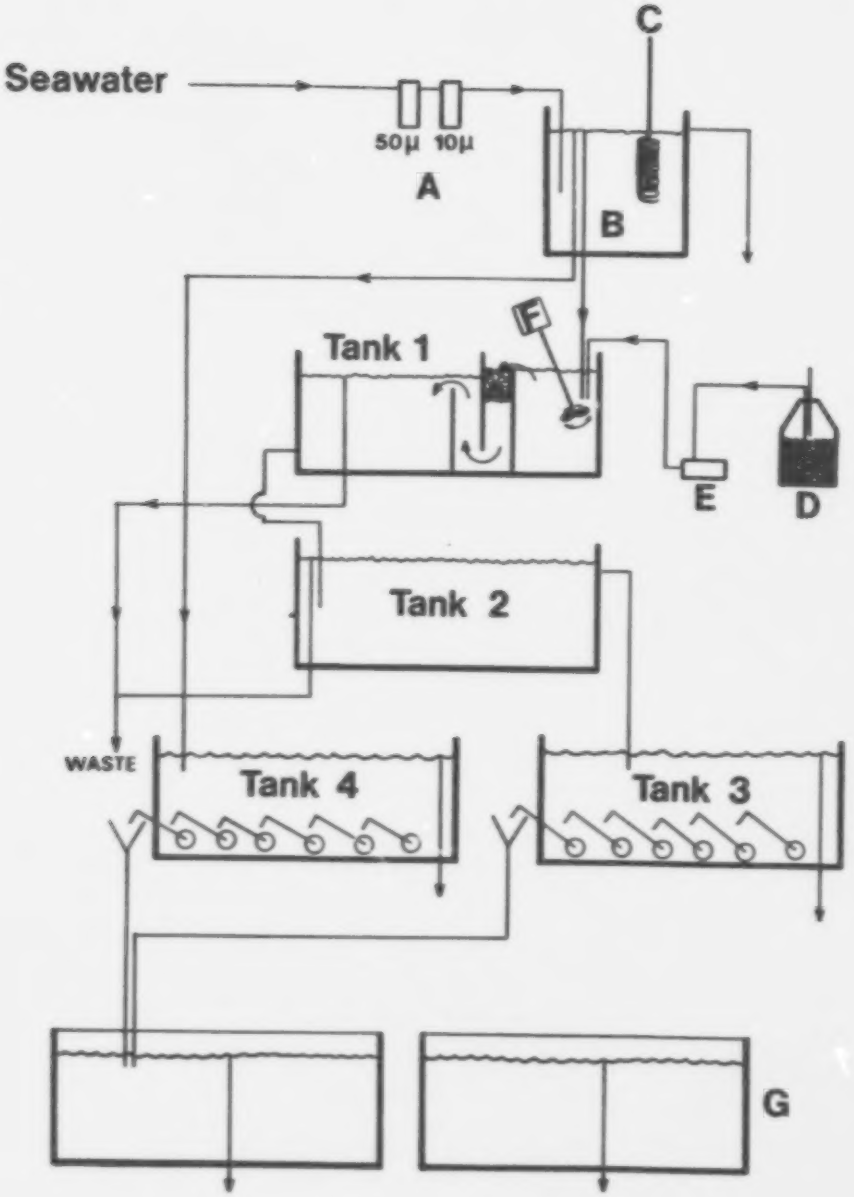
Seawater
50μ
10μ
A
C
B
F
Tank 1
E
D
Tank 2
WASTE
Tank 4
Tank 3
G

FIGURE 1. CONTINUOUS-FLOW OIL EXPOSURE SYSTEM. TANK 1 - CONTACT CHAMBER. TANK 2 - SEPARATION CHAMBER. TANK 3 - 100% WAF DISTRIBUTION TANK. A, IN-LINE FILTERS. B, CONSTANT HEAD SEAWATER TANK. C, COOLING COIL. D, OIL RESERVOIR. E, PERISTALTIC PUMP. F, VARIABLE SPEED STIRRER. G, EXPOSURE TANKS(6).

three baffles into an end chamber where surface oil is drained through a standpipe to a waste sump and the oil-water mixture leaves the tank through a sub-surface port. The mixture goes next to one end of a separation tank (Tank 2). Surface oil is drawn off through a standpipe and the oil-water mixture exits the other end of the tank to the distribution tank (Tank 3). A constant head is maintained in the distribution tank. The 100% WAF contained in the distribution tank is metered out of this tank through adjustable dipper arms which flow into glass funnels attached to 64 mm (1/4") I.D. Teflon tubing leading to exposure tanks. An identical adjacent tank receives seawater from the head tank and serves as the seawater distribution tank. By relative variation of the delivery rates of the 100% WAF and the seawater, any desired concentration of WAF between 0 and 100% can be delivered to the exposure tanks. All plumbing connections between tanks are 1.91 cm (3/4"). Circular fiberglass exposure tanks are 93 cm diameter by 50 cm high.

OIL CHARACTERIZATION

The Hibernia crude oil has been characterized by gas chromatography. The oil is separated into two fractions; F1, the non-polar hydrocarbons and F2, the aromatic and more polar compounds by chromatography on deactivated silica gel. The fractions are analyzed using a Hewlett-Packard 5830A gas chromatograph with flame ionization detection. Instrument conditions are as follows:

Column: 15 m x 0.532 mm, 1.5 um DB-5 bonded phase fused silica column (Megabore, J&W Scientific)

Carrier gas: Nitrogen, column flow 8 mL min^{-1}

Injector temp: 250°C

Temperature program: Inject sample at 40°C, hold for 5 min., heat at rate of 8°C min^{-1} to 260°C, hold for 10 min.

Detector temp: 280°C

Detector flow: Hydrogen 30 mL min^{-1}, air 240 mL min^{-1}, nitrogen makeup 22 mL min^{-1}.

The Hibernia oil is a waxy crude and the resolved components in fraction F1 (C_8-C_{18}) account for about 97% of the material eluted from silica gel. The resolved components of the aromatic F2 fraction account for 2.5% of the total.

Routine monitoring of oil concentrations in the test system is accomplished with infrared spectroscopy (IR). Samples are extracted with freon and the absorbance between 3100-2700 cm^{-1} measured. Particle size distributions are determined on a Coulter Counter.

PERFORMANCE

A number of problems were encountered during the development of the exposure system. The homogeneity and physical consistency of the crude oil were important determinants of how well the system worked. With waxy crude oils, it is important to warm and thoroughly mix the oil before decanting from larger storage containers such as oil drums and before actual use. The Hibernia crude which we used had its own complement of formation-derived particulates which often clogged the delivery tubing. In spite of attempts to mix the large drums of crude oil before distribution into smaller 20 L metal cans, the bottom of the drum always contained some particulates which would later cause problems. As the room temperature crude oil makes contact with the 10 °C water in the contact chamber, it tended to form a waxy deposit around the tip of the delivery tube. On occasion, this deposit would block the flow of oil into the contact chamber. A Venturi mixing chamber was tried initially as the primary method for mixing the water and oil. The agitation provided was not sufficient to break up the oil droplets and produce a mixture with any appreciable oil content.

Tubing lines require regular maintenance as bacterial slimes grow in them and particulate oil builds up on tubing walls over time. The adjustable dipper arms are rugged and simple but require manual calibration of flow rates. In our experience with another continuous flow delivery system for a water-soluble fraction of an oil, inline flowmeters and adjustable roller clamps such as used on medical intra-venous solution tubes provide easy and accurate determination and adjustments of flow rates.

Stirrer speed is a determinant of the total amount of oil in the 100% WAF and the amount of particulates. The most appropriate speed setting will be motor and impeller specific and should be determined for each system. For our system, the relationship between total oil content, particle concentration and size distribution and stirrer speed is illustrated in Figure 2. A small decrease in relative stirrer speed resulted in a 46% decrease in oil content (IR) of the WAF and a 91% decrease in the concentration of particles at the predominant size peak of 32 u. Clearly, reduction in the vigor of stirring puts fewer particles into the water while retaining a greater relative amount of oil in the dissolved phase. The dissolved (<0.45 u) oil concentrations at each stirrer speeds were 8 (speed 10) and 4.1 mg L^{-1} (speed 8).

The exposure system is regularly run at a stirrer speed of 8 in order to produce a WAF with total oil (IR) concentration of approximately 6-7 mg L^{-1} and low particulate concentration. The effectiveness of the separation tanks at reducing particulate oil content is illustrated in Figure 3. The particle concentration peak at 128 u is an experimental artifact which appears in the 0.45u filtered sample. Its source is yet to be determined. The particle concentration node at 32 u decreases by 40% between Tanks 2 and 3.

The absence of day-to-day variability in the oil concentration of the WAF produced is an important factor in the reliability of the system for toxicological studies. Oil concentrations in the 100% WAF during a 96 hour LC50 determination are presented in Figure 4. The mean concentration during this experiment was 7.6 ppm with a coefficient of variation of 8.7% of the mean.

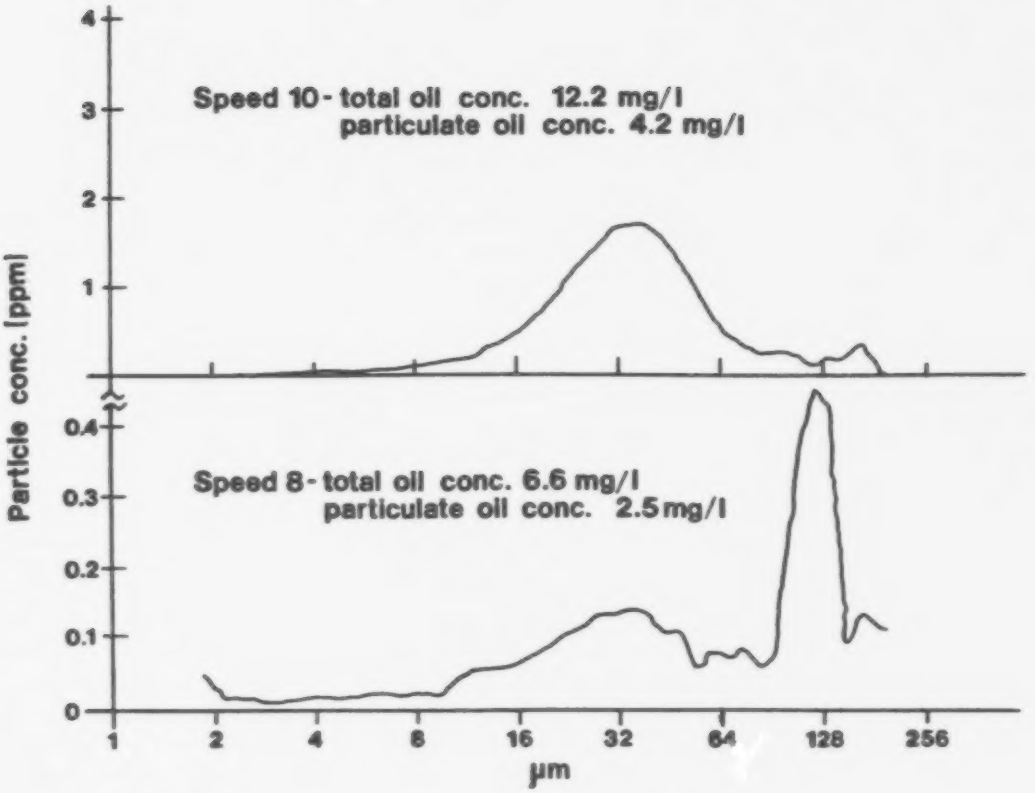

FIGURE 2. PARTICLE SIZE DISTRIBUTIONS IN 100% WAF PREPARED AT TWO STIRRER SPEEDS

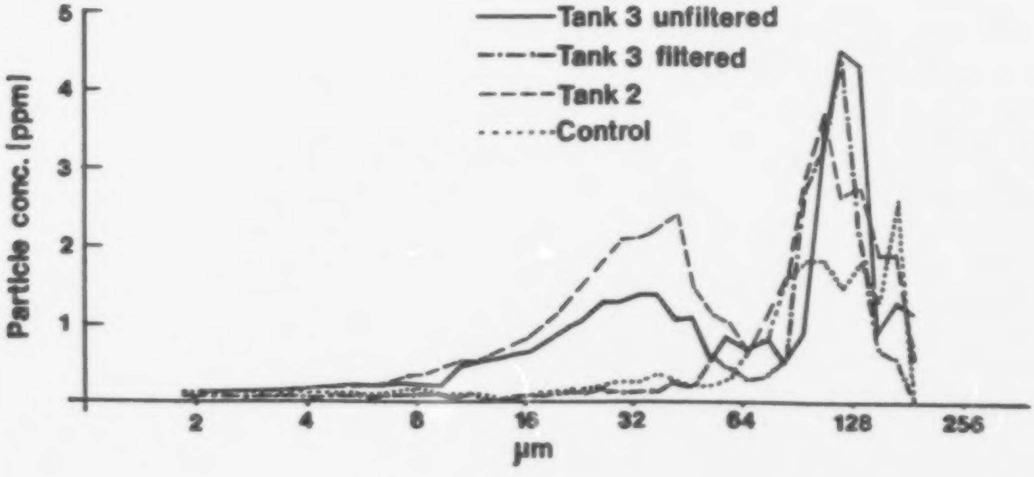

FIGURE 3. PARTICLE SIZE DISTRIBUTIONS IN TANKS WITHIN THE OIL PREPARATION SYSTEM

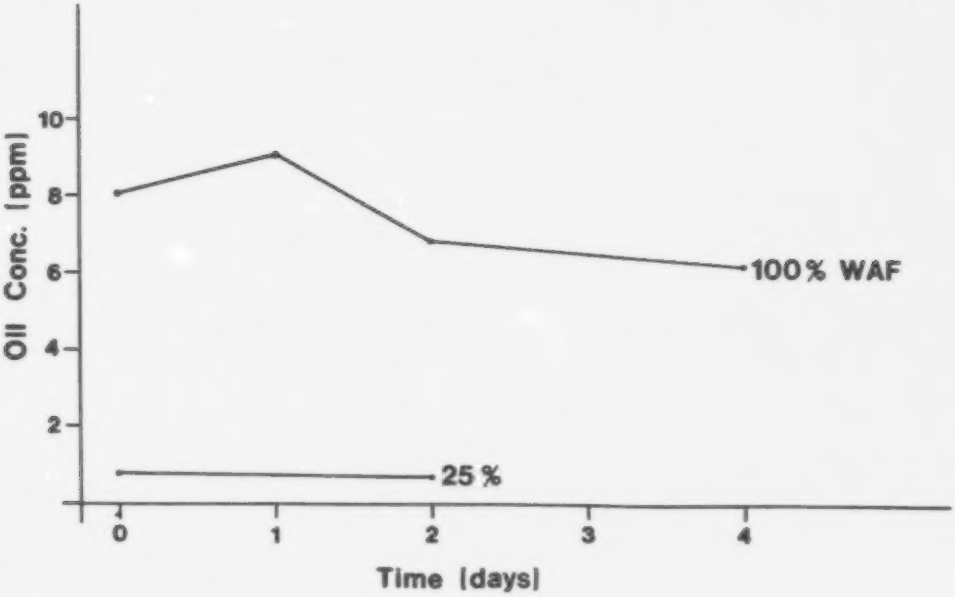

FIGURE 4. DAILY VARIABILITY IN WAF CONCENTRATIONS DELIVERED

CONCLUSION

This paper has described a continuous-flow oil exposure system which will handle waxy crude oils such as that from the Hibernia formation on the Grand Banks of Newfoundland. The availability of such systems for producing constant concentrations of water-soluble, volatile hydrocarbons is critical for the accurate determination of the aquatic toxicity of these types of substances. Exposure systems such as these are capable of delivering the toxicants in concentrations which range from the acutely lethal to the sublethal for extended periods of time. This exposure system is being used in a study of the toxicity mechanisms of Hibernia crude oil to Atlantic salmon (*Salmo salar*) juveniles in seawater.

ACKNOWLEDGMENTS

This work is being supported by the Unsolicited Proposals Program of Supply and Services Canada and the Office of Energy Research and Development, Energy Mines and Resources Canada. Mobil Oil Canada Ltd. kindly provided the Hibernia crude oil. Successful development of the exposure system has been a result of the efforts of Ms. Martha Thomson. Chemical analyses were performed by K. Deagle. Ms. Ann Orr kindly did particle size determinations.

REFERENCES

Bean, R.M., J.W. Blaylock, and R.G. Riley. 1980. Application of trace analysis techniques to a study of hydrocarbon composition upon dispersion of petroleum in a flowing seawater system. p. 233-236. *In*, L. Petrakis and F.T. Weiss, eds. Petroleum in the Marine Environment. Advances in Chemistry Series 185. Am. Chem. Soc., Washington, D.C.

Clement, L.E., M.S. Stekoll and D.G. Shaw. 1980. Accumulation, fractionation and release of oil bt the intertidal clam, *Macoma balthica*. Mar. Biol. 57:41-50.

Hyland, J.L., P. F. Rogerson, and G.R. Gardner. 1977. A continuous flow bioassay system for the exposure of marine organisms to oil. p. 547-550. *In*, Proceedings 1977 Oil Spill Conference (Prevention, Behavior, Control, Cleanup) American Petroleum Institute. Washington, D.C.

National Research Council. 1985. Oil in the Sea. Inputs, fates, and effects. National Academy Press. Washington, D.C.

Vanderhorst, J.R., C.I. Gibson, L.J. Moore, and P. Wilkinson. 1977. Continuous-flow apparatus for use in petroleum bioassay. Environ. Contamin. Toxicol. 17:577-584.

ACCINDENTALLY SPILLED GAS-OIL IN A SHORELINE SEDIMENT ON SPITSBERGEN: NATURAL FATE AND ENHANCEMENT OF BIODEGRADATION

Per Sveum

SINTEF
APPLIED CHEMISTRY DIVISION,
N-7034 TRONDHEIM
NORWAY

SUMMARY

The oil soluble fertilizer Inipol EAP22 has been used on shore as a treatment agent after an accidental marine gas oil contamination on Spitsbergen. A 60% increase in the biodegradation of the aliphatic fraction was obtained as a maximum. Due to the high rate of physical self cleaning (about 90%) the importance of the biodegradation for the total self cleaning was limited.

INTRODUCTION

On the 15th of November 1985 approx. 88 000 liters of marine gas oil was spilled from storage tanks located close to the shoreline in Ny-Ålesund, Spitsbergen. The oil was not traced any places in the fjord, except close to the shoreline adjacent to the storage tanks and in the shoreline sediment itself.

Due to the harsh environmental constrains of the arctic winter, it was impossible to start any kind of immidiate clean-up of the contaminated shoreline. A cooperating group of scientists present in the period after the spill, proposed a non-action strategy to allow for extensive studies both of oil fate and oil effects on the marine biota (Øritsland and Sveum 1985).

In late winter 1986, however, it was decided that some kind of clean-up action should be carried out. No manual or mechanical clean-up methods were considered efficient, and an alternative experimental treatment method was proposed as a suitable and labour saving treatment method. The alternative strategy comprised application of oil soluble fertilizer followed by extensive monitoring of hydrocarbon development in the shoreline sediments.

Enhancement of biodegradation of Statfjord A+B crude oil with the oil soluble fertilizer INIPOL EAP 22 has earlier been studied in a smaller scale on Spitsbergen shorelines (Halmø et al. 1986). These studies revealed interesting results in terms of biodegradation. However, those sediments studied differed considerably from the accidentally contaminated one with a lower selfcleaning potential.

Chemical treatment with dispersants, of crude oil on Spitsbergen shorelines (Sveum 1985), has also revealed interesting results giving an increase in both biodegradation and physical removal of the oil. The shoreline studied in that experiment was a mud-flat with a very low rate of water penetration.

Both these studies and the present study have been designed with the intention to develop a low cost and labour saving treatment strategy for oil contaminated remote shorelines.

MATERIAL AND METHODS

Description of experiments

The studies comprised 4 different experimental sites, each with a different time for fertilizer application. In addition to the 4 experimental sites 3 types of reference plots were studied. The experiments were carried out both on the accidentally contaminated shoreline and with back-up experiments on a test shoreline.

Table 1. Listing of reference and experiment plots studied.

Experiments	Treatment	Oil	Time of oil contamination	Time of fertilization
Exp. 1	Inipol	Yes	Nov. 15th 85	Jan. 29th 86
Exp. 2	"	"	"	June 25th 86
Exp. 3	"	"	"	July 8th 86
Exp. 4	"	"	June 10th 86	June 10th 86
Ref. 1	No treatment	Yes	Nov. 15th 85	———
Ref. 2	"	"	June 10th 86	———
Ref. 3	"	No	———	———

The microbial studies were restricted to the 2. stratum only, (i.e. 15-20 cm depth).

The locality of the contiminated shoreline is shown in figure 1.

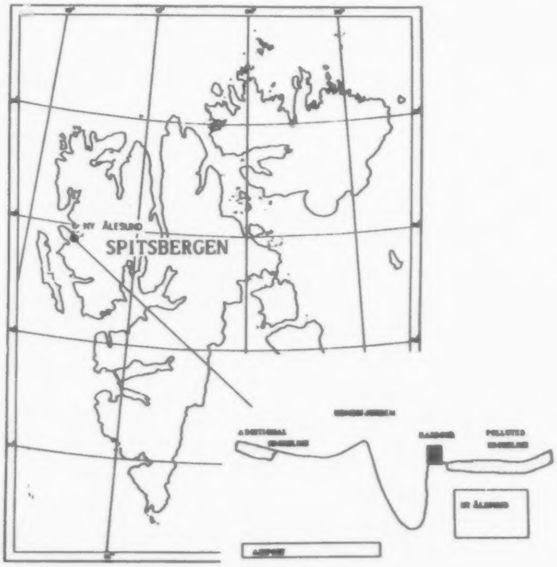

Figure 1. Location of accidentally contaminated shoreline and the additional test shoreline.

Fertilizer treatment

The fertilizer was applied to the shoreline manually using "garden watering cans" equipped with a perforated opening to allow for proper spreading of the fertilizer.

Sampling

The sampling was carried out with a small spade, as it was impossible to obtain intact sediment cores by drilling.

A hole was dug, and the different strata were carefully transferred to polyethylene bags and sealed.

Chemical analyzis

The total oil concentration was measured in dichloromethane extracts of the samples. About 500 ml of the sediment samples were transferred to 600 ml glass vessels and 500 ml $CH_2(Cl)_2$ was added. The vessels were shaken for about 24 hours at room temperature. The oil plus $CH_2(Cl)_2$ solution was decanted from the sample, and after appropriate dilution the oil content was measured by use of a Kontron 23 Spectrofluorimeter (ex=265, em=376).

The aliphatics were analyzed by use of a Perkin Elmer gas chromatograph. For the gas chromatographic analysis, the sample extraction was carried out with n-hexane instead of dichloromethane and fractionation done by use of MPLC.

Microbial analysis

The total number of bacteria was enumerated after staining with acridine orange (AO) using a Leitz dialuz 20 microscope with a Ploemopac fluorescence equipment. About 20 grams of sediment was transferred to a nutrient solution and homogenized for 3 min. on a Warring blendor at full speed. 1-5 ml of the solution was transferred to 100ml Soerensen´s phosphate puffer (pH 7.5, 0.1 M). The buffer solution was stained for 10 min. with AO and filtered through a 0.22 micrometer Polycarbonate filter (Nuclepore) on a Millipore microfilter unit. The filters were air dried and embedded on microscopical slides in a non-fluorizing immersion oil. Countings were performed through an eye piece grid. 15 squares selected at random or more than 300 bacteria were counted from each sample. The number of samples counted were adjusted to obtain a SD at about 10%, when possible.

The number of metabolically active bacteria was enumerated with the use of fluorescein diacetate (FDA), which are selectively staining esterase-producing cells. The sample preparation was identical to that described for total number of cells, except for the staining time which was about 3 min.

Total respiration was measured in vitro at 5^0C. 100 ml gas-tight bottles were filled with contaminated shoreline sediment. The bottles were analyzed for CO_2-emmision. CO_2 was measured on a Siemens Ultramat 1 infrared gas analyzer modified for septum injection. Gas samples were taken sequencially with a gas-tight syringe.

RESULTS

Changes in total oil content

The innermost parts of Kongsfjorden were covered with ice from the middle of January and until the middle of June. The iceing of the shoreline due to water plashing from the sea probably enclosed the oil within the shoreline through the winter. The ice cover and the permafrost in combination (fig. 2) constituted a possible complete enclosure for the oil.

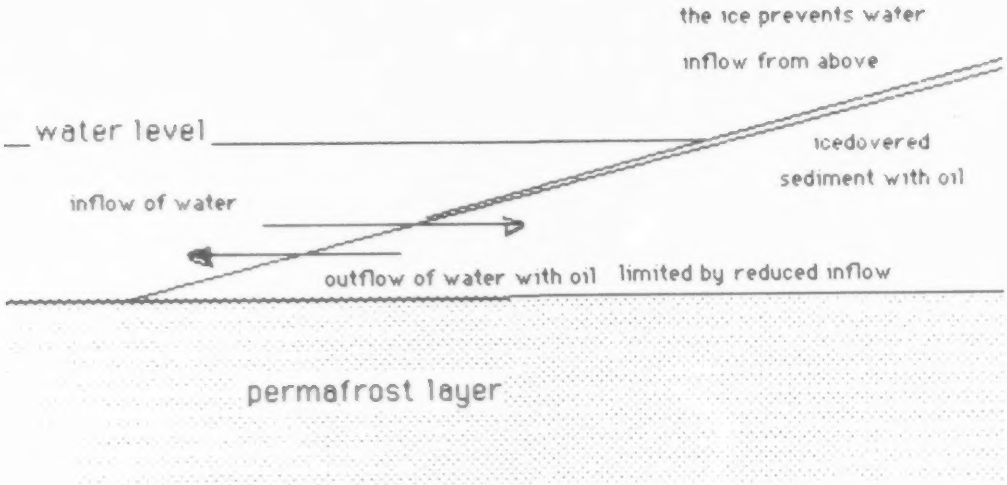
the ice prevents water
inflow from above
water level
icedovered
sediment with oil
inflow of water
outflow of water with oil
limited by reduced inflow
permafrost layer

Figure 2. Schematic presentation of the possible interaction of icecover on the shore and the permafrost layer in the shoreline.

The concentration of diesel was monitored throughout the summer season from the time of ice break-up. The fertilizer treatment was carried out on the 8 and 9th of July.

Figure 3 and 4 gives typical examples of the decrease in hydrocarbons in two sites of the shoreline.

A decrease in total oil content at a maximum level of about 90% is found in the shoreline from the time of ice break-up and until the time of freezing in the autumn. It is not possible at present to tell whether any amount of oil has been washed out of the sediment during the preceeding winter. However, the rate of removal during the summer season demonstrate a high level of selfcleaning of this type of shoreline when contaminated with marine gas oil.

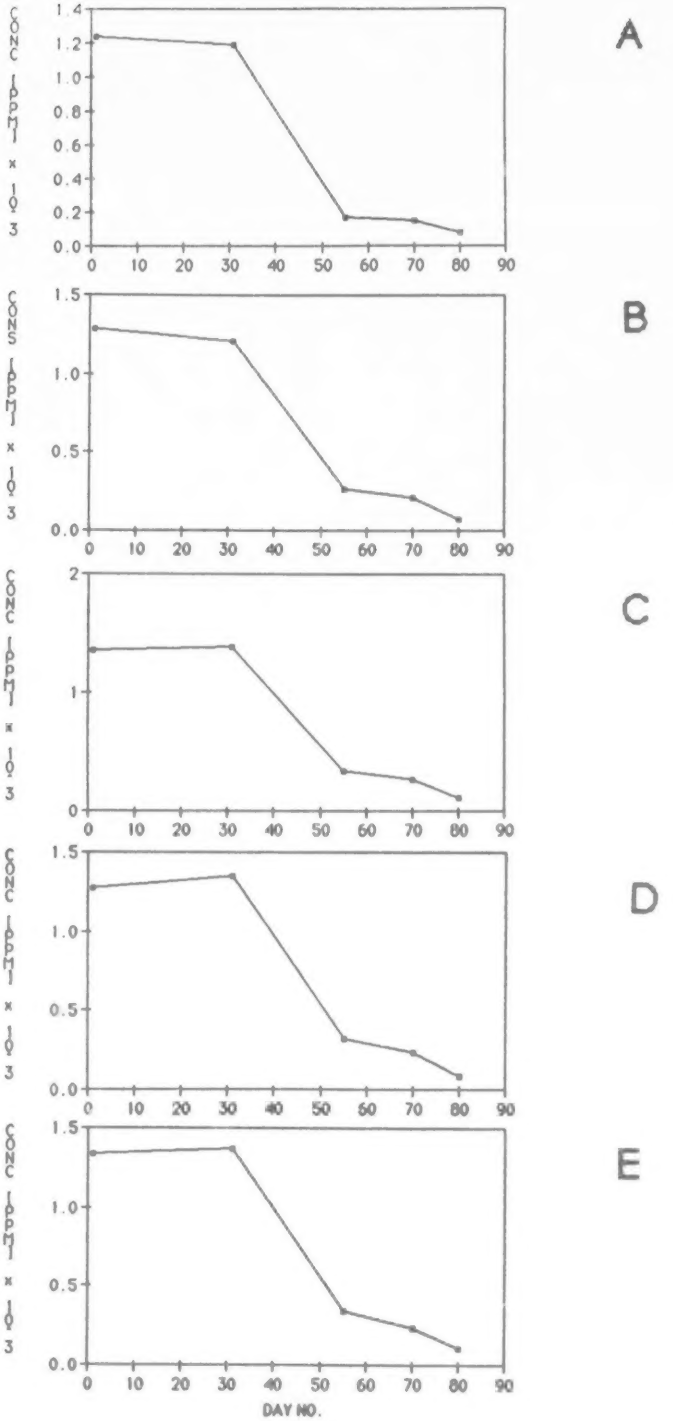

Figure 3. Total oil content in shoreline sediment at the oil contaminated shoreline at Spitsbergen. Strata: A = surface, B = 15-20 cm, C = 25-30 cm, D = 35-40 cm, E = 45-50 cm.

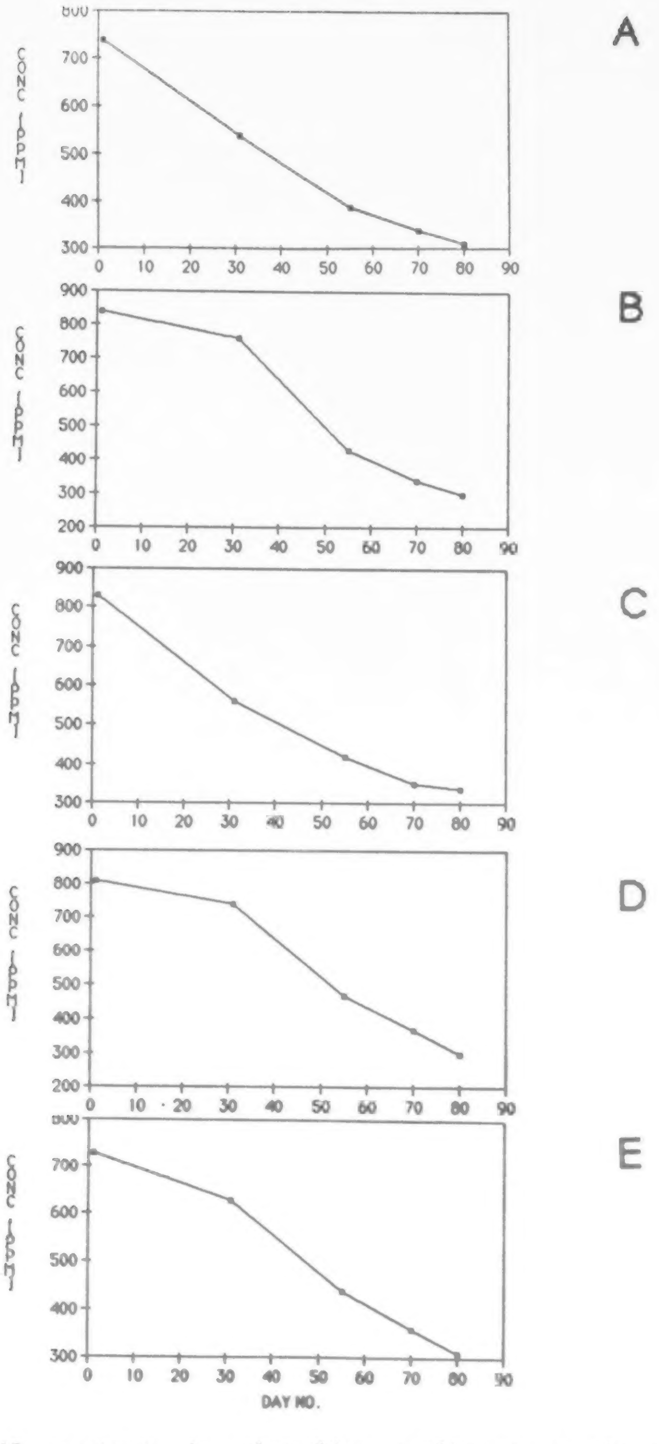

Figure 4. Total oil content in shoreline sediment at the oil contaminated shoreline at Spitsbergen. Strata: A = surface, B = 15-20 cm, C = 25-30 cm, D = 35-40 cm, E = 45-50 cm.

Microbiology

The microbial response to oil contamination and fertilization of the oil slick have been evaluated both as bacterial numbers and as total community respiration. Screening for fungal hyphae gave negative results.

The total number of bacteria and the number of metabolically active bacterial cells on selected days are given in figure 5-13. There is a significant increase in bacteria in the oil contaminated reference plots compared to the unpolluted reference. A significant increase is also found after fertilization of the accidentially polluted oil plots.

The metabolically active fraction of bacteria in the unpolluted reference is about 90% of the total number throughout the whole period.

The relative size of the active fraction decreases as a result of oil contamination. This might be due to toxic influence of microbial grazers, e.g. protozoa and nematoda. The immobilization of microbial cells further increases when fertilizer is applied to the oil contaminated sediment. However, the fertilizer has a significantly increasing effects on the number of active cells. This increase is found both relative to the unpolluted site and to the unfertilized polluted site.

As expected, when considering the microbial numbers, an increase in respiration is found. The increase in respiration is closely correlated to the metabolically active number of cells present.

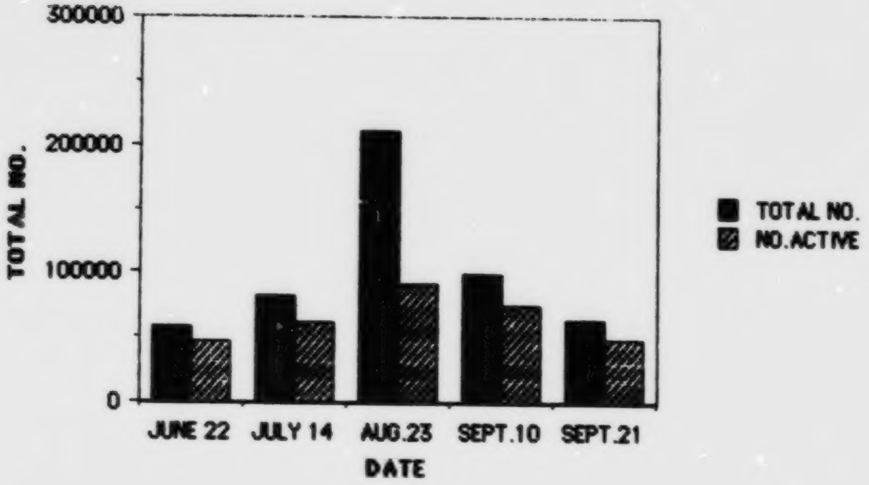

Figure 5. Total number of bacterial cells and number of metabolically active bacterial cells in the sediment of reference site 1.

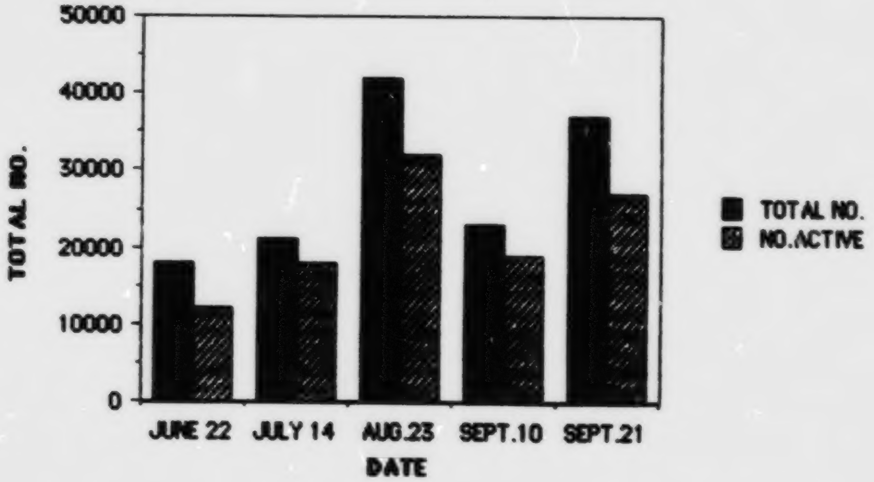

Figure 6. Total number of bacterial cells and number of metabolically active bacterial cells in the sediment of reference site 2.

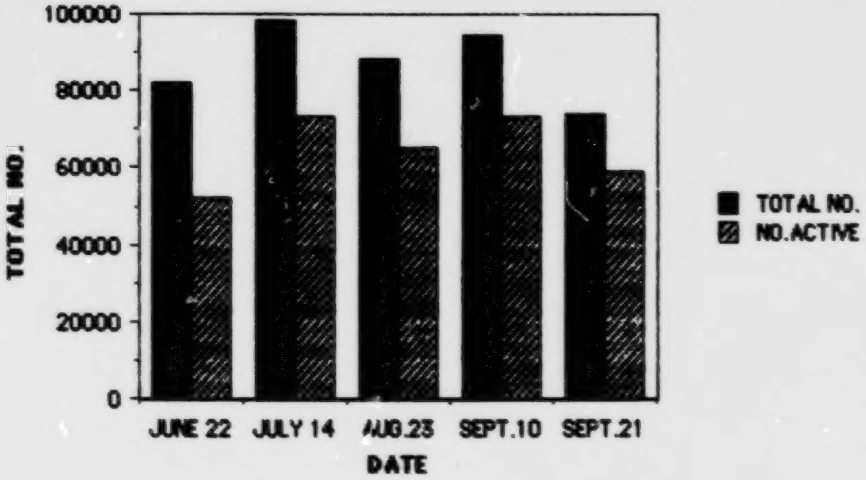

Figure 7. Total number of bacterial cells and number of metabolically active bacterial cells in the sediment of reference site 3.

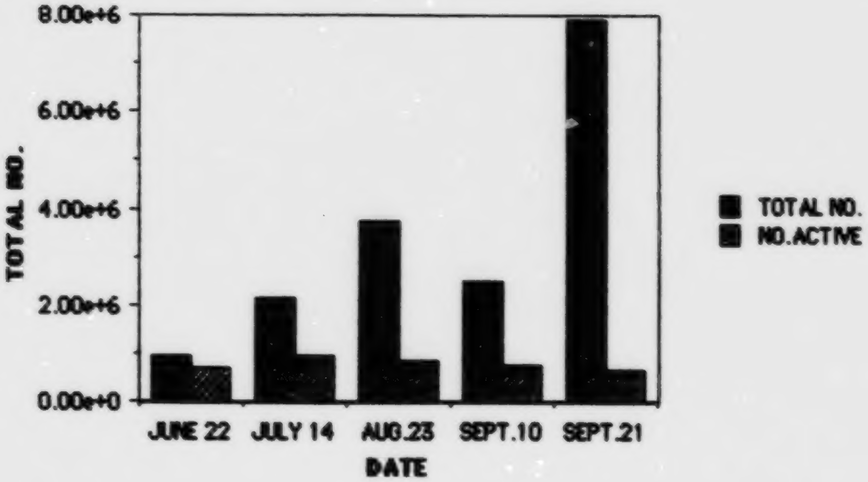

Figure 8. Total number of bacterial cells and number of metabolically active bacterial cells in the sediment of experimental site 1.

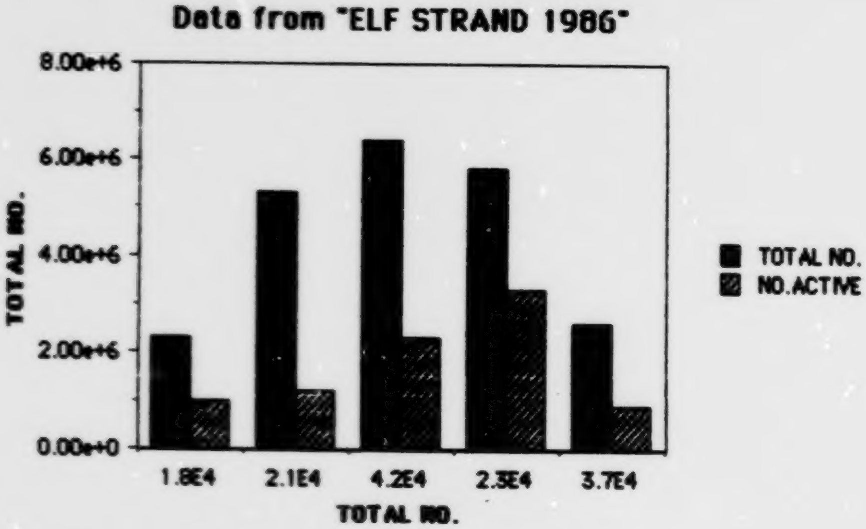

Figure 9. Total number of bacterial cells and number of metabolically active bacterial cells in the sediment of experimental site 2.

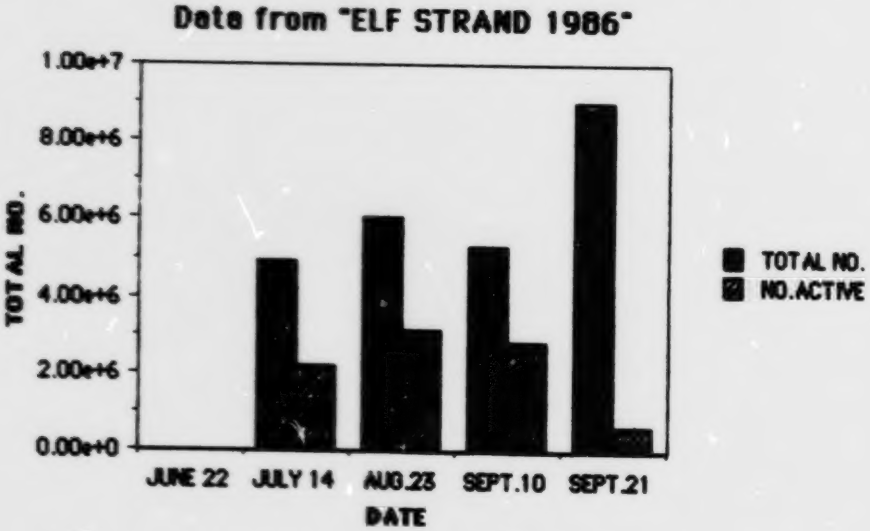

Figure 10. Total number of bacterial cells and number of metabolically active bacterial cells in the sediment of experimental site 3.

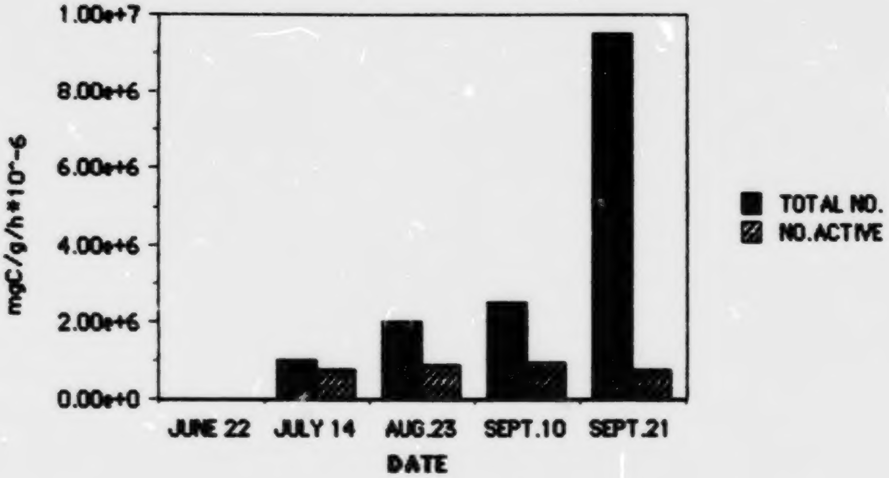

Figure 11. Total number of bacterial cells and number of metabolically active bacterial cells in the sediment of experimental site 4.

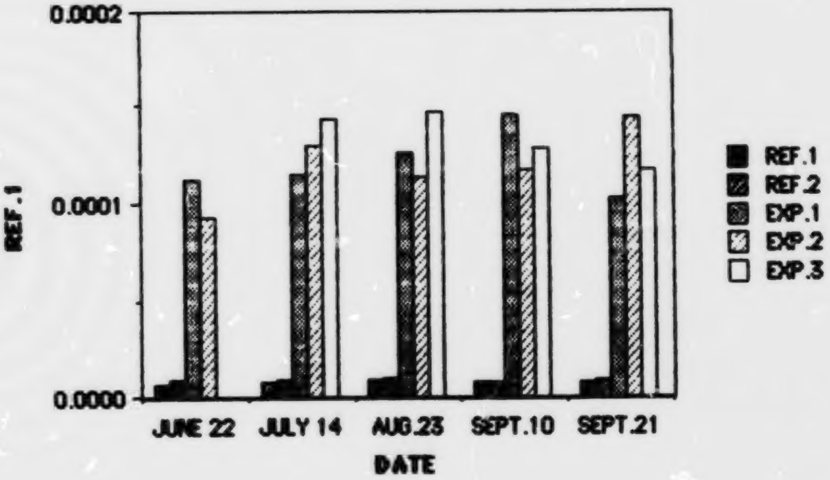

Figure 12. Comparison of total community respiration between reference site 1 and 2, and experimental site 1-3.

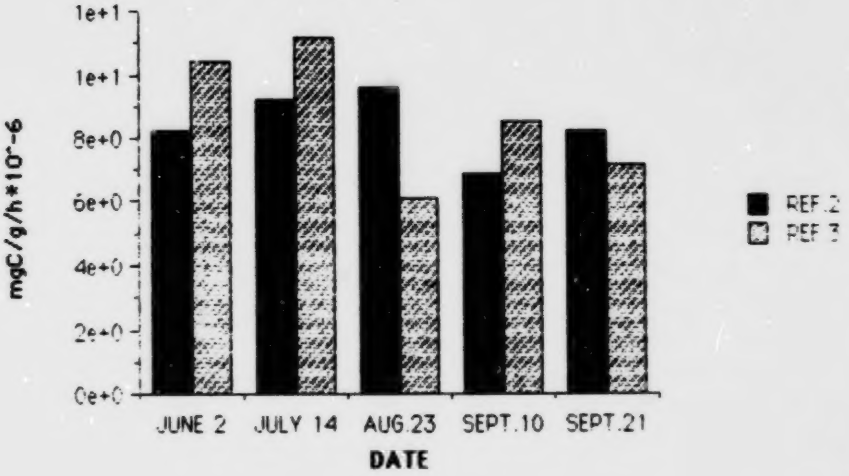

Figure 13. Comparison of total community respiration between reference site 2 and 3.

Biodegradation

The oil biodegradation has been evaluated as the decrease in the nC_{17}/pristane and nC_{18}/phytane ratios (Table 2). Both the contaminated reference sites have a limited biodegradation compared to the ratios of the fresh crude oil.

All the fertilized sites have a significant biodegradation, both compared to the fresh oil and to the references. The site fertilized in winter (end of January) (Exp. 1) has the most pronounced decrease. Within the limits of the significans of the ratios used, the biodegradation is 2-3 times that of the unfertilized sites.

The three other sites (Exp. 2-4) were fertilized at the same time, i.e. in June/July. The biodegradation is lower in this site although higher than in the reference sites.

Table 2. Biodegradation of oil evaluated as the decrease in the nC_{17}/pristane and nC_{18}/phytane ratios. Fresh oil: nC_{17}/prist. = 2.04, nC_{18}/phyt. = 2.22

Site	nC_{17}/pristane	nC_{18}/phytane
Ref. 2	2.1, 1.72, 1.91	1.96, 1.78, 2.22
Ref. 3	1.88, 1.90	2.06, 2.05
Exp. 1	0.75, 0.69, 0.86	0.71, 0.58, 0.85
Exp. 2	1.38, 1.63, 0.83	1.25, 1.68, 0.77
Exp. 3	1.33, 1.68, 1.45	1.51, 1.83, 2.00
Exp. 4	? , 1.45, 1.65, 1.66	1.24, 1.25, 1.75,1.75

DISCUSSION

The removal of oil contaminants from a shoreline sediment is carried out by the joint action of several more or less interconnected processes. These include advection, diffussion and biological and chemical degradation. If we consider the oil contaminant as a composit multicomponent mixture, where the components have different properties in terms of overall removal potential, the bulk oil can be regarded as a two state system. That is oil adsorbed to the sediment and oil in "solution". The term "solution" is used for the total amount of non-adsorbed oil without considering the mechanisms of solution i.e. whether the oil is dispersed as droplets or solubilized as molecules. The state of the system determines to a great extend whether the oil is succeptible to physical selfcleaning. Physically the most easily removed oil will be the oil in solution. Dependent on the location of the oil in solution within the shoreline sediment, the removal process can be regarded as a compartment model whereby the compartment is wasted by the entering and leaving (i.e. circulating) fluid. The clean water enters the sediment, and within the sediment the water and oil in water gradient is levelled out, whereby the water leaves with the same oil concentration as the remaining interstitial water. The concentration is levelled out by the combined action of diffusion and advective mixing.

However, the oil within the sediment is also adsorbed to the sediment and the interstitial concentration will be determined also by the rate of adsorbtion, not only by the removal. It is reasonable to assume that the desorbtion rate, when considering the bulk oil, is considerably lower than the washing of the sediment.

In terms of shoreline decontamination the desorbed oil will have a biodegradation potential related to the residence time in the sediment. In the same manner it is reasonable to consider the biodegradation to work mainly in the adsorbed part of the oil.

Studies of light crude oil contamination on Nova Scotia beaches show that bulk oil contamination was mainly removed by evaporation (Strain 1986). Components up to C_{16} were found to evaporate. The rate of evaporation was related to the water saturation of the sediment. In the type of shoreline sediment studied here a low evaporation rate could be expected.

In the Nova Scotia sediments no indices of biological degradation based on the

nC_{17}/pristane ratio were found (Strain 1986).

The possible result from fertilizer application will be enhancement of microbial degradation of the oil. The fertilizer applied for the Spitsbergen shoreline treatment is oil soluble, i.e. it contains a surfactant that increases the mixing and binding of the fertilizer to the oil. The surfactant will alter the oil properties both in terms of viscosity and in terms of diffusion properties. The present fertilizer INIPOL is thus likely to alter the contaminated oil in two ways:

1. It turns the oil from a low quality food for the microbes to a "high quality" food item.

2. It decreases the viscosity and thereby increases the possible wash-out.

3. It may neutralize polar compounds formed due to photochemical and microbial action, and may thus decrease the adsorbtion of the oil to sediment.

When considering the decrease in total oil content it is not possible to ascribe specific effects to the fertilizer. However, the shoreline sediment treated is very pourous with a high selfcleaning potential. Thus it may be assumed that despite the fertilizer application the level of hydrocarbons would have reached the level obtained here.

The strong increase in aliphatic biodegradation which was obtained in the fertilized plots shows that the application of INIPOL EAP 22 really enhances the biodegradation. It is reasonable to assume that the equilibrium between physical selfcleaning and biodegradation will be different in sediments with less water penetration and with different adsoption properties.

The results obtained with the present treatment, together with results obtained in medium scale experiments in less a porous shoreline sediment on Spitsbergen (Halmø et al. 1986), clearly indicate that the use of INIPOL EAP 22 is an available, labour saving and low cost treatment method on arctic beaches.

The transformation of urea nitrogen to a microbial available form depends on the type of bacteria present. Ureolytic bacteria, i.e. bacteria producing the enzyme urease, are found in several genera i.e. Bacillus, Pseudomonas. These genera are represented in most habitats. One might thus assume that ureolytic activity is present also in artic waters and on the experimental site.

The oil soluble properties of the nitrogen in Inipol are connected to the urea state of the nitrogen. Once mineralized to ammonium, the difference in solubility of the ion between oil and water or the microbial fate of the ammonium ions, will determine the nutritional status of the oil slick or droplets. As the solubilization will be much greater in water, osmotic forces will decrease the concentration of the ammonium ions in the vicinity of the oil. One way to maintain a nitrogen concentration higher than in the surrounding interstital water or on the solid sediment is by microbial immobilization.

In the present experiments it has been demonstrated that a large inactive microbial biomass is developed. Thus large quantities of the nutrients applied will be immobilized.

An important aspect of the fertilization efficiency will be connected to wheter the bacteria that immobilize the mineralized urea nitrogen, are able to metabolize the oil components, or whether there is one group of ureolytic bacteria and one hydrocarbonoclastic group with no or little overlap between them.

Another problem may be the spatial location of the oil components relative to the available urea fertilizer for the cell. If we concider the oil-fertilizer mixture as droplets, the arrangement of the fertilizer will determine whether a bacterial cell colonizing the droplet is able to metabolize both the oil components and the urea source of nitrogen as urea.

Whether the increased degradation of oil with Inipol in shoreline sediments are spesificly due to the oil-soluble property or to nitrogen application in general, can not be decided until the adsorption properties of ionic nitrogen has been tested versus the slow-releasing and mineralization properties of Inipol or other urea based fertilizers.

REFERENCES

Atlas, R.M. & Bartha, R. 1972. Degradation and mineralization of petroleum in natural water, limitations of nitrogen and phosphorus. Biotech. Bioeng. 14: 309-317.

Halmø, G., Sveum, P. and Danielsen, A., 1985. Enhancement of oil biodegradation in ice inferted waters. STF21 F85106.

Hauck, R.D. 1972. Synthethic slow-release fertilizers and fertilizer. amendments. In:Gring, C.A.I. and Hamaker, J.W. (eds), Organic Chemicals in the Soil Environment. Vol. 2.

Strain, P.M. 1986. The Persistence and Mobility of a Light Crude Oil in a Sandy Beach. Mar. Environ. Res. 19: 49-76.

Sveum, P. (1985). Olje på strand på Svalbard. Dispergeringsmiddel brukt på olje i littorale bløtbunnssedimenter. STF21 F85114.

Øritsland, N.A. & Sveum, P. (1985). Oljeutslipp i Ny Ålesund. Rapport Versjon I. Nov. 1985.

LABORATORY TESTING TO OPTIMIZE THE PERFORMANCE OF A HIGH PRESSURE WATERJET BARRIER

L. Phillips and A. Nawwar
ARCTEC CANADA LIMITED
311 Legget Drive,
Kanata, Ontario.
K2K 1Z8

and

F. Laperriere
Environmental Emergencies Technology Division,
Environmental Protection Service,
River Road,
Ottawa, Ontario.

ABSTRACT

The premise that an oil spill may be contained by means of a high pressure waterjet barrier has spurred research efforts towards developing an effective prototype. In this paper, laboratory tests are reported which investigate the influence of various parameters on the performance of the waterjet barrier. An existing waterjet system was set up in Arctec Canada's environmental test basin in Kanata, Ontario. During the tests, measurements of the mean velocity of the two-phase airflow were obtained using a laser doppler anemometer. The matrix of parametric variations included: manifold pressure, nozzle spacing, height above the water free surface, depression angle, and nozzle characteristics.
From the analysis of these results it has been possible to identify an optimal nozzle type and the most efficient spacing of the jets.

INTRODUCTION

The high pressure waterjet barrier has been developed as a means of containing and moving oil or other environmental contaminants which float on the water surface. The barrier consists of an array of high pressure waterjets which generate an airflow that in turn moves the oil.

Testing of various configurations of low pressure water spray barriers by a number of authors [1, 2] had shown the potential of spray barriers as a means of oil spill containment. However the low pressure spray barriers were found to be ineffective when faced with adverse currents or waves.

The basic concept for a high pressure waterjet barrier was proposed to the Environmental Protection Service [3] in 1979 by D.M. Christie (Ocean Dynamics International Limited). He recommended the use of a series of flat, fan-shaped waterjet nozzles which could be positioned on floats at a height about 15 to 20 cm above the surface of the water. Each waterjet was paired with a second nozzle pointing in the opposite direction to balance the moments acting on the float. It was believed that the airflow entrained by the high pressure water spray would be the principal mechanism moving the oil; simulating the affect of natural winds.

Preliminary tank testing of the concept was carried out at OHMSETT [4], the U.S. Environmental Agencies test facility, in 1983. The effectiveness of high pressure waterjets was examined for moving floating oil and its sensitivity examined for a number of parameters, including: jet height above the slick, nozzle flare angle, waterjet flow rate, current speed and surface conditions. These tests confirmed that the entrained airflow could be effectively used to contain, divert or move an oil spill, even in harbour waves.

As a consequence of the promising results from the OHMSETT test, it was decided by EPS to build an experimental waterjet barrier system. This consisted of a triplex pump driven by a diesel engine, a control manifold, a tether line connecting the manifold to the barrier, and 10 float-mounted waterjet pairs. The barrier was first tested without oil at Cultis Lake, B.C., in 1983 and again in 1984. Field trials were subsequently carried out in the MacKenzie River near Norman Wells in August 1984 [4]. Peat moss treated with vegetable oil was used to represent a slick.

The objective of the present study was to optimize the design of the existing barrier. This was achieved by performing systematic laboratory experiments to determine the influence of various parameters. The performance of the waterjet was believed to be directly related to the airflow generated, and therefore the entrained airflow downstream from the nozzle has been measured. A laser doppler anemometer was used to accurately determine the cross-sectional velocity distribution of the airflow at a range of distances from the nozzle. Corresponding induced surface current velocities were also measured. No oil has been introduced into the basin in these tests.

The experimental program was carried out for EPS in 1985 at Arctec Canada Limited's environment basin in Kanata, Ontario. The principal results of this work are reported here.

Experimental Set-up

The Environmental Protection Service provided their high pressure waterjet barrier system for use in these tests. It was necessary to replace the hosing between the triplex pump and manifold and to the waterjets, since a higher working and burst strength was required to handle the proposed test pressures. The flotation system was not deployed in the basin. Instead the waterjets were mounted on a support assembly that was rigidly attached to the front of the basin carriage (Figure 1). The support assembly could be adjusted laterally to different positions across the basin. Depression angle and height variations were also possible by appropriate adjustments to the support assembly. The basin carriage was also movable to change the distance between the measurement position and the nozzle.

A laser doppler anemometer (LDA) was mounted on a rigid light table at a fixed location along the basin wall. Details of the LDA system are illustrated in Figure 2. The LDA measured the mean velocity of air/water/dust droplets within the high pressure waterjet spray. It was calibrated using a disc rotating at an accurately known speed.

When the LDA was operating, its laser beam was split into two parts and then focussed through a 600 mm focal length lens. This focusing produced a fringe interface pattern at a fixed location in the basin which acted as a measuring grid for particle's moving through it. The backscattered light was monitored on a photo-multiplier to determine the airflow velocity.

The focal point of the LDA was a fixed reference point throughout the tests. The flow velocity at different positions with respect to the waterjet nozzle was obtained by moving the nozzle assembly laterally or moving the carriage along the basin. A vertical profile of airflow velocities was

FIGURE 1

ELEMENTS of TEST APPARATUS

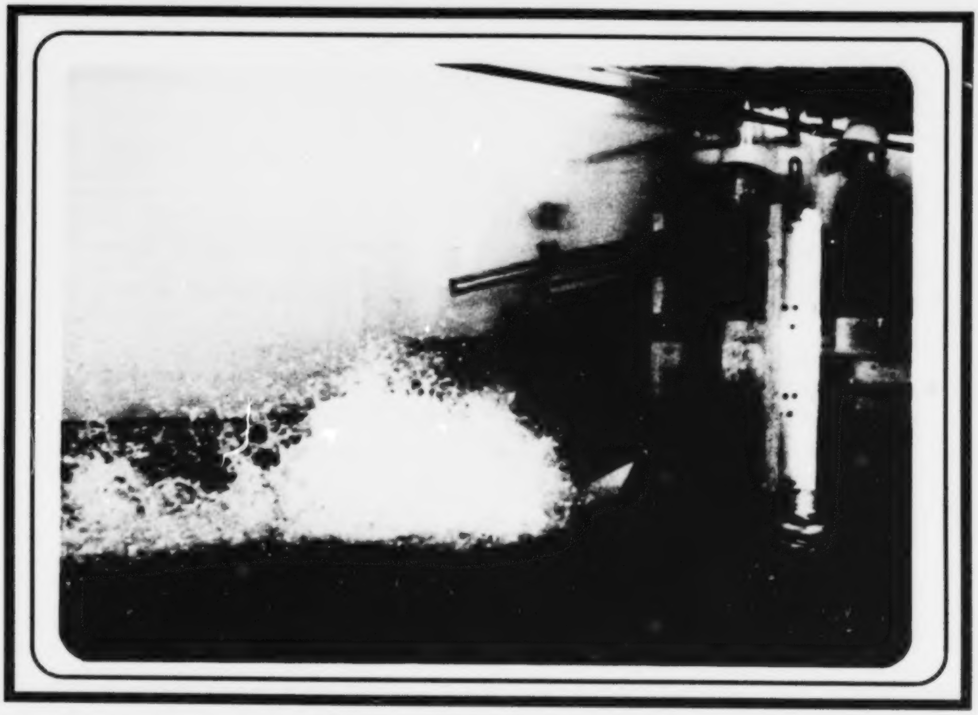

Depression Angle 30° Test

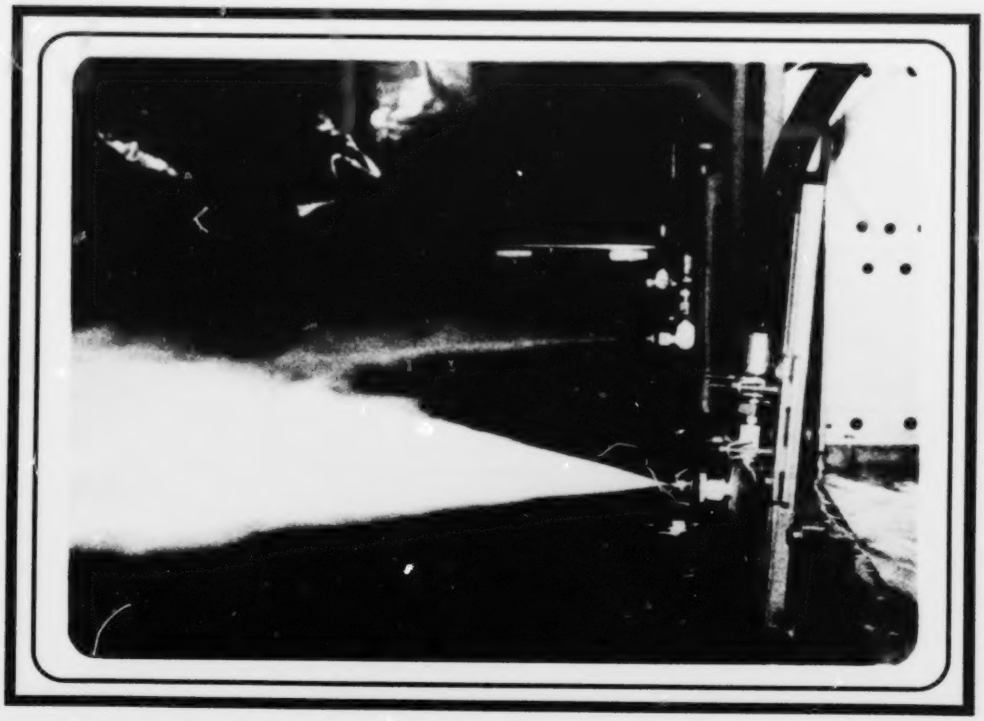

Multiple Nozzle Test

FIGURE 2

EXPERIMENTAL SET-UP: SINGLE NOZZLE AIRFLOW TESTS

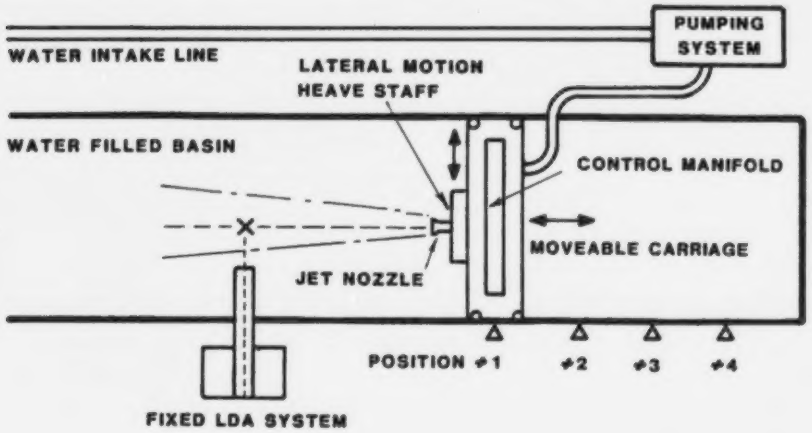
PUMPING SYSTEM
WATER INTAKE LINE
LATERAL MOTION
HEAVE STAFF
WATER FILLED BASIN
CONTROL MANIFOLD
MOVEABLE CARRIAGE
JET NOZZLE
POSITION #1
#2
#3
#4
FIXED LDA SYSTEM

DETAIL of LDA SYSTEM

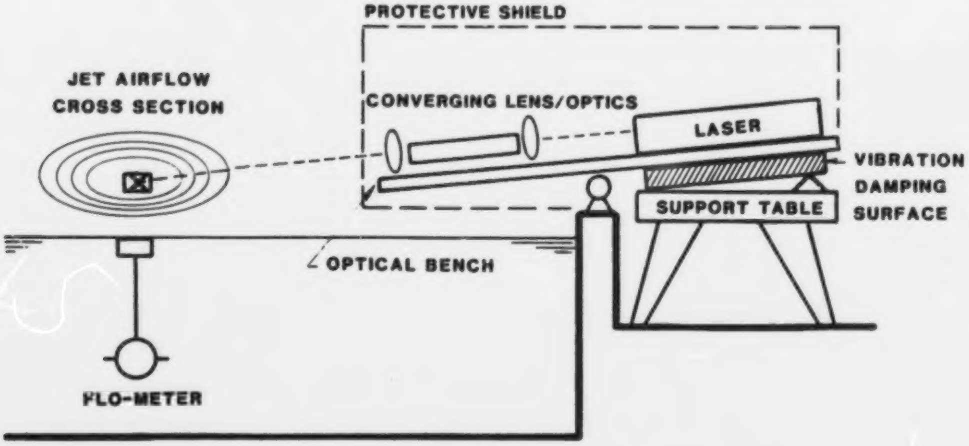
PROTECTIVE SHIELD
JET AIRFLOW CROSS SECTION
CONVERGING LENS/OPTICS
LASER
VIBRATION DAMPING SURFACE
SUPPORT TABLE
OPTICAL BENCH
FLO-METER

obtainable only by varying the basin water depth. A Dixon stream flow probe was fixed 3 cm below the water surface to measure the current velocities corresponding to the airflow velocities. The depth of the flow probe was adjusted to determine the vertical profile of the current velocity.

Test Plan

The experimental program was divided into two parts. A first phase involved single nozzle tests. The airflow velocities associated with a series of commercially available nozzle configurations were examined and trends defined for a number of barrier operating parameters. The second phase considered the spacing of waterjet nozzles. Only current flow velocities were measured in those latter tests.

A total of 34 single nozzle tests were carried out involving:

- ° nozzle flare angle and aperture
- ° waterjet height (7.5 cm - 31 cm)
- ° pressure variation (6900 kPa - 20,680 kPa)
- ° depression angle (0° - 30° down from horizontal)
- ° current depth profile

A matrix of 11 flat or fan-type nozzles were examined under fixed test conditions. Flare angles varied between 25° and 65°. Aperture diameter varied from 0.191 cm to 0.465 cm. A nominal pressure of 13,790 kPa at the manifold was maintained throughout the tests; except to study the influence of the pressure. Table 1 shows the test program matrix. Table 2 lists the nozzle configurations examined and gives their particulars.

Test Procedure

A consistent procedure was followed during testing. The testing of each nozzle consisted of approximately 15 individual measurement trials. Data was collected at 5 - 6 points along the centreline corresponding to different distance downstream from the waterjet and also at several points along cross-sections at 3.05 m and 6.1 m downstream.

During each trial the control valve on the manifold for the discharge line was closed until the requisite pressure reading in the nozzle line was attained. The velocity of the airflow at that position was then measured. The sampling time for the LDA was limited to about one minute to obtain a steady-state mean velocity. Each trial was followed by a four minute interval to allow the basin to settle.

Test Results and Discussion

A representative set of data is shown in Figure 3. It can be observed that the airflow velocities along the centreline decrease exponentially with distance from the nozzle. The corresponding cross-sectional profiles at distances of 3.05 m and 6.10 m downstream are found to be well fitted by normal distributions. As expected from the fan shape of the nozzles, the broadness of these normal distributions increased with distance from the nozzle.

Similar trends were found for each of the nozzle configurations. For the nozzles having the largest flair angle (65°) the normal curves did not fit the data accurately at 6.1 m, likely because of wall effects.

Figures 4a and 4b show the influence of nozzle flare angle and aperture on the airflow velocities. In the test region between 3.05 m and 9.15 m it was observed that airflow decreased as the flare angle was increased from 25° to 65°. Conversely the airflow increased with larger aperture nozzles. However, any increase in aperture is nearly in direct proportion to the increase in flow rate, according to the manufacturer's specifications on nozzle flow rates.

TABLE 1

A. SINGLE NOZZLE AIR FLOW TEST PROGRAM

1. NOZZLE TYPE TESTS

NOZZLE TYPE DESIGNATION: AABB where:
AA = angular spread (degrees
BB = Aperture Diameter
10 = .191 cm (.075 in.), 20 = .269 cm (.106 in.),
30 = .330 cm (.130 in.), 40 = .381 cm (.150 in.),
60 = .465 cm (.183 in.)

→ increasing aperture

↓ increasing flare angle

2510	2520	**2530	2540	
4010	4020	4030	4040	4060
**6510	6520	6530	--	

Pressure = 13790 kPa (2000 psi)
Jet Position; level, h = 15.2 cm (6 inches)
**Not Tested

2. VARIABLE HEIGHT TESTS

NOZZLE	HEIGHTS			
4030	15.2 cm (6")STD	7.6 cm (3")	22.9 cm (9")	30.5 cm (12")

Pressure = 13790 kPa (2000 psi)

3. PRESSURE VARIATION TESTS

NOZZLE	PRESSURES kPa (PSI)				
2520	6900 (1000)	10340 (1500)	13790 (2000)	17240 (2500)	20680 (3000)
4030					
6520					

Jet Position; level, h = 15.2 cm (6 inches)

4. DEPRESSION ANGLE TESTS

NOZZLE	DEPRESSION ANGLE			
6520	0° STD	7.5°	15°	30°
4030				

Pressure = 13790 kPa, (2000 psi)
Jet Position, h = 15.2 cm (6 inches)

B. MULTIPLE NOZZLE TEST PROGRAM

1. SPATIAL VARIATION TESTS

NOZZLE	NOZZLE SPACING		
4020	1.37 m (4.5')	1.98 m (6.5')	2.74 m (9.0')

Jet Position, h = 15.2 cm (6 inches), level
Pressure = 13790 kPa (2000 psi)

FIGURE 3
REPRESENTATIVE AIRFLOW DATA

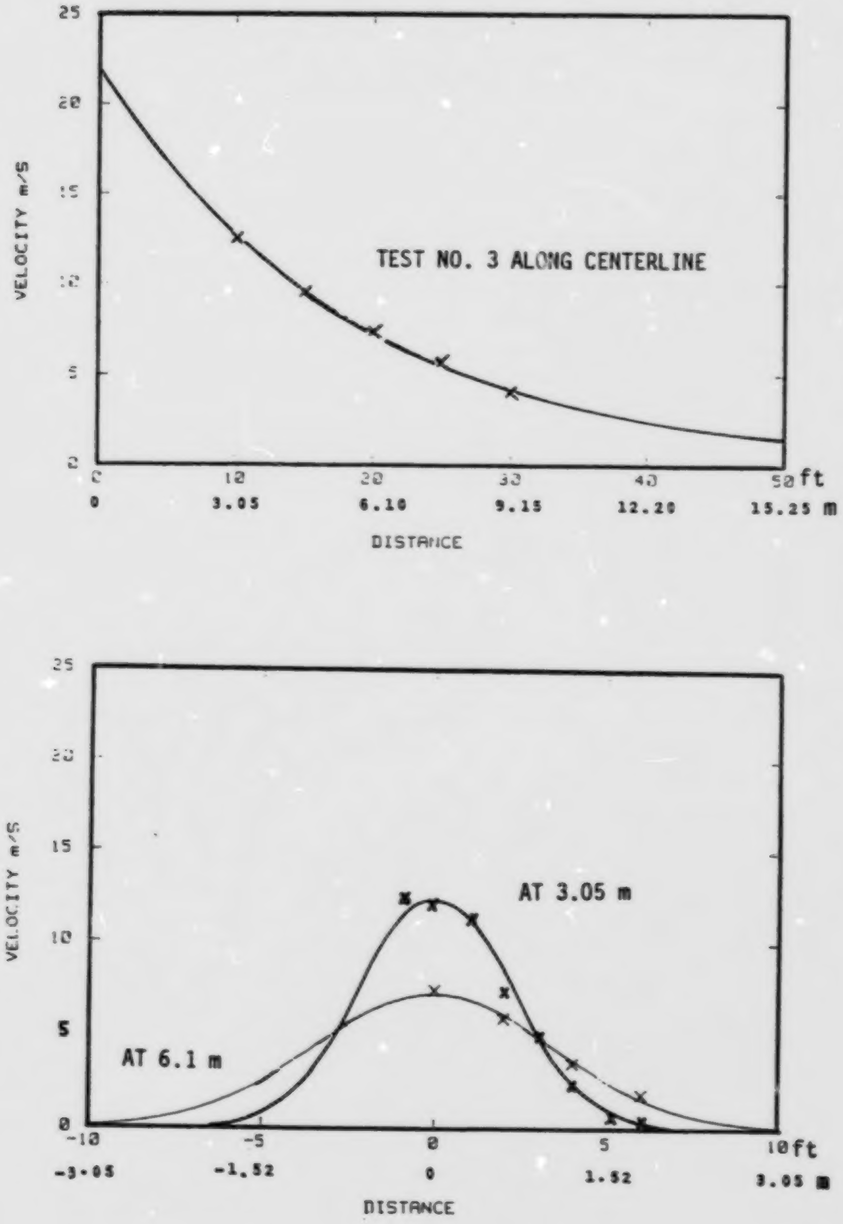

The effectiveness of the waterjet nozzles under particular operating conditions can be expressed in terms of airflow flux. The flux is a measure of airflow which is independent of concerns about different spreading characteristics of the nozzles. Flux values have been calculated for the different parametric tests by numerically integrating the normal distributions fitted to each set of velocity cross-section data. They are given by:

$$\mathrm{FLUX} = \int_{-\infty}^{\infty} \frac{A}{\sigma\sqrt{2\pi}} \exp\,[-1/2\,(Y/\sigma)^2]\,dy$$

where A and σ are the curve fit constants. Also σ, the standard deviation, is a measure of the broadness of the cross-sectional distributions.

Figure 5 illustrates the relative effectiveness of each of the nozzle types in terms of flux normalized by flow rate. The amount of flux generated at a common flow rate is observed to increase for nozzles with greater flare angle and smaller aperture. Broadness has been non-dimensionalized by angle and distance to express all of the test results in a common form. Nozzle type 4010 (40°, aperture 10 = 1.91 mm) was found to have the largest flux ratio. However it is expected on the basis of the observed trends that larger flare nozzles, such as nozzle type 6510, would be yet more efficient.

The observations of the effects of waterjet barrier parameters can be summarized as follows:

°Flare angle: At a fixed distance from the waterjet the airflow velocities decreased approximately linearly with increased flare, but velocity cross-section broadness is increased.

° Aperture: Airflow increased with greater aperture. However any advantage was mitigated by the increased pumping power required.

° Nozzle Height: The highest airflow velocities were observed at 30 cm, the maximum height tested. There was only a marginal decrease in velocities at heights between 15 cm and 30 cm. However significant reductions in airflow were observed below 15 cm. (Figure 4d).

° Depression Angle: Airflow velocities decreased rapidly with small depression angles. By beyond about 15° below the horizontal it was observed that the airflow had dropped to zero (Figure 4e).

° Pressure: Airflow velocities appeared to increase weakly with increased nozzle pressure over the range from 6,900 kPa to 20,700 kPa. However, contradictory results were obtained from tests with different nozzles. Further work is required to establish the trend in this parameter (Figure 4c).

The second phase of the experimental program involved determining the optimum spacing between waterjets. It was not possible to measure cross-sectional profiles of airflow velocity in the multiple nozzle tests. Therefore the corresponding current flow profiles were measured. Figure 6a shows the effect of increasing the nozzle spacing from 1.4 m to 3 m for a 40° nozzle. Fluctuating peaks and troughs are observed across the front, caused by the current velocity superposition. It was found that the velocity distribution became uniform at a spacing of about 2.75 m, or about twice the standard deviation (σ) of the single nozzle current profiles.

FIGURE 4
AIRFLOW RESULTS

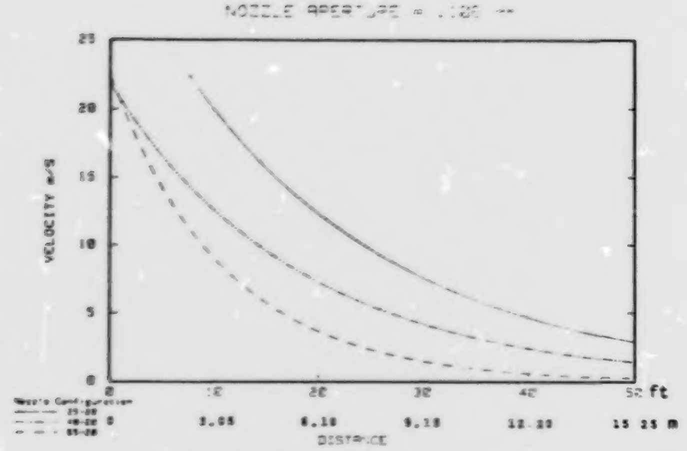

a) FLARE ANGLE VARIATION

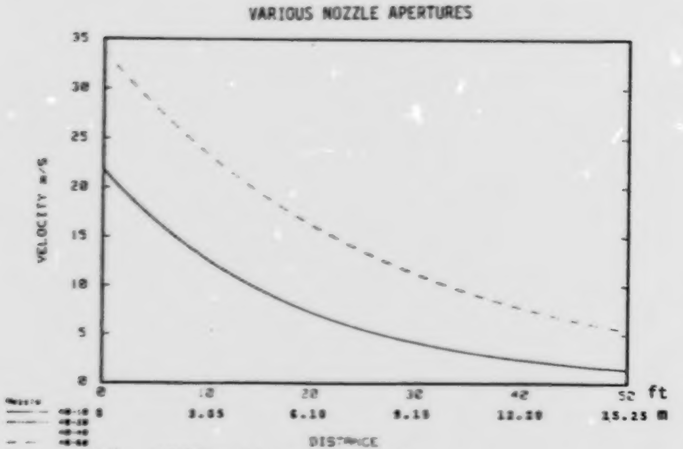

b) APERTURE VARIATION

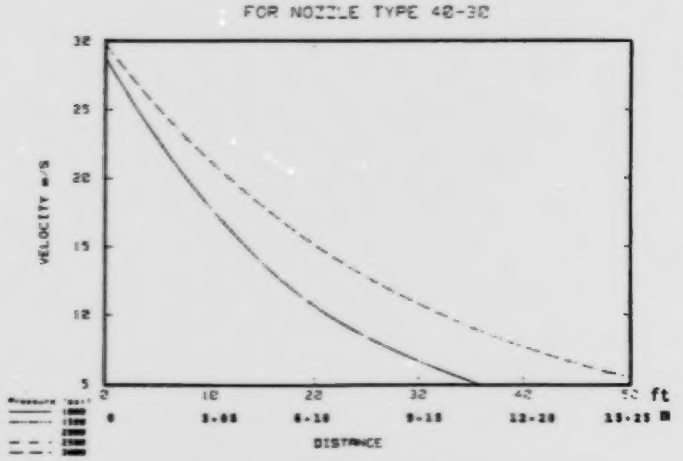

c) PRESSURE VARIATION

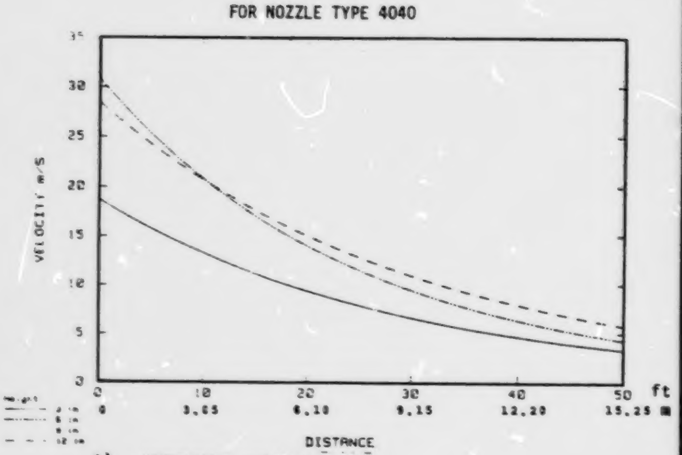

d) HEIGHT VARIATION

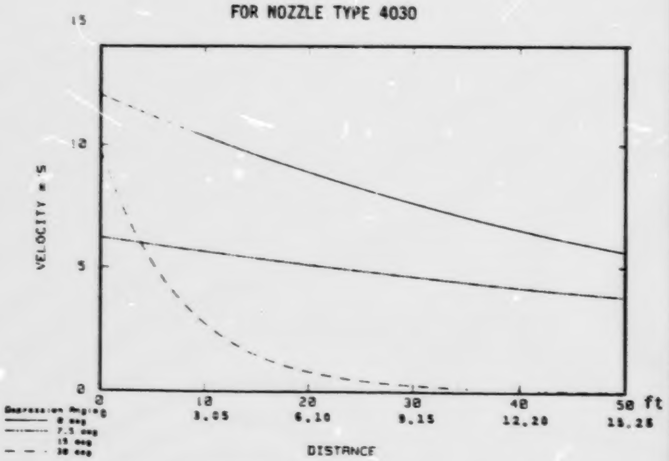

e) DEPRESSION ANGLE VARIATION

FIGURE 5

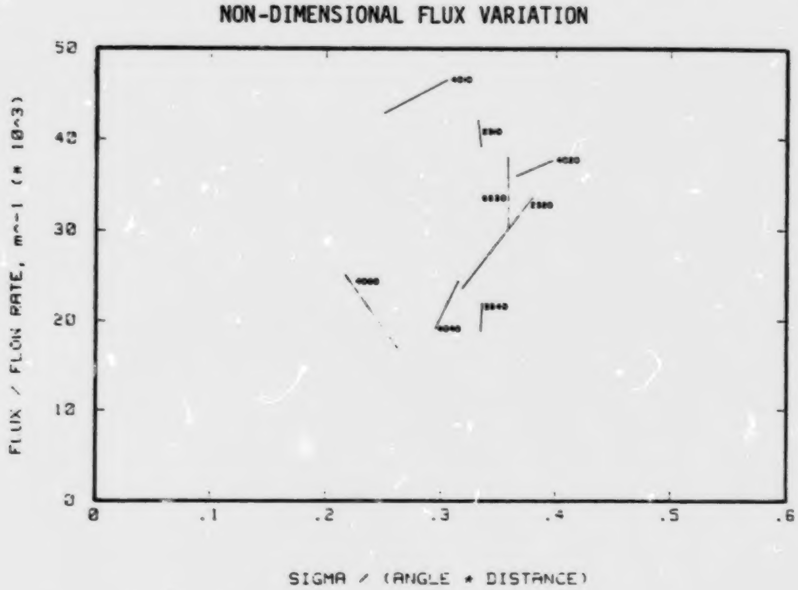

TABLE 2

NOZZLE CHARACTERISTICS

TYPES	NOZZLE SPREAD ANGLE (deg)	NOZZLE APERTURE (inch)	MAXIMUM FLOW RATE (GPM) AT PRESSURE (psi) 1000	1800	2000	2500	3000
2510	25	0.075	5.0	6.1	7.1	7.9	8.7
4010	40						
6510	65						
2520	25	0.106	10.0	12.3	14.1	15.8	19.3
4020	40						
6520	65						
4030	40	0.130	15.0	18.4	21.0	24.0	26.0
6530	65						
2540	25	0.150	20.0	24.0	28.0	32.0	35.0
4040	40						
4060	40	0.183	30.0	37.0	42.0	47.0	52.0

FIGURE 6

MULTIPLE NOZZLE SPACING RESULTS

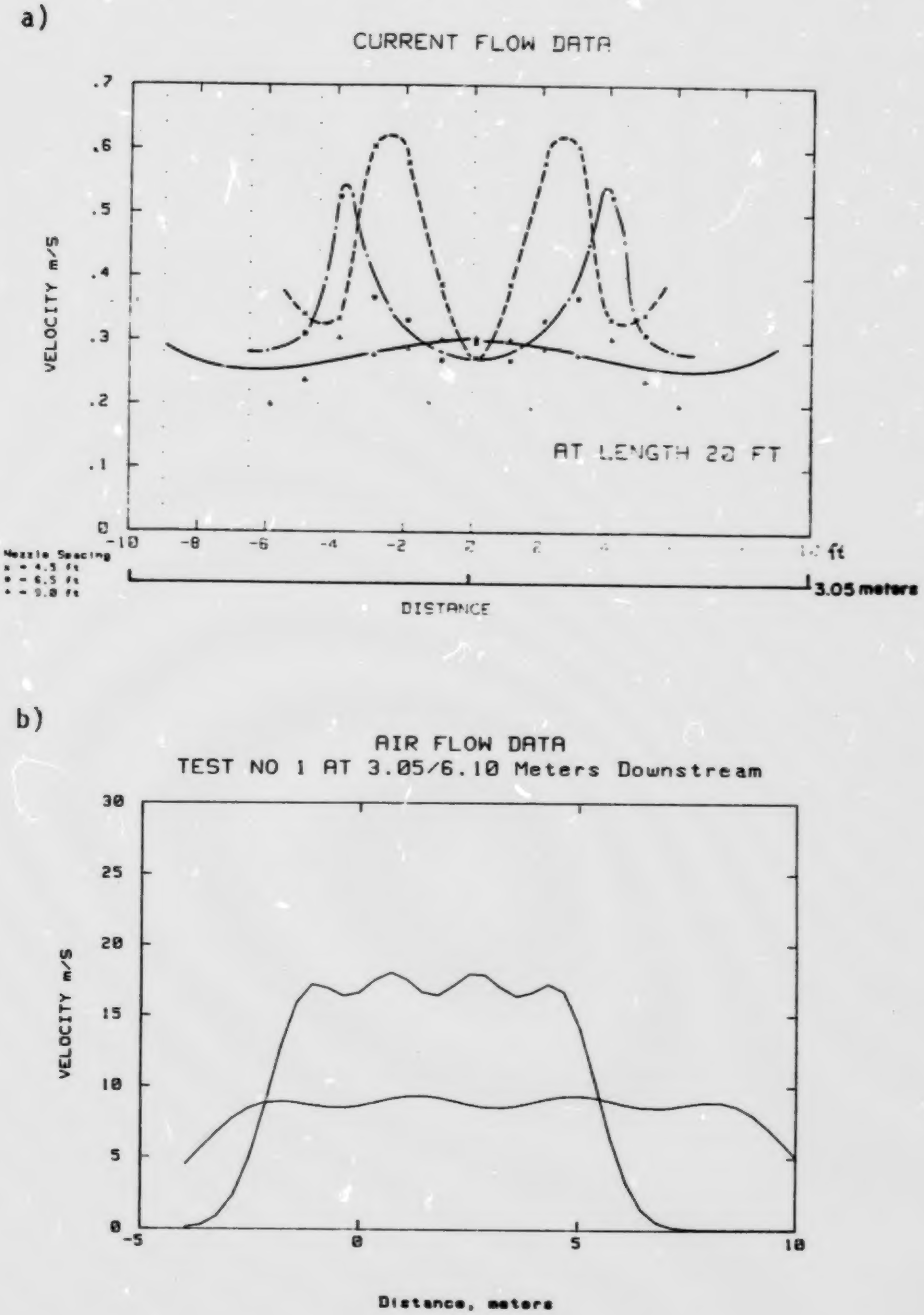

It appeared reasonable to assume that the airflow velocities would follow a similar trend to that observed for the current velocities induced in the underlying water. This assumption of simple superposition of airflow velocities has been employed in calculating the optimum spacing of the different nozzles and estimating their expected power requirements. It was important to know how many nozzles of each type would be required for a given barrier length in order to compare the total power requirements.

Table 3 provides a summary of the required spacings for each nozzle type. It was assumed in the calculations that a 10 percent fluctuation of the airflow velocities across the front was acceptable. Figure 6b shows a representative superposition of airflow curves. The airflow velocity decays in an exponential manner with distance from the nozzle, and therefore, selection of the distance at which the optimum spacing is calculated is arbitrary. Two stand-off distances being 3.05 m and 6.1 m have been selected for the calculations in Table 3.

It has been noted above that the airflow velocity at a selected distance increased with increasing aperture; and for the same aperture it decreased with increasing flare. Hence the selection of an optimum nozzle requires due consideration of the minimum required airflow velocity under any given conditions of operation.

The total hydraulic horsepower has been approximated by:

$$HHP_{max} = \frac{PQ}{1714}$$

where P is the system operating pressure (in psi) and Q is the flow rate (in gallons per minute). The results of the power requirements per meter of barrier length are given in Table 4. The power is based on a pressure of 13,790 kPa (2000 psi) and the manufacturer's specifications as to maximum flow rate. It is clearly shown by examination of the power requirements per unit length of barrier that in order to minimize the power, nozzles with smaller aperture and larger spread are preferred.

CONCLUSIONS

The problem of optimizing the operation of the high pressure waterjet barrier has been examined in this report. An experimental investigation was carried out in which the airflow velocities were measured and their variation with relevant parameters was identified. Based on the present experimental results the following conclusions may be drawn:

1. The laser doppler anemometer system proved very successful as a means of measuring the airflow velocities induced by the high pressure waterjets.
2. It was found that normal shape curves provided a good fit to the velocity cross-section data. Exponential decay curves described the longitudinal velocity profiles along the waterjet centreline. The use of normal curves allowed a convenient representation of the effectiveness of different nozzle types in terms of the velocity flux and its corresponding broadness.
3. A methodology of establishing optimum spacing of multiple waterjets was proposed which utilized the collected broadness data from the single nozzle tests. The required spacing was 2.3 times the broadness of the cross-sectional velocity profile at a given distance from the waterjet.

TABLE 3

SUMMARY OF MULTIPLE NOZZLE OPTIMUM SPACINGS

NOZZLE TYPE	TEST NO.	PRESSURE (kPa)	OPTIMUM SPACING AT 3.05 m (m)	MEAN AIRFLOW VELOCITY m/s at 3.05 m	OPTIMUM SPACING AT 10 m (m)	MEAN AIRFLOW VELOCITY m/s at 6.10 m
2510	5	13790	1.022	17.1	2.027	9.3
4010	3	13790	1.494	14.0	2.448	7.8
2520	2	13790	.973	21.5	2.323	12.8
4020	1	13790	1.942	17.2	3.577	8.9
6520	4	13790	3.868	7.9	-	-
6530	7	13790	2.852	14.0	5.690	8.8
2540	6	13790	1.024	32.3	2.056	18.9
4040	8	13790	1.442	23.3	3.084	13.9
4060	9	13790	1.061	62.6	2.565	17.5

TABLE 4

POWER REQUIREMENTS

NOZZLE TYPE	Q_{max} gpm	HHP_{max} per nozzle	SPACING, m (at 6.1 m)	HHP_{max} per meter length
2510	7.1	8.28	2.027	4.08
4010	7.1	8.28	2.448	3.38
6510	7.1	8.28	-	-
2520	14.7	16.45	2.323	7.08
4020	14.7	16.45	3.577	4.60
6520	14.7	16.45	-	-
6530	21.0	24.50	5.690	4.31
2540	28.0	32.67	2.056	15.89
4040	28.0	32.67	3.084	10.59
4060	42.0	49.01	2.565	19.11

4. An estimation of minimum power requirements was provided for each of the nozzles tested. The trends observed in the airflow analysis and power calculation suggested that selection of a small aperture, large flare angle waterjet nozzle will result in optimum performance of the barrier.

Several trends in operational parameters were identified during the course of the study:

5. ° Optimum nozzle height was observed to be between 15 cm and 30 cm above the spill. The relative insensitivity of the airflow to changes over this range suggests that greater jet heights may be practical for containment in wave environments.
° Small depression angles cause a rapid deterioration in the airflow; hence in practical operation of the waterjet barrier the stability of the floats will play a significant role.
° Increasing pressure between 6900 kPa and 20,680 kPa appeared to cause an increase in airflow velocities, although some discrepancies were observed in this data. However, the penalty in horsepower associated with increased pressure, as well as increased hosing costs would argue against pressures in excess of 10,200 kPa (1500 psi).

RECOMMENDATIONS

One consequence of the present parametric analysis is the identification of several aspects of the optimization problem which may warrant further attention:

1. The selection of an optimum nozzle type which has the smallest aperture of the group tested suggests that nozzle types with yet smaller apertures may be feasible and should be assessed. Additional laboratory testing of fixed nozzles in calm water and waves would be valuable to establish practical limits on jet height and nozzle pressure.

2. The influence of airflow on the transport of oil spread on the water surface should be analyzed for a range of parameter variations. Turbulence and oil/water emulsification may place constraints on the trends observed for parameters in the present study. Measurements of containment distances for an oil slick at varied pressures would give complimentary information as to the relative effects of wind shear and particle momentum transfer.

3. Effort may be directed at defining the airflow distributions associated with multiple nozzles and experimentally verifying the method of calculating optimum spacing. The corresponding effect of peaks and troughs in the water current velocity cross-sections of multiple nozzle configurations may also require further investigation.

4. For operation of the barrier in a deflection mode, in which nozzles are oriented at an angle from the perpendicular to the barrier line, questions remain as to optimization of the velocity cross-section and its characterization. A wide basin which can accommodate varied multiple nozzle configurations is suggested. Two dimensional measurements of current velocity or oil slick movement may be used to define the streamlines.

5. Implementation of a system configuration prediction algorithm based on the totality of parametric results would be a valuable tool in operating the barrier in a flexible and efficient manner. Site environmental data would be input and an appropriate barrier configuration would be derived.

REFERENCES:

[1] Breslin, M.K., "The Use of Coherent Waterjets to Control Oil Spills", U.S. Environmental Protection Agency, OHMSETT Report, 1980.

[2] Comfort, G., Menon, B., and Purves, W.F., "Feasibility of Water Spray Barriers as Fireproof Oil Slick Containment Devices", IEEE, 1980.

[3] Meikle, K.M., "The Use of High-Pressure Water for Spill Containment, (Environmental Protection Service). Proceedings of the 6th Arctic Marine Oil Spill Program Technical Seminar, June 1983.

[4] Meikle, K.M., Whittaker, H., Laperriere, F., "An Experimental High Pressure Waterjet Barrier", Proceedings of 8th AMOP, 1985.

[5] Laperriere, F., "High Pressure Waterjet Barrier Trials in Norman Wells", Environmental Protection Service, proc. of 7th AMOP, 1984.

ACKNOWLEDGEMENT

This research program was performed under contract No.52SS-KE145-5-0230 with the Department of Supply and Services on behalf of Environment Canada, Environmental Protection Services (EPS). The authors are grateful to Ken Meikle and Harry Whittaker of the Environmental Emergencies Technology Division of EPS for their support and active interest in this project. We would also like to thank Gordon Hadaller and Ed Ritchie of Westinghouse Canada Limited for their cooperation in making available and operating their laser doppler anemometer system.

HIGH PRESSURE WATER JET TESTING FOR OIL CONTAINMENT IN SIMULATED ENVIRONMENTAL CONDITIONS

F. Laperrière, H. Whittaker
Environment Canada
Ottawa, Ontario

M. Yanagisawa, I. Suzuki
Institute of Ocean Environmental Technology
Japan Foundation for Shipbuilding Advancement
Tsukuba, Japan

ABSTRACT

The use of conventional barriers using top and bottom tension members is limited to water currents of about 1.0 kt for containment of oil and of about 1.5 kts for deflection. A concept involving the use of water jets on the surface of the water to contain or deflect the oil was successfully tested for containment purposes in currents up to 1.5 kts, in winds up to 20 kts and in waves 0.15 m high.

This work was a joint undertaking by the Institute of Ocean Environmental Technology of the Japan Foundation for Shipbuilding Advancement and Environment Canada. The Institute's circulating channel was used to produce the different wind, wave and current conditions to determine the pressure requirements for an efficient oil containment at a distance of 2-3 m in front of the nozzle.

INTRODUCTION

Limitations of conventional barriers for containment and deflection of oil spills in fast waters promoted the study of alternative systems generating locally a horizontal surface current to oppose the movement of floating oil. Air jets were tested at EPA's OHMSETT facility (Cohen, Lindenmuth, 1979) indicating that a large pressure drop in the duct would preclude the development of an operational barrier. Plunging water jets were also tested at the same facility (Nash, Farlow, 1984). Used with low pressure (1.5 kg/cm^2) and high water volume (18 m^3/h), they show good efficiency in a deflection configuration. The logistics of their use though is increasing rapidly with the deflection distance and the current strength. Flat fan high-pressure water jets, horizontally oriented above the surface of the water, showing some potential in a tank testing at OHMSETT, were used in an array configuration in rivers and canals (Meikle, Whittaker, Laperrière, 1985). Deflection in currents of about 2 kts was possible even though the system used was not fully optimized but sufficiently operational to test the concept.

The testing discussed in this paper determined, through observations in a water circulating chanel, the limitations of a selection of high pressure water jets in wind, wave and current conditions.

TEST CONDITIONS AND PROCEDURES

Parameters and Equipment The nozzles used and the test parameters were as follows:

NOZZLE TYPE: Flat fan
NOZZLE SIZES: See Appendix A

PARAMETERS

winds:	0 - 15 m/s
currents:	0, 0.5 m/s (1 kt), 0.75 m/s (1.5 Kt)
waves:	0.15 m high x 7 m long
nozzle depression angle:	0°, 15° (6520 only)

Additional intermediate data were also recorded.

The nozzles were tested as used in the EETD prototype barrier; a pair of nozzles mounted on a floatation platform back to back in order to stabilize the platform (Figure 1).

The larger nozzles (30, 40 aperture) could not be tested in pairs because the maximun capacity of the pump was about 130 L/min. One nozzle only of these types was mounted on the float which was then fixed to a carriage. By restricting the vertical movement of the platform, testing in waves for those nozzles was made impossible.

Containment Distances and Channel Width

The basis of comparison of the jets was the power requirements to stop oil at a specific distance in front of them. This distance was outside of the area influenced by the reflection from the walls of the surface water current and the air flow generated by the jets.

The starting pressure was chosen low enough to allow the spilled oil to come close to the jet and then was adjusted to contain oil efficently at a chosen distance from it. The pressure was then recorded as the containment pressure. As mentioned in the following table, a containment distance of 2 m maximum had to be maintained while testing the nozzles of the 65 series. This distance of 2 m from the jet to the oil slick was maintained when possible for all the nozzles tested in order to be able to compare them. Variation of 0.5-1.5 m from the desired containment distance occured. All the pressure requirements were compared among them, since all were minimum pressure requirements for efficient containment.

TABLE I

Channel Length with no Wall Effects

Jet Type	Channel Width (m)	Channel Length with no Reflection in Front of Nozzle (m)
65 series	2.4	1.9
40 series	2.4	3.3
25 series	1.3	2.9

The channel width 2.4 m was chosen to reflect the present spacing of the nozzles of EETD prototype barrier after finding out that the circulating channel width 3.8 m was too large for the 65 series nozzle.

Oil was not stopped in front of the nozzle using the maximum channel width but was leaking on each side. An oil boom (30 cm of freeboard) was used to reduce the channel width. A channel width of 2.4 m being too large for the 25 series nozzles, the width was further reduced.

Test Oil In a 2.4 m water channel width 60 L of oil per test were necessary in order to observe properly the influence of the test condition variations. A theoretical slick thickness of about 5 mm was sent toward the jets with a mean slick length of 5 m. The oil was discharged all at once about 15 m away from the nozzle and 5 m up current from the wind generator.

PHYSICAL PROPERTIES OF NO. 1 TEST OIL

Specific Gravity	(15/4°C)	0.872
Kinematic Viscosity	20°C	100.0 mm^2/sec (cSt)
	40°C	36.5 mm^2/sec (cSt)
Surface Tension		30.9 dynes/cm
Interfacial Tension		46.0 dynes/cm

Wind Velocity Pattern A wind velocity pattern was determined above the water circulating channel after curtains were installed on both sides of the channel. Measurements were taken at 10 and 20 cm above the water surface every 1 m starting 10 m in front of the wind generator (Figure 2). The wind velocities just in front of the nozzle position for the different tests done are indicated in table 2. Throughout the report the wind velocity values indicated are the theoretical values, values at the generator outlet. They will be noted with a "T" except for the tables.

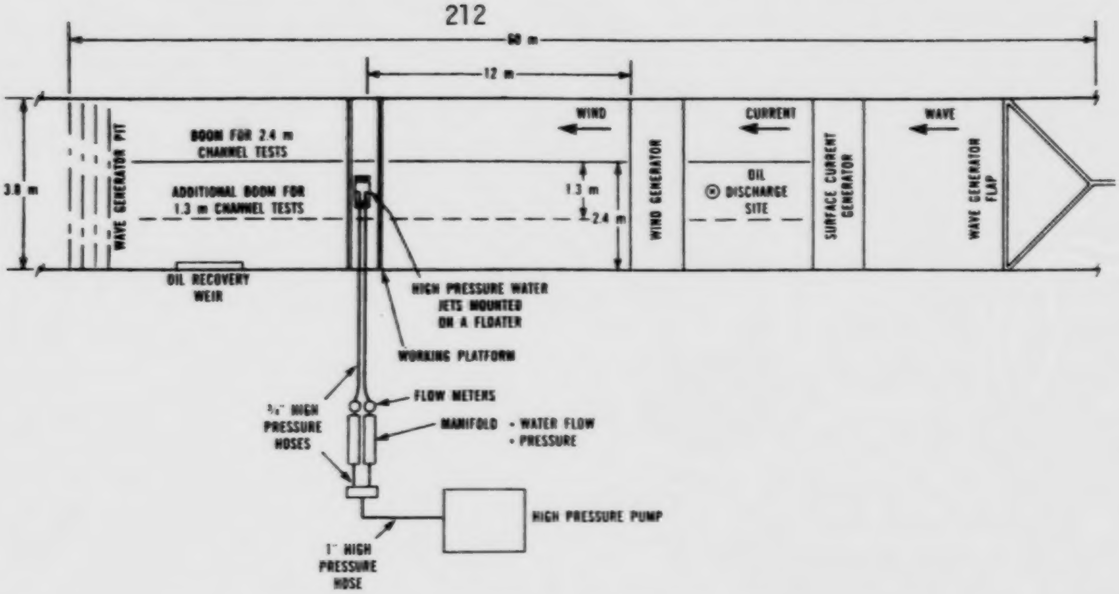
60 m
12 m
3.8 m
WAVE GENERATOR PIT
BOOM FOR 2.4 m CHANNEL TESTS
ADDITIONAL BOOM FOR 1.3 m CHANNEL TESTS
WIND
1.3 m
2.4 m
WIND GENERATOR
CURRENT
OIL ⊙ DISCHARGE SITE
SURFACE CURRENT GENERATOR
WAVE
WAVE GENERATOR FLAP
OIL RECOVERY WEIR
HIGH PRESSURE WATER JETS MOUNTED ON A FLOATER
WORKING PLATFORM
FLOW METERS
¾" HIGH PRESSURE HOSES
MANIFOLD • WATER FLOW • PRESSURE
HIGH PRESSURE PUMP
1" HIGH PRESSURE HOSE

FIGURE 1. HIGH-PRESSURE WATER JET TESTING SET UP IN THE IODET LARGE CIRCULATING WATER CHANNEL.

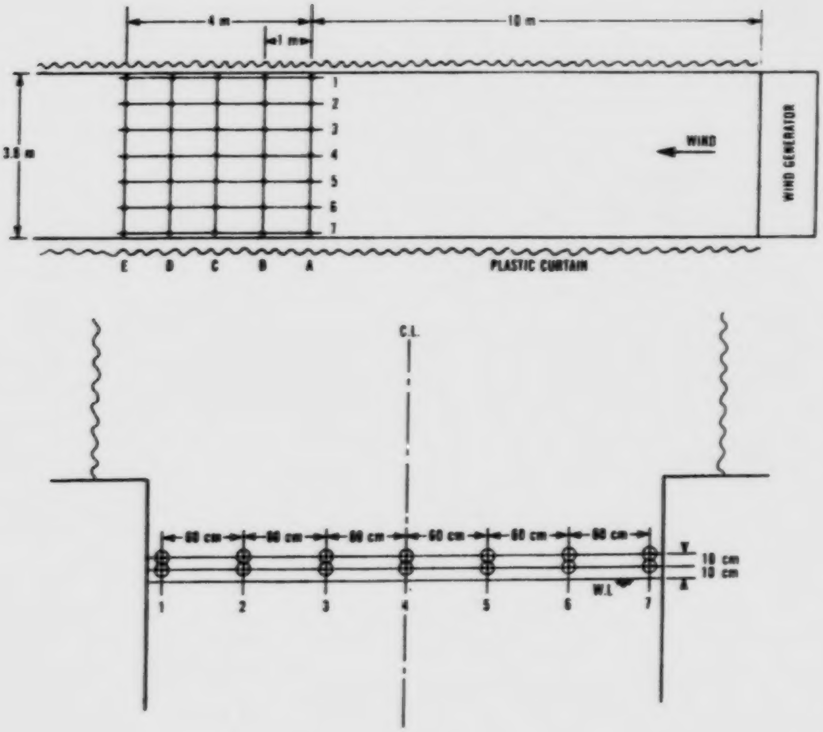
4 m
1 m
10 m
3.8 m
1
2
3
4
5
6
7
WIND
WIND GENERATOR
E
D
C
B
A
PLASTIC CURTAIN
C.L.
60 cm
60 cm
60 cm
60 cm
60 cm
60 cm
10 cm
10 cm
W.L.
1
2
3
4
5
6
7

DIAMETER OF ANEMOMETER: 10 cm Ø

FIGURE 2. MEASURING POINTS FOR THE WIND VELOCITY DISTRIBUTION ABOVE THE WATER LEVEL OF THE TESTING AREA IN THE CHANNEL.

TABLE 2

Wind Velocities in Front of the Nozzle above the Water Surface

Nozzle Position	Theoretical Wind Velocity m/s	(kt)	Real Wind Velocities upwind of the nozzle position 0m	1 m m/s (kt)	2 m
			10 cm above the water surface		
C-4	15	(29)	8.9 (17)	9.3 (18)	10.0 (20)
(tests with waves)	10	(20)	6.4 (13)	6.7 (13)	7.0 (14)
C-5	15	(29)	8.7 (17)	9.0 (18)	9.2 (18)
(tests without waves)	10	(20)	6.2 (12)	6.5 (13)	6.5 (13)
			20 cm above the water surface		
C-4	15	(29)	9.4 (18)	10.0 (20)	10.5 (21)
(test with waves)	10	(20)	6.5 (13)	6.7 (13)	7.1 (14)
C-5	15	(29)	9.2 (18)	9.4 (18)	10.0 (20)
(test without waves)	10	(20)	6.3 (12)	6.5 (13)	6.8 (13)

RESULTS ANALYSIS

The following analysis is based on the results presented in tables 3 to 9.

General Remarks

1) The containment pressure requirements in waves were found to be:

- 30-50% lower than those for calm surface water under conditions of wind
- mostly equal to those for calm surface water in current conditions
- 25-40% lower or equal to the ones in calm surface water in wind and current conditions.

2) In calm surface waters, for 5 nozzles (4020, 4040, 6510, 6530, 6520 depressed) out of 8, the containment pressure requirements in a 15^T m/s wind were about the same as for a 0.5 m/s current. The exceptions (4010, 4030, 6520 jets) required less pressure.

In waves, for 2 nozzles (6520, 6520 depressed) out of 6, the containment pressure requirements in a 15^T m/s wind was about the same as for a 0.5 m/s current. The exceptions (2510, 4010, 4020, 6510 jets) required less pressure.

3) The containment pressure requirements for the different jets tested were mainly equal or above 70 kg/cm^2 (995 psi) with the exception of the 15° depressed jet.

4) Operating pressures above 200 kg/cm^2 (2844 psi) were generating a lot of turbulence on the water surface which caused leakage through the water column and also a rapid emulsification of the oil. The volume of oil used (60 L) was emulsified, in these pressure conditions, after 5 minutes.

5) The influence of the use of a second opposing jet on containment pressure requirements was not noticeable for 2 sets of data out of 3. One set showed a 14% increase.

Wind Conditions Only 1) In a 7 m long, 0.15 m high wave condition and in a 15^{T} m/s wind, the depressed (15°) jet required half the pressure of the horizontal one for the same containment efficiency, (35 kg/cm^2 (498 psi) vs 73 Kg/ cm^2 (1038 psi)).

Without waves in a 15^{T} m/s wind, the pressurerequi- red was about the same for the horizontal jet as it was when the jet was depressed 15° (62 kg/cm^2 (882 psi) vs 70 kg/cm^2 (995 psi)).

2) With or without waves in a 15^{T} m/s wind the containment pressure increased as the jet aperture was reduced. There is not enough data to see a trend for the maximum increase but the highest occurred with the smaller jet angle and while reducing to the smallest aperture; 4020 to 4010 jet.

3) Without waves no appreciable difference in pressure requirement was noted when reducing the jet flare angle from 65° to 40°. For the chosen wave condition there is insufficient data to notice a trend, only one aperture could be tested with both flares. The 40° jet flare series had a significantly lower containment pressure than the 65° jet flare series (6520: 73 kg/cm^2, 4020: 45 kg/cm^2).

Current Conditions Only 1) Depressed and horizontal jets, both had a current limit of 0.6 m/s (1.2 k in a 7 m long, 0.15 m high wave condition. The depressed jet (15°) required 27% less pressure for about the same containment distance than the horizontal one (95 kg/cm^2 (1351 psi) vs 130 kg/cm^{2-} (1849 psi)).

Without waves the horizontal jet had a current limit of 0.6 m/s (1.2 kt) and the depressed one a current limit of 0.5 m/s (1.0 kt) with a required pressure of about 62% less (130 kg/cm^2 (1963 psi) vs 50 kg/cm^2 (711 psi))

2) An aperture influence was noticeable in both wave and calm surface water conditions.

In wave conditions, the current limit was reduced by 0.05 m/s and the pressure increased by 85 kg/cm^2 (57%)using the smaller aperture within the 65° flare jet series, 6510 instead of the next higher one, 6520 (205 kg/cm^2 (2915 psi) vs 130 kg/cm^2 (1849 psi)). It was reduced by more than 0.1 m/s using the smaller aperture with the 40°flare jet series (4010) instead again of the next higher one (4020) with a 91% pressure increase (115 kg/cm^2 (1636 psi) vs 220 kg/cm^2 (3129 psi). Lower containment pressures could probably be obtained for the 40° flare jet series with a smaller channel width.

In calm surface water conditions, within the 65° flare nozzle series (6530, 6520, 6510), the aperture reduction did not change the current limit of 0.6 m/s. The containment pressures increased by 78% and 70% for the two successive aperture reduction, reaching the maximum pressure of the pump. Within the 40° flare jet series the highest aperture nozzle tested, 4040, had a current limit lower than the other ones (4030, 4020) by 0.1 m/s. The turbulence generated by the jet on the water surface caused leakage.

Comparing their containment pressures for a 0.5 m/s current, pressure increases of 110%, 33% and 171% were required as the aperture was reduced from the 4040 jet to the 4030, the 4020 and finally to the 4010. Comparing them also for a 0.75 m/s current, only the 2 intermediate ones (20, 30) were efficient in containing the oil at about the same distance using the maximum pressure of the pump. The lower aperture was requiring higher pressure and the larger aperture was generating too much turbulence at the water surface.

3) The effect of flare angle was only noticeable during the small aperture jet tests in wave conditions. Both sizes of the 65 series (6520, 6510) jet could succeed in a 0.5m/s while only the large size of the 40 series jet tested, 4020, could contain the oil at this current and within the same channel width. The containment pressures for the highest aperture tested (20) for both jet series 65°, 40° were 13% different at the most, for the different currents tested.

In calm surface water conditions and in a 0.5 m/s current the flare angle influence was noticeable mainly for the larger aperture jet tests. The size 30 aperture required 75% more pressure to contain the oil with the 40 series jet than with the 65 series. The 4010 jet required only 3% more pressure than the 6510 jet and the 4020 required 34% less pressure than the 6520. The lower containment pressure of the 4020 jet also occurred in the wave conditions tests.

Current and Wind Conditions 1) The depressed jet (15°), both in waves and in calm surwater conditions, could not use more than 80kg/cm^2 (1138 psi) to contain oil efficiently. The turbulence generated caused the oil to leak through the water column. There was also a rapid emulsification of the oil. The current limit in the presence of a light wind (5^T m/s) was higher in waves than in calm surface water (0.5 m/s vs 0.3 m/s).

The horizontal jet could contain oil in both calm and wave conditions in a 0.6 m/s current with a slightly higher wind than with the inclined jet ($7.5-8^T$ m/s wind vs 5^T m/s wind).

2) Aperture influence is noticeable in waves and calm surface water. The jet 6510 could not withstand as high a current and wind as the 6520 did (0.5-0.55 m/s vs 0.6 m/s in a 7.5 m/s wind).

With the 40° flare series the smaller aperture jets (4010, 4020, 4030) could overcome a higher current than the large aperture jet (4040) in calm conditions with a 3^T m/s wind or less because they created less turbulence in front of the oil slick, reducing entrainment in the water column and the rapid emulsification of the slick. (0.75 m/s vs 0.66 m/s).

3) A flare angle influence was noticed in waves only. In waves the 65° and 40° jet series had the same current limit 0.6 m/s but the jet 4020 could contain as efficiently as the 6520 in stronger winds with less or equivalent pressure;

6520: 7.5^T m/s wind 0.6 m/s current, 188 kg/cm^2
6520: 10^T m/s wind 0.5 m/s current, 100 kg/cm^2
4020: 10^T m/s wind 0.6 m/s current, 130 kg/cm^2
4020: 15^T m/s wind 0.5 m/s current, 110 kg/cm^2

The jets with the 25° flare angle required less pressure for equivalent wind and current conditions than those with the 65° flare. They were also able to overcome a higher current in strong winds (0.6 m/s vs 0.5 m/s). The channel width and the oil batch volume were reduced for these tests in an effort to obtain comparable slick thicknesses.

In calm surface water, the reduced pressure requirement for the 40° flare series is not apparent for the 6530/4030 and 6510/4010 combinations but seems to apply for the 6520/4020. A reduction of the containment pressure requirements of 10-30% is noticed for the 40 series.

CONCLUSIONS

We can summarize the main findings from all the observations done as follows. We realize they are subjected to the operational conditions we used but they should apply to the behaviour of a barrier using these high pressure waterjets.

1) Small waves (0.15 m high) reduce the pressure required for containment in windy conditions.

2) In calm conditions a 9 m/s wind (18 kt) is approximately equivalent to a 0.5 m/s current based on the containment pressure.

3) Among the nozzles tested, the 6520 jet was the only one that was able to contain oil in a 0.5 - 0.6 m/s current in small waves at a pressure below 70-80 kg/cm^2 (995-1138 psi) when operated at a depression angle of 15°. It was only able to do so however if the wind was no more than 5^T m/s. The current limit is less in calm surface water conditions with the same current conditions. Finally, the pressure limit for the depressed jet was about 80 kg/cm^2. Higher pressures create too much turbulence. Subsurface leakage and emulsification were noticed operating at these pressures.

4) In wave and current conditions, the flare angle seems to be more important for the small jets (aperture 10, 20) than it is in calm conditions. In calm conditions and in a current, the containment pressure requirements for the large size jet (aperture 30) were influenced by the flare angle. In wind, wave and current the flare angle influence was the same as for wave and current conditions. The most efficient flare angle in strong winds seems to be 40°. Even though both succeeded in containing oil, the 4020 jet required 0-30% less pressure than the 6520 jet.

5) As the jet aperture was reduced, the containment pressure requirements were increased for the smaller jet sizes (aperture 10, 20). However, the largest jet size tested (aperture 40), creates excessive turbulence and rapidly emulsifies the oil. Its current limit is thus lower than it is for the smaller jet sizes (aperture 10, 20, 30).

REFERENCES

1. Cohen, S.H. and Lindenmuth, W.T. 1979. Design, Fabrication and Testing of the Air-Jet Oil Boom, EPA-600/7-79-143 U.S. Environmental Protection Agency, Cincinnati, Ohio

2. Nash, J.H. and Farlow, J.S. 1984. Field Manual for Plunging Water Jet Use in Oil Spill Cleanup, EPA-600/S2-84-045

3. Meikle, K., Whittaker, H. Laperrière, F., 1985, An Experimental High Pressure Waterjet Barrier, Proceedings of the 1985 Oil Spill Conference, Los Angeles Feb. 1985, API Publication No. 4385, p.7

TABLE 3

WATER JET TESTING IN WAVES

Wind Conditions Only (15 m/s)

Nozzle Type/ Depression Angle	Pressure kg/cm2 (psi)	Containment Distance m	Estimate of Contained Slick Thickness mm	Water Flow Rate Lpm	Power Requirements HHP/m
6520/15°	35 (498)	1.5	20	26.5	0.8
6520/0°	73 (1038)	1.2	16	38.5	2.6
6510	95 (1351)	1.7	20	22.0	1.9
4020	45 (640)	3.0	27	30.0	1.2
4010	100 (1422)	2.5	30	22.5	2.1
2510	60 (853)	1.0	20	17.0	1.7

TABLE 4

WATER JET TESTING IN WAVES

Current Conditions Only

Nozzle Type/ Depression Angle	Current m/s (kt)	Pressure kg/cm2 (psi)	Containment Distance m	Estimate of Contained Slick Thickness mm	Water Flow Rate Lpm	Power Requirements HHP/m
6520/15°	0.5 (1)	45 (640)	1.5	21	30.0	1.2
	0.6 (1.2)	95 (1351)	2.0	16	44.0	3.8
	0.75 (1.5)	105 - 180 (1493 - 2560)	LEAK	-	46.0-60.5	4.4-9.9
6520/0°	0.5	72 (1024)	2.0	12	38.5	2.5
	0.6	130 (1849)	1.5	16	51.0	6.1
	0.75	190 (2702)	LEAK	-	62.0	10.8
6510	0.5	185 (2631)	2.0	15	31.0	5.2
	0.55 (1.1)	205 (2915)	2.3	25	33.0	6.2
	0.6	220 (3129)	LEAK	-	33.0	6.6
4020	0.5	70 (996)	3.0	16	38.0	2.4
	0.6	115 (1636)	2.5	16	48.5	5.1
	0.75	200 (2845)	LEAK	-	64.0	11.7
4010	0.5	220 (3129)	LEAK	-	33.0	6.7
2510	0.5	110 (1564)	3.0	11	24.0	4.5
	0.6	140 (1991)	2.0	11	27.0	6.4
	0.75	230 (3271)	LEAK	-	33.0	12.8

TABLE 5

WATER JET TESTING IN WAVES

Wind and Current Conditions

Nozzle Type/ Depression Angle	Wind m/s (kt)	Current m/s (kt)	Pressure kg/cm2 (psi)	Containment Distance m	Estimate of Contained Slick Thickness mm	Water Flow Rate Lpm	Power Requirements HHP/m
6520/15°	5 (10)	0.5 (1)	68 (967)	2.3	13	37.5	2.3
		0.6 (1.2)	80 (1138)	2.0	16	41.0	3.0
	10 (20)	0.5	70 - 140 (995 - 1991)	LEAK	-	38.0-53.0	2.4-6.8
		0.6	85 - 185 (1209 - 2631)	LEAK	-	42.0-61.0	3.3-10.3
6520/0°	5	0.5	92 (1308)	2.0	16	43.5	3.7
		0.6	135 (1920)	1.5	12	52.0	6.4
	7.5 (15)	0.6	188 (2674)	1.5	12	62.0	10.6
	10	0.5	100 (1422)	1.5	2.5	45.5	4.1
		0.6	180 - 190 (2560 - 2702)	LEAK	-	60.5-62.0	10.0-10.8
	15	0.5	160 (2275)	LEAK	-	57.0	8.3
6510	5	0.5	160 (2275)	2.0	13	29.0	4.2
		0.55	220 (3129)	3.3	16	33.0	6.6
		0.6	220 (3129)	LEAK	-	33.0	6.6
	10	0.5	220 (3129)	2.5	16	33.0	6.6
		0.55	220 (3129)	LEAK	-	33.0	6.6
	12 (23)	0.5	220 (3129)	LEAK	-	33.0	6.6
4020	5	0.6	110 (1564)	3.0	13	47.5	4.8
	10	0.6	130 (1848)	3.0	25	51.0	6.1
	15	0.5	110 (1564)	2.5	20	47.5	4.8
		0.6	175 (2489)	LEAK	-	59.5	9.5
4010	-	-	-	-	-		
2510	5	0.5	110 (1564)	3	9	24.0	4.5
		0.6	200 (2844)	3	23	32.5	11.0
	10	0.5	140 (1991)	2.5	15	27.0	6.4
		0.6	210 (2986)	3.5	23	33.0	11.7
	15	0.5	230 (3271)	LEAK	-	33.0	12.8

TABLE 6

WATER JET TESTING WITHOUT WAVES

Wind Conditions Only (15 m/s)

Nozzle Type/ Depression Angle	Pressure kg/cm2 (psi)	Containment Distance m	Estimate of Contained Slick Thickness mm	Water Flow Rate Lpm	Power Requirements HHP/m
6520/15°	62 (882)	1.5	20	35.0	2.0
6530	50 (711)	2.5	12	47.0	2.2
6520	70 (995)	2.0	25	37.0	2.4
6510	175 (2489)	1.5	18	30.0	4.8
4040	40 (569)	2.0	22	57.0	2.1
4030	65 (925)	2.0	21	55.0	3.3
4020	80 (1138)	2.0	33	41.0	3.0
4010	150 (2133)	3.0	27	28.0	3.8

TABLE 7

WATER JET TESTING WITHOUT WAVES

Current Conditions Only

Nozzle Type/ Depression Angle	Current m/s (kt)	Pressure kg/cm2 (psi)	Containment Distance m	Estimate of Contained Slick Thickness mm	Water Flow Rate Lpm	Power Requirements HHP/m
6520/15°	0.5 (1)	50 (711)	1.5	13	32.0	1.5
6530	0.5 (1)	60 (853)	2.5	6	53.0	2.9
	0.6 (1.2)	73 (1038)	2.0	6	58.0	3.9
	0.75 (1.5)	160 - 220 (2276 - 3129)	LEAK	-	86.0-97.0	12.6-19.5
6520	0.5	107 (1522)	1.5	10	47.0	4.6
	0.75	188 (2674)	LEAK	-	62.0	10.6
6510	0.5	185 (2631)	1.5	11	31.0	5.2
	0.6	220 (3129)	1.5	13^-	33.0	6.6
	0.75	220 (3129)	LEAK	-	33.0	6.6
4040	0.5	50 (711)	2.0	16	64.0	2.9
	0.66 (1.3)	110 (1565)	4.0	10	93.0	9.4
	0.75	210 (2986)	LEAK	-	133.0	25.5
4030	0.5	105 (1493)	3.0	20	70.0	6.7
	0.75	220 (3129)	2.0	16^-	98.0	19.7
4020	0.5	70 (995)	2.0	12	38.0	2.4
	0.75	200 (2845)	2.5	16^-	64.0	11.7
4010	0.5	190 (2702)	2.0	10	32.0	5.6
	0.75	220 (3129)	LEAK	-	33.0	6.6

TABLE 8

WATER JET TESTING WITHOUT WAVES

Wind and Current Conditions

Nozzle Type/ Depression Angle	Wind m/s (kt)	Current m/s (kt)	Pressure kg/cm2 (psi)	Containment Distance m	Estimate of Contained Slick Thickness mm	Water Flow Rate Lpm	Power Requirement HHP/m
6520/15°	5 (10)	0.25 (0.5)	15 (284)	1.3	18	15.0	0.3
		0.3 (0.6)	15 (213)	1.0	16	15.0	0.2
		0.4 (0.8)	65 - 100 (924 - 1422)	LEAK	-	31.0-47.0	1.8-4.3
	10 (20)	0.3 (0.6)	100 (1422)	LEAK	-	47.0	4.3
6530	5	0.5	72 (1024)	2.0	7	58.0	3.8
	10	0.5	72 (1024)	2.0	7	58.0	3.8
	15	0.5	90 (1280)	2.5	7	65.0	5.3
6520	5	0.5	138 (1963)	2.5	14	53.0	6.7
		0.6	130 (1849)	2.0	15	51.0	6.1
	8 (16)	0.6	150 (2133)	2.0	18-	55.0	7.5
	10	0.5	160 (2276)	2.0	18	57.0	8.3
		0.6	188 (2674)	LEAK	-	62.0	10.6
	15	0.5	188 (2674)	2.0	18-	62.0	10.6
6510	5	0.5	220 (3129)	2.0	10	33.0	6.6
	10	0.5	220 (3129)	2.0	12	33.0	6.6
	12 (23)	0.5	220 (3129)	1.5	14	33.0	6.6
	15	0.5	220 (3129)	LEAK	-	33.0	6.6
4040	5	0.66	90 (1280)	3.0	20-	85.0	7.0
	10	0.66	90 (1280)	3.0	20	85.0	7.0
	15	0.5	55 (782)	2.0	11	68.0	3.4
		0.66	70 (996)	2.0	11-	76.0	4.9
		0.75	135 (1920)	LEAK	-	104.0	12.8
4030	5	0.75	220 (3129)	LEAK	-	98.0	19.7
	15	0.5	120 (1707)	3.0	27-	75.0	8.2
		0.75	220 (3129)	LEAK	-	98.0	8.2
4020	5	0.5	125 (1778)	3.5	18	50.0	5.7
	3 (6)	0.75	200 (2845)	2.5	16-	64.0	11.07
	15	0.5	125 (1778)	2.0	22	50.0	5.7
		0.75	200 (2845)	LEAK	-	64.0	11.7
4010	5	0.75	212 (3015)	3.0	13	33.0	6.4
	10	0.75	215 (3058)	2.5	14	33.0	6.5
	13 (26)	0.5	210 (2987)	2.0	15	33.0	6.3
	15	0.5	210 (2987)	LEAK	-	33.0	6.3
		0.75	215 (3058)	LEAK	-	33.0	6.3

TABLE 9

Verification of Opposing Jet Influence

Nozzle Type/ Depression Angle	Wind m/s (kt)	Current m/s (kt)	Pressure kg/cm2 (psi)	Containment Distance m	Water Flow Rate Lpm	Power Requirements HHP/m
6520/15° x 1 jet	5 (10)	0.3 (0.6)	18 (256)	1.0	18.0	0.3
6520/0° x 1 jet	0	0.5 (1.0)	110 (1565)	2.0	48.0	4.8
	10	0.5 (1.0)	140 (1991)	2.0	53.0	6.8

APPENDIX A

NOZZLE CHARACTERISTICS

				MAXIMUM FLOW RATE Lpm (US gpm) AT DIFFERENT PRESSURES									
TYPES	NOZZLE SPREAD ANGLE (deg)	NOZZLE APERTURE (cm)	(inch)	70.3 kg/cm	(1000) (psi)	105.5 kg/cm	(1500) (psi)	140.6 kg/cm	(2000) (psi)	175.8 kg/cm	(2500) (psi)	210.9 kg/cm	(3000) (psi)
2510	25												
4010	40	0.191	(0.075)	18.9	(5.0)	23.1	(6.1)	26.9	(7.1)	29.9	(7.9)	32.9	(8.7)
6510	65												
4020	40	0.269	(0.106)	37.9	(10.0)	46.6	(12.3)	53.4	(14.1)	59.8	(15.8)	65.5	(17.3)
6520	65												
4030	40	0.330	(0.130)	56.8	(15.0)	69.7	(18.4)	79.5)	(21.0)	90.8	(24.0)	98.4	(26.0)
6530	65												
4040	40	0.381	(0.150)	75.7	(20.0)	90.8	(24.0)	106.0	(28.0)	121.1	(32.0)	132.5	(35.0)

LABORATORY AND TANK TEST EVALUATION OF ELASTOL$^{T.M.}$

M.A. Bobra and P.I. Kawamura
Consultchem
Ottawa, Ontario

M. Fingas and D. Velicogna
Environment Canada
Ottawa, Ontario

Introduction

Recently, a new spill treating agent called Elastol has been manufactured, which when applied to oil, imparts a viscoelastic property. It is claimed that this viscoelastic enhancing agent increases the oil slick's resistance to spreading and breakup, and improves the performance of skimmers, collecting devices and containment barriers. Improved separation after removal of oil from the water surface is also cited.

Elastol is manufactured in the form of a white powder, 100 to 1000 microns in size, by General Technology Applications Inc. It is composed of a simple, nominally non-toxic polymer coated with a water-insoluble salt. To date, the product has shown promise in small-scale field demonstrations but the effect of many important variables has not been addressed.

The bulk of this study was undertaken on a small scale to determine the effect of Elastol on selected oil properties and physical processes to which oil slicks are subjected. The results of this study will be used as a guide towards future large-scale testing of this product.

This study was divided into three phases. The main objectives of the first phase were to determine the effect of Elastol on the following:

(i) flash point and evaporation
(ii) physical processes: emulsification, oil spreading, and increase in viscoelasticity.

The second phase explored the combined, simultaneous processes of dispersion, emulsion formation and the change in viscoelastic properties of the Elastol-treated oil slick when subjected to wave action in a small-scale test apparatus. In the final phase, a large-scale tank test was conducted at the Esso Research Laboratory.

In this report, only selected numerical results are given. Complete results are presented in Bobra et.al. (1987).

*(ELASTOL is a registered trademark of General Technology Applications Inc.)

PHASE 1: EFFECT OF ELASTOL ON OIL PROPERTIES AND PHYSICAL PROCESSES

Experimental

(i) Effect of Elastol on Flash Point and Evaporation

The effect of Elastol on flash point and rate of evaporation was measured. In the flash point study, a Pensky-Martens closed tester was employed to measure the flash points of three Elastol-treated petroleum products; Alberta Sweet Mixed Blend crude oil (ASMB), unleaded gasoline and automotive diesel. In the evaporation study, the difference in the rate of volatilization of Elastol-treated (6000 ppm) and untreated oils, was measured gravimetrically at specific time intervals. Oils were either left undisturbed or subjected to mixing by magnetic stirrers.

(ii) Effect of Elastol on Viscoelasticity

Although the viscous and elastic properties of a viscoelastic fluid are related, these properties were treated and measured separately throughout this study. All viscosity measurements were performed using the Brookfield viscometer, and a novel "die swell" apparatus was constructed to measure the elasticity.

The die swell apparatus utilizes the phenomenon of swelling of viscoelastic fluids when they are forced through a small opening. It has been established that the extent of this swelling, which is commonly referred to as the die swell phenomenon, characterizes the degree of elasticity of viscoelastic fluids (Bird et.al., 1977).

The apparatus consists of two syringes, one acting as a piston, the other as a sample holder. Air pressure is used to drive the piston, which transmits its force to the plunger of the sample syringe containing the oil sample. This action ejects the fluid through a 12 gauge needle. Photographs of the swelling were taken to determine the elasticity of the oil samples. Details of this apparatus and a background of the die swell phenomenon and elasticity are given in Bobra et.al. (1987).

In order to determine the effect of Elastol on viscoelasticity, a series of bench-scale experiments were performed in which the Elastol-treated oil samples were mixed in a shaker/incubator at a controlled temperature. Nine different oils were tested in this study. These experiments were conducted at 15 deg C and a mixing speed of 80 RPM at Elastol concentrations of 600 and 6000 ppm. Further tests were conducted with two of the nine oils in which the effect of no mixing energy and lower temperature (0 deg C) were studied. Viscosity and elasticity of the samples were measured at five selected time intervals during the 48 hour experimental period.

(iii) Effect of Elastol on the Spreading of Oil Slicks

The approach taken was to confine the oil and a specified amount of Elastol in a tube, which was positioned in the centre of a salt-water-filled 0.91 m diameter shallow pan. The top of the tube was sealed to prevent evaporation and a specific amount of Elastol was allowed to dissolve in the oil. After a defined time interval, the tube was lifted, which allowed the oil to spread out on the water. The final spill area for each experiment was then recorded. It was the extent of this spreading that was used as the criteria for the effectiveness of Elastol to retard the spread of an oil slick at a particular concentration and time interval.

The oils used were ASMB and Emulsifying Mix (50-50 volume mixture of ASMB and Bunker C). An oil volume of 4.4 mL, which produced a 2 mm "spill" in the tube, was used in all experiments. To determine the effect of Elastol concentration, Elastol was added at doses of 0, 600, 6000 ppm and 6% and left to react for 30 minutes for ASMB and 6.5 hours for the 50-50 mixture. With the reaction time as the variable, the Elastol dose was set at 6000 ppm. In addition, a control experiment was performed for each selected reaction time for the two oils.

(iv) Effect of Elastol on Emulsion Formation Tendency and Stability

These experiments focused on the emulsification behaviour of Elastol-treated oils. Elastol-treated oil and seawater were combined in glass fleakers and mixed in a tumbling emulsion apparatus for four "one-hour mixing, followed by 30 minutes of settling" cycles, as described in Mackay and Zagorski (1982) and Bobra et.al. (1987). At the end of each settling period, the height of free oil, emulsion (if any) and water phase in the fleaker were measured to determine the volume fraction of initial oil which forms an emulsion at any time, f. These measurements were also recorded after allowing the sample to settle for 24 hours following the last mixing cycle. The f values calculated at two different times, f (initial), (which is the f value at time zero (determined by extrapolating the f versus time curve to time zero)) and f (final), (which is the f value at the end of the 24 hour settling period) were used to classify the emulsion formation tendency and emulsion stability of oils, respectively (Mackay and Zagorski, 1982). The criteria for these classifications are as follows: f(initial): 0 to 0.25, Emulsion Formation Tendency: Not Likely; 0.25 to 0.75, Fairly Likely; 0.75 to 1.0, Very Likely. f(final): 0 to 0.25, Emulsion Stability: Unstable; 0.25 to 0.75, Fairly Stable; 0.75 to 1.0, Very Stable. This classification system was employed in these experiments to study the effect of Elastol addition on these two emulsion properties.

In addition, the same apparatus and procedure were employed to determine the combined effect of Brand S (an emulsion inhibitor, applied at an inhibitor-to-oil volume ratio of 1:1500) and Elastol on four selected oils.

RESULTS AND DISCUSSION

(i) Effect of Elastol on Flash Point and Evaporation

Flash point measurements showed that Elastol had no effect on this property for the three oils tested.

In the evaporation study, the Elastol-treated oil was found to have a slightly lower (less than 3%) rate of volatilization than the untreated oil. This reduced rate was more significant when the oils were subjected to mixing.

(ii) Effect of Elastol on Viscoelasticity

All oils exhibited viscoelastic properties when treated with Elastol. Untreated oils, on the other hand, showed no elastic behaviour. For most experiments, the dynamic viscosity and die swell ratio curves paralleled each other. These curves for ASMB at 15 deg C are shown in Figure 1. As expected, a higher dose of Elastol imparted a greater increase in viscosity and elasticity: at a concentration of 6000 ppm, viscosity increased by a factor of 6.2 to 35.4 after 48 hours for the oils tested; at 600 ppm, the increase was only 1.1 to 4.0 (except for Bent Horn Crude, which had a 18.3 fold increase).

Personnel performing the tests and subsequent cleaning of the apparatus had adequate opportunity to observe the physical nature of Elastol-treated oil samples. In their opinion, the magnitude of the die swells calculated from the die swell apparatus was indicative of the relative degree of observed elasticity.

In an attempt to present the results in a simplified form, each oil treated at a particular concentration and temperature was classified into one of three groups under two categories: degree of elasticity and reaction time. The criteria for classification was arbitrarily chosen as follows:

Die Swell Ratio After 48 Hours	Degree of Elasticity
> 1.75	High
1.25 to 1.75	Moderate
< 1.25	Low

Time to Reach 50% of Total Die Swell Increase	Reaction Time
0 to 1 hour	Fast
1 to 4 hours	Moderate
> 4 hours	Slow

The grouping of oils under both categories is tabulated in Tables 1 and 2. It is important to note that the classifications only provide a relative measure of the degree of elasticity increase and reaction times for the nine oils tested.

A comparison between mixed and unmixed oils showed that the mixed samples

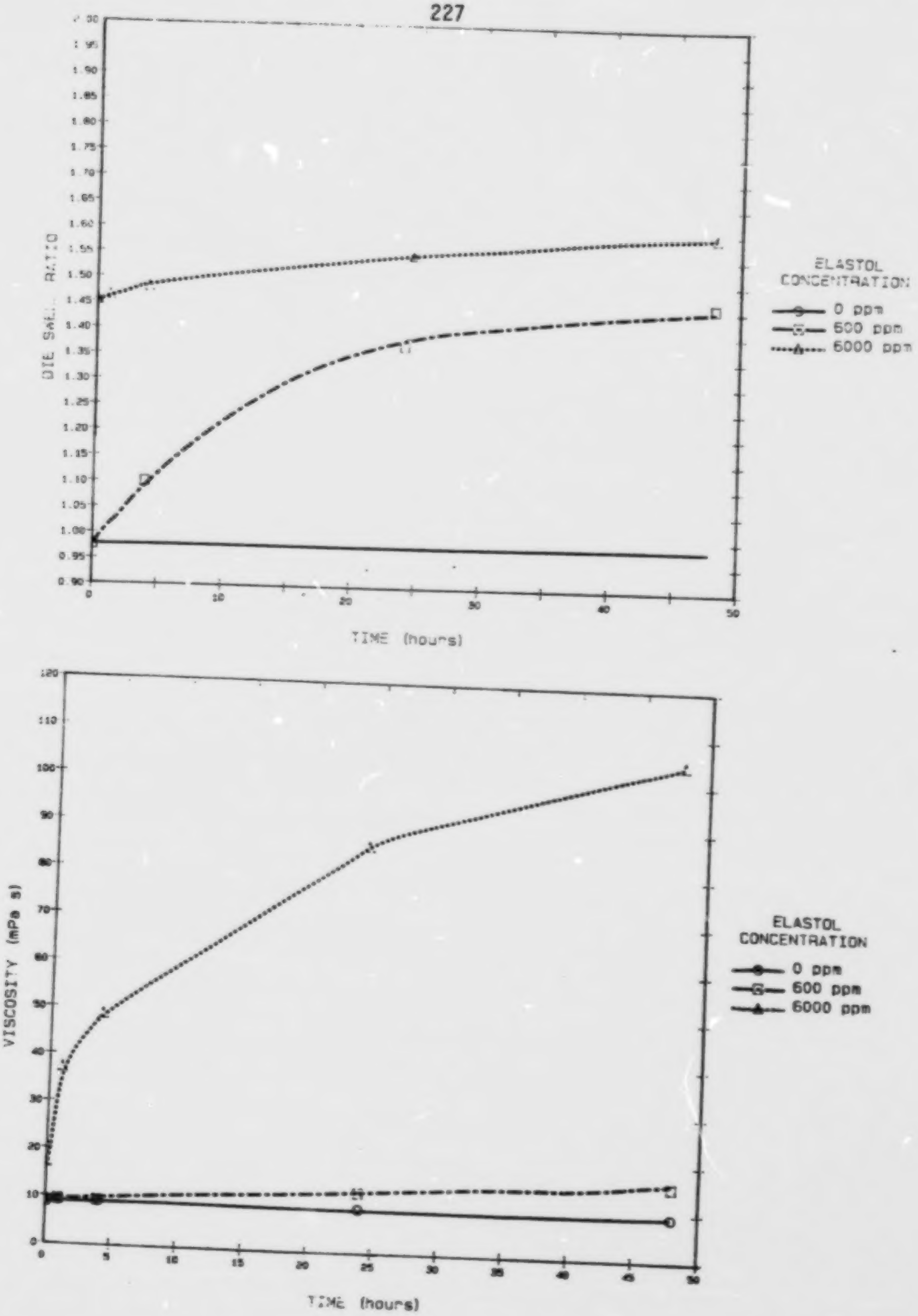

Figure 1. Die swell ratio and viscosity as a function of time for ASMB at 15 Deg. C.

Table 1: Degree of Elasticity of Test Oils

Temperature: 15 deg C

DEGREE OF ELASTICITY	ELASTOL CONCENTRATION 6000 PPM	 600 PPM
HIGH	Emulsifying Mix Norman Wells Prudhoe Bay	----
MODERATE	ASMB ASMB (no mixing) Amauligak Bent Horn Emulsifying Mix (no mixing) Hibernia Tarsiut	Emulsifying Mix Hibernia Norman Wells Prudhoe Bay
LOW	Diesel	ASMB Bent Horn Diesel Tarsiut

Temperature: 0 deg C

DEGREE OF ELASTICITY	6000 PPM	600 PPM
HIGH	----	----
MODERATE	ASMB Emulsifying Mix	----
LOW	----	ASMB Emulsifying Mix

All samples subjected to mixing at 80 RPM unless otherwise stated.

Table 2: Elastol Reaction Time for Test Oils

Temperature: 15 deg C

REACTION TIME	ELASTOL CONCENTRATION 6000 PPM	 600 PPM
FAST	ASMB Bent Horn Diesel Tarsiut	Bent Horn
MODERATE	ASMB (no mixing) Amauligak Emulsifying Mix Hibernia Norman Wells Prudhoe Bay	Diesel Prudhoe Bay
SLOW	Emulsifying Mix (no mixing)	ASMB Emulsifying Mix Hibernia Norman Well Tarsiut

Temperature: 0 deg C

REACTION TIME	6000 PPM	600 PPM
FAST	----	----
MODERATE	ASMB	----
SLOW	Emulsifying Mix	ASMB Emulsifying Mix

All samples subjected to mixing at 80 RPM unless otherwis stated.

exhibited greater viscoelasticity and faster reaction times. Oils tested at both temperatures had faster reaction times at 15 deg C. The degree of elasticity for ASMB was the same at both temperatures and slightly less at 0 deg C for the Emulsifying Mix.

(iii) Effect on Spreading

The results from these experiments were expressed as a ratio of the final spill area of the Elastol-treated oil slick to the area of the control slick. These ratios were plotted against the concentration in Figure 2 and against the reaction time, in Figure 3.

In the experiment in which concentration was varied, it is clear from Figure 2 that the greater the concentration, the smaller the extent of spreading. This is due to a greater increase in viscoelasticity of the treated oils at the higher concentrations.

In the reaction time study, it can be seen from Figure 3 that the effectiveness of Elastol (in terms of the extent of spreading) at a given concentration, increases with greater reaction time for both oils. However, the time required for Elastol to dissolve and "take effect" was found to be much shorter for ASMB than for the Emulsifying Mix.

(iv) Emulsification of Elastol-treated Oils

Tables 3 and 4 give experimental values for f(initial), f(final) and water content of the emulsions for untreated oils and oils treated with 600 and 6000 ppm of Elastol at 15 and 0 deg C.

The results from Table 3 (at 15 deg C) indicate that the emulsion formation tendency and/or stability of over half the oils were affected by the addition of Elastol. Of the oils which normally have no tendencies to form an emulsion, Amauligak and Tarsiut crudes exhibited an increase in emulsion formation with the addition of Elastol. The emulsion formed by Amauligak was found to be unstable, whereas the stability of Tarsiut increased. The opposite trend was observed for Norman Wells crude, in which a complete inhibition of emulsion formation was observed.

Of the oils which were classified as "very likely" to form an emulsion, weathered ASMB and Hibernia showed decreased emulsion stabilities. Prudhoe Bay crude formed an emulsion which could be classified as fairly stable, and the addition of Elastol at 600 ppm resulted in the formation of a completely unstable emulsion, and at 6000 ppm, completely inhibited emulsion formation. Although no change in tendency or stability was observed for the other oils, the water content of the emulsions formed by the Elastol-treated oils was, on average, 16% lower than those of the untreated oils. This would mean that for a given quantity of oil, the volume of emulsion formed is smaller when treated with Elastol.

At 0 deg C, the addition of Elastol to Amauligak and Tarsiut crudes again increased their tendencies to form emulsions. Of the oils having a high emulsion formation, only Norman Wells and Prudhoe Bay crudes' tendencies to emulsify and their emulsion stabilities were lowered by the addition of

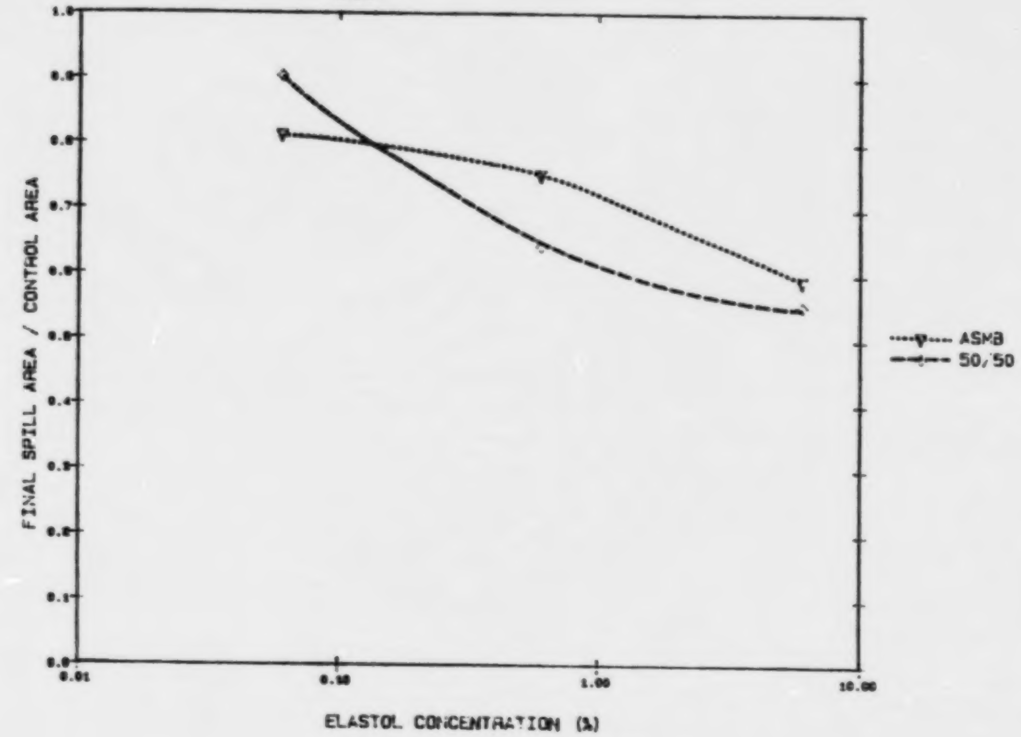

Figure 2. The extent of spreading versus concentration of Elastol for ASMB and the Emulsifying Mix at 15 Deg. C.

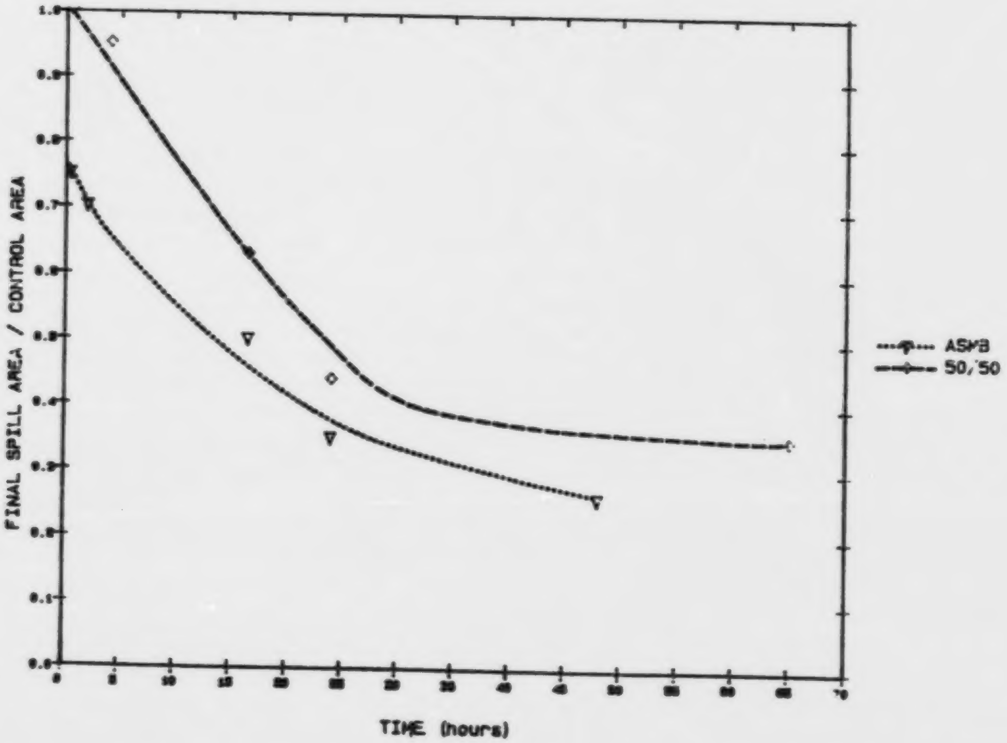

Figure 3. The extent of spreading versus time for ASMB and the Emulsifying Mix with 6000 ppm Elastol at 15 Deg. C.

Table 3: Emulsion Formation Tendency, Stability and Water Content of Test Oils

Temperature: 15 deg C.

Elastol Conc.	0 ppm			600 ppm			6000 ppm			Effect of Increasing Elastol Conc. on:		
Oil	f_∞	f	w	f_∞	f	w	f_∞	f	w	f_∞	f	w
ASMB Crude	0.9	0.4	0.96	0.9	0.31	0.96	0.9	0.34	0.78	o	-	-
ASMB, 15% Weathered	1	1	0.9	1	1	0.9	1	0.86	0.78	o	-	-
Amauligak Crude	0	0	0	0.29	0	0	0.53	0	0	+	o	o
Bent Horn Crude	0	0	0	0	0	0	0	0	0	o	o	o
Diesel	0	0	0	0	0	0	0	0	0	o	o	o
Emulsifying Mix*	1	1	0.9	1	1	0.88	1	1	0.77	o	o	-
Hibernia Crude	1	1	0.9	1	0	0	1	0	0	o	-	-
Norman Wells Crude	0.4	0.1	0.98	0	0	0	0	0	0	-	-	-
Prudhoe Bay Crude	1	0.22	0.97	1	0	0	0	0	0	-	-	-
Tarsiut Crude	0.08	0.08	0.96	0.55	0.22	0.88	1	0.4	0.94	+	+	o

Table 4: Emulsion Formation Tendency, Stability and Water Content of Test Oils

Temperature: 0 deg C

Elastol Conc.	0 ppm			600 ppm			6000 ppm			Effect of Increasing Elastol Conc. on:		
Oil	f_∞	f	w	f_∞	f	w	f_∞	f	w	f_∞	f	w
ASMB	1	1	0.9	1	1	0.88	1	1	0.82	o	o	-
ASMB, 15% Weathered	1	1	0.9	1	1	0.9	1	1	0.89	o	o	o
Amauligak Crude	0	0.29	0.91	1	0.43	0.89	1	0.75	0.65	+	+	-
Bent Horn Crude	0	0	0	0	0	0	0	0	0	o	o	o
Diesel	0	0	0	0	0	0	0	0	0	o	o	o
Emulsifying Mix*	1	1	0.86	1	1	0.88	1	1	0.68	o	o	-
Hibernia Crude	1	1	0.71	1	1	0.87	1	1	0.71	o	o	o
Norman Wells Crude	1	0.23	0.9	0.68	0.19	0.93	0.22	0.17	0.85	-	-	-
Prudhoe Bay Crude	1	1	0.9	1	0.89	0.9	0.34	0.89	0.79	-	-	-
Tarsiut Crude	0.15	0.22	0.6	0.91	0.45	0.65	0.89	0.3	0.77	+	+	+

f_∞: f initial
f : f final
w: volume fraction of water in emulsion 24 hrs after last mixing

+: increase
-: decrease
o: no change

* 50% Alberta Sweet Mix Blend; 50% Bunker C.

Elastol. The emulsions formed by Elastol-treated ASMB, Emulsifying Mix, Norman Wells and Prudhoe Bay crudes were observed to have 5 to 18% less water than emulsions formed by untreated oils.

In the experiments involving Brand S, the addition of Elastol had no effect on the effectiveness of this emulsion inhibitor. No emulsion formation was observed in the oils to which Brand S was applied.

PHASE 2: PERFORMANCE OF ELASTOL IN A SMALL-SCALE WAVE GENERATING TANK

Experimental

The experiments were performed in a small water-filled tank equipped with a variable speed oscillating hoop wave generator, as described in Bobra et.al (1987). The selected experimental parameters are listed below:

- Oil Type: Alberta Sweet Mix Blend (ASMB); Emulsifying Mix (50-50 of ASMB and Bunker C); 15% weathered ASMB
- Elastol Concentration: 0, 600, 2000, 4000, 6000 ppm
- Mixing Energy (Hoop Oscillation): 150 and 220 RPM
- Temperature: 0 and 15 deg C
- Water Salinity: fresh water and salt water (33 ppt)

Due to time limitations, only selected combinations of the above parameters were chosen.

The procedure involved pouring 150 mL of oil, which would produce an initial oil slick thickness of approximately 2 mm, into the centre of the oscillating hoop. Elastol was then uniformly distributed onto the oil slick by a salt-shaker-like applicator. At time intervals of 1/4, 1/2, 1, 2 and 3 hours, water and oil samples were collected. The water sample was analyzed for the extent of dispersion. The following measurements/analysis were conducted for the oil sample: viscosity; elasticity; water-in-oil content and the extent of weathering.

In addition, the effect of Corexit 9527, an oil dispersant, on an Elastol-treated oil slick was investigated using the same apparatus and procedure as described above. The dispersant was added at a dispersant-to-oil volume ratio of 1:100 one hour after the addition of Elastol on the oil slick.

RESULTS AND DISCUSSION

The results from the measurements/analysis were plotted as a function of time. The results for the ASMB experiments conducted at 15 deg C and at a mixing energy of 150 RPM are presented in Figure 4. These results are typical of the general trends observed in the other experiments and therefore, for the sake of brevity, are the only ones presented in this paper. For the complete set of results, refer to Bobra et.al. (1987).

(i) Effect on Weathering

At 15 deg C, the results indicate that the addition of Elastol slightly decreases the loss due to evaporation during the first two hours for both ASMB and Emulsifying Mix, which agrees with the trend observed in the earlier evaporation study in Phase 1. However, this difference in the total evaporative loss became insignificant after two hours. At 0 deg C, the effect of Elastol on weathering was negligible.

(ii) Effect on Dispersion

Elastol-treated oils were found to have a lower amount of oil dispersed in the water phase than untreated oils. This suppression of oil dispersion increased with increasing Elastol concentration. The greatest decrease occurred for ASMB at 15 deg C at 150 RPM in which a four and twenty fold decrease in oil dispersion was observed at an Elastol concentration of 600 and 6000 ppm, respectively. This reduction factor for the Emulsifying Mix under the same conditions was 2 at 600 ppm and 3 at 6000 ppm.

Experiments conducted at 0 deg C showed similar trends with respect to Elastol's ability to suppress oil dispersion. However, the magnitude of the reductions and the actual oil-in-water concentrations were found to be smaller at the lower temperature. This is in agreement with the fact dispersion is generally suppressed at lower temperatures.

(iii) Effect on Emulsification

Measured water-in-oil concentrations, which are an indication of the degree of emulsification, show that at the lower mixing energy level, 150 RPM, the addition of Elastol delays the onset of emulsion formation. Elastol-treated slicks had significantly lower water content (average of 28% and 65% less at 600 and 6000 ppm) than untreated slicks.

At 220 RPM, the rate of water entrainment for both treated and untreated oils were approximately the same for the first 15 minutes. After this period, the treated Emulsifying Mix emulsified at a slower rate and reached a constant but lower level of water content than the untreated oil. ASMB treated with Elastol, on the other hand, exhibited quite a different behaviour. The water content of the surface slick rose sharply during the initial stages and reached a maximum value at 15 minutes. This concentration then decreased for the next 15 minutes after which it remained constant. This behaviour was more evident at the higher Elastol concentration (see Figure 5).

From the water-in-oil concentrations observed for ASMB, it appears that Elastol has the ability to reverse the emulsification process and "squeeze out" water from the oil. One possible explanation for this phenomenon lies in the time required for Elastol to "react" with the oil. It was observed that the Elastol-treated ASMB did not reach its potential in terms of elasticity increase until about 1 hour into the experiment. Therefore, it is thought that during the initial stages (first 15 minutes), water enters the oil freely in the form of large droplets. As Elastol dissolves in the oil, the oil becomes progressively more cohesive, thereby impeding the introduction of additional water, and at the same time, promoting the emigration of water globules from the oil slick. This may explain the observed decrease in water content during the second 15 minute interval. From about 1 hour to the end of the experiment, a constant value of water-in-oil concentration was recorded. This is thought to indicate one or more of the following: that Elastol has "reacted" with the oil to the maximum elasticity; it has reached a point where any increase in elasticity has no effect on the net migration of remaining water droplets in the slick; and that there is no deterioration of the elastic properties of the oil with time.

The appearance of the water-in-oil emulsions formed by Elastol-free oils was a brown, stable mass, which is colloquially named "chocolate mousse". Of the Elastol-treated oils which formed a distinct emulsion at 15 deg C, none had the true appearance of "chocolate mousse". They were darker in colour and were observed to have smoother surfaces. At 0 deg C, only the Elastol-treated Emulsifying Mix approached the "chocolate mousse" appearance. These emulsions differed from stable Elastol-free emulsions by the presence of many large water droplets (> 1 mm). In addition, several small rigid "nodules", which were thought to be tightly bound clumps of Elastol polymer, were observed. The water-in-oil content of these emulsions were not significantly affected by the Elastol addition.

(iv) Effect on Slick Viscosity

Under most spill conditions, the viscosity of the spilled oil increases with time. This increase is due to the combined effect of weathering, and to a greater extent, emulsification. If Elastol is added to an oil slick, part of the increase will be due to the increase in viscoelasticity imparted by the polymer.

The viscosity measurements for the ASMB experiments show that the viscosity of the untreated oil increased by a factor of 600 to 900 after 3 hours. This dramatic increase is attributed mainly to the emulsification of oil. In comparison, the viscosities of oils treated with Elastol had a 100 to 150 fold increase. This smaller increase is the result of the ability of Elastol to decrease the extent of emulsification, as discussed previously. This also shows that the viscosity increase as a result of an increase in elasticity is small compared to the increase due to emulsification.

The measured viscosities for 15% weathered ASMB showed a similar trend. The results for the Emulsifying Mix at 15 deg C showed that the viscosities of the oil treated with 600 ppm Elastol and the Elastol-free oil were similar in magnitude. In contrast, an 81% lower viscosity was measured for the oil treated at a dose of 6000 ppm.

The viscosity measurements for the Emulsifying Mix at 0 deg C showed an opposite trend. In these experiments, the slick viscosity increased with increasing dose of Elastol. Since Emulsifying Mix has a high and stable emulsion formation tendency, a possible explanation is that the addition of Elastol merely imparted a higher viscoelastic effect on the oil's stable emulsion. In these experiments, the addition of Elastol did not significantly lower the water content of the emulsion. It should be noted that there was significant emulsion formation before the effects of Elastol were realized, since Elastol particles were still found floating on top of the oil slick 30 minutes after application.

(v) Die Swell Measurement and Observed Elasticity

The general trend of the die swell versus time plots for oils treated with 6000 ppm Elastol indicate that the maximum elasticity was reached within 15 minutes after commencement of the experiment, since the measured die swells after 15 minutes were either the same or smaller than the ratios at 15 minutes. This appears to imply that the Elastol had dissolved and imparted its full elastic potential to the oils within 15 minutes. This was not supported by recorded observations. Although the oil exhibited some degree of elasticity at 15 minutes, it was felt that a high degree of elasticity was not realized until some time later. For ASMB, it was agreed that this time was about 1 to 1.5 hours at 15 deg C and 2 to 3 hours at 0 deg C, depending on the concentration and mixing energy. For the Emulsifying Mix, and 15% weathered ASMB, a time of 2 hours was required to produce a slick exhibiting a high degree of elasticity at 15 deg C. (It should be noted that very little elasticity was observed for the Emulsifying Mix for all experiments at 0 deg C and for Elastol dose of 600 ppm at 15 deg C due to significant emulsion formation. This is discussed further in the next section.) These observations may imply that the die swell measurements taken at times greater than 15 minutes may be underestimating the true elasticity.

The most probable reason for this lack of agreement between the die swell measurement and observed elasticity is associated with the presence of water droplets in the oil phase, which has a reducing effect on the die swell.

(vi) Elasticity of Surface Oil

Despite the possible underestimation of the degree of elasticity as discussed in the previous section, the die swell measurements do illustrate some trends in the elastic behaviour for the oils tested. Untreated oils were found to exhibit no positive elastic behaviour, ie. exhibited die swell ratios approximately equal to one. Treated oils usually showed elastic behaviour within 15 minutes of Elastol application. As expected, increasing the concentration of Elastol resulted in a higher degree of elasticity.

Although the magnitude of the die swell ratios may not reflect the true elasticity of the oil slick, in this case, it is worthy to mention the differences in the range of the calculated die swell ratios for the three oils tested at 15 deg C and at the lower mixing speed. At an Elastol dose of 6000 ppm, the "average" die swell ratio for the three oils; ASMB, Emulsifying Mix and 15% weathered ASMB were found to be similar in magnitude, with the ratios for the Emulsifying Mix being slightly smaller than those of the other two oils. This difference was found to be more significant at 600 ppm. Observations of slick elasticity recorded during these experiments support this trend. Since the Emulsifying Mix was found to have the greatest emulsion

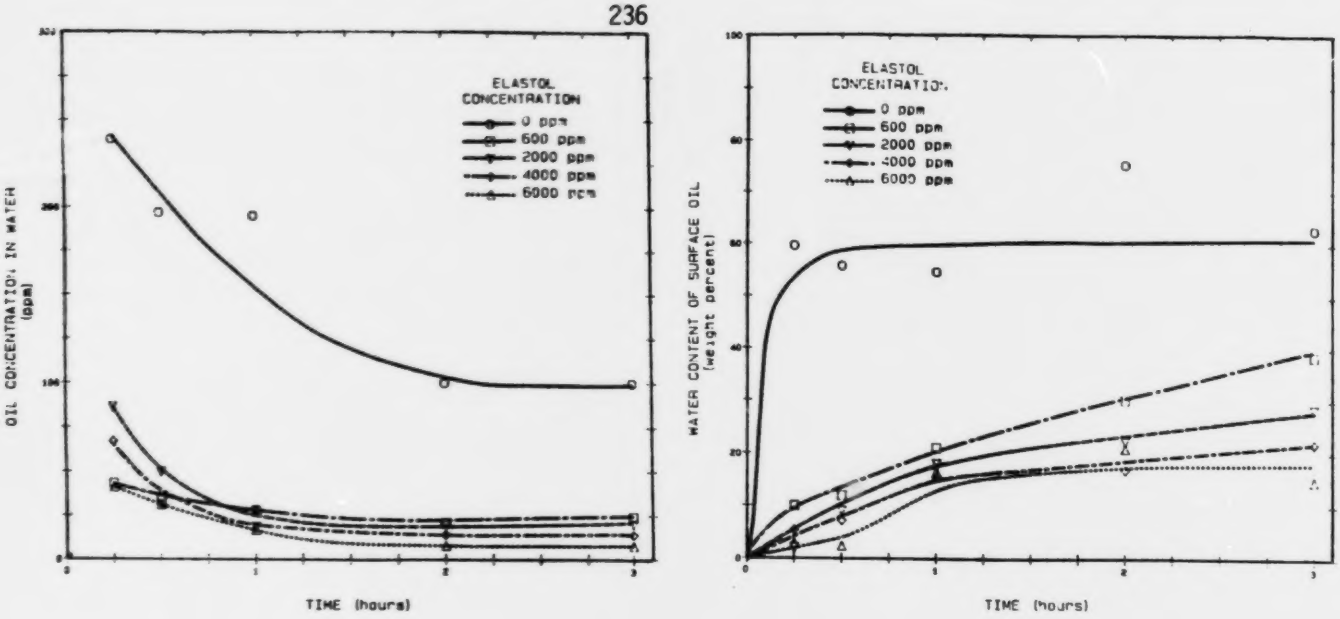

a) Dispersion versus time

b) Emulsification versus time

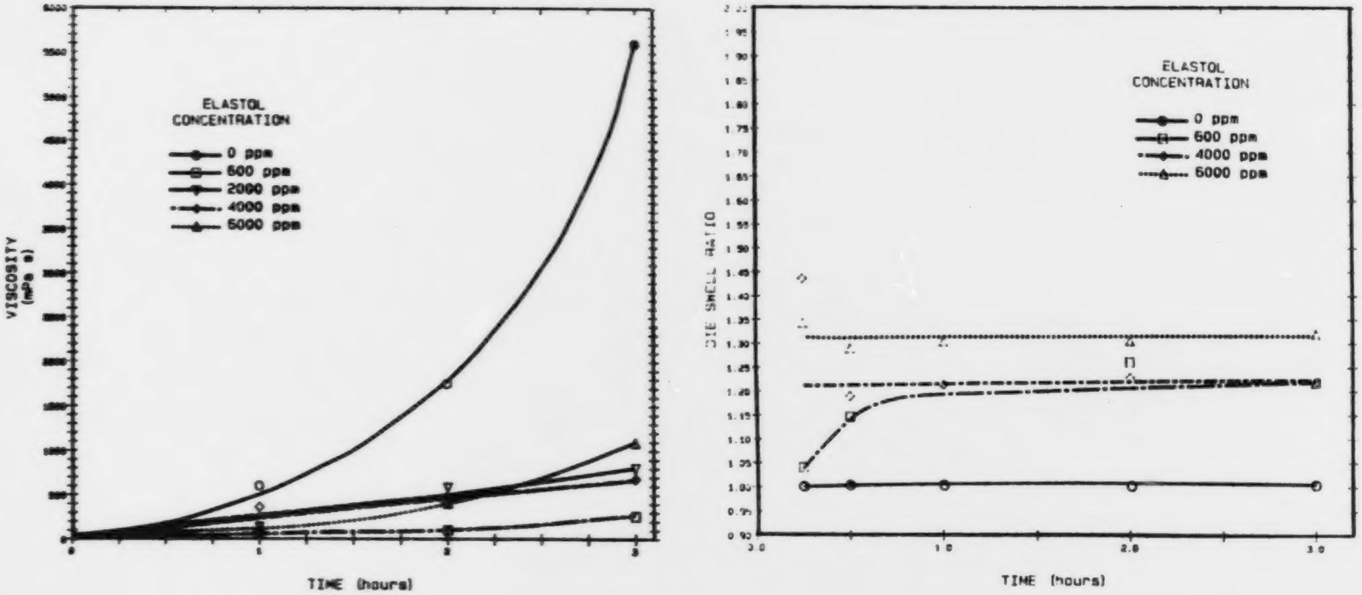

c) Viscosity versus time

d) Die swell ratio versus time

Figure 4. ASMB at 150 R.P.M. and 15 Deg. C

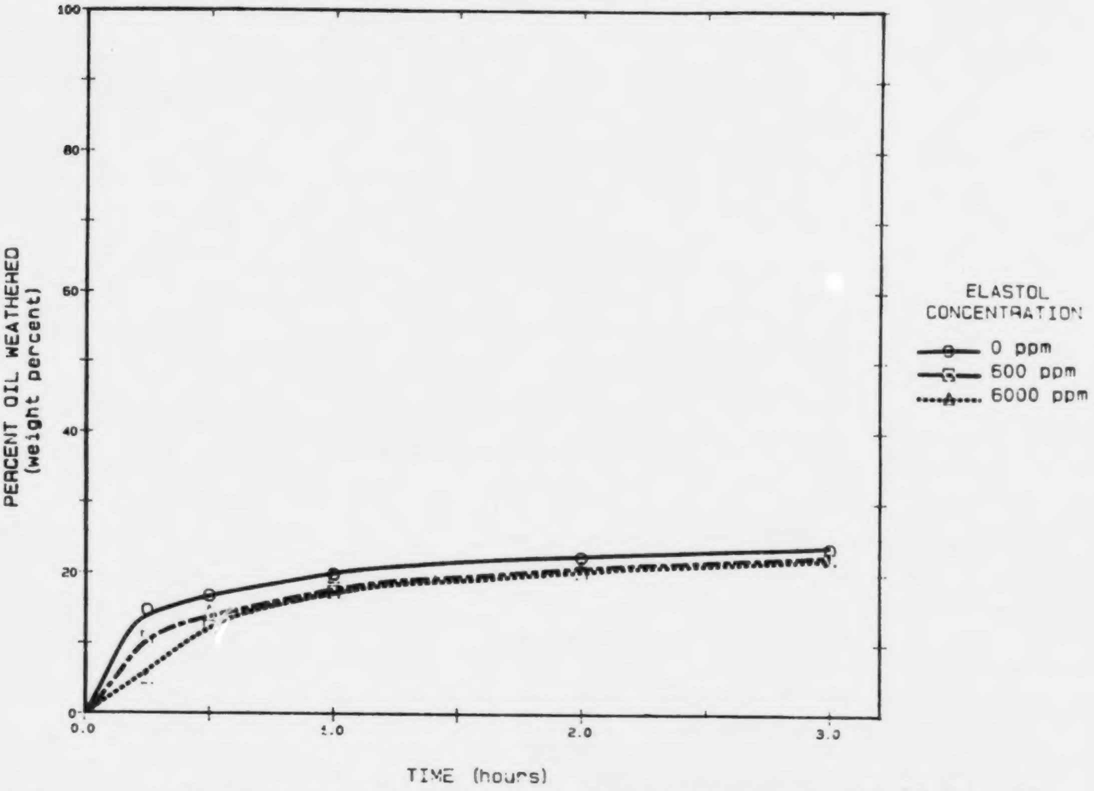

Figure 4e. Weathering versus time for ASMB at 150 R.P.M. and 15 Deg. C.

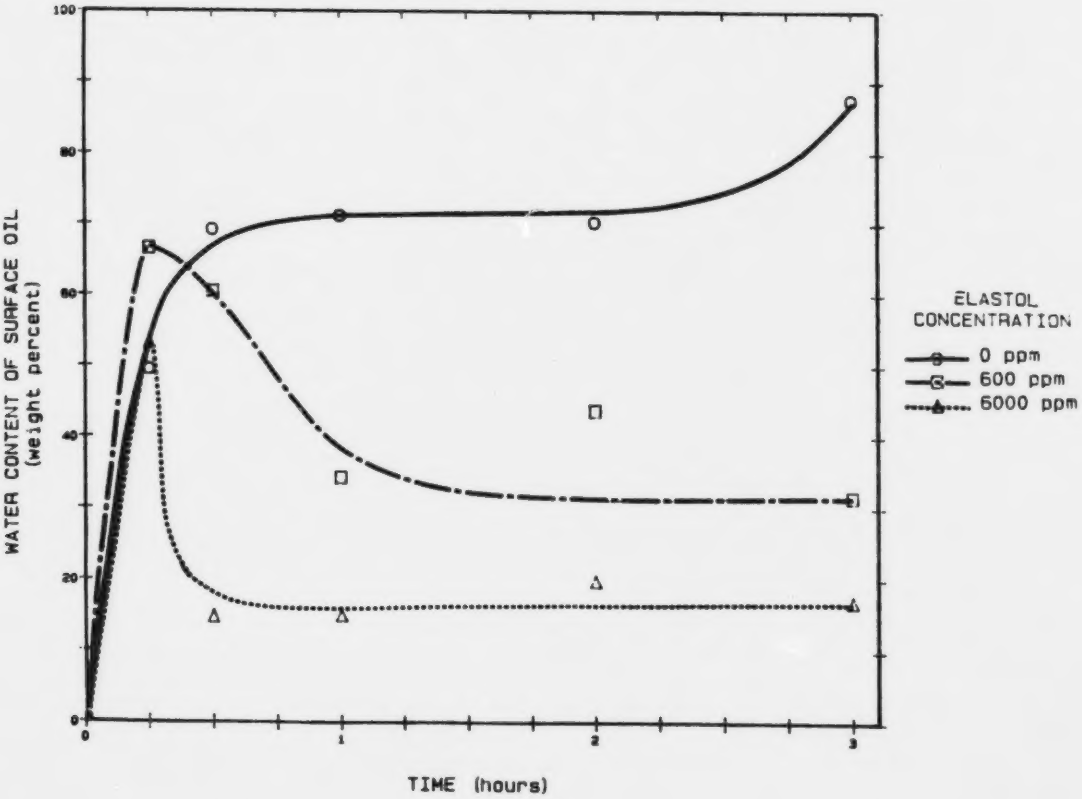

Figure 5. Emulsification versus time for ASMB at 220 R.P.M. and 15 Deg. C.

formation at both concentrations, it can be concluded that the emulsification process competes against, and discourages or masks the increase in measureable elasticity of the oil.

(a) Effect of Mixing Energy

For ASMB at 15 deg C, die swell measurements indicate that greater elasticity was imparted to the oil when mixed at a higher rate for both concentrations of Elastol. The results of the experiments involving Elastol-treated Emulsifying Mix showed that there was no significant difference in the measured die swell ratios when treated at an Elastol concentration of 600 ppm for the two mixing levels. At 6000 ppm, the die swell ratios were slightly lower for the experiment performed at the higher mixing speed. This decrease can most likely be attributed to the higher rate of emulsion formation observed at the higher mixing energy.

(b) Effect of Temperature

The die swell ratios for ASMB at both concentrations of Elastol showed that temperature had little overall effect on the measured die swells. Although the die swell ratios do not explicitly show the dependence of effective reaction time (the time required for Elastol to dissolve and impart its elastic behaviour) on temperature, the observations indicated a longer reaction time at the lower temperature.

For Emulsifying Mix treated with 600 ppm Elastol, the oil formed thick emulsions which suppressed the action of Elastol at both temperatures. This was supported, in part, by the relatively small die swell measurements. At a dose of 6000 ppm, higher die swell ratios were calculated for the experiment at 15 deg C. This is explained from the fact that the tendency for oils to emulsify increases with decreasing temperature. In the experiment conducted at 0 deg C, significant emulsion formation was observed even before the Elastol completely dissolved into the oil phase.

(c) Effect of Water Salinity

It was found that a slightly higher degree of elasticity was observed for the tests using fresh water than salt water. This was probably due to the lower degree of emulsification of the oil in the fresh water experiments.

(d) Effect of Weathered Oil

A comparison of the results for fresh ASMB and 15% weathered ASMB show that the initial die swell ratio measurement for the aged ASMB is greater than for the fresh oil. After one hour, the ratio of the fresh oil surpassed that of the weathered oil. Despite this lack of a general trend, both oils were found to exhibit considerable elasticity within one to two hours after the start of the experiment.

(vii) Effect of Dispersant on Elastol-Treated Slick

The oil-in-water concentrations for the Corexit-Elastol and Corexit-only experiments revealed that the addition of Elastol decreased the dispersant's effectiveness by 70%. However, the extent of oil dispersed was still found to be approximately 1000 times greater than the value observed from the slick treated only with Elastol. The elastic nature of the oil slick did not appear to be affected by the dispersant.

PHASE 3: PRELIMINARY LARGE-SCALE TANK TESTS AT ESSO

This section summarizes the findings of a large-scale tank test conducted by M. Fingas on March 25 and 26, 1987 at the Esso Research Facility in Calgary, Alberta.

Procedure

Seventy-five litres of Norman Wells crude oil were placed in a boom, then Elastol, at a dose of 6700 ppm, was added by casting the powder from jars. This was done in a random and unscientific manner. Samples of the oil were taken and analyzed for viscosity at 0, 20, 80 and 230 minutes after the application of Elastol. Analysis was performed using a FANN viscometer. At least two RPM settings were used and the results averaged.

The wave generators were turned on after the Elastol was applied and were turned off again for sample taking. The wave height was about 1/2 metre on the first day and about 1/4 metre on the second day. The respective temperatures of the tank water and air were 3 and 5 deg C for both days.

RESULTS AND DISCUSSION

(i) Observations Day 1:

Numerical results for both days are shown in the Table 5.

The wave energy on day 1 was very high and subsequently, much of the oil splashed over a cusp of the boom in the first few minutes. Because this occurred very rapidly, it is difficult to say what effect the Elastol had on oil containment dynamics. This loss of oil made sampling difficult as little oil was left in the boom. The oil that escaped stuck to the new steel beach and the walls of the tank. Interestingly, the oil appeared to be uniformly elastic, even though it was spread all over. At the 20 minute sampling time there was still undissolved Elastol in the samples in the boom.

At the end of the experiment, the oil was highly elastic and was very difficult to get into a bottle. The oil certainly did not break down in the waves. Very little oil remained in the booms to assess its burnability.

(ii) Observations Day 2:

The wave height was much lower than in day 1 and, with adjustments to the boom, no oil was splashed over.

The oil remained in the boom and progressively became thicker during the day. Unmixed Elastol particles were still in the oil at the 80 minute sampling time. Mixing and elasticity were much less than the previous day.

At the end of the experiment a Morris skimmer was used to recover the oil. It was too windy to attempt a burn. The skimmer recovered 70 litres (75 were spilled) and water was not evident! Obviously, the oil did not weather much or recovered water made up for the difference. The final area of the slick was estimated to be 6 to 10 square metres and this would give an average slick thickness of the 7 to 11 mm whereas 3 is the minimum for burning.

Table 5: Increase in Viscosity of the Oil Slick with Time

	Time (min)	Visc(Cp)	Ratio
Day 1	0	8	1
	20	41	5
	80	280	35
	230	2600	320
Day 2	0	8	1
	20	32	4
	80	69	17
	235	290	36

CONCLUSIONS

All oils tested (8 crudes and Diesel) exhibited viscoelastic properties when treated with 600 to 6000 ppm of Elastol. The magnitude and the time required to produce this increase in viscoelasticity was found to be different for each oil, and were enhanced by mixing and higher temperatures. Spreading studies showed that Elastol also reduced the extent of spreading of an oil slick. The addition of Elastol had no effect on flash point and slightly decreased the oil evaporation rate.

Tests performed to examine the effect of Elastol on emulsification showed that of the ten oils tested, two (Amauligak and Tarsiut), exhibited increased emulsion formation tendencies when treated with Elastol and two, (Norman Wells and Prudhoe Bay), showed a marked decrease. For the other oils, Elastol, in general, had little effect on their formation tendencies but for the oils that emulsified, the addition of Elastol lowered the resulting water content. Elastol had no effect on the performance of Brand S emulsion inhibitor.

In the small-scale tank tests, the addition of 6000 ppm of Elastol imparted a significant elastic property to all three oils tested. Oil slicks treated with Elastol showed a lower degree of emulsification and viscosity increase. Elastol also suppressed dispersion - both natural and chemically induced. In addition, it was observed that significant emulsion formation decreased the effectiveness of Elastol. This was particularly noticeable for Emulsifying Mix.

The results from the preliminary large-scale tank tests confirmed the basic trends and results observed in the laboratory testing of Elastol. Moderate wave energy appeared to enhance and speed up the elasticity development. At the conditions encountered in the second day of experiments, the thickness of the slick increased sufficiently to allow for burning. The high oil recovery rate (93%) observed in the second day and the generally favourable results obtained from this study appear to indicate that Elastol is an effective and useful oil spill treating agent. Therefore, further large-scale or ocean tests are recommended.

REFERENCES

Bird R.B., Armstrong R.C., Hassager O. Dynamics of Polymer Liquids John Wiley and Sons, New York, 1977.

Bobra M.A., Kawamura P.I., Fingas M., Velicogna D. Laboratory and Tank Test Evaluation of Elastol EPS Report, Environment Canada (to be published), 1987.

Mackay D., Zagorski W. Studies of Water-in-Oil Emulsions Report EE34, EPS, Environment Canada, 1982.

TEST AND EVALUATION OF THE HELITORCH FOR THE IGNITION OF OIL SLICKS

Alan A. Allen
Spiltec
Anchorage, Alaska

ABSTRACT

A field test and evaluation has been completed involving the use of gelled gasoline for the aerial ignition of oil under arctic conditions. This research has been conducted as the second phase of a much larger effort to identify or develop efficient, inexpensive aerial ignition concepts. All research has been conducted under the sponsorship of Alaska Clean Seas (an association of 14 oil companies with interest in Alaskan operations), with project administration handled by Shell Western E&P Inc. Results of several field tests under both temperate and Arctic conditions reveal that burning gelled gasoline can be released effectively from a helicopter-slung Helitorch and remain burning upon impact with water and/or oil. With release heights of 1 to 18 meters, burning gelled gasoline has been found to survive the splash effects upon impact and continue to burn for several minutes. Successful ignitions of fresh and weathered crude oil have been conducted with 2 1/2- to 12 1/2-mm thick oil layers on shallow water and ice, with air temperatures well below freezing, and with winds up to 29 km/h (18 mph). By varying the speed and height of the Helitorch, the distribution of burning globules at ground level can be selected involving a nearly continuous narrow swath of flame to one involving globules separated by a meter or more. Tests have been conducted with a number of nozzle configurations on the Helitorch creating ground-level distributions of burning globules with swath widths that vary from approximately 1 to 8 meters. Gelled gasoline, ignited and released from a Helitorch, appears to be an effective means of producing numerous oil ignition sources quickly, safely and at a cost of only pennies per ignition point.

BACKGROUND

This paper contains a summary of a much more extensive report prepared by Spiltec and administered by Shell Western E&P Inc. for Alaska Clean Seas (ACS). The original report, Refinement of Aerial Ignition Systems (Spiltec 1987), presents the results of one of several R&D efforts sponsored by ACS during 1986.

Various methods for the ignition of oil slicks were examined by Spiltec for Alaska Clean Seas during 1985 resulting in the publication: Survey And Analysis Of Air-Deployable Igniters (Spiltec, 1986). Five basic ignition systems were examined in the course of this project including the Canadian Environmental Protection Service (EPS) "PYROID" igniter, the Dome igniter (developed by Dome Petroleum Ltd.), laser ignition systems (under sponsorship of EPS), the Premo Aerial Ignition Device (manufactured by Premo Plastics Engineering Ltd.), and the Helitorch (manufactured by Simplex Manufacturing Co.). Each of these ignition systems represents a relatively unique approach for initiating the in-situ combustion of petroleum products.

The first two ignition systems (PYROID and Dome igniters) have had substantial exposure to actual field tests. These tests have resulted in several successful ignitions of floating oil slicks under a range of environmental conditions. These pyrotechnic devices, however, did have certain disadvantages in terms of safety, shelf-life, availability, speed of deployment and cost. The laser ignition concept, while still in the experimental stage, also showed several drawbacks associated with instability of beam-focussing from a helicopter, wind-effects during oil preheating, energy requirements, and cost.

These operational considerations and cost constraints became especially important as one examined the ignition requirements for a spill involving numerous isolated patches of oil. Should a major spill in the Arctic, for example, ever result in the uncontrolled movement of a continuous oil spill into a moving ice field, oil could conceivably surface as relatively small concentrations over an extensive region. In-situ burning could require the release of a very large number of individual ignition sources (S.L. Ross, 1981 and 1984). During such an event the cost to manufacture and deploy the igniters, as well as the speed and accuracy with which they could be distributed, would be of paramount concern.

As described in the above-referenced document (Spiltec, 1986), these operational and economic considerations highlighted the need to refine our understanding of existing aerial ignition concepts and equipment. The latter two ignition systems (Premo "AID" igniter and Helitorch*) seemed to have some of the most promising characteristics, even though they had never been used to initiate the combustion of an actual oil spill. Whether it be the use of a chemical starter (AID igniter) or the dropping of burning gelled gasoline (Helitorch), these approaches avoided the problems of finite inventories, limited shelf-life, time-consuming deployment, and high cost.

The research carried out during 1986, therefore, focussed on the feasibility of using the Premo AID igniter (or some similar configuration) and the Helitorch for the ignition of floating oil. After a few preliminary field tests it became apparent that the Helitorch offered considerable potential as an efficient aerial ignition device. Such tests also revealed that some major design changes would be needed in order to use the AID-like device. All further testing was then devoted exclusively to the Helitorch ignition system.

Igniter Performance Criteria

During the field-testing portion of this project, it was essential that igniter performance be based on the full range of actual oil spill "targets" that could be considered for in-situ burning. Such targets might be single large spills that are relatively thick and continuous (e.g., at a major tanker accident), or they might be a large number of isolated slicks such as those described above. If a major spill in the Arctic ever did occur, it is possible that during early breakup, oil-contaminated melt pools could result with irregular shapes ranging from typically 1 to 10 meters across. Some pools could be much larger, and spacings between pools could vary from a few meters to several hundred meters. The efficient ignition of such pools of oil could require a separate igniter for each pool thereby involving a very large number of individual ignition points.

---

* The Helitorch is described in detail later in this paper. The Premo Aerial Ignition Device (AID) is a polystyrene spherical container about 1¼ inches in diameter with about 3 grams of potassium permanganate inside.

In the above scenario, it would also be necessary to deliver the ignition sources to the "target" slicks with sufficient accuracy to impact most, if not all, of the spilled oil. The igniters would have to work reliably from altitudes that would ensure a reasonable degree of accuracy; they would have to survive falls onto ice and into shallow pools (including water); and they would have to operate effectively under relatively strong winds. Once in contact with an oil layer, the ignition source would need to provide sufficient heat to volatilize the oil nearby, and burn long enough and hot enough to create a self-sustaining flame over the surrounding oil. It is most desirable to have an ignition source that produces a "soft" flame; that is, one where there is a minimal disturbance of the surrounding oil. The use of gelled gasoline has considerable promise because such an ignition source can blend with and promote ignition of the surrounding oil. And, since the gelled gasoline is prepared as needed, there are no concerns regarding igniter shelf-life.

Another important criterion for effective and safe use is the need to avoid any open flame or sparks within the aircraft being used for deployment. The ignition source should be activated outside the aircraft so that any possibility of fire onboard is eliminated. And, if possible, all flammable materials should be carried outside the aircraft or at least be easily jettisoned in the event any equipment malfunctions or an emergency landing is necessary.

One final consideration involves the need to minimize and hopefully eliminate any debris following the use of an igniter. Unlike most ignition devices available to date, the Helitorch does not leave behind any structural components that could persist in the environment.

Objectives

The objectives during the Helitorch field trials (Figure 1) included an initial assessment of the survivability of burning gelled gasoline upon impact with water (Phase 1). Since burning globules from a conventional Helitorch configuration showed promise of survival, controlled low-level drop-tests were then conducted (Phase 2) to evaluate the importance of globule size, gelling-mix-to-fuel ratios, fuel type, and drop height. The influence of arctic conditions on globule/oil interactions, preheating times, ignition potential, and susceptibility to wind were also examined.

Objectives during Phase 3 involved the release of burning gelled gasoline (again under arctic conditions) from a Helitorch onto simulated melt pools with fresh and weathered crude oil. The results of these tests then led to the final field-test objectives (Phase 4) to determine the ground-level distributions of burning globules that could be achieved with different nozzle configurations at different release heights. Detailed descriptions of the environmental conditions and experimental procedures used during these four phases are contained in the final project report Refinement of Aerial Ignition Systems (Spiltec, 1987).

TEST AND EVALUATION OF THE HELITORCH
FOR THE IGNITION OF OIL SLICKS

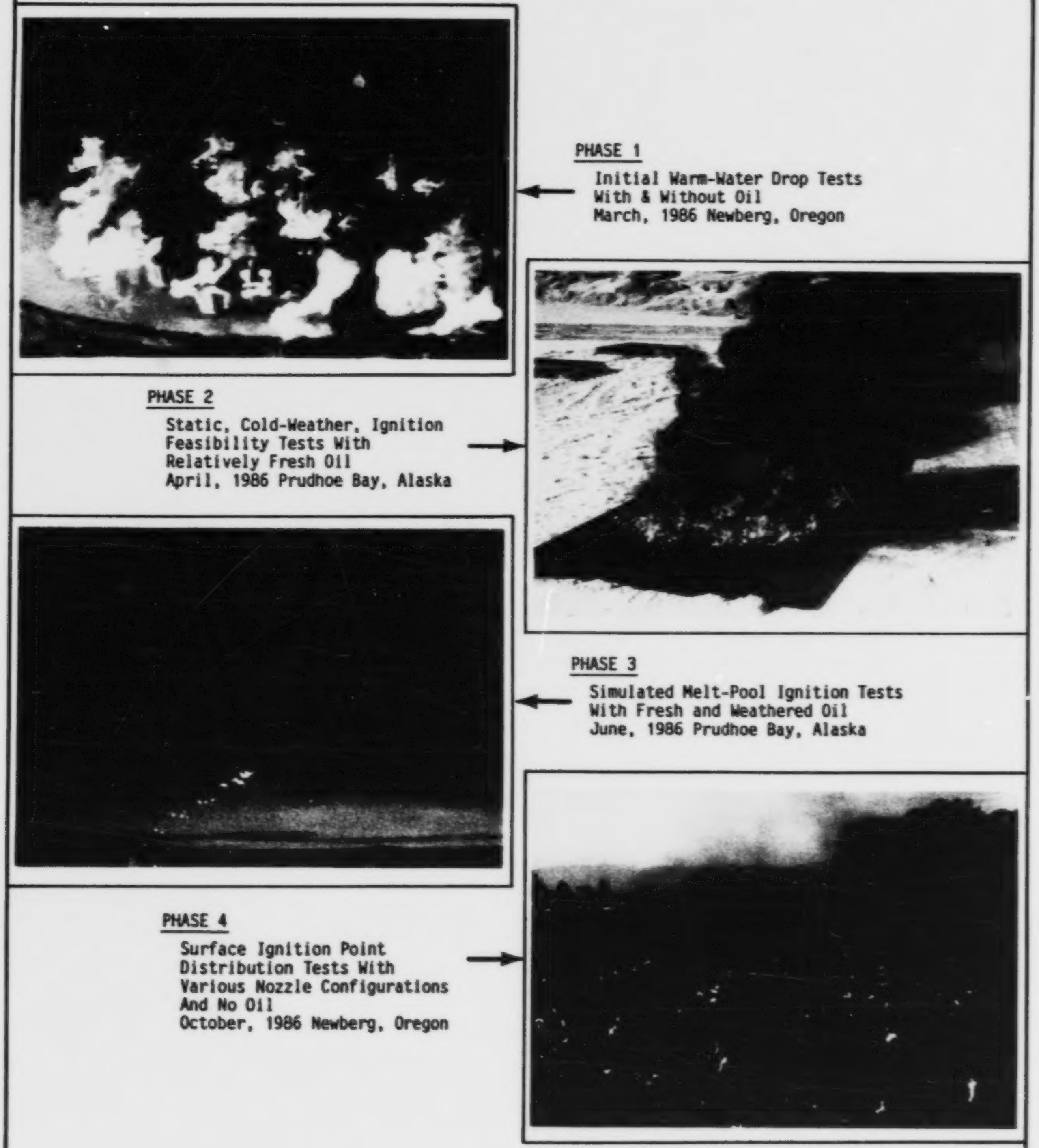

PHASE 1

Initial Warm-Water Drop Tests
With & Without Oil
March, 1986 Newberg, Oregon

PHASE 2

Static, Cold-Weather, Ignition
Feasibility Tests With
Relatively Fresh Oil
April, 1986 Prudhoe Bay, Alaska

PHASE 3

Simulated Melt-Pool Ignition Tests
With Fresh and Weathered Oil
June, 1986 Prudhoe Bay, Alaska

PHASE 4

Surface Ignition Point
Distribution Tests With
Various Nozzle Configurations
And No Oil
October, 1986 Newberg, Oregon

FIGURE 1 PHASES OF HELITORCH R&D PROGRAM -1986

Physical Description of the Helitorch

The Helitorch (Figure 2) is a proven aerial ignition system commonly used by the U.S. Forest Service and Canadian Forestry Service for the burning of forest slash and for setting backfires during fire-control operations. It is a completely self-contained unit consisting of a fuel barrel, pump, and motor assembly slung beneath a helicopter and controlled with an electrical connection from the Helitorch to a panel in the cockpit. The fuel barrel can be filled with a gelled gasoline or gasoline-and-diesel mix which is then pumped upon demand to a positive-control shut-off valve and ignition tip. The gelled fuel mixture is ignited with electrically fired propane jets as it exits one or more nozzles protected by wind shields. The burning gelled fuel falls as a highly viscous stream and quickly breaks up into individual globules before impacting the ground.

In fighting forest fires, the Helitorch is normally operated at heights and speeds much greater than those desired for the ignition of oil slicks in the Arctic. Depending upon the actual nature of the slicks to be ignited, lower altitudes and airspeeds have been found to enhance the accuracy, burn-times, and distribution of the burning globules.

The Helitorch ignition system is manufactured by Simplex Manufacturing Co. in Portland, Oregon, and is approved by the Federal Aviation Administration (FAR Part 137). Users of the system in the United States are cautioned that certain federal regulations (46 CFR) require approval by the Office of Hazardous Materials Transportation (OHMT), U.S. Department of Transportation, for transporting fuel beneath a helicopter (e.g., sling-loaded Helitorch) and for transporting the fuel to support a gelling operation at a remote site. Exemptions from these requirements have been obtained for such operations as forest fire control; however, application for exemption involving oil spill control must be requested.

The Helitorch (Figure 2) can be carried by any helicopter with a cargo hook and a 24- to 28-volt power supply. When the single-point suspension cable system is used with helicopters carrying swivel cargo hooks (e.g., Bell 205, 212, 412), the Helitorch may experience certain degrees of freedom during flight that may alter its globule-distribution (or swath-generating) capabilities.

The weight of the Helitorch with a full 55-gallon (208-liter) drum is approximately 242 kilograms (534 pounds). As illustrated in Figure 2, the entire unit is connected to a helicopter with a support cable assembly that can be jettisoned quickly from the helicopter's cargo hook. The electrical cable has a quick-disconnect plug near the helicopter, allowing the plug to be pulled apart if the unit is released in an emergency.

Depending upon the helicopter used (i.e., with fixed or swivel cargo hook), the Helitorch support assembly may be rigged to include a self-releasing horizontal support arm or stabilizing bar to keep the Helitorch oriented properly. The stabilizing bar can be suspended at one end directly below the cargo hook, with the other end of the bar resting on one of the helicopter's skids. The Helitorch's support cable assembly is then connected directly to the stabilizing bar. This approach provides a stable two-point connection while permitting the Helitorch to be jettisoned if necessary. Both support systems (i.e., with and without the stabilizing bar) were used during the field trials described in this report.

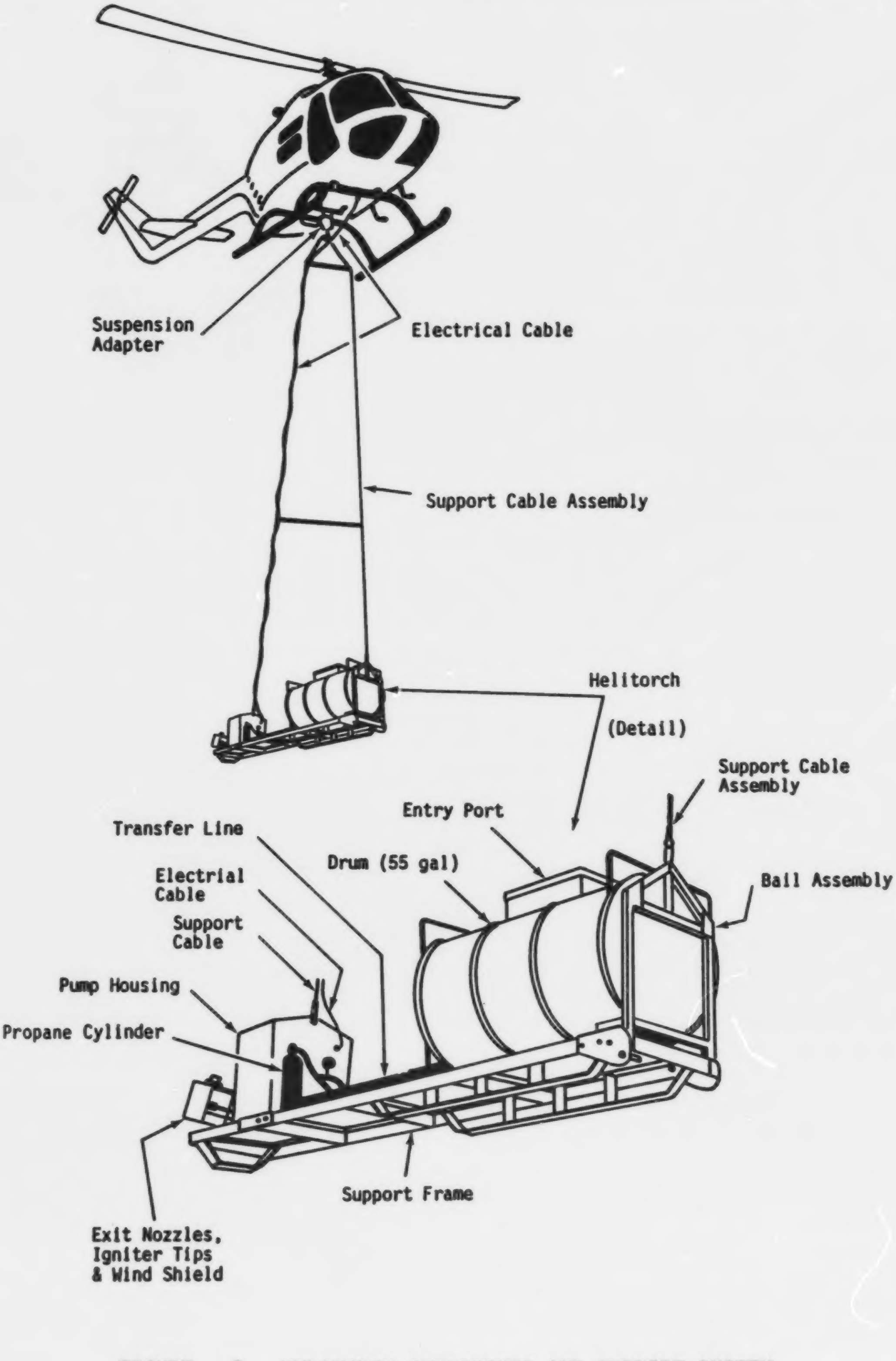
Suspension Adapter
Electrical Cable
Support Cable Assembly
Helitorch
(Detail)
Support Cable Assembly
Entry Port
Transfer Line
Drum (55 gal)
Bail Assembly
Electrial Cable
Support Cable
Pump Housing
Propane Cylinder
Support Frame
Exit Nozzles, Igniter Tips & Wind Shield

FIGURE 2 HELITORCH COMPONENTS AND SUPPORT SYSTEM

Throughout this project the gelling mix used to thicken the gasoline (or diesel in some cases) was SUREFIRE, a gelling agent available from Simplex, (Portland, Oregon) and from FIREFLEX MFG. LTD. (Langley, B.C.). SUREFIRE is a very fine powder which when mixed with liquid fuel produces a smooth, viscous gel. When typical ratios of 4 to 6 pounds of SUREFIRE to 55 gallons of fuel are used, (i.e., 9 to 13 grams/liter), adequate viscosities for Helitorch use can normally be achieved within a matter of minutes at room temperature. The gelling mix is poured through the entry port of the Helitorch fuel storage drum, which is equipped with a hand crank for mixing. Experiences gained in handling SUREFIRE at different ratios and under different temperatures during this project are presented below.

SUMMARY OF FIELD TEST RESULTS

The results of field tests conducted during the four phases of this project have been synthesized and categorized as follows:

- Gelled Gasoline Performance on Water
- Ignition of Crude Oil with Gelled Gasoline
- Helitorch Operational Performance
- Nozzle Performance
- Preparation of Gelled Fuel

Based on the findings of this R & D effort, it can be concluded that the Helitorch does provide an effective tool for the aerial ignition of combustible oil accumulations even under arctic conditions. Key advantages of the Helitorch include improved safety, speed and efficiency during deployment; no shelf-life constraints; no post-use debris; and low cost.

Gelled Gasoline Performance On Water

(a) Burning gelled gasoline globules released from heights ranging from 1 meter to 18 meters remained burning after impact with water alone. Even without oil on the water's surface, splash effects were tolerable, and elongated "pancakes" of gelled burning fuel resulted.

(b) Burning globules released to an oil-free water surface produced floating "pancakes" with areas (if expressed as a circular mass) typically 13 to 18 centimeters in diameter. When the globules were released from the higher altitudes of 15 to 18 meters, the surface areas were reduced slightly due to globule breakup at times and due to the reduction of volume while burning and falling a greater distance.

(c) Controlled drop tests in Phase 2 revealed that for globule volumes between 1/4 cup (59.3 cc) and 2 cups (474 cc), the thicknesses and burn times are relatively insensitive to the volume of the globule.

(d) The accumulated experiences from all four phases of this project suggest that the average globule sizes produced by the Helitorch with its standard nozzle at heights of 18 meters or less will be between 60 and 120 cc. With gelling-mix-to-gasoline ratios of 5-1/2 to 11 pounds per 55 gallons of fuel (i.e., 12 to 24 grams/liter), such globules will likely achieve thicknesses of 0.5 to 0.8 centimeters on oil-free water surfaces. The resulting burn times are typically between 4 and 6 minutes.

Ignition Of Crude Oil With Gelled Gasoline

(a) Cook Inlet and Prudhoe Bay crude oils (2-1/2 to 12-1/2 millimeters thick) have been ignited successfully with gelled gasoline released from heights of from 0 to 8 meters (Figures 3 and 4). Field data suggest that such ignitions should also be successful at heights of from 8 to 18 meters or higher. Most of the actual ignition tests with a Helitorch were conducted with Prudhoe Bay crude oil weathered from 0 to 14 days, on shallow water and/or ice, and with air temperatures well below freezing.

(b) In most cases a single globule of burning gelled gasoline was sufficient to preheat and ignite the surrounding crude oil within 30 to 60 seconds following impact. During controlled experiments, it was found that burning globules or surface "pancakes" needed to be at least 4 to 5 centimeters in diameter to insure ignition under relatively calm conditions.

(c) The ignition of the fresh and weathered crude oil layers in Phase 2 was possible with winds of 10 to 15 mph (16 to 24 kilometers/hour); however, surface globules approximately 60 to 120 cc in volume (i.e., surface areas approximately 13 to 18 centimeters in diameter) were necessary to prevent a blowout of the flame. During several successful ignitions of crude oil layers in Phase 3, surface winds had reached speeds of 18 mph (29 kilometers/hour).

(d) Controlled drop tests in Phase 2 revealed that average "pancake" thicknesses of dropped globules were two to three times greater (i.e., 1 to 2 centimeters or more) with a surrounding oil layer than with oil-free water. Had such tests failed to ignite the surrounding oil (ignition typically occurring in 10 to 15 seconds under calm conditions), the thickened globules could have burned for periods in excess of 10 minutes.

(e) During the above-referenced controlled drop tests under calm conditions, there was no noticeable difference in the efficiency of igniting oil with various gelling-mix-to-fuel ratios. Nor was there any significant difference in ignition time with different globule volumes, as long as the surface area was more than 4 to 5 centimeters in diameter. This critical area represents a volume of about 0.05 cup (or 12 cc) for the average thicknesses experienced.

(f) The results of the oil-ignition tests suggest that for the oils and environmental conditions experienced during this project, the standard Helitorch configuration is capable of producing adequate ignition sources for crude oil weathered up to 2 weeks during spring conditions in the Arctic. Ignition tests were conducted under warm (18°C) and cold (-16°C) weather conditions, on water (with and without ice), and with winds from 0 to 18 mph (29 kilometers/hour).

Helitorch Operational Performance

(a) Minor modifications are needed to the electrical cable and connector on the Helitorch to prevent the connector from opening too easily during

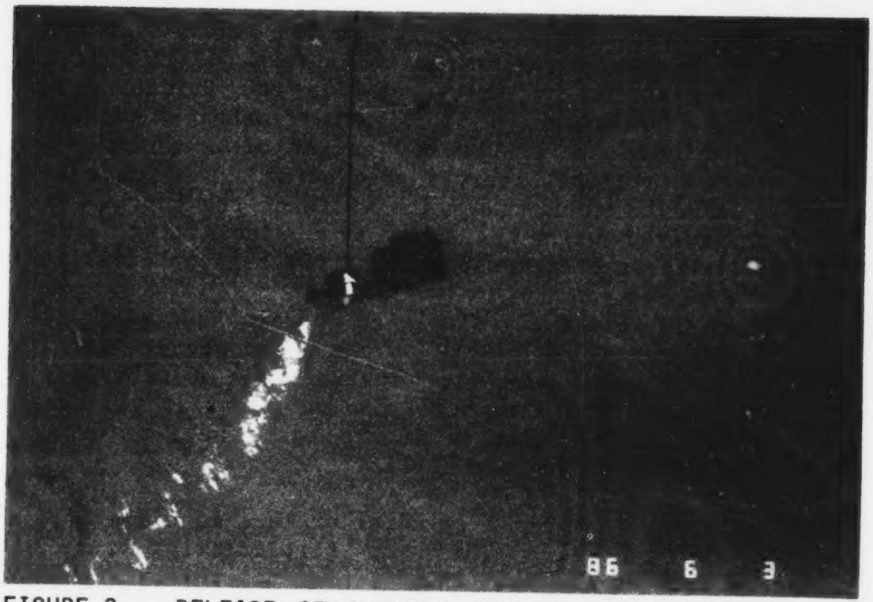

FIGURE 3 RELEASE OF BURNING GELLED GASOLINE FROM HELITORCH DURING SIMULATED MELT-POOL IGNITION TESTS

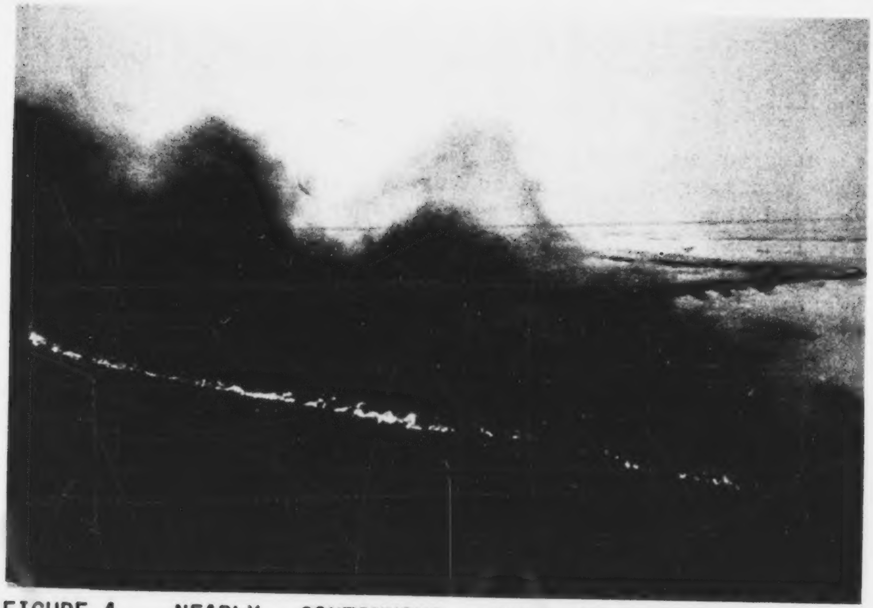

FIGURE 4 NEARLY CONTINUOUS PATH OF BURNING GELLED GASOLINE FOLLOWING SLOW, LOW-LEVEL PASS OF THE HELITORCH

flight. When the single-point suspension cable system is used with helicopters carrying swivel cargo hooks (e.g., Bell 205, 212 and 412), the resulting freedom of movement for the Helitorch can pull the connector open prematurely. This same freedom of movement can also allow the Helitorch to assume any number of orientations relative to the direction of flight, thereby presenting a problem should alternate nozzles be used to widen the swath width of the torch. These problems can be eliminated with the use of a stabilizing bar between the Helitorch's support cable assembly and the helicopter's landing skid.

(b) The Helitorch is relatively simple to operate, and very little instruction is required for the pilots of the helicopter to use it safely and effectively. Considerably more instruction is necessary for ground support and maintenance crews to mix and transfer gelled gasoline, to service the Helitorch, and to insure that the Helitorch is properly handled before and after each sortie.

(c) When target slicks are small (1 meter or less in diameter), accuracy is difficult to achieve. This is particularly true with larger helicopters such as the Bell 212. Improved accuracy should result with a) smaller helicopters, b) helicopters with good downward visibility, c) a two-point suspension assembly to arrest rotation of the Helitorch unit, and d) pilots experienced with the equipment.

(d) Experience has shown that the Helitorch should be flown at altitudes of 3 and 8 meters and with speeds in excess of 15 mph (24 kilometers/hour). The suggested altitude range is to provide accuracy during the release, to reduce the loss of gelled fuel while burning in the air, and to prevent the blowout of smaller globules on the surface when the helicopter is flying at low speeds. Speeds of 24 kilometers/hour or more are recommended to prevent the blowout of burning globules on the surface with the helicopter's downwash.

(e) When used at altitudes of 3 to 8 meters, the Helitorch with standard nozzle configuration produced burning globules that fell within a swath at ground level that was less than 1 meter wide. When it was flown at approximately 24 kilometers/hour over the ground, individual globules would usually be separated by less than 1/2 meter. If the system is flown at slower speeds and higher altitudes (to prevent the blowout of surface flame), a nearly continuous line of burning gel can be produced at ground level. Greater swaths can be achieved with different nozzle configurations, as described below.

Nozzle Performance

(a) It is possible to remove the standard Simplex Solid Stream nozzle (orifice = 7/16 inch or approximately 1.11 centimeters), which at recommended altitudes (for igniting oil slicks) produces a narrow swath of burning gelled globules typically between 1/4 cup (60 cc) and 1/2 cup (120 cc) in volume. Three multiple nozzle configurations were tested in Phase 4 (Figure 5) resulting in a variety of globule distributions and swaths ranging from 5 to 27 feet (i.e., approximately 1-1/2 to 8.2 meters).

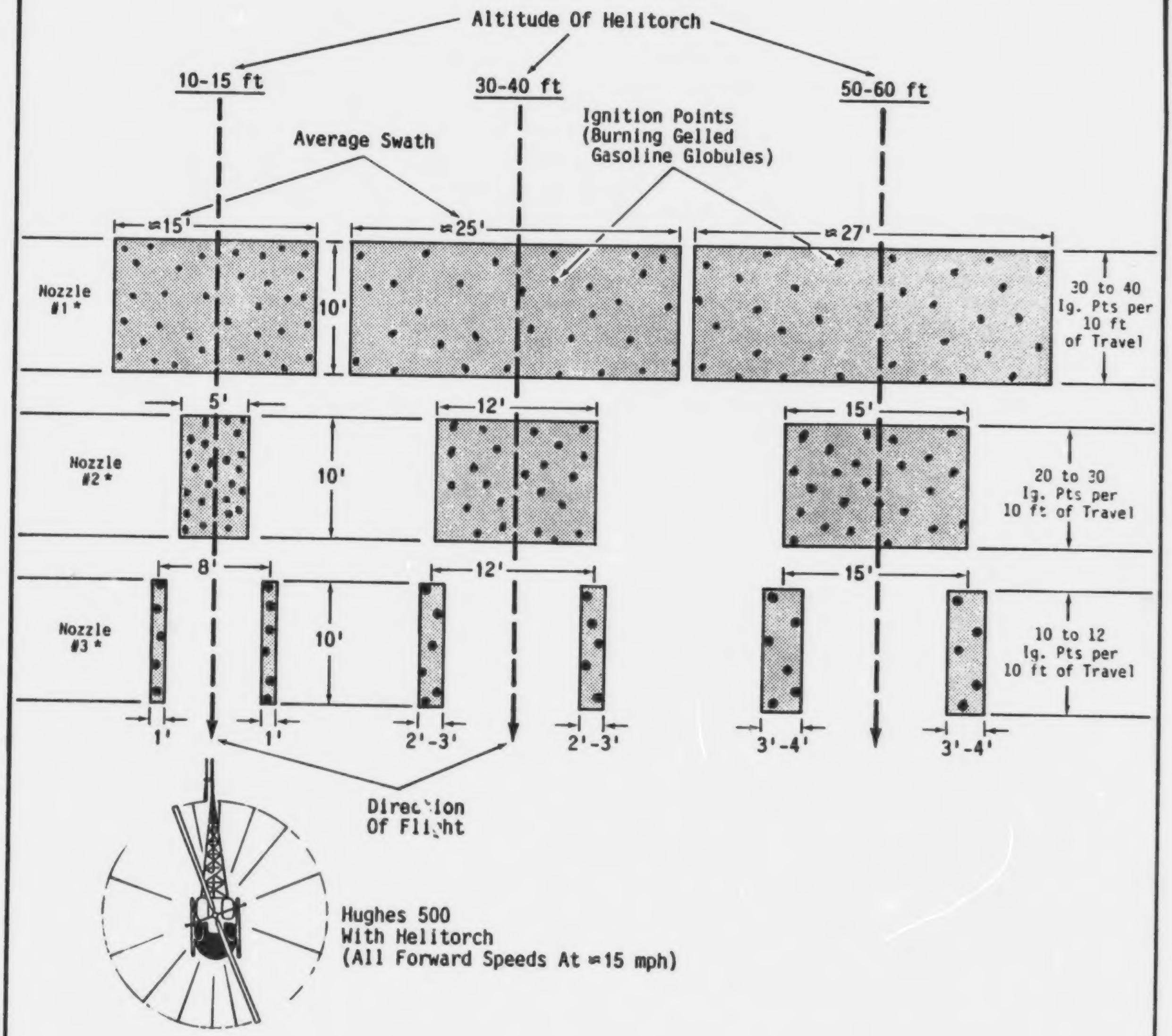
Altitude Of Helitorch
10-15 ft
30-40 ft
50-60 ft
Average Swath
Ignition Points (Burning Gelled Gasoline Globules)
≈15'
≈25'
≈27'
Nozzle #1*
10'
30 to 40 Ig. Pts per 10 ft of Travel
5'
12'
15'
Nozzle #2*
10'
20 to 30 Ig. Pts per 10 ft of Travel
8'
12'
15'
Nozzle #3*
10'
10 to 12 Ig. Pts per 10 ft of Travel
1'
1'
2'-3'
2'-3'
3'-4'
3'-4'
Direction Of Flight
Hughes 500
With Helitorch
(All Forward Speeds At ≈15 mph)

*Nozzle Configuration 1: Six VeeJet Solid Stream nozzles (three nozzles mounted on each of two triple spray manifold assemblies); manifolds positioned so that nozzles, with 15° between each nozzle, cover a full 75°. Nozzle orifice = 3/16 inch.

*Nozzle Configuration 2: Two TeeJet Off-Center OC150 (flat spray) nozzles mounted with 30° between nozzles. Nozzle orifice = 3/8 inch.

*Nozzle Configuration 3: Two Simplex Solid Stream nozzles mounted with 30° between nozzles. Nozzle orifice = 7/16 inch.

FIGURE 5 SWATH WIDTHS AND IMPACT POINT DISTRIBUTIONS FOR THREE DIFFERENT NOZZLE CONFIGURATIONS AND THREE RELEASE ALTITUDES

(b) Nozzle Configuration 1 (six VeeJet Solid Stream nozzles - Figures 6 and 7), operating from altitudes of 30 to 60 feet (9 to 18 meters), resulted in uniformly dispersed globules typically 3 to 4 feet (approximately 1 meter) apart over a swath of 25 to 27 feet (about 8 meters). From elevations of 10 to 15 feet (3 to 4-1/2 meters), the globules were a little less than 1 meter apart, within an average swath of 4-1/2 meters. Globules with an average volume of 0.05 cup (or approximately 12 cc) were produced leaving about 30 to 40 separate ignition points per 10 feet (3 meters) of travel when the system was flown at 15 mph (24 kilometers/hour). Such ignition sources are comparable to the smallest globules found to be successful in igniting cold, fairly fresh crude oil with light wind.

(c) Nozzle Configuration 2 (two VeeJet off-center nozzles) produced swaths of from 5 to 15 feet (1-1/2 to 4-1/2 meters) for altitudes of 10 to 60 feet (3 to 18 meters), with uniformly distributed globules approximately 1 to 2 feet apart (about 1/2 meter or less). Average globule sizes were approximately 0.072 cup (or about 17 cc). Again, such ignition sources are at the lower range of acceptable sizes for igniting cold, fairly fresh crude oil under light wind conditions.

(d) Nozzle Configuration 3 (two Simplex Solid Stream nozzles) resulted in the formation of two separate swaths separated by distances of 8 to 15 feet (2.4 to 4.5 meters), depending upon the Helitorch's height (10 to 60 feet, or 3 to 18 meters). Each of the swaths comprising a pair (made by a single pass) was between 1 and 4 feet wide (0.3 to 1.2 meters), again increasing with the altitude up to 60 feet (18 meters). Average globule sizes of about 0.18 cup (or about 43 cc) were produced, with approximately 10 to 12 ignition points per 10 feet (3 meters) of travel when the globules were released at 15 mph (24 kilometers/hour). This volume is well within the range of acceptable sizes for igniting cold, fresh and weathered crude oils even under light to moderate winds.

Preparation Of Gelled Fuel

(a) SUREFIRE gelling mix was used as the thickening agent throughout this project. SUREFIRE was found to be effective in producing adequately thickened fuel (gasoline or diesel) within a matter of a few minutes following contact with the fuel during all indoor mixing operations (16°C to 18°C). Mixture ratios varied from 5-1/2 pounds of gelling mix per 55 gallons of fuel to 18-1/3 pounds per 55 gallons (i.e., 12 grams/liter to 40 grams/liter). The higher ratios were used simply to expose any differences in globule spreading and ignition processes associated with greater viscosities in the gelled medium. It was found that there is very little advantage (from an ignition standpoint) in using higher gelling mix ratios; however, the higher ratios could reduce the gelling time at very cold fuel temperatures.

(b) SUREFIRE was used with gasoline that had been left outside at ambient air temperatures of -18°C to -12°C. During these gelling operations it was observed that weights of approximately 14 to 18 pounds per 55 gallons (30 to 40 grams/liter) of fuel were needed in order to achieve

FIGURE 6

RELEASE OF BURNING GELLED GASOLINE FROM HELITORCH WITH NOZZLE CONFIGURATION 1. NOTE THAT ONE OF SIX NOZZLES IS PLUGGED DURING THIS PASS.

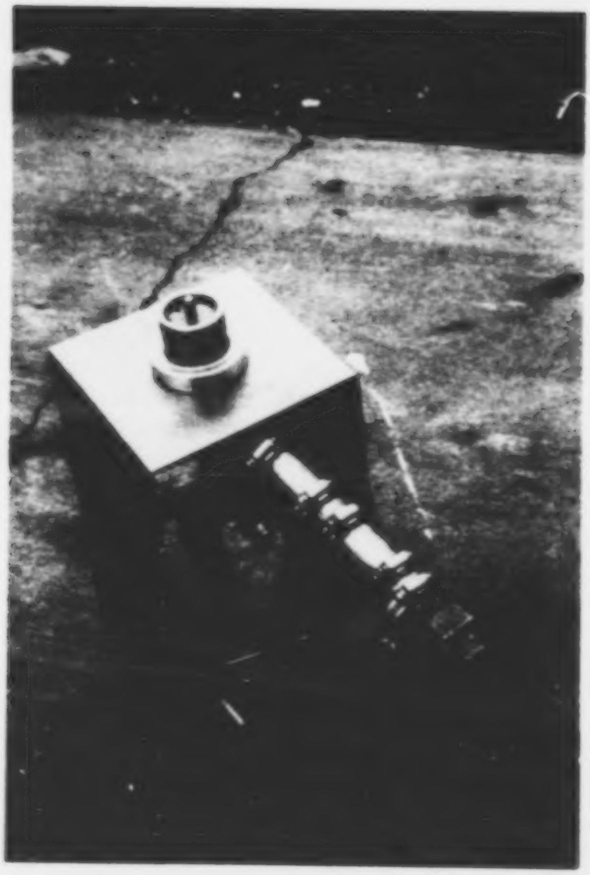

FIGURE 7

SIX VEEJET SOLID STREAM NOZZLES (CONFIGURATION 1) MOUNTED WITHIN STANDARD HELITORCH WIND-SHIELD ASSEMBLY. NOTE PROPANE EMISSION TUBE AND ELECTRICAL IGNITION TIP BELOW THE VEEJET NOZZLES.

adequate "torching" viscosities within 15 to 20 minutes. Using 11 pounds per 55 gallons (24 grams/liter), adequate viscosity was achieved within 30 to 40 minutes; and with 7-1/3 pounds per 55 gallons (16 grams/liter), a usable mixture required well over an hour.

(c) During all cold-weather tests (Phases 2 and 3), it was found that fuels gelled at room temperature retained their thickened properties without any noticeable change even after several hours of exposure to temperatures well below freezing.

(d) During all gelling operations it is essential that the thickening agent be applied at a moderate rate to a fuel that is free of water. As little as 2% water in the gasoline can seriously degrade the gelling process. A proper rate and mode of dispersion is needed to ensure a uniform distribution within the fuel, while completing the injection of powder prior to any noticeable thickening. Improper mixing, particularly with the higher mixture ratios, will result in the formation of stable lumps that can plug nozzles.

OPERATIONAL CONSIDERATIONS

The Helitorch has been shown to be an effective means of deploying ignition sources from the air onto floating oil. Burning gelled gasoline globules from the Helitorch can be applied as a narrow band with a swath width of a few feet or less, or they can be applied in a "broadcast" mode with swaths of nearly 30 feet (8 to 9 meters). Although not tested during this project, it is conceivable that much greater swaths could be achieved with a single helicopter using two or more Helitorches, higher pump rates, and/or a modified discharge and ignition assembly.

Depending upon the nature of the oil concentrations to be ignited, the Helitorch can be used to deliver a continuous stream of ignition sources, or it can be turned off and on for short bursts of burning fuel. Several examples of each type of application are illustrated in the following section.

It should be recognized that independent of the application mode, the Helitorch is operated with a positive-displacement pump producing a flow of approximately 15 gpm (56.8 liters/min). When operated with a 55-gallon-capacity holding drum (208 liters), the Helitorch can therefore provide a total application time of about 3 minutes and 40 seconds. The drum would then have to be refilled with gelled fuel or replaced with another drum already filled. The Helitorch is rigged so that an empty drum can be removed from the support frame and replaced with a full backup drum quickly and safely.

The distance over the ground, areal coverage, and number of ignition points that can be achieved during an application time of 3-2/3 minutes is dependent on a number of variables, including the speed and altitude of the Helitorch as well as the nozzle configuration used. The nozzle configuration will determine the number and size of ignition points created, which together with the speed and altitude of the Helitorch will determine the distribution of burning globules at ground level.

Using the fixed pump rate of 15 gpm (56.8 liters/min) and 55 gallons (208 liters)/drum, the resulting 3-2/3 minutes for application per drum can be used with any Helitorch speed (over the ground) to determine the distance achievable during continuous application. For example, at a speed of 15 mph (24 kilometers/hour) the distance (D) that can be achieved with a single drum and continuous application would be:

D = 15 mi/hour x 3.67 min/drum x 1 hr/60 min
= 0.92 mi/drum (or approximately 1-1/2 kilometers/drum of gelled fuel)

When the Helitorch is operated with nozzles that produce various swaths and distribution patterns, one might want to know the coverage rate at which the Helitorch can distribute such globules. A common expression for the areal coverage rate ($\dot{A}$) of any application system is:

$\dot{A}$ (acres/min) = speed (kt) x swath (ft) ÷ 430
or
$\dot{A}$ (acres/min) = speed (mph) x swath (ft) ÷ 494.5

If, for example, the Helitorch were to be operated at approximately 15 mph (24 kilometers/hour) with a nozzle configuration and altitude that resulted in a swath of 15 feet (4-1/2 meters), the Helitorch would cover the ground at about 1/2 acre per minute (0.18 hectares/min). That is:

$\dot{A}$ = 15 x 15 ÷ 494.5 = 0.45 acre/min (0.18 hectares/min)

The total area (T.A.) covered with a single drum under these conditions would therefore be:

T.A. = 0.45 acre/min x 3.67 min/drum
= 1.66 acres/drum (0.67 hectares/drum)

This area represents the size of the zone within which burning globules would be deposited. The area of oil concentration that might ultimately be ignited, of course, could be considerably greater depending upon the size and distribution of the original pools of oil.

Some additional calculations may be of interest recognizing that various nozzle configurations produced fairly consistent numbers of ignition points (Figure 5). For example, Nozzle Configuration 2 typically produced 20 to 30 ignition points per 10 feet (3 meters) of travel when flown at 15 mph (24 kilometers/hour). If the Helitorch were then flown at an altitude of 50 to 60 feet (15-18 meters), these 20 to 30 globules per 10 feet (3 meters) of travel would be distributed over a swath of about 15 feet (4-1/2 meters). If the helicopter were to double its speed to 30 mph (48 kilometers) and then to 60 mph (96 kilometers/hour), the resulting concentrations would correspondingly drop from an average of 25 ignition points per 10 feet (3 meters) of travel to 12 and 6 ignition points per 10 feet (3 meters) respectively. Table 1 shows how each of the above parameters would vary for a single Helitorch flown at 15, 30, and 60 mph with swaths of 5, 15, and 25 feet. (Conversions for metric units are provided at the bottom of the table.)

Use of the Helitorch in a "broadcast" mode over an extensive region would require a carefully planned application program involving the potential for many staging areas. With application times of less than 4 minutes

TABLE 1

HELITORCH PERFORMANCE APPROXIMATIONS FOR SELECTED VALUES OF SWATH AND GROUND SPEED DURING CONTINUOUS OPERATION

(Single Helitorch with fixed pump rate of 15 gpm)

	Swath = 5 ft			Swath = 15 ft			Swath = 25 ft		
	Speed			Speed			Speed		
	15mph	30mph	60mph	15mph	30mph	60mph	15mph	30mph	60mph
Areal Coverage Rate $\dot{A}$ (acres/min)	0.15	0.30	0.61	0.45	0.91	1.82	0.76	1.52	3.03
Application Time T (min/drum)	3.67	3.67	3.67	3.67	3.67	3.67	3.67	3.67	3.67
Total Area* Covered T.A. (acres/drum)	0.55	1.11	2.24	1.65	3.34	6.68	2.79	5.58	11.12
Distance Covered D (miles/drum)	0.92	1.84	3.68	0.92	1.84	3.68	0.92	1.84	3.68
Ignition Points per 10' of Travel (Avg. #/10')	≈25	≈12	≈6	≈25	≈12	≈6	≈25	≈12	≈6

* T.A. = $\dot{A}$ x T [Because of rounded-off values for $\dot{A}$ and T, T.A. values do not reflect exact multiples for speed and swath comparisons. (Example: when comparing T.A. for 15-ft swath @ 60 mph with T.A. for 5-ft swath @ 60 mph, T.A. (15') is not exactly 3 times T.A. (5').]

1 acre = 0.4047 hectare
1 foot = 0.3048 meter
1 mph = 1.6093 kilometers/hour
1 gpm = 3.785 liters/minute

per drum, it may be necessary to provide gel-preparation and reloading sites, as well as helicopter refueling stations, at a number of locations as close as possible to the region being treated. During open water, it may be possible to use a barge as such a staging platform. Depending upon the width and length of the oiled zone, "D" values of only a few miles (5 to 6 kilometers) or less per drum suggest that staging sites also be separated by comparable distances if possible. Such logistical considerations will be addressed in the following section for a hypothetical region of contamination approximately 100 miles (161 kilometers) in length.

One final consideration relates to the cost to conduct an in-situ burning operation with the Helitorch. The cost for the helicopter will obviously represent a substantial portion of the overall expense, running from hundreds to thousands of dollars per hour depending upon the type of helicopter used.

Deployment costs will also vary with the company and location from which the aircraft is obtained. Other costs, however, can be anticipated such as the purchase price of the Helitorch (approximately $5,000 U.S. as of January, 1987) and the price for gelling agent (approximately $4.00 U.S./lb for SUREFIRE as of January, 1987).

Using current gasoline prices, an estimate can be made of the application cost (less helicopter and ground support expenses). As discussed in detail in the original report (Spiltec, 1987), one could achieve a nearly continuous path of burning gelled gasoline (with more than 12,000 ignition points) for approximately $50 U.S. per kilometer (less than $100 U.S./mile). With Nozzle Configuration 3, producing the largest but least number of ignition points, the cost still remains on the order of a penny per ignition point.

POTENTIAL SCENARIOS

Figures 8 through 13 are provided as examples of spill situations during which a Helitorch could be used to support an approved in-situ burning program. While other scenarios can be envisioned, those illustrated here are representative of ones which could conceivably take place in Alaska and other cold-weather regions. Two scenarios are provided for solid (decaying) ice conditions, two are given for broken ice conditions, and two are also provided for open water environments (one as an open lead). Figure 12 could apply to temperate and tropical areas as well.

In the spill scenario illustrated in Figure 8, the Helitorch could be especially effective in covering an extensive area of isolated patches of oil. As discussed earlier, this kind of spill scenario could occur during the early melt period in the Arctic. Oil from a massive spill could have been released during breakup or during the winter months into moving broken ice or beneath moving solid ice. A response of this magnitude involving tens to hundreds of miles of oiled ice in a relatively narrow swath would require careful logistical planning involving:

- Helicopter and Helitorch nozzle selection,
- Ground speed and altitude required for efficient ignition,
- Number and location of staging areas for gelled fuel and helicopter fuel,

DECAYING ICE

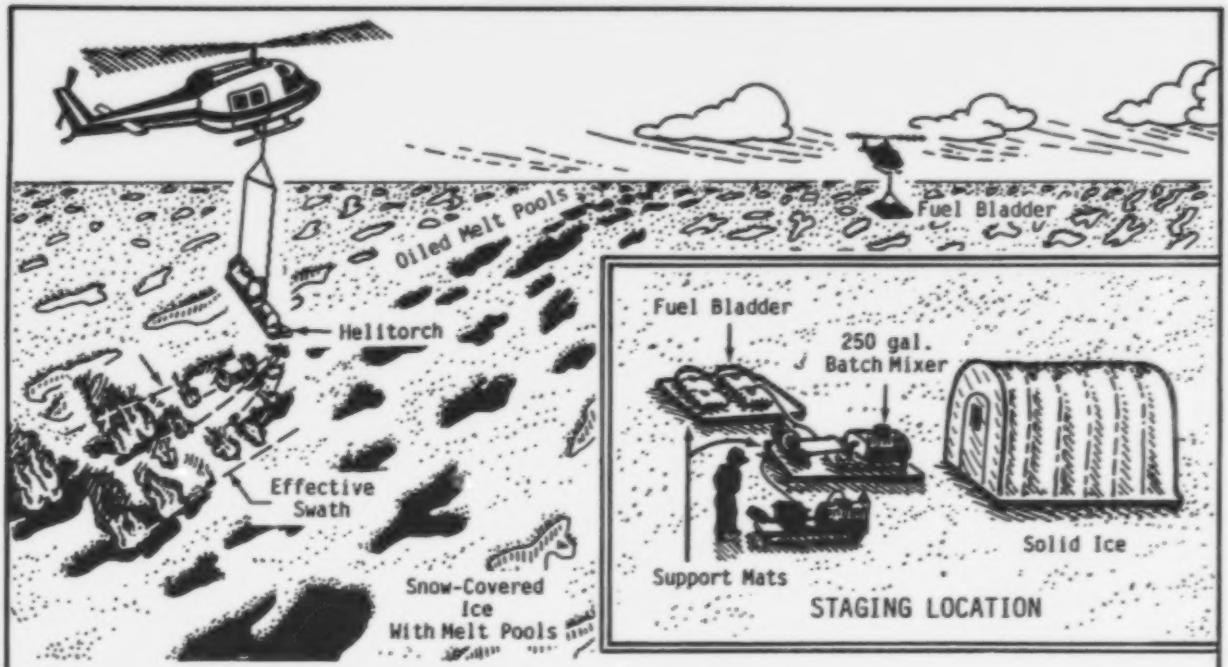
Oiled Melt Pools
Fuel Bladder
Helitorch
Effective Swath
Snow-Covered Ice With Melt Pools
Fuel Bladder
250 gal. Batch Mixer
Solid Ice
Support Mats
STAGING LOCATION

FIGURE 8 APPLICATION OF BURNING GASOLINE FROM A HELITORCH OVER A CONTINUOUS ZONE OF OILED MELT POOLS (BROADCAST MODE)

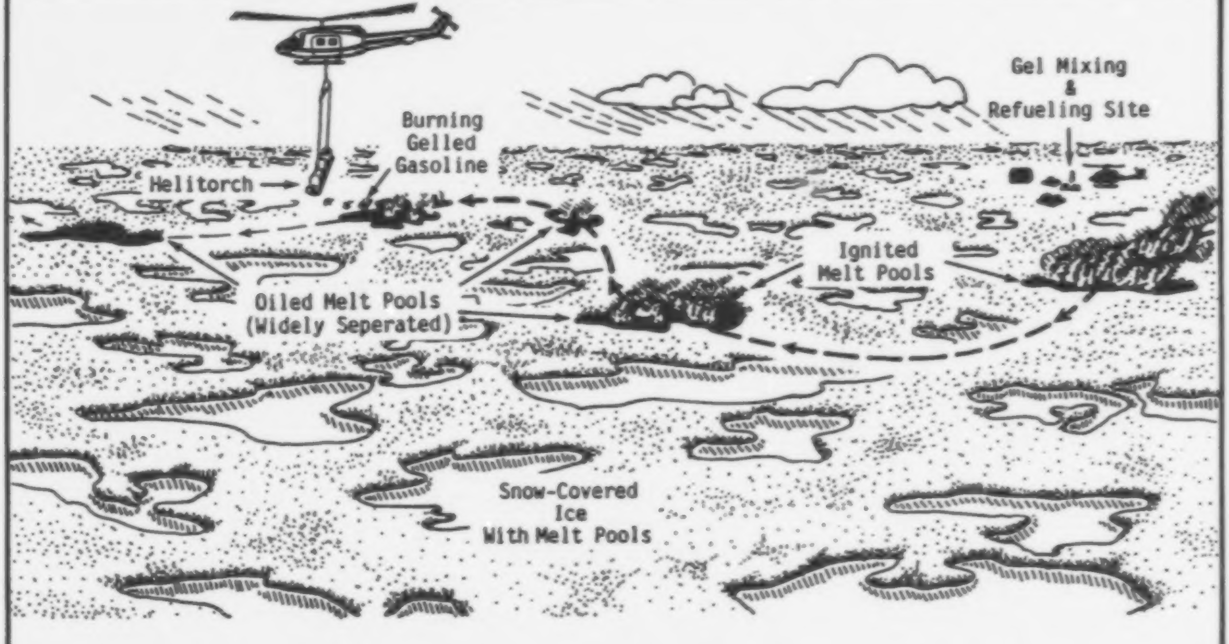
Gel Mixing & Refueling Site
Burning Gelled Gasoline
Helitorch
Ignited Melt Pools
Oiled Melt Pools (Widely Seperated)
Snow-Covered Ice With Melt Pools

FIGURE 9 APPLICATION OF GELLED GASOLINE WITH A HELITORCH OVER INDIVIDUALLY-TARGETED MELT POOLS WITH OIL (SINGLE-TARGET MODE)

BROKEN ICE

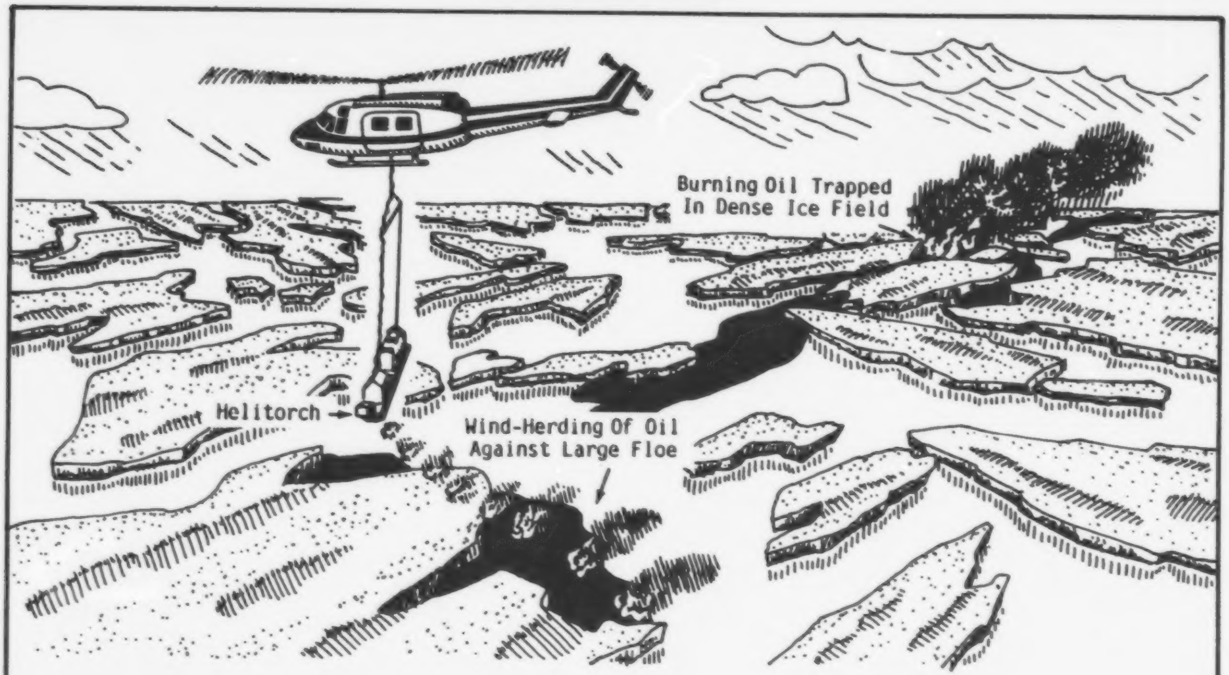
Burning Oil Trapped
In Dense Ice Field
Helitorch
Wind-Herding Of Oil
Against Large Floe

FIGURE 10 USE OF A HELITORCH OVER POOLS OF FLOATING OIL TRAPPED WITHIN OR AGAINST MOVING ICE FLOES

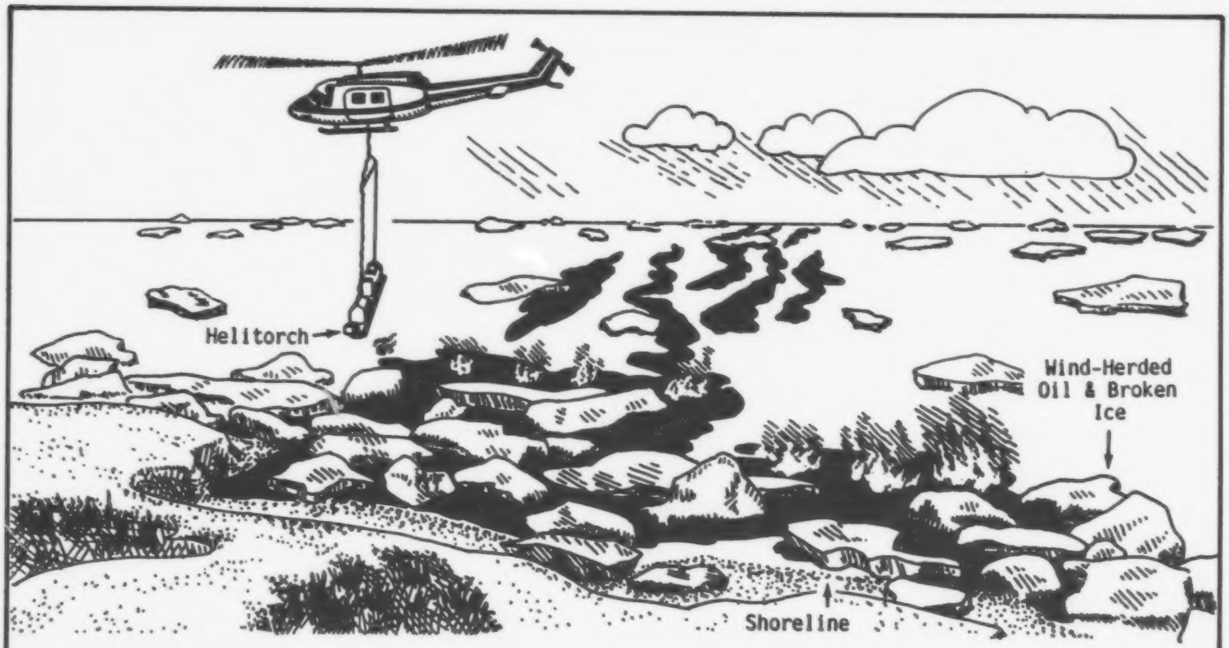
Helitorch
Wind-Herded
Oil & Broken
Ice
Shoreline

FIGURE 11 USE OF A HELITORCH OVER OIL AND ICE TRAPPED ALONG A SHORELINE

OPEN WATER

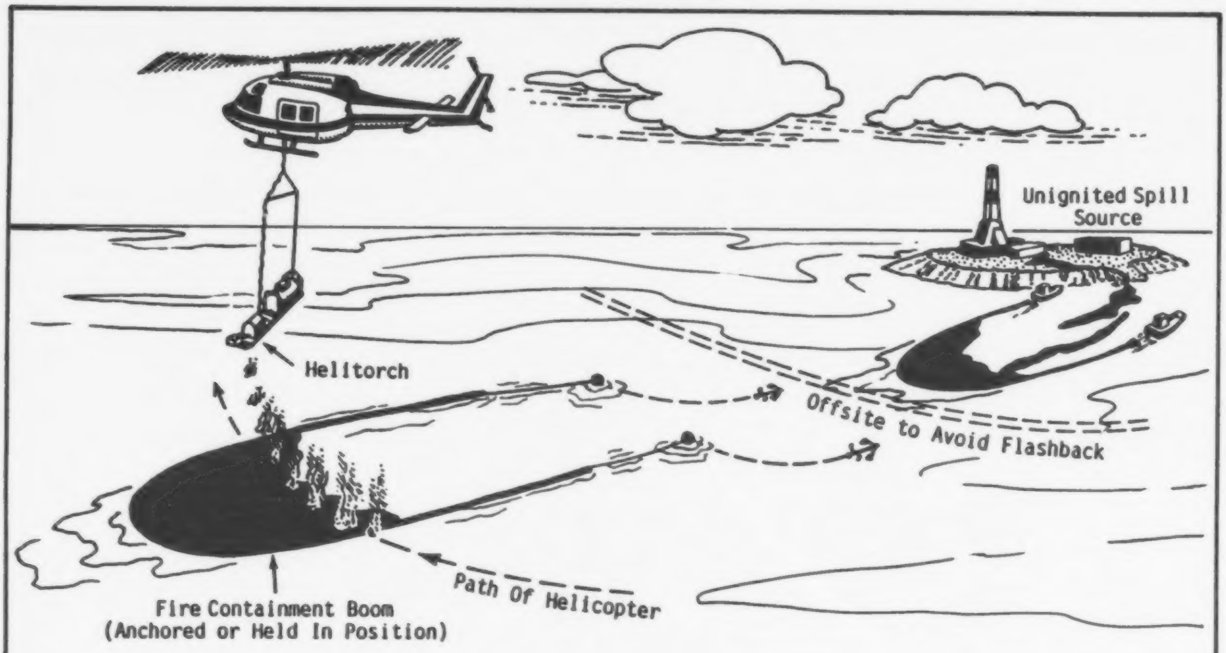
Unignited Spill
Source
Helitorch
Offsite to Avoid Flashback
Path Of Helicopter
Fire Containment Boom
(Anchored or Held In Position)

FIGURE 12 USE OF A HELITORCH IN IGNITING AND POSSIBLY RE-IGNITING OIL TRAPPED IN FIRE CONTAINMENT BOOM

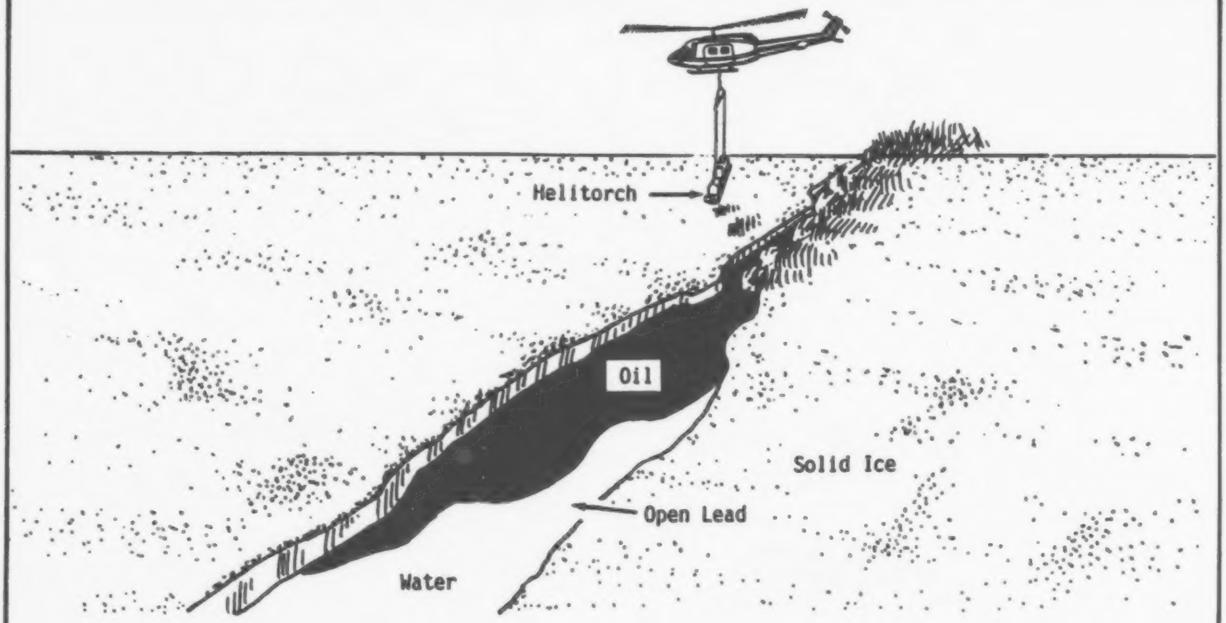
Helitorch
Oil
Solid Ice
Open Lead
Water

FIGURE 13 USE OF A HELITORCH IN IGNITING OIL TRAPPED IN AN OPEN LEAD

- Volume of fuel for helicopter and gelling operations at each staging site, etc.

These choices would depend on the actual location and extent of the oiled ice, the nature of the oil and ice, and the feasibility of staging personnel and equipment on the ice. Ideally, one would attempt to locate staging sites as close as possible to the oiled zone in order to minimize transit times following the depletion of each gelled payload. If safe and practical to do so, such locations would be positioned so that each sortie with a full Helitorch could begin or end very near each staging site.

These and other staging considerations can best be explained with the use of a hypothetical spill scenario. Assume, for example, that a response as depicted in Figure 8 is to be carried out using the assumptions provided below. (Normally, weeks to months would be available for such planning and staging preparations.)

- Length of oiled ice zone = 100 miles (161 kilometers).
- Width of oiled ice zone is approximately 50 to 60 feet (15 to 18 meters).
- A nozzle configuration comparable to Nozzle 2 in this report is used providing an effective swath of approximately 15 feet (4-1/2 meters) when flown at an altitude of 50 to 60 feet (15 to 18 meters).
- The Helitorch is flown with an estimated ground speed of 30 mph (48 kilometers/hour), thereby providing an estimated 12 ignition points per 10 feet (3 meters) of travel.

Using the above assumptions and data generated in the previous section, a single Helitorch could be flown continuously (without reloading) a distance of 1.84 miles (2.96 kilometers) in this scenario and cover about 9/10 acre (0.37 hectare) per minute. With an effective swath width of 15 feet (4-1/2 meters), it will be assumed that 4 passes will be required to cover the full area of oiled ice, which is 50 to 60 feet (15 to 18 meters) wide.

In Figure 14, such application distances per drum are illustrated along with one suggested mode of staging fuel and transiting to/from the oiled ice zone. The distance between staging sites using this method would be about 3.7 miles (5.95 kilometers). This mode would minimize overall transit time and allow the helicopter to conduct its longest transits with an empty Helitorch. Should conditions such as the wind require application in the same direction during each run, four of the eight longest transits would be conducted with a full load. This should not increase the overall time significantly.

If this staging mode was used along the entire 100 miles (161 kilometers), it would be necessary to stock fuel at 27 locations (i.e., 100 miles ÷ 3.7 miles per site). Each site would need at least 8 drums of gelled fuel, requiring approximately 216 drums to stock all 27 locations.

An estimate of the time to complete each grouping of 8 runs (or sorties) covering 3.7 miles (5.95 kilometers) of the oiled zone can be made as follows:

Application time = 3.67 min/drum x 8 passes = 29.4 minutes

Long-transit time (assuming avg. transit speed of 80 mph) = (2 mi/run x 8 runs)÷(80 mi/hr x 1 hr/60 min)

= 12 minutes

Time for turns, relocation, take-offs and landings = 12 minutes (assume equal to long-transit time)

Time for refueling = approx. 15 minutes for every hour of flight time (in this case, 1 fuel stop per staging site)

Time for reloading gelled fuel = 24 minutes (assume 3 minutes per change of drum)

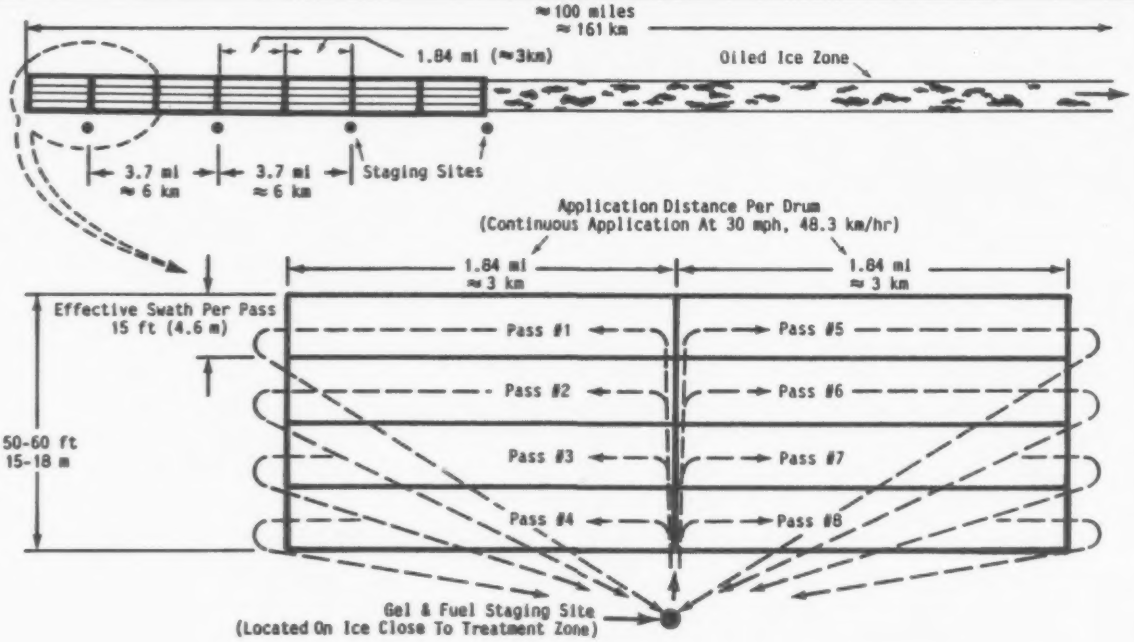
≈ 100 miles
≈ 161 km
1.84 mi (≈3km)
Oiled Ice Zone
3.7 mi ≈ 6 km
3.7 mi ≈ 6 km
Staging Sites
Application Distance Per Drum
(Continuous Application At 30 mph, 48.3 km/hr)
1.84 mi ≈ 3 km
1.84 mi ≈ 3 km
Effective Swath Per Pass
15 ft (4.6 m)
50-60 ft
15-18 m
Pass #1
Pass #5
Pass #2
Pass #6
Pass #3
Pass #7
Pass #4
Pass #8
Gel & Fuel Staging Site
(Located On Ice Close To Treatment Zone)

FIGURE 14 SAMPLE LOCATION OF STAGING SITES FOR CONTINUOUS TREATMENT OF A 100 MILE LONG OILED ICE ZONE WITH A HELITORCH

These rough estimates add up to 92.4 minutes per staging location (or per 3.7 miles along the 100-mile oiled zone). The total time to complete the entire 100 miles (161 kilometers) with a single Helitorch would therefore be about:

27 x 92.4 minutes = 2,495 minutes or nearly 42 hours.

The cost (U.S. dollars) for the gelled gasoline (assuming $1/gal gasoline, $4/lb of gel mix and 5.5 lb mix/drum) would be about $77/drum x 216 drums, or $16,632. Added to this cost would be all costs for the helicopter, for ground personnel, and for equipment.

If each staging site in the previous scenario is located at 7.4-mile (11.9-kilometer) intervals, the number of staging sites can be reduced from 27 to 13 or 14 over the entire 100-mile (161-kilometer) drop-zone. The same amount of gelling agent would be required (216 drums); however, each site would need to have 16 drums of gelled fuel and enough helicopter fuel for potentially two refuelings per site. With this mode of operation, the additional transit time (and corresponding turn and relocation time) could add as much as 7 hours, bringing the total application time to about 49 hours.

An operation of this nature would very likely be accomplished during the spring when there are nearly 24 hours of usable light each day. If the size and location of the oiled ice zone are monitored before the spring thaw, an operation could be planned with the optimum number and location of staging areas for that response. Additional helicopters and Helitorches could be used along with batch mixing equipment to reduce the total response time to less than a day.

REFERENCES

S.L. Ross Environmental Research Ltd., 1981. The Use of Aerially-Deployed Igniters for an Oil Blowout in the Southern Beaufort Sea. Prepared for Dome Petroleum Ltd.

S.L. Ross Environmental Research Ltd., 1984. Igniter Requirements for a Major Oil Spill from a Vessel in the Canadian Arctic. Prepared under contract to Research and Development Division, Environmental Emergency Branch, Environmental Impact Control Directorate, Environmental Protection Service, Environment Canada. Ottawa, Ontario.

Spiltec, 1986. Survey and Analysis of Air-Deployable Igniters. Prepared under contract to Shell Western E&P Inc. for Alaska Clean Seas. Anchorage, AK.

Spiltec, 1987. Refinement of Aerial Ignition Systems. Prepared under contract to Shell Western E&P Inc. for Alaska Clean Seas. Anchorage, AK.

EVALUATION OF SURFACE DRIFTERS FOR SATELLITE TRACKING OF OIL ON THE SEA

M. Reed, C. Turner and M. Spaulding
Applied Science Associates, Inc.
70 Dean Knauss Drive
Narragansett, Rhode Island 02882
and
Don Dorson
Bathy Systems
Gardiner Road
West Kingston, Rhode Island 02892

ABSTRACT

The purpose of this study is to evaluate satellite-tracked surface drifters for use in simulating the movement of spilled crude oil and assessing the skill of oil spill trajectory models. The results of this study may form the basis for future Minerals Management Service (MMS) initiated field testing and any necessary modifications of the recommended drifter(s). MMS may then procure drifters to be used in deployments in Outer Continental Shelf (OCS) lease areas where complex, near-shore circulation features exist, or where there exists a significant probability of oil contacting important coastal resources.

There are three key questions to be addressed in this study:

1. What do we know about the drift velocity of crude oil spilled at sea, as a function of oil type and environmental conditions, and how do various weathering processes affect this velocity?
2. What characteristics should a surface drifting buoy have in order to reproduce the drift velocity of spilled crude oil?
3. Which available drifter(s), capable of carrying an ARGOS certified transmitter, will result in the greatest return of good data for the least overall cost?

To answer the first question, automated searches were applied to several computer data bases. Requests for information were also sent to over 70 members of the international oil spill research community. We then synthesized the resulting information with a focus on advances in our understanding of surface drift of oil slicks. In response to the second question, we created a detailed list of specifications for an ideal oil spill tracking drifter. We then identified candidate drifters and subjected them to a set of selection criteria, to arrive at a final recommendation.

INTRODUCTION

One goal of the U.S. Department of Interior Minerals Management Service (MMS) Outer Continental Shelf (OCS) Environmental Studies Program has been to develop a capability for estimating hypothetical oil spill trajectories. The MMS uses an Oil Spill Risk Analysis (OSRA) model (Smith et al, 1980) to estimate the probability of spill occurrence, and to model potential spill movement. Critical inputs to the oil spill trajectory component of the OSRA model are wind and surface current representations which incorporate the influences of major surface and subsurface circulation features.

The purpose of this study is to evaluate satellite-tracked surface drifters for use in simulating the movement of spilled crude oil and assessing the skill of the OSRA model. The results of this study may form the basis for future MMS-initiated field testing and any necessary modifications of the recommended drifter(s). MMS may then procure drifters to be used in deployments in OCS lease areas where complex, near-shore circulation features exist, or where there exists a significant probability of oil contacting important coastal resources.

There are three key questions to be addressed by this study:

1. What do we know about the drift velocity of crude oil spilled at sea, as a function of oil type and environmental conditions, and how do various weathering processes affect this velocity?

2. What characteristics should a surface drifting buoy have in order to reproduce the drift velocity of spilled crude oil?

3. Which available drifter(s), capable of carrying an ARGOS certified transmitter, will result in the greatest return of good data for the least overall cost?

To answer the first question, automated searches were applied to several on-line data bases. Requests for information were also sent to over 70 members of the international oil spill research community. We then synthesized the resulting information with a focus on advances in our understanding of the surface drift of oil slicks. In response to question (2), we created a detailed list of specifications for an ideal oil spill tracking drifter. We then identified candidate drifters, and subjected them to a set of selection criteria to come up with a final recommendation. The present paper represents a summary of the work accomplished to date. A final report on this study will be completed in the summer of 1987 (Reed et al, 1987).

FACTORS INFLUENCING THE MOVEMENT OF SPILLED OIL ON THE SEA SURFACE: LITERATURE REVIEW AND SYNTHESIS

The purpose of this section is to summarize recent research relevant to the understanding of surface slick drift. Because quite thorough reviews exist for the period up to 1980 (Stolzenback et al, 1977; Huang and Monastero, 1982; Huang, 1983; Davidson and Lawrence, 1982; Murray, 1982), we focus here primarily on work reported during the principal period 1980-1986. The key results of a recent review by Spaulding (1986) are incorporated here.

We have relied on four major sources of information for identification of published and unpublished literature. First, we searched the computerized Applied Science Associates, Inc. (ASA) library, containing several thousand volumes relevant to oil spill research. The second was the DIALOG Information Retrieval Service, which provides access to over 250 data bases containing in excess of 119 million records. A review of the DIALOG data base descriptions indicated that the Oceanic Abstracts, Pollution Abstracts, and Aquatic Sciences Abstracts represented the most promising sources of relevant citations.

These three data bases were therefore searched under a variety of logical constructs to tailor the retrieved list as closely as possible to the subject of interest. The third was a published search of the National Technical Information Service data base (NTIS, 1985).

Our fourth source of information was by direct mail contact with over 70 oil spill researchers throughout the world. The purpose of this portion of the effort was to provide a check on the thoroughness of our computer searches, and to provide access to unpublished research results as well as work in progress. The response rate was approximately 30%, but we received information from all researchers whom we know to be most active.

The movement of spilled oil on the sea surface is a function of wind, wave, and current forcing. Recent reviews of slick drift modeling procedures cited above, model hindcasting tests (URI and ASA et al, 1982; Anderson, 1983 a,b; Dippner, 1983), and observations of test spills (Audunson et al, 1984; Johansen, 1984) confirm that the functional relationship is complex. The reasons for this complexity are several. In the first place, winds, waves, and currents are not independent environmental parameters, and interdependences among them remain incompletely understood. Secondly, the oil itself changes character as a function of time, so that aero- and hydrodynamic effects are also variable. As the oil weathers and changes density, for example, the effect of the wind can be expected to change relative to the ocean current and wave forcing.

Figure 1 summarizes the approximate state-of-the-art in the numerical representation of the various processes acting on spilled oil pre 1980, at present and projections for the near future. Advection was typically taken as 2% to 4% of the wind speed, with some veering angle due to the Coriolis effect. Pre 1980 those few models which included evaporation capabilities linked spreading and evaporation through surface area. Dispersion, spreading, and evaporation were all interconnected by conservation of mass. Although research had been performed on other processes, these were not included in oil spill behavior and fate models. Advection was completely decoupled from any of the other processes represented.

The conception of oil slicks as flat, round, elliptical, or rectangular (e.g., Amstutz and Samuels, 1986) pancakes, to which one could apply stresses to the air-oil and oil-water interfaces to estimate the resultant motion, continues for the moment to dominate oil spill trajectory modeling endeavors. This is not to say that the research community has been unaware of the three dimensional physical and weathering dynamics of oil in the marine environment, but that virtually no effort has been made until quite recently to couple vertical motion or weathering phenomena with surface slick transport and distribution.

Presented below are brief summaries of the more important advances in oil spill research over the last six years. The primary focus of the discussion is on how our understanding of spill transport at the sea surface has improved.

Advection and Spreading

Perhaps the most significant advance in our understanding of surface oil transport and distribution is reflected in the work of Elliott et al (1986), Elliott (1986), and Johansen (1984, 1985, 1987). These authors demonstrate through theoretical and field work that temporary entrainment of oil from a surface slick into the water column and a velocity shear at

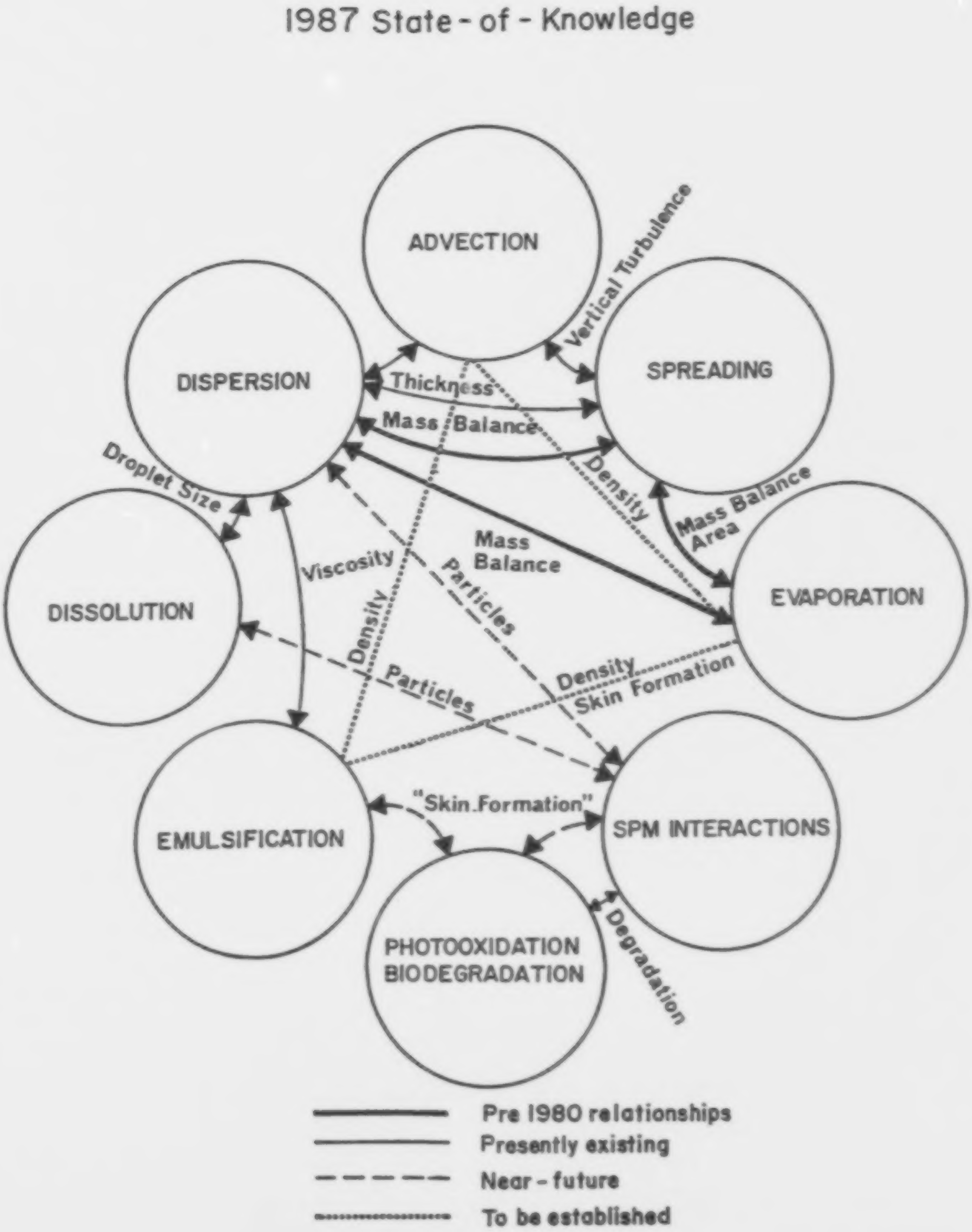
1987 State - of - Knowledge
ADVECTION
DISPERSION
SPREADING
DISSOLUTION
EVAPORATION
EMULSIFICATION
SPM INTERACTIONS
PHOTOOXIDATION
BIODEGRADATION
Vertical Turbulence
Thickness
Mass Balance
Density
Droplet Size
Mass Balance
Area
Viscosity
Mass
Balance
Particles
Density
Particles
Density
Skin Formation
"Skin Formation"
Degradation
Pre 1980 relationships
Presently existing
Near - future
To be established

FIGURE 1. STATE-OF-KNOWLEDGE IN 1987 (AND THE NEAR FUTURE) OF SURFACE SLICK ADVECTION, AND LINKAGE TO OTHER PROCESSES.

the water surface, combine to produce realistic distributions of oil at the sea surface. The basic concept is that wind driven currents and surface waves together produce a horizontal current field with relatively strong vertical shears. Oil which is entrained into the water column will be transported horizontally at lower speeds than oil which remains at the sea surface. Representation of an oil slick by a large number of discrete particles allows a model to produce surface oil patterns which correctly reflect the occurrence of thicker oil towards the leading (downwind) edge of slick, and are aligned in the direction of the wind. This modeling approach will likely replace earlier primitive algorithms, as typified by the Fay and Hoult (1972) or Mackay "thick-thin" (Mackay and Patterson, 1980) approaches. For example, it is being incorporated into a coastal zone oil spill model presently being developed for MMS by ASA, E-TECH, and Coastal Science and Engineering (Reed et al, 1986).

Dispersion, Dissolution, and Submergence

A number of research groups have been studying the processes by which surface oil enters the underlying water column. Dispersion, or the entrainment of oil droplets or particles into the water column, has received the most attention. Dissolution, either directly from the surface or from entrained droplets, accounts for only a small portion of the total mass of a spill, but is important from the standpoint of biological effects estimation. Gross submergence of oil is most commonly observed in tropical or sub-tropical environments, but may be important for small "pans" of oil in more temperate environments.

Scientists at the University of Rhode Island and Applied Science Associates, Inc. (URI and ASA, 1982) have derived an empirical relationship which gives dissolution rates for various hydrocarbon constituents from oil particles. The procedure also explicitly includes the effects of waves on the oil dissolution rates.

This approach is particularly interesting because of the natural interface (through particle diameter) between it and the Elliott-Johanson particle-based modeling approach. These methodologies are being coupled in the coastal zone oil spill model now being developed for MMS (Reed et al, 1986).

Two entrainment rate algorithms are in common use. The first (Mackay et al, 1982) is discussed in Huang and Monastero (1982). The second, which is also based on the square of the wind speed, employs a simple exponential decay term to reflect the reduction in entrainment as a function of time due to mousse formation (Spaulding et al, 1982). The Mackay et al (1982) and Spaulding et al (1982) formulations behave similarly for the first few days. Thereafter, the former continues to entrain oil until the surface slick disappears, whereas the latter virtually ceases entrainment after about 5 days.

Mackay et al (1986) report some results from two research projects concerning the dispersion and submergence of oil spills on ocean surfaces. The authors study the process of chemical dispersion of oil slicks, but no quantitative algorithms are reported. They also report on the factors which result in an oil slick breaking up into discrete droplets and "pans", and how these formations tend to become submerged and therefore invisible to remote sensing systems. Although the studies were performed with the implications for remote sensing of oil spills as an impetus, the implications for advection are also important. For that fraction of the time that a "pan" is under the surface, no direct wind shear stress will be applied, and the pan will lag behind the leading edge of the slick.

Emulsification

Mackay et al (1982) calibrated a model developed earlier (Mackay et al, 1980) for No. 2 fuel oil, home heating oil, and Prudhoe Bay crude. Most of the algorithms used have been reviewed by Huang and Monastero (1982). The dispersion emulsion formation equations, however, deserve some mention here, since they provide a linkage among spreading dispersion and emulsion formation through the viscosity and the slick thickness. The mousse formation and viscosity ratio algorithms appear to behave reasonably well (Mackay et al, 1982). The weak link appears to be the dispersion formulation, which tends to drive the entire surface slick into the water in a few days at wind speeds much in excess of 5 m/sec.

Evaporation

Payne et al (1984) developed an open ocean weathering model based primarily on the work of Mackay et al (1980, 1982). The most significant contribution arising from this work is the representation of crude oil and petroleum products by a series of boiling point fractions. The use of multiple fractions, each with its own chemical characteristics, is not new in oil spill modeling. Cornillon et al (1979) used fractionation based on carbon number to resolve the evaporation process. The boiling point fraction data, however, is much easier to obtain for a wide variety of crude oils and petroleum products. Reijnhart and Rose (1982) also use a boiling point representation very similar to that of Payne et al (1984), and with equally good results. The main drawback of this approach is the difficulty in tracking specific oil components (e.g., benzene and toluene, for toxic effects estimation). This difficulty arises from the fact that such components are generally arrayed across several "cuts" of the parent oil.

Suspended Particulate Matter Interactions

Sedimentation of oil can result from three processes: increased density of the oil as weathering proceeds, incorporation into fecal pellets via zooplankton ingestion or adhesion to or flocculation of the oil with the heavier suspended particulate matter (SPM). Sinking of oil through weathering alone is not expected in colder northern waters, although this has been observed in Gulf of Mexico and Persian Gulf blowouts. Numerous studies have been performed on the adhesion of oil to SPM, but it remains difficult to adequately express the detailed dynamics of the process in a qualitative manner. Variability in bulk oil characteristics is one confounding factor, but the key controlling variable appears to be percent clay in the SPM population (Button, 1969; Meyers and Quinn, 1973; Payne et al, 1981, 1984; Meyers and Oas, 1978; Bassin and Ichiye, 1977). Work in progress by Payne et al (1986) should contribute further to our understanding of oil-SPM interaction processes.

Oil-Ice Interaction

Summaries of the fate and behavior of oil in the Arctic environment are included in Walter (1975), Bobra and Fingas (1986), Payne and McNabb (1985), and Reed et al (1986a,b). The interested reader is referred to one of these publications for an overview.

Extension of spill models to handle oil-ice interactions has been extremely limited. ASA (1984) has formulated a menu-driven model on a personal computer based on the existing state-of-knowledge for Arctic waters. The model addresses oil-ice interactions for spills under ice and in ice infested waters, but excludes freezing and thawing situations.

Data on ice and on temperature conditions is derived from available atlases (LaBelle et al, 1983; Brower et al, 1977) or model predictions.

When oil is located under ice, we have a reasonable set of algorithms to describe its motion (advection), and based on the work of Sayed and Abdelmour (1982), Uzuner et al (1979), and Cox and Schultz (1981a,b), and trapping in under ice roughness elements (Kovacs, 1977, 1979). If oil is incorporated in a broken ice field, we know from Thomas (1983), Allen (1983), Coon and Pritchard (1979), and Reimer (1981) that the oil drifts with the ice.

The spreading and evaporative and dispersive losses of oil in broken ice fields is poorly known at best. The consensus is that medium to heavy oils exhibit a hearding effect and that the evaporative and dispersive losses decrease due to sheltering from the wind by the ice field (Cox et al, 1981a,b,; Free et al, 1981; Reimer, 1981). The behavior of oil under freezing and thawing conditions is just beginning to be studied with a view toward modeling. The recent work of Wilson and Mackay (1986) and on-going studies (J. Payne, personal communication) should add to our understanding of these processes.

Summary

The linkages which have been quantitatively made among the above processes since 1980 are shown in Figure 1 by heavy solid lines. The light solid lines correspond to linkages in place before 1980. Heavy broken lines indicate linkages which are probably imminent as a result of present research. Light broken lines indicate relationships which are probable in the next few years. Comparison between the interconnections in time suggests that considerable progress has been made in the past seven years with increasing understanding of the interconnections between the various processes.

The major implications of this new knowledge relevant to the use of surface drifters for the simulation of oil slick trajectories are:

1. The desired drift speed remains, as before, on the order of 3.5% of the wind speed; with a drift angle typically 10-30° clockwise (northern hemisphere) from the wind directions.

2. A buoy drifting at 3.5% of the wind speed will best track the leading edge of a slick; the center of mass of the slick will be considerably behind this point. A significant wind shift during a trajectory could reverse this situation (i.e., the buoy would suddenly be at a point in the middle of or behind the main body of the slick).

3. A buoy which is ideal for tracking oil in open water conditions may be inadequate for tracking oil in broken ice fields, or in ice-covered waters since ice transport processes may dominate the spill movement.

SPECIFICATIONS FOR AN IDEAL DRIFTER FOR OIL SPILL MOVEMENT SIMULATION

The selection of one or more buoys for simulating or tracking oil spill trajectories requires the accommodation of several criteria. These considerations are dictated by the proposed mission of the buoy to simulate the motion dynamics of an oil spill under the widest possible set of weather and sea conditions, the ease with which the buoy may be used to accomplish this mission, and its durability.

This section focuses on specifying the characteristics of the ideal drifter. The discussion classifies these criteria into two general areas: engineering and dynamic.

Engineering Criteria

The engineering design criteria are dictated by mission-related conditions and by the requirements of the ARGOS system (specified by the Sponsor). The mission-related criteria cover:

1. ease of deployment and recovery
2. ease of use and limited requirements for highly trained personnel
3. durability and reliability of the drifter
4. ease of maintenance
5. low production costs

The first two criteria are related to the suitability of the drifter for use at sea. It is expected that each deployment will consist of the release of one to three dozen drifters from a ship, helicopter, or fixed wing aircraft. The weight and size of the drifter should also be suited for handling by one person at sea in order to reduce manpower requirements.

The drifter's shape is also an important factor in deployment or recovery. The absence of a drogue, antenna or a skirt makes recovery easier and reduces the probability that the buoy will be damaged. A simple buoy shape is also easier to store before and after the deployment. These considerations indicate that the buoy should be as small, light and as simple as possible.

The drifters selected by this study will be exposed to a variety of harsh environments during their use. It is, therefore, important that the drifter be as reliable and durable as possible. The outer body of the drifter must be as resistant as possible to rough handling, beaching, marine organism attack, and collisions with ships. Materials used in the hull, fasteners and penetrations must be compatible for use in the sea. The drifter should also be resistant to biofouling and ice build-up. The use of a skirt or drogue is probably disadvantageous from the standpoint of reliability. For example, the fatigue failure of drogue tethers is a common problem for drogued buoys.

Minimal drifter size and weight, and simplicity of hull design are also desirable from the point of view of reliability, durability, and cost. This may be illustrated using the sphere as an example. In order to double the volume of a thin-walled sphere, its radius must be increased by 26%. In order for the strength of the sphere to remain the same, its wall thickness must be increased by 60 percent, since collapse pressure is proportional to the ratio of thickness to radius squared. This means that in order to double the volume of the sphere while maintaining its strength, the weight of the hull must be increased by a factor of 2.5.

The lower limits of size and weight must be considered in light of the requirements of the ARGOS transmitter, power supply, electronics and the reserve buoyancy desired for the drifter. Assuming a weight of 10 kg for the buoy hull and ballast, and a reserve buoyancy of 10 kg to reduce antenna submersion, the necessary volume of the drifter should be about 28 liters. Assuming that half of the drifter's volume is submerged, its total displacement would then be about 15 kg.

The size and weight of the drifter would be increased by the addition of a supplementary VHF tracking system. The accuracy of the ARGOS system is typically on the order of a few kilometers and position updates are separated by several hours. The addition of a VHF transmitter would permit the buoy to be located more easily during the recovery phase of an operation and would also allow some redundancy for tracking and recovery. An additional option which would increase the weight and size of the drifter to a lesser degree would be the addition of a skirt or mat to aid in coupling the buoy to the surface layer or to an oil slick.

The reliability and durability of the buoy's electronics package is only partially controlled by ARGOS certification standards. Testing by Service ARGOS is designed to examine the following characteristics of the PTT (Service ARGOS):

1. Interference with other PTT's
2. Compatibility with satellite-borne equipment
3. Compatibility with the ARGOS data processing center
4. Accuracy of fixes provided by the PTT.

The ARGOS certification, therefore, does not examine a number of variables which are vital to the performance of the drifter. These factors include the adequacy of the power supply for powering the electronics package during a typical 60 day deployment. Electronic components must be securely mounted onto printed circuit boards. Circuit boards, wiring runs, power supplies and the antenna must also be securely mounted to the buoy's hull to reduce the chances of vibration-induced failure.

The ease with which the buoy may be operated and maintained is also important. Preparation for deployment should be simple and require no special training. Activation and deactivation of the transmitter at sea should only involve activating a switch. Battery replacement and servicing procedures should also be simple. Documentation provided by the manufacturer on maintenance and operation of the drifter must be complete and concise.

The final engineering criterion requires little explanation. The cost of each drifter should be as low as possible.

Dynamical Criteria

The dynamical drifter selection criteria pertain to the performance characteristics of a drifter in a seaway which are controlled by the buoy's shape, size and weight. The most important dynamical characteristic which the buoy should have is the ability to accurately track an oil spill and serve as a suitable platform for the ARGOS transmitter under a variety of wind and sea conditions.

It is easy to see that in order to effectively simulate an oil spill, the drifter should resemble a thin sheet which would float on the ocean surface. The requirements of the ARGOS PTT, its power supply and antenna make this shape impractical, however, so a compromise should must be arrived at through an examination of the desirable buoy characteristics dictated by the requirement for matching oil slick drift and carrying the ARGOS system. The following discussion will lay a foundation for this compromise by outlining the characteristics which are needed to satisfy each requirement.

It is critical that the drifter selected be able to simulate the drift of an oil slick. Present knowledge about oil slick motion was summarized earlier and indicates that the ideal drifter should move down wind at 3.5% of the surface wind speed. To reproduce oil slick motions, the buoy must be configured so that, as closely as possible, it is subjected to the same forces as a slick. Disparate forcing arises because vertical shear exists in winds and near-surface currents. Penetration of the buoy hull and appendages into the air and water should, therefore, be minimized. The use of a drogue is not desirable, because the buoy should be coupled with the layer of water at the air/water interface. For the same reason, the drifter should be a good surface follower. Excessive heave motions cause the drifter to be exposed to the effects of shear. Heave and roll motions may also produce changes in the shape of the wetted volume, producing a time-varying coefficient of drag which produces excessive down-wind motion.

This means that the buoy must be able to follow the free surface. Heave motions should be small to minimize submersion of the antenna. To prevent large heave displacements from occurring near the natural heave frequency the buoy should have a damping mechanism. Changes in buoyant restoring force about the still waterline should be large. The natural heave frequency of the buoy should also be high so that the buoy will be able to follow the free surface in wind generated waves.

Roll motions of the buoy should be minimal in order to prevent immersion of the antenna. The buoy should have adequate static stability to enable it to right itself if overturned by a wave.

IDENTIFICATION OF CANDIDATE DRIFTERS

The process of selecting the best drifter or group of drifters for oil slick tracking began with the identification of all existing drifters and their manufacturers. This search was initiated by contacting organizations which are or had been actively involved with ARGOS-certified buoys. The MMS specified that the drifter buoys must be ARGOS certified or at the minimum have the capability to be certified.

This effort produced the names of the better-known buoy manufacturers. The names of additional manufacturers were obtained by contacting the principal investigators of recently published drifter studies. The editors of the _Oil Spill Intelligence Report_ (OSIR), assisted us by publishing an article outlining the purpose of the project and soliciting information from ARGOS-certified drifter manufacturers.

The names of the manufacturers along with their candidate buoy models are listed in Table 1. Some of the drifters in the table are not ARGOS equipped, but were included because they had been used in the past to track spills in the ocean and could potentially be equipped with an ARGOS PTT.

FIELD TESTS OF BUOYS IN OIL

Lacking strong theoretical understanding of free buoy drift dynamics, except for a few simple cases (Chhabra, 1976; Baumgartner and Nath, 1984), test results in which buoy trajectories were compared with those of real slicks was considered a valuable indicator of the relative performance of different classes of buoy shapes. A search uncovered several experiments where drifters were deployed in spills. Several of the experiments are summarized below focussing on the drifter's ability to track oil spills.

Halifax Harbor and Bay of Fundy, 1977

This study evaluated two drifters, an Orion Electronics, Ltd. device similar to its current model OST 2100, and 1.3 x 1.3 m sheets of painted plywood. Two weights of the Orion device were used. The heavier buoy was used with an aged, emulsified Arabian Crude. The lighter buoy was used with a light Arabian Crude. The study found that the buoy tracks were identical to those of the slicks during tests lasting a few hours. The plywood sheets moved significantly slower than the slicks, however, with deviations of the plywood sheets from the centroid of the slick as great as 0.11/hr. (expressed

TABLE 1. LIST OF DRIFTERS EVALUATED.

BERGEN OCEAN DATA/SEATEX

- SURFACE DRIFTING BUOY

CEIS ESPACE

- ECOMAR
- ECOCAP

COASTAL CLIMATE

- SPHERICAL DRIFTER

DOBROCKY SEA TECH

- ELLIPSOID (1.3) (LORAN-C)
- LIGHT BULB (2') (LORAN-C)

DRAPER LABS

- LCD

FERRANTI O.R.E.

- ARGOSPHERE
- TORPEDO DRIFTER

HERMES

- CONICAL DRIFTING BUOY

HORIZON

- FAR HORIZON DRIFTER 'A' AND 'B'

METOCEAN

- CMOD
- STANDARD DRIFTER

NOVATECH

- RF700A

ORION ELECTRONICS

- OST 2100 (VHF)

POLAR RESEARCH LABORATORY (PRL)

- MINI TOD
- TOD
- TMD

SEA DATA

- ARGONAUT

SEIMAC

- FLOODED CYLINDER

SCRIPPS

- LOW WETTED SURFACE AREA

SIPRO A/S

- ICE DRIFTER

TECHNOCEAN

- FLOODED SPHERE

as the ratio of displacement of the sheet away from the centroid to the total displacement of the slick in one hour). The study concluded that the Orion device was excellent for the purpose of simulating the movement of oil slicks, whereas the plywood sheets were unsuitable (Fingas, 1977).

Tromsoflaket, 1978

Four Bergen Ocean Data drifters equipped with ARGOS and DECCA positioning systems were deployed during the Tromsoflaket experiment (Andunsen et al, 1979). One was released with the oil, the other three slightly later along a transect perpendicular to the coastline to assist in determination of current patterns in the area. Only the track of the drifter released with the oil is discussed here.

The buoy tracked the slick fairly well for a period of 3.5 days. During this time, the greatest separation between the slick centroid and the buoy was 8 km. At this point, the oil slick was sufficiently dispersed so that it could no longer be tracked and the test was stopped.

It is worth noting that the determination of the "slick centroid" is a subjective process which is affected by the observers' ability to accurately delineate slick outlines, as well as the ability to delineate the centroids of discontinuous, irregular slicks. In addition, as discussed elsewhere, we expect a drifter to track most successfully the leading edge of a slick, rather than the centroid.

North Sea Tests, Warren Springs Institute, 1977-1979

Tests were performed in the North Sea to evaluate the performance of the Orion OST 2100 drifter and other remote sensing techniques for tracking oil slicks by researchers at Warren Springs Institute.

A specific goal was to find the method which would permit a spill to be located on mornings subsequent to the spill or following a storm. The methodology and results were never documented. The information presented here was obtained from interviews with one of the researchers (Hurford, personal communication 1987).

The tests were conducted during summer months in an area of the North Sea 50 km east of Lowestost (52° 13'N, 2° 25'E). Winds were typically 5-10 m/s. Ten tons of light North Sea crude were released into the ocean, and the buoy was placed at the centroid of the slick about two hours later. The spill and buoy were monitored for about 6 hours. At the end of this time, the buoy was generally observed to move out of the slick. Upon returning to the area the next day, researchers found the buoy to be 3-5 km distant from the slick. The researchers concluded that the Orion OST 2100 buoy was not effective as a means of pinpointing oil slicks.

IXTOC, 1979

Polar Research Laboratory (PRL) TOD drifters were used by the U.S. Coast Guard to track the IXTOC oil spill in the Gulf of Mexico. One undrogued drifter was deployed near the slick for the purpose of tracking the spill. Five other drifters drogued at 15 m were deployed one to five weeks later to provide information on circulation patterns in the general vicinity, (Mountain et al, 1980).

The undrogued buoy was deployed in the northern edge of a large mousse concentration on 27 July 1979. After a period of two weeks, the buoy was still within or closely associated with the northernmost mousse concentration, although it moved significantly more slowly than the oil. Mountain et al (1980) reports that the difference between oil slick and buoy speed was about 1.5% of the wind speed. Since the mean wind was southeasterly with a speed of

5 m/s, the oil moved approximately 90 km further than the buoy during this period. The principal author of the study indicated that the size of the spill made it easy for the buoy to perform well, since "the oil was everywhere" (Mountain, personal communication 1987).

Newfoundland, 1981

This evaluation was carried out in conjunction with a series of trials conducted by the Canadian Offshore Oil Spill Research Association (COOSRA) to evaluate the effects of dispersants on oil spills (Lea, 1982; Fingas and Lea, 1981). A pair of controlled oil spills were conducted on each of two days at a point near the mouth of Conception Bay, Newfoundland. Each spill consisted of 1900 liters of Lago-medio crude oil. One of the spills released each day was treated with a dispersant, COREXIT 9527. The second was left untreated for comparison.

Four types of drifters were used for the study: the Orion OST 2100, the Orion 4800, a cylindical drifter which is no longer on the market, the Novatech RF 700B, and 1.8 x 3.7 m sail drogues. The drifters were traced visually at one to three hour intervals. Their positions were transferred to aerial photographs of the spill to provide a picture of the drifters movement relative to the oil.

Results show that the Novatech RF 700B performed quite well throughout the test. The Orion OST 2100 moved downwind more quickly than the slick, while the Orion 4800 and sail drogues moved more slowly than the oil. It was concluded that the Novatech RF 700B and Orion OST 2100 were suitable for use in tracking the slick, while the Orion 4800 apparently was not.

Lake Michigan, 1982

The Great Lakes Environmental Research Laboratory, Gros Ille, Michigan conducted experiments as part of a study to evaluate means of tracking chemical spills in the Great Lakes. The main focus of the study was tracking chemicals which would mix with water, such as sulfuric acid and ammonia. For this purpose, four Polar Research Laboratory Mini-TOD drifters equipped with cruciform and windshade drogues centered at a depth of 4 m were used to track fluorescent dye patches. The tests found that the drifters worked quite well. During a 3 hour test, Pickett et al (1983) report that the drifter moved 10 m downwind relative to the dye patch, while both the drifter and dye moved a net distance of 1.2 km during that period. Wind speeds during this period were not documented. The authors concluded that the drifter was well suited for this use.

Pickett et al (1983) also briefly documents the use of an undrogued Mini-TOD for tracking an intentional spill of cooking oil during a 3 hour test. The report states that the drifter "stayed near the center of an oil slick moving at 0.5 m/s during a 3 hour test".

Haltenbanken, 1982

The 1982 experimental oil spill on Haltenbanken (Audunsen et al, 1984) provides the most comprehensive picture of buoy performance of all tests which were evaluated. Data collected in the spill was used to evaluate existing methods of calculating the drift and spread of oil and to provide insight for their improvement.

The spill consisted of 100 tons of Statfjord Crude released from a point 150 km off the coast of Norway (65° 02'N, 7° 33'E) on 25 July 1982. The experiment continued for 7 days. Environmental conditions were mild during this period: wind speeds were less than 12 m/s, and significant wave heights varied from 1 to 2 m.

Two Bergen Ocean Data drifters were launched at the initiation of the spill. Both buoys were ARGOS equipped. One of the drifters was additionally equipped with a DECCA positioning system.

The DECCA-equipped drifter was found to perform significantly better than the drifter equipped only with ARGOS. The separation between the DECCA drifter and the front edge of the slick was only 11 km after 1 week. This separation represents only 12% of the slick's net movement over the same period (Figure 2).

The performance of the drifter carrying only the ARGOS transmitter was significantly poorer. Unfortunately, a direct comparison of slick and ARGOS trajectories is not contained in the final report, however, it does present a comparison of the trajectories of the two drifters, and shows that the ARGOS drifter lags the DECCA drifter throughout the experiment and slows down considerably during the last two days. At the end of the 7 day period, the separation between the ARGOS drifter and the leading edge of the spill appears to be about 28-30 km. The poorer performance of this drifter was attributed to the lower windage of the ARGOS drifter. The drifter containing only the ARGOS has one antenna mast, while the drifters carrying both ARGOS and DECCA have two masts.

Observations of the oil slick movement during the experiment revealed that the slick moved at 3.5% of local wind speed and approximately 12 degrees to the right of the downwind direction. Similarly, the ARGOS and DECCA/ARGOS drifters moved at 2.5% and 2.8% of the wind speed. the report concludes that the drifter provided an effective means of simulating the motion of the spill. The drifters were found to be especially useful for determining the position of the spill following periods of fog or in the morning.

PRELIMINARY DRIFTER SELECTION

Table 2 provides a list of all buoys, by manufacturer and model that were potentially applicable for oil spill tracking. Drifters that were not ARGOS compatible have been eliminated. Also included in the table is summary information on the buoy's draft, freeboard, reserve buoyancy, aspect ratio, weight, length, cost, and references to any field tests performed.

An objective scoring scheme was devised to evaluate all drifters. For each parameter noted in Table 2, a score was given ranging from 0 to 10. The smaller the parameter the higher the score (except for reserve buoyancy). For instance a drifter with a weight of 10 kg or less scores a 10 while a drifter with a weight of 50 kg or more scores a 0. The scores for each parameter were summed to obtain a total score for the drifter. In addition, results of field performance tests were also used in the evaluation. The primary basis of this evaluation is hence seen to be on dynamic considerations (shape, weight, reserve buoyancy) and some simple measures of easy of transport, deployment and retrievability (i.e. size, weight, aspect ratio).

Based on this review six drifters were selected for more detailed evaluation. They were:

BERGEN OCEAN DATA
COASTAL CLIMATE
DRAPER: LCD
FERRANTI: ARGOSPHERE
PRL: MINI TOD
TRITON: MINI-D

The majority of the other drifters were eliminated on the basis of weight or geometric (width/length) constraints. These constraints were primarily

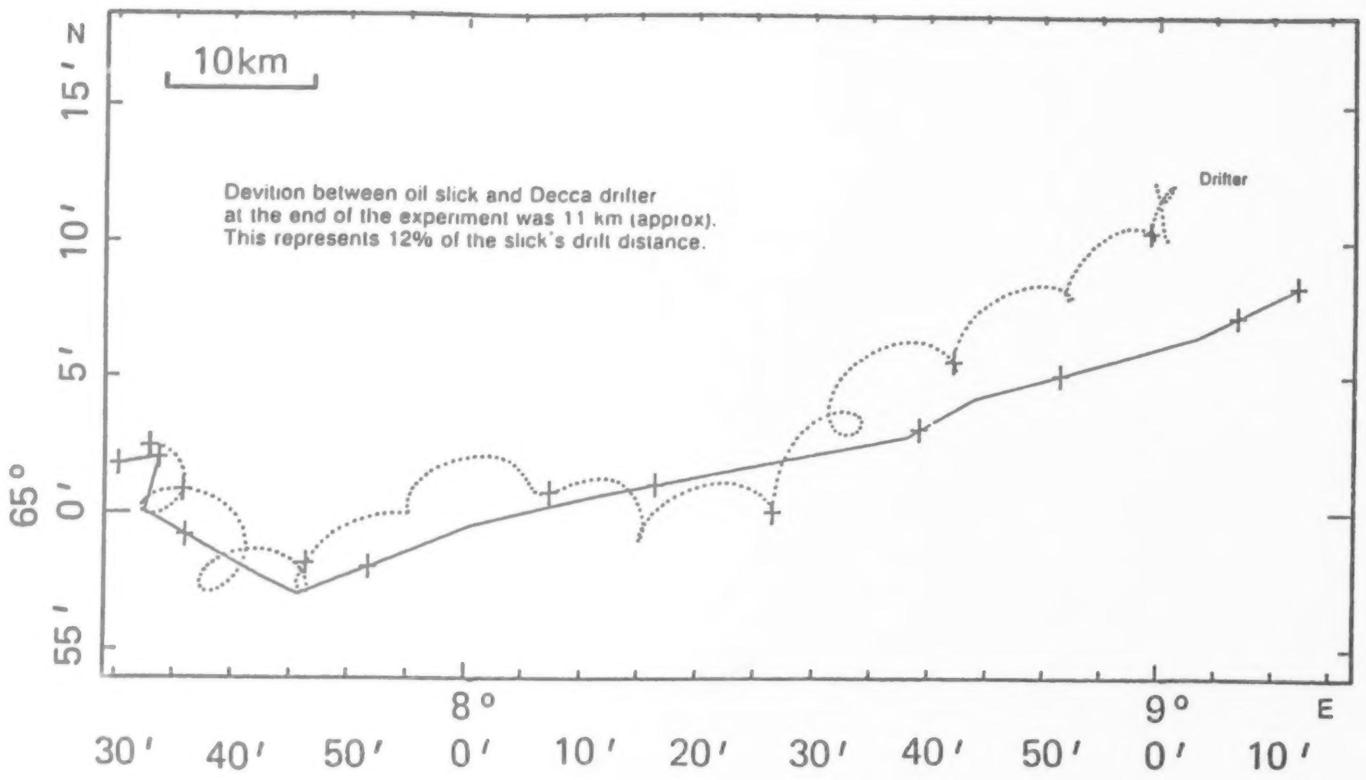

FIGURE 2. THE ROUTES OF DRIFT OF THE OIL SLICK AND THE DECCA-DRIFTER (AUDUNSON ET AL, 1979).

TABLE 2. SUMMARY OF SELECTED PHYSICAL CHARACTERISTICS AND COST OF DRIFTERS.

MANUFACTURER: MODEL	SHAPE	LENGTH/WIDTH (m)	(m)	WEIGHT (kg)	ASPECT RATIO	DRAFT (m)	FREEBOARD (m)	RESERVE BUOYANCY (kg)	FIELD TESTS	COST (1987,USA DOLLARS)
BERGEN OCEAN DATA	CYLINDRICAL	1.2	0.6	50	0.5	0.2	0.4	20	Audunson, 1978,82,85&86	$8,000
CEIS: ECOMAR/ECOCAP	SPAR	1.2	0.3	50	5.5	-	-	-	-	-
COASTAL CLIMATE	SPHERE	0.7	0.38	15	1.0	0.35	0.5	12	-	2,500
DRAPER: LCD	DISK	0.4	0.2	5	0.5	0.1	0.1	7	-	2,000
FERRANTI: ARGOSPHERE	SPAR	0.5	0.5	26	1.0	0.2	0.2	26	-	3,400
FERRANTI: TORPEDO	BOAT	1.2	0.5	90	2.4	0.2	0.2	95	-	3,900
HERMES: CONICAL	SPAR/COLLAR	2.0	0.9	74	2.7	1.2	0.8	35	-	6,000
HORIZON: FHD 'A'	CYLINDER	1.0	0.12	8	10.5	0.65	0.25	3	Pickett et al, (1983)	2,500
METOCEAN: CMOD	SPAR/COLLAR	2.25	0.4	13.6	3.5	0.7	1.4	16	Pickett et al, (1983)	2,750
METOCEAN: STANDARD	SPAR/COLLAR	3.5	0.7	95	5.0	-	-	50	-	10,000
PRL: MINITOD	SPAR/COLLAR	1.5	0.3	42	3.5	0.9	0.7	30	Pickett et al, (1983)	3,300
SCRIPPS	DROGUE	1.7	1.0	3.3	-	1.2	0.5	1.0	-	-
SEA DATA: ARGONAUT	SPAR/COLLAR	1.6	0.5	32	4.4	1.1	0.5	23	-	4,000
TRITON: MINI-D	SPAR/COLLAR	1.2	0.3	10	4.5	0.68	0.52	5	-	3,000
TRITON: TOGA	SPAR/COLLAR	2.6	0.7	136	3.7	-	-	50	-	12,000

NOTES:

1. The NOVATECH: RF700B and ORION OST 2100 are not ARGOS compatible and hence have not been included. The SEIMAC AST and TECHNOCEAN are submerged volume drifters and are not suitable for the present application.
2. The COASTAL CLIMATE and FERRANTI drifters require ballast. The table entries reflect ballasted conditions.
3. Aspect ratio defined as: draft/(0.5 Beam at SWL).
4. Quoted are approximate unit costs.

determined by the requirement to be able to air deploy multiple drifters from helicopter or fixed wing aircraft.

FINAL DRIFTER EVALUATION AND SELECTION

The final drifter evaluation process is currently in progress. Presented below is the basic strategy that is being employed.

Each of the six drifters that were selected as a result of the preliminary evaluation will undergo a rigorous engineering evaluation. All available information for each buoy will be obtained from the manufacturer/designer.

In addition a member of the ASA project team will visit each manufacturer to discuss their drifter and its design and manufacturing in detail. A check list for the site visits is shown in Table 3. It is the intent of this site visit and information collection exercise to gather as much information as possible about each drifter.

Based on a review of this data, two or three drifters will be recommended to MMS as possible candidates for oil spill tracking. It is hoped that the final candidates will be tested in a subsequent field program to document their ability to perform the desired task.

CONCLUSIONS

A review of the oil spill fates literature since 1980 has revealed considerable progress, particularly in how the various fate processes interact with one another to determine the behavior of spilled oil. From the oil spill tracking point of view, the most important advance is in better understanding the role of entrainment and near surface current shear in spreading and transporting the slick. However, even with this progress the leading edge of the slick is well approximated by the well know 3.5% of the wind speed rotated typically 10-30° to the wind direction (clockwise in northern hemisphere) rule. The center of mass of the slick will be considerably behind this point although a significant wind shift could markedly alter this situation. While a drifter may perform well in tracking a spill in open water, spill situations perform well in ice covered waters where oil spill transport can be significantly influenced by the movement of ice.

Candidate drifters to track oil were identified by contacting manufacturers noted in trade journals, by personal knowledge, by talking with researchers who have been actively involved in drift tracking experiments and by solicitation in the Oil Spill Intelligence Report (OSIR). Drifters were subjected to a preliminary evaluation to narrow the field of applicable drifters. At this stage, weight, geometry (length, width, aspect), reserve buoyancy, draft, and freeboard were employed to compare the identified drifters. Documented drifter performance in field tests comparing drift and oil trajectories was also used to evaluate the candidate drifters. All drifters, at the sponsor's specification, were required to be ARGOS certified or have the potential to be certified without major redesign. This preliminary evaluation consisted of assigning a score to each parameter, summing the scores for each drifter and then determining those drifters with the total highest score. In general the smaller the value of the parameter (except reserve buoyance) the higher the score. The rationale is that small, low weight drifters are easily handled and readily deployed from helicopter or fixed wing aircraft. Such a platform should also be readily able to store a dozen or more drifters with ease. In addition, minimizing draft freeboard will allow the drifter to more closely resemble a spill slick and hopefully respond in a similar manner to wind, wave, and current forcing. This process is fairly subjective and it is important to note that the ultimate oil spill

TABLE 3. SITE VISIT CHECK LIST.

Engineering Criteria

1. Ease of Deployment and Recovery

Length and width.........................
Weight...................................
Shape (simplicity)
Suitability for deployment and
recovery by aircraft.....................
Ease of storage..........................

2. Ease of Use

Pre-deployment checkout..................
Energizing and de-emergizing.............
ARGOS transmitter........................

3. Reliability and Durability-Mechanical

Hull design..............................
Hull materials-strength..................
Hull materials-corrosion resistance......
Hull materials-corrosion compatibility...
Number of hull penetrations..............
Adequacy of of seals.....................
Adequacy of hull fasteners...............
Hull surface finish......................
Resistance to icing & biofouling.........
Skirt or mat used?.......................
Fatigue failure modes....................

4. Reliability and Durability-Electronics

Power Supplies:

Dependability of the type used...........
Number required..........................
Weight...................................
Discharge characteristics................
Failure modes............................

Electronics:

Assembly quality.........................
Component quality........................
Connections..............................
Design margins...........................
Power requirements.......................
Failsafes................................
Wiring mountings.........................
Board mountings..........................

ARGOS Transmitter

Power requirements.......................
Antenna Design...........................
Software interface.......................
I.D. and timing setup....................

5. Cost

Initial unit cost........................
Deployments costs........................
Auxillary equipment needs................
Electronics repair.......................
Hull and mechanical repair...............

6. Maintenance

Amount of pre-and post-deployment
maintenance required.....................
Ease of routine maintenance..............
Location and assessibility of
manufacturer's repair facility...........
Spare parts inventory....................
Ease of repair by other facilities.......
Documentation - Completeness.............
Documentation - Clarity..................

tracking drifter may not be the one with the lowest score in this evaluation. For instance, a deeper draft may be compensated by higher a freeboard to maintain the appropriate balance between wind, wave and current forcing of the drifter. The evaluation, however, provides a useful first cut on selecting candidate drifters.

The six drifters selected during this preliminary review will be subjected to an extensive engineering evaluation. Engineering criteria include ease of deployment and recovery, ease of use, reliability and durability (mechanical, electronic, and ARGOS transmitter), cost, and maintenance requirements. For each drifter all the engineering and test literature will be collected. In addition, a member of the project team will visit the manufacturer to perform an in depth review of all engineering, design, and manufacturing aspects of the drifter. We will also attempt to contact any organizations that have operational experience with the drifter. Based on this review two or three drifters will be recommended to the sponsor as final candidates for use in tracking oil spills. If warranted a field evaluation may be performed under a subsequent contract to compare the drifter behavior to an actual spill.

ACKNOWLEDGEMENTS

This work was sponsored by the U.S. Department of Interior Minerals Management Service. Mr. Newell Stiles serves as the technical contract monitor.

BIBLIOGRAPHY

Allen, A.A., 1983. Oil Spill Response in the Arctic, Part 2. Field Demonstrations in Broken Ice, Spiltec, Anchorage, Alaska.

Amstutz, D. and W. Samuels, 1986. Oil Weathering Literature Review and OSRA-II Model Analysis. Report to Minerals Management Service. Req. #6-4340-0108.

Anderson, E., 1983. Study of Wind and Current Data sets for IXTOC Oil Spill Hindcast, 1983 Oil Spill Conference (Prevention, Behavior, Control, Cleanup), San Antonio, Texas, February 28-March 3, 1983, Paper #002.

Anderson, E., 1983b. Oil Spill Hindcast Simulation of the IXTOC I, Gulf of Mexico, M.S. Thesis, Department of Ocean Engineering, University of Rhode Island, Kingston, RI

Applied Science Associates, Inc. (ASA), 1984. Oil spill trajectory model for St. George Basin. Prepared for Alaska Clean Seas, Anchorage, Alaska.

Audunson, T., B. Fossum, J. Haldorson, P. Steinbekke, 1979. Drift of Satellite and DECCA Positioned Buoys During the Experimental Oil Spill on Tromsoflaket, September 1978 (in Norwegian). Continental Shelf Institute, Report No. P195/3/79, Trondheim, Norway. 54 p.

Audunson, T., H. Celius, O. Johansen, P. Steinbakke, S.Sortrom, 1984. The Experimental Oil Spill on Haltenbanken, 1982. Continental Shelf Institute, Trondheim, Norway. Pub #112. 109.

Bassin, J. and T. Ichiye, 1977. Flocculation Behavior of Suspended Sediments and Oil Emulsions. J. Sed. Petrology 47(2):671-677.

Baumgartner, C. and J. Nath, 1984. Lagrangion Drifting Buoy Validation Program, NOAA Data Buoy Center National Space Technology Laboratories, Contract NA-82-QA-C-134. 22 p.

Bobra, A.M., and M.F. Fingas, 1986. The behavior and fate of Arctic oil spills. Water Sci. Tech, 18:13-23.

Brower, W.A., H.F. Diaz, A.S. Prechtel, H.W. Searby, and J.L. Wikse, 1977. Climatic atlas of the outer continental shelf waters and coastal regions of Alaska. Arctic Environmental Information and Data Center, University of Alaska, Anchorage, Alaska and U.S. National Climatic Center, Asheville, North Carolina. 3 Volumes.

Button, D., 1969. The Influence of Clay and Bacteria on the Concentration of Dissolved Hydrocarbon in Saline Solution, Geochemical et Cosm. Aeta 40:435-440

Chhabra, N.K., 1976. Mooring Mechanics - A Comprehensive Study, Vol. II. Three Dimensional Dynamic Analysis of Moored and Drifting Buoy Systems. Charles Stark Draper Laboratory, Inc. Cambridge, Massachusetts, 277 p.

Coon, M.D. and R.S. Pritchard, 1979. The transport and behavior of oil spilled in and under sea ice. Report prepared for Minerals Managment Service NOAA/OCSEAP, Research Unit 567, prepared by Flow Research Company, Inc., Kent, Washington.

Cornillon, P.C., M.L. Spaulding and K. Hansen, 1979b. Sample Application of the Oil Spill Model: Georges Bank Spill Simulation and User's Manual, Part V in Environmental Assessment of Treated Versus Untreated Oil Spills: Final Report United States Department of Energy Contract No. E(11\-1) 4047. 274 p.

Cox, J.C. and L.A. Schultz, 1981a. The mechanics of oil containment beneath sea ice. Proceedings of the Fourth Arctic Marine Oilspill Program Technical Seminar, Edmonton, Alberta, June 16-18, 1981, :3-44.

Cox, J.C. and L.A. Schultz, 1981b. The containment of oil spilled under rough ice. 1981 Oil Spill Conference, Atlanta, Georgia, :203-208.

Davidson, L. and D. Lawrence, 1982. Review of Existing Oil Spill Trajectory Scenario Models. Canadian Dept. Oceans and Fisheries Tech. Report #9. 62 p.

Dippner, J.W., 1983. A hindcast of the Bravo Ekofisk blow-out. Veroff. Inst. Meeresforsch, Bremerh, 19:245-257.

Elliott, et al, 1986. Shear diffusion and the spread of oil in the surface layers of the North Sea. Unit for Coastal and Estuarine Studies, Marine Science Laboratories, Menai Bridge Angelesy U595EY, GroBbritannien, pp. 113-137.

Elliott, A.J., N. Hurford, and C.J. Penn, 1986. Shear diffusion and the spreading of oil slicks. Marine Pollution Bulletin, 17(7); pp. 308-313.

Fay, J.A. and D.P. Hoult, 1971. Physical Processes in the Spread of Oil on a Water Surface, U.S. Coast Guard Research and Development, Report No. 714107/A/001.

Fingas, M. 1977. The Evaluation of an Oil Spill Tracking Buoy, Spill Technology Newsletter, January-February 1977.

Fingas, M.F. and B. Lea, 1981. Evaluation of three oil spill tracking buoys, Spill Technology Newsletter, Vol 6(6) November-December 1981.

Free, A.P., J.C. Cox, and L.A. Schultz, 1981. Laboratory studies of oil spill behavior in broken ice fields. Final Report. Prepared for U.S. Coast Guard Research and Development Center, Contract No. DTCG 39-80-C-80138.

Huang, J.C. and F.C. Monastero, 1982. Review of the State of the Art of Oil Spill Simulation Models, Final Report to American Petroleum Institute, Washington, D.C. Vitvs 350 p.

Huang, J.C., 1983. A review of the state-of-the-art of oil spill fate/behavior models. In Proceedings of the 1983 Oil Spill Conference. American Petroleum Institute :313-322.

Johanson, O., 1984. The Haltenbank experiment - observations and model studies of drift and fate of oil in marine environment. Proc. 7th Arctic-Marine Oil Spill Program Techn. Seminar, Edmonton, Alberta, :18-36.

Johanson, O., 1985a. Drift and spread of oil from the Troll field. IKU, Sintef-Gruppen, Trondheim, Norway, Reg. No. 85.050, p.1-31.

Johanson, O., 1985b. Particle in fluid model for simulation of oil drift and spread, Part I: Basic concepts. Oceanographic Center, Sintef Group, Norway. Note Number 02.0706.40/2/85, 34 p.

Johansen, O., 1987. DOOSIM - A new simulation model for oil spill management. 1987 Oil Spill Conference, Papter 169 (preprint).

Kovacs, A., 1977. Sea ice thickness profiling and under-ice oil entrapment. Proceedings, 1977 Offshore Technology Conference, Houston, Texas, Vol. III, :547-554

Kovacs, A. 1979. Oil pooling under sea ice. Environmental Assessment of the Alaskan Continental Shelf, Annual Reports, Vol. VIII, Transport, :310-353.

LaBelle, J.C., J.L. Wise, R. Voleker, R. Schulze, and G. Wohl, 1983. Alaska marine ice atlas. Artic Environmental Information and Data Center, University of Alaska, Anchorage, Alaska. 302 p.

Lea, B.N., 1982. Field evaluation of oil spill tracking devices, Environmental Protection Service, Ottawa, Ontario Canada, Report EE-28, February, 1982.

Mackay, D., and S. Paterson, 1980. A Mathematical Model of Oil Spill Behavior, Report Prepared for Environmental Emergencies Branch, Environmental Protection Service, Publication EE-7.

Mackay, D., W. Shui, K Hossain, W. Striver, D. McCurdy, and S. Paterson, 1982. Development and Calibration of An Oil Spill Behavior Model, U.S. Coast Guard Research and Development Center, Groton, Connecticut 06340, Report No. CG-D-27-83.

Mackay, D., 1984. Uses and abuses of oil spill models. Proceedings of the 7th Arctic Marine Oil Spill Program, Technical Seminar, Edmonton, Alberta, Environment Canada, Ottawa, :1-17.

Mackay, D. et al, 1986. The dispersion and submergence of oil spills. Proceedings of the Ninth Arctic Marine Oilspill Program Technical Seminar, Edmonton, Alberta, June 10-12, 1986, pp. 101-112.

Meyers, P. and J. Quinn, 1973. Organic Matter on Clay Minerals and Marine Sediments - Effects on Adsorption from Saline Solutions. Chem: Geol. 13:63-68.

Meyers, P. and T. Oas, 1978. Comparison of Associations of Different Hydrocarbons with Clay Particles in Simulation Seawater. Env. Sci Tech. 12:934-937.

Mountain, D. G. and K.A. Mooney, 1980. Operational use of Satellite

Tracked current drifters, Proceedings of the 1983 Synposium on Buoy Technology. News Orleans, Louisiana, April 27-29, 1981.

Murray, S.P., 1982. The Effects of Weather Systems, Currents, and Coastal Processes on Major Oil Spills at Sea. In Kullenberg, G (ed) Pollutant Transfer and Transport in the Sea. CRC Press, Baton Rouge, Florida. p. 169-227.

NTIS (National Technical Information Service), 1985. Citations from the selected Water Resources Abstracts DataBase. Oil Spills: Environmetal Effects (1977-May 1985). PB85-860559.

Payne, James R., Bruce E. Kirstein, G. Daniel McNabb, Jr., James L. Lambach, Robert Redding, Randolph E. Jordan, Wilson Hom, Celso de Oliveira, Gary S. Smith, Daniel M. Baxter, and Russel Gaegel, 1984. Final Report, Multivariate analysis of petroleum weathering in the marine environment - sub arctic, Vol, 1 - Technical Results. In: Enviromental Assessment of the Alaskan Continental Shelf, Final Reports of Principal Investigators, Vol 21, U.S. Department of Commerce, U.S. Department of the Interior, Minerals Management Service, p. 670.

Payne, J.R. and G.D. McNabb, Jr., 1985. Weathering of petroleum in the marine environment. Marine Technology Society Journal, Vol. 18, No. 3.

Payne, J., B. Kirstein, et al, 1986. Integration of Suspended Particulate Matter and Oil Transportation. Quarterly Progress Report to Minerals Management Service Contract #14-12-0001-30146 94 p.

Pickett, R.L., R.M. Partridge, A.H. Clites, and J.E. Campbell, 1983. Great Lakes Satellite tracked current drifters, Proceedings of the 1983 Symposium on Buoy Technology. New Orleans, Louisiana, April 27-29, 1983.

Reed, M., M. Spaulding, E. Gundlach, T. Kana, S. Siah, 1986. Formulation of a Shoreline/Oil Spill Interaction Model Proc. Ninth AMOP Seminar, Edmonton, Alberta. p. 77-100.

Reed, M., D. French, J. Calambokidis, and J. Cubbage, 1986a. Simulation modeling of the effects of oil spills in population dynamics of northern fur seals. OCS Study MMS 86-0045, Minerals Management Service, Anchorage, Alaska.

Reed, M., K. Jayko, A. Bowles, E. Anderson, S. Leatherwood, and M. Spaulding, 1986b. Computer simulation of probability that endangered whales will interact with oil spills. OCS Study 86-0044, Minerals Management Service, Anchorage, Alaska.

Reed, M, C. Turner, M. Spaulding, D. Dorson, and O. Johanson, 1987, Evauation of Surface Drifters for Satellite Tracking of Oil on the Sea Surface prepared for Minerals Management Service prepared by Applied Science Associates, Inc., Narragansett, Rhode Island

Reijnhart, R. and R. Rose, 1982. Evaporation of crude oil at sea. Water Resources, Vol. 16, pp. 1319-1325.

Reimer, E.M., 1981. Anticipated Oil Dispersion Rates in Pack Ice, 1981 Oil Spill Conference, Atlanta, Georgia, pp. 199-202.

Sayed, M. and R. Abdelmour, 1982. Oil movement under ice. Arctec Canada Ltd., Kanata, Ontario, Canada, Report No. 1117C.

Smith, R.A., J.R. Slack, T. Wyant and K.J. Lanfear, 1980. The Oil Spill Risk Model of the U.S. Geological Survey, U.S. Geological Survey, U.S. Geological Survey Survey Open-File Report 80-687, 107 p.

Sorstrom, S. and O. Johansen, 1985. Experimental Oil Spill at Haltenbanken, Data Report No 85.136. Oceanographic Center. Trondheim, Norway.

Spaulding, M.L., S.B. Saila, M. Reed, E. Lorda, H. Walker, T. Isaji, J. C. Swanson, E. Anderson, 1982. Assessing the impact of oil spills on a commercial fishery. Final Report to Minerals Management Service. Contract No. AA851-CTO-75. NTIS No PB83-149104.

Spaulding, M.L., 1986. A State-of-the-Art Review of Oil Spill Trajectory and Fate Modeling. International Seminar on Chemical and National Dispersion of Oil inot the Sea, 10-11 November 1986, Heimdal, Norway.

Stolzenback, K.D., O.S. Madsen, E.E. Amdams, A.M. Pollock and C.K. Cooper, 1977. A Review and Evaluation of Basic Techniques for Predicting the Behavior of Surface Oil Slicks, Massachusetts Institute of Technology, Report MITSG77-8, 323 p.

Thomas, D.R., 1983. Interaction of oil with Arctic sea ice. RTD Report No. 258, Flow Industries, Inc., Kent, Washington, 27 p.

URI and ASA (University of Rhode Island and Applied Science Associates, Inc.), 1982. Assessing the Impacts of Oil Spills on a Commercial Fishery. Final Report to U.S. Department of Interior, Contract #AA851-CTO-75. 241 p.

Uzuner, M.S., F.B. Weiskopg, J.C. Cox and L.A. Schults, 1979. Transport of Oil Under Smooth Ice, Environmental Protection Agency, Report EPA-600/3-79-0412, 49 p.

Walker, F.R., 1975. Oil, Ice and Climate in the Beaufort Sea, Beaufort Sea Technical Report #35, Beaufort Sea Project, Victoria, B.C. 40 p.

Wilson, D. and D. Mackay, 1986. The behavior of oil in freezing situations. Spill Technology Newsletter, September 1986, :87-100.

CCRS REMOTE SENSING OF THE
BEAUFORT SEA DISPERSANT TRIALS 1986

W.D. McColl, CCRS Data Acquisition Division

M.F. Fingas, Environment Canada
Environmental Emergencies Technology Division

R.A.E. McKibbon, CCRS Data Acquisition Division

S.M. Till, CCRS Data Acquisition Division

ABSTRACT

The Canada Centre for Remote Sensing with the Environmental Emergencies Technology Division, Environment Canada participated in a co-operative project to provide remote sensing measurements of the Beaufort Sea Dispersant Trials in August 1986.

CCRS has considerable expertise in the development of sensor systems and data interpretation for the remote sensing of oil pollutants acquired from research participation in the AMOP program and data acquisition of accidental oil spills. The research sites included Baffin Bay 1978, Wallops Islands 1978, and Newfoundland Dispersant Trials 1981. The accidental spills measured were the Kurdistan shipwreck 1979 and the Vinland natural gas blowout off Sable Island 1984.

The aircraft configuration for the Beaufort Trials was the basic Falcon electro-optical system, including the DS 1260 MSS with UV/IR, dual IR and multi-spectral/IR interchangeable detectors, the RC 10 camera, inertial navigation with the MAID data logger, ALICE real-time display system with the video cassette recorder and the high density tape recorder. This system provided the capability to satisfy both operational and research objectives.

Operationally the task required temporal mapping of the distribution and relative thickness of the oil at the multiple test sites to document the effects of the various dispersant applications.

Research objectives included the utilization of dual infrared detectors at 5 and 10 micrometres, for fringe detection, to provide additional oil thickness information and the test of the MSS spectrometer for imaging the dispersed oil in the water column.

The on-location analysis of the real-time video cassette recording of the UV/IR data verified success in documenting each test slick and the relative effectiveness of the dispersant applications for the trial date. In addition the remnants of the four test slicks were located and mapped two days later.

Subsequent analysis of multispectral image data recorded on the high density tape has provided position and area information of each test slick with time for the complete trial period.

For the research data, post-flight analysis and imagery examples document the sensor sensitivity requirements for both the dual band infrared fringe measurements and the detection of the dispersed oil yellow cloud.

TRIAL PROTOCOL AND REMOTE SENSING FLIGHT PLANNING

The dispersant trial protocol planned for two trial days in the Beaufort Sea north of Tuktoyaktuk. Each trial scheduled four oil sites comprised of two control sites and two test sites. One control site was to be untreated, the other control to be sprayed with dispersant once and the two test sites each to receive multiple applications of different dispersants. Primary evaluation of the trials would be by remote sensing providing temporal mapping of the four sites to document the effects of the dispersants. The scheduled time period for the trials was August 11-15, 1986.

To accommodate both the operational and research remote sensing objectives a minimum of three airborne sorties would be required for different sensor configurations. The CCRS Falcon 20 aircraft was scheduled to be based in Inuvik which has a paved runway required for Falcon operation.

AIRCRAFT SENSOR CONFIGURATION

The CCRS Falcon 20 aircraft (Fig. 1) was equipped with an electro-optical sensor configuration.

The prime sensor was the Daedalus MSS 1260 with the Alice MSS processor and Real Time Display Systems (Fig. 2). The MSS sensor head mounted in the nose of the aircraft (Fig. 3) accommodates optional detector configurations including ultraviolet/infrared (UV/IR), dual IR, and multispectral I/R. The spectral bands for each of these configurations are listed in Table 1.

The multiband digital MSS data were recorded on a Bell and Howell M14F high density digital tape recorder (HDTR). The colour real time display data were recorded on a Canon portable VCR for on-site review of the remote sensing data.

In addition to the MSS, a Wild RC-10 camera using Aero-negative 2445 film provided selected photo coverage of the trial sites.

The primary system for aircraft navigation was a Litton 51 inertial navigation system (INS). The INS aircraft position and attitude data are interfaced to both the MAID navigation processor and the MSS sensor. MAID data are recorded on a Kennedy CCT recorder mounted in rack with HDTR and INS systems (Fig. 4). In addition, the MAID flight line data including time, position, altitude, aircraft heading, track angle, attitude and event marker are output to a line printer mounted in the navigation/camera rack (Fig. 5). The line printer record is part of the permanent flight log.

The overall aircraft interior configuration is shown in Fig. 6 as seen from the aft of the aircraft.

REMOTE SENSING OBJECTIVES

The remote sensing plan included both operational and research objectives.

Operational Objective

The primary objective, to operationally document the dispersant trials, required the application of proven methodology for data acquisition and the MSS sensor configuration. Dual band registered imaging using the UV/IR detectors has been demonstrated, particularly for the Newfoundland Dispersant Trials 1981, to provide excellent oil imaging providing oil thickness discrimination to three levels: thick oil, areas that are solar heated; medium thickness,

FIGURE 1. CCRS FALCON 20 AIRCRAFT

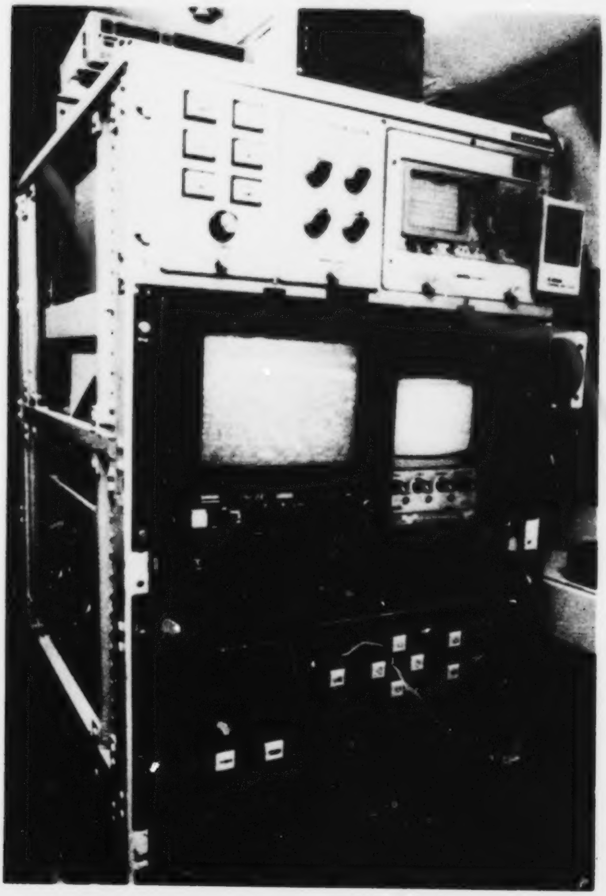

FIGURE 2.
DAEDALUS 1260
MULTISPECTRAL SCANNER
AND ALICE REAL TIME
COLOUR DISPLAY

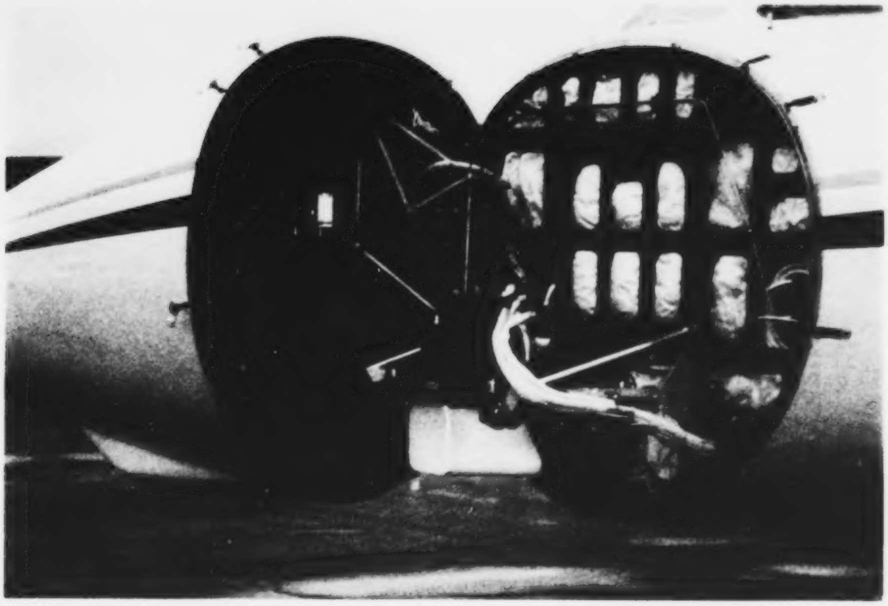

FIGURE 3. MSS SCAN HEAD MOUNTED IN THE NOSE OF THE FALCON AIRCRAFT

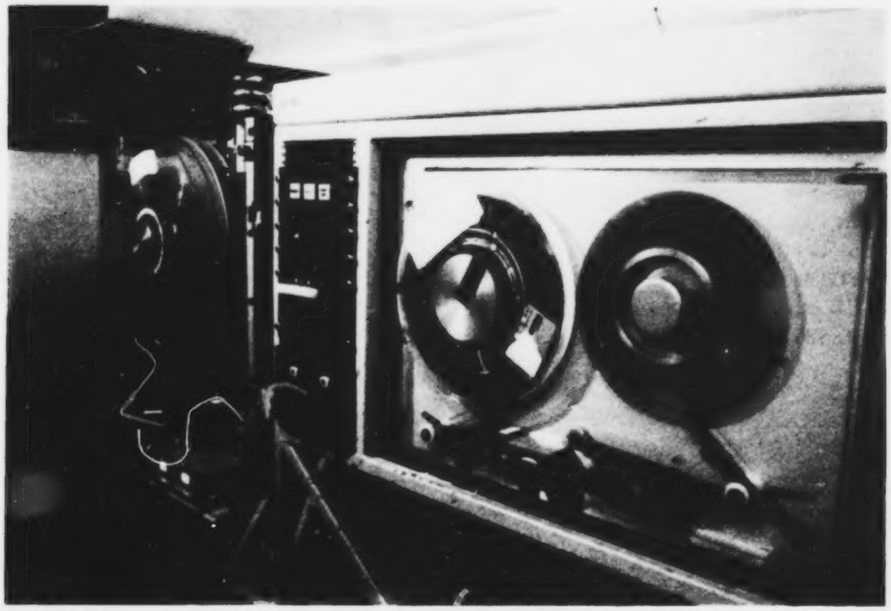

FIGURE 4. HIGH DENSITY IMAGE DATA AND COMPUTER COMPATIBLE NAVIGATION DATA TAPE RECORDERS

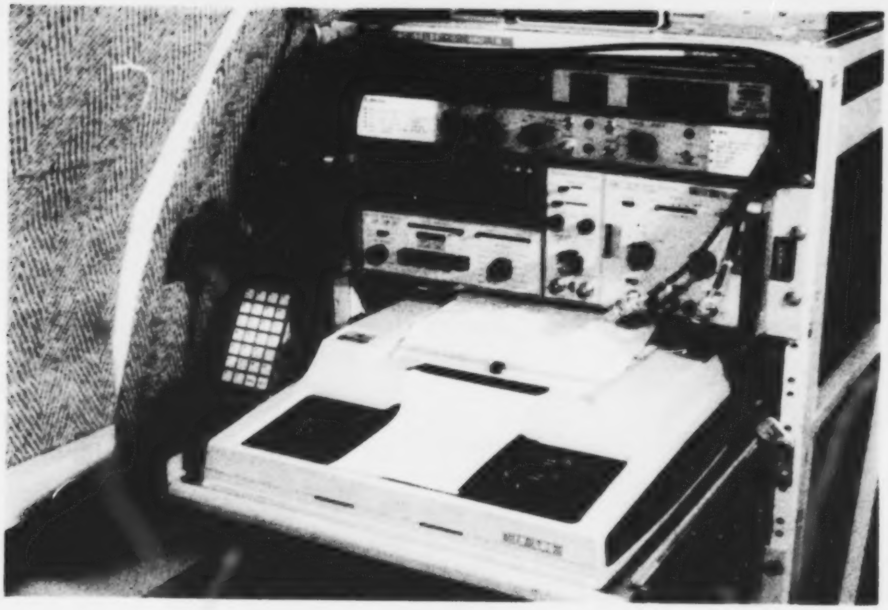

FIGURE 5. NAVIGATION DATA CONSOLE AND FLIGHT LOG DATA LINE PRINTER

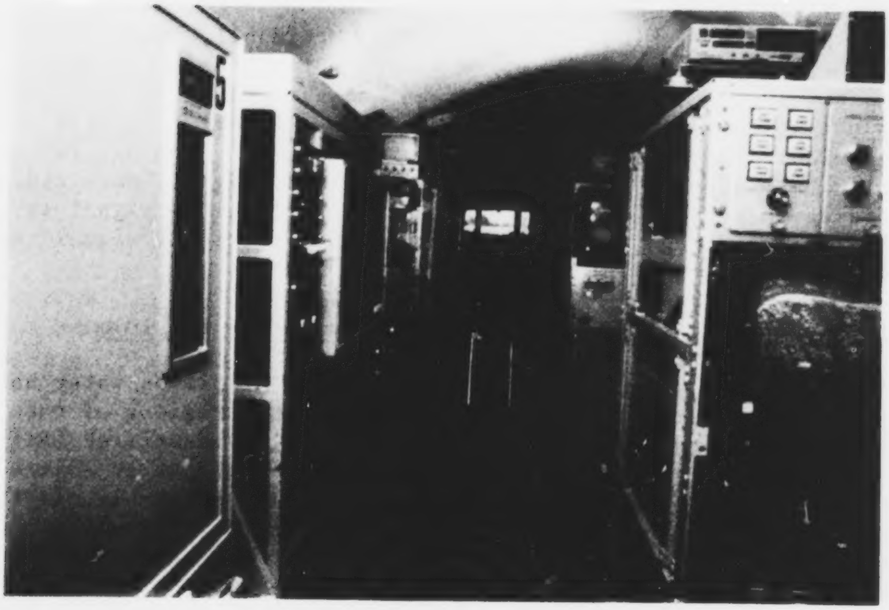

FIGURE 6. OVERALL SENSOR CONSOLE CONFIGURATION VIEW FROM THE AFT OF THE AIRCRAFT

TABLE 1. MSS DETECTOR SPECIFICATIONS

DETECTOR	BAND NO.	50% TRANSMISSION WAVELENGTH	BANDWIDTH
Spectrometer	1	390-415 nm	25 nm
	2	415-450 nm	35 nm
	3	445-495 nm	50 nm
	4	500-550 nm	50 nm
	5	550-595 nm	45 nm
	6	590-645 nm	55 nm
	7	625-695 nm	70 nm
	8	680-780 nm	100 nm
	9	765-895 nm	130 nm
	10	865-1035 nm	170 nm
Ultraviolet		275-365 nm	90 nm
Infrared Indium Antimonide		4.5-5.0 μm	0.5 μm
Infrared Mercury Cadmium Telluride		8.5-12 μm	3.5 μm

identified by areas of minimum IR signal; and thin oil, imaged as high contrast areas in the UV. Combining the UV/IR images into a three colour image by assigning the IR signal to blue and green and assigning the UV signal to red, provides the following colour coded imagery for the oil thickness discrimination: white, corresponding to regions where the oil is thick enough to be solar heated providing an increase in the IR signal, dark red, corresponding to regions of medium thickness where the IR signal is suppressed; and pink, corresponding to areas of thin oil, where the UV signal remains high and the IR signal is that of the water background.

Research Objective No. 1 - Dual IR Detectors at 4 μm and 10 μm

Previous research and analysis of IR imagery of oil on water has identified apparent fringing of the IR signal within regions of the imagery that show as solar heating of the oil. R.A. Neville identified (Ref. 1) that the fringing could be attributed to interference of the water emitted IR signal by the thin oil film. In this case the thinnest IR detectable oil film would correspond to ¼ the wavelength of the IR signal in the oil medium. For light crudes this would correspond to approximately 2 μm for the 10 μm wavelength IR detector.

Based on these observations, one of the research objectives was the trial of dual registered IR detectors; one at 5 μm wavelength and one at 10 μm to image a thin oil film, of appropriate spatial thickness gradient, to determine if the interference fringes corresponding to the ¼ wavelength transmission minima signals of each IR band were visible. Assigning each IR signal to a separate image colour would produce colour separation of any fringing pattern.

Research Objective No. 2 - Imaging of Dispersed Oil Within the Water Column

Low level RC-10 colour photography of the Newfoundland Trials provided evidence of a very limited spatially distributed "yellow cloud" attributed to dispersed oil within the water column following the application of the dispersant.

This second research objective was the trial of the MSS spectrometer in imaging the dispersed oil in the water column. The digital dynamic range and the spectral separability for the MSS spectrometer data exeeds that of the colour film, however the spatial resolution of the MSS is inferior to that of colour film requiring that the dispersed oil signature be measurable over an extended region for non-ambiguous identification.

DATA ACQUISITION DESCRIPTION

Remote sensing flights were provided on three days, the Aug. 11, Aug. 14 trial dates, and a reconnaissance flight on Aug. 16, 1986, two days after the main trial. Two airborne sorties were required on Aug. 14th to cover the trial time period. A data catalog (Table 2) provides a listing of all the data acquired per sortie by flight line, time, target, dispersant application and the CCRS imagery and MAID data CCT numbers.

August 11th

For this trial the MSS primary sensor was configured in the dual IR detector mode to accommodate the first research objective.

Two oil slicks were deployed and imagery acquired on eight flight lines. Failure of the helicopter mounted dispersant spray rig caused this trial to be aborted. Total flight time was 1.8 hours, with 0.8 hours on target.

August 14th

For the first airborne sortie on this date the MSS sensor was configured in the spectrometer/IR detector mode to accommodate research objective number two.

Two oil slicks, Cl and Tl, were down and dispersant application had begun at the start of data acquisition at 19:53 hrs. GMT. The third slick, T2, was put down at 20:30 hrs., just prior to flight line 8. Data of each site were acquired sequentially in 14 flight lines during the time of dispersant application. The aircraft returned to Inuvik at 21:17 hrs. for sensor reconfiguration and aircraft refueling.

For the second sortie on the 14th, the MSS was configured in the operational IR/UV mode. Data acquisition recommenced at 23:06 hrs. The main control slick, C, was put down at approximately 00:15 hrs. Application to Tl and T2 continued in this period. Treatment of the four test slicks as per the protocol was as follows: Cl was treated with a single application of BPMA700; Tl received multiple applications of BPMA700; T2 received multiple applications of CRX-8; C was not treated.

Seventeen flight lines acquired data in the second sortie, ending at 00:45 hrs., providing a complete data set for this dispersant trial. Total flying time for the two sorties was 4.8 hrs. with 3.1 hrs. on target.

August 16th

A reconnaissance flight was carried out on August 16th approximately 40 hours after the trial termination on August 14 to determine if any oil from the four test sites remained undispersed as detectable oil slicks. Four separate thin oil slicks were detected in a region north west of the trial site. Ten flight lines at 3 altitudes (975 m, 2000 m, 3800 m) acquired data in the IR/UV spectral bands to resolve and document the area of the residual oil slicks. Total time on the reconnaissance flight was 2.1 hours with 1.2 hours on target.

DATA ANALYSIS

Analysis of this very large data set was carried out primarily on the Alice Real Time Display. This system provides the capability to read three selectable bands simultaneously from the high density digital tape (HDDT) and to display the data or scrolling colour monitor. Data manipulation includes contrast enhancements by histogram equalization or linear stretch and selectable image roam, zoom, and freeze-frame functions. Selected flight lines, as indicated in the data catalog, documenting the trials events, were analysed in detail. Area measurements were made from the display zoom imagery by pixel count. Selected multiband data were imaged in colour hard copy on the CCRS FIRE colour image recorder and single data were imaged in black and white hard copy on the Honeywell strip image recorder.

Research Objective No. 1

Dual IR imaging at 5 μm and 10 μm respectively to determine if IR transmission interference fringes were separable in the two bands provided non-conclusive results. Infrared data from both bands did not show fringing within the region of medium oil thickness where the IR signal is suppressed, however this region that surrounded areas of solar heated oil was spatially limited during this test. The two slicks were put down at the beginning of the flight period and perhaps had not spread sufficiently to provide conditions for IR fringing that have been observed in previous measurements. This research requires additional testing.

Research Objective No. 2

Multiband spectrometer data from sortie 1 (Aug. 14/86) were analysed to determine if a dispersed "yellow cloud" were detectable within the water column after the dispersant had been applied to the slick. Imagery from bands 3, 4, 5, 6, and 7 centered at 470 nm, 525 nm, 575 nm, 625 nm and 66 nm respectively, were examined separately and in combination on the colour analysis system for evidence of any dispersed yellow cloud. This data showed no visible evidence that the feature was detectable if it existed in the water column in areas not obscured by the surface oil slick. For these trials the helicopter application of the dispersant concentrated the application quite accurately on the thicker portions of the slick and not on the thinner extremities where the dispersant creates the visible dispersed oil in the water column as was evident in the

Newfoundland trials. In addition the spatial resolution of the data, approximately 2 m pixels, may have been too large to image this feature.

The multiband spectrometer did show a strong signal in the red bands 625 nm and 660 nm from the thicker parts of the oil slick. It was confirmed that the oil provided this spectral signature, and not an oil dispersant combination, by comparison with data from site T2 on flight line 8 at 23:53 hrs. when no dispersant had been applied. Additionally, the correlation of the red response and the areas of thicker oil was made by comparison of the red signal with that of the IR band that delineates thicker areas of the slick.

Operational Analysis

Seventeen flight lines from Aug. 14/86, the main trial date, and ten flight lines from Aug. 16/86 were analysed to determine the effects of the dispersant applications. In general, this determination depends on the ability to measure the areas and estimate the volume of the residual non-dispersed oil remaining in each site after the dispersant application. Measureable differences in the residual slicks for each of the control and test sites would provide a rating for the dispersant types and application techniques.

The four test slicks were put down at times and positions as follows: P1 are the approximate positions where the slicks were put down and P2 are the respective positions of the slicks at end of the observations of sortie 2.

SLICK	TIME GMT	P1	P2
C1	19:16	N 70:03 W 133:21	N 70:05 W 133:27
T1	19:42	N 70:04 W 133:21	N 70:08 W 133:25
T2	20:27	N 70:05 W 133:22	N 70:07 W 133:26
C	00:21	N 70:10 W 133:21	N 70:10 W 133:21

During this time period the slicks are moving westward with the wind as indicated by the direction of the slick and northward with the current as indicated by the relative positions at P1 and P2.

Each slick, after it was put down and allowed to spread, developed the detectable three thickness characterized by areas of thicker solar heated oil, surrounded by a thinner area where the infrared signal is suppressed, and very thin areas where the oil is detectable only in the UV.

The dispersant spray applications as documented caused a detectable reduction in the areas of the slick, particularly in the thicker regions, however between the dispersant applications these detecable areas of thicker oil increased. This phenomenon is consisten with that observed in the Newfoundland Trials.

Throughout the trial period, temporal measurements of the solar heated areas of each slick (C1, T1, T2) show similar and overall reductions of these areas. However, during the period from 20:30 GMT, solar noon, to 00:30 GMT, the zenith angle changes from 57.7° to 65°. As the solar heating has a cosine of the zenith angle dependence, this would indicate a factor of 0.79 reduction in solar heating.

In comparison to a reduction in the areas of solar heated oil, the thinner oil areas delineated by suppression of the infrared signal, showed no consistent reduction in any of C1, T1 or T2 sites. These are areas within the medium thickness region that are identified by a reduced suppression of the IR signal.

Based on the above, reasonable estimates of the residual volume for sites C1, T1 and T2 are very difficult, however one may estimate a reasonable minimum residual oil. Using the IR transmission interference to estimate the minimum oil thickness in the areas of IR signal suppression provides an estimate between 2 μm and 6 μm, between ¼ wavelength and ¾ wavelength for the IR signal in the medium. In that there are areas where the signal is not at the minimum, a reasonable estimate for the oil thickness would be 4 μm. The measured residual areas of thin oil are C1 21,422 sq. m, T1 15,244 sq. m and T2 19,137 sq. m. The residual volumes are C1 0.086 cu. m, T1 0.061 cu. m, and T2 0.077 cu. m.

August 16 Reconnaissance

Four continuous and extensive thin oil slicks were identified and mapped in a region north west of the trials area. These slicks have been labelled 1, 2, 3 and 4, centered at the following approximate positions:

SLICK NO.	POSITION	
1.	N 70:14,	W 133.57
2.	N 70:11	W 133.52
3.	N 70:06	W 133:49
4.	N 70:05	W 133:37

If these slicks are in fact the residuals of the trials, and the northwest drift maintained the respective positions of the residual test sites, then the correspondence would be as follows:

SLICK NO.	TRIAL SITE
1.	C
2.	T2
3.	T1
4.	C1

The four slicks are thin, detectable in the UV signal, with no IR response. An estimate of their thickness based on a ¼ wavelength reflection maximum of UV signal is 70 nm.

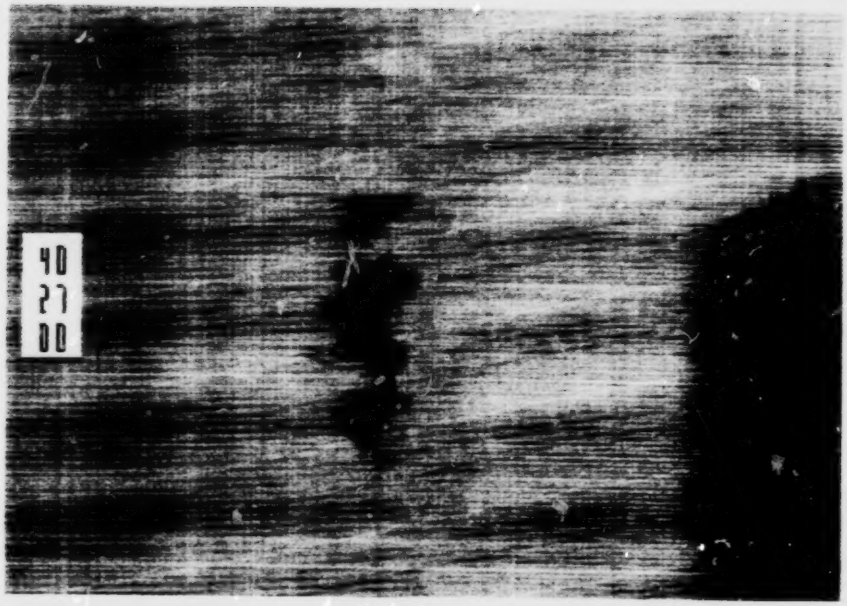

FIGURE 7. SITE C1 AREA OF RESIDUAL OIL THERMAL SIGNATURE

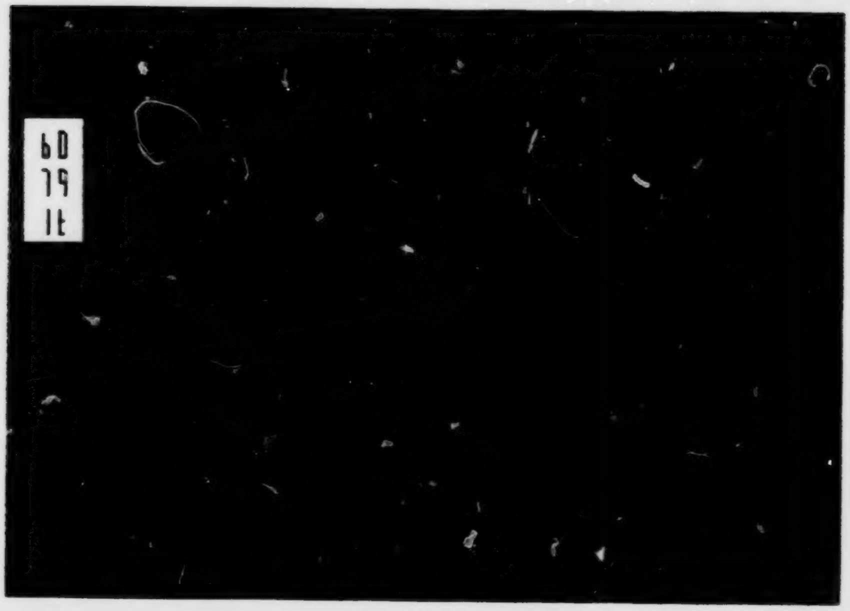

FIGURE 8. SITE T1 AREA OF RESIDUAL OIL THERMAL SIGNATURE

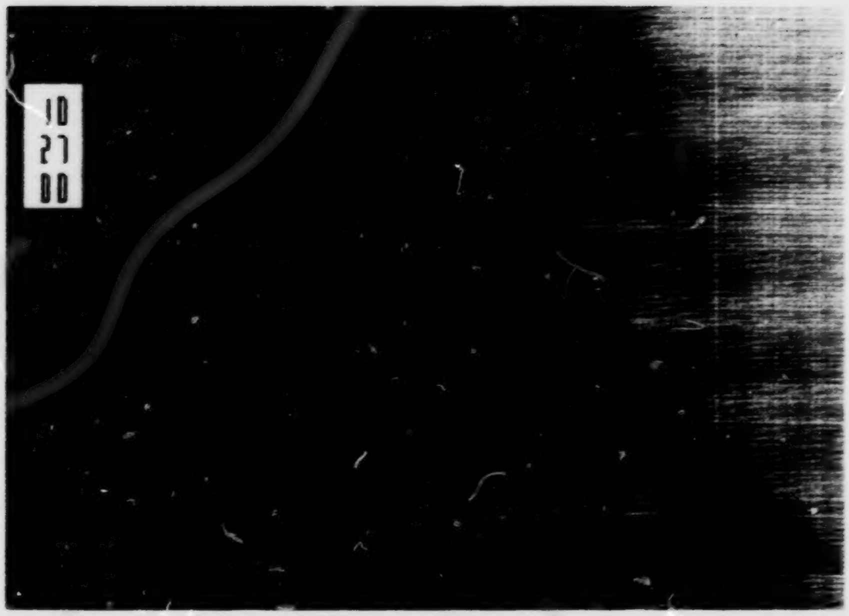

FIGURE 9. SITE T2 AREA OF RESIDUAL OIL THERMAL SIGNATURE

The areas of these slicks are:
1. 1.95×10^6 sq. m, 2. 626,945 sq. m, 3. 381,618 sq. m, 4. 436,135 sq. m.
The estimated oil volumes of the four slicks are:
1. 0.136 cu. m, 2. 0.044 cu. m, 3. 0.027 cu. m, 4. 0.031 cu. m.

The location of the four slicks is near a zone of strong thermal gradients. Slick no. 2 is partially entrapped by a thermal boundary shear zone of water at 4°c, maximum density, and the warmer over-riding water. The identifiable thermal mixing and circulation patterns within this region make the slick correlation by position questionable.

TABLE 2. DATA CATALOGUE

Flight Date Aug. 11 SORTIE 1 Arrival 212624 Departure 221157

LINE NO.	TIME GMT	ALT. (M)	SLICK ID	POSITION LAT.	POSITION LONG.	TIME	RMK.	CCT#
1 S	212624	1097		N70:05	W133:19	212702		RS5823
2 S	213131	1097		N70:05	W133:19	213210		"
3 S	213649	1067		N70:05	W133:19	213722		"
4 S	214214	1067		N70:05	W133:19	214250		"
5 S	214729	1067		N70:06	W133:18	214748		"
				N70:05	W133:18	214811		"
6 S	215317	1097		N70:06	W133:18	215339		RS5824
				N70:05	W133:18	215406		"
7 S	220021	1067		N70:06	W133:18	220055		"
				N70:05	W133:18	220121		"
8 S	221020	1097		N70:06	W133:17	221117		"
				N70:05	W133:18	221144		"

NAV TAPE ZAP398

TABLE 2. DATA CATALOGUE

Flight Date Aug. 14 SORTIE 1 Arrival 195327 Departure 211717

LINE NO.	TIME GMT	ALT.	SLICK ID	POSITION		TIME	RMK.	CCT#
				LAT.	LONG.			
1 S	195327	975M	T1	N70:04	W133:21	195334	LAID 1942	RS5746
1 1			C1	70:04	133:21	195352	LAID 1916 SPRAY 1950	"
2 SE	195848		T1	N70:04	W133:21	195904		RS5747
2 SE			C1	70:03	133:22	195927		"
3 S	200409		T1	N70:04	W133:21	200430	SPRAY 2000	RS5749
3 S			C1	70:03	133:22	200452		"
4 SW	200954		T1	N70:04	W133:21	201025		RS5751
4 SW			C1	70:03	133:22	201051		"
5 S	201537		T1	N70:04	W133:21	201610		RS5752
5 S			C1	70:03	133:21	201635		RS5758
6 S	202115		T1	N70:04	W133:21	202138		RS5771
6 S			C1	70:03	133:21	202200		"
7 S			T1	N70:05	W133:21	202722		RS5773
7 S			C1	70:03	133:21	202749		RS5774
8 S	203406		T2	N70:06	W133:21	203439	LAID 2027	RS5778
8 S			T1	70:05	133:22	203519		RS5779
8 S			C1	70:04	133:22	203544		"
9 S	204121		T2	N70:07	W133:21	204200		RS5780
9 S			T1	70:05	133:22	204245		RS5784
9 S			C1	70:04	133:22	204310		"
10 SW	204828		T2	N70:07	W133:22	204901		RS5785
10 SW			T1	70:05	133:22	204944		RS5789
10 SW			C1	70:04	133:23	205005		"
11 SW	205512		T2	N70:07	W133:22	205552	SPRAY 2050	RS5795
11 SW			T1	70:05	133:22	205632		RS5798
11 SW			C1	70:04	133:23	205659		"
12 S	210216		T2	N70:07	W133:22	210245		RS5799
12 S			T1	70:05	133:23	210325		RS5802
12 S			C1	70:04	133:23	210350		"
13 S	210851		T2	N70:07	W133:23	210930		RS5813
13 S			T1	70:05	133:23	211010		RS5815
13 S			C1	70:04	133:23	211037		"
14 S	211522		T2	N70:07	W133:22	211539		RS5821
14 S			T1	70:05	133:23	211618		RS5822
14 S			C1	70:04	133.23	211643		"
	2235		T2				SPRAY	

NAV TAPE ZAP398

Flight Date Aug. 14 SORTIE 2 Arrival 230650 Departure 004520

LINE NO.	TIME GMT	ALT.	SLICK ID	POSITION LAT.	POSITION LONG.	TIME	RMK.	CCT#
1 S	230650	975M	T2	N70:08	W133:25	230720	SPRAY 2050	RS5728
1 S			T1	70:06	133:26	230750	SPRAY 2235	"
1 S			C1	70:05	133:26		SPRAY 1950	"
2 SE	231335		T2	N70:07	W133:24	231405		RS5728
2 SE			T1	70:06	133:25	231437		"
2 SE			C1	70:05	133:27	231500		"
3 S	232022		T2	N70:07	W133:25	232050		RS5729
3 S			T1	70:06	133:25	232122		"
3 S			C1	70:04	133:26	232145		"
4 S	232717		T2	N70:07	W133:26	232740		RS5729
4 S			T1	70:06	133:26	232809		"
4 S			C1	70:04	133:26	232837		"
5 SW	233355		T2	N70:07	W133:25	233415		RS5732
5 SW			T1	70:05	133:26	233446		"
5 SW			C1	70:04	133:27	233510		"
6 SW	234011		T2	N70:07	W133:25	234038	SPRAY 2337	RS5732
6 SW			T1	70:06	133:26	234109		"
6 SW			C1	70:04	133:26	234136		"
7 S	234632		T2	N70:07	W133:25	234651		RS5735
7 S			T1	70:06	133:25	234719		"
7 S			C1	70:04	133:25	234748		"
8 SW	235244		T2	N70:08	W133:24	235308		RS5735
8 SW			T1	70:06	133:27	235341		"
8 SW			C1			NO COVERAGE		--
9 SW	235802		T2	N70:08	W133:25	235820		RS5736
9 SW			T1	70:06	133:27	235855		"
9 SW			C1			NO COVERAGE		--
10 SE	000302		T2	N70:08	W133:25	000327		RS5736
10 SE			T1	70:06	133:27	000400		"
10 SE			C1			NO COVERAGE		--
11 SW	000826		T2	N70:08	W133:24	000847		RS5736
11 SW			T1	70:07	133:27	000924		
11 SW			C1			NO COVERAGE		--
12 S	001415		T2	N70:08	W133:25	001435		RS5740
12 S			T1	70:07	133:25	001501		"
12 S			C1	70:05	133:26	001535		"
13 SE	002034		C	N70:10	W133:21	002053	LAID 0004	RS5740
13 SE			T2	70:08	133:24	002145	SPRAY 0018	"
13 SE			T1	70:07	133:26	002219		"
14 SE	02655		T1	N70:06	W133:28	002708		RS5743
14 SE			C1	70:05	133:27	002738		"
15 SE	003148		T1	N70:06	W133:28	003206		RS5743
15 SE			C1	70:05	133:27	003238		"
16 SE	003732		C	N70:09	W133:21	003803		RS5744
16 SE			T2	70:08	133:25	003855		"
17 S	004427		T1	N70:06	W133:29	004435		--
17 S			C1	70:05	133:28	004506		--

NAV. TAPE ZAP 399

TABLE 2. DATA CATALOGUE

Flight Date Aug. 16 SORTIE 1 Arrival 164809 Departure 174134

LINE	TIME	ALT.	SLICK	POSITION		TIME	RMK.	CCT#
NO.	GMT	(M)	ID	LAT.	LONG.			
1 SE	164809	1981	2	N70:11	W133:32	164934		RS5661
2 W	165438	1006	4	N70:05	W133:38	165517		"
			3	N70:06	W133.48	165634		"
3 ESE	170134	1006	2	N70:12	W133:52	170209		RS5662
4 W	170420	975	1	N70:14	W133:57	170503		"
5 S	170810	1006	2	N70:13	W133.53	170942		RS5663
6 E	171236	1006	3	N70:07	W133:50	171321		RS5670
7 S	171802	975	2	N70:06	W133.39	171833		RS5727
8 ESE	172607	3780	1	N70:14	W133:57	172711		"
9 NW	173208	3750	4	N70:05	W133:37	173248		"
			3	N30:06	W133:49	173330		"
10 ESE	173828	3749	3	N70:06	W133:49	173951		-
			4	N70:05	W133:37	174035		-

NAV TAPE ZAP399

Reference: W.D. McColl, R.A. Neville, C.A. Bonke and D.C. Knudsen, Remote Sensing of the Vinland Natural Gas Blowout, Proceedings of the 9th Canadian Symposium on Remote Sensing, pg. 245, 1984 .

BEAUFORT SEA OIL SPILL DISPERSANT TRIAL

J.J. Swiss and N. Vanderkooy
DOME PETROLEUM LIMITED

S.D. Gill
Canada Oil and Gas Lands Administration

R.H. Goodman and H.M. Brown
Esso Resources Canada Ltd.

INTRODUCTION

The Beaufort Sea Dispersant Trial was the culmination of a number of years of testing of oil spill dispersants to determine their effectiveness under field conditions (Gill, 1981; Gill and Ross, 1982; Swiss and Gill, 1984). The Canadian Offshore Aerial Application Task Force (COAATF) has been conducting such trials since the mid '70's and has demonstrated that effectiveness values achieved routinely under laboratory and mesoscale conditions cannot be easily duplicated in the field. The 1983 Halifax field trial, for example, was able to achieve a maximum dispersant effectiveness of only 40%, far lower than necessary to adequately protect the environment (Myers and Corry, 1984). Analysis of these results suggested that the low effectiveness values were a function of the nonhomogenous nature of the slicks and the manner in which the dispersant was applied (i.e., single pass). A direct conclusion from that trial was the belief that during an actual spill response operation, dispersant effectiveness rates could be increased significantly by the judicious application of dispersant to the thicker portions of the slick using more than one spray pass.

To test this hypothesis, the Beaufort Sea Oil Spill Dispersant Trial was conceived. The intent was to develop a plan that would more realistically simulate an operational application of dispersants. It was also decided that the dispersant would again be applied by helicopter and that the trial would be conducted in the Arctic where conditions could be expected to be more strenuous (5°C water temperature, remote location) than those encountered at more southern latitudes. The main purpose of the trial was to determine the percentage of oil that could be removed from the water's surface under simulated operating conditions. In addition, it was intended that the trial be the basis for the development of a number of operational procedures as a guide to the most effective way of using dispersants during an actual spill response.

TRIAL COORDINATION AND FUNDING

Overall responsibility for the planning and conduct of the trial rested with Dome Petroleum Ltd. under the auspices of the Canadian Offshore Aerial Applications Task Force (COAATF). The complete planning process including specific details of the trial are documented in the "Revised Operational Protocol for the Beaufort Sea Dispersant Trial," (COAATF,1986) Funding for the trial was provided by: The Environmental Studies Revolving Fund (ESRF); the Panel on Energy Research and Development (PERD); the Arctic and Marine Oilspill Program (AMOP); and the Petroleum Association for the Conservation of the Canadian Environment (PACE). In addition, materials, equipment, and logistic support was provided by EXXON, British Petroleum International, Esso Resources Canada Ltd; Gulf Canada Corporation and Dome Petroleum Limited.

TRIAL OBJECTIVES

Primary and secondary objectives for the experiment were developed as follows:

Primary

1. to determine the field effectiveness of two aerially applied dispersants under Arctic conditions;

2. to determine and test the operating parameters of a multihit dispersant application and document a strategy for applying dispersants under operational conditions so that all or most (90 - 95%) of the oil in a slick is removed from the surface of the water;

3. to define the logistic and cost requirements to support a dispersant operation in which a large percentage (90-95%) of a slick is removed from the water's surface.

Secondary

1. to obtain a long term record of dispersed and undispersed oil slicks at sea in order to determine their ultimate fate.

This paper will only address objectives 1 and 2.

TRIAL SETTING

Site and Timing

The site selected for the trial was an offshore location northeast of Esso's Arnak artificial island located in the Beaufort Sea at approximately 70°05'N; 133°22'W (Figure 1). The depth of water at this site was approximately 20 m and it was approximately 40 km from the nearest shore. In addition, the location was well outside the influence of the Mackenzie River plume in an open ocean environment.

The time window selected for the trial was August 11-17, 1986 and operations were conducted on August 11 (aborted effort) and August 14 (successful attempt).

Operating Constraints

The following weather/seastate/logistic conditions were used to make a GO/NO GO decision on a daily basis. If any of these factors were limiting, the trial was delayed until acceptable conditions prevailed:

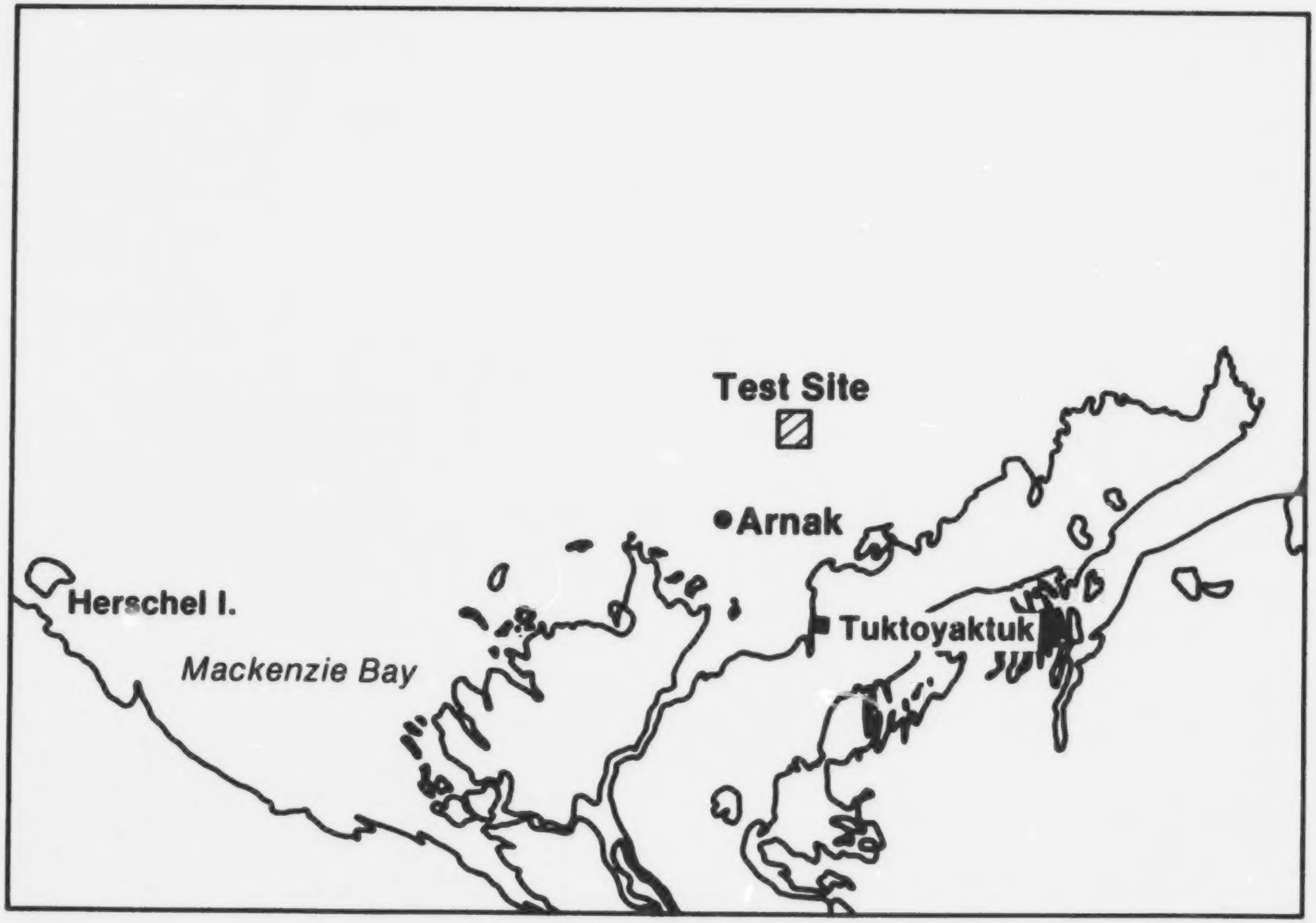
Test Site
Arnak
Herschel I.
Mackenzie Bay
Tuktoyaktuk

Figure 1

Trial Location

1. Unacceptable flying conditions
2. Less than five miles visibility at sea
3. Rain
4. Snow
5. Waves less than 0.5 m
6. Greater than 1/10 ice cover
7. Presence of wildlife in the vicinity of the trial
8. Onshore winds
9. Canmar operating constraints

Weather and Sea State Conditions

The following table provides a summary of the weather and seastate conditions that existed on the day of the trial (August 14).

Wind Direction	ENE
Wind Speed	10 - 15 knots
Visibility	24 km
Ceiling	unlimited
Significant Wave Height	1.0 - 1.5 m
Water Temperature	6°C
Air Temperature	10°C
Ice	None

LOGISTIC SUPPORT

Successful conduct of the trial would have been impossible without logistic support from Canadian Marine Drilling (Canmar), Gulf and Esso. Support was provided in the way of ships, aircraft and personnel. The details of this support are outlined in the following sections and depicted in Figure 1a.

Ship Support

Offshore Supply Vessel

The major marine support for the trial was supplied by Canmar's *Tugger 1*. This ship is an ice-strengthened seagoing tug 35.86 m in length and 10.36 m wide. It has a displacement of 805 tons and is rated at 3050 BHP. *Tugger 1* was used during the trial to release the oil, collect oceanographic data, provide a spill response capability if required and to act as a safety vessel and escort for the *M.V. Herschel*.

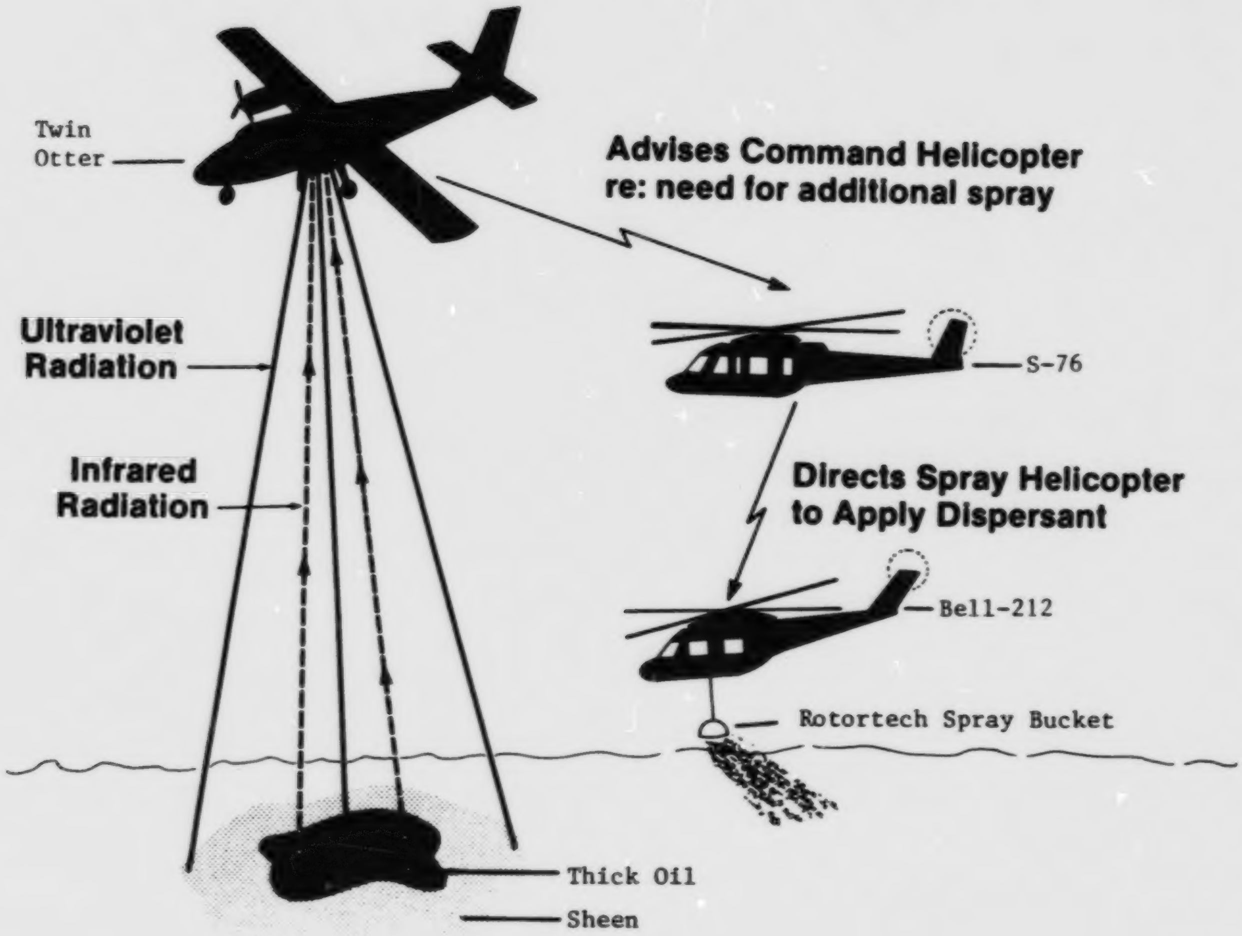
Twin
Otter
Advises Command Helicopter
re: need for additional spray
Ultraviolet
Radiation
Infrared
Radiation
S-76
Directs Spray Helicopter
to Apply Dispersant
Bell-212
Rotortech Spray Bucket
Thick Oil
Sheen

FIGURE 1a: Equipment and Technique used to Apply Dispersant.

M.V. Herschel

The M.V. Herschel was provided through contract with Gulf Canada Corporation. This vessel was to be used as a platform for the EPS towed fluorometer. Unfortunately, wave conditions on site and the design of the fluorometer combined to damage the unit and no subsurface fluorometric data were collected.

Aircraft Support

Bell 212

The Bell 212 helicopter was supplied under contract by Gulf Canada Corporation as the spray aircraft. A similar arrangement was also in place with Esso Resources Inc. and had the trial taken place on another day, the spray helicopter would have been provided by Esso.

The role of the spray aircraft was to pick up a full spray bucket from Esso's Arnak Island, transport it to the spill site and, under the direction of the command helicopter, apply dispersant to the slicks.

Sikorsky S-76

The command helicopter supplied under contract by Dome was a Sikorsky S-76. Although originally viewed as being larger than necessary for the job, it was proven to be a very suitable aircraft. Not only did it act as the command platform from which operational direction was provided, but it was also able to provide a vantage point for the Ocean Dumping Inspector and the Hunter's and Trapper's Association (HTA) representative. Two additional observers were also able to get a first hand view of the operation from this aircraft.

The function of the aircraft was to provide a location from which direction could be given for discharging the slicks, applying the dispersant and sampling the subsurface water column with the towed fluorometer.

Twin Otter

The Twin Otter used in the trial was contracted from Ken Borek Airlines Ltd. It's main function was to act as a platform for remote sensing activities, but it was also used to do the initial wildlife survey prior to the trial and as an advance aircraft to check weather conditions at the site prior to mobilizing the entire fleet of aircraft. This aircraft was outfitted with the remote sensing gear (see page 8). It was mobilized in Inuvik prior to the trial, and spent the week of the trial on standby in Tuktoyaktuk.

Falcon

The fourth aircraft involved in the trial was the Canada Centre for Remote Sensing Desault Falcon. It provided infrared and ultaviolet remote sensing support.

Spray System

The spray system used during the trial was the Rotortech Limited TC-3 underslung spray bucket. It consists of a 680 litre fibreglass bucket, a gasoline engine, centrifugal pump, fuel and spray booms. Dispersant was carried in the bucket and pumped to the spray booms when dispersant was required. Switches for starting the engine and turning the spray booms on and off were located on a small control box situated in the cockpit of the helicopter. The bucket was attached to the aircraft hook and a simple plug-in arrangement was used for the switch connections.

Two spray buckets were used for the trial. This was done to provide back-up in case of mechanical failure. They were on loan from East Coast Spill Response Incorporated (ESRI) in St. John's Newfoundland.

MATERIALS AND METHODS

The original experimental design for this trial is described in detail in the 'Revised Operational Protocol for a Beaufort Sea Dispersant Trial', July 3, 1986 (COAATF, 1986). This protocol was prepared by COAATF and served as the working document by which the trial was conducted. Because of weather and mechanical problems at the time of the trial, the original experimental design had to be modified. The revised design is described below.

Experimental Design

The trial was conducted from three locations: 1) Esso's ARNAK artificial island (Figure 1) where the dispersants were stored and loaded; 2) the test site approximately 10 km northeast of Arnak; and 3) Tuk Base/Airport which was the operational centre and home base for aircraft support, respectively.

The basic components of the trial are outlined out as follows:

- The experiment took place on August 14, 1986.
- Two dispersants (Exxon's experimental product CRX-8 and British Petroleum's Enersperse 700) were tested.
- The test oil was Alberta Sweet Mixed Blend weathered to remove 15-20% by volume.
- Four slicks were released (2.5 m^3/slick) approximately two kilometres apart.
- One slick (C) was an unsprayed control with no dispersant applied. The second slick (C_1) was a control sprayed once with Enersperse 700 applied at a nominal ratio of 1:10 dispersant to oil. The third slick (T_1) was a test slick and was sprayed three times with Enersperse 700. The fourth slick (T_2) was also a test slick and was sprayed three times with CRX-8.

- During the first spray passes of the test slicks, the entire slick was sprayed. They were then monitored by the remote sensing aircraft and after a period of time any remaining thicker lenses of oil were resprayed. This procedure was repeated until most of the oil had been dispersed (as determined by infrared imagery). A diagramatic representation of this procedure is shown in Figure 2.

- Effectiveness was monitored by remote sensing aircraft and judged on the basis of disappearance of "thick" ($>$ 100 μm) lenses of oil.

Oil Discharge

The discharge of the oil was one of the most crucial operations for the success of the trial. The slick size had to be optimized for sampling, remote sensing and, most importantly, dispersant application by the careful release of the oil.

The discharge of the oil took place while the vessel (Tugger 1) was moving at the slowest possible speed upwind. Discharging while steaming upwind eliminated the possibility of the vessel being oiled and improved the chances of controlling the slick geometry.

Ten cubic metres of oil was carried on the aft deck of Tugger 1 in three pressurized tanks that had been constructed to form three separate 2.7 m^3 storage sections. Once the oil was placed into these tanks, the tanks were pressurized to a small degree (less than 240 Pa) using compressed air. This pressurization aided the movement of oil from the tanks through the floating hoses and onto the sea surface. In addition, a small pump was placed in-line between the tank and the hose to increase the speed at which the oil could be pumped onto the surface of the water.

In order to minimize propwash effects and oiling of the discharge vessel, the hose was deployed from the side of the aft deck of Tugger 1 through the scuppers. The use of a 10 m length of hose permitted the end of the hose to trail slightly astern of the vessel. Once released, the oil was allowed to spread for approximately 20 minutes prior to initiation of dispersant spraying.

Dispersant Application

Based on a series of trials undertaken by COAATF in 1981, an S-76 helicopter flying a Rotortech TC-3 bucket at a height of 8 to 25 m was shown to create a dispersant swath some 15 m wide. It was assumed that a similar swath width and droplet density would be achieved using the Bell 212 aircraft.

Using the design dispersant to oil ratio (1:10), 250 L of dispersant are required to make one complete spray pass; however, considering the possible dimensions of the slick to be dispersed (approximately 150 m x 150 m) and the appropriate flying speeds for the dispersant helicopter (80 knots = 40 m/s), it was assumed that 20

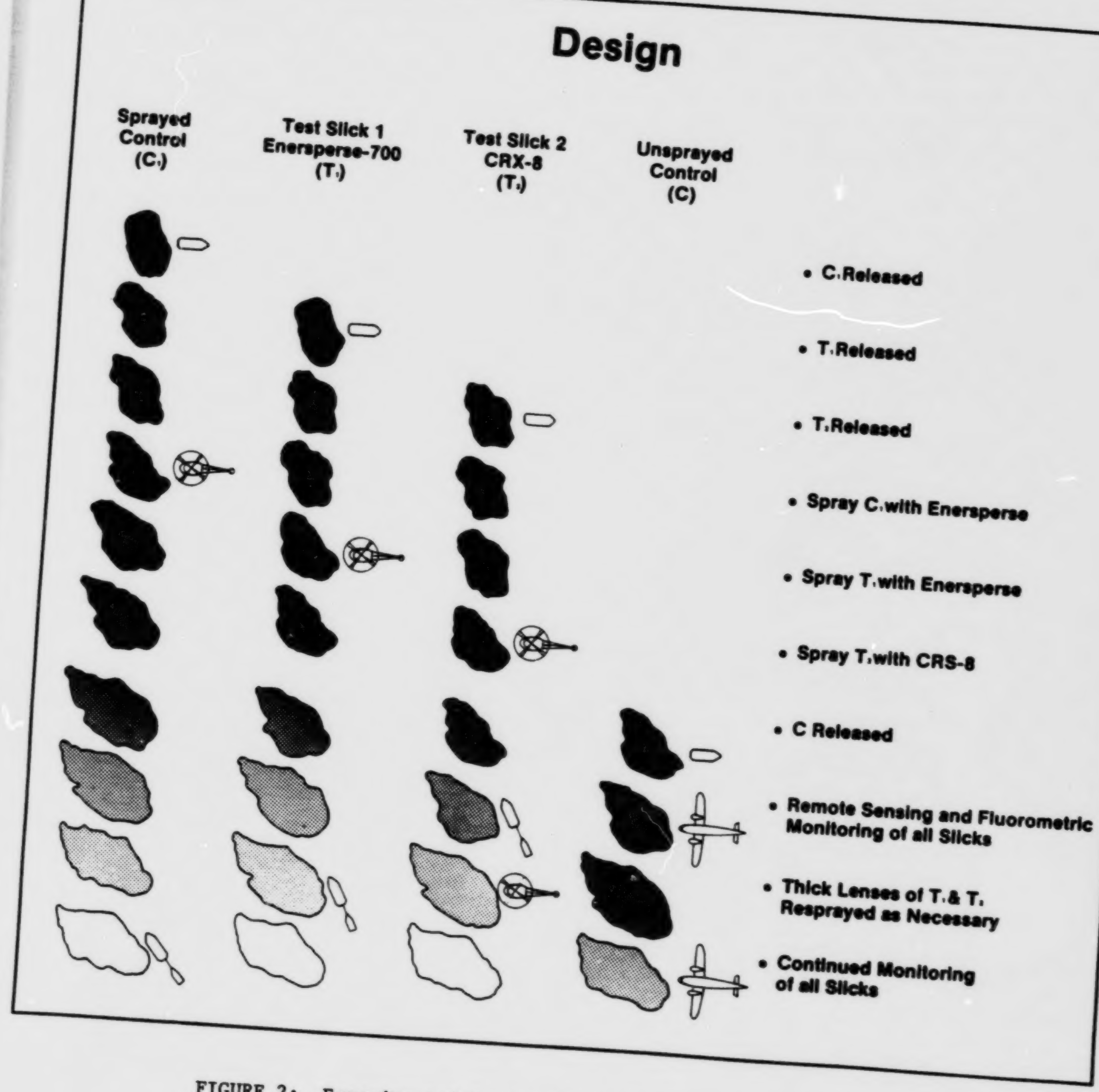
Design
Sprayed Control (C_1)
Test Slick 1 Enersperse-700 (T_1)
Test Slick 2 CRX-8 (T_2)
Unsprayed Control (C)
• C_1 Released
• T_1 Released
• T_2 Released
• Spray C_1 with Enersperse
• Spray T_1 with Enersperse
• Spray T_2 with CRS-8
• C Released
• Remote Sensing and Fluorometric Monitoring of all Slicks
• Thick Lenses of T_1 & T_2 Resprayed as Necessary
• Continued Monitoring of all Slicks

FIGURE 2: Experimental Design Used in Dispersant Trial

to 35% of the dispersant would not hit the desired target (the thick portions of the slick). Therefore, to more accurately simulate an operational application of dispersants, a full load of dispersant (416 L) was carried in the bucket.

The helicopter picked up full spray buckets from Arnak when additional dispersant was required. Since two buckets were available, there was always a full one awaiting pick-up. The total quantity of dispersant (in litres) remaining in each bucket, after each bucket exchange was completed, was measured and recorded. No dye was added to the dispersant.

The helicopter was advised to fly with the bucket at an altitude between 10 and 15 m and a forward speed of approximately 150 km/h. The dispersant was applied via the 10 m spray bar with the pump at full speed. During the initial dispersant application the helicopter made parallel passes upwind over the slick commencing at one side of the slick. Spray overlap was avoided as much as possible. During subsequent passes, the helicopter was directed to spray only the thicker lenses of oil remaining in the test slick. Each pass of the dispersant helicopter was coordinated by the command helicopter.

Evaluation of Dispersant Effectiveness

Remote Sensing

Unlike previous trials, which relied heavily on water column sampling, this experiment used a remote sensing aircraft as the prime method for determining dispersant effectiveness. This approach had a number of advantages as follows:

1. It reduced the need for people in small boats, and therefore relaxed the restriction on upper wave heights allowing the trial to be conducted under more realistic conditions;

2. It eliminated the requirement for a large chemical analysis component which is both time consuming and costly;

3. It focused attention on removal of oil from the water's surface (the prime concern) and deemphasized the need for measuring extremely patchy concentrations of oil in the three dimensional water column; and

4. Remote sensing provided almost immediate feedback to the command helicopter which was essential for determining the need for additional application of dispersant and for determining when the desired level of dispersion was reached.

The remote sensing program had three functions: 1) to monitor the slicks during the spray period; 2) to determine the percentage of oil removed from the water surface and provide the information to the command aircraft; and 3) to locate and evaluate the slicks after they had drifted for 12 to 48 hours.

The program used an imaging IR/UV system mounted in a Twin Otter aircraft (Goodman, 1985). The UV channel was used to define the extent of the sheen, while the IR channel defined the areas of thick oil.

The flight altitudes ranged from 300 m to 2000 m above sea level. As the slick increased in size, it was necessary to increase the altitude to cover the total slick in one image. The output of the IR camera was fed into an airborne image analyzer (Compuheat VIPS 300C), which calculated the area of the thick part of the slick. This area, and the location of the thicker lenses within the slicks, were transmitted to the command helicopter, which used the information to guide the spray helicopter (Fitch et al, internal report to Dome).

In addition to the real time analysis, the oil slick images and navigational information from the aircraft were recorded on a 3/4" video recorder. The 3/4" tapes were analyzed after the trial using a spectral data analyzer located in Calgary. The unit performed a density slicing function and provided integrated areas of both the thick lenses and thin sheens as a function of time.

On the day after the trial, the aircraft was used to find any remnants of the slicks. The probable locations of the slick's remnants was determined through trajectory modelling.

Water Column Sampling

As mentioned previously, water column hydrocarbon sampling was to be done at a much reduced scale compared to previous studies. Only one sampling vessel was deployed (M.V. Herschel) and attempts were made to sample both test and control slicks.

The sampling system was Environment Canada's towed fluorometer (Fingas, 1986). This system consists of a modified TURNER flo-through fluorometer which was pulled behind the Herschel. The in-water components of this sampling system are streamlined to facilitate manoeuvring of the vessel.

The fluorometer was to be towed at a depth of 1-3 m beneath each slick to produce a continuous record of subsurface oil concentrations. The initial pass through each slick was to be along the longitudinal axis with a second pass perpendicular to the first at the centroid of the slick. Passes were to be made beneath the two control slicks (C and C_1), once near the start of the operation and once near the end. The test slicks (T_1 and T_2) were to be sampled as many times as possible during the operation.

Data was to be recorded on a Compaq computer system to provide a continuous record of the concentration of oil (in ppb) along the sampling path. These data were to be analyzed after the trial and a data report produced for incorporation into the overall project report.

Unfortunately, the fluorometer was damaged at the outset of the trial and no data were collected.

Oceanographic Data

Background information describing the oceanography of the test site was provided by operators working in the vicinity. This information was supplemented by measurements taken on-site by the crew of Tugger 1. The data produced by these two sources were used for making daily decisions on the conduct of the trial and to interpret the dispersant effectiveness information collected during the trial.

Weather Forecasting and Trajectory Modelling

Weather and seastate forecasting for the trial was provided by the Beaufort weather office. Forecasts were initiated three days prior to commencement of the trial and were provided every six hours. They included 12, 24, 36 and 48 hour forecasts with outlooks to 96 hours. A weather briefing was held at the Operations Base at 0700 and 1900 daily. An oilspill trajectory model (Esso/AES) was used to predict the slick size and oil centroid location at 6, 12, 18, 24, 36 and 48 hours after an assumed release time. This information was used to predict the movement of the slicks for the purposes of the go/no go decision, to assist the remote sensing aircraft in monitoring the remnants of the slicks and to verify the accuracy of the Esso/AES model.

RESULTS

This section includes a description of the initial release and spreading of the oil; application of dispersant; visual observations of dispersant effectiveness; and a real time evaluation of dispersant effectiveness using infrared imagery. A post operational evaluation of effectiveness using infrared and ultra violet imagery is underway, but is not part of this paper.

Oil Discharge and Spreading

The decision to proceed with the trial was made at approximately 1000 LT (Local Time) on August 14th. All personnel were notified and advised to congregate on-site. Table 1 summarizes information on the release of the 4 slicks.

TABLE 1

SUMMARY OF DATA FOR RELEASE OF FOUR SLICKS ON AUGUST 14

Slick	Code	Time of Release (LT)	Location	Pumping Time	Orion Buoy #	Thick Oil Area after Spreading
Unsprayed Control Slick	C	1804	70°08'30"N 133°23'00"W	2 min 50 sec	2	790m^2
Sprayed Control Slick	C1	1216	70°02'24"N 133°22'00"W	2 min 45 sec	4	1600m^2
Enersperse Test Slick	T1	1242	70°04'00"N 133°22'00"W	2 min 15 sec	5	1870m^2
CRX-8 Test Slick	T2	1427	70°06'06"N 133°23'12"W	2 min 45 sec	6	750m^2

Dispersant Application

The number of spray passes made for each slick varied and was dependent on the size and shape of the thick oil lens and the decisions of those in the command helicopter regarding the need for additional spray. Since there was no attempt to collect spray droplets at sea level, the dispersant to oil (D:O) ratio was calculated based on the amount of dispersant used for each spray sortie (ie. the initial bucket load minus the amount remaining after spraying.) Although this approach would be less than desirable if the intent was to do a rigarous evaluation of various dispersant to oil ratio's, it is completely in line with the prime objective of the trial which was to evaluate the effectiveness of an operational application of dispersant.

The type and amount of dispersant sprayed on each slick and the cumulative D:O ratio after each spray pass is shown in the following table. Calculations of the D:O ratios were based on the assumption that the total amount of oil available for spraying was 2,500 L (2.5 m^3) and that all of the sprayed dispersant contacted oil.

Table 2 Amount of Dispersant Sprayed on each Slick

Slick	Spray Pass	Dispersant	Amount Sprayed	Cumulative Dispersant to Oil Ratio
C_1	1	Enersperse 700	261 L*	1:9
T_1	1	Enersperse 700	261 L*	1:9
	2	Enersperse 700	409 L	1:3.5
	3	Enersperse 700	364 L	1:2
T_2	1	CRX-8	273 L	1:8
	2	CRX-8	559 L	1:3
	3	CRX-8	409 L	1:2

* Assume 50% of first load applied to each slick.

These values are of course over estimates of the actual dispersant to oil ratios. Because some of the dispersant would probably evaporate en route to the slick, miss the slick entirely, or pass through the oil into the water, the actual D:O ratio would be somewhat less than those calculated above.

Visual Observations

Visual observations of the trial were carried out both from the air and from the surface of the sea. These observations provide insight into the effectiveness of the two dispersants and to the mechanisms operating during the post spray periods.

In all cases, the oil spread after initial release to form large 'tear drop' shaped slicks that became aligned with the prevailing wind (ENE). This took approximately 20 minutes a allowed the slicks to stabilize prior to spraying.

The initial spray passes for all three treatments produced similar visual effects. After these first applications, an obvious coffee coloured cloud of dispersed oil developed which seemed to be at or under the surface of the sea and which tended to remain at the upwind end of the slicks as time passed. In addition, definite lenses of thick oil remained on the surface of the water and moved down wind from the clouds of dispersed oil. This effect was observed on both previous COAATF Trials (Gill and Ross, 1982; Gill et al, 1985).

When the thick oil lens of the T_1 slick was sprayed a second time with Enersperse 700 there was a very dramatic increase in the quantity of dispersed oil. In this case, the size and intensity of the cloud was much greater than that observed in the initial spray passes. This effect was not noticed for the third Enersperse 700 pass nor for either of the second or third CRX-8 spray passes. In these cases, there was additional dispersed oil present, but the increase was far less dramatic than for the second T_1 spray and was similar to the results observed for the initial spray applications of Enersperse. As with the initially observed dispersed oil, the submerged clouds gradually became less intense and tended to stay at the upwind end of the remaining surface slicks. A dispersed oil cloud was not observed in the unsprayed control slick.

On the water's surface, another phenomenon was observed. In addition to the clouds of emulsified oil that were observed from the air, the sea surface observers also reported a large number of 'grape-sized' balls of oil which covered the surfaces of the sprayed slicks. These 'balls' have been variously referred to as 'herdy balls' 'pea floc' and 'emulsion balls' and have been observed in previous offshore trials (Fingas, Personal Communication and Bocard, Personal Communication). The term emulsion balls will be used throughout the rest of this paper.

Since no sea surface observations of slick C were made, the emulsion ball effect was not observed in the unsprayed control.

Although attempts were made to collect samples of these emulsion balls, it was found that upon being touched, they burst apart leaving no remnants of the original structure.

Real Time Analysis

The real time analysis of the infrared images produced by each slick provided an indication of the areas of thick oil within each of the four slicks. Post trial analyses of the data collected in the field was carried out to minimize any possible error in field calculations. These calculations are shown in Table 3. The decrease in area of thick oil in each slick was calculated as a percentage reduction over time. These values were plotted against time after initial release and are shown in Figure 3. The points at which dispersant was applied are also shown in this figure.

Table 4: Real Time Slick Area Calculations

Slick C		Slick T_1		Slick T_2		Slick C	
Area(M^2)	Elapsed Time	Area(M^2)	Elapsed Time	Area(M^2)	Elapsed Time	Area	Elapsed
755		755		680		791	
796	:03	1874		835	:04	734	:04
1031	:07	SPRAY 1	:02	751	:09	398	:20
1570	:10	1040	:08	749	:14	365	:25
1748	:13	1068	:12	SPRAY 1	---	168	:51
1690	:16	1030	:15	795	:19	180	1:18
1697	:20	1103	:28	721	:24	299	1:21
1608	:24	1142	:32	752	:42		
SPRAY	:30	926	:52	792	:46		
1704	:42	764	:56	670	1:11		
1059	1:02	728	1:00	835	1:15		
794	1:15	723	1:16	SPRAY 2	2:58		
928	1:18	692	1:20	425	3:00		
751	1:42	754	1:24	401	3:04		
778	1:46	706	2:06	361	3:27		
857	1:50	649	2:12	236	3:39		
668	2:07	SPRAY 2	2:30	317	4:13		
589	2:11	633	2:37	220	5:30		
535	3:05	351	2:42	SPRAY 3	5:44		
533	3:10	437	4:31	242	5:47		
179	5:45	227	4:46				
		269	4:58				
		71	5:21				
		94	5:28				
		SPRAY 3	5:30				
		160	5:53				

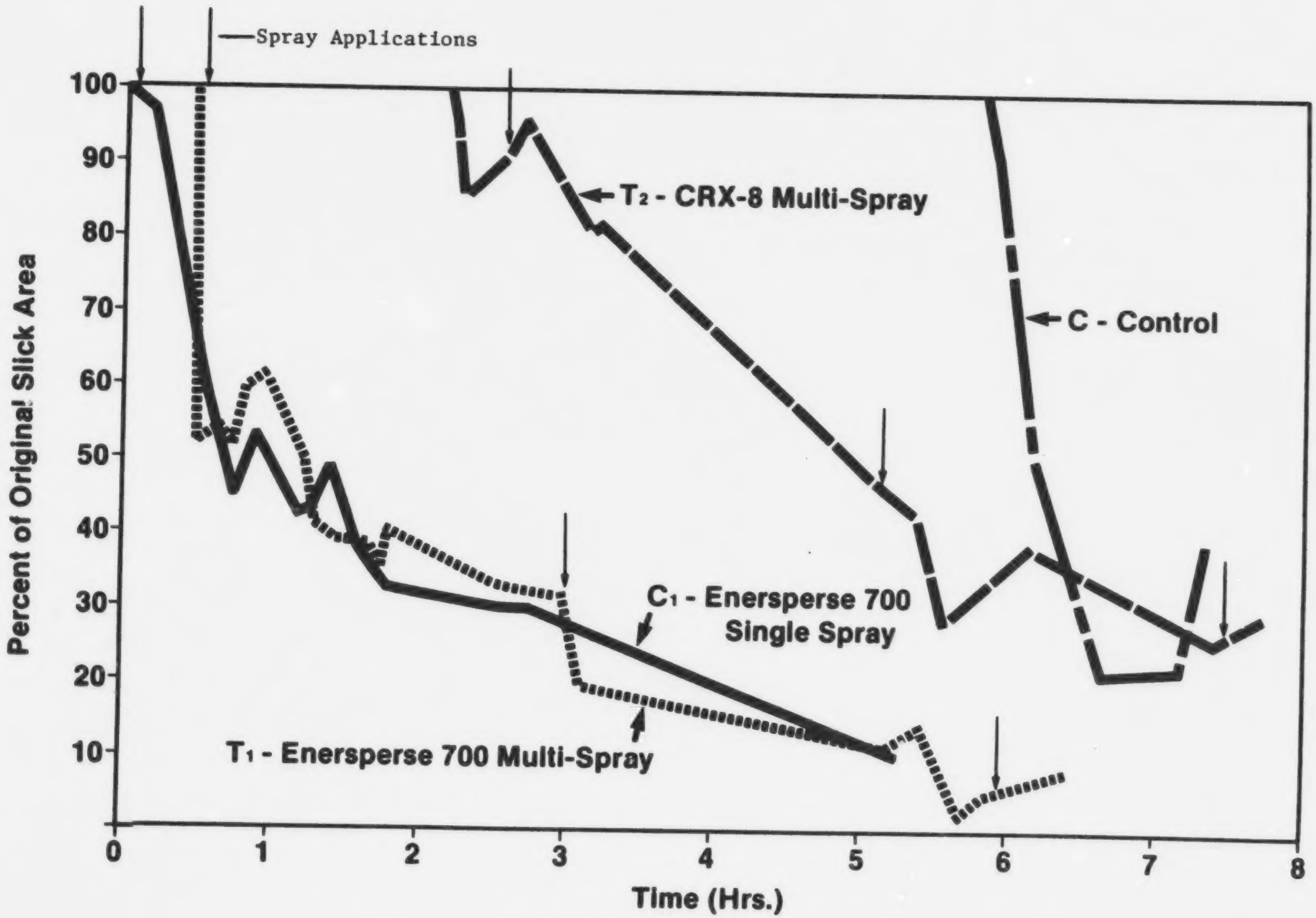

Figure 3

Change In Slick Area Over Time

Analysis of figure 3 indicates that 50 percent reductions in areas of thick oil occurred at approximately 40 and 50 minutes respectively for slicks C_1 and T_1. The reduction to 50% of initial thick area for the T_2 slick took approximately three hours. In contrast the 50% reduction in thick oil areas for the unsprayed control slick (C) was achieved in only 15 minutes. Over the five to six hour period of the trial, the C_1 and T_1 slicks were reduced by approximately 90% while the T_2 and C slicks attained maximum reductions of 75% and 80% respectively; the reductions in C occuring in less than one hour.

It is interesting to note that the dramatic visual effect described in the previous section, immediately after slick T_1 was sprayed a second time with Enersperse 700, can be seen in the graph of area reductions in figure 3. On this graph, the second spray of T_1 is shown at three hours and immediately after this spray there is a sharp reduction in area of approximately 12 percent over a period of seven minutes.

No further data were collected on the day of the trial, however the remote sensing aircraft returned to the vicinity of the trial on the next day and found remnants of all four slicks. At this time most of the slicks were visible only as a sheen although a small amount of thick oil was also observed. A final reconaissance by the CCRS jet occurred on August 16 and only sheen was observed.

Discussion

It is difficult to imagine applying more dispersant to a slick than what was applied to test slicks T_1 and T_2 in this trial. The nominal dispersant to oil ratio for these two slicks after three spray passes was approximately 1:2. Even if the assumption is made that half of the sprayed dispersant did not reach the desired target then the D:O ratio would still be in the order of 1:4; far more than is theoretically necessary to completely disperse the slicks.

As in previous experimental spills, (COAATF, 1986-1983; Bocard 1987) the visual observations of this trial support the belief that significant dispersion was occurring upon application of the chemicals. After each spray pass, in all three slicks, the formation of a coffee coloured dispersed cloud was observed. This effect was most dramatic after the second spray of Enersperse 700 on slick T_1. These visual observations would lead the observer to the conclusion that a significant amount of oil had been dispersed. The fact that the second application of dispersant produced such a marked effect also indicates that there was significant oil left on the surface after the first spray pass which had not interacted with dispersant. This view is also supported by the fact that there were obvious lenses of thick oil left on the surface of the water even after three spray passes had been completed.

The presence of the emulsion balls on the surface of the water in the sprayed slick suggests that some mechanism other than dispersion was at work. It is possible that treated oil rather than going directly into the water column formed emulsion balls instead. Some initial laboratory work done after the trial suggests that these balls form only in the presence of dispersant and are a water-in-oil-in-water emulsion. (TANG, Personal Communication)

Initial comparison of the real time curves of thick oil area reduction does not provide a covincing argument for the use of dispersant as a countermeasures technique. Although all three treated slicks seemed to quickly diminish in size after being sprayed, the unsprayed control slick exhibited an even greater rate of reduction than the treated slicks. It would be tempting to dismiss the control slick because it was released in a manner different than the treated slicks and at a time when the wave energy was considerably higher (1.5 m vs 1.0 m). However, two unsprayed slicks which were released properly and at lower sea states earlier in the week exhibited similar reductions in thick oil area with time.

It doesn't seem logical that the unsprayed slick should disperse more quickly than the sprayed test slicks. Two possible explanations for this discrepancy are: 1) The oil lost from the thick area of the control slick was bleeding into the surrounding sheen whereas the sprayed slicks were actually being dispersed; or 2) The creation of the emulsion balls retarded the dispersion process in the sprayed slicks. It is unclear how these balls would appear to the infrared detector, but since they contained considerable oil and floated at the water's surface (Fingas Personal Communication) it is probable that they would appear to the detector as thick oil. Since these balls readily broke apart upon contact it is possible that over a period of time they would release their oil to the sea in the form of dispersed oil.

A further point worth noting is that the single treatment with Enersperse 700 seemed to be as effective as the multiple Enersperse spray and somewhat more effective than the CRX-8 multi-spray.

Based on the foregoing, no strong conclusions on the efficacy of using dispersants as a countermeasures tool can be drawn. Although it is clear that some type of dispersant action occurred when the slicks were sprayed; it is unclear why the sprayed slicks did not dissipate more quickly than the control nor why the addition of more dispersant, achieving very high D:O ratios, didn't increase the observed effect.

The results of these trials are similar to others conducted around the world (Nichols and Parker, 1985). In most cases there is a strong visual sense that slicks react rapidly and dramatically to the application of the dispersant. However, the subsequent data analysis do not confirm the visual observations. In these experiments, the rate of reduction of surface oil for the control slick was as rapid or more rapid than for the sprayed slicks.

Is this an artifact of the remote sensing? It is assumed that the thickness of the oil varies with time in the same manner for both treated and untreated slicks. This may not be true! The wave heights were slightly larger during the later part of the day; the solar heating was less. These are possible reasons for the observations to be in error, but there is inadequate data to calculate the magnitude of the errors involved.

There are clearly many unresolved problems in terms of the interpretation of remote sensing data including: the effect of emulsion balls, the correction for solar input energy variation with time and the cause of the different temperature regions found in the slick.

While the results of the experiment do not provide conclusive data on dispersant effectiveness, it is clear that from visual observations these chemicals do enhance initial dispersion of oil at sea. There is still much to understand of the processes involved. Until there is an adequate technology to obtain a true and complete mass balance, the field measurements of dispersant effectiveness will have a very large error and uncertainty. A combination of laboratory and wave basin experiments are needed to develop these measurement techniques.

CONCLUSIONS

1. It is logistically possible to conduct an aerial dispersant operation in the Arctic.
2. Alberta Sweet Mixed Blend (ASMB) can be dispersed at relatively low water temperatures (6°C).
3. The thick areas of the unsprayed control slick became smaller much more quickly than anticipated.
4. The interpretation of the infrared data is more complex and difficult than anticipated.
5. Further analysis is required to properly interpret infrared imagery of dispersed slicks.

Acknowledgements: The authors would like to express their gratitude to the funding organizations, the companies supplying logistic support and materials, and to the many individuals who participated in this project.

REFERENCES

1. Bocard, Personal Communication

2. Bocard, C., G. Castaing, J. Ducreux, C. Gatellier, Protecmar: The French Experience From a Seven Year Dispersnat Offshore Trials Program. Proceeding of the API Oilspill Conference, Baltimore MD. 1987.

3. Canadian Offshore Aerial Applications Task Force, The Effectiveness of Three Aerially Applied Dispersants in a Offshore Field Trial, COOSRA final report January, 1986.

4. Canadian Offshore Aerial Application Task Force, Revised Operational Protocol for the Beaufort Sea Dispersant Trial, Dome Petroleum Ltd. Calgary, Alberta, 1986.

5. Fingas, M. Personal Communication

6. Fitch, R.C., R.L. Wheatley, and J.E. McComiskey, Beaufort Sea Dispersant Trial Remote Sensing: Determination of Dispersant Effectiveness, Internal Reports to Dome Petroleum Ltd. September, 1986.

7. Gill, S.D., The Sulfield Trial of Aerially Applied Oil spill Dispersants, PACE Report Nv. 81-6, 1981.

8. Gill, S.D. and C. W. Ross, 1981 Dispersant Application Field Trial, St. John's Newfoundland, AMOP Technical Seminar Proceedings, Edmonton, Alberta, 00255-263, 1982.

9. Gill, S.D., J.J. Swiss, and R.H. Goodman, Halifax '83 Sea Trial of Oil Spill Dispersant Concentrates. Proceedings of the API Oil Spill Conference, Los Angeles Ca., 1985.

10. Goodman, R.H. and J.W. Morrison, A Simple Remote Sensing System for the Detection of Oil. Proceedings of the API Oil Spill Conference, Los Angeles Ca., 1985.

11. Myers, R.D. and K. Corry, Surface and Subsurface Hydrocarbon Concentrations Measured During an Offshore Dispersant Trial, AMOP Technical Seminar Proceedings, Edmonton, Alberta, 1984.

12. Nichol's, J.A. and H.D. Parker, Dispersants: Comparison of Laboratory Tests and Field Trials with Practical Experience at Spills. Proceedings of the API Oil Spill Conference Los Angeles Ca., 1985.

13. Swiss, J.J. and S.D. Gill, Planning, Development and Execution of the 1983 East Coast Dispersant Trials, AMOP Technical Proceedings, Edmonton, Alberta, 00443-453, 1984.

MID-SCALE TESTING OF DISPERSANT EFFECTIVENESS

R. Belore

S.L. Ross Environmental Research Limited
Ottawa, Ontario

INTRODUCTION

Ever since chemical dispersants were produced to treat offshore oil spills, many have attempted to develop a simple laboratory test with which to predict their effectiveness under actual field conditions. A number of dispersant effectiveness tests are available but several reviewers have shown these to be poor simulators of the chemical dispersion process in field situations (Wells and Harris 1979, Delvigne 1982, Lichtenthaler and Daling 1983, Nichols and Parker 1985, and Fingas 1985). Reasons for inconsistent results between the various effectiveness tests and shortcomings in testing procedures have been analysed in some detail by these reviewers.

The problem with most tests is that, in trying to keep them simple, inexpensive, and short, several key elements that are known to be crucial to the dispersion process in the field have been compromised.

The purpose of this project was to develop a mid-scale test for dispersant effectiveness that would incorporate all factors believed to be important in field applications. The result would be a more accurate simulation of the offshore dispersion process, and would permit a realistic evaluation of dispersant effectiveness prior to expensive offshore tests. Ideally, the need for such tests might actually be obviated.

LITERATURE REVIEW

A quantitative comparison of results from the various, existing dispersant effectiveness tests was not performed in this study because other researchers have shown convincingly that such a comparison yields little valuable information (Nichols and Parker 1985). However, an extensive review of published literature on dispersant effectiveness testing, dating back to the 1970s, was undertaken to identify the essential components of the tests and the many problems and successes that have been encountered.

KEY FACTORS IN THE SIMULATION OF CHEMICAL DISPERSION PROCESS

Four main processes or events must be considered when attempting to simulate the chemical dispersion of marine oil spills:

a) The oil is spilled and spreads and ages prior to the application of dispersant.
b) The dispersant is applied in a spray form to the surface of the oil slick and interacts and mixes with the oil-and-water system.
c) Natural wind and wave mixing energy (or artificial mixing by breaker boards, high-pressure water, propeller wash and so on) breaks the slick into an oil dispersion comprising a range of drop sizes.

d) Smaller droplets are entrained into the water column; larger drops eventually re-surface and re-coalesce if the ocean's turbulence is insufficient to retain these within the water mass.

The mid-scale test used in this study can address all but the last of these processes. The tank surface is large enough to generate realistic oil slicks (at least the thick portion of an actual oil slick can be simulated in the large test tank). Dispersant application can be made by full-scale spray booms similar to those that would be used during a ship based dispersant spraying operation. Wind and wave mixing is also possible through the use of wind tunnels and wave paddles. Although accurate simulation of oceanic diffusion or the movement of the oil once dispersed is not possible in tests of this size, the mid-scale test does move a few steps closer to simulating more realistically an actual offshore dispersant operation when compared to shaker or even hoop-tank scale experiments. By incorporating more realistic slick behaviour, dispersant application methods and surface mixing energy it is hoped that a more accurate prediction of dispersant effectiveness in a field situation can be made in the laboratory.

DISPERSANT EFFECTIVENESS TEST DESIGN

The following is a list of the many parameters that can affect dispersant effectiveness. While not all of these may be important for a given test, they should be considered when conducting a test program and analysing the subsequent results.

Environmental conditions

- temperature of water, oil, dispersant, and air
- water salinity
- water quality (surfactant free)
- surface-mixing
- larger-scale ocean-mixing processes (not likely scaleable in a laboratory study).

Oil properties and distribution

- oil thickness
- oil distribution
    - patchiness
    - thick-to-thin area ratios
- oil properties
    - viscosity
    - density
    - wax content
    - indigenous surfactants
- oil aging
    - evaporation
    - emulsification
    - photo-oxidation.

Dispersant

- type
- dispersant-to-oil application ratio
- dispersant drop-size distribution
- dispersant fallout timing
- velocity of dispersant drops on contact
- dispersant drop spacing and coverage
- dispersant loss to water column
  - direct
  - partitioning from oil.

EXPERIMENTAL SET-UP AND DESIGN

In this section the test apparatus, measurement techniques, and test procedure selected for use in the mid-scale test are outlined.

Test Apparatus

The testing made use of a wind-wave tank that measures 11 m x 1.2 m x 1.2 m excluding the detachable overhead wind tunnel. The tank was filled to the 85-cm level during these tests. The amount of water used per test was about 11,000 litres. Figure 1 shows the tank with the wind tunnel in place. The glass viewing panels, sampling access doors in the wind tunnel, and fan are all visible in the photo. The wave paddle is located at the opposite end of the tank from the fan and is driven by a 3-hp, variable-speed D.C. motor to provide a wide range of wave energy conditions (Figure 2). Control of the wind speed is attained by simply choking off the inlet side of the fan using a perforated insert (Figure 3).

Water samples are taken from three levels in the tank through a series of tubes whose inlets are located 15 cm, 40 cm, and 65 cm below the calm water surface. One set of tubes directs water by gravity to a set of viewing cells to monitor the presence of oil in the water (Figure 4). Photographs of the oil-in-water dispersions passing through these cells are taken for subsequent determination of oil drop-size distribution. The second set of tubes is used to take water samples for subsequent oil extraction and concentration analysis.

Dispersant was applied to the oil-water surface by a full-size spray boom using conventional nozzles. The boom was mounted about 1 m above the calm water surface on a cart that traveled on a linear bearing that extends the length of the tank.

Measurement Techniques

The following data were collected during each test:

- in-water oil concentration;
- dispersed oil drop-size distributions;
- surface oil area and thickness; and
- oil-water interfacial tensions.

The methods used to determine each are outlined below.

Oil concentrations in the water were determined by extracting the oil in each of the grab samples with a colourless solvent (toluene). The quantity of oil in the solvent was then determined by a spectrophotometer.

Oil-water interfacial tensions were measured by a duNuoy ring apparatus. In this technique a small platinum ring is drawn through the water-oil-air interfaces of a sample from the test tank. The force required to pull the ring through an interface is then used to estimate the interfacial tension. The method works well for uniform, clean, non-viscous oils but encounters problems with thicker, less homogeneous products. Another problem occurs when the oil slick becomes too thin for a large enough sample to be collected for use in the test.

The mixing energy levels used during the testing program were measured after the tests were completed using a turbulence probe device provided by Environment Canada. This was developed by Canpolar Consultants (1985) for ocean turbulence measurements.

Test Procedure

The major steps taken to complete a test are outlined below.

1) The tank is filled with salt water (32 ppt) at the required temperature.
2) The dispersant application gear is readied. The dispersant reservoir is filled, the air cylinder is charged to 100 psi, the cart is positioned at the end of the tank and is connected to the drive cable, and the switches used to start and stop the dispersant spray are set.
3) The water sampling ports are opened temporarily to clear them of air and to ready them for sampling.
4) The oil is placed on the water and spread to the desired coverage and thickness.
5) A known area of oil is picked up by an oil-spill sorbent for oil thickness estimation. A pre-test oil and water sample is taken for interfacial tension determination.
6) The wind and wave action is started and the wave frequency is fine-tuned to maintain the oil in the centre of the tank at the wind speed set for the test.
7) The dispersant is applied by the motorized boom system.
8) Another set of oil and water samples is taken immediately after the application of dispersant for interfacial tension analysis.
9) At first sight of oil in the viewing cells oil drop-size photos and water samples are taken from three depths in the tank.
10) The test continues for one hour with a new set of measurements taken every 15 min. Each measurement set consists of a surface oil and water sample for interfacial tension, water samples and oil drop size photos from the three sampling depths, oil thickness samples (sorbent pads), and an estimate of the area of the surface slick.
11) After taking the samples at one hour the test is stopped and the tank is drained and cleaned for the next test.
12) The in-water oil concentration and surface slick thickness samples are analysed between sampling periods. The oil-drop size photos and interfacial tension samples are analysed in batches after a number of tests are completed.

RESULTS

Test Parameters

A total of 16 different tests were completed during the experimental program. These were intended to investigate the ability of the test procedure to determine dispersant effectiveness as a function of oil type, dispersant type, oil thickness, and mixing energy level. The variables used in the testing program are listed below.

* oil type (2) - Fresh Alberta Sweet Mixed Blend
  - aged Alberta Sweet Mixed Blend (15% loss by volume)
* dispersant type (2) - Corexit 9527
  - Enersperse 700
* oil thickness (2) - 1 mm
  - 0.5 mm
* energy level (2) - high (as defined in Belore 1987)
  - low.

Because of time and cost constraints it was not possible to carry out a more varied test matrix. It was felt, however, that this limited series would demonstrate the potential of the test set-up and procedures.

Conditions that were kept constant during the testing are listed below.
* dispersant-to-oil ratio - 1:20
* dispersant drop size - 800 μm VMD
* water salinity - 30 ppt
* water temperature - 15°C
* air temperature - 20°C.

Alberta Sweet Mixed Blend crude oil and Corexit 9527 and Enersperse 700 dispersants were used in the experimentation because of their common use in effectiveness testing in Canada. These products were also used during the 1983 offshore dispersant trial in Canada (Gill et al. 1985). This allowed comparison and validation of the laboratory results with those from a field test.

Data Collection

As stated, during each test data were collected on:
* oil-water interfacial tension;
* dispersed oil drop-size distributions;
* surface oil thickness and area; and
* in-water oil concentration.

In a separate set of tests the mixing energies used in the experiments were also evaluated.

A discussion of the general trends identified within these five data groups follows.

Mixing Energy

The mixing energies used in the study have been measured with a turbulence probe developed by Canpolar Consultants Ltd. (1985). The technique employs a space domaine measurement technique that uses a pair of fixed-velocity sensors operated in a differential mode. These sensors measure the instantaneous velocity shear in the fluid between the probes but are not sensitive to coherent water motions or to the relative motion of the sensor pair.

The probe was used to measure the turbulent energy developed in the test tank at the two mixing levels used in the study. The average values recorded by the system were 6.8×10^{-4} Joules/kg (high energy) and 6.3×10^{-4} J/kg (low energy). These values can be compared to the limited data collected in the Canpolar study where the probe was deployed next to a wharf in Conception Bay during light seas and winds and with no swell. The average turbulence values measured during this program ranged from 1 x 10^{-5} J/kg up to 8.8 x 10^{-5} J/kg. Apparently the mixing energy developed in the test tank exceeded that measured during a relatively calm period at a nearshore location by an order of magnitude. Unfortunately sufficient field data are not available to enable us to estimate the type of offshore condition which the test simulated. What these measurements do tell us, however, is that the two energy levels used in the study did not differ greatly. The probe was not available at the beginning of the testing and was, therefore not used to set the two levels of mixing energy but only to measure them after they had been established.

Oil-Water Interfacial Tension. Oil and water samples for interfacial tension measurements were taken prior to the addition of dispersant, immediately after the dispersant application, and 15 min, 30 min, and 60 min thereafter for all but two of the tests. The results were disappointing. In many cases the oil sample was not large enough for performing the interfacial tension test or was viscous and lumpy. The lumpy consistency of the sample resulted in an uneven force on the ring used in the duNuoy technique and, therefore, yielded questionable results. The only significant observation that can be made from these data is that a drop in interfacial tension was noted after the addition of dispersant and that this lowered interfacial tension persisted for at least the first half hour of the test.

Dispersed Oil-Drop Size Distributions. During every sampling period in each test, photographs were taken of the oil-in-water dispersions at all sampling depths. The oil-drop diameters in these photos were then digitized and stored on computer files for analysis. For each photograph the oil-drop size distributions were evaluated. The volume median diameters calculated for each test at each sampling depth (averaged from three data sets collected over the entire test period) are summarized in Table 1. The volume median drop diameters ranged from 60 to 100 um. As would be expected the oil drop diameters were largest at the water surface and decreased in size with depth. The larger drops are more buoyant and therefore are not driven to as great a depth. In most cases the higher mixing energy gave a slightly smaller volume median drop diameter. The difference is small likely because the two energy levels used were not drastically different. The oil drops generated in the tests using Enersperse 700 were generally smaller than those measured for the Corexit 9527 tests. The oil-drop diameters generated with the weathered oil were consistently smaller than for the fresh oil. The reason for this is not clear.

Surface Oil Slick Thickness and Area. Three samples of surface oil-slick thickness were taken prior to the addition of dispersant and about 15 minutes after the dispersant was applied and averaged to provide an estimate of oil-slick thickness. At the time that each surface sample series was taken a visual estimate of the oil coverage and overall slick extent was made to permit the estimation of the volume of surface oil present at the time of sampling. The results of this sampling and analysis were inconsistent and provided little useful information. The greatest error in the procedure was undoubtedly the determination of the total oiled area by a simple visual estimate. The patchiness of the oil slick also made it difficult to estimate average thickness by using only three samples. If estimates of surface oil quantity are to be used in future tests a more accurate method of determining the total oiled area will be required.

In-Water Oil Concentrations. Dispersed oil concentrations versus time for the three sampling depths have been plotted for all tests and these results are presented in our final report. Figure 5 has been derived from these plots and illustrates the general behaviour of the dispersion process that occurred during the testing. For most of the tests the upper sampling location recorded a high initial oil concentration but this quickly dropped off as oil diffused both to greater depth and laterally within the tank. Diffusion to greater depths is illustrated by comparing the times at which maximum oil concentrations occurred at the three sampling depths and noting the lag time that exists between peaks at successively deeper sampling points.

Lateral diffusion of oil to each end of the tank also takes place as the oil moves deeper, which further reduces the measured oil concentrations. This lateral diffusion and dilution occurs because the initial oil slick is confined to the central third of the tank and, therefore, any dispersed oil also originates in the centre of the tank. Complete lateral diffusion from a central point source was found to occur within 15 to 20 minutes.

For many of the experiments the oil concentrations throughout the tank became fairly uniform after 15 to 20 minutes but continued to increase steadily over the remainder of the test. Because of this slow but steady dispersion most of the experiments resulted in very high overall dispersion efficiencies (50-100%) over the full one hour duration of the test. It is likely that this ultimate, high degree of dispersion results from the fact that, unlike field conditions, this system is a closed one in which the dispersant is always present in the water in sufficient concentrations to maintain a low interfacial tension between the oil and the water and thus enhance dispersion over the long term.

As a result dispersant effectiveness is over-estimated if the test duration is excessive. In our mid-scale test we believed that the dispersion efficiencies measured at the 15-minute point are most indicative of the likely efficiencies of the dispersant in a field application.

TABLE 1
Dispersed oil-drop sizes:
average volume median drop diameters
(micometres)

Oil Type	**Fresh ASMB**				**Weathered ASMB**			
Oil Thickness	**0.5 mm**		**1.0 mm**		**0.5 mm**		**1.0 mm**	
Energy Level	**high**	**low**	**high**	**low**	**high**	**low**	**high**	**low**
Enersperse 700								
overall	78	79	77	100	68	68	62	74
top	97	90	82	112	80	87	71	86
middle	76	76	81	94	61	66	58	72
bottom	68	69	67	84	66	45	51	60
Corexit 9527								
overall	82	105	91	81	---	90	---	---
top	111	102	102	101	---	96	---	---
middle	66	108	99	79	---	105	---	---
bottom	66	105	73	61	---	76	---	---

--- data not collected.

Dispersed oil quantities were estimated by plotting the dispersed oil concentrations versus water depth, calculating the areas under these curves, and finally by multiplying this value by the areal extent of the dispersed cloud at the time of measurement. For the 15-min estimate of dispersion efficiency, two-thirds of the tank was assumed to be filled with dispersed oil at the concentration profile measured in the centre of the tank.

TABLE 2
Estimates of dispersion efficiency using dispersed oil concentrations (%)

Oil Type	**Fresh ASMB**				**Weathered ASMB**			
Oil Thickness	**0.5 mm**		**1.0 mm**		**0.5 mm**		**1.0 mm**	
Energy Level	**high**	**low**	**high**	**low**	**high**	**low**	**high**	**low**
Enersperse 700								
15 min	67	62	38	46	61	19	36	41
Corexit								
15 min	30	28	44	27	33	9.3	17	45

The effect of the test parameters (oil thickness, oil age, mixing energy, and dispersant type) can now be discussed based on the results of this table. There appears to be very little difference in dispersion efficiency for the two thicknesses studied. The fresh oil was dispersed slightly better than the weathered oil. The high-energy tests generally resulted in higher levels of dispersion but in many cases these were only marginal differences. The experiments with Enersperse 700 resulted in a slightly higher dispersal efficiency than that resulting from the Corexit 9527 experiments. To investigate these trends further a statistical comparison of means was undertaken to determine if there was any statistically valid difference in dispersant effectiveness for the above comparisons (Guttman et al. 1971; Spiegel 1961). The results of the analysis are shown in Table 3.

The null hypothesis assumes that there is no difference between the tested conditions. When t measured is greater than the t statistic at the desired confidence level the null hypothesis is disproven and the means are considered different. These results indicate that without question (i.e., >99.5% probability) the Enersperse 700 tests resulted in higher dispersion efficiencies than the Corexit 9527. The thick and thin slick dispersion results are essentially the same because the null hypothesis can be accepted only at the 65% confidence level.

TABLE 3
Results of statistical comparison of means

		Hypothesis	t measured	Rejection Level
1)	Ho:	$\mu_{thick} = \mu_{thin}$	0.3662	$t_{65} = 0.390$
2)	Ho:	$\mu_{fresh} = \mu_{weathered}$	1.11	$t_{85} = 1.059$
3)	Ho:	$\mu_{high} = \mu_{low}$	1.396	$t_{90} = 1.318$
4)	Ho:	$\mu_{Enersperse\ 700} = \mu_{Corexit\ 9527}$	7.567	$t_{99.5} = 2.707$

The two remaining comparisons, fresh versus weathered and high energy versus low energy, are not as definitive, but the null hypothesis for these two parameters can be accepted at the 95% and 90% level respectively. Although normal practice is to use a 95% or higher confidence level before rejecting the tested hypotheses, we know from other test programs that these parameters do affect dispersion efficiency. For this reason we are reasonably confident in assuming that the data are indeed unique and that the small differences result from the small differences in mixing energy levels and weathered states used for this testing program.

Because the thick and thin slick results are essentially from the same population these results can be averaged to simplify the presentation of the final results. The data in Table 2 can thus be reduced to the values shown in Table 4. The overall average value is included in the table as a distillation of all of the data (i.e., assumes that all of the null hypothesis of Table 3 except for dispersant type are valid).

The average results have been compared to the data collected during the 1983 COAATF dispersant trial (Gill et al. 1985) in which both Enersperse 700 and Corexit 9527 were used. As seen in the Table 4, the laboratory results for Enersperse 700 compare favourably to the offshore test results. The Corexit 9527 laboratory test results show a higher dispersion efficiency than was measured in the field. This can be attributed to the under-dosing of the oil slick in the field study.

TABLE 4
Averaged dispersion efficiencies
(% at 15 minutes)

Oil Type	**Fresh ASMB**		**Weathered ASMB**		**Overall Average**	***1985 COAATF Results**
Energy Level	**high energy**	**low energy**	**high energy**	**low energy**		
Enersperse 700	52	54	48	30	46	41
Corexit 9527	37	28	25	7	24	3.75

* Gill et al. 1985.

CONCLUSIONS AND RECOMMENDATIONS

Test Design

The equipment and procedures used during the test program generally worked well and allowed two persons to conduct each test without difficulty. The following modifications to the test procedure and equipment are recommended to improve the test design.

1) This test should be shortened to 15 minutes because dispersion after this time likely results from the presence of dispersant in the water rather than from dispersant in the oil. In an ocean environment dispersant quickly diffuses away from the upper water layers and no longer affects the dispersion of oil. If this laboratory test lasts longer than 15 minutes unrealistically high dispersion efficiencies will likely result. A longer test could be used if the tank's water were continually diluted with dispersant-free water but this would be difficult with the large tank volume used in the study.
2) Water samples for measuring oil concentration should be taken at more locations in the tank to provide more accurate oil mass balance and dispersion efficiency determinations.
3) The fan used for the wind tunnel should be controlled by a variable-speed motor to permit the generation of a wider range of wind speeds. Because the wind is used to hold the oil in the centre of the tank (by opposing the movement due to waves) a wider range of wind speeds would also allow the tests to be carried out over a wider range of wave energies.

Test Measurement Methods

The techniques used to measure oil concentration in the water column and dispersed oil-drop size distribution provided the most consistent and useful data collected during the study.

The determination of surface oil quantities by sorbent sampling and oiled area estimation was inaccurate, primarily, because of poor area estimates. A method of accurately quantifying surface oil volumes in tests such as this would be extremely useful.

Interfacial tension measurements were reasonable when the oil was relatively fresh and fluid and when enough oil could be sampled from the tank. If the oil sample was too small or too viscous or lumpy the device used to measure the interfacial tension (duNuoy ring apparatus) gave questionable results. An inexpensive method is needed to determine the concentration of dispersant in both the oil and the water over the duration of the test. This information would improve our understanding of the interaction of the dispersant, oil, and water and the overall chemical dispersion process.

The turbulence probe used to measure the mixing level in the tank performed as expected but similar measurements have not been made in actual ocean environments over a wide enough range of sea states to enable us to compare the mixing levels in our tests to those under actual field conditions. The probe should be used to establish the mixing generated during the range of sea states considered acceptable for dispersant application.

Dispersant Effectiveness

The averaged estimate of percentage of oil dispersed by Enersperse 700 in our tests compares favourably with those measured during the 1985 COAATF dispersant trials (46% (test) vs 95 to 41% (field) for Enersperse 700. The estimated dispersion efficiency for Corexit 9527 in our tests was higher than that measured in the offshore trial (24% vs 1 to 3.75%). This may be due to underdosing of the oil slick with dispersant in the field test (Gill et al. 1985).

Dispersant effectiveness was the same for the two oil thicknesses used in the study (0.5 mm and 1.0 mm). There were only slight differences in effectiveness for the different mixing energies and for the two oil types (fresh and weathered) used in the testing. These findings may result from insufficient differences in the test parameters to affect the dispersant's performance.

ACKNOWLEDGEMENTS

This work was funded by and carried out for the Environmental Studies Revolving Funds. The author is grateful to Mr. M. Fingas of Environment Canada for his guidance and suggestions throughout the study.

REFERENCES

Belore, R.C. 1987. Mid-scale testing of dispersant effectiveness. Environmental Studies Revolving Funds, Report No. 068, Ottawa. p.82.

Canpolar Consultants Ltd. 1985. Surface energy and oil spills: investigation of an instrumental technique for surface energy measurement. Report prepared for EPS Environment Canada.

Delvigne, G.A.L. 1982. Effectiveness of natural and chemical dispersion of oil slicks. Review and evaluation of measuring methods. Report on Investigation R1786-1 Delft, P.O. Box 177, 2600 mh Delft, The Netherlands.

Fingas, M.F. 1985. The effectiveness of oil spill dispersants. Spill Technology Newsletter Vol. 10(4-6), Environment Canada, Ottawa. p.47.

Gill, S.D., R.H. Goodman and J. Swiss. 1985. Halifax 1983 sea trial of oil spill dispersant concentrates. Proceedings of the 1985 Oil Spill Conference. American Petroleum Institute, Washington, D.C. p.4769

Lichtenthaler, R.G. and P.S. Daling. 1983. Dispersion of chemically treated crude oil in Norwegian offshore waters. Central Institute for Industrial Research. Report No. 1406 and 1407 PFO Oil Pollution Control. Research and Development Program, Oslo, Norway.

Nichols, J.A. and H.D. Parker. 1985. Dispersants: comparison of laboratory tests and field trials with practical experience at spills. Proceedings of the 1985 Oil Spill Conference. American Petroleum Institute, Washington, D.C. p.421.

Wells, P.G. and G.W. Harris. 1979. Dispersing effectiveness of some oil spill dispersants: test with the Mackay apparatus and Venezuelan Lago Medio crude oil. Spill Technology Newsletter (July-Aug.)

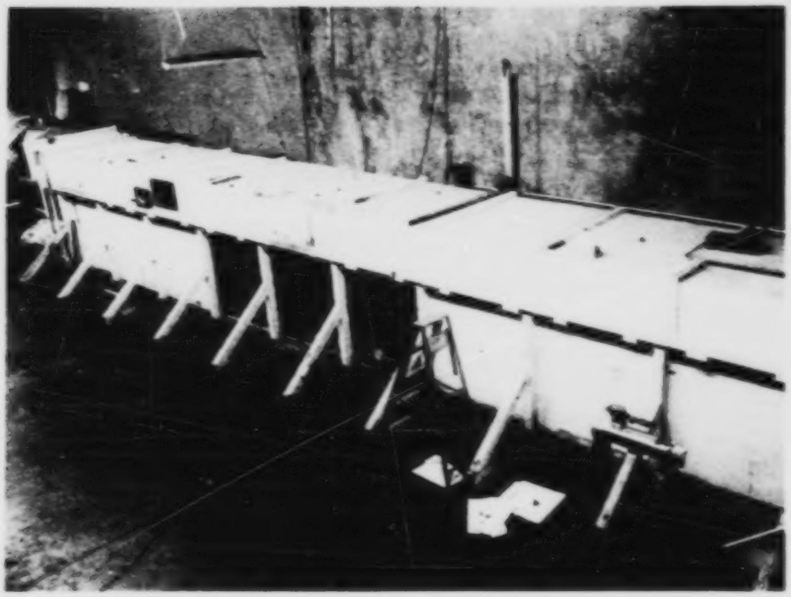

Figure 1. Test Tank

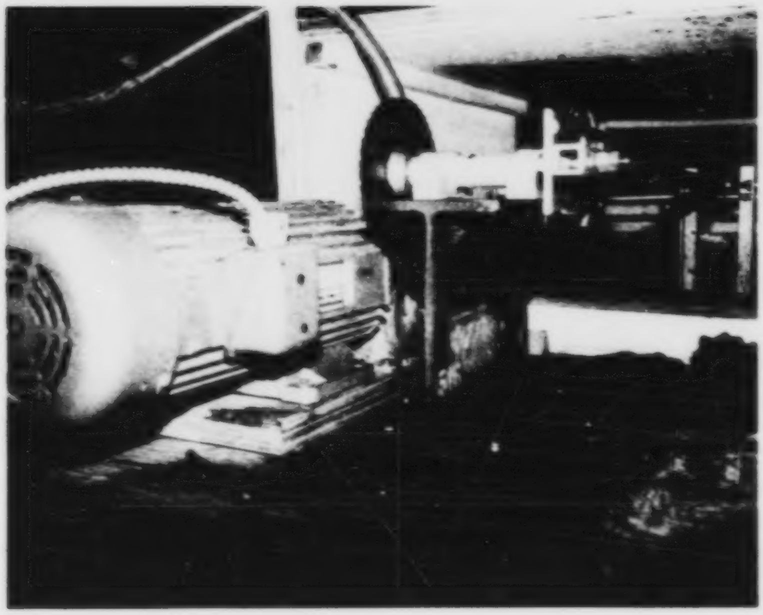

Figure 2. Wave paddle and drive mechanism

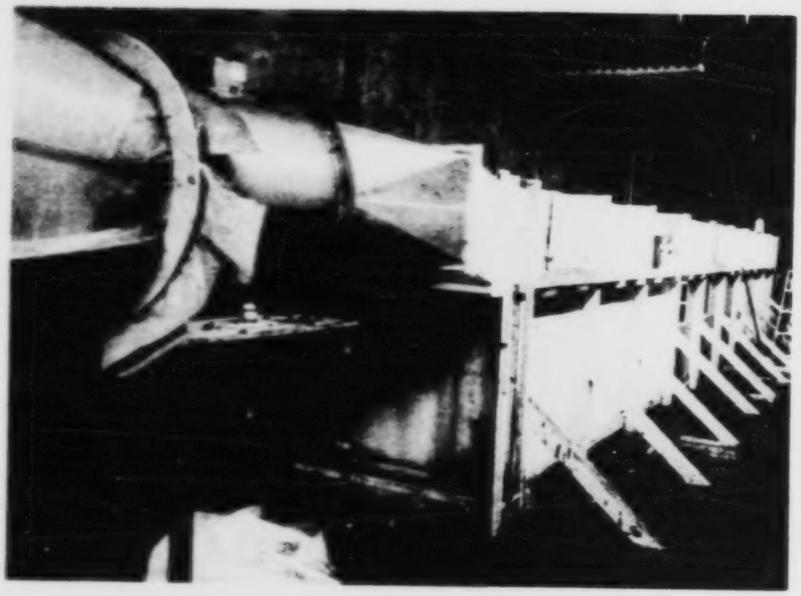

Figure 3. Fan and choking template

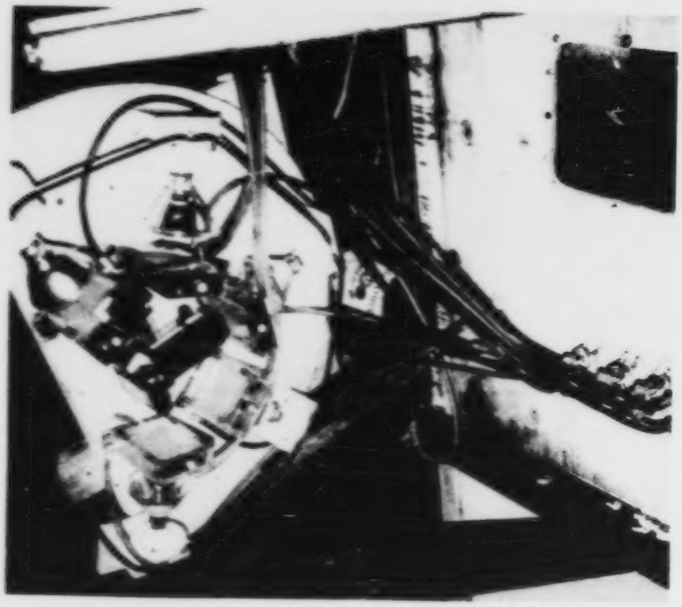

Figure 4.
Cells used in oil dispersion photography

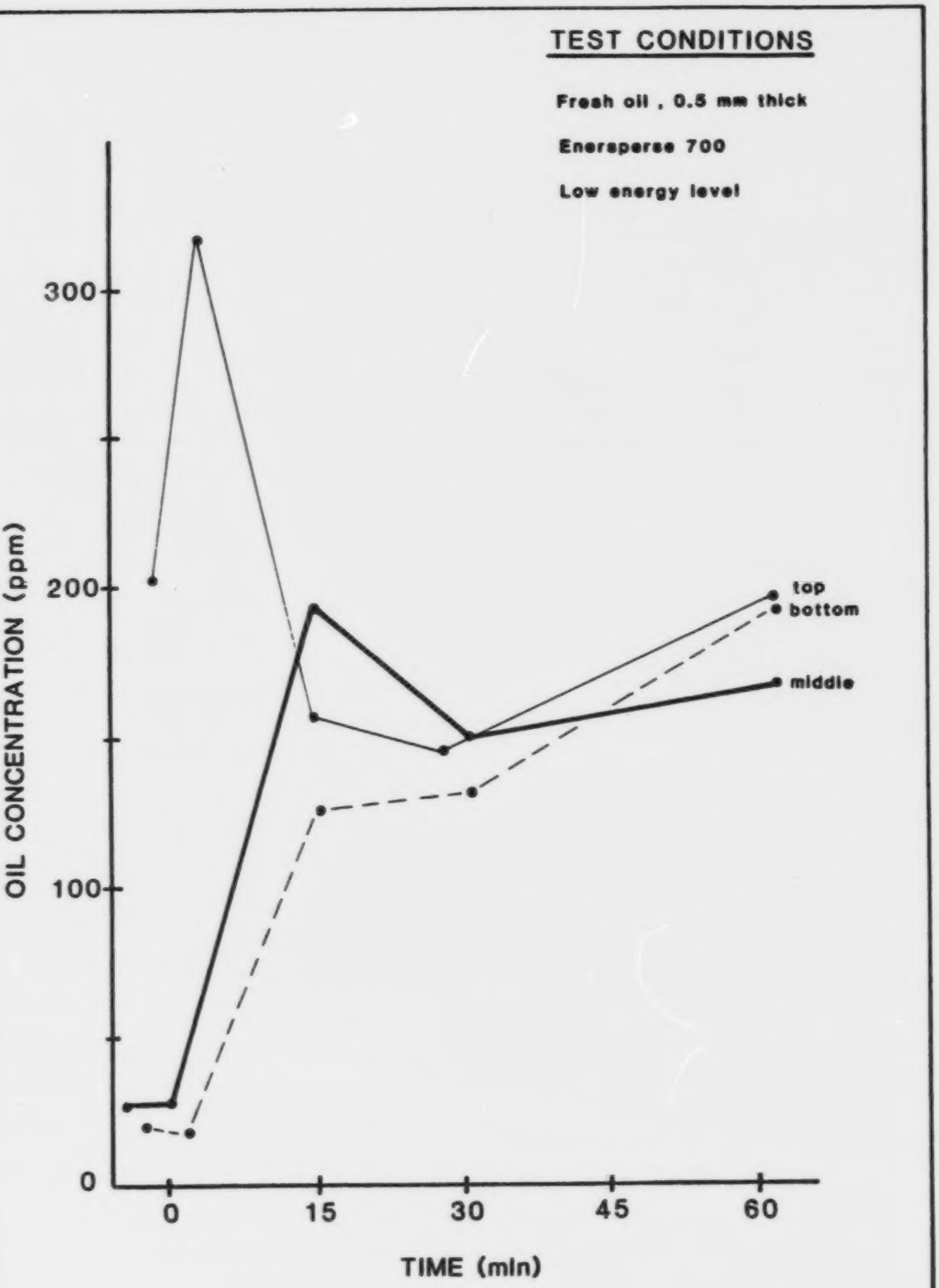

Figure 5 Example plot of oil concentration vs time

DISPERSANT TESTING AT THE ENVIRONMENTAL EMERGENCIES TECHNOLOGY DIVISION

Merv F. Fingas, Kathy A. Hughes and Melodie A. Schweitzer
Environmental Emergencies Technology Division
Conservation and Protection
Environment Canada
Ottawa, Ontario K1A 0E7

INTRODUCTION

Environment Canada has maintained a testing laboratory devoted to looking at dispersant testing and many other aspects related to dispersants. Over the past few years, the laboratory has conducted a number of specific studies. These include:

1. A study of the chemical and natural dispersability of oils.
2. A re-examination of the Mackay test.
3. An examination of some new dispersant formulation ideas.
4. A comparison of some dispersant testing means.
5. A study of new possible testing devices.
6. A re-examination of the analytical techniques used for dispersant tests.
7. Development of a new swirling flask test.
8. Examination of the use of dispersants in sewers and for flushing spills down sewers.

Some of these studies have been reported in other literature and will only be briefly summarized here.

A Study of the Natural and Chemical Dispersability of Oils

A number of oils were tested in the Mackay apparatus for dispersability. These results have been discussed in the literature.[1] The method used for dispersant effectiveness was that of the EPS guideline procedures.[2] This, in summary, uses six litres of sea water placed in the test vessel and a wave of the appropriate height is achieved through the use of the high velocity air. Ten millilitres of oil is put into a containment ring and released after dispersant is added. The water is sampled while the unit operates and this water extracted and analyzed colorimetrically. Some of the results are shown in Table 1.

TABLE 1. DISPERSABILITY RESULTS - PERCENT DISPERSED INTO WATER COLUMN

	Blank Run (Natural Dispersability)		Chemical Dispersability (with Corexit 9527)	
Oil Type	0°C	15°C	0°C	15°C
Automotive diesel	7	5	92	94
Automotive gasoline	38	38	54	46
Bent Horn (20.4% evaporated)	0	0	12	80
Bent Horn (32.9% evaporated)	0	9	0	69
Bunker C	0	0	0	3
Electrical transformer oil	21	21	72	94
Fuel oil No. 2	26	24	86	75
Hibernia	0	0	10	48
Hibernia (18.2% evaporated)	0	0	4	46

TABLE 1. (... cont.)

Oil Type	Blank Run (Natural Dispersability) 0°C	Blank Run (Natural Dispersability) 15°C	Chemical Dispersability (with Corexit 9527) 0°C	Chemical Dispersability (with Corexit 9527) 15°C
Hibernia (23.0% evaporated)	0	0	0	19
Issungnak	0	34	16	91
Issungnak (15% evaporated)	0	0	0	99
Issungnak (25% evaporated)	0	0	0	85
Lagomedio	1	2	73	81
Lagomedio (8.8% evaporated)	1	5	62	69
Lagomedio (14.8% evaporated)	0	2	20	85
Norman Wells	5	8	79	75
Tarsiut (12.4% evaporated)	16	22	57	53
Tarsiut (16.4% evaporated)	17	39	62	72
Transmountain blend	0	1	40	84
Transmountain blend (18.5% evaporated)	0	0	0	80
Transmountain blend (28.5% evaporated)	0	0	0	83

Anomalous results were achieved with lighter oils (20-200 mPa.S) due to an effect known as viscous shearing. The effect might be better known as viscosity-dependent shearing as the lighter oils shear. Essentially what occurs is that the lighter oils are under sufficient strain in the MNS apparatus to break into droplets and enter the water. These droplets are not small and thus are unstable. After the energy is removed from the apparatus, the particles re-surface and re-form a slick. The droplets are generally large enough to be seen visually. The shearing occurs mostly at 0°C. Table 2 shows results of MNS tests where viscosity shearing is evidenced.

TABLE 2. VISCOUS SHEARING RESULTS

Oil type	Dispersal type	Dispersability (percent) 0°C	Dispersability (percent) 15°C	Viscosity (cSt or mm^2/s) 0°C	Viscosity (cSt or mm^2/s) 15°C
Adgo	natural	63	20	172	65
Adgo (2.6% evaporated)	chemical	88	74	229	76
Amauligak	natural	50	15	28	16
Amauligak (13.4% evaporated)	chemical	83	65	46	23
Amauligak (19.4% evaporated)	natural	22	6	74	36
Amauligak (19.4% evaporated)	chemical	74	67	74	36
Bent Horn	chemical	86	68	31	15
Electrical Lubricating Oil	chemical	49	28	397	165
Tarsiut	natural	38	30	14	9

The results of these tests show that, aside from the viscosity shearing phenomenon, Beaufort oils are highly dispersable - both chemically and naturally.

Re-examination of the Mackay Apparatus

Our laboratory has conducted extensive testing with the Mackay apparatus in the past two years. Results of these tests have been published separately and in data collections. The test has been observed to have a number of problems, as noted below in perceived order of importance.

1. Values of effectiveness from the apparatus are uniformly high. The values produced are so high that they do not always represent achievable values in the field, nor do they discriminate clearly between good and bad dispersants, nor between oils that are difficult and less difficult to disperse.
2. The apparatus is expensive to operate in that it is time consuming. Our laboratory's experience is that one person can perform an average of three runs per day. Allowing for replicates and blank runs, many days are required to complete a table. The results for a one-page table have consumed more than six man-months of testing time.[1] Additionally, the mere fact that tests are so time consuming, has meant that difficulties with the apparatus were not noted until after many organizations and countries, including Canada, had adopted it as a standard.
3. The apparatus is difficult to replicate. Several experimenters, including ourselves, had difficulties constructing the apparatus and achieving results comparable to results already published. The apparatus is intricate and its operating conditions can easily change if slightly different components are substituted. In 1984, we participated in a round-robin series of tests with three laboratories. One of them was the developer of the test and one of them was another Environment Canada laboratory. Results could only be replicated after three weeks of work by four laboratory personnel. During this time, a number of components for two sets of the apparatus were altered or changed. Similar results were obtained in Sweden and Norway.[3]
4. Test protocols for the apparatus do not include a settling time. Oil is sampled while the unit is running. Thus, even unstable dispersions show high effectiveness. The apparatus does not lend itself to sampling in another manner. Even visually, one can see that some emulsion or dispersion rapidly disappears when the apparatus is shut down; however, the sample was taken when the oil was "artificially" suspended. Daling and Nes performed studies of this phenomenon in the Labofina test and found that effective percentage dropped by as much as an order of magnitude if settling time was increased from one minute to eight minutes.[4]
5. Wave damping with the apparatus is a large problem. The device is, in practice, operated with wave height as an indicator of energy. Even though the device is calibrated by an oxygen transfer experiment when initial setup is performed, the actual energy during a given test run is directly related to the wave height. We have found, in our laboratory, that wave damping or a decrease in energy often occurs after an oil is released. As could be expected, the energy falloff decreases the measured effectiveness compared to a run where this does not occur. This problem has been noted by Mackay in previous literature.[5] We have noted an additional source of wave damping in our laboratory; that is the damping caused by surface roughness of glassware. In fact, after repeated

experiments we found that certain glass vessels could not be used reliably to perform the test. Out of six vessels, we were able to use only three. Age and previous history of the glass did not appear to be the cause, and all glassware was purchased from the same manufacturer. The slight roughness difference in vessels could barely be discerned visually.

6. Viscous shearing of droplets occurs, producing incorrect dispersability or effectiveness results for medium viscosity oil. It is observed visually with oils that have a viscosity between 30 and 200 cSt (mm^2/s) that large drops shear from the oil mass and become entrained in the sample path. These are then picked up during sampling and counted as being dispersed. These droplets are not stable and immediately resurface when the apparatus is shut down. This particular problem is analyzed in depth earlier in this paper.
7. The position of the sampling port on the apparatus is critical. The current drawings call for the position of the sampling tube at a location where particles are observed to congregate. The fact that the droplets are not homogeneously distributed across the diameter of the cylinder is evidenced by the frequent results of over 100 percent effectiveness. We have, in fact, measured up to 120 percent in our laboratory.
8. The air stream creates an unrealistically high energy regime in the apparatus. A one horsepower (745 watt) blower is used to create the air stream in a vessel 31 cm high by 31 cm diameter.
9. The high velocity air induces high evaporative loss of any volatile test fluids. In our laboratory, we have noted that it is difficult to test volatile products, and we must compensate for the high expected losses by first measuring the loss rate.

Despite these shortcomings, the Mackay apparatus is a marked improvement over the SET (Simulated Environment Test) formerly used by our laboratory for regulatory testing of dispersants.[6] The SET test apparatus consists of a 55 gallon drum and a centrifugal pump. Most of the above disadvantages apply to the SET apparatus also, and in many cases the problems were more severe. We have also performed a number of Labofina experiments and noted many similar problems, although the apparatus is simpler than the Mackay setup and tests can be performed more quickly. The energy applied to the oil and water is even higher than in the Mackay apparatus as Lewis and co-workers found upon performing droplet size analysis.[7]

In general, laboratory tests of all types now in common use share the following shortcomings.

1. The oil/water ratio is too high. In fact, in some tests this is sufficient for the dispersant to function from the water to the oil, evidenced by the fact that some authors have been able to get analogous results whether the dispersant is put in the oil or the water.
2. The oil comes into contact with glassware. In fact, we may be measuring the detergency of products or how well the dispersant removes the oil from the glass rather than puts it into the water column (dispersancy).
3. Most current apparatus impart too much energy to the oil/water system.

It is important that the limitations of any given dispersability test be understood before the results are used in making critical assessments.

An Examination of Some New Dispersant Formulation Ideas

A study is still underway to examine a variety of surfactants and the effect of the solvent on dispersant effectiveness. Studies to date indicate that more oleophilic dispersants have greater effectiveness in low energy testing devices but not necessarily in high energy test devices. It is suspected that the effect of high energy, plus low oil-to-water ratios, lead results to be favorable towards hydrophilic products of high detergency.

A Comparison of Some Dispersant Tests

Several investigators have reported results of dispersant apparatus comparison tests.[3,7,8,10,12,13,14] In the papers reviewed here, all authors have concluded that the laboratory test results do not correlate well, but do agree on many of the rankings assigned to dispersants. Daling and Nes have evaluated a number of oils and dispersants using both the Mackay and Labofina tests, and they conclude that the Mackay test is less useful for more viscous oils.[13] Both Canevari and Lee have found that the Labofina tests could be used to study the effects of viscosity on dispersant effectiveness.[9,12] Lehtinen and co-workers focused on temperature and salinity effects.[10] Other than these efforts, little has been done to investigate the differences among types of apparatus as they relate to other physical properties of the oil or other operating conditions.

The two most commonly used dispersant effectiveness test methods in the world are the Mackay and Labofina.[5] The Labofina test is also known as the rotating flask test, Warren Spring Laboratory test, or the rolling flask test. The basic operating procedure is as follows: 250 millilitres (mL) of sea water is put into a separatory funnel along with 5 mL of oil and 0.2 mL of dispersant. The separatory funnels are rotated for 2 minutes at 33 rpm. After one minute of resurfacing time, a 50 mL aqueous sample is drawn, extracted with chloroform, and analyzed colorimetrically.[12]

The Mackay apparatus, otherwise known as the Mackay-Nadeau-Steelman (MNS) apparatus, is a more recent development, but has been adopted by a number of countries as their disperant-testing standard.[5] A detailed description of the apparatus is found in the literature.[2,5,16] The test procedure is as follows: 6 litres of sea water is placed in the cylindrical glass vessel and an air flow is turned on and adjusted until a wave amplitude of 3.5 centimeters (cm) is maintained. Ten mL of oil is put into a small containment ring in the center of the water surface, an amount of dispersant (usually calculated to give a dispersant-to-oil ratio of somewhere between 1:10 and 1:50) is added, and the oil is released. After 10 minutes, a 500 mL sample of water is removed from a fixed point on the diameter of the apparatus. The sample is extracted with methylene chloride and analyzed colorimetrically.

Table 3 presents the results of an apparatus intercomparison using ten different oils and Corexit 9527, an Exxon dispersant product. All results shown are the average of at least two determinations. The Mackay and Labofina tests were run according to protocols described in the literature.[2,15] The swirling flask test was operated according to the procedure described below. The physical properties of the test oils are given in Table 5 and are taken from Bobra and Chung.[17] As is evident from the results, the correlation between the three sets of values is poor. The dispersability rank is not necessarily maintained among the three tests, although those oils that disperse well or very poorly do so in all three tests.

A series of test runs were conducted using the swirling flask test to measure natural dispersability. Little or no oil was detected, and it was concluded that the test procedure would have to be modified to measure natural dispersability. The energy imparted to the oil is insufficient to yield the minimum 0.5 percent reading. Work on this measurement technique

TABLE 3. APPARATUS EFFECTIVENESS COMPARISONS FOR COREXIT 9527

Oil type	Dispersant Effectiveness (in percentage)* Mackay test	Labofina	Swirling flask
Adgo	96	87	4.7
Alberta Sweet Mixed Blend	90	40	8.1
Amauligak	71	98	9.0
Amauligak (13.4% evaporated)	65	77	6.7
Bent Horn	68	18	2.0
Hibernia	48	39	3.1
Issungnak	91	52	10.1
Lagomedio	81	45	3.2
Norman Wells	75	52	6.8
Tarsiut	81	86	8.2

* Using Corexit 9527 at 1:20 by volume in the Mackay test and 1:25 in the other tests; temperature was 15°C in the Mackay test and 20°C in the other tests.

continues.

The differences in error and repeatability of all three apparatus were examined. For the data set presented in this paper, deviation for all apparatus is similar and not significantly different. The swirling flask test produces a lower average deviation; however, since the numbers are much smaller, the average absolute deviation is larger. Since value differences between the three experiments cannot be attributed to error alone, each device must have unique characteristics which contribute to the different values.

The data presented in this paper show that the three test methods each produce their own unique data sets. The correlation between data sets is poor, although trends are discernable. Oils that disperse well generally do so in all apparatus and vice versa. In the absence of extensive field data, no apparatus can be said to be more correct than another, nor is there any correlation that could resolve the issue. The results from the swirling flask test correlate better with viscosity and interfacial tension data. There is no theory at this time which describes dispersion in terms of viscosity or interfacial tension alone, which would resolve the issue.

A Study of New Testing Devices

A number of tests have been performed to find new test devices which do not show the problems experienced previously. Modifications have been made to a number of devices and the devices rerun with oil and dispersants. To date, the only device that has shown significant promise is the swirling flask test. Results from this test have been presented above and a detailed description of the device and its operating procedure are presented below.

A Re-examination of the Analytical Techniques Used for Dispersant Tests

Most tests used to date employ an extraction procedure (usually with methylene chloride, sometimes with carbon tetrachloride) and then the extract is analyzed colorimetrically. This is the reading of the color intensity which is dependent on the concentration of the oil as well as the type of oil. A survey of techniques showed that the following wavelengths have been recommended: 340, 370, 400, 530, 540, 580, 620 and 650 nanometers.[11] Some procedures call for the use of different wavelengths depending on the oil, for example 370 nanometers (nm) for light oil and 470 for heavy oil. Most analysis to date has been performed on low-resolution instruments.

A series of experiments were run in our laboratory to determine the detectability of oil in methylene chloride by the colorimetric procedure, the best wavelength to use, and an assessment of the accuracy of the method. A higher resolution UV/visible spectrometer, Perkin Elmer Model No. 552A was used in a series of experiments to answer the above quesiton. Table 4 summarizes the results of these studies.

TABLE 4. SUMMARY OF WAVELENGTH STUDY RESULTS

	Oil Type			
Wavelength (nm)	Alberta	Alberta plus dispersant	Issungnak	Overall
200	not linear	not linear	not linear	not usable
235	not linear	not linear	usable	not usable
255	not linear	not linear	usable	not usable
340	good	good	best	usable
370	good	good	low	usable
390	good	good	low	usable
400	good	good	low	usable
470	good but low	noisy	low	usable, but noisy
530	linear but low discrimination	low	low	poor
540	linear but low discrimination	low	low	poor
580	linear but low discrimination	low	low	poor
620	linear but low discrimination	low	low	poor
650	linear but low discrimination	low	low	poor
720	linear but low discrimination	low	low	poor

Overall, it was determined that the most usable wavelengths were from 340 to 470 nanometers. Subsequent tests employed only 340, 370, 400 and 470 nanometers. The latter of these was dropped when it was found that it produced very poor results in terms of repeatability. Examination of the oil spectra shows that 470 nanometers is on the shoulder of a major peak and thus a small wavelength change changes the absorbance dramatically. This effect would not be as dramatic as in the medium resolution used in this experiment.

A study of the sensitivity range of the procedure showed that the procedure produces linear results between 0.17 and 2.1 microlitres of oil per millilitre of methylene chloride. Below this critical level, little discrimination is apparent and above, saturation occurs.

A variety of tests show that the analytical noise is as high as 40% alone and typically is around 10-15%. This is due to extraction errors, spectrometer inconsistencies, minor cuvette differences, spots on cuvettes, and reagent (including water) differences. These can be controlled to the lower value with some extra effort. It has been found that analytical error is a very significant variant and should not be ignored in dispersant testing.

Development of a New Swirling Flask Test

As noted above, a new test was developed and tested at Environment Canada. The vessel component is very simple; a small flask with a side spout to drain bottom contents without including the surface oil. Water, then oil and dispersant are placed in the flask. The flask is mechanically shaken and, after a time, a sample of water is drained from the bottom and analyzed. In designing the test a number of criteria were followed.

1. The prime criteria were simplicity and speed of analysis.
2. As many as possible of the problems found with other apparatus were to be avoided.
3. Only low energy levels would be used.
4. Simplicity and repeatability were more important than visual simulation of real phenomena.

A 125 mL Erlenmeyer flask was chosen as the vessel. The primary reason for this is the ready availability of biological and chemical shakers designed to carry this size of flask. Because the shaker imparts a swirling motion to liquid in the flask, the test has been dubbed the "swirling flask test". The flask is fitted with a side arm of ¼ inch ID which follows the flask's outer profile.

Initially, a layer of methylene chloride was placed in the apparatus before putting it in the water. The intent was to obtain direct analysis of the oil in the solvent by colorimetry without extracting the water column. It was found, however, that the oil was not rapidly taken up by the methylene chloride layer; in fact, the entry of the oil into the layer was the limiting factor. Runs up to 18 hours long with a number of oil and dispersant combinations confirmed that fact.

Experiments conducted with other heavier-than-water solvents including carbon tetrachloride and trifluorotrichloromethane produced similar results. In addition, these latter products had a tendency to lose droplets into the water. Since such action would produce anomalous results, the use of the heavier-than-water extractant in the vessel was abandoned.

Testing was performed to determine the best shaker energy level in revolutions per minute (rpm). This was done by using the methylene chloride noted above, but only as an indicator of the depth of mixing. Various combinations of oil and dispersant were placed on the water layer, and the rpm were noted at which the oil layer on top breaks through to the methylene chloride layer. For ten oil and two dispersant combinations this occurred at 170 to 250 rpm, and was characteristic of the oil/dispersant combination. 150 rpm was chosen as the highest practical rpm before excessive (to the bottom) mechanical mixing occurred. Similarly, the amount of oil used was the minimum amount that gave a linear colorimetric analysis response for the volume of extractant (20 mL) chosen. The volume of oil that met this requirement was 0.1 mL (100 microlitres). The use of this amount of oil yields an oil-to-water ratio of 1:1200, which is lower than that of both the Mackay apparatus (1:600) and the Labofina apparatus (1:50). Preliminary tests with different sets of glassware do not show sensitivity to exact dimensions or roughness.

For the results reported in this paper, the following procedure was used. 120 mL of artificial sea water is placed in the test vessel. The water and vessels are brought to temperature. For tests with dispersants, the dispersant is added to the oil and 0.1 mL of the mixture is placed on the water in each vessel. The dispersant is premixed with the oil to ensure that differences in application do not alter results. The shaker (New Brunswick Scientific G-27) is started (at 150 rpm) and agitation is continued for ten minutes. After five minutes of settling time 20 mL of water is poured from the test flask and extracted with two 10 mL portions of methylene chloride. The methylene chloride extract is analyzed colorimetrically at 400 nanometers and percent effectiveness assigned on the basis of a calibration curve. The latter is prepared by adding oil directly to methylene chloride in progressively increasing amounts to a maximum of 0.017 mL. It is assumed that the oil is homogeneously distributed in the water; that is, for 100 percent effectiveness, all of the 0.1 mL of oil is distributed evenly throughout the water and the 20 mL drawn off contains 20/120 or 1/6 of this oil.

Since these results were reported, further optimization was performed on the test and the oil increased to 150 microlitres, lowering the oil/water ratio to 1:800. This is necessary to allow colorimetric analysis. Now 30 mL of water is extracted and the mixing time increased to 20 minutes and the settling time increased to 10 minutes. The latter times have been chosen as they are the shortest times producing the same dispersant effectiveness withing a number of tests. Currently also, the extract is analyzed at 340, 370 and 400 nanometers and the results averaged.

A Study of the Use of Dispersants for Flushing Fuel Spills Into Sewers

A model sewer was constructed with a number of objectives.

1. To study the use of dispersants in flushing fuel into and in sewers.
2. To study the behaviour of fuels in the sewer.
3. To examine other countermeasures for sewer explosions.

The system was constructed as follows: A head box of approximate dimensions 1 m x 1 m x 0.3 m high which runs into a 3.8 cm ABS pipe (1½") which extends downwards for 110 m (360 ft) at an approximate slope of 0.8 cm per m (3/32 inch per foot) to simulate a realistic sewer system. Manholes were installed at intervals of 18 m maximum, however near the source these were installed at shorter intervals. This permitted vapour measuring devices (HNUs calibrated to the fuel which was used, either gasoline or diesel) to be installed at approximately logarithmic intervals (4.5, 9.0, 18.0, 51.4 and 104 m). The vapour measuring devices were directly coupled to a Tekmar convertor as part of a Compaq computer. This provided a real time display of vapour concentrations at each manhole as well as recording and computation of data.

Figure 1 shows a typical real time trace of vapour concentrations at the various manholes with time. This particular figure shows gasoline which as a volatile fluid behaves in a different manner when spilled in a sewer. The vapour concentrations show two peaks. The first one, appearing in Figure 1, is due to vapour from the fuel floating down on the water. This vapour peak appears at the same rate as the water flow. The second peak is from vapours released near the point of entrance and contains mostly the volatile components up to C-8. This was established by performing gas chromatography analysis on the two peaks. The vapour associated with this peak moves much slower down the sewer and the time difference between the two peaks increases

figure 1

CONCENTRATION AT EACH MANHOLE - gasoline only

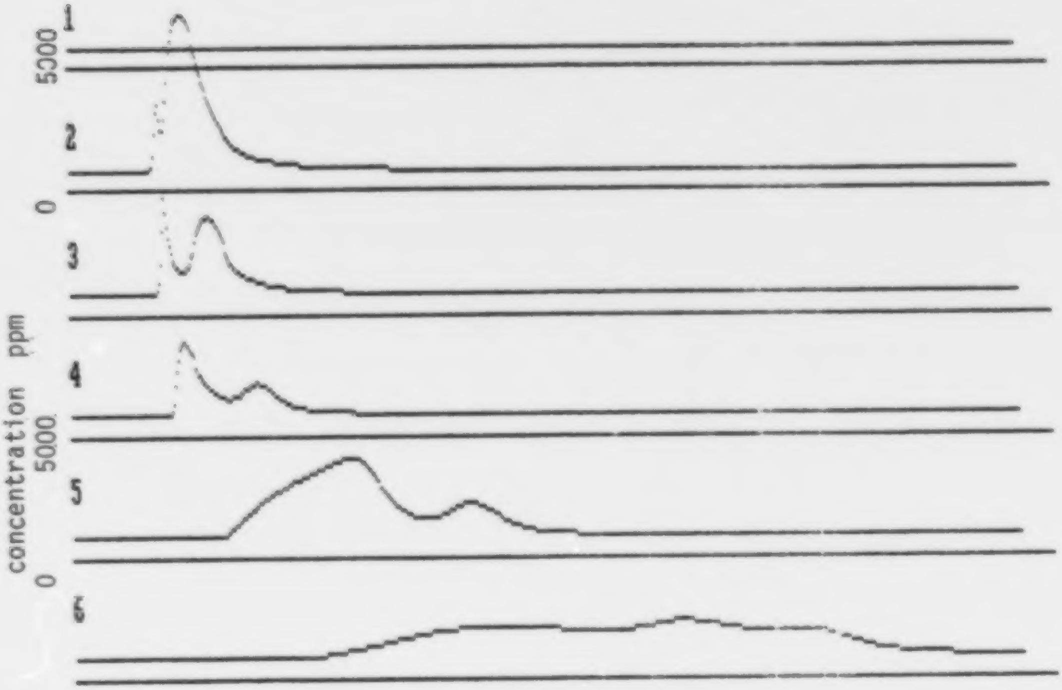

figure 2

concentration at each manhole - dispersant flushed

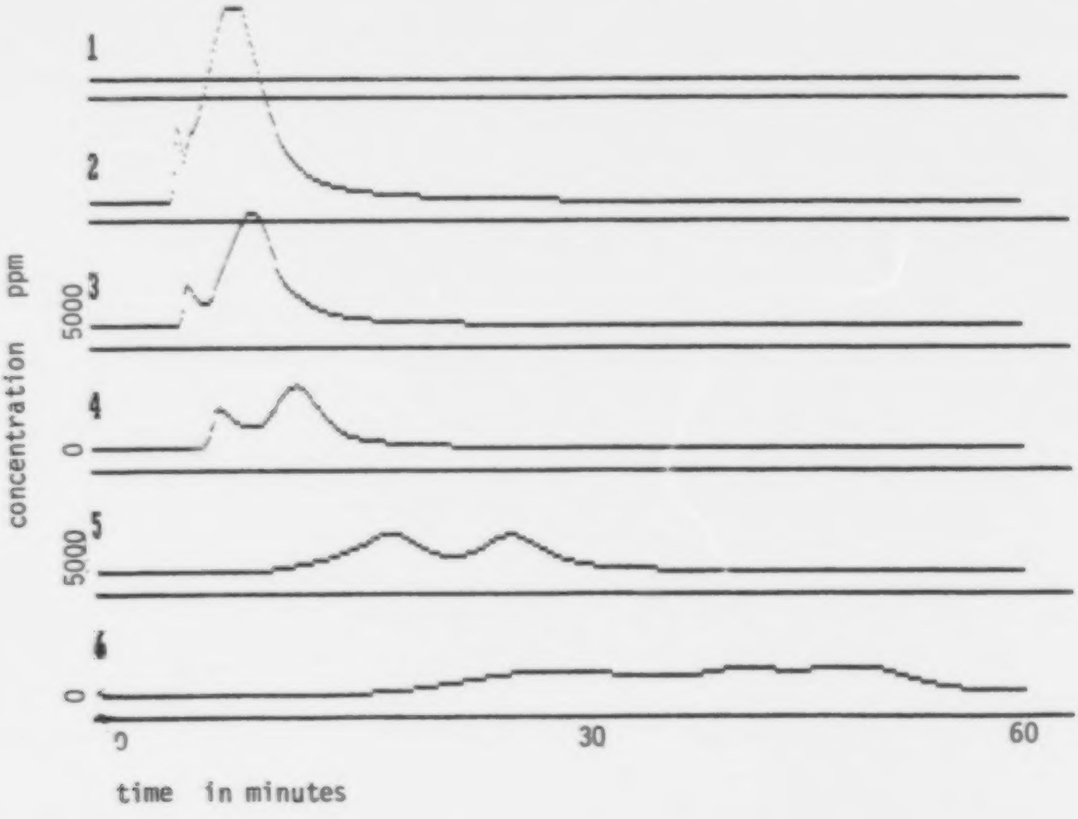

until two peaks are no longer differentiated. Diesel fuel behaves somewhat similarly; however, the amount of volatile components below C-10 is sufficiently small to prevent two peaks from being visible.

A number of researchers have studied the evaporation of petroleum with the addition of dispersant.[18,19] This experiment has shown the same effect. Vapour concentration is increased by the addition of dispersants. This is illustrated by comparing the vapour concentration difference between Figure 1 and Figure 2. In addition to increasing the concentration, the time that a higher concentration is achieved is also increased. This implies that the use of dispersants increases the vapour explosion potential in sewer systems. This effect was observed throughout 130 runs involving many different configurations and operating conditions. The effect was observed despite the mixing mode as well (direct injection, pre-mixing and flushing down from a surface).

As a footnote to these studies it might be noted that a number of other countermeasures for vapours in sewers were tried, and the addition of a heavy gas will dramatically reduce the vapour concentration. The best countermeasure of this type was the addition of dry ice or solid carbon dioxide.

Figure 3 shows the peak concentrations versus distance as a result of dispersant use. The peak concentration is increased most at the first manhole (4.5 m) and decreases down the system until it nearly approaches the gasoline-only values. A number of products were tested as can be seen from the graphs including the dish detergent "Sunlight" and the common household cleaner "Lestoil". Little differentiation exists between the various products in this type of application. Figure 4 shows the increasing total vapour released with increasing flushing volumes. This refers to the addition of volumes of dispersant solution (here 5% in tap water in every case) compared to the volume of fuel released. Increasing the flushing volumes actually increased the total vapour released into the sewer system until a ratio of 1:5 is reached and then the effect is diminished somewhat. In all cases, the addition of the dispersant increases the total vapour released in the sewer and thus also increases the explosion potential.

REFERENCES

1. Fingas M., M. Bobra and J. Doran, 1986. Recent Petroleum Dispersability Results. Spill Technology Newsletter, v11, n2. Environmental Protection Service, Environment Canada, Ottawa, Ontario, pp34-36.
2. Anonymous, 1984. Guidelines on the Use and Acceptability of Oil Spill Dispersants, 2nd Edition. Report EPS 1-EP-84-1. Environmental Protection Service, Environment Canada, Ottawa, Ontario.
3. Nes, H., 1984. Effectiveness of Oil Dispersants: Laboratory Tests. PFO Project Report No. 1410. Trondheim, Norway.
4. Daling, P.S. and H. Nes, 1986. Laboratory Effectiveness Testing of Dispersants: Correlation Studies Between Two Test Methods. Poster Session presented at Arctic and Marine Oilspill Program Technical Seminar held in Edmonton. Environment Canada, Ottawa, Ontario, p3.
5. Mackay, D. and F. Szeto, 1981. The Laboratory Determination of Dispersant Effectiveness: Method Development and Results. Proceedings of the 1981 Oil Spill Conference, American Petroleum Institute, Washington, D.C., pp11-17.

FIGURE 3 PEAK CONCENTRATION AT MANHOLES

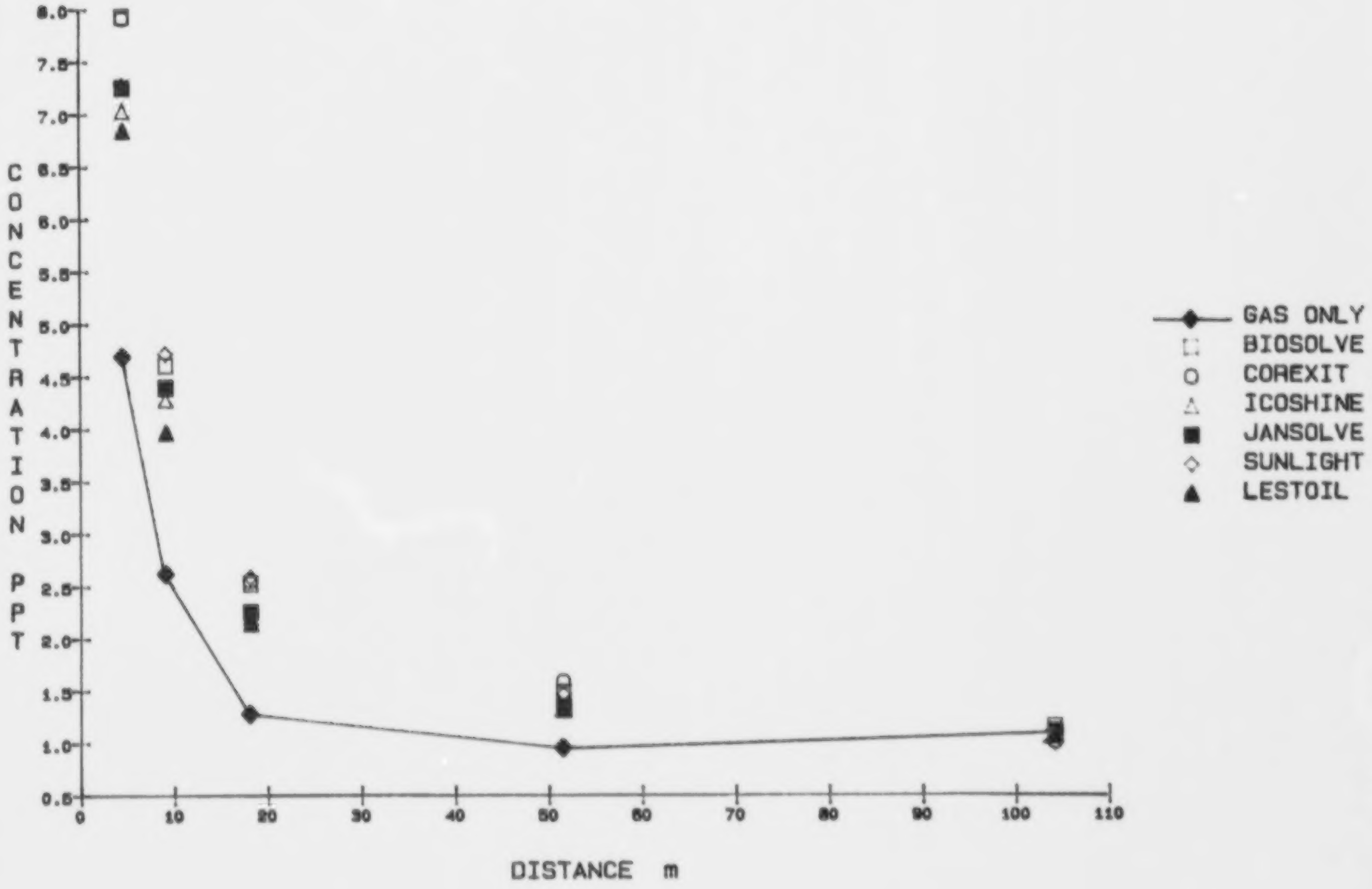

FIGURE 4 TOTAL VAPOUR RELEASED INTO SEWER

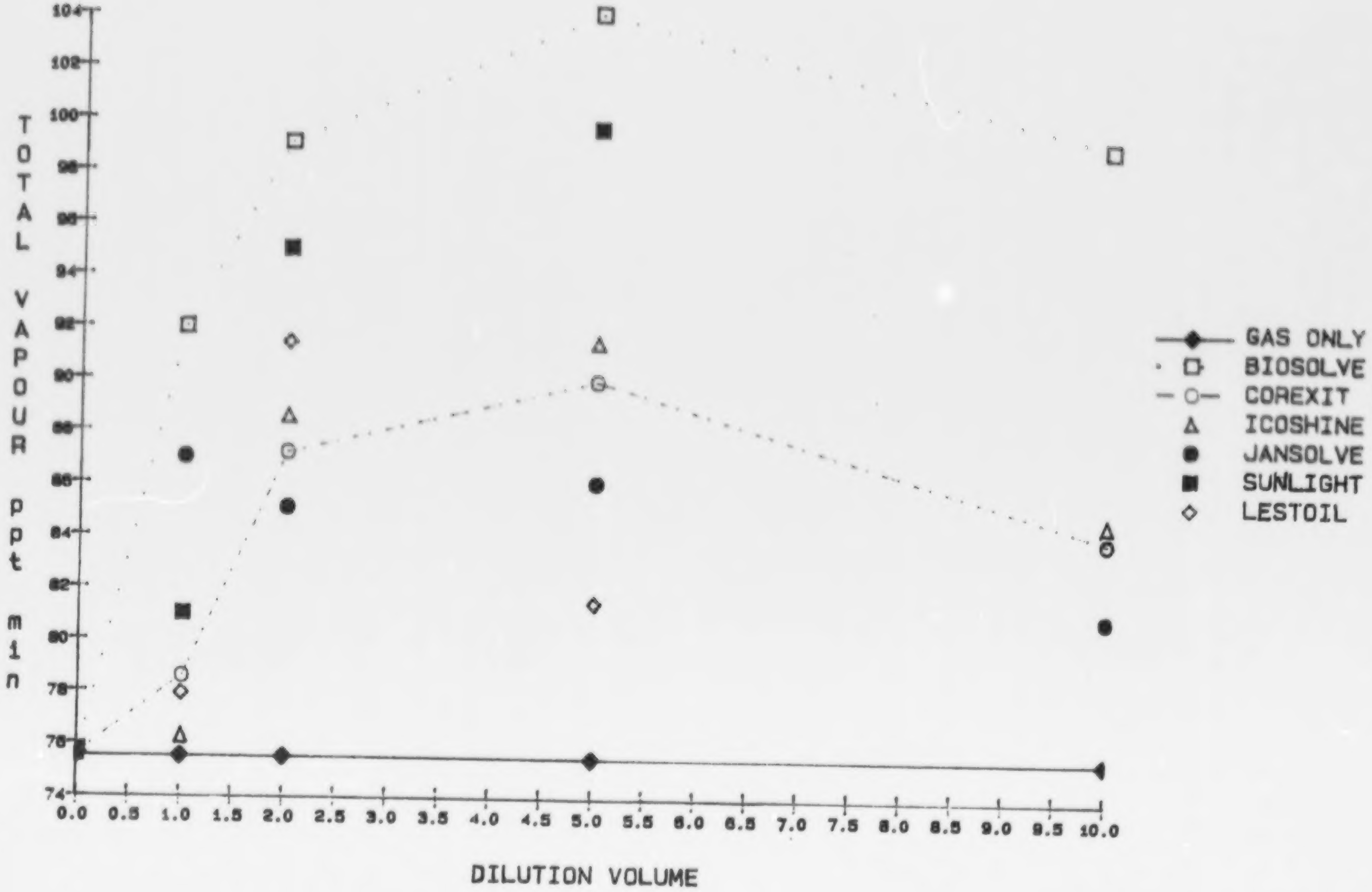

6. Anonymous, 1973. Guidelines on the Use and Acceptability of Oil Spill Dispersants. Report EPS 1-EE-73-1. Environmental Protection Service, Environment Canada, Ottawa, Ontario.
7. Lewis, A., D.C. Byford and P.R. Laskey, 1985. The Significance of Dispersed Oil Droplet Size in Determining Dispersant Effectiveness Under Various Conditions. Proceedings of the 1981 Oil Spill Conference, American Petroleum Institute, Washington, D.C., pp433-440.
8. Byford, D.C. and P.J. Green, 1984. A View of the Mackay and Labofina Laboratory Tests for Assessing Dispersant Effectiveness with Regard to Performance at Sea. Oil Spill Chemical Dispersants: Research, Experience and Recommendations, Tom E. Allen, ed. STP 840. American Society for Testing and Materials, Philadelphia, Pennsylvania, pp69-86.
9. Canevari, G.P., 1985. The Effect of Crude Oil Composition on Dispersant Performance. Proceedings of the 1985 Oil Spill Conference, American Petroleum Institute, Washington, D.C., pp441-444.
10. Lehtinen, C.M. and A-M. Vesala, 1984. Effectiveness of Oil Spill Dispersants at Low Salinities and Low Water Temperatures. Oil Spill Chemical Dispersants: Research, Experience, and Recommendations, Tom E. Allen, ed. STP 840. American Society for Testing and Materials, Philadelphia, Pennsylvania, pp108-121.
11. Meeks, D.G., 1981. A View of the Laboratory Testing and Assessment of Oil Spill Dispersant Efficiency. Proceedings of the 1981 Oil Spill Conference, American Petroleum Institute, Washington, D.C., pp19-25.
12. Lee, M., F. Martinelli, B. Lynch and P.R. Morris, 1981. The Use of Dispersants on Viscous Fuel Oils and Water in Crude Oil Emulsions. Proceedings of the 1981 Oil Spill Conference, American Petroleum Institute, Washington, D.C., pp31-35.
13. Nes, H. and S. Norland, 1983. Effectiveness and Toxicity of Oil Dispersants. Proceedings of the Sixth Annual Arctic and Marine Oilspill Technical Seminar, Environment Canada, Ottawa, Ontario, pp132-139.
14. Rewick, R.T., K.A. Sabo, J. Gates, J.H. Smith and L.I. McCarthy, Jr., 1981. An Evaluation of Oil Spill Dispersant Testing Requirements. Proceedings of the 1981 Oil Spill Conference, American Petroleum Institute, Washington, D.C., pp5-10.
15. Martinelli, F.N., 1984. The Status of the Warren Spring Laboratory's Rolling Flask Test. Oil Spill Chemical Dispersants: Research, Experience and Recommendations, Tom E. Allen, ed. STP 840. American Society for Testing and Materials, Philadelphia, Pennsylvania, pp55-68.
16. Mackay, D., J.S. Nadeau and C. Ng, 1977. A Small Scale Laboratory Effectiveness Test. Department of Chemical Engineering and Applied Chemistry, University of Toronto, Toronto, Ontario.
17. Bobra, M.A. and P.T. Chung, 1986. A Catalogue of Oil Properties. Report EE-77, Environmental Protection Service, Environment Canada, Ottawa, Ontario.
18. Bowler, B., A. Knapstad, A. Due and M. Sandstad, 1985. Laboratory Studies on the Effect of Oil Dispersant on Evaporation and Dissolution. Centre for Industrial Research, Trondheim, Norway.
19. Wilson, M.P., et al, 1981. Assessment of Treated vs Untreated Oil Spills: Final Technical Report. Department of Energy Report DOE/EV/04047-T3, Washington, D.C.

A STUDY OF DISPERSANT EFFECTIVENESS USING AN ULTRA-UNIFORM DROP-SIZE GENERATOR

Randy Belore

S.L. Ross Environmental Research Limited
Ottawa, Ontario

INTRODUCTION

An interesting mathematical model has been developed by Dr. Don Mackay of the University of Toronto concerning the prediction of the effectiveness of oil spill dispersants when applied to oil spills under field conditions (Mackay 1986). The model recognizes the importance of dispersant-oil interaction and predicts the likely effectiveness of a dispersant based primarily on the mean dispersant drop size and the oil slick's thickness distribution. The model defines two dispersion regimes which are controlled by these parameters (see Figure 1).

The performance-limited regime describes the situation in which the dispersant is used to its maximum potential. This occurs when dispersant is applied to thick oil slicks (relative to dispersant drop diameter) and is able to disperse "X" volumes of oil per volume of dispersant. The performance factor "X has been estimated to be about 40 for good dispersants on readily dispersible oils.

The access-limited regime occurs when dispersant is applied to thin slicks or sheens, in which case the dispersant is unable to contact "X" times its volume of oil. Mackay postulates that these drops of dispersant can "access" a circle of the oil slick only "M" times the drop diameter. This less efficient use of dispersants has been described by Mackay as a "first-order" process with an exponential decrease in oil remaining as a function of increasing dispersant dosage. Although theoretical values of "M" based on maximum potential drop spreading can exceed 20, a typical value of 5 has been estimated by Mackay for field application of dispersants where herding effects are present.

The primary objective of this study was to evaluate the validity of this model by conducting a series of controlled lab-scale tests. The experiments were intended to determine the performance factors "M" and "X" and the transition oil thickness between the two dispersion regimes (see Figure 1) for a range of dispersants and oils.

EXPERIMENTAL DESIGN, APPARATUS, AND PROCEDURE

Design

In developing the test procedure to meet the experimental objectives, certain criteria had to be met:

i) Very uniform dispersant drop size distributions and oil slick thicknesses would be needed if the final data were to be useful in estimating the performance factors "X" and "M" and the transition between performance and access limited dispersion regimes.

ii) The test would have to be conducted at a mixing level sufficiently low to not mask the effects of the dispersant and sufficiently high to enable the dispersants to function at reasonable dose rates.

iii) The dispersant dosage would have to be set such that an excess of dispersant was not present to overwhelm the effect of dispersant drop size on effectiveness.

iv) A reliable method of measuring the overall effectiveness of the dispersant would have to be developed.

We were able to satisfy these criteria with varying degrees of difficulty. By far the most difficult task was the design of a uniform drop generator for the dispersant application; this took several months to perfect. We feel that the effort was justified since the end product was a unique system capable of delivering the applied dispersant in a spray composed of virtually identical sized droplets.

Uniform oil slick thicknesses were achieved by placing the oil in a containing ring and mechanically spreading the oil to achieve a "uniform" thickness. The slick was considered uniform when a light shining through the slick resulted in a consistent colouring throughout the slick.

The mixing level was set such that the fresh, untreated oils would not disperse (i.e., <5% dispersion) during the 10-minute test. The mixing level was varied in a series of tests to establish this upper bound on mixing energy.

The dispersant dosages used in the study were established by conducting a series of pre-mixed dispersant-in-oil tests at the mixing energy selected for the oil. The dispersant-to-oil ratio was increased from 1:100 up to as high as 1:5 while measuring the dispersant's effectiveness in the 10-minute test. The pre-mixed dispersant concentration resulting in 75 to 90% dispersion was selected for use in the final test program. This assured that an excess of dispersant was not added.

The dispersion efficiency was measured by taking water samples from the centre of the test tank, extracting the oil with a colourless solvent and determining the oil concentration colorimetrically. Preliminary tests, in which oil concentrations were measured 3, 6 and 10 minutes after the application of dispersant, indicated that the main effect of the dispersant was finished within six minutes. This allowed the sampling program to be reduced to only one sample at the 10-minute mark. To improve the reproducibility of the test all of the oil remaining on the surface of the tank at ten minutes was removed with a sorbent pad, and the test vessel was completely mixed with a paddle to ensure that the one sample was indeed representative of the average oil concentration in the tank.

While this method for determining the dispersed oil concentration and dispersant efficiency seems quite simple it evolved as a result of much testing and analysis and several failed techniques.

Apparatus

The major apparati used in the testing program were the hoop tank, used to hold the test water and oil and to provide the mixing energy to the system, and the dispersant application apparatus.

The hoop tank is illustrated in Figure 2. The tank was filled with 125 litres of salt water for each test. Mixing energy was applied via the cantilevered hoop supported above the tank by an off-centre cam. The cam can be adjusted to increase the stroke length of the mixing hoop and the stroke frequency can be varied by the D.C. motor powering the cam. Water samples are taken from the centre of the vessel via a sampling tube which passes through the tank bottom. A light is shone through the clear tank bottom to assist in the viewing of the dispersion and surface slick characteristics.

A schematic drawing of the dispersant application apparatus is presented in Figure 3. The major components of the system are a supply of pressurized air with a stable pressure regulator, a pressure vessel to hold the dispersant supply, a filter to clean the dispersant to prevent orifice clogging, a pressure gauge to monitor the fluid pressure being delivered to the nozzle, a nozzle body, precision orifices, and a method of vibrating the liquid in the nozzle body at a specific frequency. The quantity of dispersant reaching the oil slick was controlled by a mechanical shutter placed in the path of the dispersant spray. A high quality stroboscope is also needed to view the spray being generated to ensure that the equipment is operating properly.

The strobe is triggered by the signal generator (which also controls the liquid oscillation), via a variable frequency divider to enable stop-action viewing of the drop-stream generated at each orifice. To prevent coalescence of the drops downstream of the orifice a high voltage charging ring is placed around the spray pattern close to the nozzle head to charge the particles exiting the orifices. Not only did this prevent coalescence, due to particle repulsion, it provided a method of adjusting the spray pattern reaching the oil slick. By altering the charging voltage, and thus charge on the drops, the divergence of the spray pattern can be controlled.

This basic technique for mono-disperse (i.e., uniform drop) drop generation was brought to our attention by researchers at the National Research Council's National Aeronautics Establishment in Ottawa. Several papers by other researchers were also consulted during the development of our system (Threadgill et al. 1974, Lindbland and Schneider 1965, Sakai et al. 1982, Goedde and Yuen 1970). The system works as follows: Normally, if a liquid is forced through a nozzle orifice the resulting stream disintegrates into a series of droplets having a relatively wide size distribution. If, however, the liquid is vibrated or oscillated at a regular, given frequency, the liquid stream exiting the orifice will "neck" uniformly and break into a series of equal sized droplets. In this application the fluid in the nozzle body is kept at a constant pressure (thus providing a steady exit velocity from the nozzle orifice) and is oscillated at a particular frequency to achieve the desired uniform size of droplets after the liquid exits the orifice.

Dispersant drop diameters of 0.30, 0.65 and 1.10 mm were generated for this study. Figure 4 is a photograph of a multiple-orifice nozzle generating 300 μm drops.

The speed of the shutter used to control the amount of dispersant reaching the oil slick (see Figure 3) was controlled by varying the weight used to pull the shutter across the spray opening. The size of the shutter opening was also adjusted to vary the quantity of dispersant passing through to the slick.

The orifices used were purchased from a manufacturer of precision jewel bearings. The high voltage charging system was built by us based on a system developed for insecticide spraying in confined areas. Suitable high speed strobe lights and frequency dividers are commercially available but because of their high cost these were also designed and constructed by us. Most of the remaining components of the drop generator were off-the-shelf items. These include the pressurized air supply and regulator, pressure gauge, pressure vessel, filters, signal generator and amplifier. The nozzle body was fabricated from brass plumbing fittings to eliminate machining costs.

Procedure

The final test procedure used for the testing program is briefly summarized below.

1) The hoop tank was filled with approximately 125 litres of 32 ppt salt water. The water was brought up to the level of the hoop when resting in its central position on the off-centre cam.

2) The oil slick thickness for the test was chosen and the volume of oil needed to create a slick of a certain diameter was calculated. The quantity of dispersant needed for the test was then calculated.

3) The dispersant spray nozzle, high voltage charging circuit and shutter were set such that the dispersant spray pattern would hit only the oil slick and the quantity of dispersant passing through the shutter was the amount necessary for the test.

4) The quantity of dispersant passing through the shutter was verified by operating the spray system prior to the final test and catching the dispersant on a pre-weighed sorbent. The quantity of dispersant passing by the shutter was determined by weighing the dispersant soaked sorbent.

5) The oil was then carefully placed in a containing ring of appropriate diameter and spread to fill the ring evenly.

6) The spray nozzle was started by pressurizing the fluid line to the nozzle, the piezoelectric transducer was turned on at the appropriate frequency and voltage, the droplet charging circuit was energized at the pre-set voltage and the entire set-up allowed to equilibrate for a few seconds with the dispersant being caught by the closed shutter.

7) The oil retaining ring was lifted.

8) The shutter was activated to allow passage of the pre-determined quantity of dispersant.

9) The agitating hoop was started.

10) The dispersant spray equipment was turned off.

11) Observations of the behaviour of the oil slick were recorded periodically throughout the test.

12) After ten minutes of agitation any remaining surface oil was removed by an oil sorbent.

13) The tank's contents were completely mixed by a large hand paddle to ensure that any dispersed oil was evenly distributed.

14) A 250 ml sample was then taken from the centre of the tank for oil extraction and colorimetric analysis.

15) The hoop agitation was stopped and the tank cleaned in preparation for the next test.

RESULTS

Tests were conducted with three dispersants, Corexit 9527, Enersperse 700 (EN700) and Finasol OSR5, and four crude oils, Alberta Sweet Mixed Blend (ASMB), Uviluk, Norman Wells and Redwater. Some of the basic physical and chemical properties of these oils are provided in Table 1. Some preliminary testing was also conducted using Corexit 9550 but, because of its low effectiveness on most of the oils and the difficulty of forcing this viscous product through the small orifice of the drop generator, the dispersant was not studied in the final test matrix. Table 2 summarizes the main tests which were carried out in the study. The dispersant effectiveness measurements are summarized in Figures 5 to 12.

Discussion of Results. Figures 5, 6 and 7 strongly suggest that the simple "performance-access" theory of dispersant effectiveness put forth by Mackay cannot be applied in a general manner to all oils. For example, in the case of Enersperse 700 applied to Norman Wells crude oil (see Figure 5) an "access limited" regime did not seem to materialize (at least not for oil slicks as thin as 200 microns with dispersant drops as large as 1100 microns in diameter). Instead, the dispersant performed similarly at all oil thicknesses. While this does not directly contradict Mackay's theory, one would have expected the transition between the "access and performance" regimes to occur within the range of oil slick thicknesses tested, at least for the largest dispersant drop size.

TABLE 1
PHYSICAL AND CHEMICAL PROPERTIES OF TEST OILS+

Oil	Density [g/ml]	Viscosity [sCt]	Oil-Water Interfacial Tension
Alberta Sweet Mixed Blend	0.84	11	21.5
Uviluk	0.90	15	21.4
Norman Wells	0.83	6.1	16.4
Redwater (Coldlake)	0.90	70.7	--

+ Note: these data were taken from Bobra and Chung 1986.

The results for the ASMB oil are even less encouraging with respect to the support of the proposed dispersion theory. For both Finasol OSR5 and Corexit 9527 a reverse trend to that proposed by Mackay was noted in the testing (Figure 6 and 7). As the oil slick thickness increased the dispersant efficiency dropped. The reason for this is not known.

TABLE 2
SUMMARY OF TEST CONDITIONS

Oil Type	Dispersant	Dispersant Drop Size (microns)	Oil Thickness (microns)
ASMB	Corexit	300	200*, 400, 1300
	9527	650	200, 1000, 2000, 3000
	C1:50	1100	500, 1000, 2000, 3000
	Enersperse	300	200, 400, 1200
	700	650	200, 700, 2200
	C1:40	1100	200, 1000, 2500
	Finasol OSR5	650	200, 700, 2200
	C1:25	1100	200, 1000, 2000
Uviluk	Corexit	300	200, 400, 1300
	9527	650	200, 500, 1000, 2000
	C1:50	1100	500, 1000, 2000, 3000
	Enersperse	650	200, 700, 2200
	700	1100	200, 1000, 2500, 3000
	C1:40		
	Finasol	650	200, 700, 2200
	OSR5	1100	200, 1000, 3000
	C1:50		
Norman	Enersperse	300	200, 400, 1500
Wells	700	650	200, 700, 3000
	C1:75	1100	200, 1000, 2000
Redwater	Enersperse	300	200,400, 1000
	700	650	200, 700, 1500
	C1:15	1100	200, 1100

* Note: This was the thinnest slick which could be generated in this test tank

The ASMB, EN700 results (Figure 8) are also difficult to interpret. There was no significant variation in dispersant effectiveness for the 650 um dispersant drop size over a wide range of oil thicknesses; however, for both the 300 and 1100 um drop sizes a sharp reduction in effectiveness was noted for the thin oil slick tests. We attribute this drop in measured efficiency to wall effects. In these tests involving thin slicks, only small quantities of oil were utilized; therefore, any oil that adhered to the tank wall resulted in in-water oil concentration estimates of dispersion far less than 100% even when no slick was observed at the end of the test period. Unfortunately, we had no way to quantify accurately the small volumes of oil attached to the side wall at the end of each test. While we have plotted the measured efficiencies on all of the curves in this paper, we feel that the low efficiencies measured for most of the thin slick cases are not accurate and that the 100% dispersion, based on the visual observations, is likely a more correct indication of the dispersant's effectiveness. Therefore, we do not believe that the low dispersant efficiencies measured for the thin oil slicks (200 um) represent an "access-limited" dispersion regime.

This same problem occurred during the tests on Uviluk crude oil with all three dispersants (Figures 9, 10 and 11). While the measured data plotted for these tests indicate a reduced efficiency at the 200 um slick thickness, our observations again indicated that little or no surface oil was present at the end of all of these tests except for the 1100 um Corexit 9527 test where an incomplete dispersion was noted. All of the dispersants applied on Uviluk gave similar dispersion efficiencies close to the pre-mixed efficiency.

The Redwater crude and EN700 dispersant results differ from all others in that a linear increase in dispersion efficiency occurred with an increasing slick thickness even in the zone where the "performance" of all dispersants was constant for the other oils (Figure 12). This may somehow be due to the more viscous nature of the Redwater crude.

In summary, the results of this testing program generally do not support the "performance-access" theory of dispersant effectiveness. Tests conducted with ASMB using Corexit 9527 and Finasol OSR5 and Redwater using EN700 resulted in trends very different from those proposed in this theory. The remaining tests on Norman Wells, Uviluk and ASMB did not identify a transition between a performance and access dispersion regime for oil slicks greater than 200 um (the thinnest uniform oil slick that we could generate in the test) and dispersant drops as large as 1100 um in diameter. For the field cases used by Mackay to test his model the estimated thick slick thicknesses generally exceeded 200 um, sheens were assumed to be 10 microns thick, dispersant drop sizes were 400 to 1000 microns and transition thicknesses ranged anywhere from 30 to 2000 microns. The tests conducted for this study bracket the input conditions used by Mackay to test his model but do not identify a transition between "access and performance" limited dispersion as his model suggests. If such a transition exists for these oils it must occur at even thinner oil thicknesses. If it applies only to very thin slicks or sheens (i.e., 50 microns or less) then the problem is academic since the oil volume is small in slicks of these thicknesses and natural dispersion is generally fairly rapid for thin slicks.

The dispersion efficiencies achieved with the mono-disperse application system equaled the pre-mixed results for many of the tests at all dispersant drop-sizes studied. This indicates that the dispersant application system used was very efficient at delivering the dispersant to the oil.

ACKNOWLEDGEMENTS

This study was funded by the Environmental Studies Revolving Funds. Valuable guidance and insight into the study was provided by the scientific adviser for the project, Dr. Ron Goodman. The extensive laboratory work was performed by L. Rinaldo.

REFERENCES

Bobra, M.A. and P.T. Chung. 1986. A catalogue of oil properties. Environmental Emergencies Technology Division, Environment Canada, Ottawa. EE-77.

Mackay, D., A Chau, Y.C. Poon. 1986. A study of the mechanism of chemical dispersion of oil spills. Environmental Emergencies Technology Division, Environmental Protection Service, Environment Canada. EE-76.

Mackay, D. 1985. Chemical dispersion: a mechanism and a model. Proceedings of the 8th Annual Arctic Marine Oilspill Seminar. Environment Canada. P.260-268.

Lindblad, N.R., J.M Schneider. 1965. Production of uniform-sized liquid droplets. Journal of Scientific Instrumentation, Vol. 42. p.635-638.

Sakai, T., M. Sadakota, M. Saito, N. Hoshino and S. Senuma. 1982. 2nd International Conference on Liquid Atomization and Spray Systems. Madison, Wisconsin. p.32-45.

Goedde, E.F. and M.C. Yuen. 1970. Experiments on liquid jet instability. Journal of Fluid Mechanics. Vol. 40, part 3. p.495-511.

Threadgill, E.D., R.E. Williamson and G.E. Miles. 1974. Development of controlled-size droplet generators. Transactions of the ASAE. p.837-840.

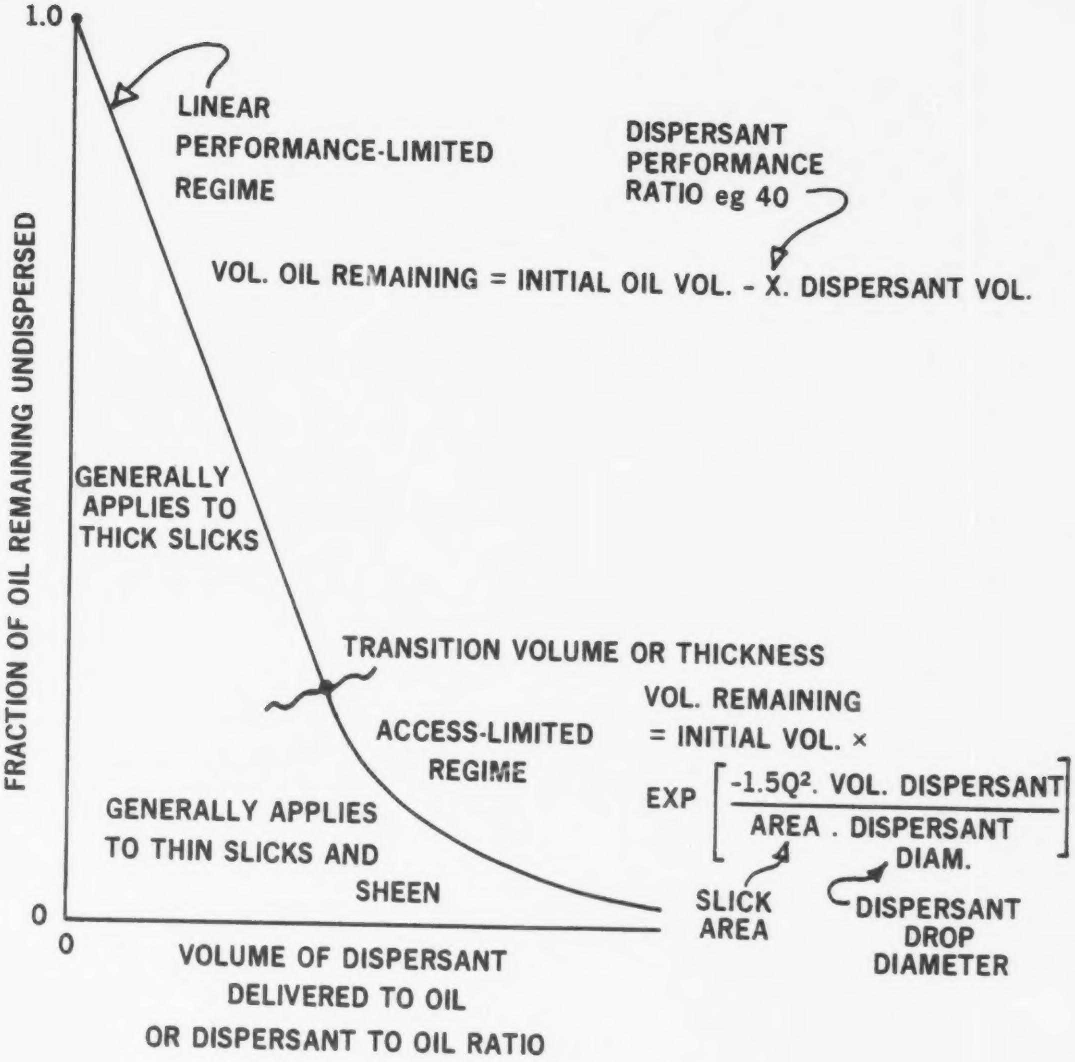

FIGURE 1 - SCHEMATIC DIAGRAM SHOWING THE TWO REGIMES OF DISPERSION, ie INITIAL LINEAR REGIME AND LATER LESS-EFFICIENT ACCESS-LIMITED REGIME

(from Mackay, 1985)

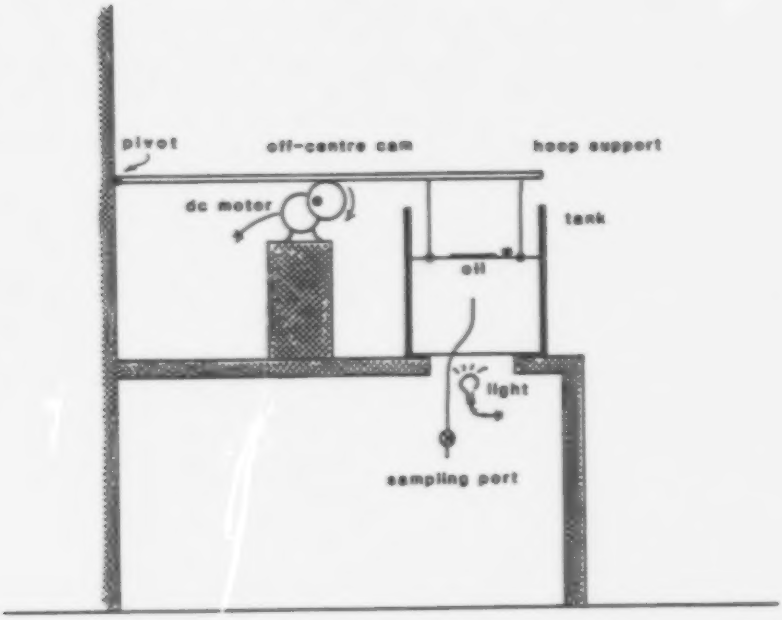
pivot
off-centre cam
hoop support
dc motor
tank
oil
light
sampling port

FIGURE 2

Hoop Tank (side view)

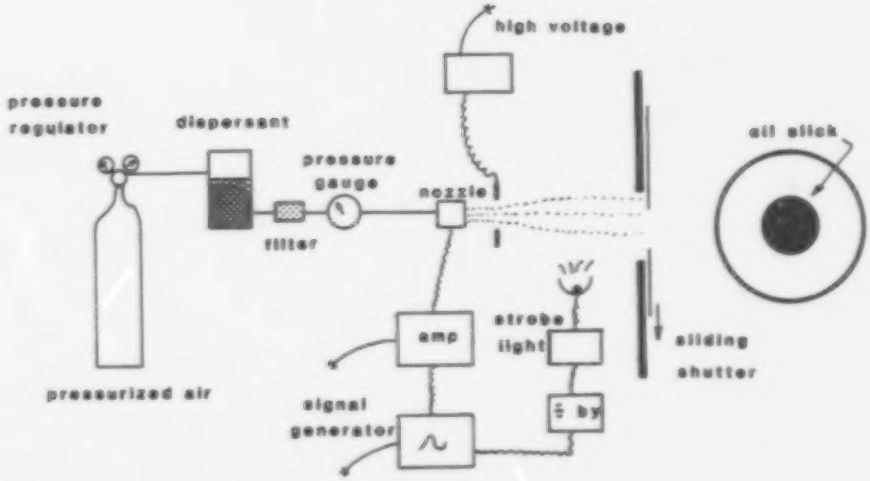
high voltage
pressure regulator
dispersant
pressure gauge
nozzle
oil slick
filter
strobe light
amp
sliding shutter
pressurized air
signal generator
÷ by

FIGURE 3

Mono-Disperse Drop Generator Layout

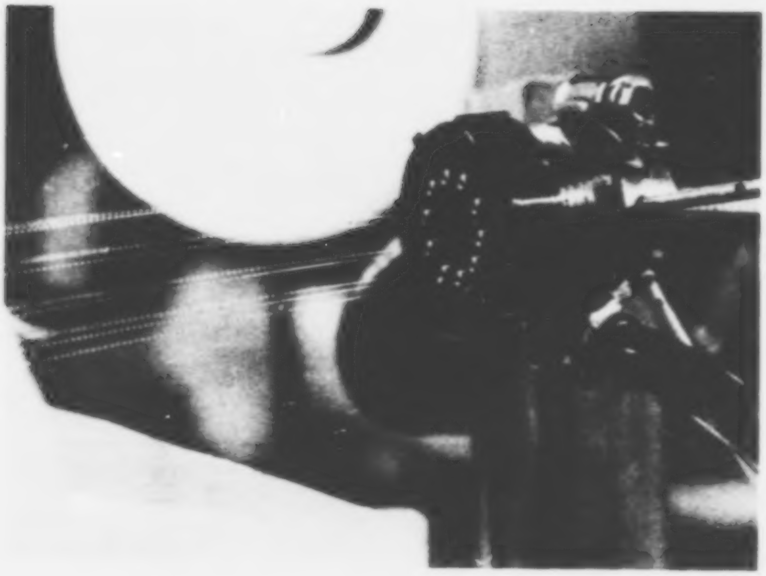

FIGURE 4

Multiple-orifice nozzle generating
300 um dispersant drops

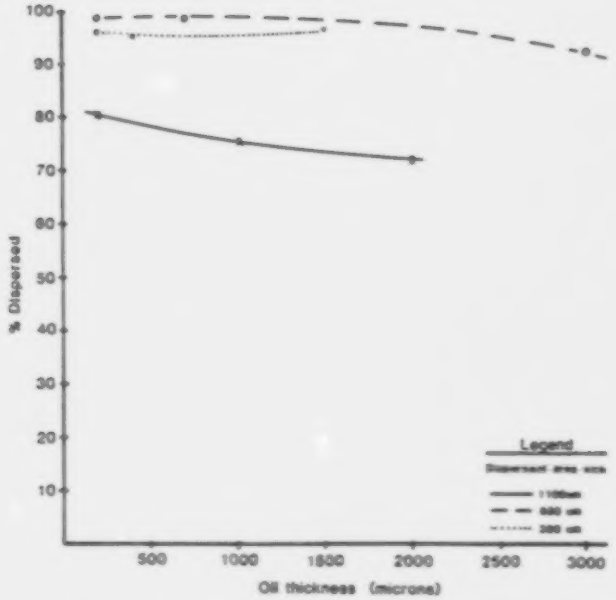

Figure 5 Dispersion efficiency vs oil thickness and dispersant drop size : EN700 at 1:75 on Norman Wells

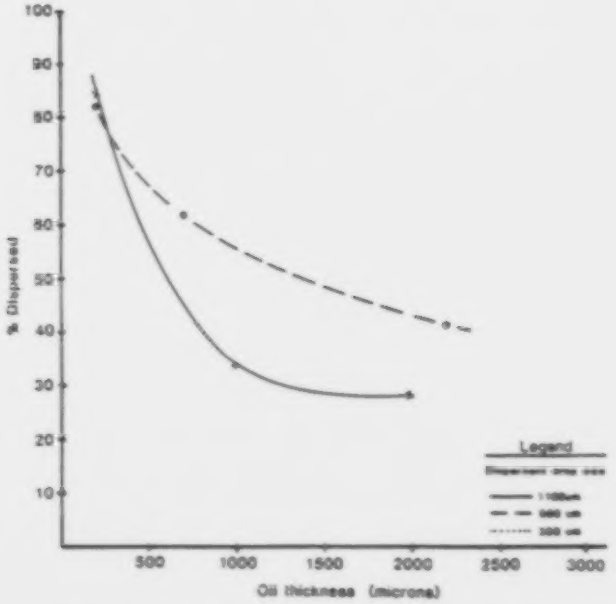

Figure 6 Dispersion efficiency vs oil thickness and dispersant drop size : Finasol at 1:25 on ASMB

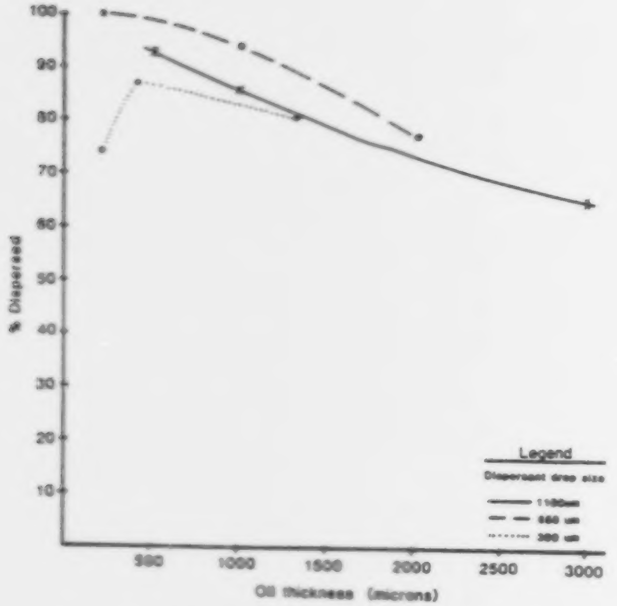

Figure 7 Dispersion efficiency vs oil thickness and dispersant drop size : Corexit 9527 at 1:50 on ASMB

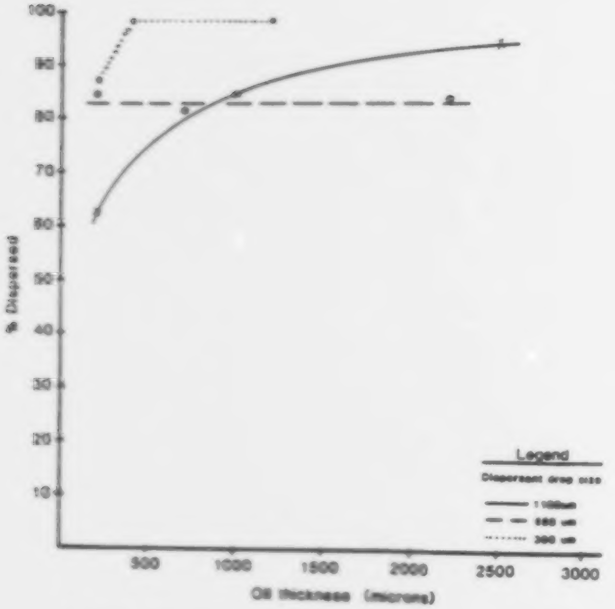

Figure 8 Dispersion efficiency vs oil thickness and dispersant drop size : EN700 at 1:40 on ASMB

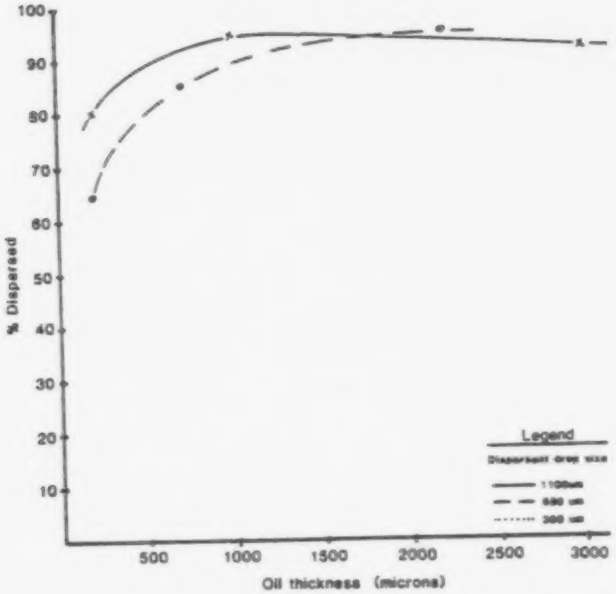

Figure 9 Dispersion efficiency vs oil thickness and dispersant drop size : Finasol at 1:50 on Uviluk

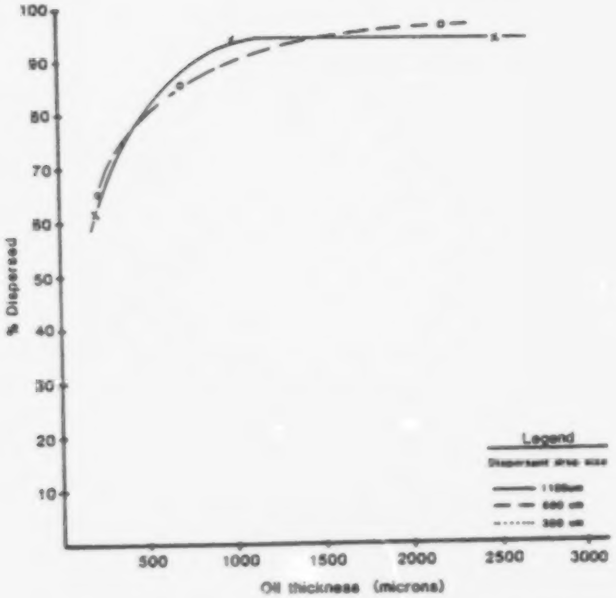

Figure 10 Dispersion efficiency vs oil thickness and dispersant drop size : EN700 at 1:40 on Uviluk

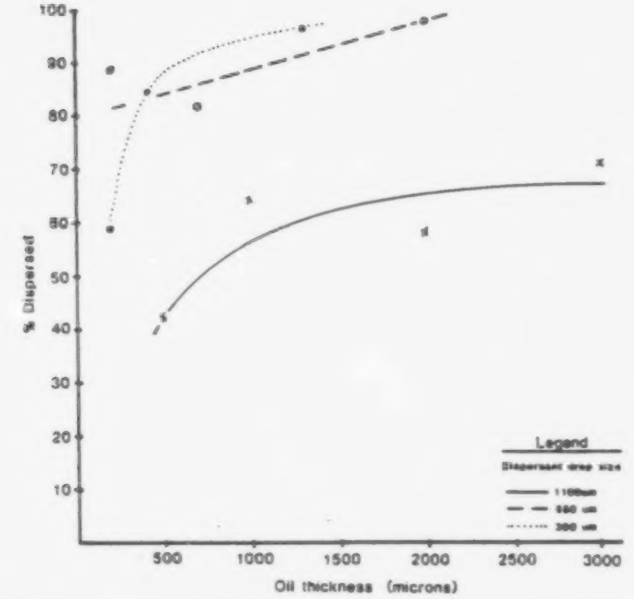

Figure 11 Dispersion efficiency vs oil thickness and dispersant drop size : Corexit 9527 at 1:50 on Uviluk

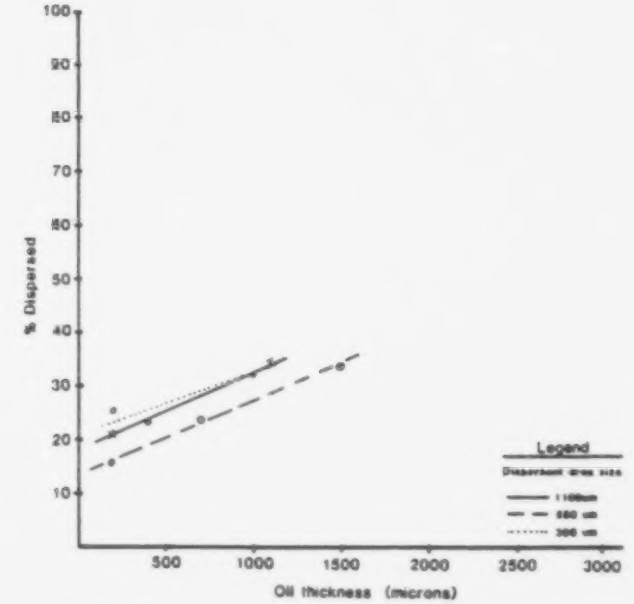

Figure 12 Dispersion efficiency vs oil thickness and dispersant drop size : EN700 at 1:15 on Redwater

A STUDY OF OIL DISPERSION:
THE ROLE OF MIXING AND WEATHERING

Alfred Chau
Donald Mackay
Department of Chemical Engineering
and Applied Chemistry
University of Toronto, Toronto, Ontario M5S 1A1

INTRODUCTION

As has been discussed widely in the literature, laboratory dispersion test systems demonstrate convincingly that relatively small quantities of chemical dispersants can have dramatic effects on the dispersability of crude oils. Results from large scale experimental spills have, however, often been less satisfactory. It appears that when dispersant is added in appropriate quantities to a slick at sea, there is often less dispersion than expected (Nichols and Parker, 1985). Part of the difficulty has been the problem of measuring accurately, the amount of oil which has actually been dispersed, or the amount which has remained on the surface. But it is increasingly apparent that there are fundamental factors which adversely affect oceanic dispersant performance. In this report we discuss and investigate three possible factors: dispersant delivery, oil weathering, and oil-dispersant mixing. The delivery aspect has been discussed previously (Mackay et al., 1986) and will only be reviewed briefly here. The weathering issue has been largely ignored, and it is thus appropriate to devote more attention to it here. The mixing issue is very difficult to investigate, and is the subject of some study as part of this work. The primary purpose is to address the weathering issue in a systematic manner in the hope that future studies may elucidate its true importance. Fortunately, the weathering issue is amenable to reproducible laboratory investigation.

The Mechanism of Dispersion

It is becoming increasingly clear that there are three stages which must be successfully completed for dispersion to occur.

First, a reasonable volume of dispersant must be delivered to the oil. It is generally accepted that a reasonable volume is 1 part dispersant to 20 parts oil, recognizing that much of this dispersant may not eventually usefully disperse the oil. Some factors which influence this delivery process are as follows:

(a) Oil of thickness 1 mm is equivalent to 10000 L/ha, thus to achieve a 20:1 ratio requires 500 L/ha of dispersant. Generally only 10 to 20% of this dosage can be achieved, thus thick patches of oil are generally starved of dispersant. This can be overcome by multiple application but at the same cost.

(b) The tendency of oil slicks to separate into thick and thin patches may result in over- and under-dosing. This is illustrated in Figure 1 which is a simulation of the delivery to the 1984 Norwegian W1 test spill as described by Lichtenthaler and Daling (1985). The thin oil received approximately a 1:1 dosage, whereas the thick oil only received a 1:73 dosage. The average dosage was 1:22. It is believed that this type of under-over-dosing phenomenon is quite common.

(c) The dispersant drop size is often large (eg. 400 um) compared to the thinner parts of the oil slick (eg. 50 um), thus the dispersant drops may break the oil film and induce herding. This will result in much of the oil being unexposed to dispersant. Unfortunately, the larger dispersant drops will fall faster and strike the oil first resulting in this phenomenon being most prevalent initially.

(d) Although it is relatively easy to calculate dispersant dosage from delivery rate, swath width, and aircraft or boat velocity, in practice there are numerous uncertainties which can combine to create a considerable error in dosage. Uncertainties about oil thickness contribute to an even greater error in the estimated delivered dispersant to oil ratio.

Unfortunately, this delivery factor can only be investigated in expensive full scale tests. It is not amenable to laboratory testing. As has been discussed by Lindblom (1986), it is probably a major reason for poor performance.

Second, the dispersant must mix into the oil, and probably must form a reasonably homogeneous solution. It is suspected that this process is facilitated by having small dispersant drops (with a high area to volume ratio), by matching the viscosities of the oil and dispersant, by there being available sufficient time for this mixing-dissolution process to occur, and by sufficient mixing energy being available. Particularly important are believed to be the relative dimensions of the slick and the dispersant drops and their relative viscosities. If the oil viscosity is large, the dispersant may flow over the oil surface and eventually roll off or wash off. If the dispersant drop viscosity is larger, the drop may retain its integrity as it drops through the slick, and possibly through the oil-water interface into the water. In some cases, we have observed the dispersant to form a layer below the oil, separating the oil and water phases. It is also possible that the dispersant dissolves in the water, establishing a critical micelle concentration, then causing the oil to emulsify, ie. dispersion can be from the water side. In any event, the passage of surfactant to and through the oil-water interface causes intense local turbulence and emulsification. The complexity of these phenomena is discussed in the text by Eicko and Parfitt (1987).

Third is the weathering issue. It has been shown experimentally in laboratory and field that under reasonably energetic conditions 1 volume of dispersant can disperse 50 to 100 volumes of oil provided that it is first well mixed into the oil. This suggests that of the dispersant added initially (eg. 5 parts dispersant per 100 parts oil) much fails to achieve a well mixed condition (eg. 4 parts per 100 part of oil fail to disperse, while 1 part mixes and disperses). Obviously, the chemistries of the oil and dispersant are important variables, as is the oil viscosity. It appears that when the oil viscosity exceeds 5000 cp there is insufficient quantity or quality of energy to shear off the oil droplets. Another complicating factor may be the presence of an oil film adjacent to the interface with water which is sufficiently rigid to prevent dispersant from migrating to the interface.

It is this third factor which we have addressed in some detail in this study. The task is to determine if the oil has weathered to a state such that it has become poorly dispersable or even non-dispersable. It is well established that when oil evaporates to the extent that its viscosity reaches some 5000 cp, it becomes very difficult to disperse. The oil may take up water to form water-in-oil emulsion which further increases the viscosity. These two processes can be quantified by laboratory testing.

The approach taken in the study, which is only briefly outlined here, has been to devise and conduct experiments which have the aim of answering the following questions:

(a) How does a drop of dispersant mix into the oil? Does it flow over the oil, penetrate through it, or mix with it?

(b) How is effectiveness related to dispersant drop size and how does drop size influence mixing?

(c) Is it possible that effectiveness is impeded by a "skin" of more hydrophilic material which accumulates in the oil at the oil-water interface and "blocks" access to the dispersant? How can this skin be detected?

(d) Does oil weathering (evaporation) play a more important role that has been previously appreciated? How can this be quantified?

(e) Can an improved dispersion model be developed which is consistent with the observed physical and chemical phenomenon?

SUMMARY OF RESULTS AND DISCUSSION

Dispersant-Oil Mixing

Test solutions were prepared of various densities and viscosities by mixing water, sodium chloride, and glycerol. Dropes of one solution were added to a layer of another. It was striking that despite the fact that both liquids were aqueous and thus, in principle, easily miscible, the drop often retained its integrity for a considerable time, and fell a considerable distance before it broke up. The behaviour was influenced by the relative densities and viscosities of the drops. Surprisingly, the higher the drop viscosity the more rapidly it broke up and dispersed, possibly because it could not circulate internally.

It appears that the dispersant drop lands on the oil surface and tends to penetrate it, accelerating towards a terminal velocity. If the oil is very viscous, the terminal velocity is so low that the dispersant drop merely spreads over the oil surface. For example, on oils of viscosity approximately 1000 cp, the dispersant drop falling velocity is of the order of 0.05 mm/s, thus it is not likely that the dispersant drop can retain its integrity for long. If penetration does occur, the dispersant drop may tend to disintegrate into smaller drops because of the low oil-dispersant interfacial tension.

If the oil viscosity is too low, the dispersant will rapidly penetrate the oil in an intact form and reach the water. This may be the explanation of the maximum in dispersant effectiveness which has been frequently observed, eg. by Martinelli and Lynch (1980).

The most rapid breakup occurred with the most viscous drops, suggesting that it may be desirable to use more viscous dispersants or dispersants containing solvents which will evaporate. A major limitation of dispersant viscosity is the ability to pump the fluid through the fine dispersing jets.

Figure 2 shows one result of an experiment in which an ice cube was immersed in oil, a "film" allowed to form, and the cube withdrawn and placed in water. The results were encouraging in that it appears that a film was formed and could be easily identified. Work is proceeding to establish a better more reproducible method of determining if the film-forming tendency of various crude oils can be tested in this way.

Photographs were taken of various stages of a typical dispersion process under static conditions in the double tube system. When the dispersant drop landed on the oil surface, it rapidly penetrated through the oil layer and then located itself at the oil-water interface. After a few seconds, the dispersant started herding the oil. It was noted that some of the dispersant was lost into the water column. Regions of oil-water interface were observed to be unstable and subject to emulsification. If no mixing was applied, little or no oil dispersion could be seen.

When the oil-dispersant mixing was enhanced with air blowing on to the oil surface, the treated oils were better dispersed from the interface and formed clouds of oil near the top of the water column.

Other experiments were done varying dispersant drop size, slick thickness, and viscosity.

It had been hoped that the mixing tests would yield an equation or model describing the fraction of a dispersant drop which is retained in the oil or sufficiently close to it to cause dispersion. That fraction (F) is presumably related to the variables:

* dispersant drop size
* dispersant drop viscosity
* dispersant drop density
* oil viscosity
* oil density
* oil thickness
* dispersant drop terminal velocity

We are unable to write such an equation because the roles of some key variables are not yet clear.

The results indicate that a high value of F is promoted by

- small dispersant drop size
- large oil viscosity

The effects of the other variables are still not clear. Particularly puzzling is the effect that thinner oil slicks are often more easily dispersed. It had been thought that the opposite would occur.

In previous studies, we have suggested that, provided that there is sufficient oil available, the "captured" dispersant is capable of dispersing perhaps 50 time its volume of fresh oil. This performance factor (N) of 50 probably falls as the oil becomes very viscous and if a film precipitates at the oil-water interface. A key capability would be to relate this quantity to the extent of weathering but to do this requires that the extent of weathering be quantified. This issue is addressed later.

The performance factor N is also influenced by the extent of turbulence at the oil-water interface as quantified, for example, by sea state.

Weathering

In the oil pollution literature, several criteria of weathering have been used, namely

- volume fraction of oil evaporated
- mass fraction of oil evaporated
- distillation temperature
- time of exposure to evaporation
- evaporative exposure

We prefer the use of dimensionless evaporative exposure E as defined by Stiver and Mackay (1984). It can be defined as either KAt/V or Gt/V where K is an evaporation mass transfer coefficient (m/h), A is the oil area (m^3) and G is flowrate of gas (m^3/h) which may be sparged through the oil and becomes saturated with oil vapour. The first definition is most convenient when the oil is evaporated from a tray with a wind stream, and the second when gas sparging or bubbling is used. E is an accurate determinant of extent of evaporation at a specified temperature and can be readily converted to a time if K, A, and V are known. V/A is of course Z the initial oil thickness. Time alone is not a meaningful criterion since the extent of evaporation is sensitive to oil thickness. If time is used, thickness and K must also be specified.

E can be related to F, the volume fraction of oil evaporated by an equation developed by Stiver and Mackay (1984)

$$F = (1/Q \ln (1 + H_0 Q E)$$

where $Q = 10.3\ T_G/T$

and $H_0 = 6.3 - 10.3\ T_0/T$

and T is the environmental temperature (K), T_O is the oil's initial boiling point (K), and T_G is the gradient of the boiling point vs F line (K). The constants 6.3 and 10.3 were fitted from experimental data for five crude oils.

F can be related to T_B by the simpler linear equation

$$T_B = T_O + FT_G$$

It is also possible by substitution to relate E to T_B.

We prefer to use E as a criterion of weathering since it is easily related to time, F, and hence T_B. Often in experimental studies the oil is "topped" to a specific value of T_B.

If the spill is of constant area, E is simply KAt/V or Kt/Z. If A varies with time, ie. the spill spreads, then the time dependence must be included. Often A varies with $t^{1.5}$ thus we can write

$$A = kt^{1.5}$$
$$E = KA/Vdt = Kkt^{1.5}/Vdt = Kkt^{2.5}/(2.5V)$$

It is striking that E now varies with the t to the large power of 2.5, thus in equal time increments 1, 2, 3, 4, 5, E will vary in the proportions 1, 5.6, 15.6, 32, 56, ie. it increases very rapidly. The reason for this is that as the slick thins, its area/volume ratio increases resulting in faster evaporation. It is often not appreciated that very thin slicks are subject to very rapid composition change as a result of evaporation. If, for example, a 1 cm layer of oil loses 10% by evaporation after 10 hours, then a 1 mm slick will lose 10% in 1 hour, and a 0.1 mm slick 10% in 6 minutes and a sheen of 0.01 mm or 10 um will require only 36 seconds. It follows that we can expect thin parts of a slick to be very heavily weathered.

It is relatively straightforward to measure the dependence of oil density, viscosity, and pour point as a fraction of E. Using a laboratory test such as the MNS, Double Tube, WSL/VL, or IFP procedures it is possible to determine the dependence of dispersability on extent of evaporation. There are two general approaches.

If a dispersant to oil ratio (DOR) is specified of say 1:50, the dispersion efficiency can be measured and plotted against E. Alternately, test DOR values can be sought which yield about 50% dispersion and the volume of oil (N) dispersed per unit volume of dispersant is then calculated. Usually N decreases as the oil evaporates and becomes more viscous. N usually approaches low and uneconomic values when the oil reaches a viscosity of several thousand centipoise.

The advantage of the latter "50% dispersion" approach is that it better separates or "spreads out" the performance of different dispersants. The use of a fixed DOR may result in all the high performance products giving effectiveness figures in the 85 to 100% range with inadequate discrimination. In principle, the 50% approach is similar to the search for a lethal concentration to 50% of the test organisms in an aquatic bioassay.

It is also possible to test the emulsion (mousse) formation tendency of the weathered oils by a standard shaking-settling procedure and determine the dispersability of the resulting emulsions. An illustrative plot of N versus E for fresh and emulsified oil is given in Figure 3.

A complete picture of the oil's dispersability can now be obtained by compiling all these data in the form illustrated in Figure 4. The oil properties and dispersability data apply at a specified temperature. If the area-time histories of thick and thin parts of the oil slick are known, it becomes possible to include time scales using the appropriate E-time relationships.

In bringing together all the weathering factors, this figure highlights two problems which correspond to the opening and closing of dispersant application "time windows".

At short exposure times, it may not be feasible to disperse the oil because the response time is not adequate. Further, the thick oil (eg. greater than 1 mm) requires, at least in principle, a dosage of approximately 500 L/ha which may be too large to be feasible. Lower dosages could be applied and probably would have some desirable effect, but the risk remains of underdosing this thick oil. This thick oil, which is relatively small in area, may also be difficult to target.

For these reasons, it may be difficult to apply dispersant effectively to the area to the left of Figure 4, ie. it is a region in which the time window has not yet opened.

A more serious problem arises to the right of Figure 4 when the time window closes. A point (with a specified E) will be reached at which the oil viscosity is too high and an excessive amount of dispersant (N) must be added, to achieve reasonable dispersion. The problem may be related to the oil's chemistry, viscosity, pour point, or susceptibility to emulsion formation. If this E can be identified, the corresponding times can be deduced and the time of "closure of the dispersion time window" determined. It is suspected that for some oils which spread and evaporate rapidly to give viscous residues, this window may be quite short. Indeed in extreme cases it may not be open at all.

We suggest that what is needed is a series of determinations of diagrams such as Figure 4 for selected oils to build up a knowledge base as to how important and variable this effect may be. At present, information on the time window is fragmentated and inadequately documented.

In the analysis of data from experimental spills, it would be useful to sample the surface slick from time to time, obtain GC analyses, and thus estimate the exposure which each part of the oil has experienced. If the dispersant dosage is also known, it should be possible to determine if the oil was inherently dispersable at the time of application. The capability could be built up of relating experimental spill dispersion to laboratory test dispersion.

Although it is unwise to speculate on the results of such tests, if it can be demonstrated that dispersant effectiveness remains lower than expected, even when delivered dispersant dosage is correct and the oil is not excessively weathered, then the only remaining factor is the nature of air-sea mixing/turbulence phenomena. It is conceivable that the turbulence present in the slick and potentially available to promote dispersion is not of the desired nature in terms of frequency, intensity, or length scale. Laboratory systems may fortuitously generate the desired type of turbulence. If this is the case (and it is hoped that it is not) then the entire issue of chemical dispersion as a countermeasure will require rethinking. Fortunately, the UK experience described by Turner and Hurford (1986) suggests that dispersants do result in mitigation of the adverse effects of oil spills, provided that the technical and decision infrastructure is in place well in advance of the emergency.

CONCLUSIONS

A series of exploratory tests have been conducted to elucidate the mixing phenomena which occur when dispersant drops land on, penetrate into, and mix with oil. The results show that the phenomena are quite complex, but it is believed that it should be possible to calculate F, a "fraction of dispersant which intimately mixes with the oil".

Dispersion tests have been conducted with the Double Tube and MNS apparatus and the results interpreted in terms of a performance factor N. ie. the volume of oil dispersed per unit volume of dispersant. It is believed that N is influenced by the nature of the dispersant and that of the oil, but that it falls as the oil weathers and increases in viscosity. It may also fall as a result of formation of a film or skin of viscous oil at the oil-water interface. Attempts have been made to identify and study this interface.

A method of quantifying N in terms of evaporative exposure has been devised which suggests that the time window for effective dispersion is quite short in some cases.

It is believed that if F and N can be quantified then reliable dispersion models or predictive capability could be devised, similar to that devised in earlier phases of this research program. Until this is done, there will remain doubt about the feasibility of using dispersion as a countermeasure.

Figure 1

Illustration of over-under-dosing for the 1984 Norwegian W1 experimental spill assuming 400 um diameter dispersant drops.

	THICK SLICK	SHEEN	TOTAL OR AVERAGE
SLICK VOLUME (m3)	9.72	.28	10
SLICK AREA (m2)	4510	27690	32200
SLICK THICKNESS (mm)	2.16	.01	.31
FRACTIONAL AREAS	.14	.86	
DISPERSANT APPLIED (m3)	.133	.311	.444
DISPERSANT FRACTIONS APPLIED	.3	.7	
OIL TO DISPERSANT RATIO	73.0	.89	22.5
NUMBER OF DROPS (MILLIONS)	3977	9279	13256
DROPS PER SQUARE CM	88.2	33.5	41.2
DROP SPACING (mm)	1.06	1.73	1.56
DISPERSANT DOSAGE (L/ha)	295	112	138

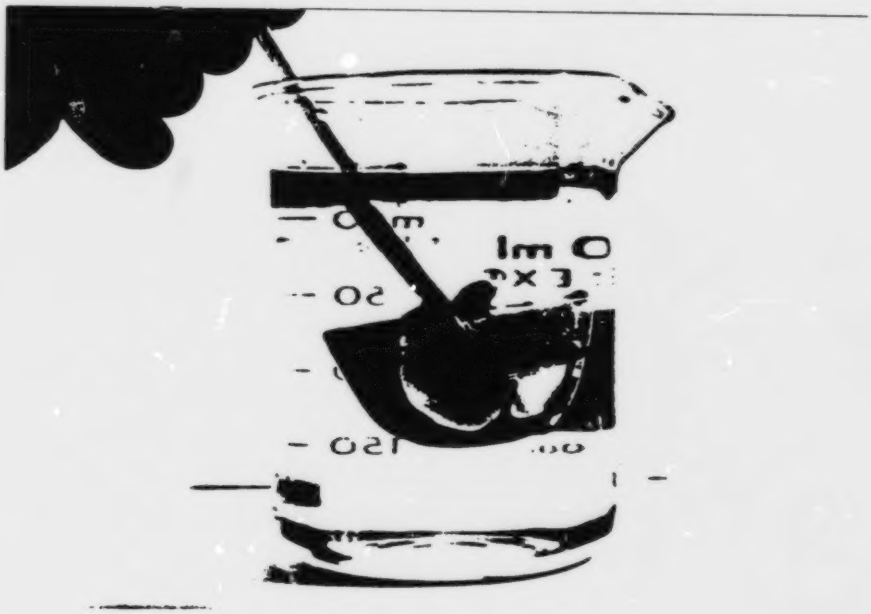

Figure 2 Ice cube experiment, showing the oil film formation

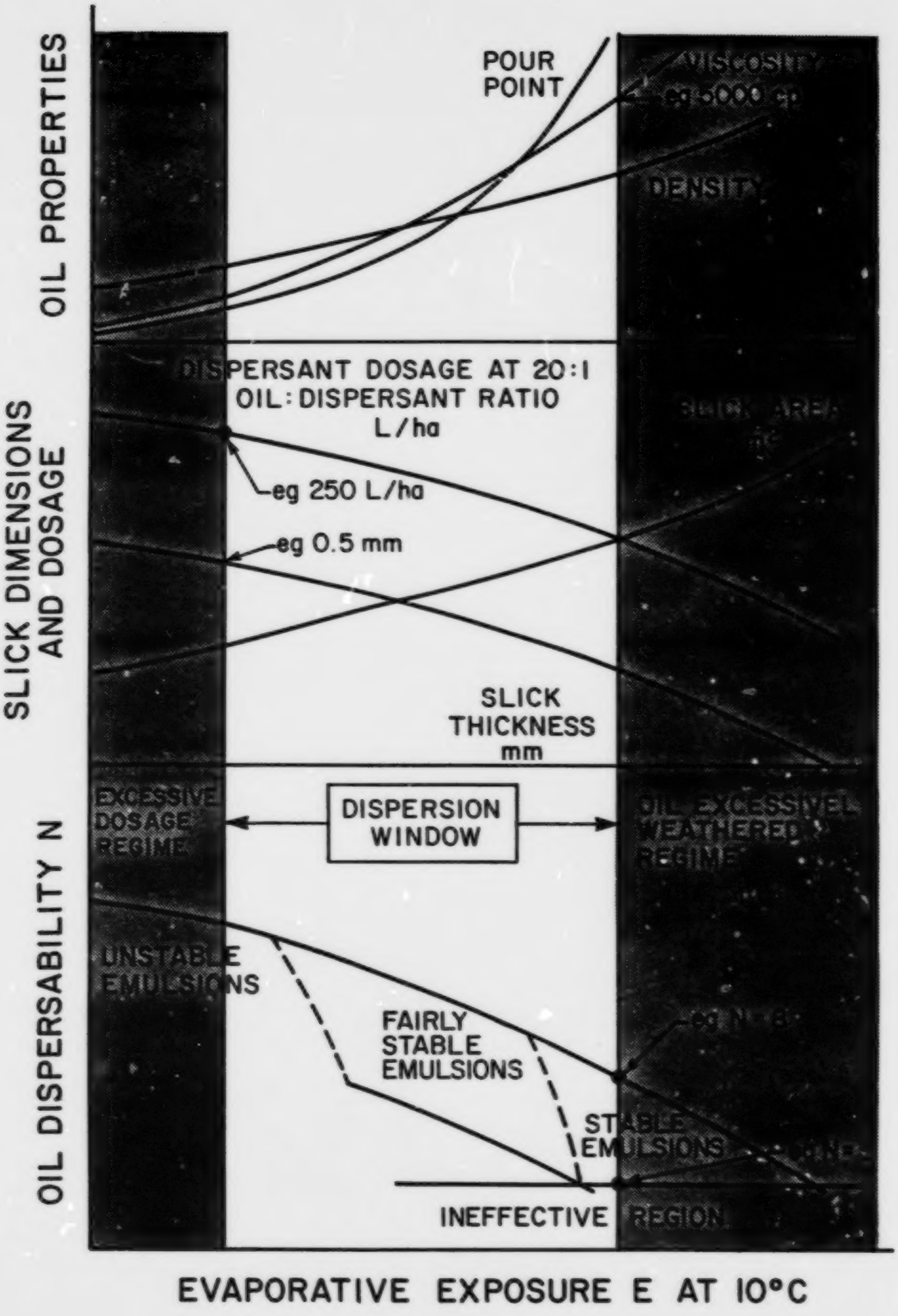

Figure 4

Plot of various quantities affecting oil dispersion as a function of exposure or time illustrating the dispersion window concept

Figure 3

Plot of decreasing effectiveness as a function of exposure or time as the oil weathers

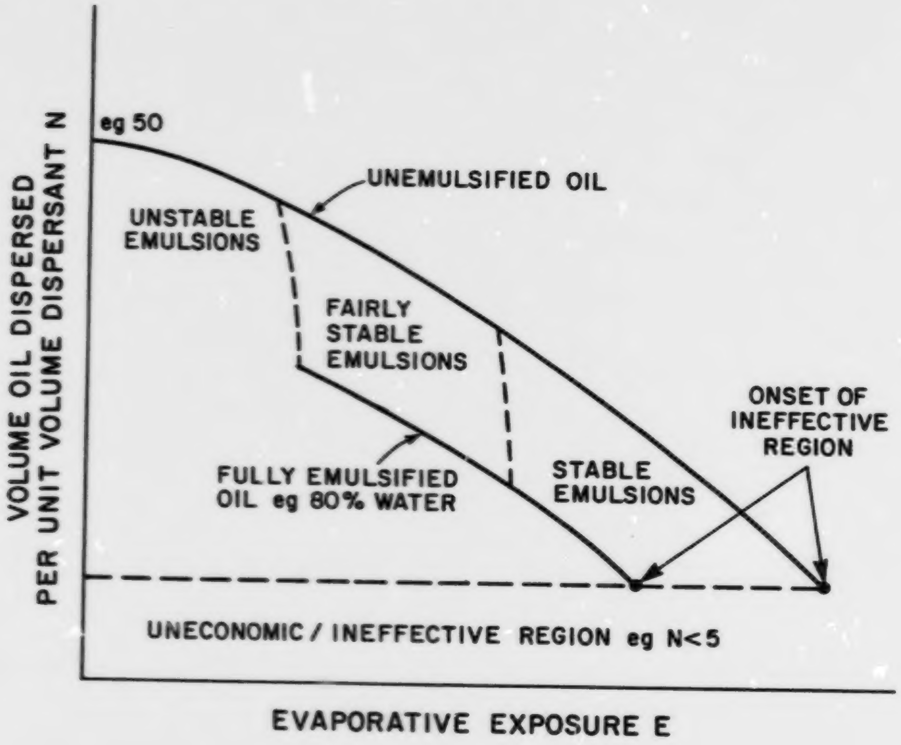
eg 50
VOLUME OIL DISPERSED PER UNIT VOLUME DISPERSANT N
UNEMULSIFIED OIL
UNSTABLE EMULSIONS
FAIRLY STABLE EMULSIONS
STABLE EMULSIONS
FULLY EMULSIFIED OIL eg 80% WATER
ONSET OF INEFFECTIVE REGION
UNECONOMIC / INEFFECTIVE REGION eg N<5
EVAPORATIVE EXPOSURE E

REFERENCES

Chau, A., Sproule, J., and Mackay, D., 1986, A Study of the Fundamental Mechanism of Chemical Dispersion of Oil Spill. Report to Environment Canada, Environmental Emergencies Branch, Ottawa.

Eicko and Parfitt 1987, Interfacial Phenomena in Apolar Media, Sufactant Series No. 21, Marcel Dekker Inc., N.Y.

Lichtenthaler, R.G. and Daling, P.S., 1985, Chemical Application of Dispersants Comparison of Slick Behavior of Chemically Treated versus Non-treated Slicks, 1985 Oil Spill COnference Proceedings, pp. 471-478, Amer. Petrol. Inst., Washington, D.C.

Lindblom, G., 1986, Dispersants and Their Application as Currently Perceived in the United States. Paper presented at the International Seminar of Chemical Dispersion of Oil on Sea, DOOS Proceedings. Trondheim, Norway.

Mackay, D. and Chau, A., 1986, The Effectiveness of Chemical Dispersants: A Discussion of Laboratory and Field Test Result. International Seminar on Chemical and Natural Dispersion of Oil on Sea, DOOS Proceedings 1986, Trondheim, Norway

Nichols, J.A. and Parker, H.D., 1984, Dispersant Comparison of Laboratory Tests and Field Trials with Practical Experience at Spills, 1985 Oil Spill Conference Proceeding, pp. 421-427, Amer. Petrol. Inst., Washington, D.C.

Turner, A. and Hurford, N., The use of Oil Spill Dispersants - Some views from U.K. 1986 Paper presented at the International Seminar of Chemical Dispersion of Oil on Sea, DOOS Proceedings. Trondheim, Norway

Stiver, W., and Mackay, D., 1984, Evaporation Rate of Spills of Hydrocarbons and Petroleum Mixtures, Environ. Sci. Technol. 18, pp 834-840

THE ARCO ANCHORAGE OIL SPILL, A REVIEW

D. W. Chamberlain, J. Lindstedt-Siva, E. R. Mancini
Atlantic Richfield Company, 515 South Flower Street
Los Angeles, California 90071

R. A. Levine
ARCO Marine Incorporated, 300 Oceangate
Long Beach, California 90802-4341

J. A. Miller
GeoEngineers Incorporated, 2405 - 140th Avenue, N.E.
Bellevue, Washington 98005

ABSTRACT

On 21 December 1985 the oil tanker ARCO Anchorage grounded in Port Angeles Harbor, Washington, USA, spilling 5690 barrels of Prudhoe Bay crude oil. Oil eventually spread east and west of Port Angeles Harbor. Localized intertidal areas of the Strait of Juan de Fuca were lightly to heavily oiled, with the heaviest oiling on the inside of Ediz Hook, Port Angeles Harbor, and on the outer edge of Dungeness Spit, a National Wildlife Refuge.

About 2000 seabirds were oiled. Spill response included setting up oiled bird collection stations, an oiled bird cleaning and rehabilitation center, the use of conventional skimmers, booms and sorbents, etc., inshore and open water cleanup. Unique problems encountered included cleaning of bundles of oiled logs and contaminated shore sediments involving the invention of special cleaning methods and equipment. A field screening procedure for the analysis of crude oil in beach sediments was developed.

Monitoring the fate and effects of the spilled oil began immediately following the spill and is continuing. Results of beach sediment agitation for crude oil removal *demonstrate a significant reduction of oil concentrations in affected sediments. Elevated tissue levels of hydrocarbons in affected invertebrates oiled by the spill also show a decrease since the event. Elevated levels of petrogenic hydrocarbons in captive fish exposed to the spill were not observed.*

INTRODUCTION

At 4:25 p.m. on Saturday afternoon, December 21, 1985 the tanker *ARCO Anchorage* (operated by ARCO Marine Inc. [AMI], a subsidiary of Atlantic Richfield Company) ran aground in Port Angeles Harbor, Washington (Figure 1). The grounding ruptured the hull (tanks 5 Port and 5 Center) of the tanker releasing approximately 5,690 bbl (239,000 gal) of Alaska North Slope crude oil into the water. Immediately, crude oil was smelled by the crew, who notified the U. S. Coast Guard of the accident. At the same time, the ARCO Marine Inc. Spill Contingency Plan and the ARCO Marine Spill Response Team were activated. Heavy fog throughout the area closed down local airports, delaying arrival of the response team and hampering overflights of the spill area. Calm seas, however, aided the deployment of containment booms and oil skimmers (Levine, 1987; Miller, 1987; Siva, et al., 1987).

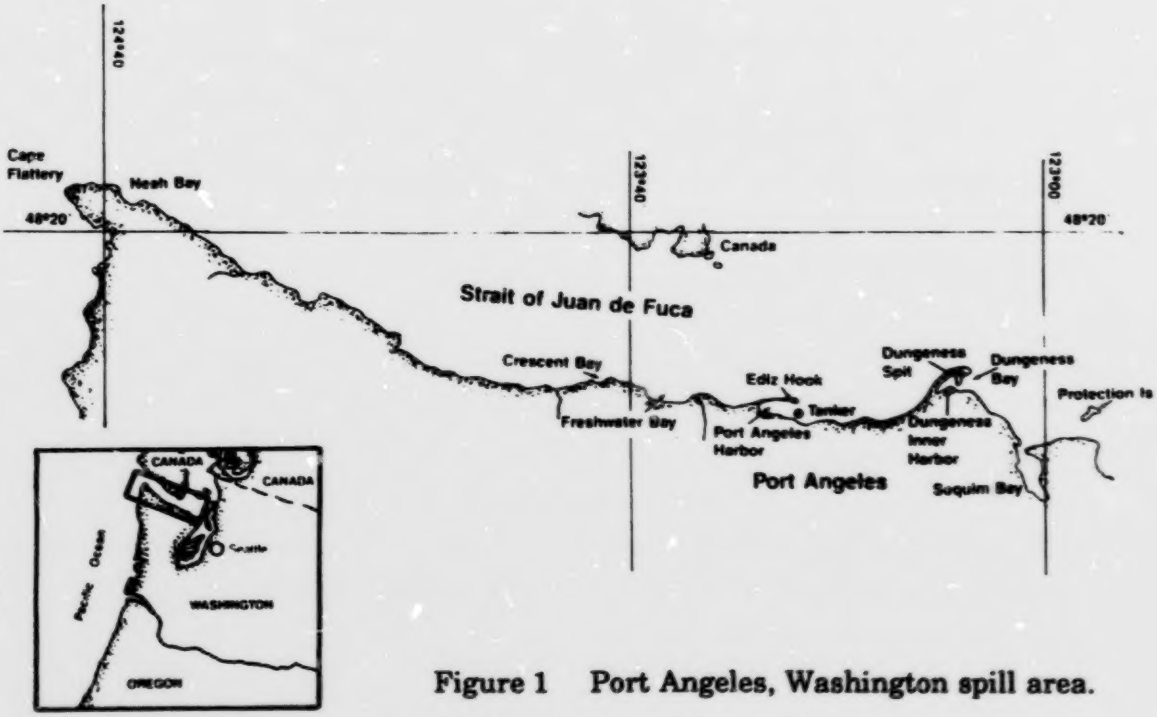
124°40
123°40
123°00
48°20'
48°20
Cape Flattery
Neah Bay
Canada
Strait of Juan de Fuca
Crescent Bay
Freshwater Bay
Ediz Hook
Tanker
Port Angeles Harbor
Port Angeles
Dungeness Spit
Dungeness Bay
Dungeness Inner Harbor
Sequim Bay
Protection Is
CANADA
CANADA
Pacific Ocean
Seattle
WASHINGTON
OREGON

Figure 1 Port Angeles, Washington spill area.

Primary response priorities were, 1) concern for Public safety and, 2) mitigating environmental impacts.

Initially, the oil spread within Port Angeles Harbor coming ashore on the south shore of Ediz Hook (Figure 2).

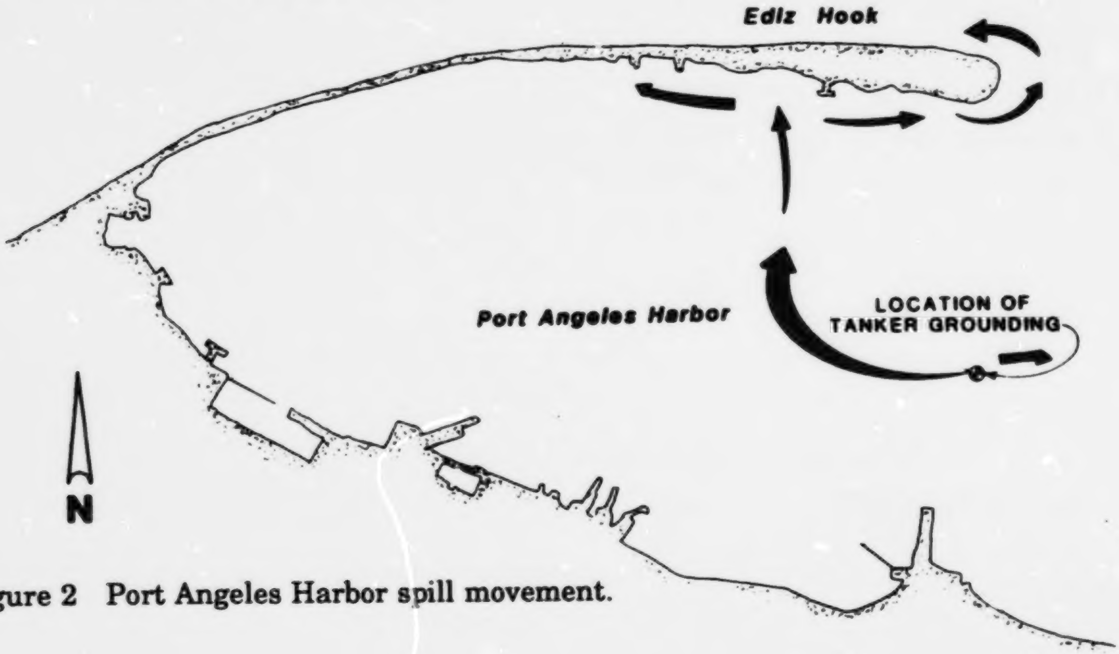
Ediz Hook
Port Angeles Harbor
LOCATION OF TANKER GROUNDING
N

Figure 2 Port Angeles Harbor spill movement.

The oil then spread out of the harbor as far east as Dungeness Bay and west to Neah Bay. Heaviest contamination occurred along the south shore of Ediz Hook and the north shore of Dungeness Spit (Figure 3).

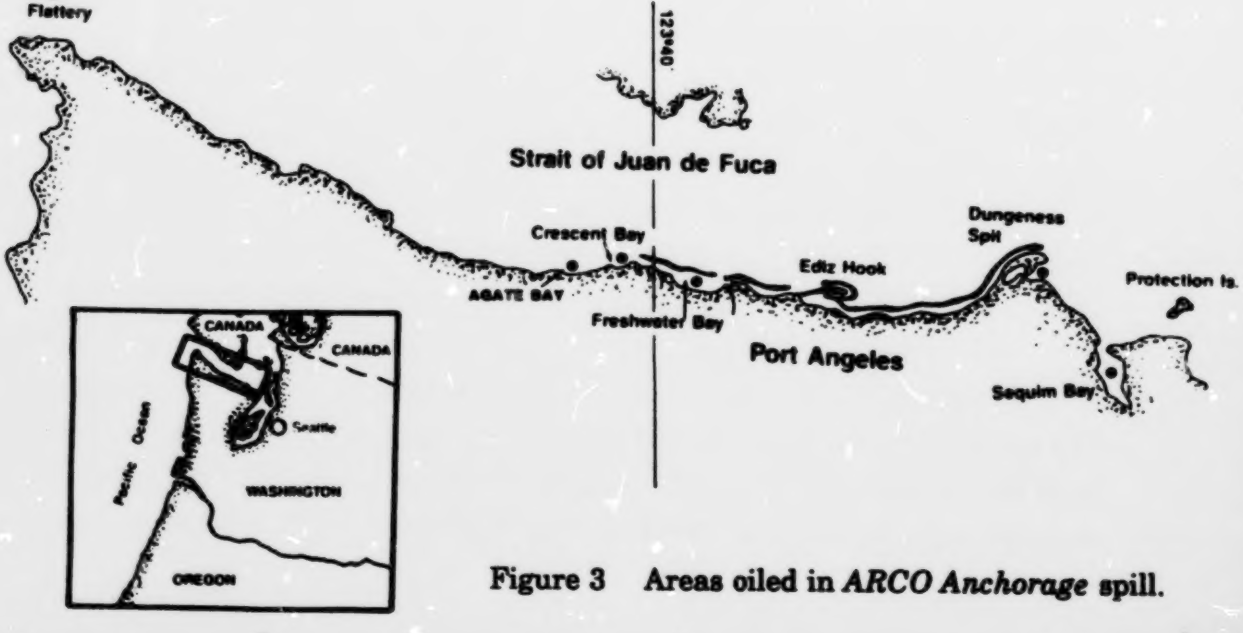
Cape Flattery
123°40'
Strait of Juan de Fuca
Crescent Bay
AGATE BAY
Freshwater Bay
Ediz Hook
Port Angeles
Dungeness Spit
Protection Is.
Sequim Bay
CANADA
CANADA
Pacific Ocean
Seattle
WASHINGTON
OREGON

Figure 3 Areas oiled in *ARCO Anchorage* spill.

ENVIRONMENTAL ASPECTS

Description of the Area

The Strait of Juan de Fuca is located along the Canada/United States border between British Columbia and Washington (Figures 1 and 2). The physical setting of the area, as summarized by the Washington State Department of Ecology, describes the Strait as a deep estuary connecting inland waters with the Pacific Ocean. The climate is maritime with cool summers and mild winters, has a tidal range of 4-10 feet, and current speeds up to 2-4 knots. High energy areas are north and west facing beaches (Kittle et al., 1987).

This area is characterized as being very productive, supporting significant populations of fish, molluscs, crustaceans, birds and mammals. It is one of the major habitats for marine birds on the west coast of North America. Just to the east of Port Angeles is the Dungeness Wildlife Refuge (Kittle et al., 1987).

Spill Response

It is AMI philosophy to assume responsibility for a spill if it occurs from a vessel owned or operated by AMI, regardless of cause or fault (Levine, 1987). The first priority was to protect the Dungeness National Wildlife Refuge which included Dungeness Spit, Dungeness Bay, and inner Dungeness Harbor. Additional concerns were Protection Island and Sequim Bay previously identified as important Pacific herring spawning areas and also supporting large populations of seabirds, fishes, and invertebrates (Siva, et al., 1987). Containment booms and skimmers were deployed to protect the bay and inner harbor and also Protection Island. This was successful although some oil rounded the end of the Dungeness Spit. No oil entered Sequim Bay or reached Protection Island. Later, skimmers and booms were deployed in Port Angeles Harbor and skimmers operated in various areas along the coast to the west of Port Angeles.

A bird cleaning facility was set up by local volunteers, aided by the local county emergency services, to handle the oiled birds coming ashore. Birds were collected by local volunteers. The bird cleaning facility was operated by Alice Berkner (International Bird Rescue Research Center, Berkely, California) until January

14, 1986. More than 2,000 volunteers aided the bird rescue over the course of the spill (Siva, et al., 1987).

Spill Documentation

A sampling program was initiated two days following the spill to document fate and effects of the spilled oil. This developed into a more comprehensive effort to include sampling of sediments and the water column where oil was reported.

Salmon and trout from a commercial mariculture faiclity in the spill area in Port Angeles were sampled monthly and analyzed for hydrocarbons. No increase in fish mortality over the normal rate was observed. Fish tissue analyses showed no significant amounts of petroleum hydrocarbons present (Page, 1987).

Impacts

Marine birds were affected by the spill; 1,917 were known to have been oiled. Almost 60 percent (1,118) of these were grebes and another 25 percent (475) were ducks. Alcids, cormorants, gulls, loons, and shorebirds were affected in lesser numbers. Eighty percent (1,243) of the birds treated at the bird center died before release. Eighteen percent (281) birds were released after cleaning.

High mortality among cleaned birds was attributed to a large number being received at the cleaning center in a short time and the difficulty of maintaining quality control because of the large numbers of volunteers doing the cleaning (Siva, et al., 1987).

The State of Washington Department of Ecology's short-term damage assessment concluded that the contamination of the south side of Ediz Hook resulted in the stressing of hardshell clam and crabs, and the killing of starfish, jellyfish, and nudibranchs. They documented no impacts outside of Ediz Hook except for waterbirds. The state estimated about 4,000 waterbirds were oiled and died from the spill (ca. 2000 oiled birds were actually observed). Nesting marine bird populations in the spill area appear unaffected (Kittle, et al., 1986).

Fate of Oil

Siva, et al. (1987) give oil concentrations in various regions of the spill area listing concentrations as high as 8,300 ppm in the heavily oiled sediments of outer Dungeness Spil. Very high oil concentrations were also found on the southern shore of Ediz Hook, up to 20,000 ppm. These figures were produced from 239 sediment samples analyzed by infrared spectrophotometry (IR) and gas chromatography (GC). Water and animal tissue samples were also analyzed by GC. Oil concentrations in other areas were present in trace amounts or at background levels. The results of a reconnaissance survey (Word, et al., 1986) of the spill area show the following:

-No oil contamination of sediments at Protection Island, Sequim Bay, Port Williams, Jamestown, Three Crabs, Green Point, Freshwater Bay, Agate Beach, or Whiskey Creek.

-Trace amounts of oil observed at Crescent Bay and outer Dungeness Bay.

-Significant contamination at outer Dungeness Spit, Ediz Hook, and Port Angeles Harbor in December, but not in January.

-GC analysis of water samples from Port Angeles Harbor and off Dungeness Spit showed no detectable dissolved petroleum hydrocarbons from the *ARCO Anchorage*, even at 1 m beneath a slick.

Following the removal of oiled debris from Ediz Hook, oil continued to leak from the sediments. Sampling revealed oil in varying concentrations between 2 to 12 inches below the surface (Siva et al., 1987). Special cleanup methods were developed to address this problem. (discussed below). Before beach cleanup sediment oil concentrations ranged from less than 100 to about 20,000 ppm. Following cleanup the mean oil concentration (2,900 ppm) for all sites was reduced 67 percent to a mean of 550 ppm for all sample sites. Sediment cleaning procedures were generally very effective where sediment oil concentrations were above 1,000 ppm and generally ineffective at lower concentrations. Highest oil concentrations remained in those areas where the cleaning methods devised for this particular situation were not employed because of structures present.

Monitoring Program

A sampling program is being conducted periodically to monitor the fate and effects of the oil in the sediments of Ediz Hook on an extended time basis. This program will continue for up to three years or until oil concentrations reach background levels. Results to date show significantly reduced levels of oil in the sediments compared to levels before the sediment cleanup started. Previous work on the oil degrading activity of microorganisms in the Port Angeles area suggests that this trend will continue (Westlake and Cook, 1980). Our most recent data give a mean oil sediment level for all sites of 255 ppm (Miller, et al., 1987).

OPERATIONAL ASPECTS

Spill Response

Within about ten minutes of the spill, the industry spill cooperative, Clean Sound, had been notified. By 9:25 p.m., about 5 hours following the spill, 4,500 feet of containment boom had been deployed from local storage. Because of the extent of the spill five different major cleanup contractors were called in to assist in the cleanup response (Levine, 1987).

In addition to the environmental concerns addressed above, a number of other factors complicated the spill response. These included the extensive use of the harbor as a lumber port, large areas of land and water storage for export lumber, and the many lumber and lumber-related industries. In Port Angeles Harbor there is also a public marina with docking for both pleasure boats and commercial fishing boats.

Along with the environmental priorities, economic priorities for protection and cleanup were established. In descending order of economic sensitivity, these were Port Angeles Harbor, Dungeness Bay, Agate Bay, Crescent Bay and Freshwater Bay (Levine, 1987).

Cleanup Plan

Cleanup was divided among the cleanup contractors to minimize the spill effects. Two contractors provided offshore cleanup, stored recovered oil, and did most of the oil containment. Another contractor provided cleanup along the Ediz Hook beaches. The State of Washington Conservation Corps was brought in to assist in cleaning the beaches at Dungeness Spit in the wildlife refuge. Two additional contractors handled the cleanup of the logs oiled in Port Angeles Harbor and cleanup of the beaches to the west of Port Angeles.

Levine (1987) points out three major problems that were encountered which had a significant impact on cleanup duration and cost, and which could not have been anticipated. These were 1) the weather, 2) the floating log bundles in the harbor, and 3) the oil penetrating the sediments of Ediz Hook Beach.

Although at the time of the spill the weather was clear and calm with good visibility, immediately and for almost a month following it deteriorated to light easterly winds and fog. Fog was the primary problem and created severe conditions for locating the oil and for the operation of skimming equipment. Because aircraft overflights were restricted, skimming vessel operators predicted oil slick locations by their knowledge of local currents and trajectories. This was very effective and kept the skimming operations going 24 hours per day for five weeks (Levine, 1987). Also the use of radar on the skimmer boats allowed for safe operation and without it working offshore would not have been possible.

Other important factors in maintaining the skimming operation were the presence of additional skimmers, equipment repair crews and an inventory of spare parts to reduce the down time for reparis, etc.

As Port Angeles is a center for lumber export to many foreign countries, logs are stored on both land and on the water awaiting loading onto bulk carriers. About 20 million board feet were stored in the waters of the harbor at the time of the spill. Of this amount 15 million board feet were oiled, with 10 million of it heavily oiled. Subsequent cleanup of the logs was slow. Lightly oiled logs were cleaned by spraying with fire hoses. Bundles containing 10 to 20 logs were found to have oil drawn into spaces between the logs and held there well below the water surface. Though not obvious at first, the holding of oil by the log bundles was later suspected when large amounts of new uncontained oil was observed on the water surface following a squall. This was confirmed and the log bundles, averaging about 45 tons each, were cleaned utilizing large logging barges. The bundles were lifted out of the water, dipped below the water surface 3-4 times to release any trapped oil, and then sprayed by high pressure fire hoses. This process freed the trapped oil which was contained and recovered. In this manner the logs were cleaned sufficiently for most owners (Levine, 1987).

Well into the cleaning operations the Ediz Hook beach was observed to have been re-oiled with fresh oil following rough weather. It was determined that this was oil that had penetrated into the beach aided by the very porous coarse grain sand and cobble sediments and the 6-10 food tidal variations that drained the beach sediments. In various places the beach sands were saturated with oil that remained about as fresh as when it was spilled. This oil appeared to be a layer 4-6 inches thick, 2-3 inches below the surface of the sediment. This penetration of oil was found along a 7000 foot length of moderately to heavily oiled beach. Estimtes of trapped oil were as high as 75 barrels per 100 yds of beach. A unique system was devised to efficiently release the trapped oil (Levine, 1987). Figure 4 shows the apparatus (called "Muck Monster III") that provided good mechanical agitation of the sediments releasing the trapped oil. This apparatus consisted of bulldozers equipped with ripper blades fitted with high pressure water spray nozzles. The nozzles were mounted behind each ripper blade and the combination of hydraulic and mechanical energy provided by this arrangement proved to be fast and efficient. Oil released in this manner was contained and recovered preventing re-oiling of the beach. Heavily oiled portions of the beach required up to 40 passes of the bulldozer, with the agitation apparatus, over two days time to decrease visible oil to small amounts.

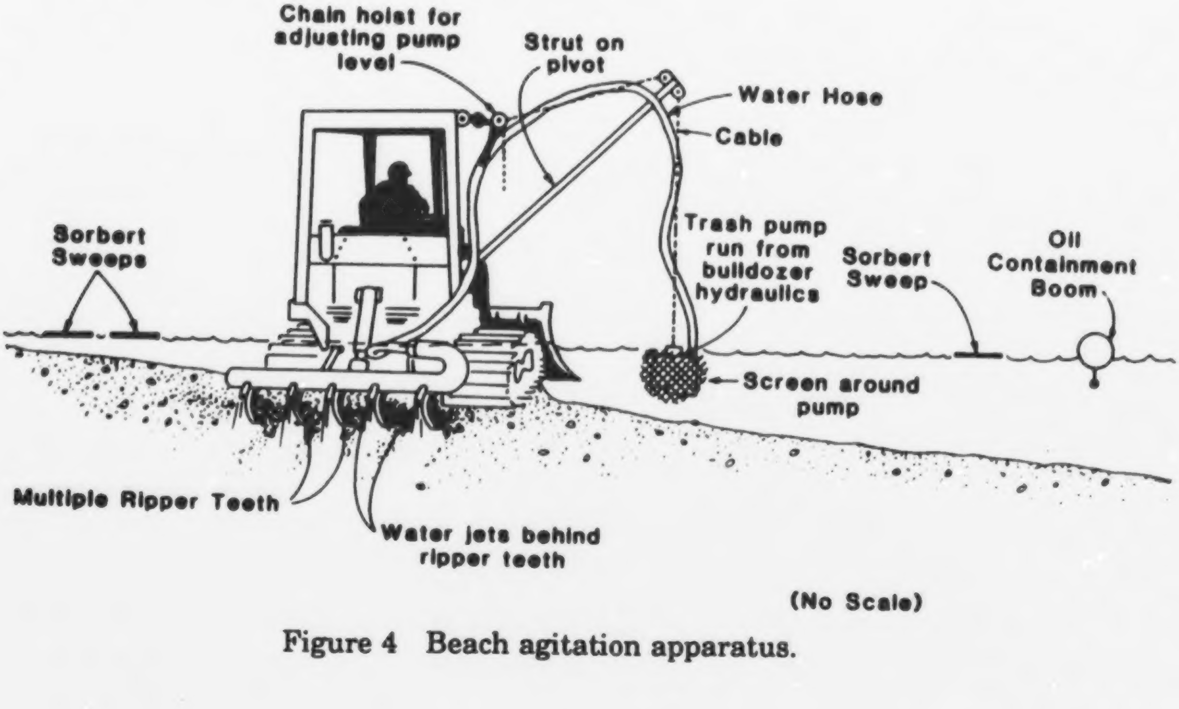
Chain hoist for adjusting pump level
Strut on pivot
Water Hose
Cable
Sorbert Sweeps
Trash pump run from bulldozer hydraulics
Sorbert Sweep
Oil Containment Boom
Screen around pump
Multiple Ripper Teeth
Water jets behind ripper teeth
(No Scale)

Figure 4 Beach agitation apparatus.

Approximately 55 percent (3,126 barrels) of the spilled oil (5,690 barrels) was ultimately recovered and refined (Levine, 1987). Approximately 2,800 cubic yards of debris was collected and 2,300 cubic yards of this burned. The remainder was cleaned and used as fill for road building or placed in a landfill. Additionally, 2,180 tons of abandoned logs were removed from Ediz Hook and used for waste fuel.

BEACH SEDIMENT RESTORATION

Miller (1987) has reviewed the geology of the Port Angeles area, described the origin of Ediz Hook and the composition of its sediments that facilitated the oil penetration mentioned above. Test excavations at various locations in the oiled sediments of Ediz Hook showed that most of the oil was in the upper 5 inches and that the trapped oil would float to the surface of the water in the excavations, especially if the sediment was agitated. Interestingly, the oil would not emerge from the sediments during tidal fluctuations (Miller, 1987). As far as is known, this phenomenon has not been reported before. The information was the basis for implementation of the beach agitation procedure described.

Oil concentrations in the beach sediments before and after the agitation were determined by thin layer chromatography (TLC) and checked with gas chromomatography (GC) and gas chromatography/mass spectrophotometry. The TLC data was examined to determine the effectiveness of the beach agitation program (Miller, 1987). The resulting data revealed that the upper beach had the greatest degree of contamination, the mean reduction of oil concentration was 74 percent in areas where the concentration was above 1,000 ppm, and beach agitation reduced the mean concentration of oil from about 2,900 ppm to 550 ppm.

DISCUSSION AND CONCLUSIONS

The environmental goal of the spill response was to minimize the ecological impacts of the spill and consequently response efforts prevented or reduced the amount of oil reaching the identified environmentally sensitive areas (Siva, et al., 1987). A conscious decision to deploy resources to more ecologically sensitive areas was made.

Bird impacts probably would have been reduced if chemical dispersants could have been used to remove oil slicks on the water surface. Also, the use of a stable work force in place of volunteers would most probably result in more oiled birds surviving the cleaning process.

The spill's most severe impacts were to the marine birds that were oiled. The most heavily oiled area, Ediz Hook, showed short-term impacts on intertidal fauna.

The agitation of oiled beach sediments utilizing a combination of mechanical and hydraulic energy proved very successful in removing oil from between the sediment pore spaces. It was apparently ineffective in removing adsorbed oil.

Thin layer chromatography technique proved, for the purpose of reclamation monitoring, a cost-effective and reliable technique.

Cleanup of the Port Angeles spill showed it is possible to clean a spill efficiently, effectively while minimizing environmental impacts.

REFERENCES

Kittle, L. J., R. Burge, R. Butler, W. Cook, K. Fresh, M. Kyte, R. Lowell, R. Pease, D. Penttila, A. Scholz, S. Speich, R. Steelquist, and J. Walton. 1987. The Washington State Department of Ecology Marine Resource Damage Assessment Report for the *ARCO Anchorage* oil spill, December 21, 1985 into Port Angeles harbor and the Strait of Juan de Fuca. State of Washington Department of Ecology, Olympia, WA. 97p. + appendices.

Levine, R. A. 1987. Operational aspects of the response to the *ARCO Anchorage* oil spill, Port Angeles, Washington. Proceedings of the 1987 Oil Spill Conference, American Petroleum Institute, Washington, D. C., pp 3-7

Miller, J. A. 1987. Beach agitation for crude oil removal from intertidal beach sediments. Proceedings of the 1987 Oil Spill Conference, American Petroleum Institute, Washington, D. C., pp 85-90.

Miller, J. L., J. K. Farr, W. B. Blaylock, J. P. Houghton, and R. N. Dexter. 1987. First annual report, Ediz Hook monitoring program, Port Angeles Harbor, Washington. Draft report to ARCO Marine, Inc., Long Beach, CA. 31 p + appendices.

Page, D. W. 1987. An analysis and interpretation of tissues hydrocarbon data for fish sampled from the *ARCO Anchorage* oil spill impact zone. Draft report to ARCO Marine Inc., February 1987. 31 p + appendices.

Siva, J. L., D. W. Chamberlain, E. R. Mancini. 1987. Environmental Aspects of the *ARCO Anchorage* oil spill, Port Angeles, Washington. Proceedings of the 1987 Oil Spill Conference, American Petroleum Institute, Washington, D. C. pp. 407-410.

Westlake, D. W. S. and F. D. Cook. 1980. Petroleum biodegradation potential of northern Puget Sound and Strait of Juan de Fuca environments. Report to U. S. Environmental Protection Agency, EPA-600/7-80-133. 133 p.

Word, J. Q., W. H. Pearson, J. R. Skalski, J. M. Gurtisen, R. B. Lucke, and J. A. Strand. 1986. Reconnaissance of petroleum contamination from the *ARCO Anchorage* oil spill at Port Angeles, Washington, and its influence on selected areas of the Strait of Juan de Fuca. Report to ARCO Marine, Inc. 93 p.

ACS ALASKAN BERING SEA COASTAL RESOURCES MANUAL

Sharon O. Hillman, Standard Alaska Production Company
William F. Gusey, Shell Oil Company
Dee W. Chamberlain, Atlantic Richfield Company

ABSTRACT

Coastal resource documentation is an important element of contingency planning. The Alaska Clean Seas (ACS) Alaskan Bering Sea Coastal Resources Manual, which was authored by oil industry biologists, presents a compilation of pertinent resource data for selected areas of the Bering Sea coastline. The two areas covered in the manual are the Norton Sound region (which includes St. Lawrence Island) and the Alaska Peninsula North Coast region (which includes the Pribilof Islands and part of the eastern Aleutian Islands). The purpose of the manual is to provide biological, cultural and historical information; shoreline types; and spill response and logistical considerations for specific shoreline segments.

The manual is composed of three major sections. The first part is a general section which discusses the purpose and organization of the manual, and provides general information on shoreline characteristics and spill response considerations for contingency purposes. These sections are further supplemented by the detailed information provided in the ACS Contingency Planning Manual, Core Document and CPA Documents. The second and third sections are the two regional manuals. Each of these sections provides, in narrative format, a detailed, area-specific review of the physical environment and the biological resources. Each review is in turn followed by an atlas section, which provides individual maps, each with an accompanying facing page. These maps and facing pages provide site-specific information for each sector of the coastline in the region. Seasonal information is provided where it is available. All information is documented and references are in the bibliography.

This paper provides an overview of the manual. Final technical reviews of the manual have been completed, and the document will be published in 1987 following final ACS approval.

PURPOSE AND ORGANIZATION OF THE MANUAL

The Alaskan Bering Sea Coastal Resources Manual is the result of several years of resource data compilation, synthesis, and cartographic design and production by representatives of several oil companies and their contractors. These oil companies are members of Alaska Clean Seas (ACS), an oil spill response association representing many of the oil companies operating in Alaska. The manual is a continuation of ACS' effort to provide its member companies with the information they need to effectively plan for and respond to oil spills.

The original project was proposed in early 1984 when upcoming oil and gas lease sales where scheduled for parts of the Bering Sea. Technical representatives studied possible oil trajectories from various sale locations, and the areas where shoreline impacts could occur were delineated. A project was proposed to the ACS organization to provide for a coastal resource manual for contingency planning and prioritization assignment should a spill occur. The original proposal provided for the use of U. S. Geological Survey (USGS) base maps (scale 1:63,360, or whatever was available in areas with limited coverage).

A project team of ACS member company biologists was selected to prepare this in-house document. The biologists were chosen in part based on their participation in similar coastal resource data compilation efforts for spill contingency purposes. The team started with an analysis of available information for the area and concluded that the manual should include existing published and unpublished data on biological resources and use areas, cultural areas, and historical sites. Additionally, several publications provided documentation of the type and character of the shoreline. General bird, terrestrial and marine mammal use areas were included along with commercial and subsistence fishing areas and locations identified as having limited access due to gold claims.

Most information on spill response considerations and logistics was provided by the authors, though some references were available. Some very important resources in this work included: Alaska Department of Fish and Game's Alaska's Wildlife and Habitat, Vol. I (1973) and Vol. II (1978); U.S. Fish and Wildlife Service Catalogue of Alaskan Seabird Colonies (1978); National Oceanic and Atmospheric Administration's (NOAA) Sensitivity of Coastal Environments and Wildlife to Spilled Oil of the Bristol Bay Area of the Bering Sea, Alaska (Gundlach et al., 1982) and Oil Spill Sensitivity of Coastal Environments and Wildlife, Norton Sound and the Pribilof Islands, Alaska (Gundlach et al., 1981); and the Alaska Department of Natural Resources Historical Site Inventory.

Purpose of the Manual

The purpose of the Alaskan Bering Sea Coastal Resources Manual is to provide the ACS member companies with a reference manual and contingency planning tool with detailed information on the physical environment, biological resources, historical/cultural resources, and logistical considerations for the selected portions of the Bering Sea coastline. This information can be used in developing site-specific oil spill contingency plans and in planning for response operations in the event of an oil spill. Portions of the Bering Sea coastline were selected for inclusion in the coastal resource analysis and documentation based on their location in relationship to potential exploration operations associated with lease sales. Figure 1 show the geographical locations covered in the two regions addressed in the manual.

Organization of the Manual

This manual is divided into three major parts: the Introduction and Overview, the Norton Sound Regional Overview and Atlas, and the Alaska Peninsula North Coast Regional Overview and Atlas. The first part discusses in general terms, biological, environmental, logistical, and spill response information for contingency planning purposes. Additional information to supplement these discussions is contained in the ACS Contingency Planning Manual and in the references cited in the manual.

The second and third sections contain regional manuals for the Norton Sound Region and for the Alaska Peninsula North Coast Region, which includes the Eastern Aleutians Region and the Pribilof Islands. Figure 1 shows the two areas currently covered in the Alaskan Bering Sea Coastal Resources Manual. Each of the regional manuals provides a detailed discussion of the region's physical environment, biological resources, and cultural/historical

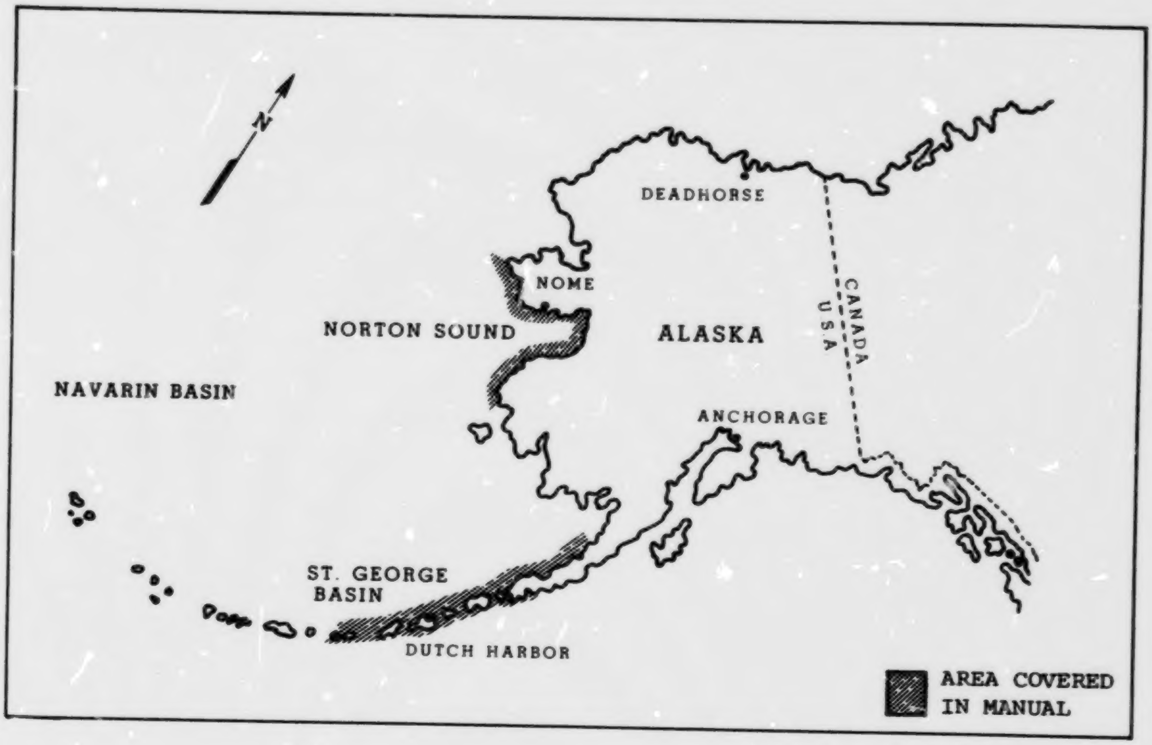

FIGURE 1

AREAS COVERED IN THE TWO REGIONAL ATLASES OF THE ALASKAN BERING SEA COASTAL RESOURCES MANUAL

resources. Following the overview is a regional map atlas. Each map in the atlas section is accompanied by a facing page which provides a description of biological resources and uses, cultural and historical data, shoreline types, and spill response considerations and logistics of the area shown on the map. The maps themselves depict the locations of these resources (See Figures 2 and 3).

The atlas section for each region includes three key maps followed by a short explanation of how to use and interpret the maps. Clearly identifiable symbols have been used to designate resources and shoreline types on the maps (see Figure 4).

The manual depicts the distribution of living resources along the Bering Sea coast. However, biologists and cartographers are limited by the quality and quantity of the data base existing at the time of the manual development. It is not possible to illustrate the continual shifts in the distribution of animals that are influenced by changing environmental conditions from year to year. General habitat data or resource use areas have been depicted with area markers such as long arrows on one or several sides of the resource symbol.

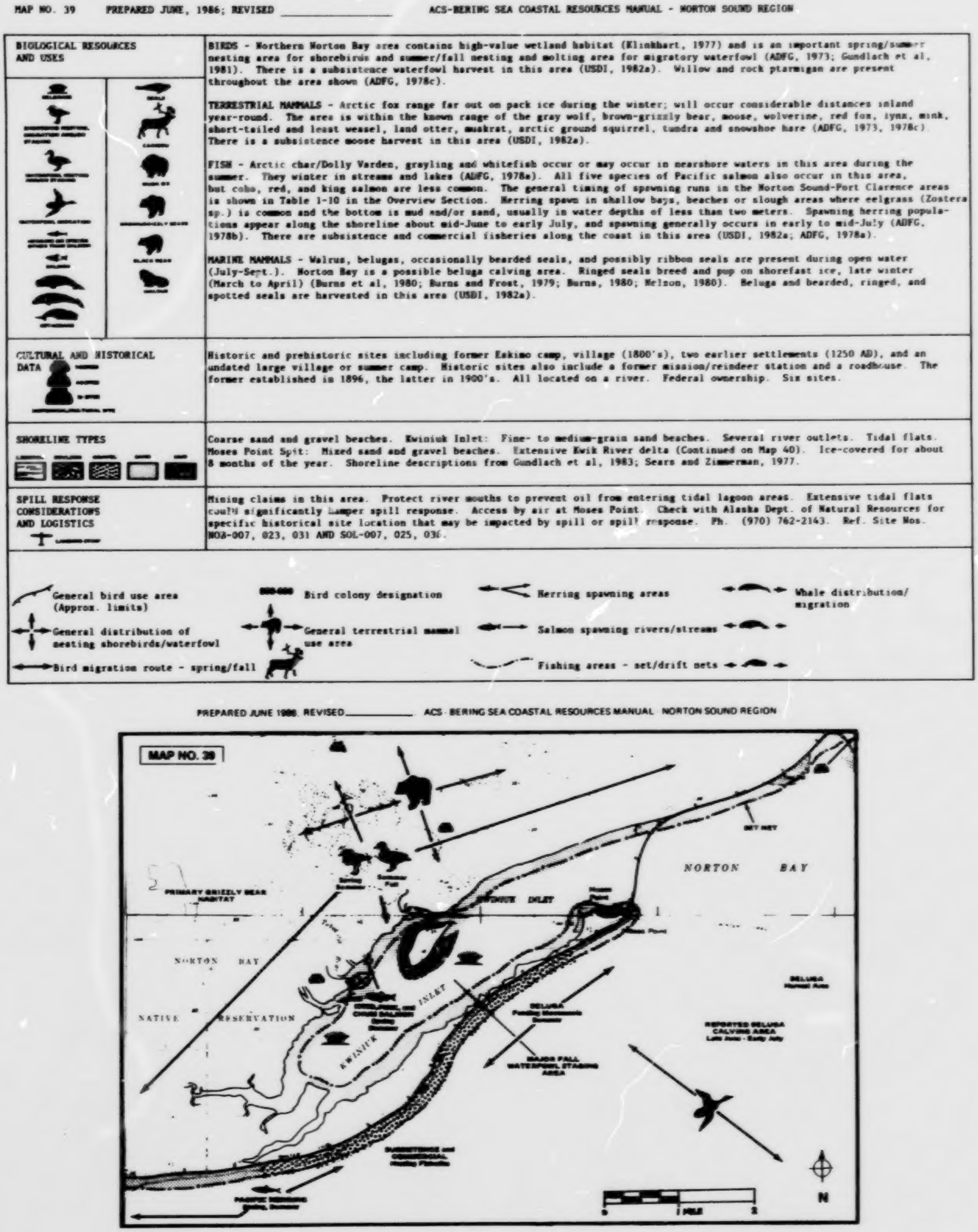

MAP NO. 39 PREPARED JUNE, 1986; REVISED ________________ ACS-BERING SEA COASTAL RESOURCES MANUAL - NORTON SOUND REGION

BIOLOGICAL RESOURCES AND USES	BIRDS - Northern Norton Bay area contains high-value wetland habitat (Klinkhart, 1977) and is an important spring/summer nesting area for shorebirds and summer/fall nesting and molting area for migratory waterfowl (ADFG, 1973; Gundlach et al, 1981). There is a subsistence waterfowl harvest in this area (USDI, 1982a). Willow and rock ptarmigan are present throughout the area shown (ADFG, 1978c). TERRESTRIAL MAMMALS - Arctic fox range far out on pack ice during the winter; will occur considerable distances inland year-round. The area is within the known range of the gray wolf, brown-grizzly bear, moose, wolverine, red fox, lynx, mink, short-tailed and least weasel, land otter, muskrat, arctic ground squirrel, tundra and snowshoe hare (ADFG, 1973, 1978c). There is a subsistence moose harvest in this area (USDI, 1982a). FISH - Arctic char/Dolly Varden, grayling and whitefish occur or may occur in nearshore waters in this area during the summer. They winter in streams and lakes (ADFG, 1978a). All five species of Pacific salmon also occur in this area, but coho, red, and king salmon are less common. The general timing of spawning runs in the Norton Sound-Port Clarence areas is shown in Table 1-10 in the Overview Section. Herring spawn in shallow bays, beaches or slough areas where eelgrass (Zostera sp.) is common and the bottom is mud and/or sand, usually in water depths of less than two meters. Spawning herring populations appear along the shoreline about mid-June to early July, and spawning generally occurs in early to mid-July (ADFG, 1978b). There are subsistence and commercial fisheries along the coast in this area (USDI, 1982a; ADFG, 1978a). MARINE MAMMALS - Walrus, belugas, occasionally bearded seals, and possibly ribbon seals are present during open water (July-Sept.). Norton Bay is a possible beluga calving area. Ringed seals breed and pup on shorefast ice, late winter (March to April) (Burns et al, 1980; Burns and Frost, 1979; Burns, 1980; Nelson, 1980). Beluga and bearded, ringed, and spotted seals are harvested in this area (USDI, 1982a).
CULTURAL AND HISTORICAL DATA	Historic and prehistoric sites including former Eskimo camp, village (1800's), two earlier settlements (1250 AD), and an undated large village or summer camp. Historic sites also include a former mission/reindeer station and a roadhouse. The former established in 1896, the latter in 1900's. All located on a river. Federal ownership. Six sites.
SHORELINE TYPES	Coarse sand and gravel beaches. Kwiniuk Inlet: Fine- to medium-grain sand beaches. Several river outlets. Tidal flats. Moses Point Spit: Mixed sand and gravel beaches. Extensive Kwik River delta (Continued on Map 40). Ice-covered for about 8 months of the year. Shoreline descriptions from Gundlach et al, 1983; Sears and Zimmerman, 1977.
SPILL RESPONSE CONSIDERATIONS AND LOGISTICS	Mining claims in this area. Protect river mouths to prevent oil from entering tidal lagoon areas. Extensive tidal flats could significantly hamper spill response. Access by air at Moses Point. Check with Alaska Dept. of Natural Resources for specific historical site location that may be impacted by spill or spill response. Ph. (970) 762-2143. Ref. Site Nos. NOB-007, 023, 031 AND SOL-007, 025, 036.

General bird use area (Approx. limits)

General distribution of nesting shorebirds/waterfowl

Bird migration route - spring/fall

Bird colony designation

General terrestrial mammal use area

Herring spawning areas

Salmon spawning rivers/streams

Fishing areas - set/drift nets

Whale distribution/migration

PREPARED JUNE 1986. REVISED__________ ACS - BERING SEA COASTAL RESOURCES MANUAL - NORTON SOUND REGION

FIGURE 2

SAMPLE ATLAS MAP/FACING PAGE, NORTON SOUND (REDUCED SIZE)

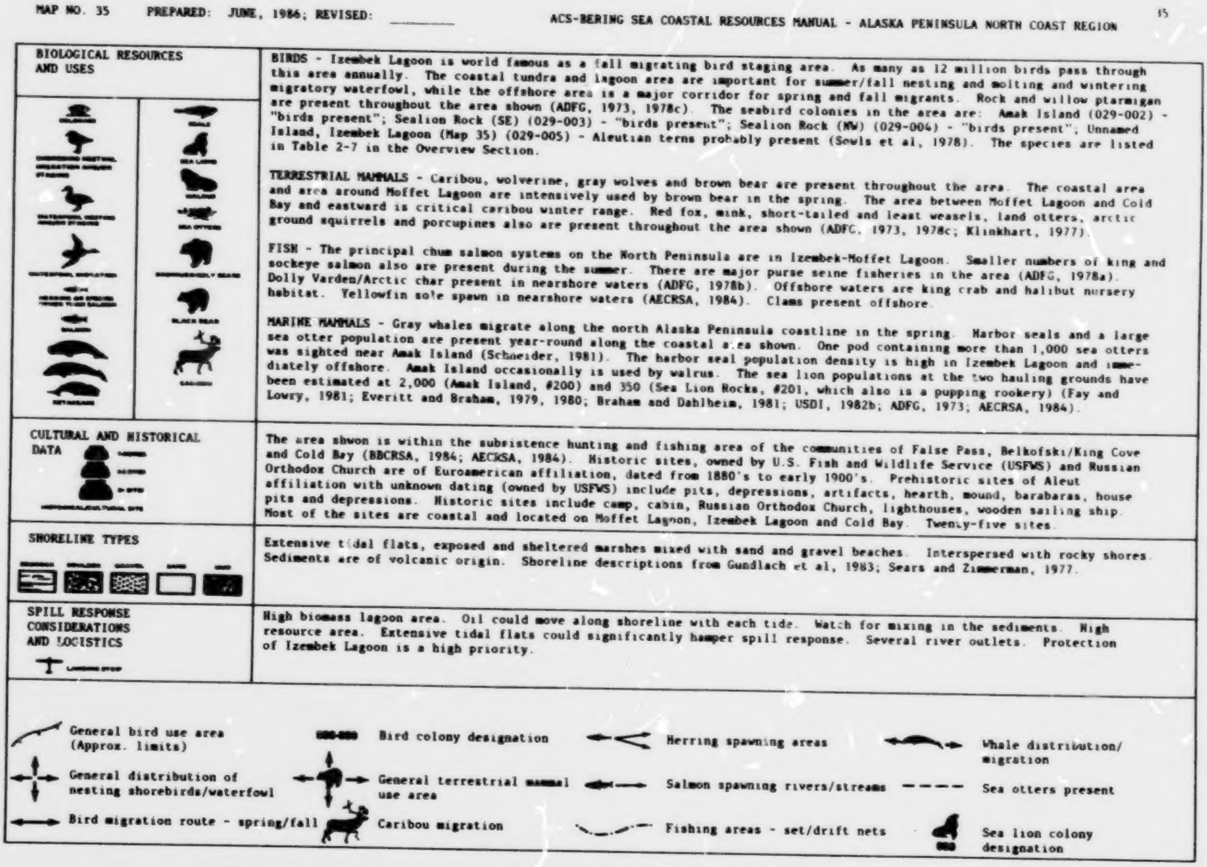

MAP NO. 35 PREPARED: JUNE, 1986; REVISED: ________ ACS-BERING SEA COASTAL RESOURCES MANUAL - ALASKA PENINSULA NORTH COAST REGION 35

BIOLOGICAL RESOURCES AND USES	BIRDS - Izembek Lagoon is world famous as a fall migrating bird staging area. As many as 12 million birds pass through this area annually. The coastal tundra and lagoon area are important for summer/fall nesting and molting and wintering migratory waterfowl, while the offshore area is a major corridor for spring and fall migrants. Rock and willow ptarmigan are present throughout the area shown (ADFG, 1973, 1978c). The seabird colonies in the area are: Amak Island (029-002) - "birds present"; Sealion Rock (SE) (029-003) - "birds present"; Sealion Rock (NW) (029-004) - "birds present"; Unnamed Island, Izembek Lagoon (Map 35) (029-005) - Aleutian terns probably present (Sowls et al, 1978). The species are listed in Table 2-7 in the Overview Section. TERRESTRIAL MAMMALS - Caribou, wolverine, gray wolves and brown bear are present throughout the area. The coastal area and area around Moffet Lagoon are intensively used by brown bear in the spring. The area between Moffet Lagoon and Cold Bay and eastward is critical caribou winter range. Red fox, mink, short-tailed and least weasels, land otters, arctic ground squirrels and porcupines also are present throughout the area shown (ADFC, 1973, 1978c; Klinkhart, 1977). FISH - The principal chum salmon systems on the North Peninsula are in Izembek-Moffet Lagoon. Smaller numbers of king and sockeye salmon also are present during the summer. There are major purse seine fisheries in the area (ADFG, 1978a). Dolly Varden/Arctic char present in nearshore waters (ADFG, 1978b). Offshore waters are king crab and halibut nursery habitat. Yellowfin sole spawn in nearshore waters (AECRSA, 1984). Clams present offshore. MARINE MAMMALS - Gray whales migrate along the north Alaska Peninsula coastline in the spring. Harbor seals and a large sea otter population are present year-round along the coastal area shown. One pod containing more than 1,000 sea otters was sighted near Amak Island (Schneider, 1981). The harbor seal population density is high in Izembek Lagoon and immediately offshore. Amak Island occasionally is used by walrus. The sea lion populations at the two hauling grounds have been estimated at 2,000 (Amak Island, #200) and 350 (Sea Lion Rocks, #201, which also is a pupping rookery) (Fay and Lowry, 1981; Everitt and Braham, 1979, 1980; Braham and Dahlheim, 1981; USDI, 1982b; ADFG, 1973; AECRSA, 1984).
CULTURAL AND HISTORICAL DATA	The area shwon is within the subsistence hunting and fishing area of the communities of False Pass, Belkofski/King Cove and Cold Bay (BBCRSA, 1984; AECRSA, 1984). Historic sites, owned by U.S. Fish and Wildlife Service (USFWS) and Russian Orthodox Church are of Euroamerican affiliation, dated from 1880's to early 1900's. Prehistoric sites of Aleut affiliation with unknown dating (owned by USFWS) include pits, depressions, artifacts, hearth, mound, barabaras, house pits and depressions. Historic sites include camp, cabin, Russian Orthodox Church, lighthouses, wooden sailing ship. Most of the sites are coastal and located on Moffet Lagoon, Izembek Lagoon and Cold Bay. Twenty-five sites.
SHORELINE TYPES	Extensive tidal flats, exposed and sheltered marshes mixed with sand and gravel beaches. Interspersed with rocky shores. Sediments are of volcanic origin. Shoreline descriptions from Gundlach et al, 1983; Sears and Zimmerman, 1977.
SPILL RESPONSE CONSIDERATIONS AND LOGISTICS	High biomass lagoon area. Oil could move along shoreline with each tide. Watch for mixing in the sediments. High resource area. Extensive tidal flats could significantly hamper spill response. Several river outlets. Protection of Izembek Lagoon is a high priority.

General bird use area (Approx. limits)

General distribution of nesting shorebirds/waterfowl

Bird migration route - spring/fall

Bird colony designation

General terrestrial mammal use area

Caribou migration

Herring spawning areas

Salmon spawning rivers/streams

Fishing areas - set/drift nets

Whale distribution/migration

Sea otters present

Sea lion colony designation

PREPARED JUNE 1986, REVISED ________ . ACS-BERING SEA COASTAL RESOURCES MANUAL ALASKA PENINSULA NORTH COAST REGION

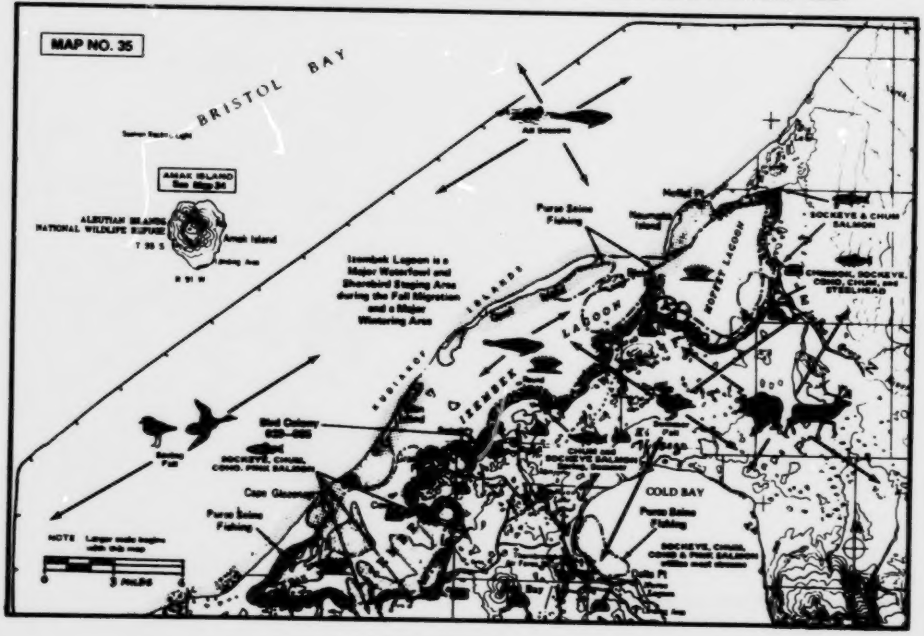
MAP NO. 35
BRISTOL BAY
AMAK ISLAND
See Map 34
ALEUTIAN ISLANDS
NATIONAL WILDLIFE REFUGE
Amak Island
T 55 S
R 91 W
All Seasons
Purse Seine Fishing
Izembek Lagoon is a Major Waterfowl and Shorebird Staging Area during the Fall Migration and a Major Wintering Area
ISLANDS
LAGOON
IZEMBEK
MOFFET LAGOON
SOCKEYE & CHUM SALMON
CHINOOK, SOCKEYE, COHO, CHUM, and STEELHEAD
Bird Colony
Spring Fall
SOCKEYE, CHUM, COHO, PINK SALMON
Cape Glazenap
Purse Seine Fishing
CHUM and SOCKEYE SALMON
COLD BAY
Purse Seine Fishing
SOCKEYE, CHUM, COHO & PINK SALMON
NOTE Larger scale begins with this map
3 MILES

FIGURE 3

SAMPLE ATLAS MAP/FACING PAGE, ALASKA PENINSULA NORTH COAST (REDUCED SIZE)

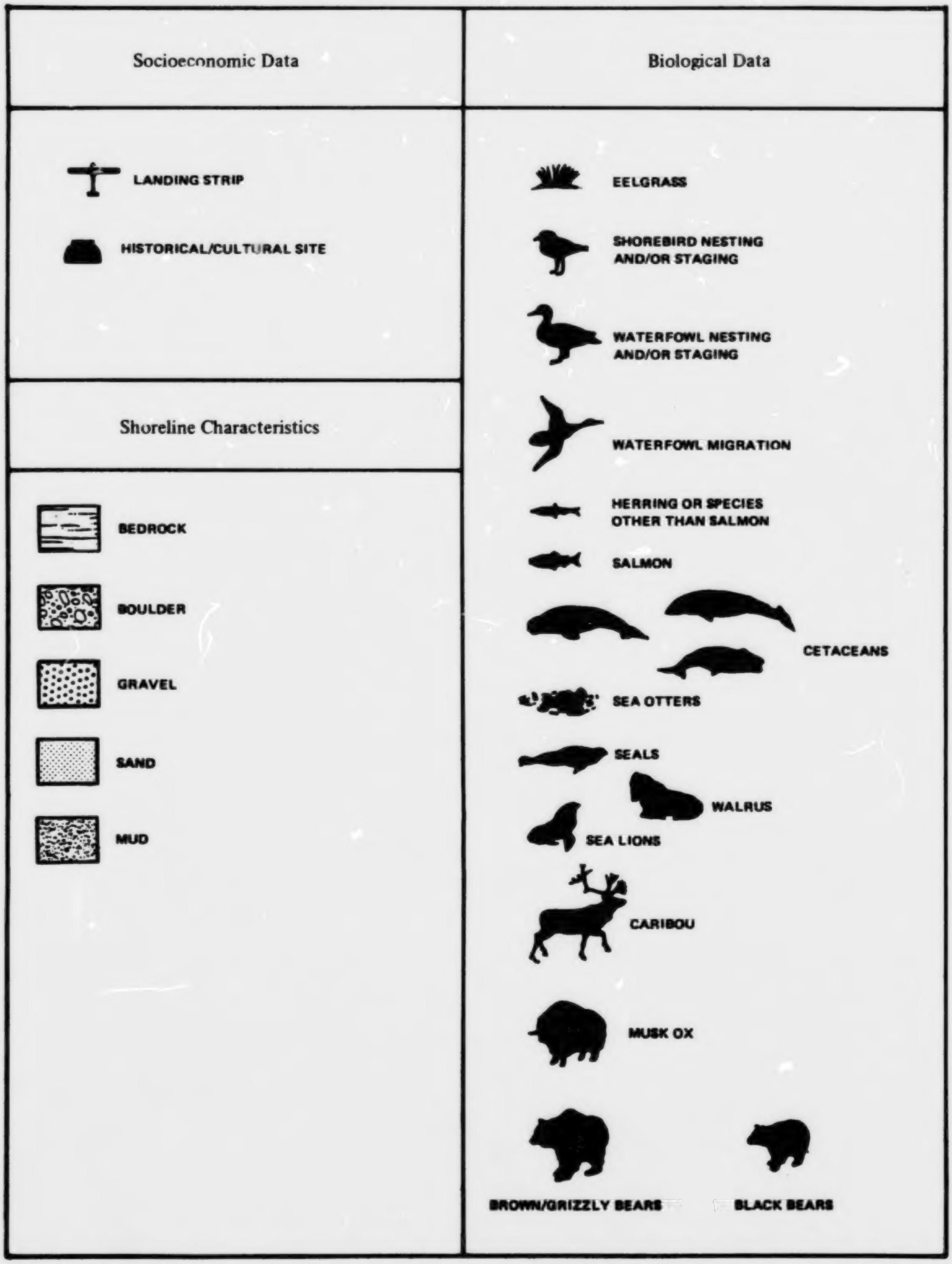
Socioeconomic Data
Biological Data
LANDING STRIP
HISTORICAL/CULTURAL SITE
Shoreline Characteristics
BEDROCK
BOULDER
GRAVEL
SAND
MUD
EELGRASS
SHOREBIRD NESTING AND/OR STAGING
WATERFOWL NESTING AND/OR STAGING
WATERFOWL MIGRATION
HERRING OR SPECIES OTHER THAN SALMON
SALMON
CETACEANS
SEA OTTERS
SEALS
WALRUS
SEA LIONS
CARIBOU
MUSK OX
BROWN/GRIZZLY BEARS
BLACK BEARS

FIGURE 4

LEGEND AND SYMBOLS USED IN THE ATLAS SECTION OF THE MANUALS

The potential for oil and gas leasing in the Bering Sea raised concern among archaeologists about possible impacts by industry activities on coastal and submerged historic and prehistoric sites. Many of these sites are the only representatives of maritime cultures of a particular period and are very important for developing correlations with cultural remains found in inland freshwater bodies. On the maps in the two atlas sections, the precise location of each site intentionally is not given in order to protect the site from vandalism. However, reference numbers are provided so that for individual contingency planning efforts or for an actual spill response, specific information about any noted sites could be obtained.

General Overview

The overview section reviews the information presented in the regional sections and highlights considerations that are not region-specific but would apply to contingency planning and spill response anywhere on the West Coast of Alaska. Discussions are provided in the manual on the following topics:

- Biological resources and uses,
- Cultural and historical sites,
- Shoreline characteristics,
- Spill response considerations,
- General guidelines for oil spill countermeasures, and
- Spill response staging locations.

The first two topics are discussed in detail in the overview sections of the regional atlases and highlighted briefly in the general overview. The remaining four subjects are covered in depth to provide, in one place along with the shoreline maps, general information that is common to all contingency planning for the West Coast of Alaska.

REGIONAL SECTIONS

Biological Resources and Uses

Detailed information is provided in the biological sections of each regional atlas to help spill contingency planners with the complexities of the region's various biological resources and habitats. This information, which includes bird colony statistics and locations, subsistence and commercial fisheries, and the distribution of major terrestrial mammals, is provided in the overview sections for each region. This same information is summarized in the atlas section on the facing pages to each map. This allows for quick and ready access to summary information pertinent to spill response, along with the visual portrayal of the areas of concern. These pages may be reproduced easily, separate from the manual, for on-site use and reference, or may be distributed among many response team members in various locales, with action notations and cautions.

Cultural and Historical Sites

On the maps in this series, the basket symbols have been chosen to indicate the locations of cultural resources of various types recognized by both federal and state agencies. The relative size of the basket symbol indicates the number of cultural sites in the immediate area. A small basket indicates 1 to 3 sites, a medium-sized basket 4 to 8 sites, and a large basket more than 8 sites. The precise location of each site is not provided to protect the site from vandalism.

Brief descriptions of the cultural resources are provided in the facing page text for each map where data are available, including age, ownership, types of structures, and natural environment. Any spill response activity that might disturb these important cultural resources would receive consideration early in response planning and be coordinated with the Alaska Division of Parks, Department of Natural Resources, so that any necessary mitigation can be accomplished.

Shoreline Characteristics

The shoreline characteristics section of each map and facing page provides information on the physical nature of the shoreline and the shoreline wave energy regime, which together control the natural dispersion and degradation of oil on an impacted shoreline. For example, steep, exposed bluffs generally are least affected by an oil spill due to the high rate of natural dispersion and may require little or no cleanup or protection. On the other hand, low-energy sheltered tidal flats or lagoons may be sensitive to oil approaching the shoreline and could retain oil for many years. In addition, almost any cleanup activity in these areas would disturb the vegetative mat, could cause erosion, and could increase the ecological impacts of a spill. Some areas of the coastline have not been characterized or the data reported shows conflicts. Because these areas were not field-checked, on-site verification would be advisable during an actual spill response.

General Guidelines for Spill Response

If an oil spill occurs from industry drilling operations in the Bering Sea, not all spilled oil may be immediately contained and picked up offshore. Under some circumstances and environmental conditions, oil could escape and reach a portion of the shoreline if an onshore trajectory exists. One or another interest group could consider resources of the entire coastline important, "sensitive", and/or worthy of protection. Therefore, priority response procedures must be developed so that the most sensitive areas threatened by a spill will be protected first. Further, in order to minimize the impact of the spill on the remaining areas, spill response and cleanup methods must be characterized for each area in the contingency planning phase. This allows for the factors of probable spill trajectories, seasonal environmental characteristics, and constraints and logistical requirements to be considered.

Each facing page contains a description of information which may be useful in responding to a spill involving that particular stretch of shoreline. General information was provided in the overview; however, not too much detail was provided since ACS has extensive documentation available on spill response.

Spill cleanup practices for coastal arctic and subarctic regions of the Bering Sea are similar to spill cleanup concerns throughout the world. The first rule (sometimes referred to as the BLACK GOLD rule) is always that each incident must be individually evaluated relative to the potential for human and environmental impact, biological disturbances, containment and cleanup techniques which will work in the area, cultural resources that may be impacted, logistical requirements and availability, and the potential for long-term impacts from the spill. Another major factor is how long the spilled material will remain in the environment, especially in a given location. Natural dispersion in a high-energy environment such as exists in many Bering Sea locations can dissipate all of a spill in a few short days.

CONCLUSION

Knowledge of the resources in an area is an essential component of an effective response operation because such knowledge is needed for responsible decisions. The information presented in the Alaskan Bering Sea Coastal Resources Manual provides an on-scene coordinator with immediate knowledge of resources which may be impacted and the seasonality of the resource use. The shoreline type will affect the oil/shoreline interaction, and both the shoreline and backshore character will influence the type of response. Long-term impact will be the function of a number of factors, including seasonal presence of the biological species, patterns of distribution and abundance, life-stage and physiological conditions, behavioral patterns, species characteristics, habitat characteristics, ecosystem factors, pathways of impact, subsistence importance and economic or aesthetic value.

It is not the role of the Alaskan Bering Sea Coastal Resources Manual to dictate cleanup methods for various areas or types of shoreline. Rather, the manual is designed to provide the necessary information for contingency planners and on-scene coordinators to allow for appropriate, informed decision-making during a real or simulated spill event.

REFERENCES

Alaska Clean Seas, 1987, Alaskan Bering Sea Coastal Resources Manual, Anchorage, Alaska (in press).

Alaska Department of Fish and Game, 1973, Alaska's Wildlife and Habitat, Vol. I, Anchorage, Alaska.

Alaska Department of Fish and Game, 1978, Alaska's Wildlife and Habitat, Vol. II, Anchorage, Alaska.

Gundlach, E.R., J.L. Sadd, G.I. Scott, L.C. Thebeau, and D.J. Maiero, 1981, Oil Spill Sensitivity of Coastal Environments and Wildlife, Norton Sound and the Pribilof Islands, Alaska, prepared for the National Oceanic and Atmospheric Administration by Research Planning Institute, Inc., Columbia, South Carolina.

Gundlach, E.R., J.L. Sadd, G.I. Scott, and L.C. Thebeau, 1982, Sensitivity of Coastal Environments and Wildlife to Spilled Oil in the Bristol Bay Area of the Bering Sea, Alaska, prepared for the National Oceanic and Atmospheric Administration by Research Planning Institute, Inc., Columbia, South Carolina.

CONTINUING THE PROGRAM:
ALASKA CLEAN SEAS RESEARCH, DEVELOPMENT AND ENGINEERING

Richard V. Shafer, P.E.
Alaska Clean Seas

Introduction

Alaska Clean Seas (ACS) is a spill response organization sponsored by oil companies interested in petroleum operations in Alaskan waters. The organization has a commitment to investigate, acquire, and maintain appropriate spill response equipment and materials, and to develop training programs for personnel who may be involved in the cleanup of oil spills. ACS also does research, development and engineering (RD&E) work directed at improving response capabilities in Alaskan waters. This paper provides an overview of the ACS RD&E program to date.

ACS RD&E Projects Initiated Prior to 1986.

The research, development and engineering projects described below were initiated by ACS prior to 1986 (Hillman and Shafer, 1983; Hillman, 1985; Shafer, 1986; Shafer, 1987):

ARCAT skimming vessel design.

This project covered the design of the ARCAT II, a 65-ft catamaran vessel utilizing a rope-mop skimming system as well as a weir skimmer. The vessel was designed specifically for use during broken ice and open water periods in the Alaskan Beaufort Sea. Hull sections are specially strengthened to resist ice forces (Williams, 1982).

Experiments involving oil in ice.

Samples of selected oils (either diesel fuel or hot Prudhoe Bay crude oil) were introduced beneath sea ice at various times throughout the winter at a total of 15 sites in Prudhoe Bay. In each case, the behavior of the oil and its sea ice matrix were observed. As a part of this experiment, thermal insulation material was placed in selected areas on the ice surface to reduce freezing rates beneath. The resulting irregularities in the under-ice surface helped provide oil containment. Research also involved laboratory observations of oil-ice interactions, and field tests of oil detection and recovery techniques (Nelson and Allen, 1981, 1982; Allen and Nelson, 1981).

Coastal resource manuals for the Beaufort and Bering Seas.

ACS prepared and published an extensive coastal resource manual for the Alaskan Beaufort Sea (Morson, *et al.*, 1983) providing information on biological and cultural resources, and on how to protect them from an oil spill. A similar manual covering critical portions of the Bering Sea coast is now being published (Gusey, Hillman and Chamberlain, in press).

Spill trajectory models for Beaufort and Bering Sea areas.

ACS developed spill trajectory models which run on an IBM-PC. The models can be used for contingency planning and for real-time predictions of oil spill movement (*Alaska Beaufort Sea Oil Spill Trajectory Analysis*, 1983; *Norton Sound Oil Spill Trajectory Model*, 1985; and *St. George Basin Oil Spill Trajectory Model*, 1984).

Dispersant effectiveness in cold water.

Several commercially available dispersants were tested in the laboratory to assess their ability to disperse oil under low temperature conditions.

Research on the use of air-cushion vehicles for logistic support.

ACS sponsored the preparation of a synthesis of available information on air-cushion vehicles, with emphasis on their utility for logistics and operational uses in the event of an oil spill in the Arctic.

In situ combustion.

ACS contributed funds to support research on fireproof containment boom and air deployable igniters under development by Canadian operators (Pistruzak, 1981).

Flare burner equipment.

ACS evaluated disposal of recovered oil using flare burner equipment on long-term loan from the U. S. Coast Guard..

Oily refuse incineration.

ACS examined various incinerator systems for arctic use.

Transfer and storage systems.

ACS evaluated several pumps, hoses and temporary storage tanks for use in the Arctic.

Beach cleaning.

ACS helped support the development of the prototype Moorhead beach cleaning system for removal of oil from beaches.

Containment booms.

ACS conducted evaluations of selected deep-draft spill containment boom systems.

Fire containment boom.

A number of special containment booms have recently been developed which are resistant to damage by fire. Such booms can be used to facilitate disposal of spilled oil by *in situ* burning. Fire containment boom must be designed to provide containment of spilled oil in a layer sufficiently thick to support combustion, while resisting the effects of heat well enough to functionally survive exposure to the burning oil. This project was conducted to assess survivability, containment capability, and other characteristics of various designs and configurations of fire containment boom. In all, seven burn tests were performed. They demonstrated that several boom types are available which will survive a 24-hour exposure to burning oil and still be capable of containing burning oil. (*Test and Evaluation of Fire Containment Boom*, 1986.)

Bubble Barrier.

If air bubbles are injected into the water column at some depth beneath the surface, the resulting water mass containing bubbles, being less dense than water alone, will tend to be buoyed up by the surrounding water. Anything floating on the surface nearby--such as oil--will tend to be pushed away from the area of the bubbles, (1) because surface currents will be set up which flow away from the bubbly area, and (2) because the surface over the bubbly area will be elevated somewhat above the surrounding water surface.

This project was designed to evaluate the concept of a flexible bubble barrier, fitted with ballast so it does not float to the surface, and supported in the water column from a system of floating buoys. Initial tests of a prototype bubble barrier were conducted in open water. Additional tests involved oil together with ice in a test tank. These tests showed that the prototype was an effective barrier to oil yet allowed floating ice to pass. The system also worked well as a fire containment barrier.

Field tests involving the *ARCAT* were to be conducted at Prudhoe Bay during the 1986 open water season (Garlow, *et al.*, November 1986). Unfortunately the prototype bubble barrier system sustained extensive damage by being dragged along the sea bottom by wave action. It should be noted that the damage occurred during the night after the system had been put in the water but before deployment for testing. The damage was not associated with any operational tests of the equipment. The system is being redesigned to improve its resistance to such damage. A reconstructed system is to be evaluated at Prudhoe Bay this year. (See discussion of 1987 ACS RD&E program later in this paper.)

Plunging Water-Jet Boom.

A jet of water directed downward into the surface of the sea will tend to entrain air and inject it into the upper part of the seawater column. The rising air bubbles produce water currents on the surface which flow away from the point where the jet impinges. This water current will tend to move any floating oil away with it. Also, the injected air will make the affected water buoyant relative to surrounding water, and it's surface will be higher, creating an additional barrier to movement of oil on the surface. (The concept of an oil containment system using plunging water jets is covered by a patent held by the U. S. Environmental Protection Agency.)

A system of plunging water jets arranged in a "V" configuration ahead of the *ARCAT* skimming vessel, as diagrammed in Figure 1, will enhance the vessel's skimming capability by providing a greater swath width. The water jets should also help rinse oil off floating ice in the area covered by the jets.

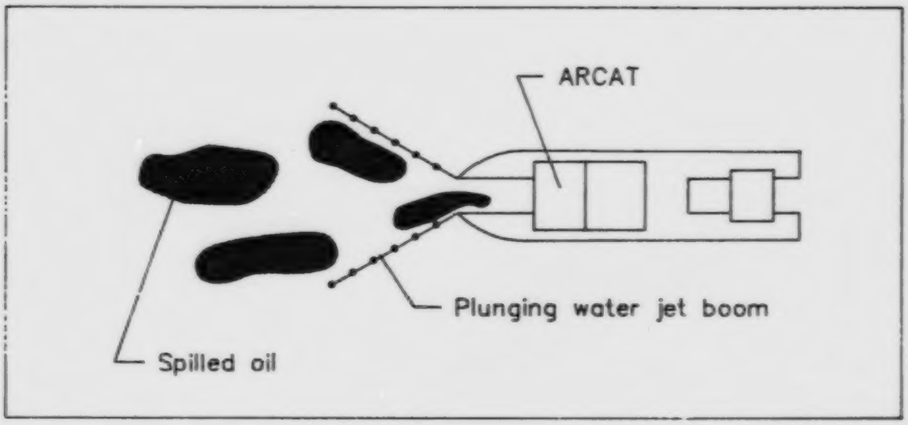

Figure 1. Plunging water jet boom system installed on the ARCAT.

This project was designed to assess different jet configurations, and provide a guide for the design and operation of water jet booms systems. A prototype jet boom system has been fabricated and its performance was evaluated in a test tank. Subsequent full scale tests of the system were performed in Galveston Bay. The system was installed on the *ARCAT* during the summer of 1986 and field tested in the Prudhoe Bay area. It is now ready for use in an actual spill response operation (Garlow, *et al.*, October 1986).

Air Deployable Igniters.

Alaska Clean Seas has a sizeable inventory of air deployable igniters of a design developed by Canadian operators (with some financial support from Alaska Clean Seas) to help initiate *in situ* combustion of spilled oil. Such igniters would ordinarily be applied to a spill area by dropping them by hand from a helicopter as illustrated in Figure 2. While igniters of this type have been demonstrated to be effective, several improvements are desirable.

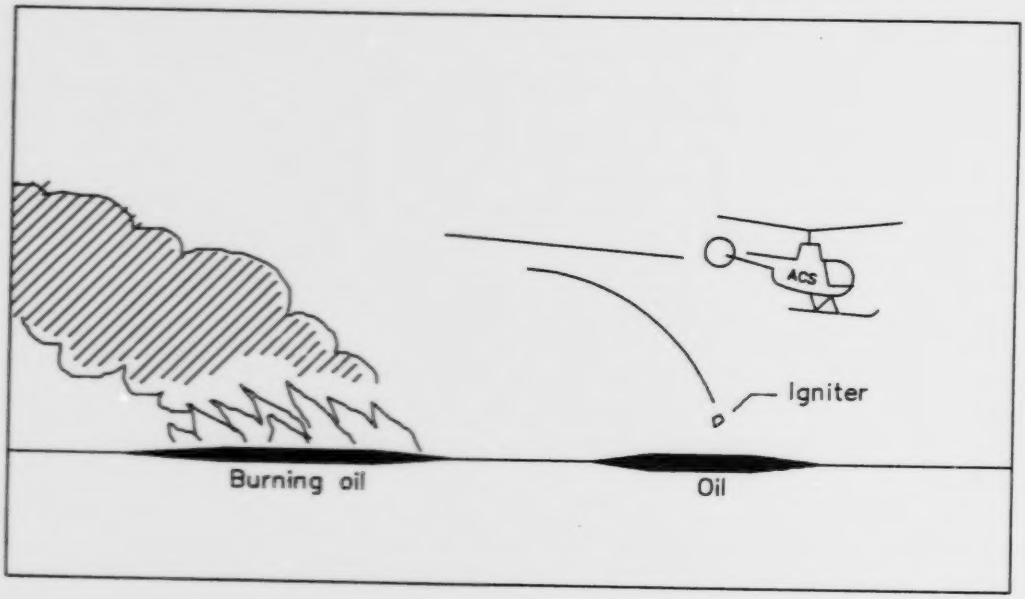

Figure 2. Air deployable igniter.

The objective of this project, was to review available information on alternative igniter designs, seeking a design with smaller size and weight, improved performance in thin or weathered oils, greater simplicity and safety of use, and lower cost. Project scope included review and analysis of existing design details and problems, examination of ignition promoters, investigation of mechanisms to minimize splash effects, and proposal of new igniter concepts if applicable. The study evaluated five devices. The results of this study, which were published in April, 1986 (Allen, April, 1986), provided the basis for decisions regarding further igniter RD&E work.

Oil Spill Chemical Application Manual.

A substantial amount of information is available regarding the use of dispersants and other spill response chemicals in the Arctic. However, this information has not been in a form readily available for spill response planners or those who must direct spill response operations in an emergency. This project synthesized available information on spill response chemicals and various related environmental and logistics data into a single oil spill chemical application manual for use by response planners and managers concerned with operations in Alaska. (Allen, June, 1986)

The manual presents data on dispersants which are stockpiled in Alaska, equipment which could be used for dispersant application, and potential logistical support bases. Included also is detailed information on how to estimate coverage rates and application times based on these data. Example calculations are given.

Logistics Support for U. S. Coast Guard Spill Trajectory Study.

In addition to the research and development projects with which Alaska Clean Seas was directly involved, substantial logistics support was provided to the U. S. Coast Guard during the course of field work on a spill trajectory study. Alaska Clean Seas and member companies provided vessels and crews plus office space and living quarters for Coast Guard personnel to use while acquiring data for the study. (St. Martin and Lissauer, 1986)

The 1986 Research and Development Program

Alaska Clean Seas undertook the following new research, development and engineering projects in 1986:

Shoreline Protection Using Porous Netting.

When an oil spill impacts a beach, the cleanup methods commonly used are labor intensive and may themselves be damaging to the environment. Furthermore, conventional beach cleanup techniques are slow, especially in remote areas; and the longer oil remains in a wildlife habitat, the greater the potential for biological harm.

This project was designed to assess the concept of using a thin, lightweight, fine mesh material to help protect a threatened shoreline. The material could be delivered to a remote shoreline by helicopter and quickly deployed by a small number of workers. Long sheets of this material would be applied at or near the next expected high tide elevation where most of the oil would be deposited. Figure 3 illustrates how such material might be deployed. When oil or oily

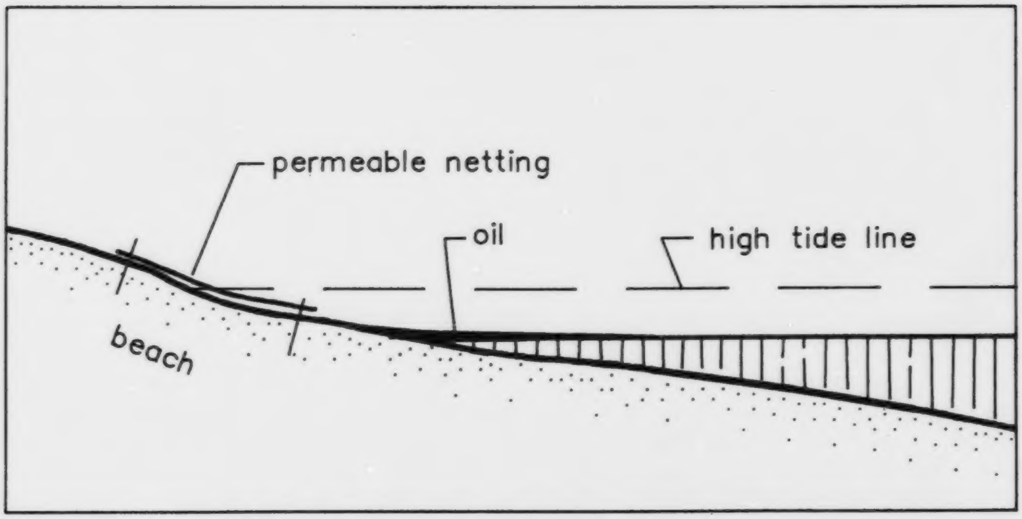

Figure 3. Beach protection material.

emulsion is deposited on the shoreline it will settle on top of the porous material. The surface characteristics of the material must be designed to allow water to seep through the fabric into the soil but to retain oil. On a receding tide, the material could be rolled up, thereby capturing virtually all of the oil or emulsion but not robbing any substantial quantity of beach sand. The rolled up material would then be disposed of in an approved manner. Work is under way on this project, and a final report is expected during the third quarter.

Refinement of Aerial Ignition System.

As discussed earlier in this paper, the hand held igniter units ACS has provided for igniting spilled oil for *in situ* disposal have been shown to be effective, but inventories are finite, application rates could be improved, costs are high, and their use involves some risk of fire on board the helicopter used for release of the igniters.

This project involved: (a) testing of innovative ignition systems for igniting and burning oil *in situ*, (b) initial field testing of

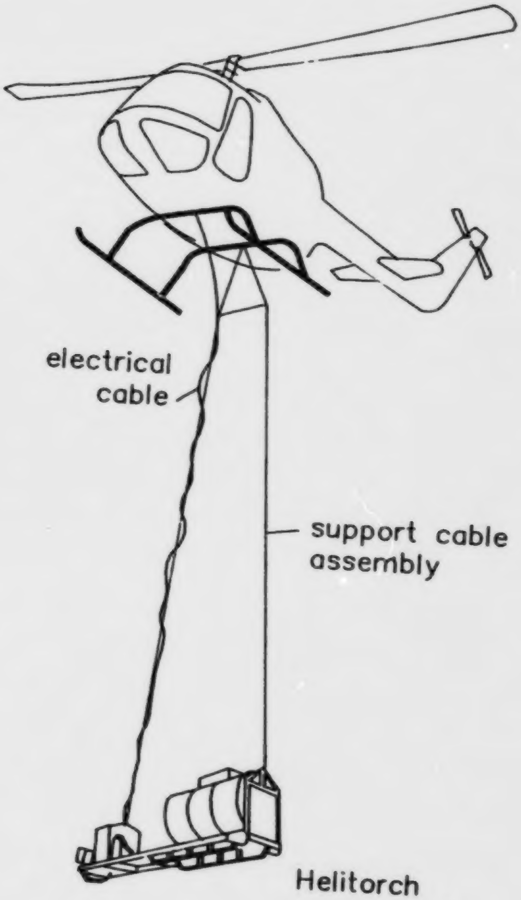

Figure 4. Helitorch system.

selected concepts under various conditions, and (c) larger scale tests of the most promising design(s). Field tests are now complete, and the survey has identified the Helitorch ignition system is the most promising igniter for use in the Arctic. The Helitorch is a device which can simultaneously release and ignite discrete globules (on the order of 100 - 500 ml) of gelled hydrocarbon fuel onto an ignition target such as an oil slick. In operation the Helitorch unit is suspended by cable from a helicopter. Release of burning fuel is controlled by the helicopter pilot. (See Figure 4.)

The Helitorch was originally developed for the purpose of igniting backfires to help control forest fires and grass fires. It was not known at the outset of this investigation whether releases into water would provide sustained burning and be capable of igniting a floating oil slick, however field tests performed as part of this project demonstrated that with release heights up to 60 ft, burning gelled gasoline could survive splash effects upon impact and continue to burn for several minutes. Floating oil in layers 0.1 to 0.5 in. thick were successfully ignited even in the presence of broken ice, subfreezing temperatures and winds up to 18 mph. The project provides information on how to use the equipment to achieve various application rates and swath widths.

The Helitorch unit which ACS had leased for testing has now been purchased and is a permanent addition to inventory. ACS will include coverage of this equipment in future training programs and contingency manual updates (Allen, in press).

Dispersant Effectiveness Test in Cold Water.

Laboratory work conducted in 1980 demonstrated that the dispersant chemicals presently stockpiled by Alaska Clean Seas are effective for use on Prudhoe Bay crude oil under arctic conditions. However, larger scale tests conducted in a wave basin would provide more realistic test conditions and provide a better basis for recommending procedures and practices to be included in the *Alaska Oil Spill Chemical Applications Manual* recently published by Alaska Clean Seas (Allen, June 1986). Furthermore, since 1980 additional dispersants have been developed that are expected to be more effective for cold water applications, and these new chemicals can be included in the experiments.

Three commercially available dispersant products have been selected for evaluation. The chemicals selected have characteristics which are typical of the range of products on the market. Dispersability tests were conducted in an experimental wave basin. The final report is expected to be completed in the third quarter of 1987.

Detection of Oil Under Ice by Induced Fluorescence.

Present methods for detecting oil encapsulated within sea ice or trapped beneath it are either slow and inefficient, or virtually ineffective for thin deposits of oil. However, ACS is pursuing one promising approach to detection of oil in ice, involving the phenomenon of induced fluorescence.

Crude oil fluoresces strongly in the visible spectrum when it is illuminated with ultraviolet light. Conceptually, as shown in Figure 5, a compact, portable, pulsed ultraviolet light source, similar to a photographic strobe light, could be used to flash an intense beam of ultraviolet light onto a small area of the surface of the sea ice. The light would need to be sufficiently intense to penetrate several feet of snow cover and ice, and illuminate an underlaying layer of oil. When exposed to ultraviolet light, oil fluoresces strongly at a much longer wave length in the visible spectrum. A suitable sensing device mounted adjacent to the ultraviolet light source should detect fluorescence from any oil present.

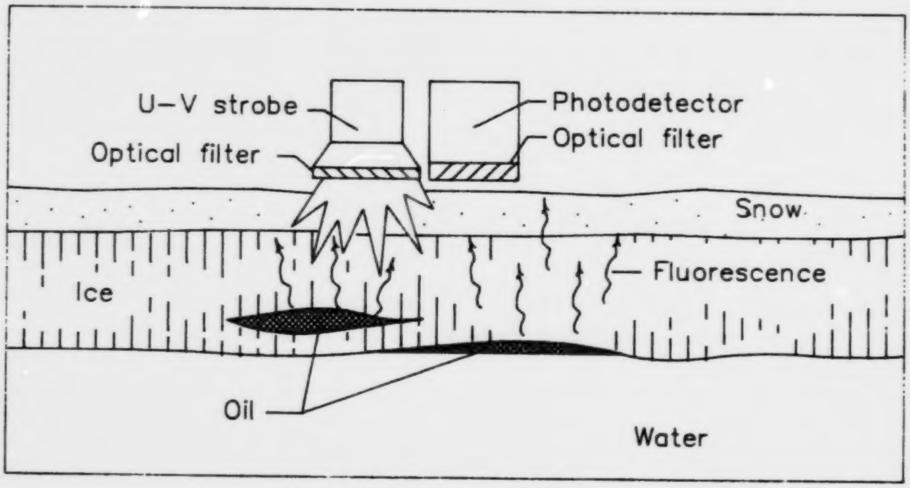

Figure 5. Through-ice detection system.

A high intensity UV flash system and a sensitive photodiode detector have been purchased which meet ACS criteria. Several suitable optical filters for the light source and detector have also been purchased. Experiments are now under way to evaluate the performance of the components working together as a detection system.

Multiple boom Strategies for Use in Arctic Waters.

Virtually all booms have oil underflow losses when the local normal flow velocity vector exceeds 1 to 1.5 knots. In the presence of waves, underflow begins at lower velocities, and wind-driven choppy waves can also cause oil to splash over the tops of booms, particularly with low profile booms such as the more massive fire containment booms. Short-period waves also inhibit the ignition and subsequent incineration of oil, significantly reducing the effectiveness of the *in situ* burning disposal technique. In arctic waters the possibility of collision with moving ice threatens the structural integrity of the booms.

A promising concept for extending the use of booms into these more severe conditions involves use of multiple boom arrays. The concept utilizes a configuration of specially designed booms placed upstream of the final boom. This boom assemblage establish a quiescent containment region, isolated from choppy waves and high currents. This enclosed portion of the boom system will accumulate a thick, relatively undisturbed pool of oil which can be skimmed or burned efficiently.

Selected multiple boom configurations were tested for performance with an irregular wave condition which consisted of a significant wave height of 0.62 ft and a mean wave length of 9.1 ft. (This is the condition that OHMSETT researchers refer to as a "harbor chop" wave condition, and their previous experience has established it as a severe test of a boom's retention capability.) An additional irregular wave condition of 1.0 ft wave height and a mean frequency of 0.5 Hz has also been used. Tests were performed at the Shell wave tank at Westhollow Research Center in Houston, Texas. Polybutylene pellets were used to simulate oil in preliminary tests, followed by confirming tests with actual oil with selected standard characteristics.

The best multiple boom configuration found during these tests consisted of a rear boom and a special single lead (forward) boom constructed by placing three booms adjacent to one another and tying them together with nylon rope every few feet. Each of the three booms had a different size and mass, with the largest and heaviest boom used in the front and the smallest and lightest boom in the back. Each of the three booms were skirtless, since in each of the multiple boom tests the presence of a skirt on the lead boom was found to increase the underflow losses at the rear boom.

Salmon Tainting Study.

In the latter part of 1986, ACS joined with the Cook Inlet Response Organization (CIRO) in sponsoring a study of the potential for tainting of salmon as a result of the use of dispersant chemicals on an oil spill in salmon habitat. From previous experimental work, the concentrations of dispersed oil and dispersant chemicals in the environment can be reliably predicted. In this study salmonid specimens are placed in tanks containing seawater and dispersant-treated oil at concentrations typical of what fish would experience in an actual oilspill dispersion operation. Tanks containing (1) plain seawater, and (2) seawater with undispersed oil are to provide experimental controls. This work is being performed under contract with the University of Washington. Results are to be published later in 1987.

The ACS 1987 Research and Development Program

Alaska Clean Seas has selected the research, development, and engineering projects described below to be initiated in 1987.

Development of a high-capacity rotating brush/rope mop skimmer for oil recovery in ice-laden waters.

Preliminary development work by Exxon Production Research on this new skimming system concept is promising, especially for use with viscous oils in arctic waters. The system uses a rotating cylindrical brush to help move floating oil to a central collection point. As the rotating brush sweeps the water surface it generates a surface current which moves floating oil toward the brush. In preliminary tests, oil many feet away from the brush was observed being "pulled" toward it. Equipment to be constructed and tested under this project will use a system of rotating brushes to move oil toward the skimmer, and rope mops to remove the oil from the water. (See Figure 6.) The system with rotating brushes as well as mops is expected to be more effective than a rope mop system alone. It should be noted that both the rotating brush and the rope mop units are highly compliant and are not damaged by repeated contact with floating solids such as ice.

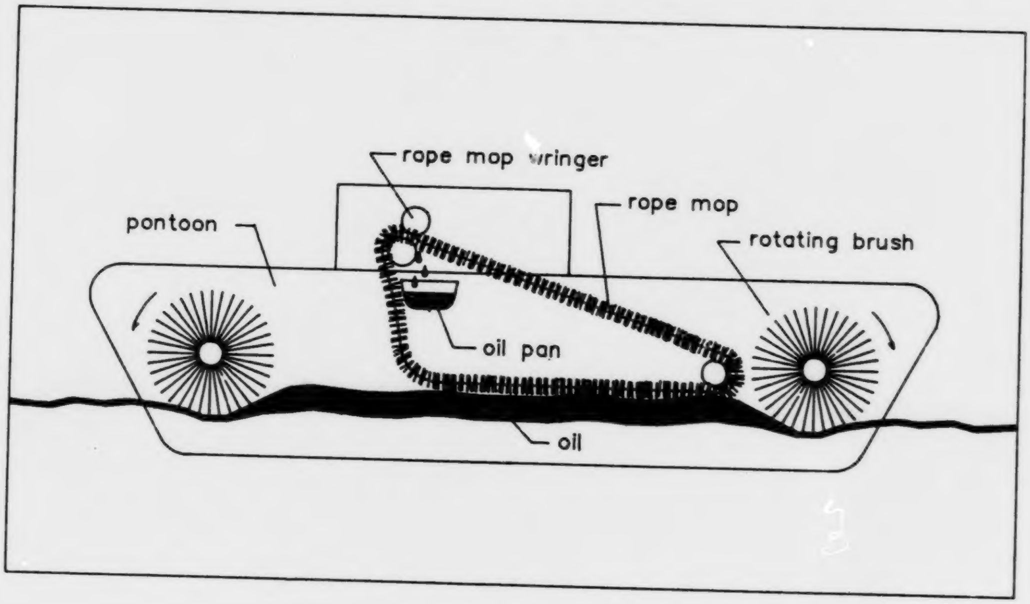

Figure 6. Rotating brush skimmer.

Additional experiments will be performed in which a dense array of stationary rope mops will be placed directly in the path of a flowing stream of oil and water. The array of ropes will act both as a wave damper to calm the fluid stream and as an oil coalescer to help in recovery of the oil. Oil released by the rope mop coalescer will collect in a calm sump area where it can be removed with a simple pump. (See figure 7.)

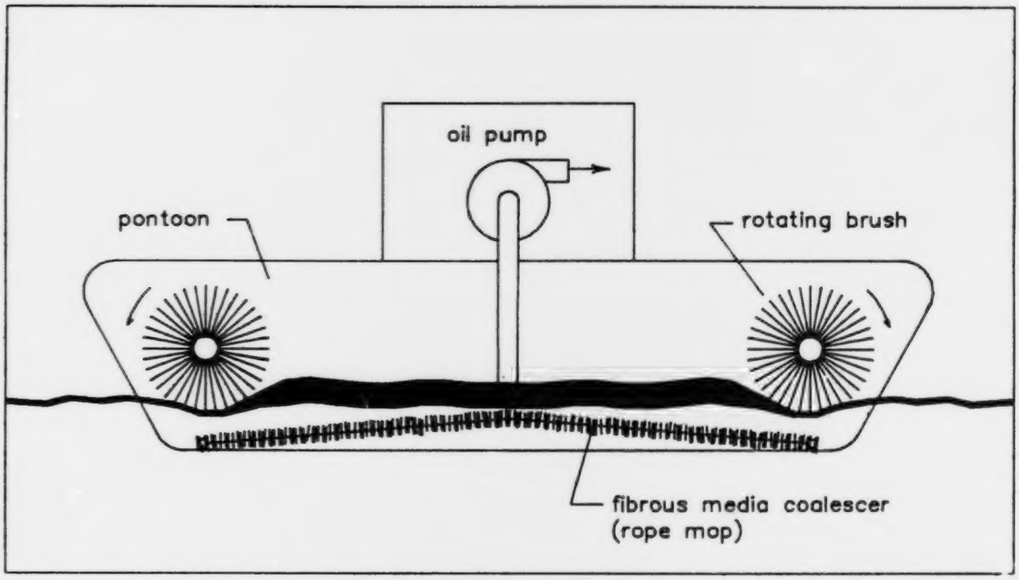

Figure 7. Rotating brush skimmer with fibrous media coalescer.

Bubble barrier field tests.

This project will continue the development and evaluation work which has been under way in previous years. A new bubble barrier unit will be constructed to replace the one which was severely damaged in 1986. The new unit will be designed to resist damage. After construction the boom will be deployed, towed to a suitable location, and tested by operating it in a broken ice environment.

Development of a high tensile strength containment boom.

Standard Alaska Production Company has conducted independent tests involving a special high tensile strength containment boom. The main component of the boom is a section of heavy duty conveyor belt material. Standard has developed a system for connecting sections of the boom to one another. This project, which will be jointly accomplished by Standard and the ACS staff, will include the following steps: 1) design of floatation, ballasting, and end connection systems; 2) procurement of materials and fabrication of boom system; 3) field testing of assembled boom system, including an assessment of its operating characteristics in broken ice; and 4) preparation of project report.

Arctic Skimmer Prototype Development.

Under this project, the ACS staff is to develop and test a prototype skimming device for use with the *ARCAT* or the *NorthStar* in broken ice conditions. The concept to be tested is to be similar to that of the SOCK device used by ACS in Bering Sea waters, however it will include provisions for deflecting broken ice.

The project will involve the following steps: 1) design of the skimmer, ice deflector, mounting system for the NorthStar, and ancillary equipment; 2) procurement of materials and fabrication of equipment and mounting system; 3) Field testing in a broken ice environment; and 4) report preparation.

Shallow Water Access Mop Platform (SWAMP).

Access to near-shore environments in the lagoonal systems south of the Beaufort Sea barrier islands is limited because of the shallow water. Under this project a shallow-draft pontoon hull skimming vessel will be designed, assembled and tested. Project steps include the following: 1) design of system including hull, propulsion, skimmer, oil/water separator, transfer equipment, temporary storage, and life support subsystems. (alternately, select suitable commercially produced components if they are on market, otherwise design from scratch.); 2) procure materials and components; 3) fabricate and assemble vessel and ancillary equipment; 4) conduct operational tests; and 4) prepare report.

Literature study on effects of in situ burning.

This project includes review of technical literature to assess the state of knowledge on the potential environmental and health effects of *in situ* combustion of crude oil. Considerations regarding further study needs will be covered in the report.

Computer Assisted Dispersant Application (CADA) Planning System.

This project covers the preparation of a computer program to assist in the planning of dispersant application operations. The program is to be based on computation and decision systems described in the Alaska Oilspill Chemical Application Manual published by Alaska Clean Seas in 1986. Rapid but accurate decisions would be critical to the successful application of chemical dispersants. The program will be written in Pascal and/or Prolog, and will initially be prepared for use on computers using the MS-DOS operating system. If there is demand, versions of the program could also be implemented for the CP/M operating system and for the Apple Macintosh.

Oil and Oily Debris Disposal Guidelines.

This project will examine options and prepare written guidelines for disposal of recovered oil and oily debris associated with a spill response operation in the Alaska Clean Seas areas of operation.

Conclusion

The Alaska Clean Seas research and development program continues to help advance the state-of-the-art for oil spill response in arctic waters. Knowledge gained through this ongoing program is used to update contingency planning manuals and the ACS training curriculum to help member companies maintain and improve the quality and effectiveness of their spill countermeasures.

REFERENCES

Alaska Beaufort Sea Oil Spill Trajectory Analysis, prepared for Alaska Clean Seas by Northern Technical Services; July 1983.

Alaska Oil Spill Chemical Application Manual, prepared by Spiltec for Alaska Clean Seas, 1986.

Norton Sound Oil Spill Trajectory Model; Prepared for Alaska Clean Seas by Applied Science Associates, Inc., January 1985.

St. George Basin Oil Spill Trajectory Model; Prepared for Alaska Clean Seas by Applied Science Associates, Inc., September 1984.

Survey and Analysis of Air-Deployable Igniters, prepared by Spiltec for Alaska Clean Seas, 1986.

Test and Evaluation of Fire Containment Boom, prepared by Spiltec for Alaska Clean Seas, 1986.

Allen, Alan A.; *Test and Evaluation of Fire Containment Boom*; Prepared by Spiltec under contract to Shell Western E&P, Inc. for Alaska Clean Seas; Anchorage, February, 1986.

Allen, Alan A.; *Survey and Analysis of Air-Deployable Igniters*; Prepared by Spiltec under contract to Shell Western E&P, Inc. for Alaska Clean Seas, Anchorage, April, 1986.

Allen, Alan A.; *Alaska Oil Spill Chemical Application Manual*; Prepared by Spiltec under contract to Standard Alaska Production Company for Alaska Clean Seas; Anchorage, June, 1986.

Allen, A. A. and W. G. Nelson; "Oil Spill Countermeasures in Land Fast Sea Ice", *Proceedings of the 1981 Oil Spill Conference;* API, 1981.

Allen, A. A. and W. Simpson; "Alaska Clean Seas Test and Evaluation of Fire Containment Boom", *Proceedings of the Ninth Arctic Marine Oilspill Program Technical Seminar*; Environment Canada; June 1986.

Allen, A. A., "Alaska Clean Seas Survey and Analysis of Air-Deployable Igniters"; *Proceedings of the Ninth Arctic Marine Oilspill Program Technical Seminar*; Environment Canada; June 1986.

Allen, A. A.; "Alaska Clean Seas Development of a Chemical Application Manual"; *Proceedings of the Ninth Arctic Marine Oilspill Program Technical Seminar*; Environment Canada; June 1986.

Allen, Alan A.; *Refinement of Aerial Ignition Systems (Test and Evaluation of the Helitorch for the Ignition of Oil Slicks)*; prepared by Spiltec under contract to Shell Western E&P Inc. for Alaska Clean Seas. In press.

Frish, M. B., P. E. Nebolsine, M. A. Defaccio, H. Scholaert, W. Kung and J. Wong; "Laser Ignition of Arctic Oil Spills: Engineering Design"; *Proceedings of the Ninth Arctic Marine Oilspill Program Technical Seminar*; Environment Canada; June 1986.

Garlow, R. E., R. E. Steele, and R. E. Williams; *Development of a Bubble Barrier Boom for Oil Spill Containment in Broken Ice*, Exxon Production Research Co., November 1986.

Garlow, R. E., R. E. Steele, and R. E. Williams; *Development of a Water-Jet Boom for ARCAT II Skimmer Vessel; Exxon Production Research Co., October 1986.*

Gusey, W. F., S. O. Hillman, and D. W. Chamberlain; ACS Alaskan Bering Sea Coastal Resources Manual; Alaska Clean Seas, in press.

Hillman, Sharon O., "Arctic Spill Response Improvements: A 1985 Review of Arctic Research and Development", *Proceedings, 1985 Oil Spill Conference*, American Petroleum Institute, February 1985.

Hillman, Sharon O., and Richard V. Shafer, "ABSORB: A Three Year Update in Arctic Spill Response", *Proceedings, 1983 Oil Spill Conference*, American Petroleum Institute, February, 1983.

Morson, Barbara J.,*et al.*, *Alaskan Beaufort Sea Coastal Region*, Alaska Clean Seas, June, 1983.

Nelson, W. G. and Allen, A. A.; "Oil Migration and Modification Processes in Solid Sea Ice"; *Proceedings of the 1981 Oil Spill Conference;* API, 1981.

Nelson, William G. and Alan A. Allen, "The Physical Interaction and Cleanup of Crude Oil with Slush and Solid First Year Sea Ice", *Proceedings of the Fifth Arctic Oilspill Program Technical Seminar*, Environment Canada, 1982.

Neve', Richard A. and Esther C. Wunnicke, *Final finding and Decision of the Commissioners Regarding the Oil Industry's Capability to Clean Up Spilled Oil during Broken Ice Periods in the Alaskan*

Beaufort Sea, State of Alaska Departments of Environmental Conservation and Natural Resources, June 1984.

Pistruzak, W. M.; "Dome Petroleum's Oil Spill Research and Development Program for the Arctic"; *Proceedings, 1981 Oil Spill Conference*; API, 1981.

Ross, S. L., *Evaluation of Industry's Oil Spill Countermeasures Capability in broken ice conditions in the Alaskan Beaufort Sea*, S. L. Ross Environmental Research Limited, September 1983.

St. Martin, J, and I. Lissauer; Satellite Buoy Trajectories - 1982, 1985"; *Proceedings of the Ninth Arctic Marine Oilspill Program Technical Seminar*; Environment Canada; June 1986.

Shafer, R. V.; "The Alaska Clean Seas Research, Development and Engineering Program"; *Proceedings of the Ninth Arctic Marine Oilspill Program Technical Seminar*; Environment Canada; June 1986.

Shafer, R. V.; "Alaska Clean Seas: Meeting Response Needs for 1987 and Beyond", *Proceedings, 1987 Oil Spill Conference*, API, April 1987.

Williams, R. E., "The ARCAT, ABSORB's New Catamaran Oil Skimmer", *Proceedings of the Fifth Arctic Marine Oilspill Program Technical Seminar*, Environment Canada, 1982.

ENVIRONMENTAL ATLAS FOR BEAUFORT SEA OIL SPILL RESPONSE

David F. Dickins
DF Dickins Associates Ltd.
Vancouver, B.C.

Linda C. Martin
ESL Environmental Sciences Limited
Vancouver, B.C.

Ingrid E. Bjerkelund
DF Dickins Associates Ltd.
Vancouver, B.C.

Stephen G. Potter
S.L. Ross Environmental Research Limited
Ottawa, Ontario

David C. Tilden
Environmental Protection Service
Environment Canada
Yellowknife, N.W.T.

INTRODUCTION

Project Background

An abundance of environmental data and knowledge has been generated over the past decade as a result of Beaufort Sea hydrocarbon exploration and development. Much of this knowledge is relevant to the development, selection, and implementation of oil spill countermeasures. Unfortunately, this information is not always readily accessible or available to those responsible for planning and implementing oil spill countermeasures.

The concept of developing the Environmental Atlas for Beaufort Sea Oil Spill Response arose in 1985 as a result of the following factors and identified needs:

- there is a need to condense currently existing environmental data and information into a concise, atlas format suitable for ready reference;
- the advent of year-round drilling in the offshore regions of the Beaufort, due to new and improved technology, emphasizes the need for response planning and countermeasures in ice covered or ice infested waters;
- the existing Worbets' (1979) "Shoreline Oil Spill Protection and Cleanup Strategies" manual is restricted to open water

conditions along the southern Beaufort Sea coast;
- there is a need to increase public awareness and understanding of the environmental features of the Beaufort Sea Region which influence planning and implementation of oil spill countermeausres;
- there is a general consensus among government and industry personnel that a common information base is required for planning and implementing marine oil spill countermeasures to reduce misunderstandings and duplication of efforts (e.g. for developing environmental operating conditions and contingency plans, for evaluating regulatory permits, and for drilling program approvals);
- spill response personnel from both government and industry require a concise reference guide which will provide practical, operations-oriented information (e.g. logistics constraints, shoreline types, and locations of critical human and biological resources); and
- a number of Beaufort Sea EARP Panel recommendations stressed the need for continuing research and development in the field of oil spill countermeasures by industry and governments. The development of the atlas is consistent with these recommendations.

Objectives

The primary objective of the atlas is to provide a synthesis of environmental information relevant to the planning and implementation of year-round oil spill countermeasures in both coastal and offshore areas of the Beaufort Sea. **The atlas is intended to be used as a link between the environmental characteristics of the region and the practical considerations of providing an effective response to marine oil spills, but not as an oil spill manual.** Hopefully this work will lead to better utilization of available resources and to reduced environmental impact in an actual Beaufort Sea spill incident.

The emphasis throughout the atlas is on the presentation of selected information in a concise, graphic form with important supporting text. The selection of information is intended to satisfy a wide variety of perceived user groups, including: government scientists, Coast Guard and industry response teams, policy directors, regulatory agencies, Beaufort Sea community organizations, and land use planners.

Worbets' (1979) manual provided a model for the atlas in terms of physical layout, operational map scales, and general concepts of sensitivity ranking. In addition, "A Manual for the Preparation of Shoreline Protection and Cleanup Plans" prepared by F. Beech (1981) was used as a guide for general format and map presentation. Apart from these similarities, the current atlas represents a completely new information base, which is organized, mapped, and presented entirely as computer generated product. The atlas can be updated at any time by entering new information to replace or augment the existing files.

The atlas is useful in three major areas: first to assist in the development of the most effective contingency plans for a specific area; second to provide a source document on which to base realistic oil spill training exercises; and third to act as a basic field reference to important environmental factors in an actual spill situation. Information contained in the atlas must be supplemented by local knowledge and real time information in the event of a spill.

ATLAS OVERVIEW

The study area covers the southern Canadian Beaufort Sea from the United States/Canada border on the west to Baillie Islands on the east. The actual coastline exceeds 2,700 km in length while the direct east-west distance across the study area is only 520 km (Worbets, 1979). The northerly extent of the study area is based on the median location of the polar pack edge (≥ 5/10 old ice). The southern boundary of the area is determined by the backshore limits of potential contamination from a marine oil spill. These limits are defined as the maximum area of inundation which could occur during positive storm surge events (onshore winds).

The atlas is organized by map scale, moving from the summary to the regional to the operational scale. The bulk of the atlas information is presented at the operational scale of 1:150,000 using maps derived from the Canadian Hydrographic Service (1986) charts of the Beaufort Sea. Figure 1 shows the areas covered by the operational maps.

Information is grouped as follows according to the different map scales:

SUMMARY MAPS
Scale 1:2,500,000

- Oil and Gas Discoveries and General Bathymetry
- Overview - Areas of High Environmental Sensitivity
- Offshore Environmental Sensitivity
- Areas of Special Status
- General Ice Conditions:
    - Winter Ice Zones
    - Cape Bathurst Polynya
    - Summer Ice Zones
    - Ice Clearing Dates
    - Open Water Season

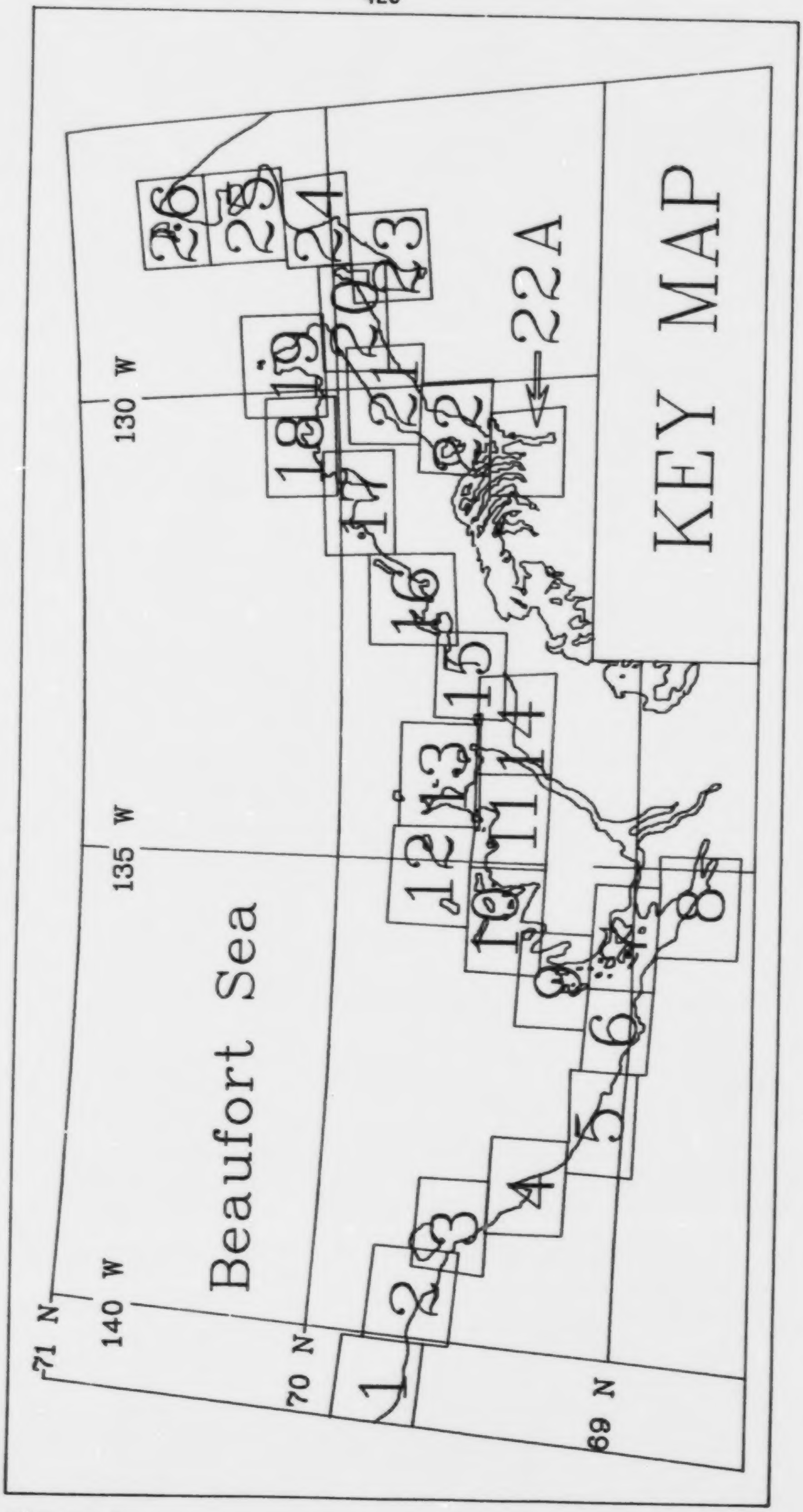
Beaufort Sea
KEY MAP
71 N
70 N
69 N
140 W
135 W
130 W
1
2
3
4
5
6
7
8
9
10
11
12
13
14
15
16
17
18
19
20
21
22
22A
23
24
25
26

Figure 1

Ice and Water Movement
- Offshore Access and Countermeasures Information

REGIONAL MAPS
Scale 1:1,000,000

- Offshore Environmental Sensitivity During Winter and Spring
- Offshore Environmental Sensitivity During Summer and Fall
- Landfast Ice Conditions:
    Landfast Ice Development
    Winter Landfast Ice
    Landfast Ice Break-up
    Ice Growth and Ablation Curves
    Ice Bearing Capacity
    Ice Ridge Frequency
- First Dates Ice Free - Examples of Early and Late Ice Clearing

OPERATIONAL MAPS
Scale 1:150,000

- Shoreline Environmental Sensitivity:
    Biological Resources
    Resource Harvesting Areas
    Resource Harvesting Camps
    Archaeological Sites
    Heritage Sites (locally identified)
    National or Territorial Parks
- Sensitivity Rankings
- Occurrence of Species and Resource Use
- Environmental Description

Physical Environment and Logistics:
- Shoreline Type
- Areas Inundated During Storm Surge Events
- Locations of Artificial Islands
- Airstrips and Anchorages
- Inlet Widths
- Spot Soundings **(Not to be used for navigation)**
- Oil Disposal Sites
- Shore Access for Barge Offloading
- Description of Countermeasures and Access Limitations

Tactical maps are inserted into the operational map series at different scales for specific areas where more detailed charts are available (Workboat Passage, Tuktoyaktuk Harbour, McKinley Bay, and Nicholson Island).

The following pages extracted from the atlas show the Users' Guides for the physical environment and logistics maps, and for the environmental sensitivity maps.

PHYSICAL ENVIRONMENT AND LOGISTICS

Legend

▦	**Tundra Cliffs**
▴▴▴	**Inundated Tundra**
⁘	**Barrier Beaches & Spits**
▤	**Deltas**
E	**Estuaries and Bays**
→	**Net Longshore Sediment Transport**
≋	**Areas Inundated During Positive Storm Surges**
......	**Low Water Line**
⊠	**Artificial Islands**
⚓	**Anchorage**
╲	**Shore Access** (Barge Offloading)
✈	**Airstrip suitable for STOL**
✈	**Airstrip suitable for F27, HS748**
✈	**Airstrip suitable for Hercules**
⊕	**Ice Runways** (Winter Only)
( )	**Inlet Width (m)**
×	**Potential Debris Storage** - Temporary
⊗	**Potential Disposal Site** - Permanent
....	**Summer Access** (Disposal Sites)
----	**Winter Access** (Disposal Sites)

Nearest Airstrip -

Hydrographic Chart -

Video Tapes -

Coastal Type Descriptions

Information on coastal types mapped on the operational maps is derived from 1:50,000 coastal resource maps originally prepared by Dobrocky Seatech (4).

Tundra Cliffs:
Cliffs cut into unconsolidated, but frozen coastal plain sediments; usually rapidly retreating (1 to 2 m/yr); narrow, fringing gravel beaches are frequently asscociated with the cliffs.

Inundated Tundra:
Very low tundra that has been inundated such that the tundra surface is now below mean sea level; in effect a tundra mat extends below the water surface; coastal retreat rates are characteristically high (1 to 2 m/yr), although this coastal type frequently occurs within low wave exposure embayments.

Barrier Beaches and Spits:
Frequently interspersed with tundra cliffs along the coast; the barrier islands and spits are low in elevation, usually less than 2.5 m above mean water level; substrate is most commonly a mixture of sand and gravel; coastal stability is usually controlled by the rate of headland retreat of nearby tundra cliffs although some barrier spits are actually prograding.

Deltas:
Include several coastal landforms such as tidal flats, low tundra areas, and channel complexes that are found at the seaward terminus of rivers; on the main portion of the Mackenzie River delta, coastal retreat is rapid (>2 m/yr).

Estuaries/Embayments:
May include all of the above-mentioned coastal types with the common attribute that they all occur in very low wave energy environments (wave fetch less than 10 km) and are likely to have lengthy potential residence periods. Limited space precludes mapping individual coastal types within an estuary. Estuaries associated with major rivers are predominantly deltas. Examples are the Wood, Mason, Running, and Babbage Rivers which are marked only as Estuaries on the maps.

Net Longshore Sediment Transport

This information is intended only as a guide to where sediment transport is likely to occur and, on average, in which direction. Net directions are determined from geomorphological indicators, such as elongated spits, and aerial photo interpretation. Most longshore transport is due to breaking waves and occurs in water depths from less than 4 m to 5 m. Short term, high energy storm events are responsible for most coastal sediment transport in the Beaufort Sea (4).

Areas Inundated During Positive Storm Surges

The natural tidal range in the southern Beaufort Sea is between 0.3 and 0.5 m. Much greater water level variations are associated with wind driven pile-ups of water in shallow water areas and are called storm surges. Between the years 1962 and 1973, there were 5 negative surges (offshore winds leading to a drop in sea level by up to 1 m) and 22 positive surges (onshore winds leading to a rise in sea level of up to 3 m). The frequency of storm surges is greater during good ice years when sufficient fetch is available to generate the necessary wind driven waves. Positive storm surge events cause extreme coastal erosion and inland flooding of low lying areas, such as Ellice Island (5). The historical limits of storm surge inundation are indicated by log and driftwood debris lines mapped from aerial photographs (6). These lines are used here to delineate the maximum backshore limits of the shoreline sensitivity areas which could be affected by a marine oil spill.

Low Water Line

Shoreline exposed at low tide is mapped (3).

Artificial Islands

These features are abandoned, man-made islands used for oil exploration. Not all islands will be visible as wave action can rapidly erode an island to a level several metres below sea level.

Anchorage

Anchorages described in the Sailing Directions, Arctic Canada (7) are noted.

Shore Access

Arrows denote known locations of shallow draft barge access for direct cargo transfers to and from a beach or shoreline area (7). Note: Winter ice roads are mapped on Regional Maps 4 West and 4 East.

Airstrips

Locations of all existing land airstrips and selected ice runways used in the past are based on information provided by the Canadian Armed Forces Northern Region (Air). Each land site is marked by a particular aircraft symbol to indicate the approximate runway length and condition as follows:

Twin Otter Symbol:

Indicates runways less than 800 m (2,600 ft) or abandoned strips suitable for light aircraft or STOL aircraft in the 6,000 kg weight category and up (Twin Otter, Dash 7, Buffalo). Surface conditions may vary from tundra to sand or gravel. Any symbol marked Aband(oned) should be considered suitable only for Twin Otter aircraft on high flotation tyres until further inspection.

Fokker (Fairchild) F.27 (F227) Symbol:

Indicates primarily Distant Early Warning (DEW) runways approximately 1,100 m (3,600 ft) in length designed specifically to accommodate F27 type aircraft used for routine DEW resupply (also suitable for Hawker Siddely HS 748 as used in the Baffin Region of the NWT). Note: Permission is required to use DEW facilities. Contact Canadian Armed Forces (Air), Northern Region Headquarters, Yellowknife. The DEW Line will be referred to as the North Warning System in the future. Radar and communications equipment are in the process of being upgraded.

Lockheed Hercules (CC130) Symbol:

Indicates runways in excess of 1,500 m (5,000 ft) able to accommodate a heavy lift freight aircraft (Hercules, Electra, B737). The only land airfield in the study region that this applies to is at Tuktoyaktuk.

Ice Runways:

A circled aircraft symbol is used to denote those sites where ice runways have been used for regular operation in the past. Symbols are not meant to imply that these are the only sites available for ice landing. Given suitable conditions (smoothness, snow, ice thickness) there is no physical limit on the size of aircraft that can be accommodated throughout the nearshore area of the study region within the landfast ice zone. Winter fixed wing operations are also possible within the transition ice zone and the polar pack. Operations in these rougher ice areas are usually limited to Twin Otters on skis or large tyre/ski combination undercarriages (see Regional Maps 4 West and 4 East for locations of ice zones and information relating to ice bearing capacity for aircraft operations).

Inlet Widths

Inlet widths are from the 1986 1:150,000 Canadian Hydrographic Service charts for the Beaufort Sea (3).

Temporary Debris Storage Sites and Permanent Disposal Sites

Potential disposal sites are identified for the temporary stockpiling and permanent disposal of oiled debris and sediments. The sites were first selected by previous researchers (8) based mainly on geotechnical considerations, and identified largely through air-photo interpretation. An attempt was made to identify sites as close as possible to sand and gravel beaches that would be cleaned in the event of a spill. The main criteria for permanent disposal site selection are acceptable geological conditions, and that the sites are inland of the maximum storm surge zone and accessible from the shoreline via summer or winter access roads. As some sites cannot be accessed during summer, temporary stockpile locations are also identified at which debris could be temporarily stored before ultimate disposal. In this atlas, some potential sites of each type were rejected for reasons of proximity to archaeological sites, regional camps, and heritage sites. It is accepted that field verification at the time of a spill will be required to confirm site acceptability, and that other considerations, such as proximity to other human-use areas, might preclude the use of certain sites. Nonetheless, inclusion of potential sites in the atlas is considered useful as a tool for countermeasures planning.

Summer and Winter Access (Disposal Sites)

Where possible, summer access is identified to permanent disposal sites, otherwise summer access is identified to temporary storage sites. Temporary sites can be used until winter access over frozen tundra or frozen lakes permits access to permanent disposal sites.

Hydrographic Charts

Current charts at 1:150,000 are available from the Canadian Hydrographic Service (CHS). Note: Although the operational maps in this atlas have been computer generated directly from the CHS digital chart data base, many important navigational features (buoys, beacons, markers, etc.) have not been included. **Maps in this atlas should not be used for navigational purposes and are not intended as substitutes for the original charts.**

Video Tapes

Tape numbers refer to codes for a series of video tapes of the Beaufort Sea coast available through two sources: Dome Petroleum Limited, Calgary, and Atlantic Geoscience Centre (AGC), Geological Survey of Canada, Dartmouth.

Access and Countermeasures

Access and countermeasures information is specific for each operational and tactical map.

References

References are indicated by numbers in brackets (see Sections 5.2 and 5.3 for references relating to Physical Environment and Access and Countermeasures, respectively).

ENVIRONMENTAL SENSITIVITY MAPS

Legend

Shoreline Environmental Sensitivity*

■ **High Sensitivity Ranking > 68.70**

Moderate Sensitivity Ranking 35.10 - 68.70

▨ **Low Sensitivity Ranking < 35.10**

* See Appendix A. See Regional Maps for Offshore Sensitivity

Area No.	Area Name	Sensitivity Ranking
50	Nicholson Island	21.25
51	Cliff Point	20.50
52	Anderson River	102.30
62	Mason River	64.45

- ● **Archaeological Site**
- ■ **Heritage Site - locally identified**
- ♦ **Major Resource Harvesting Camp**
- ▲ **Other Resource Harvesting Camp**
- —·— **National or Territorial Park**

Resource Harvesting Areas

Highly Important R

Important R

Birds

Diving Ducks & Loons DL

Dabbling Ducks DD

Geese Ge

Swans Sw

Shorebirds & Cranes SC

Seabirds Se

Mammals

White Whale WW

Bowhead Whale Bh

Polar Bear PB

Ringed Seal RS

Bearded Seal BS

Arctic Fox AF

Reindeer Re or Caribou Ca

Fish

Anadromous Fish & Pacific Herring F

Site Specific

Environmental Sensitivity

Appendix A provides the background information and the detailed rankings necessary to interpret the summary values and relative sensitivity rankings (High, Moderate, Low) shown on the maps. The entire study area is divided into sensitivity areas. There are 69 shoreline environmental sensitivity areas shown on the operational maps. Shoreline area boundaries extend from approximately 1 km offshore to the maximum extent of storm surges in the backshore. Environmental sensitivity areas for the offshore were determined separately for the winter/spring and summer/fall periods by using ice and open water zones to define the area boundaries. Sensitivity was determined for 15 offshore areas during winter/spring and 11 areas for summer/fall. Offshore environmental sensitivities are shown on Summary Maps 3 and 4 and Regional Maps 1 West, 1 East, 2 West, and 2 East.

Seasons

The following seasonal definitions apply throughout the Atlas:

Shoreline Sensitivity (Summer/Fall)
- refers to the period late May to October 1, which corresponds to the maximum time span when oil could be exposed in an unfrozen state along the shore. It should be noted that there will be no opportunity for fresh oil to reach the shoreline from a marine spill until landfast ice break-up in early July.

Offshore Sensitivity (Summer/Fall)
- refers to the period July 17 to October 1, which corresponds to the duration of significant open water extent offshore. The variability in ice clearing dates throughout the study area is shown in Summary Map 9.

Offshore Sensitivity (Winter/Spring)
- refers to the period October 2 to July 16, which corresponds to the duration of extensive ice cover.

Archaeological Sites were identified from the Archaeological Survey of Canada (ASC) inventory and are shown on the operational maps. In the event of an oil spill, the ASC should be contacted for information on the contents and status of these sites.

Heritage Sites are those areas that Inuvik workshop participants identified as having the greatest cultural or historic significance to local residents (shown only on the operational maps).

Major Resource Harvesting Camps are locations that are used every year as a base for resource harvesting activities and are considered of primary importance by regional residents (shown only on the operational maps).

Other Resource Harvesting Camps are locations that often serve as a fishing or hunting camp or as a temporary camp in bad weather. These camps have only been identified within areas considered to be important for resource harvesting by regional residents (shown only on the operational maps).

National or Territorial Park Boundaries are shown on the operational maps and Summary Map 5.

Black Animal Symbols on the regional and operational maps indicate the general area where: (1) a significant proportion of a regional population; (2) a significant proportion of a group of bird species; (3) an important resource harvesting area; or (4) a large number of important fish species occurs. Fewer numbers of these species or other harvesting activities may occur in other areas, but symbols have been placed only where significant numbers of individuals have been observed over a period of several years or in areas that were identified by workshop participants as being important for resource harvesting. See Appendix A for detailed information.

Coloured Symbols on the regional and operational maps indicate a very site-specific area (less than approximately 50 km^2) that is used by a significant proportion of a regional population.

References are indicated by numbers in brackets (see Sections 5.4 and 5.5 for references relating to Offshore Environmental Sensitivity and Shoreline Environmental Sensitivity, respectively).

ENVIRONMENTAL SENSITIVITY

The sensitivity ranking system is based on a total of 20 environmental elements ranked within three categories: (1) human use sensitivity; (2) biological sensitivity; and (3) shore zone oil residence category or marine oil residence category. The marine oil residence category was developed specifically for this atlas to allow the overall sensitivity of offshore areas to be determined. This category effectively parallels the shore zone oil residence category that was developed to determine the sensitivity of coastal areas. The above three categories were assigned a Weighting Factor (WF) that quantitatively represents the relative importance of each category within the entire ranking system. The Weighting Factors range from 1.5 to 2.00.

Human use sensitivity received the highest Weighting Factor of 2.00 because the protection of human life, life style and property is considered the highest priority during an emergency response (Worbets, 1979). The biological sensitivity category was assigned a Weighting Factor of 1.75 to reflect the importance of these resources. The marine and shore zone oil residence categories received a lower Weighting Factor (1.50) and relate to the persistence of oil in the environment.

Selection of specific environmental elements within each of the categories was necessary to develop a relatively simple ranking system that still adequately considered the complex environment of the Beaufort Sea. The rationale for the inclusion and ranking of the individual elements was based on:

1. a review of the literature regarding the sensitivity and vulnerability of resources to the effects of oil;
2. those resources that were identified through the Beaufort Environmental Monitoring Project (Indian and Northern Affairs Canada and Environment Canada, 1985) as being of the highest profile in the region;
3. research on the fate and persistence of oil in cold, ice-infested water and in northern coastal environments;
4. results of a workshop conducted in Inuvik on 14 January 1987 regarding the use of the land and renewable resources by residents of the region; and
5. the consensus of the study team and Steering Committee members regarding the relative ranking of each environmental component or element.

The environmental elements within each category were given an Assigned Value (AV) between 1 and 10, where 10 represents the component or element most sensitive to oil. For example, the habitat of rare or endangered birds is the most sensitive in the biological category, while estuaries and bays with low wave exposure are the most sensitive in the shore zone oil residence category.

The sensitivity of a specific shoreline or offshore area to oil was determined by reviewing the 20 elements from the different categories, identifying which ones apply to the area, and then summing the Assigned Values (AV) multiplied by their Weighting Factor (WF) for each of those elements. For example, a stretch of shoreline may (1) have tundra cliffs; (2) support a significant portion of the population of rare or endangered birds; and (3) be within a territorial park. For each of these three elements, the Assigned Value is multiplied by the Weighting Factor of its category to produce a Priority Index (PI) for that element (i.e., AV x WF = PI). The priority indices of all elements that apply to the area are then summed to produce a single number that represents the sensitivity of that particular area to oil (Worbets, 1979).

The entire study area is divided into sensitivity areas to enable the application of the 20 sensitivity elements and to determine the overall environmental sensitivity. Environmental sensitivities for 69 shoreline areas are shown on the operational maps. Sensitivity rankings for 11 offshore areas in the summer and fall, and 15 offshore areas in the winter and spring are presented on summary and regional maps.

Shoreline environmental sensitivity area boundaries are indicated on each operational map. Each area extends approximately one kilometre offshore and backshore to include the maximum extent of positive storm surges. Shoreline environmental sensitivity values apply only for the period late May through October, when oil could be exposed in an unfrozen state along the shore.

Offshore environmental sensitivity was determined independently from shoreline sensitivity, and was analyzed for two periods: (1) summer and fall (July 17 to October 1) and (2) winter and spring (October 2 to July 16). The numbers and boundaries of offshore sensitivity areas are dictated by typical seasonal locations of distinct ice and open water zones. In the event of an actual spill, the offshore sensitivity area boundaries may differ greatly from those shown in the atlas depending on the ice conditions present at the time.

Ranking of the shoreline and offshore areas was simplified to three degrees of sensitivity (LOW, MODERATE, AND HIGH) to allow quick determination of their relative sensitivity to an oil spill, and eliminate judgements on the significance of small differences in the rankings.

The divisions between low, moderate and high were based on an even division of the absolute range in the rankings for winter/spring and for summer/fall. The rankings for the shoreline and offshore areas during summer/fall ranged from 1.5

to 102.3, while the rankings for the offshore areas during winter/spring ranged from 7.5 to 73.26.

The purpose of the ranking system is to provide an On-Scene-Commander and others in charge of responding to an oil spill with a system that priorizes areas for protection and cleanup when a large area is threatened. It does not imply that a "low-sensitivity" area should not be protected or cleaned in the event of a spill. A detailed list of all the elements which were combined to form the sensitivity ranking for each area is provided in the atlas. This list should be used to supplement the summary information shown on the maps in order to determine the environmental resources in each area and to select the most appropriate contingency strategies.

In conclusion, the sensitivity ranking system provides a scheme to compare the sensitivity of particular areas of the Beaufort Sea region with respect to oil spill effects, and to determine priorities for protection and cleanup. There will always be a degree of subjectivity and uncertainty associated with sensitivity ranking systems because of the complexity of natural systems and the uniqueness of circumstances surrounding any specific oil spill event. Despite the limitations of the ranking system, the atlas incorporates the best available knowledge of the Beaufort Sea environment and the effects of oil on northern resources.

Summary Map 2 shows the areas ranked using the system described above as being of high environmental sensitivity to oil spills. The accompanying pages, extracted from the atlas, summarize the different environmental elements that contribute to the sensitivities of the areas shown on the map.

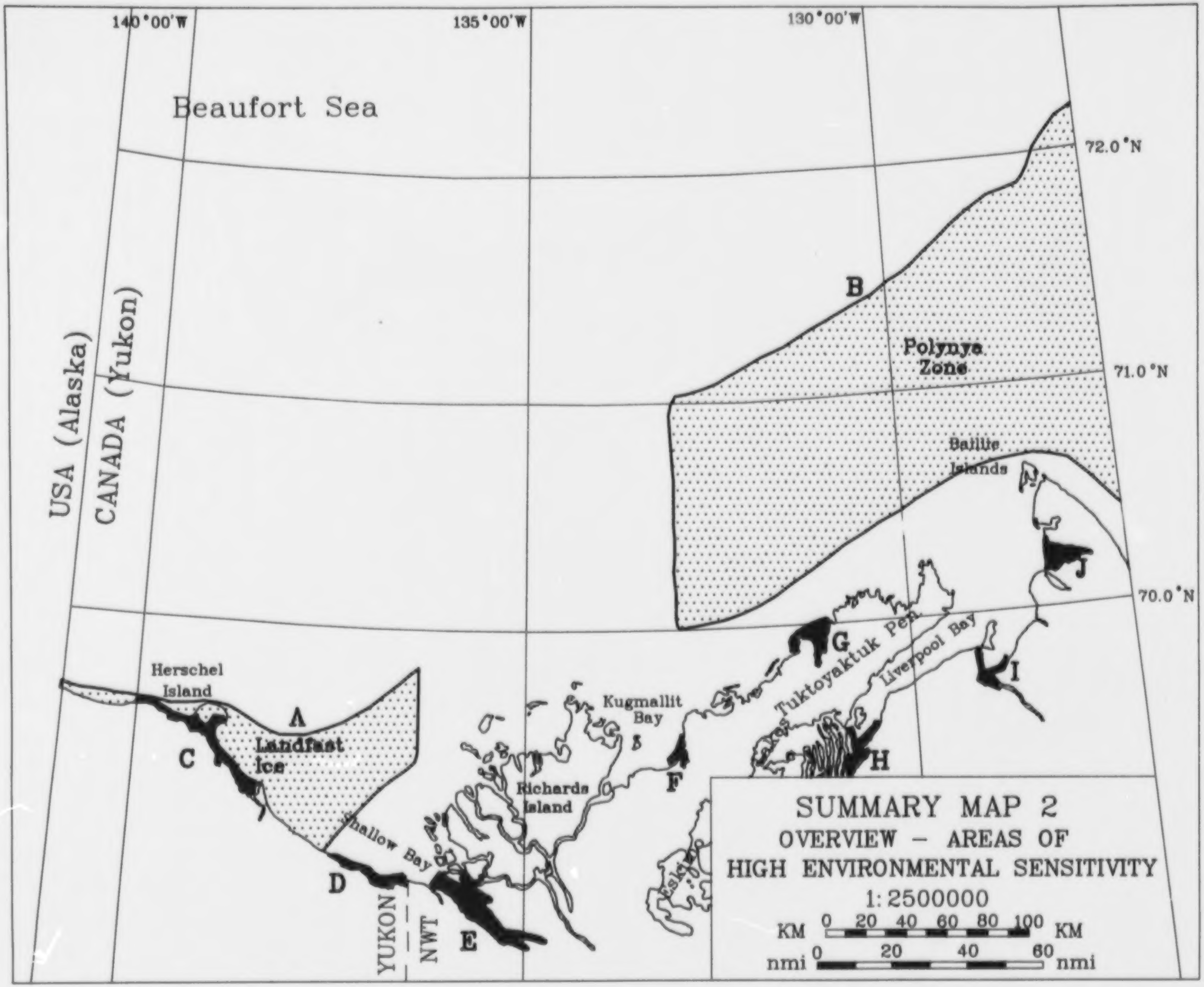

SUMMARY MAP 2
OVERVIEW – AREAS OF
HIGH ENVIRONMENTAL SENSITIVITY
1:2500000

140°00'W
135°00'W
130°00'W
72.0°N
71.0°N
70.0°N
Beaufort Sea
USA (Alaska)
CANADA (Yukon)
B
Polynya Zone
Baillie Islands
J
G
Tuktoyaktuk Pen
Liverpool Bay
I
Herschel Island
A
Landfast Ice
C
Kugmallit Bay
F
H
Richards Island
Shallow Bay
D
E
YUKON
NWT
KM 0 20 40 60 80 100 KM
nmi 0 20 40 60 nmi

OVERVIEW – AREAS OF HIGH ENVIRONMENTAL SENSITIVITY

SUMMARY MAP 2
BEAUFORT SEA

INTRODUCTION

This map presents a summary of areas of high environmental sensitivity to oil spills based on available data and the environmental sensitivity ranking scheme described in Appendix A. Depending on actual environmental conditions at the time of a spill, other areas may be more or less sensitive than those shown here. A number of areas ranked six points or less below the range defining the "High" category are not indicated on this map. These "borderline" areas are Kendall Island (Area No. 24), Kittigazuit Bay (Area No. 34), Hutchison Bay (Area No. 41), and Mason River (Area No. 62).
Users should refer to detailed information regarding the human use, biological, and physical environmental factors that contribute to the sensitivity of all areas before deciding on a response plan. This information is provided on the maps and accompanying text throughout the atlas. Appendix A contains a complete list of the environmental elements for each sensitivity area, sensitivity ranking calculations, and a full explantion of the sensitivity ranking scheme.

A summary of the environmental elements that contribute to the high sensitivity of the areas shown on Summary Map 2 is presented below.

A. Landfast Ice off the Yukon Coast During Winter/Spring (October 2 to July 16)

See Regional Map 1 West, Environmental Sensitivity Area 209

- Black guillemots (a rare and endangered bird) breed, rear broods, feed, moult and rest in and adjacent to nearshore waters northeast of Herschel Island.
- Polar bears and seals are hunted on the landfast ice between Phillips Bay and Herschel Island.
- White whales travel along the landfast ice edge to Mackenzie Bay and Kugmallit Bay.
- Marine fish overwinter under ice, and anadromous species migrate along the coast in spring.
- Oil spilled in landfast ice after freeze-up in early October will be quickly incorporated within the growing ice and remain encapsulated until the following spring when the oil will migrate to the surface and be exposed as slicks on melt pools from late May to ice break-up in July.
- The time period when the simultaneous occurrence of most of these elements may occur is late May through mid July.

B. Polynya Zone off Tuktoyaktuk Peninsula and Baillie Islands During Winter/Spring (October 2 to July 16)

See Regional Map 1 East, Environmental Sensitivity Areas 207 and 208

- Polar bears are hunted from mid January to the end of May.
- Several thousand diving ducks congregate in leads from mid May until early June.
- Substantial numbers of polar bears occupy areas in the transition zone.
- Bearded seals are abundant in the transition zone and pup in April and May.
- White whales travel along the landfast ice edge to concentration areas in Kugmallit and Mackenzie Bays.
- Oil in the polynya zone could be available for exposure to wildlife at any time during the winter.
- Increasing opportunity for oil exposure will be associated with the typical progression of polynya expansion from the Baillie Islands to the north and west beginning in March (see Figures 1 and 2, Summary Map 7).
- Simultaneous occurrence of most of these elements is most likely to occur from mid May to the end of May.

C. Yukon Coast from Nunaluk Spit to Phillips Bay, late May to October 1

See Operational Maps 2, 3 and 4, Environmental Sensitivity Areas 4,6, 8, 9, 10 and 11

- A number of human use elements contribute to the sensitivity of this area. These include resource harvesting, heritage sites, camps, archaeological sites and parks.
- Diving ducks, shorebirds, black guillemots and brant use various coastal areas in this region during the period May to September.
- Use of the region by Arctic foxes and caribou contribute to the sensitivity.
- Nearshore areas provide important migration corridors for anadromous fish and feeding and rearing habitat for marine and anadromous species.
- Estuary/embayment shore zone types are common along this coast and have the highest oil retention capacity.

D. Trent Bay and Shoalwater Bay, late May to October 1

See Operational Maps 5 and 6, Environmental Sensitivity Areas 16 and 17

- Regional residents indicated that these areas were of greatest importance for resource harvesting.
- Glaucous gulls breed and rear broods on Escape Reef and swans and geese use coastal areas from Trent Bay to the mouth of West Channel.
- White whales concentrate in Shoalwater Bay during late June to mid July.
- Nearshore areas are important for summer feeding, migration and rearing for fish.
- Caribou use nearshore areas to feed during mid June.

E. Shallow Bay, late May to October 1

See Operational Maps 7 and 8, Environmental Sensitivity Areas 19 and 20

- Whale and bird hunting occurs in these areas.
- Swans and geese (including brant) use Shallow Bay and adjacent wetlands and river channels.
- Mackenzie River channels are important migration corridors for fish. Some fish may overwinter where there is flow under ice.
- Estuary/embayment shore zone type in Shallow Bay have the highest oil retention capacity.

F. Tuktoyaktuk, late May to October 1

See Operational Maps 14 and 15, Environmental Sensitivity Area 37

- Tuktoyaktuk is the only community located within the study area and is an important base for many harvesting activities.
- Tuktoyaktuk Harbour provides an important year-round fish habitat.
- Archaeological sites and the Pingo Landmark Site contribute to the sensitivity of the area.
- Estuary/embayment shore zone type is predominant in this region and has a high oil retention capacity.

G. McKinley Bay and Atkinson Point, late May to October 1

See Operational Maps 17 and 18, Environmental Sensitivity Area 43

- This area is important for residents of Tuktoyaktuk throughout the year. There are also a number of archaeological sites and a heritage site located in the area.
- Diving ducks and brant moult and stage in the McKinley Bay area. The latter species also nests and rears broods in this area.
- Nearshore areas provide summer rearing and feeding habitat

and are important migration corridors for fish.

- Reindeer use nearshore areas to escape from flies from late July to early September.
- Estuary/embayment is the predominant shore zone type and it has a high oil retention capacity.

H. Entrance to Eskimo Lakes and Kugaluk River, late May to October 1

See Operational Maps 22 and 22A, Environmental Sensitivity Areas 57, 58 and 59

- This is an important spring and summer resource harvesting area. There are also a number of archaeological sites located along the coast.
- Large numbers of birds (swans, diving ducks and brant) use these areas.
- Pacific herring spawn in shoreline areas during spring. The Kugaluk River supports large populations of anadromous coregonids.
- Caribou use some nearshore areas to escape from flies during July.
- Shore zone types vary, but near the Kugaluk River the predominant type is estuary/embayment.

I. Wood Bay and Anderson River Delta, late May to October 1

See Operational Map 23, Environmental Sensitivity Area 52

- This area is important to residents of Tuktoyaktuk, and a camp is often established in the area for resoruce harvesting. Several archaeological sites and a heritage site are located in the area.
- This area is used by thousands of birds including diving ducks, dabbling ducks, swans and geese. The most recent confirmed sighting of an Eskimo curlew occurred in this area.
- Nearshore habitat is important for anadromous fish from the Anderson River.
- Caribou use nearshore areas to escape from flies during July.

J. Harrowby Bay, late May to October 1

See Operational Map 25, Environmental Sensitivity Area 65

- The North Star Harbour area is an important resource harvesting area and a number of archaeological sites are located on the shore of the bay.
- Thousands of diving ducks and geese use nearshore and shoreline areas from mid July to mid September.
- Nearshore areas provide important summer fish habitat.
- Caribou use nearshore areas to escape from flies during July.
- Estuary/embayment is the predominant shore zone type and it has a high oil retention capacity.

PHYSICAL ENVIRONMENT

Physical environment information presented in the atlas was selected on the basis of its relevance to oil spill countermeasures response. As the atlas is intended for the planning and implementation of year-round oil spill countermeasures, knowledge of the changing ice and climatic conditions in the study area is essential. The main effect of ice cover is to drastically change the area affected by an oil spill, the behavior of oil, and the opportunity for oil impact on the shoreline on a seasonal basis.

For example, oil spill response decisions for a spill occurring in early or mid-winter depend on the winter ice conditions. The ice zone in which the spill occurs will determine whether oil will be encapsulated in-situ within the stable, landfast ice zone, or whether oil will be incorporated within the dynamic, drifting ice cover of the transition zone or polar pack.

In the first case, countermeasures response can be delayed until spring. As the landfast ice sheet deteriorates in June and early July, the oil appears in melt pools on the surface of the ice and can be effectively burned. The following page from the atlas is the facing page for Regional Map 5 West of Mackenzie Bay showing an example of landfast ice break-up patterns. The data presented on landfast ice ablation and ice bearing capacity are to be used as guidelines for determining when it is safe to have people and equipment on the ice for oil cleanup in spring.

In the second case, an immediate response is required to ensure adequate surveillance and tracking of the oil. Representative data on seasonal pack ice drift and surface water speeds, as well as sample winter and summer buoy trajectories, are presented in the atlas at the summary scale.

Climatic data relevant to oil spill countermeasures response are also presented in the atlas in an appendix. Two shore stations were chosen to be representative of climate along the Beaufort Sea coast: Shingle Point and Tuktoyaktuk. Offshore climatic data, collected from drillships, are also presented. All data were obtained from Atmospheric Environment Service's (1986) computer archives.

An example of the format of the climatic data contained in the atlas is shown in the following pages. In this case, air temperature, wind chill, and frequencies of fair weather and flying weather for Shingle Point are shown. Air temperature and wind chill affect the performance of people and equipment during cleanup operations. Visibility (as fair weather and as flying weather) affects surface travel and aircraft operations for surveillance, aerial photography, and cleanup activities.

Other information presented on climate in the atlas includes wind speeds, wind directions, wave heights, daylight hours, sea surface temperatures, and freezing spray potential.

LANDFAST ICE BREAK-UP – 1976 EXAMPLE

REGIONAL MAP 5 WEST MACKENZIE BAY

Legend

░	**Polynya (open water area), June 18, 1976 (1).**
—	**OpenWater Following Flooding of the Mackenzie River prior to Landfast Ice Break-up, June 13-15, 1976 (2).**
—	**Landfast Ice Limit prior to Ice Break-up, June 13-15, 1976 (2).**
--	**Landfast Ice Remaining on July 4, 1976 following Fracturing of the Landfast Ice Sheet across Mackenzie Bay and Kugmallit Bay (21).**
......	**Landfast Ice Remnants on July 11, 1976 (21).**

Notes:

1. Cracked Ice Bearing Capacity, Figure 10
   Use this chart for aircraft landing only if weight is less than that predicted from Figure 7 modified with regard to crack type as follows (23):
   - non-intersecting wet cracks Wt. x 0.5
   - intersecting wet cracks Wt. x 0.25.

2. General Modifiers to Spring Ice Bearing Capacity
   For rapid temperature drops:
   - 5° C/day use Wt. x 0.5
   - 10° C/day use Wt. x 0.25
   - >10° C/day suspend operations.
   For operations with average daily temperatures > -1.8° C use Curve 5 (Figure 7) until surface deterioration prevents operations. Expect maximum one week to ten days further use after surface water drains. Suspend operations when average daily temperature exceeds 5° C (23).

Figure 9. Examples of Landfast Ice Ablation (22)

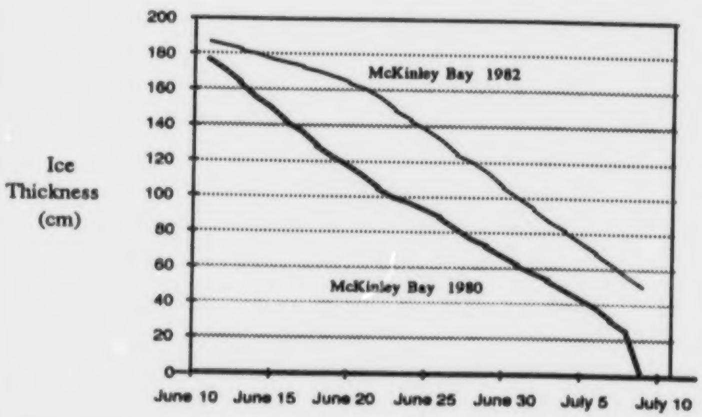

Figure 10. Ice Bearing Capacity for Cracked Ice Sheets (23)
For Given Ice Crack Spacings

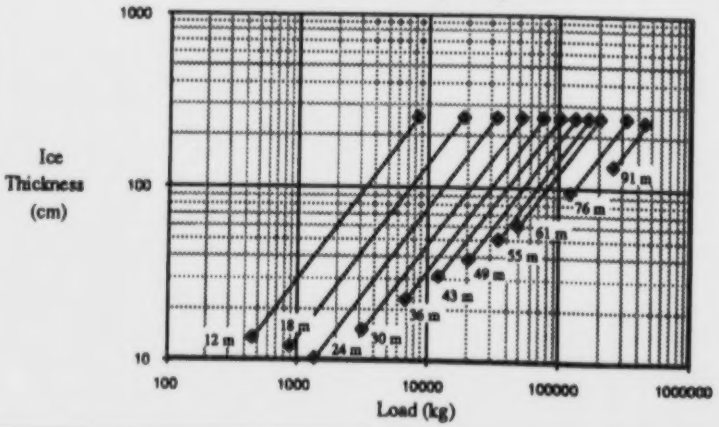

CLIMATIC DATA FOR LOGISTICS

SHINGLE POINT

Figure 1. Air Temperature

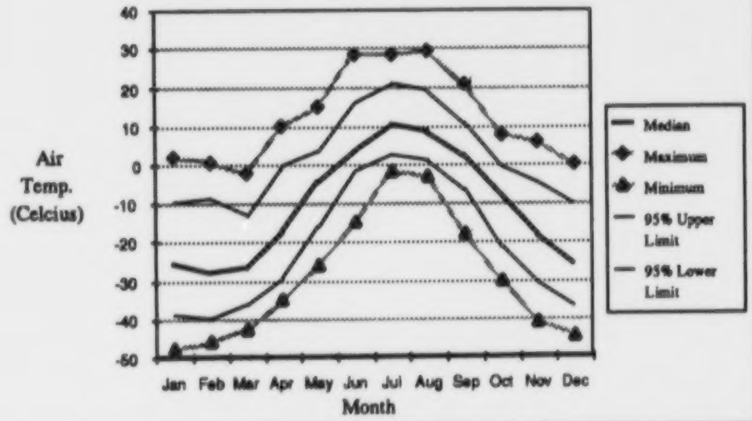

Figure 3. Frequency of Fair Weather

Visibility Greater Than 2 miles and Winds Less Than 25 knots

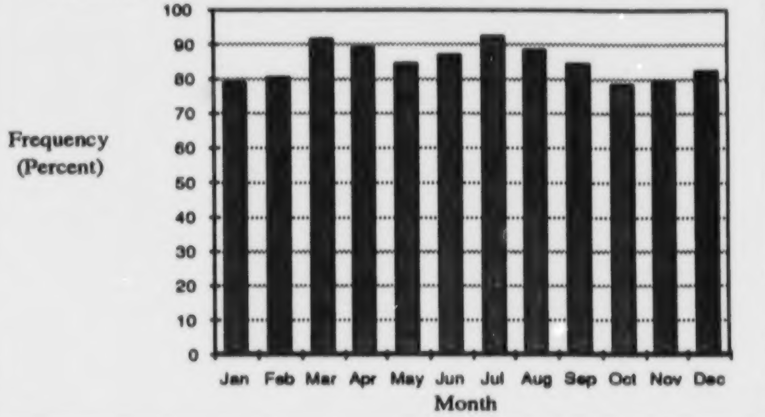

Figure 2. Frequency of Wind Chill Classes

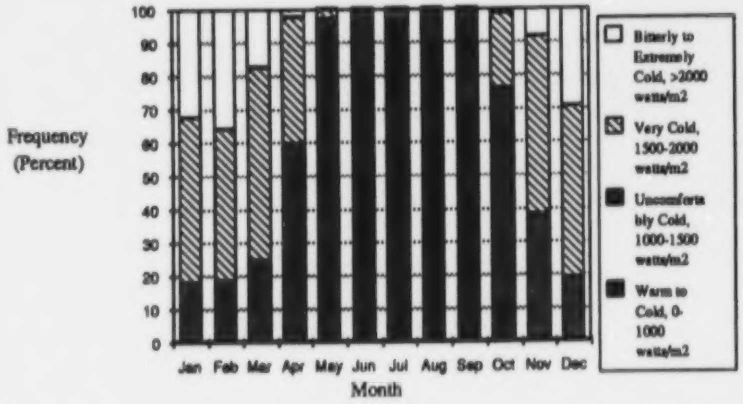

Figure 4. Frequency of Flying Weather

Visual Flight Rules, Ceiling > 1000 ft and Visibility > 2.5 miles

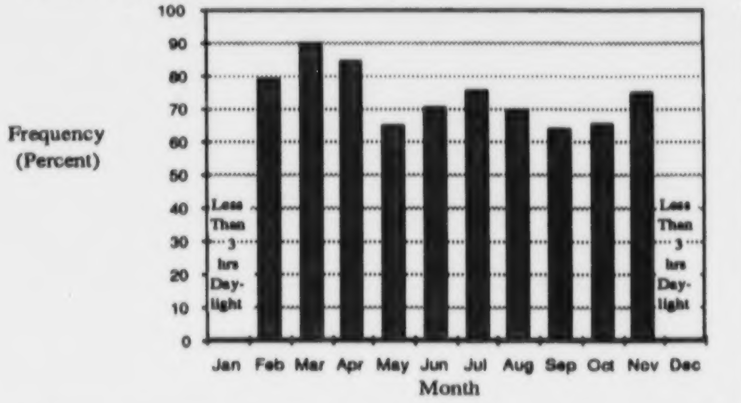

ACCESS AND COUNTERMEASURES

Countermeasures and access information is provided for each of the operational and tactical scale maps. The countermeasures information is intended as a guide to the applicability of protection and cleanup techniques as they relate to local conditions, rather than as a comprehensive spill cleanup manual. The access information is intended as a guide to the local conditions that may influence the choice and performance of logistics support for countermeasures activities.

The countermeasures information is presented in three parts: marine countermeasures, shoreline protection, and shoreline cleanup. The first part has notes on the applicability of offshore and nearshore countermeasures and the ecological applicability of dispersant use, and may suggest nearby locations for basing operations.

The second part lists possible protection strategies that apply to particular shoreline resources and nearshore conditions, and also notes, where applicable, which protection actions are of high priority. In this instance, the designation of high priority relates directly to the identified environmental sensitivity ranking.

The third part notes the applicability of shoreline cleanup techniques to the area in question, the existence of access points for delivering cleanup equipment, and the location of potential sites for temporarily or permanently disposing of spill debris. In some cases, the priority of cleanup as dictated by shoreline exposure, degree of contamination, or proximity to sensitive resources is noted.

The access information is presented, in order, following the coastline of each map from west to east. The information includes, where applicable:

- nearshore water depths and variability;
- access to inshore areas and channel depths;
- ice freeze-up and break-up dates for bays and harbours;
- tidal variations;
- safe anchorages and depths;
- access points for beaching shallow draft barges;
- high, or unusual currents;
- airstrips, floatplane access, and areas where winter runways have been built; and
- fresh water sources.

As an example, the facing page for Operational Map 20 of Nicholson Island is shown here to demonstrate how the information on countermeasures and access is presented in the atlas.

PHYSICAL ENVIRONMENT AND LOGISTICS

OPERATIONAL MAP 20
NICHOLSON ISLAND

Legend

▦	**Tundra Cliffs**
∴	**Inundated Tundra**
⁘	**Barrier Beaches & Spits**
▤	**Deltas**
E	**Estuaries and Bays**
→	**Net Longshore Sediment Transport**
≋	**Areas Inundated During Positive Storm Surges**
......	**Low Water Line**
⊠	**Artificial Islands**
⚓	**Anchorage**
↘	**Shore Access** (Barge Offloading)
✈	**Airstrip suitable for STOL**
✈	**Airstrip suitable for F27, HS748**
✈	**Airstrip suitable for Hercules**
⊕	**Ice Runways** (Winter Only)
( )	**Inlet Width (m)**
×	**Potential Debris Storage** - Temporary
⊗	**Potential Disposal Site** - Permanent
········	**Summer Access** (Disposal Sites)
----	**Winter Access** (Disposal Sites)

Nearest Airstrip - Nicholson Island, Map 20

Hydrographic Chart - 7664

Video Tapes - AGC 2, Dome 17, 18, 24, 25

Access:

Shoal water extends as far as 5 km offshore from Johnson Bay northwards. South of this region shallow-draft barges can be beached along most of the coast. Liverpool Bay has fairly constant mid-channel depths of between 9.1 and 12.8 m to within 7 km of Campbell Island (Map 22). The 750 m inlet at the south end of Nicholson Island provides access into Wood Bay for vessels drawing less than 2 m. A DEW Line station is located about 3 km south from the northern extremity of Nicholson Island. A wind cone and a hut are located at the northwest end of Hepburn Spit.

Niarkrok Harbour and Hepburn Spit (Nicholson Island) provide protected anchorage at a depth of 1.5 m. The normal range of tide is reported to be about 0.5 m. When entering the inside of Hepburn spit, stay clear of breakers that extend 2 km southeast from the sand spit. The depth of water in the harbour formed between the spit and the island varies from 0.9 to 2.1 m. Landing craft can dry-ramp at the beach; barges drawing about 1.5 m are berthed bows-to a bulldozed gravel ramp. Deeper draft vessels can anchor close off the outer side of the spit in 4.9 m of water.

A gravel airstrip on Hepburn Spit is 1045 m long and suitable for year-round use. Wood Bay, to the SE, is suitable for landing floatplanes. Fresh water is available from a lake 3 km SW of Hepburn Spit. Ice in Liverpool Bay normally begins to break-up in the first week of July, clearing two weeks later; freeze-up normally begins in the second week of October, the ice becoming consolidated four weeks later. Break-up and freeze-up dates can vary by up to three weeks.

Countermeasures:

Offshore countermeasures, dispersion or at-or near-source containment for recovery or in-situ burning, are the first options for protecting the Liverpool Bay area. Relatively calm conditions within Liverpool Bay should allow fairly effective nearshore recovery operations. Dispersant use within this area is ecologically warranted when oil threatens waterfowl concentrations or waterfowl habitats.

In terms of shoreline protection, diversion booms may be used to concentrate slicks at accessible sand beaches, thus limiting the extent of shoreline contamination. If threatened, the channel at Nicholson Point and the entrance to Johnson Bay should be sealed with booms.

Beached oil may persist for some time in this relatively low wave energy environment; oiled beaches, especially those in the vicinity of the Anderson River Bird Sanctuary, should be cleaned in a timely manner. Except for Johnson Bay and a few areas with fronting mud flats, most beaches can be accessed by shallow draft barge for the delivery of cleanup machinery. Two potential disposal sites on the north half of Nicholson Island are preferred over the more southerly sites that lie within the bird sanctuary.

CONCLUSIONS

The Environmental Atlas for Beaufort Sea Oil Spill Response constitutes a major milestone in synthesizing available environmental data of the Beaufort Sea region. The atlas will advance both government and industry's level of preparedness and capability to respond to spills. This project has had widespread support and participation from many Federal government departments, both Territorial governments and Land Use Planning Commissions, the oil industry, and native organizations from the Beaufort region. The production of the atlas is consistent with many of the Beaufort Sea EARP Panel recommendations, as well as with the stated policy objectives of Environment Canada, Environmental Protection Service. In light of Gulf Canada Resources' plans for Beaufort Sea production, the release of the atlas is timely.

The scientific framework on which the Beaufort Sea Atlas is based can be applied with local modifications to other arctic areas where marine oil spill response is required. Two regions where similar atlases may be developed in the future are Lancaster Sound and the Mackenzie Valley. Funding for such projects is contingent on the perceived need within government and industry to improve preparedness in advance of development. Planning now for future atlas volumes is appropriate, considering the lead time required to secure funding and develop an atlas into a printed product.

STUDY TEAM DESCRIPTION

DF Dickins Associates Ltd. was the prime contractor with overall responsibility for production of the atlas. David Dickins directed the project in association with the study team managers in the key scientific areas of biological resources, physical environment, human use and oil spill countermeasures, and developed a marine oil residence category for environmental sensitivity ranking.

Linda Martin of ESL Environmental Sciences Limited was responsible for all aspects of the atlas concerned with biological resources and environmental sensitivity. Stephen Johnson of LGL Limited and Pamela Norton of PN Research Projects compiled biological resource information and provided sensitivity rankings for birds and marine mammals, respectively. Patricia Vonk of ESL provided research support and compiled information relating to archaeological sites, park boundaries, and special status areas.

Diane Erickson of Erickson Associates developed the information base on human coastal and offshore use of the region and interpreted the sensitivity elements related to resource harvesting and locally identified cultural sites.

Ingrid Bjerkelund of DF Dickins Associates Ltd. prepared all information describing the physical environment (ice and climate) and logistics, developed the overall atlas layout and assisted with final production of the atlas.

Stephen Potter of S.L. Ross Environmental Research Limited developed the text sections concerned with shore access and countermeasures, and selected potentially acceptable oil disposal sites.

John Harper of Dobrocky Seatech Ltd. mapped shoreline types and backshore inundation limits, and developed and applied a shore zone oil residence category for environmental sensitivity ranking.

John McDonald of ESL Environmental Sciences Limited managed the computer production of all maps contained in the atlas. Peter Brouwer was in charge of digitization of map bases and overlay information and final plotting. Rod Olafson carried out specialized software development, including modifications to enable downloading of the Canadian Hydrographic Service digital chart data base for the Beaufort Sea.

David Tilden with the Environmental Protection Service, Yellowknife was the Scientific Authority for the project and chairman of the project steering committee.

PROJECT FUNDING

The main funding for the atlas was provided by the Northern Oil and Gas Action Program (NOGAP). NOGAP is a Department of Indian Affairs and Northern Development sponsored research program with the objective of advancing the state of Federal and Territorial government preparedness for major hydrocarbon development north of 60°N.

Considerable effort was expended in obtaining additional funding to complete the atlas. Supplementary funding was received from: the Environmental Protection Service, the Department of Indian Affairs and Northern Development, the Canadian Coast Guard/Department of Transport, the Canada Oil and Gas Lands Administration, the Yukon Territorial Government, the Government of the N.W.T., the Beaufort Sea Oil Spill Co-op (Dome Petroleum Limited, ESSO Resources Canada Limited, and Gulf Canada Resources Ltd.), the Yukon and N.W.T. Land Use Planning Commissions, the Department of Fisheries and Oceans, Chevron Canada Resources Limited, the Committee for Original Peoples Entitlement-Land Use Planning, and the Beaufort Mackenzie Delta Development Impact Zone Society.

REFERENCES

ATMOSPHERIC ENVIRONMENT SERVICE. 1986. Climatic data from MAST and DUST Computer Programs. Scientific Services Division, Western Region, Environment Canada, Edmonton.

BEECH, F. and E. OWENS. 1981. Manual for the Preparation of Shoreline Protection and Cleanup Plans. Regional Program Report 81-17. Environmental Protection Service, Environment Canada, Vancouver.

CANADIAN HYDROGRAPHIC SERVICE. 1986. Nautical Charts 7661, 7662, 7663, 7664, 7608, 7685, 6433, 6434, 6436, and 6441. Department of Fisheries and Oceans, Sidney, B.C.

INDIAN AND NORTHERN AFFAIRS CANADA and ENVIRONMENT CANADA. 1985. Beaufort Environmental Monitoring Project 1984-85 Final Report. Unpublished report by ESL Environmental Sciences Limited, LGL Limited, ESSA Limited, Arctic Laboratories Limited, and Arctic Sciences Limited.

WORBETS, B.W. 1979. Shoreline Oil Spill Protection & Cleanup Strategies: Southern Beaufort Sea. Manual and Appendix. Arctic Petroleum Operators' Association Report No. 136, Calgary.

A NEW APPROACH TO EMERGENCY INCIDENT RESPONSE

by

R.H. Goodman
Esso Resources Canada Ltd.
Calgary, Alberta

and

R. J. Woznow
Esso Petroleum Canada
Toronto, Ontario

and

W.F. MacKay
Esso Chemical Canada
Toronto, Ontario

ABSTRACT

The Imperial Oil family of companies has developed a new National Emergency Team, which will assist local facility response teams to handle any major spill or emergency situation that should occur as the result of company activities in Canada. This paper will describe the development of this team concept, it's implementation and structure.

1 Introduction

This paper will discuss the development of a new Imperial Oil response team with national responsibilities, which will be used in the event of chemical or petroleum emergency situations which cannot be handled by the local facility response team.

2 Analysis of Present Situation

In 1984, the Imperial Oil group of companies established four regional response teams across Canada to respond to spill situations that were larger or more complex than could be handled by local facility teams. The organization chart for each of these teams is shown in figure 1. Each of the core positions have three members, and the remaining positions have one or two members depending on the region. The core positions are shown in bold face in the diagram (figure 1).

The technical positions on each of these teams were occupied by local staff who were backed up by company experts from the operating affiliates. A total of about 270 staff were involved in these teams across Canada.

In order to train these staff members in spill response, a five-day training program was developed by Esso. Each training session had about 40 pupils, and a total of four sessions were conducted during 1984-86 in Vancouver and Sarnia.
The material covered in this course included sessions on Company policy, the disciplined approach, hazardous materials handling, containment and recovery and fate and effects. Boom deployment in both an ocean and a river situation and a simulated chemical spill were involved in the hands on exercises. Two paper simulations were conducted which involved both a river and major ocean scenario. These programs were very successful and provided Imperial with a staff of more than 160 workers trained in spill response.

3 Study of Response team needs

A review of this response structure was initiated in the first half of 1986, as a component of the restructuring of Esso Petroleum. This restructuring lead to a reduction in staff due to retirement and other incentive programs. As a result, there was a significant reduction in the availability of staff trained in spill response, both due to staff leaving and the reassignment of people to different positions. Therefore, a new major training program would be needed to bring our response capability to acceptable standards and to optimize our utilization of staff for emergency response. A study was initiated to determine

FIGURE 1

REGION MAJOR SPILL RESONSE TEAM

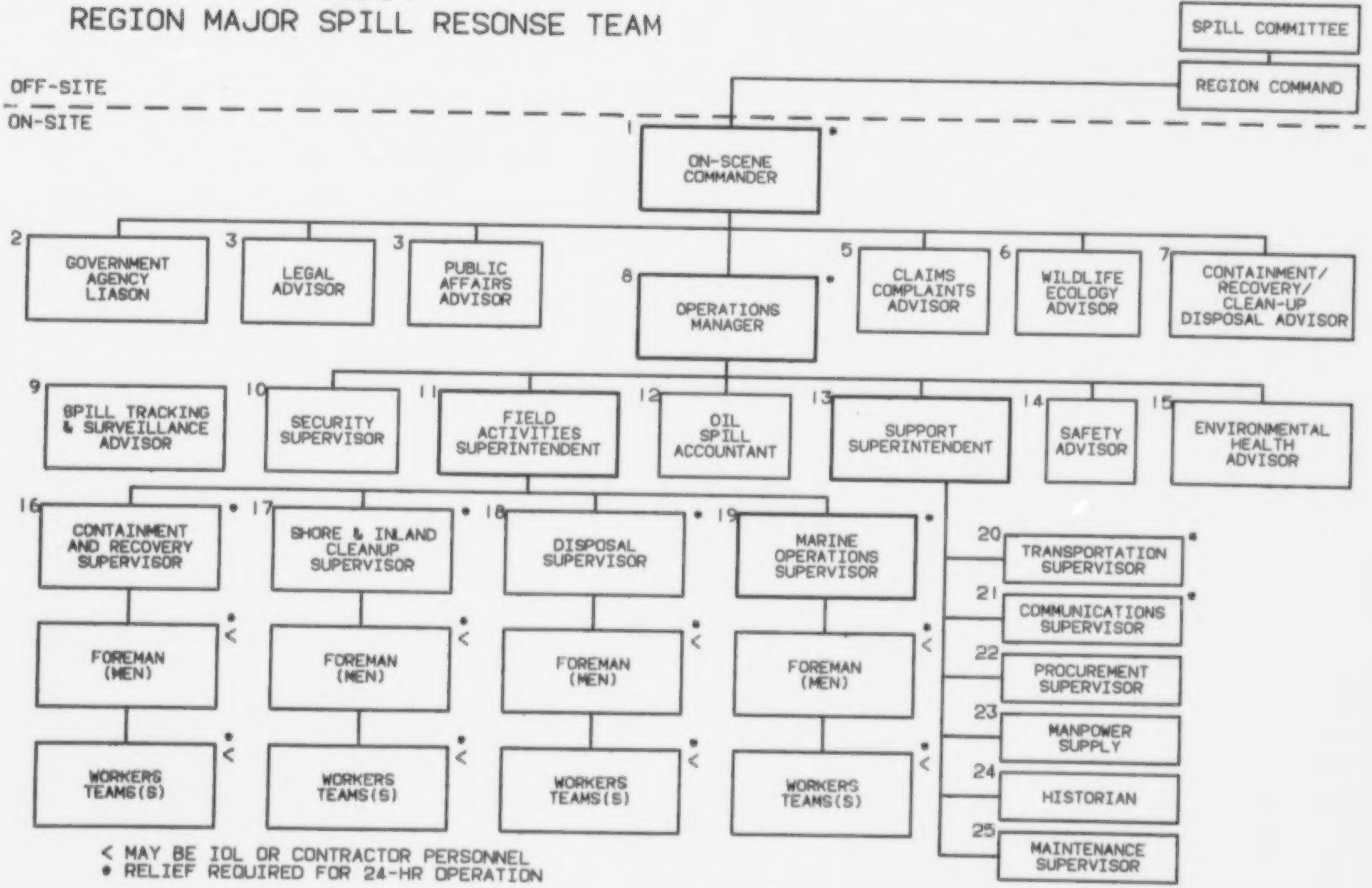
SPILL COMMITTEE
REGION COMMAND
OFF-SITE
ON-SITE
1 ON-SCENE COMMANDER •
2 GOVERNMENT AGENCY LIASON
3 LEGAL ADVISOR
3 PUBLIC AFFAIRS ADVISOR
8 OPERATIONS MANAGER •
5 CLAIMS COMPLAINTS ADVISOR
6 WILDLIFE ECOLOGY ADVISOR
7 CONTAINMENT/ RECOVERY/ CLEAN-UP DISPOSAL ADVISOR
9 SPILL TRACKING & SURVEILLANCE ADVISOR
10 SECURITY SUPERVISOR
11 FIELD ACTIVITIES SUPERINTENDENT
12 OIL SPILL ACCOUNTANT
13 SUPPORT SUPERINTENDENT
14 SAFETY ADVISOR
15 ENVIRONMENTAL HEALTH ADVISOR
16 CONTAINMENT AND RECOVERY SUPERVISOR •
17 SHORE & INLAND CLEANUP SUPERVISOR •
18 DISPOSAL SUPERVISOR •
19 MARINE OPERATIONS SUPERVISOR •
FOREMAN (MEN) • <
WORKERS TEAMS(S) • <
20 TRANSPORTATION SUPERVISOR •
21 COMMUNICATIONS SUPERVISOR •
22 PROCUREMENT SUPERVISOR
23 MANPOWER SUPPLY
24 HISTORIAN
25 MAINTENANCE SUPERVISOR
< MAY BE IOL OR CONTRACTOR PERSONNEL
• RELIEF REQUIRED FOR 24-HR OPERATION

F120,807,01,870514,894 AMH

whether there were other organizational structures which could be developed that would be equally effective, and would optimize the utilization of staff for emergency response within the company.

A number of alternatives were considered in this study. These included:

1. The training of staff to maintain the existing response organization.

2. Use existing major co-ops across the country to manage the response.

3. The use of external contractors and a small team of supervisors from Imperial Oil. This is the "project manager" option.

4. The development of a small national major response team which would provide emergency response for all of the country.

Discussions were held with those responsible for emergency across the country and a list of musts and wants was developed during these meetings. The musts for the organization were:

1. Maintain or improve existing response capability.
2. Meet all legal obligations.
3. Cost the same or less than the existing organization.
4. Be responsive to Imperial Oil needs for emergency response.

As a result of a detailed analysis, it was concluded that option 4, the development of a single major response met all the wants, and could be operated and maintained at a lower cost than the present structure.

4 Structure of New Response Team

The new response team was developed which had two parts: a major response team known as NET (National Emergency Team) and a number of regionally-based support advisors.

The NET operates in support of local response teams. The team members generally serve as advisors to the local team members. In some situations, such as a response in a remote area, the team may function by itself and assume the total responsibility for the spill. The organizational structure for this is shown in figure 2. It is not a hierarchical structure, but rather a matrix structure which is consistent with the expert nature and specialized roles of the response team.

The major response team has seven positions, each of which has three members. The positions are:

FIGURE 2

NET RESPONSE ORGANIZATION

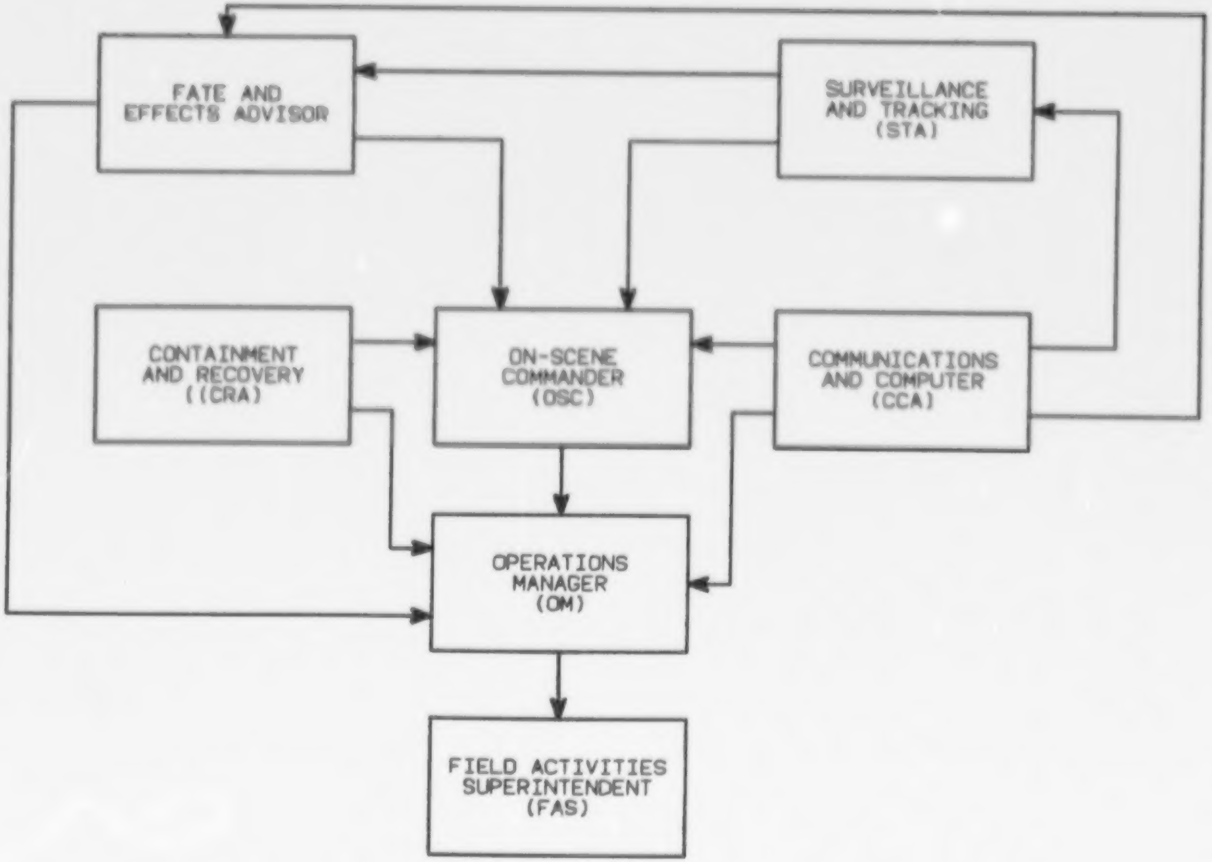
FATE AND EFFECTS ADVISOR
SURVEILLANCE AND TRACKING (STA)
CONTAINMENT AND RECOVERY ((CRA)
ON-SCENE COMMANDER (OSC)
COMMUNICATIONS AND COMPUTER (CCA)
OPERATIONS MANAGER (OM)
FIELD ACTIVITIES SUPERINTENDENT (FAS)

F120.807.03.870514.894 AMM

1. On-Scene Commander (OSC): The On-Scene commander is responsible for the conduct of the response, and the coordination of all aspects of the operation. He is the most senior person from NET at the spill scene. The OSC advises local staff on communications with the local media, as well as public and government officials. He is responsible for liaison with Head Office Spill committee, prompt attention to claims. The OSC coordinates activities with the Salvage Operations coordinator, and has regular meetings with the Operations manager.

2. Operations Manager (OM): The operations manager acts as a deputy on-scene commander, and implements the decisions of the on-scene commander. Coveys all appropriate information and relays orders to the Field Activities Superintendent. The OM is responsible for safety and security at the spill site, with advice from the Safety and Security advisors. The Operations Manager ensures that adequate records are kept using the services of the Historian.

3. Field Activities Superintendent (FAS). The field activities superintendent is responsible for the undertaking of all the response operations. He follows a plan of action developed by the On-Scene Commander and the Operations Manager and coordinates the functions of the various response teams. The FAS ensures that all operations are conducted in a safe manner, and that adequate records are maintained. He coordinates the procurement of equipment and personnel from local contractors and company facilities.

The above three positions are essentially managerial in nature, and provide the basis for the structure and control of a response. The next four positions are those of specialist technical advisors.

4. Surveillance and Tracking Advisor (STA). The Surveillance and Tracking advisor is responsible to the On-Scene Commander, and provides technical expertise in the monitoring of the location of the spill, its concentration and probable movement. The STA prepares large scale maps and charts of the affected areas, showing the current position of the spill. He provides actual and predicted concentration information to the Fate and Effects, Medical, and Public Affairs Advisors as required.

5. Fate and Effects Advisor (FEA). The Fate and Effects advisor is responsible for an analysis of the consequences of the spill, and assists in the technical assessment of clean-up priorities. The FEA coordinates wildlife cleaning and rehabilitation and acts as a liaison with government officials on environmental

issues. The FEA assists the OSC in responding to questions from the media relating to environmental issues.

6. Containment and Recovery Advisor (CRA). The Containment and Recovery Advisor provides technical advice on the capabilities of various equipment that may be used in response to the spill to the On-Scene Commander and Operations Manager. Advises on countermeasures including the use of dispersants, and monitors the effectiveness of response strategies and techniques.

7. Communications and Computer Advisor (CCA). The communications advisor is responsible for providing the communications and the computer needs of the team during an incident. Develops a communication system for alerting the teams and call-out to an incident. The CCA is responsible for advising the local facility teams on their communication needs.

The above positions require particular expertise and ability in response to a spill incident. There are a number of other functions needed for response to an incident which require special expertise. These include:

1. Legal
2. Accounting
3. Historian and Record Keeping
4. Public Affairs
5. Industrial Hygiene
6. Safety
7. Security
8. Purchasing
9. Metallurgical
10. Hot Tapping
11. Medical

Experts in these fields have been chosen from various operating regions of the company. They will not receive the same level of training as the NET team since the skills needed to handle a spill situation are the same as that needed for the normal activities undertaken by these people.

5 Training of New Response Team

The training of the new response team will be undertaken during the next year. Since many of the members of the team have had considerable training and hands-on experience in spill response, it was decided that most of the training would use the expertise of the team. A number of meetings of the team will be held at various locations across the country in order to familiarize all team members with the variety of Imperial facilities. These meetings will serve to provide a training function, during which simulations, and technology transfer will take place.

Specialist training programs will be conducted as required to familiarize team members with the use of equipment, computer programs and other technology. In order for the team to function effectively, there will be a good deal of cross training between positions so that one team member can serve in a number of positions as required for a specific incident.

6 Call out procedure

The national emergency team (NET) can be activated in a number of ways. The decision to use this team is based on the evaluation of an incident by the manager of the facility responsible for the incident. He can call out any member of the team or the total team at his discretion. He may elect to have some team members present on site, and others providing assistance from their work locations.

The procedures used to activate the team, in the case of an incident involving chemicals, are shown in figure 3. The same procedures would be used for a hydrocarbon spill except for the involvement of TEAP. This is only one procedure for obtaining the services of team members. A list of all team members, with their business and home numbers, pager numbers and other methods of contact have been supplied to all Imperial Oil facilities in Canada. This list provides another method of obtaining team services.

In order to facilitate a quick response to an incident, all team members are supplied with pagers. This serves as a primary warning mechanism. The details of the incident will be placed on ENVOY 100 and will be automatically transmitted to all NET members. ENVOY 100 provides all team members with the same information, in a written form, and does not require the initial contactor to repetitively relay the same information to all team members.

7 Conclusions

The new national response team, NET, was established in January 1987. Its mandate has been established and the twenty-one member team selected. Three team meetings have been held and a training program established. The team has not yet had to respond to an incident, but all the members are confident that they are prepared for any incident that may occur.

8 Acknowledgments

The authors would like to thank Imperial Oil for permission to publish this paper and for the company's continued support of the emergency response program.

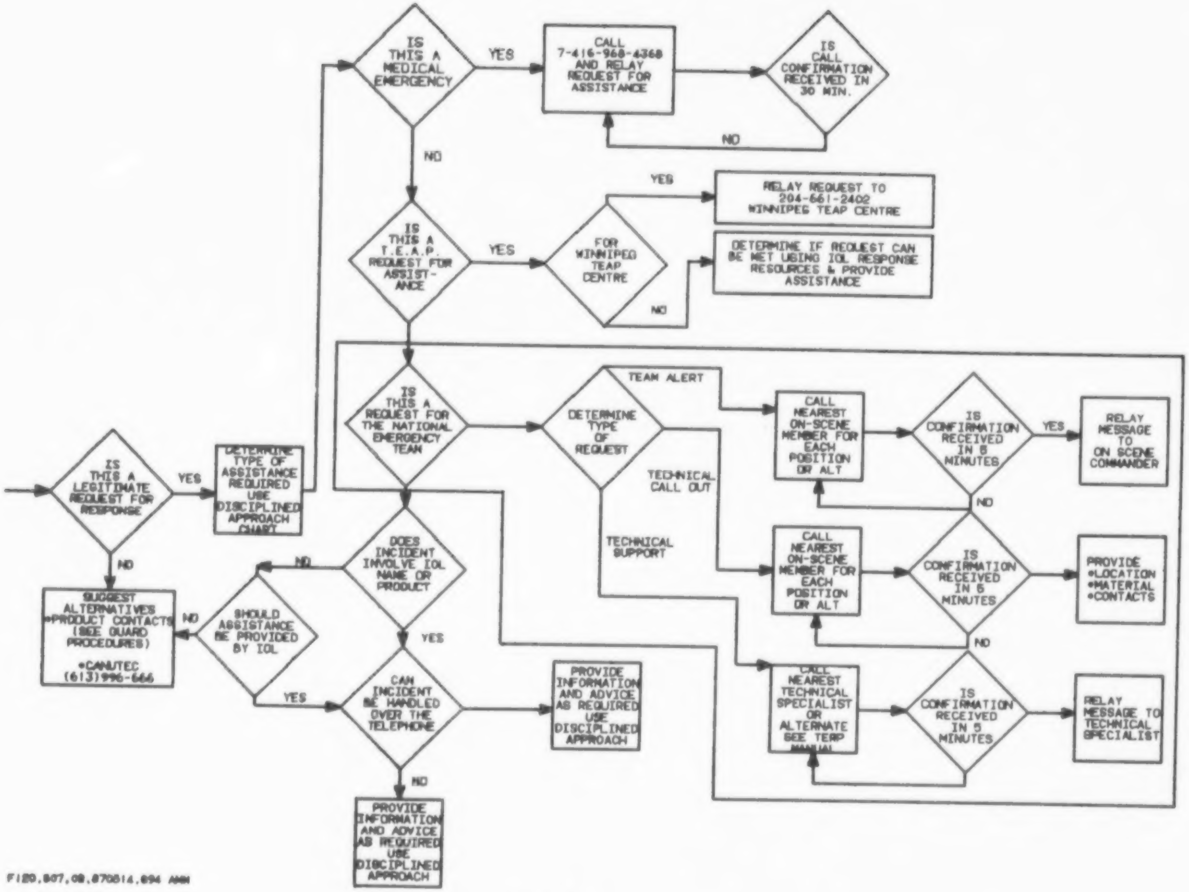
IS THIS A LEGITIMATE REQUEST FOR RESPONSE
YES
NO
DETERMINE TYPE OF ASSISTANCE REQUIRED USE DISCIPLINED APPROACH CHART
SUGGEST ALTERNATIVES •PRODUCT CONTACTS (SEE GUARD PROCEDURES) •CANUTEC (613)996-666
IS THIS A MEDICAL EMERGENCY
YES
NO
CALL 7-416-968-4368 AND RELAY REQUEST FOR ASSISTANCE
IS CALL CONFIRMATION RECEIVED IN 30 MIN.
NO
IS THIS A T.E.A.P. REQUEST FOR ASSIST-ANCE
YES
FOR WINNIPEG TEAP CENTRE
YES
NO
RELAY REQUEST TO 204-661-2402 WINNIPEG TEAP CENTRE
DETERMINE IF REQUEST CAN BE MET USING IOL RESPONSE RESOURCES & PROVIDE ASSISTANCE
IS THIS A REQUEST FOR THE NATIONAL EMERGENCY TEAM
DETERMINE TYPE OF REQUEST
TEAM ALERT
TECHNICAL CALL OUT
TECHNICAL SUPPORT
CALL NEAREST ON-SCENE MEMBER FOR EACH POSITION OR ALT
IS CONFIRMATION RECEIVED IN 5 MINUTES
YES
NO
RELAY MESSAGE TO ON SCENE COMMANDER
CALL NEAREST ON-SCENE MEMBER FOR EACH POSITION OR ALT
IS CONFIRMATION RECEIVED IN 5 MINUTES
NO
PROVIDE •LOCATION •MATERIAL •CONTACTS
CALL NEAREST TECHNICAL SPECIALIST OR ALTERNATE SEE TERP MANUAL
IS CONFIRMATION RECEIVED IN 5 MINUTES
RELAY MESSAGE TO TECHNICAL SPECIALIST
DOES INCIDENT INVOLVE IOL NAME OR PRODUCT
NO
YES
SHOULD ASSISTANCE BE PROVIDED BY IOL
NO
YES
CAN INCIDENT BE HANDLED OVER THE TELEPHONE
NO
PROVIDE INFORMATION AND ADVICE AS REQUIRED USE DISCIPLINED APPROACH
PROVIDE INFORMATION AND ADVICE AS REQUIRED USE DISCIPLINED APPROACH
F120,807,08,870814,894 AMH

FIGURE 3
CALL OUT PROCEDURE

THE USE OF POLYSULPHIDE RUBBER MOLDS TO MEASURE OIL STORAGE VOLUMES

by

R. H. GOODMAN and A. G. HOLOBOFF
Research Department
Esso Resources Canada Limited
Calgary, Alberta, Canada

ABSTRACT

The roughness of the upper surface of Arctic sea ice has been measured in a number of studies, but there are few measurements of the ice roughness at the ice-water interface. Some data has been obtained using impulse radar and using boring, but this information is at a size scale of several meters. It is well known from the observations of divers that the ice is rough at a scale of a few centimeters with an amplitude of a few millimeters.

This small scale roughness has been proposed as having a major role in the storage of oil under the ice, and is therefore of concern to those involved in oil spill response countermeasures.

1 INTRODUCTION

In this paper, when ice surface or ice roughness is used, it refers to the surface at the ice-water interface, unless otherwise stated.

There have been a number of studies on the top surface roughness of Arctic sea ice using a variety of techniques. Several of these were initiated during project AIDJEX with the purpose of determining the forces on sea ice, since the top-surface roughness is a major component of determining the coupling of wind energy to the ice surface. Similarly, the sub-surface roughness couples the ocean regime to the ice.

A number of experiments have been conducted which measured the under-ice roughness. Various techniques have been used including the drilling of holes (Comfort, 1986), impulse radar (Kovacs, 1981), acoustic sounding and under-ice photography using divers. The values obtained vary greatly and seem to depend on location and time of year (that is the stage of the ice growth).

2 THEORY AND MODELS

Ice roughness can be characterized by the root mean square deviation of the ice surface. It order to specify the roughness, it is necessary to state the linear scale of the features. Most measurements have a spatial resolution of from a few meters to several tens of meters, and the roughness scale is measured in terms of these lengths.

If the ice is smooth at these size scales, there is still a roughness of amplitude in the order of a few centimeters, with length scales of several centimeters. This will be called the meso-scale roughness. The meso-scale roughness is important to the storage volume in the event of an incident involving the release of oil under the ice. Observations of divers have confirmed that there are significant features occurring at this size scale, but no suitable measuring technique was available to measure these features.

3 EXPERIMENTAL PROGRAM

The site chosen for the experimental program was near the Esso artificial island ARNAK, located in the Canadian Beaufort Sea (lat 69^{o} 50' N, long 139^{o} 52' W).

Since this project was designed to demonstrate a new technique, it was considered more important to have good logistic support than to select a particularly unique or critical sea ice situation.

The sea ice in the area was landfast, and had experienced little movement during the winter. The experiments were conducted just before break-up, so that a vehicle could be used for access. At this time of year, the ice was at its maximum thickness (about 2m.) and was stable. There was little ablation and the ice was not growing rapidly.

The details of the experimental program have been previously described by Goodman et al (1987). A total of 12 molds were made in the field and returned to the Esso Research Lab in Calgary for analysis.

4 ANALYSIS OF MOLDS

Positive replicates were obtained from the polysulphide molds using resin and fiberglass material. All the analysis of the ice roughness characteristics was undertaken using these positive molds.

4.1 Stereo Photography

Stereo photography was used to prepare a contour map of each of the molds. The methodology used was based on that used for terrestrial mapping. The vertical resolution achieved was better than 0.1cm. and the contour interval was selected as 0.1cm.

The rms roughness, average roughness and variance were calculated from the stereo images using standard computer analysis techniques.

4.2 Progressive Flooding

While the stereo photography was a useful technique for determining the average surface roughness, it does not address the interconnectivity of the channels and thus the spreading of oil on the under-ice surface. It order to study this characteristic, a series of progressive flooding experiments were conducted.

The experimental program used the positive molds. The molds were painted white and the flooding fluid was black so as to present a high contrast image. The molds were carefully leveled and then flooded in 250 ml. increments. After each addition of fluid, the image was captured using the video camera, and recorded as a digital image for subsequent computer image analysis.

The digitized images were analyzed using a Robot image analyzer connected to an IBM PC-XT. A plot of the area flooded as a function of volume is shown in figure 1.

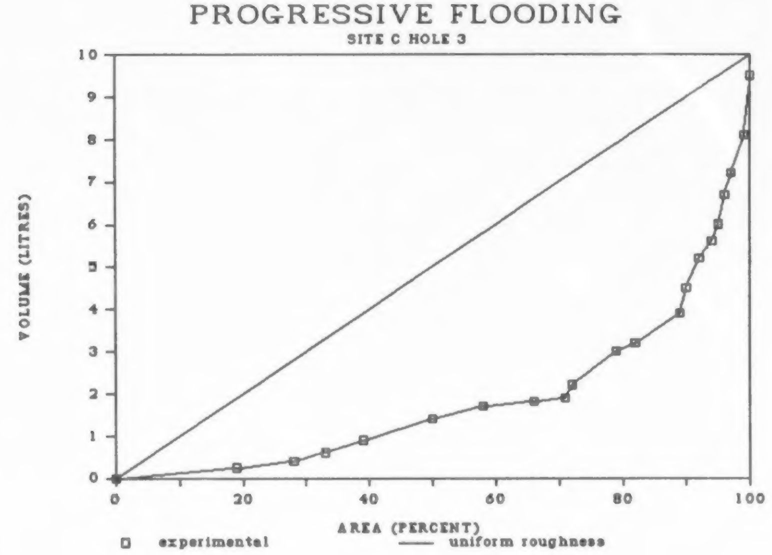

Figure 1. Storage volume as a function of area flooded

The final (100%) coverage thickness is related to the rms roughness by the equation;

$$R_{rms} = \sqrt{2} \times \overline{thickness}$$

$where:$

$$R = rms \quad roughness$$

$$\overline{thickness} = average \quad thickness$$

The value of roughness measurements, obtained from these two techniques is shown in Table 1. The estimated errors are 20%, and the two methods are in essential agreement.

TABLE 1

Average Ice Roughness Values

Location	Average Roughness Photogrammetric m^3/m^2	Average Roughness Volumetric m^3/m^2
Site A		
Hole 1	0.009	0.008
2	0.013	0.014
3	0.010	0.010
4	0.011	0.012
Site B		
Hole 1	0.012	0.011
2	0.013	0.014
3	0.014	0.013
4	0.011	0.010
Site C		
Hole 1	0.010	0.011
2	0.011	0.010
3	0.018	0.016
4	0.010	0.011

5 INTERPRETATION

As shown in figure 1, the experimental values are always less than the linear assumption. This indicates that the surface roughness of the ice does not have a continuous spectrum, but rather consists of a few large features which occur on a generally flat surface. This is collaborated by observations of the mold.

6 COMPARISON WITH OTHER DATA

The values of oil storage volume have been published by a number of workers (Comfort 1986, Kovacs 1981). This data and the results of these experiments are shown in Table 2.

Table 2

COMPARISON WITH OTHER DATA

Location	Storage Volume m^3/m^2	Reference
Tigvariak Island	0.032	Kovacs (1981)
West Dock Site	0.0605	Kovacs (1981)
Reindeer Island (Flat Ice)	0.010	Kovacs (1981)
Site A	0.0248	Kovacs (1981)
Site B	0.0239	Kovacs (1981)
Site C	0.0574	Kovacs (1981)
Seal Island	0.130 0.023	Comfort (1986)
Thunder Bay Harbour	0.062 0.022	Comfort (1986)
Mold Experiments	0.012	This work

7 ICE ROUGHNESS AND STORAGE VOLUMES

The total area of ice that will be oiled for a given volume of hydrocarbon is directly related to the ice-roughness by the equation:

$$D = 2 \times \sqrt{\frac{(V \times R_{rms})}{\pi}}$$

where D is the diameter in meters

V is the spill volume in m3

R_{rms} is the ice roughness

π is 3.14

This is plotted in figure 2.

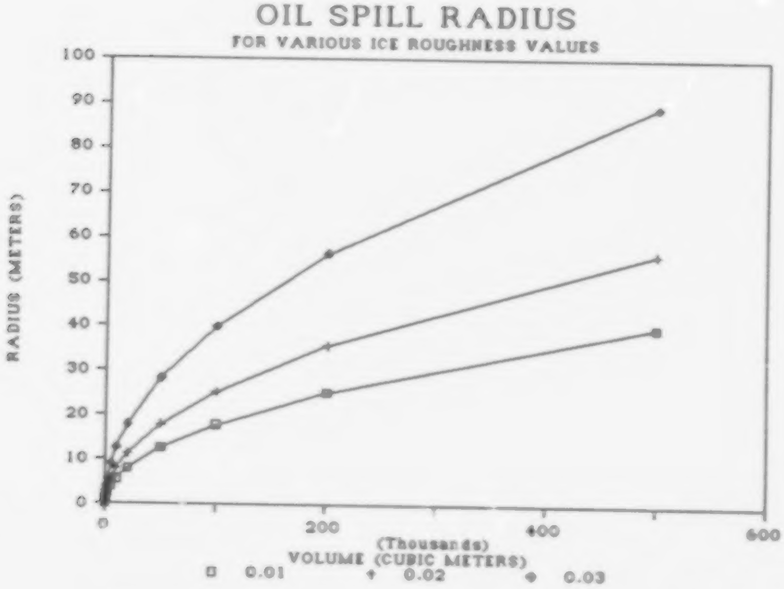

Figure 2. Radius of oil as a function of spill volume

The area contaminated is:

$$A = V \times R_{rms}$$

where A is the area in m^2

This is plotted in figure 3.

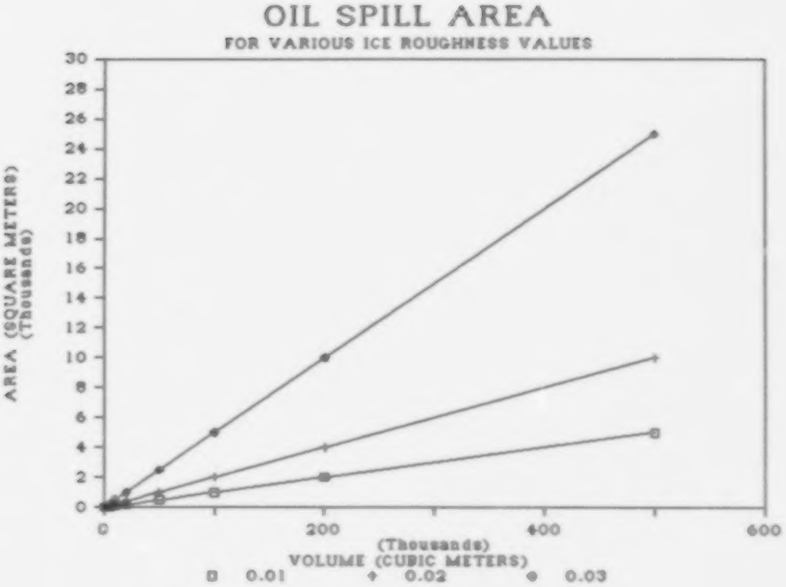

Figure 3. Area of oil as a function of spill volume

8 CONCLUSIONS

These initial experiments have shown that it is technically and logistically possible to use a polysulphide rubber molding technique to produce a high-quality replicate of the under-ice features. Initial observations in the field showed that there was a significant structure at a length scale of several centimeters, with a roughness of a few centimeters.

This roughness contributes to the ability of ice to store oil spilled under the ice.

9 ACKNOWLEDGMENTS

The authors would like to thank Esso Resources Canada Limited for its support of this project. Funding was provided by Esso Resources Canada and the Environmental Emergencies Technology Division of Environment Canada. The initial development of the molding technique was undertaken by Parks Canada, who provided this technology to the program.

10 REFERENCES

Comfort,G., 1986 Under Ice Roughness Measurements Arctec Canada ESRF Study 2041 Part 2.

Goodman, R. H., A. G. Holoboff, T. W. Daley, P. Waddell, L.D. Murdock and M. Fingas 1987. "A Technique for the Measurement of Under-ice Roughness to determine Oil Storage Volumes" Proceedings of 10th Oil Spill Conference (Baltimore); American Petroleum Institute, Washington, D.C. pp395-398.

Kovacs, A., 1981. Pooling of oil under ice. Proceeding of POAC, Quebec City

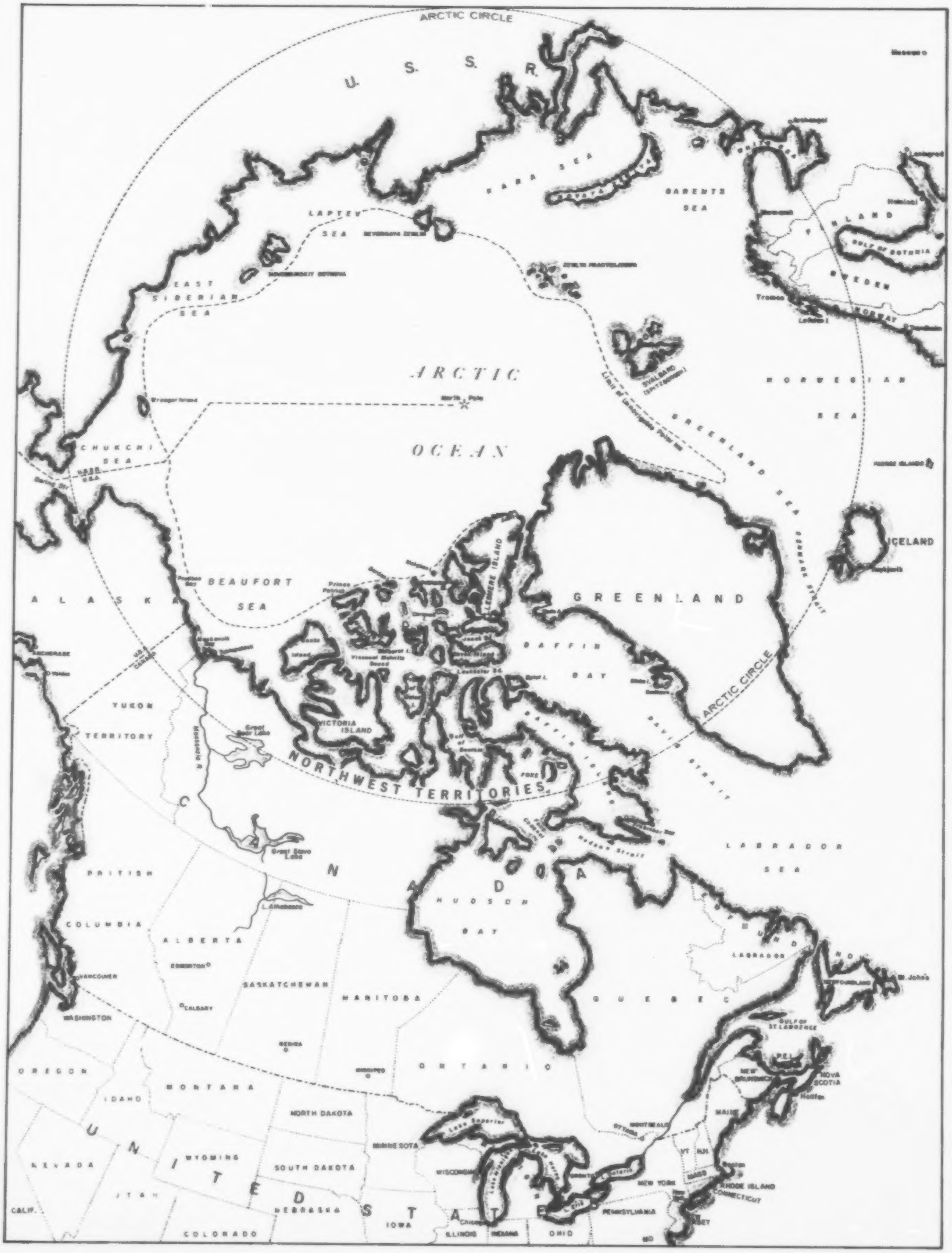
ARCTIC CIRCLE
U. S. S. R.
Moscow
KARA SEA
BARENTS SEA
LAPTEV SEA
Severnaya Zemlya
Archangel
WHITE SEA
Leningrad
Helsinki
FINLAND
GULF OF BOTHNIA
SWEDEN
NORWAY
Tromsø
Lofoten I.
Zemlya Frantsa-Iosifa
EAST SIBERIAN SEA
Novosibirskiye Ostrova
ARCTIC OCEAN
North Pole
Wrangel Island
SVALBARD (SPITZBERGEN)
Limit of Undergrowth Pack Ice
NORWEGIAN SEA
Faeroe Islands
GREENLAND SEA
DENMARK STRAIT
ICELAND
Reykjavik
CHUKCHI SEA
U.S.S.R.
U.S.A.
Bering Str.
BEAUFORT SEA
Prudhoe Bay
ALASKA
Anchorage
Mackenzie Bay
U.S.A.
CANADA
ELLESMERE ISLAND
GREENLAND
BAFFIN BAY
Prince Patrick I.
Banks Island
Viscount Melville Sound
Lancaster Sd.
Devon Island
VICTORIA ISLAND
Gulf of Boothia
BAFFIN ISLAND
DAVIS STRAIT
ARCTIC CIRCLE
Foxe Basin
YUKON TERRITORY
Mackenzie R.
Great Bear Lake
NORTHWEST TERRITORIES
Great Slave Lake
Hudson Strait
LABRADOR SEA
CANADA
HUDSON BAY
BRITISH COLUMBIA
ALBERTA
L. Athabasca
Edmonton
SASKATCHEWAN
MANITOBA
Calgary
Vancouver
WASHINGTON
Regina
Winnipeg
ONTARIO
QUEBEC
LABRADOR
NEWFOUNDLAND
St. John's
GULF OF ST. LAWRENCE
P.E.I.
NEW BRUNSWICK
NOVA SCOTIA
Halifax
MAINE
Montreal
Ottawa
OREGON
IDAHO
MONTANA
NORTH DAKOTA
MINNESOTA
Lake Superior
WISCONSIN
Lake Michigan
Lake Huron
Lake Ontario
Lake Erie
Toronto
VT
N.H.
MASS
Boston
RHODE ISLAND
CONNECTICUT
NEW YORK
New York
NEW JERSEY
PENNSYLVANIA
MD
NEVADA
WYOMING
SOUTH DAKOTA
UNITED STATES
UTAH
CALIF.
NEBRASKA
IOWA
Chicago
ILLINOIS
INDIANA
OHIO
COLORADO